

Erlangen Program at Large

Vladimir V. Kisil

SCHOOL OF MATHEMATICS, UNIVERSITY OF LEEDS, LEEDS LS2 9JT, UK

Email address: kisilv@maths.leeds.ac.uk

URL: <http://v-v-kisil.scienceontheweb.net/>

2010 *Mathematics Subject Classification*. Primary 43A85; Secondary 30G30, 42C40, 46H30, 47A13, 81R30, 81R60.

Key words and phrases. Erlangen program, $SL(2, \mathbb{R})$, special linear group, Heisenberg group, symplectic group, Hardy space, Segal-Bargmann space, Clifford algebra, dual numbers, double numbers, Cauchy-Riemann-Dirac operator, Möbius transformations, covariant functional calculus, Weyl calculus (quantization), quantum mechanics, Schrödinger representation, metaplectic representation

ABSTRACT. The **Erlangen programme** of F. Klein (influenced by S. Lie) defines geometry as a study of invariants under a certain transitive group action. This approach proved to be fruitful much beyond the traditional geometry. For example, special relativity is the study of invariants of Minkowski space-time under the Lorentz group action. Another example is complex analysis as study of objects invariant under the conformal maps.

These notes systematically apply the Erlangen approach to various areas of mathematics. In the first instance we consider the group $SL_2(\mathbb{R})$ in details as well as the corresponding geometrical and analytical invariants with their interrelations. Consequently the course has a multi-subject nature touching algebra, geometry and analysis.

This work is licensed under a **Creative Commons** “Attribution-NonCommercial-ShareAlike 4.0 International” licence.



Contents

List of Figures	ix
Preface	xiii
Part I. Geometry	1
Lecture I.1. Erlangen Programme: Preview	3
I.1.1. Make a Guess in Three Attempts	3
I.1.2. Covariance of FSCc	7
I.1.3. Invariants: Algebraic and Geometric	8
I.1.4. Joint Invariants: Orthogonality	10
I.1.5. Higher-order Joint Invariants: Focal Orthogonality	11
I.1.6. Distance, Length and Perpendicularity	13
I.1.7. The Erlangen Programme at Large	14
Lecture I.2. Groups and Homogeneous Spaces	17
I.2.1. Groups and Transformations	17
I.2.2. Subgroups and Homogeneous Spaces	19
I.2.3. Differentiation on Lie Groups and Lie Algebras	22
I.2.4. Integration on Groups	25
Lecture I.3. Homogeneous Spaces from the Group $SL_2(\mathbb{R})$	29
I.3.1. The Affine Group and the Real Line	29
I.3.2. One-dimensional Subgroups of $SL_2(\mathbb{R})$	31
I.3.3. Two-dimensional Homogeneous Spaces	33
I.3.4. Elliptic, Parabolic and Hyperbolic Cases	36
I.3.5. Orbits of the Subgroup Actions	37
I.3.6. Unifying EPH Cases: The First Attempt	39
I.3.7. Isotropy Subgroups	40
Lecture I.4. The Extended Fillmore–Springer–Cnops Construction	45
I.4.1. Invariance of Cycles	45
I.4.2. Projective Spaces of Cycles	47
I.4.3. Covariance of FSCc	49
I.4.4. Origins of FSCc	51
I.4.5. Projective Cross Ratio	53

Lecture I.5. Indefinite Product Space of Cycles	55
I.5.1. Cycles: an Appearance and the Essence	55
I.5.2. Cycles as Vectors	57
I.5.3. Invariant Cycle Product	60
I.5.4. Zero-radius Cycles	62
I.5.5. Cauchy–Schwarz Inequality and Tangent Cycles	65
Lecture I.6. Joint Invariants of Cycles: Orthogonality	69
I.6.1. Orthogonality of Cycles	69
I.6.2. Orthogonality Miscellanea	71
I.6.3. Ghost Cycles and Orthogonality	76
I.6.4. Actions of FSCc Matrices	79
I.6.5. Inversions and Reflections in Cycles	82
I.6.6. Higher-order Joint Invariants: Focal Orthogonality	84
Lecture I.7. Metric Invariants in Upper Half-Planes	89
I.7.1. Distances	89
I.7.2. Lengths	92
I.7.3. Conformal Properties of Möbius Maps	93
I.7.4. Perpendicularity and Orthogonality	94
I.7.5. Infinitesimal-radius Cycles	96
I.7.6. Infinitesimal Conformality	98
Lecture I.8. Global Geometry of Upper Half-Planes	101
I.8.1. Compactification of the Point Space	101
I.8.2. (Non)-Invariance of The Upper Half-Plane	104
I.8.3. Optics and Mechanics	106
I.8.4. Relativity of Space-Time	109
Lecture I.9. Invariant Metric and Geodesics	113
I.9.1. Metrics, Curves' Lengths and Extrema	113
I.9.2. Invariant Metric	117
I.9.3. Geodesics: Additivity of Metric	118
I.9.4. Geometric Invariants	120
I.9.5. Invariant Metric and Cross-Ratio	122
Lecture I.10. Conformal Unit Disk	125
I.10.1. Elliptic Cayley Transforms	125
I.10.2. Hyperbolic Cayley Transform	126
I.10.3. Parabolic Cayley Transforms	127
I.10.4. Cayley Transforms of Cycles	129
Lecture I.11. Unitary Rotations	135
I.11.1. Unitary Rotations—an Algebraic Approach	135
I.11.2. Unitary Rotations—a Geometrical Viewpoint	137
I.11.3. Rebuilding Algebraic Structures from Geometry	139
I.11.4. Invariant Linear Algebra	141

I.11.5. Linearisation of the Exotic Form	143
I.11.6. Conformality and Geodesics	144
Lecture I.12. Cycles Cross Ratio: an Invitation	147
I.12.1. Preliminaries: Projective space of cycles	147
I.12.2. Fractional linear transformations and the invariant product	149
I.12.3. Cycles cross ratio	151
I.12.4. Discussion and generalisations	156
Lecture I.13. An Extension of Möbius–Lie Geometry with Conformal Ensembles of Cycles	159
I.13.1. Introduction	159
I.13.2. Möbius–Lie Geometry and the cycle Library	161
I.13.3. Ensembles of Interrelated Cycles and the figure Library	164
I.13.4. Mathematical Usage of the Library	170
I.13.5. To Do List	173
Lecture I.14. Poincaré Extension of Möbius Transformations	177
I.14.1. Introduction	177
I.14.2. Geometric construction	177
I.14.3. Möbius transformations and Cycles	180
I.14.4. Extending cycles	182
I.14.5. Homogeneous spaces of cycles	184
I.14.6. Triples of intervals	186
I.14.7. Geometrisation of cycles	188
I.14.8. Concluding remarks	190
Lecture I.15. Conformal Parametrisation of Loxodromes by Triples of Circles	193
I.15.1. Introduction	193
I.15.2. Preliminaries: Fractional Linear Transformations and Cycles	194
I.15.3. Fractional Linear Transformations and Loxodromes	198
I.15.4. Three-cycle Parametrisation of Loxodromes	199
I.15.5. Applications of Three-Cycle Parametrisation	202
I.15.6. Discussion and Open Questions	204
Lecture I.16. Continued Fractions, Möbius Transformations and Cycles	207
I.16.1. Introduction	207
I.16.2. Continued Fractions	208
I.16.3. Möbius Transformations and Cycles	209
I.16.4. Continued Fractions and Cycles	210
I.16.5. Multi-dimensional Möbius maps and cycles	213
I.16.6. Continued fractions from Clifford algebras and horocycles	214

Part II. Harmonic Analysis 217

Lecture II.1. Elements of the Representation Theory	219
---	-----

II.1.1. Representations of Groups	219
II.1.2. Decomposition of Representations	222
II.1.3. Invariant Operators and Schur's Lemma	223
II.1.4. Induced Representations	224
Lecture II.2. Wavelets on Groups and Square Integrable Representations	227
II.2.1. Wavelet Transform on Groups	227
II.2.2. Square Integrable Representations	230
II.2.3. Fundamentals of Wavelets on Homogeneous Spaces	233
Lecture II.3. Hypercomplex Linear Representations	241
II.3.1. Hypercomplex Characters	241
II.3.2. Induced Representations	242
II.3.3. Similarity and Correspondence: Ladder Operators	245
Lecture II.4. Covariant Transform	249
II.4.1. Extending Wavelet Transform	249
II.4.2. Examples of Covariant Transform	250
II.4.3. Symbolic Calculi	254
II.4.4. Contravariant Transform	256
II.4.5. Composing the Co- and Contravariant Transforms	260
Lecture II.5. Analytic Functions	265
II.5.1. Induced Covariant Transform	265
II.5.2. Induced Wavelet Transform and Cauchy Integral	268
II.5.3. The Cauchy-Riemann (Dirac) and Laplace Operators	270
II.5.4. The Taylor Expansion	272
II.5.5. Wavelet Transform in the Unit Disk and Other Domains	272
Lecture II.6. Affine Group: the Real and Complex Techniques in Harmonic Analysis	275
II.6.1. Introduction	275
II.6.2. Two approaches to harmonic analysis	276
II.6.3. Affine group and its representations	278
II.6.4. Covariant transform	280
II.6.5. The contravariant transform	284
II.6.6. Intertwining properties of covariant transforms	287
II.6.7. Composing the covariant and the contravariant transforms	289
II.6.8. Transported norms	294
Part III. Functional Calculi and Spectra	299
Lecture III.1. Covariant and Contravariant Calculi	301
III.1.1. Functional Calculus as an Algebraic Homomorphism	301
III.1.2. Intertwining Group Actions on Functions and Operators	302
III.1.3. Jet Bundles and Prolongations of ρ_1	304
III.1.4. Spectrum and Spectral Mapping Theorem	305

III.1.5. Functional Model and Spectral Distance	307
III.1.6. Covariant Pencils of Operators	309
Part IV. The Heisenberg Group and Physics	313
Lecture IV.1. Preview: Quantum and Classical Mechanics	315
IV.1.1. Axioms of Mechanics	315
IV.1.2. “Algebra” of Observables	316
IV.1.3. Non-Essential Noncommutativity	317
IV.1.4. Quantum Mechanics from the Heisenberg Group	318
IV.1.5. Classical Noncommutativity	319
IV.1.6. Summary	321
Lecture IV.2. The Heisenberg Group	323
IV.2.1. The Symplectic Form and the Heisenberg group	323
IV.2.2. Lie algebra of the Heisenberg group	325
IV.2.3. Automorphisms of the Heisenberg group	326
IV.2.4. Subgroups of \mathbb{H}^n and Homogeneous Spaces	328
Lecture IV.3. Representations of the Heisenberg Group	331
IV.3.1. Left Regular Representations and Its Subrepresentations	331
IV.3.2. Induced Representations on Homogeneous Spaces	332
IV.3.3. Co-adjoint Representation and Method of Orbits	333
IV.3.4. Stone–von Neumann Theorem	334
IV.3.5. Shale–Weil Representation	334
Lecture IV.4. Harmonic Oscillator and Ladder Operators	337
IV.4.1. p-Mechanic Formalism	339
IV.4.2. Elliptic characters and Quantum Dynamics	341
IV.4.3. Ladder Operators and Harmonic Oscillator	346
IV.4.4. Hyperbolic Quantum Mechanics	347
IV.4.5. Parabolic (Classical) Representations on the Phase Space	353
Lecture IV.5. Wavelet Transform, Uncertainty Relation and Analyticity	359
IV.5.1. Induced Wavelet (Covariant) Transform	359
IV.5.2. The Uncertainty Relation	360
IV.5.3. The Gaussian	361
IV.5.4. Right Shifts and Analyticity	361
IV.5.5. Uncertainty and Analyticity	363
IV.5.6. Hardy Space on the Real Line	363
IV.5.7. Contravariant Transform and Relative Convolutions	364
IV.5.8. Norm Estimations of Relative Convolutions	365
Appendix A. Open Problems	369
A.1. Geometry	369
A.2. Analytic Functions	369
A.3. Functional Calculus	370

A.4. Quantum Mechanics	371
Appendix B. Supplementary Material	373
B.1. Dual and Double Numbers	373
B.2. Classical Properties of Conic Sections	373
B.3. Comparison with Yaglom's Book	375
B.4. Other Approaches and Results	375
B.5. FSCc with Clifford Algebras	375
Appendix C. How to Use the Software	379
C.1. Viewing Colour Graphics	380
C.2. Installation of CAS	380
C.3. Using the CAS and Computer Exercises	383
C.4. Library for Cycles	388
C.5. Predefined Objects at Initialisation	389
Bibliography	391
Index	407

List of Figures

I.1.1	Actions of the subgroups A and N by Möbius transformations	4
I.1.2	Action of the subgroup K	5
I.1.3	K -orbits as conic sections	6
I.1.4	Decomposition of an arbitrary Möbius transformation	6
I.1.5	Cycle implementations, centres and foci	8
I.1.6	Different σ -implementations of the same $\check{\sigma}$ -zero-radius cycles	9
I.1.7	Orthogonality of the first kind in the elliptic point space	11
I.1.8	Focal orthogonality for circles	12
I.1.9	Radius and distance for parabolas	13
I.1.10	The perpendicular as the shortest route to a line.	14
I.3.1	Actions of isotropy subgroups	41
I.3.2	Actions of the subgroups K , N' , A'	42
I.5.1	Linear spans of cycle pairs in EPH cases	59
I.5.2	Positive and negative cycles	62
I.5.3	Intersection and tangency	68
I.6.1	Relation between centres and radii of orthogonal circles	69
I.6.2	Orthogonal pencils of cycles	74
I.6.3	Nine types of cycle orthogonality	77
I.6.4	Three types of inversions of the rectangular grid	81
I.6.5	Focal orthogonality of cycles	87
I.7.1	Zero-radius cycles and the “phase” transition	98
I.8.1	Compactification and stereographic projections	102
I.8.2	Continuous transformation from future to the past	104
I.8.3	Hyperbolic objects in the double cover	105
I.8.4	Double cover of the hyperbolic space	106
I.8.5	Some elementary optical systems and their transfer matrices	107

I.9.1 Lobachevsky geodesics and extrema of curves' lengths	116
I.9.2 Region where the triangular inequality fails	120
I.9.3 Geodesics and equidistant orbits in EPH geometries	124
I.10. Action of the isotropy subgroups under the Cayley transform	129
I.10. Cayley transforms in elliptic, parabolic and hyperbolic spaces	130
I.10. EPH unit disks and actions of one-parameter subgroups	133
I.11. Rotations of algebraic wheels	136
I.11. Geodesics as spokes	145
I.12. Cycles cross ratio for two conjugated cycles	153
I.12. Construction for Möbius invariant distance between two cycles	154
I.13. Equivalent parametrisation of a loxodrome	167
I.13. Action of the modular group on the upper half-plane.	171
I.13. An example of Apollonius problem in three dimensions.	171
I.13. The illustration of the conformal nine-points theorem	174
I.13. Animated transition between the classical and conformal nine-point theorems	175
I.14. Poincaré extensions	179
I.15. A logarithmic spiral and a loxodrome	193
I.15. Elliptic and hyperbolic pencils	196
I.15. Loxodromes and pencils of cycles	202
I.16. Continued fractions for e and π visualised. The convergence rate for π is pictorially faster.	208
I.16. Various arrangements for three cycles	212
II.2. The Gaussian function	228
II.3. Rotations of wheels	242
II.3. The action of hyperbolic ladder operators on a 2D lattice of eigenspaces	247
II.6. The correspondence between different elements of harmonic analysis.	297
III.1. Three dimensional spectrum	306
III.1. Spectral stability	308
IV.4. Quantum probabilities: the blue (dashed) graph shows the addition of probabilities without interaction, the red (solid) graph present the quantum	

interference. Left picture shows the Gaussian state (IV.4.23), the right—the rational state (IV.4.26)	345
IV.4.2 Hyperbolic probabilities: the blue (dashed) graph shows the addition of probabilities without interaction, the red (solid) graph present the quantum interference. Left picture shows the Gaussian state (IV.4.23), with the same distribution as in quantum mechanics, cf. Fig. IV.4.1(a). The right picture shows the rational state (IV.4.26), note the absence of interference oscillations in comparison with the quantum state on Fig. IV.4.1(b).	350
B.1 Classical definitions of conic sections	374
B.2 The correspondence between complex, dual and double numbers	377
B.3 Comparison with the Yaglom book	378
C.1 Initial screens of software start up	382
C.2 Initial screens of software start up	383
C.3 Example of figure library usage	387

Preface

Everything new is old... understood again.

Yu.M. Polyakov

The idea proposed by Sophus Lie and Felix Klein was that *geometry is the theory of invariants of a transitive transformation group*. It was used as the main topic of F. Klein's inauguration lecture for professorship at Erlangen in 1872 and, thus, become known as the **Erlangen programme** (EP). As with any great idea, it was born ahead of its time. It was only much later when the theory of groups, especially the theory of group representations, was able to make a serious impact. Therefore, the EP had been marked as "producing only abstract returns" (©Wikipedia) and laid on one side.

Meanwhile, the 20th century brought significant progress in representation theory, especially linear representations, which was requested by theoretical physics and supported by achievements in functional analysis. Therefore, a "study of invariants" becomes possible in the linear spaces of functions and associated algebras of operators, e.g. the main objects of modern analysis. This is echoed in the saying which Yu.I. Manin attributed to I.M. Gelfand:

Mathematics of any kind is a representation theory.

This attitude can be encoded as the *Erlangen programme at large* (EPAL). In this book, we will systematically apply it to construct geometry of two-dimensional spaces. Further development shall extend it to analytic function theories on such spaces and the associated co- and contravariant functional calculi with relevant spectra [197]. Functional spaces are naturally associated with algebras of coordinates on a geometrical (or commutative) space. An operator (non-commutative) algebra is fashionably treated as a non-commutative space. Therefore, EPAL plays the same rôle for non-commutative geometry as EP for commutative geometry [172, 176].

EPAL provides a systematic tool for discovering hidden features, which previously escaped attention for various psychological reasons. In a sense [176], EPAL works like the **periodic table of chemical elements** discovered by D.I. Mendeleev: it allows us to see which cells are still empty and suggest where to look for the corresponding objects [176].

Mathematical theorems once proved, remain true forever. However, this does not mean we should not revise the corresponding theories. Excellent examples are given in *Geometry Revisited* [71] and *Elementary Mathematics from an Advanced Standpoint* [221, 222]. Understanding comes through comparison and there are many excellent books about the Lobachevsky half-plane which made their exposition through a contrast with Euclidean geometry. Our book offers a different perspective: it considers

the Lobachevsky half-plane as one of three sister conformal geometries—elliptic, parabolic, and hyperbolic—on the upper half-plane.

Exercises are an integral part of these notes¹. If a mathematical statement is presented as an exercise, it is not meant to be peripheral, unimportant or without further use. Instead, the label “Exercise” indicates that demonstration of the result is not very difficult and may be useful for understanding. Presentation of mathematical theory through a suitable collection of exercises has a long history, starting from the famous Polya and Szegő book [287], with many other successful examples following, e.g. [111, 164]. Mathematics is among those enjoyable things which are better to practise yourself rather than watch others doing it.

For some exercises, I know only a brute-force solution, which is certainly undesirable. Fortunately, all of them, marked by the symbol \heartsuit in the margins, can be done through a Computer Algebra System (CAS). The DVD provided contains the full package and Appendix C describes initial instructions. Computer-assisted exercises also form a test case for our CAS, which validates both the mathematical correctness of the library and its practical usefulness. Usage of computer-supported proofs in geometry is already an established practice [275] and it is naturally to expect its further rapid growth.

All figures in the book are printed in black and white to reduce costs. The coloured versions of all pictures are enclosed on the DVD as well—see Appendix C.1 to find them. The reader will be able to produce even more illustrations him/herself with the enclosed software.

There are many classical objects, e.g. pencils of cycles, or power of a point, which often re-occur in this book under different contexts. The detailed index will help to trace most of such places.

Chapter I.1 serves as an overview and a gentle introduction, so we do not give a description of the book content here. The reader is now invited to start his/her journey into Möbius-invariant geometries.

Odessa, July 2011

¹This is one of several features, which distinct our work from the excellent book [339], see also App. B.3. Kolmogorov [225] criticised Yaglom’s book for an insufficient number of exercises.

Part I

Geometry

Erlangen Programme: Preview

The simplest objects with non-commutative (but still associative) multiplication may be 2×2 matrices with real entries. The subset of matrices of *determinant one* has the following properties:

- It is a closed set under multiplication since $\det(AB) = \det A \cdot \det B$.
- The identity matrix is in the set.
- Any such matrix has an inverse (since $\det A \neq 0$).

In other words, these matrices form a *group*, the $SL_2(\mathbb{R})$ group [240]—one of the two most important Lie groups in analysis. The other group is the *Heisenberg group* [138]. By contrast, the $ax + b$ group, which is used to build wavelets, is only a subgroup of $SL_2(\mathbb{R})$ —see the numerator in (I.1.1) below.

The simplest non-linear transforms of the real line—*linear-fractional* or *Möbius maps*—may also be associated with 2×2 matrices, cf. [10; 26, Ch. 13; 262, Ch. 3]:

$$(I.1.1) \quad g : x \mapsto g \cdot x = \frac{ax + b}{cx + d}, \quad \text{where } g = \begin{pmatrix} a & b \\ c & d \end{pmatrix}, \quad x \in \mathbb{R}.$$

An enjoyable calculation shows that the composition of two transforms (I.1.1) with different matrices g_1 and g_2 is again a Möbius transform with a matrix equal the product $g_1 g_2$. In other words, (I.1.1) is a (left) action of $SL_2(\mathbb{R})$.

According to F. Klein's *Erlangen programme* (which was influenced by S. Lie), any geometry deals with invariant properties under a certain transitive group action. For example, we may ask: *What kinds of geometry are related to the $SL_2(\mathbb{R})$ action (I.1.1)?*

The Erlangen programme has probably the highest rate of $\frac{\text{praised}}{\text{actually used}}$ among mathematical theories, not only due to the large numerator but also due to the undeservedly small denominator. As we shall see below, Klein's approach provides some surprising conclusions even for such over-studied objects as circles.

I.1.1. Make a Guess in Three Attempts

It is easy to see that the $SL_2(\mathbb{R})$ action (I.1.1) also makes sense as a map of complex numbers $z = x + iy$, $i^2 = -1$, assuming the denominator is non-zero. Moreover, if $y > 0$, then $g \cdot z$ has a positive imaginary part as well, i.e. (I.1.1) defines a map from the upper half-plane to itself.

However, there is no need to be restricted to the traditional route of complex numbers only. Less-known *double* and *dual* numbers, see [339, Suppl. C] and Appendix B.1, also have the form $z = x + iy$ but with different assumptions for the imaginary unit ι : $\iota^2 = 0$ or $\iota^2 = 1$, respectively. We will write ε and j instead of ι within dual and

double numbers, respectively. Although the arithmetic of dual and double numbers is different from that of complex numbers, e.g. they have divisors of zero, we are still able to define their transforms by (I.1.1) in most cases.

Three possible values $-1, 0$ and 1 of $\sigma := v^2$ will be referred to here as *elliptic*, *parabolic* and *hyperbolic* cases, respectively. We repeatedly meet such a division of various mathematical objects into three classes. They are named by the historic first example—the classification of conic sections—however the pattern persistently reproduces itself in many different areas: equations, quadratic forms, metrics, manifolds, operators, etc. We will abbreviate this separation as the *EPH classification*. The common origin of this fundamental division of any family with one parameter can be seen from the simple picture of a coordinate line split by zero into negative and positive half-axes:

$$(I.1.2) \quad \begin{array}{c} \text{---} \quad \text{0} \quad \text{---} \\ \text{hyperbolic} \quad \uparrow \quad \text{elliptic} \\ \text{parabolic} \end{array}$$

Connections between different objects admitting EPH classification are not limited to this common source. There are many deep results linking, for example, the ellipticity of quadratic forms, metrics and operators, e.g. the **Atiyah–Singer index theorem**. On the other hand, there are still many white spots, empty cells, obscure gaps and missing connections between some subjects.

To understand the action (I.1.1) in all EPH cases we use the Iwasawa decomposition [240, § III.1] of $SL_2(\mathbb{R}) = ANK$ into three one-dimensional subgroups A , N and K :

$$(I.1.3) \quad \begin{pmatrix} a & b \\ c & d \end{pmatrix} = \begin{pmatrix} \alpha & 0 \\ 0 & \alpha^{-1} \end{pmatrix} \begin{pmatrix} 1 & v \\ 0 & 1 \end{pmatrix} \begin{pmatrix} \cos \phi & -\sin \phi \\ \sin \phi & \cos \phi \end{pmatrix}.$$

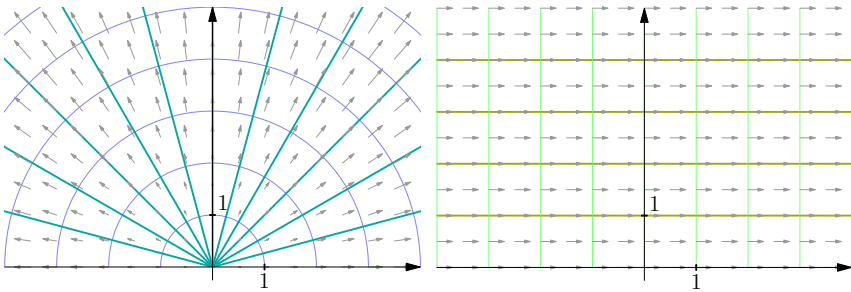


FIGURE I.1.1. Actions of the subgroups A and N by Möbius transformations. Transverse thin lines are images of the vertical axis, grey arrows show the derived action.

Subgroups A and N act in (I.1.1) irrespective of the value of σ : A makes a dilation by α^2 , i.e. $z \mapsto \alpha^2 z$, and N shifts points to left by v , i.e. $z \mapsto z + v$. This is illustrated by Fig. I.1.1.

By contrast, the action of the third matrix from the subgroup K sharply depends on σ —see Fig. I.1.2. In elliptic, parabolic and hyperbolic cases, K -orbits are circles, parabolas and (equilateral) hyperbolas, respectively. Thin traversal lines in Fig. I.1.2 join

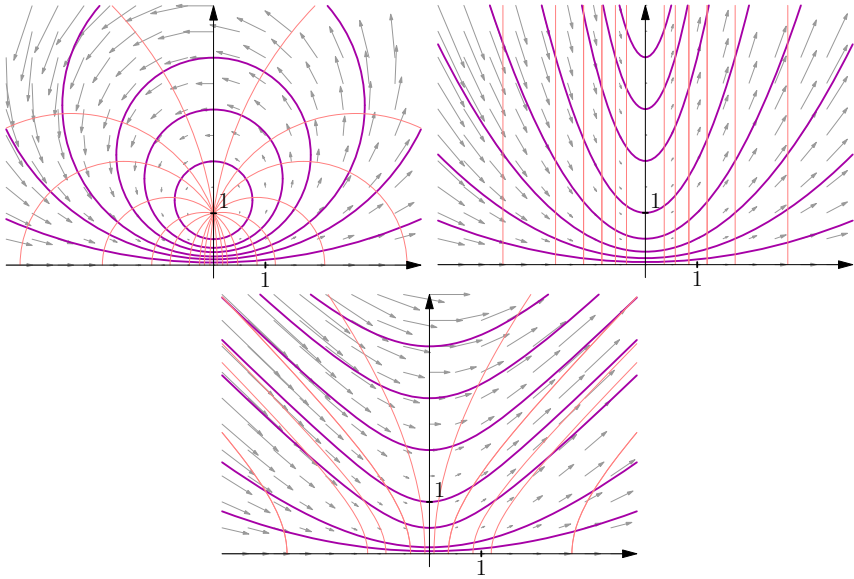


FIGURE I.1.2. Action of the subgroup K . The corresponding orbits are circles, parabolas and hyperbolas shown by thick lines. Transverse thin lines are images of the vertical axis, grey arrows show the derived action.

points of orbits for the same values of ϕ and grey arrows represent “local velocities”—vector fields of derived representations.

DEFINITION I.1.1. The common name *cycle* [339] is used to denote circles, parabolas and hyperbolas (as well as straight lines as their limits) in the respective EPH case.

It is well known that any cycle is a *conic section* and an interesting observation is that corresponding K -orbits are, in fact, sections of the same two-sided right-angle cone, see Fig. I.1.3. Moreover, each straight line generating the cone, see Fig. I.1.3(b), is crossing corresponding EPH K -orbits at points with the same value of parameter ϕ from (I.1.3). In other words, all three types of orbits are generated by the rotations of this generator along the cone.

K -orbits are K -invariant in a trivial way. Moreover, since actions of both A and N for any σ are extremely “shape-preserving”, we find natural invariant objects of the Möbius map:

THEOREM I.1.2. *The family of all cycles from Definition I.1.1 is invariant under the action (I.1.1).*

PROOF. We will show that, for a given $g \in \mathrm{SL}_2(\mathbb{R})$ and a cycle C , its image gC is again a cycle. Figure I.1.4 provides an illustration with C being a circle, but our reasoning works in all EPH cases.

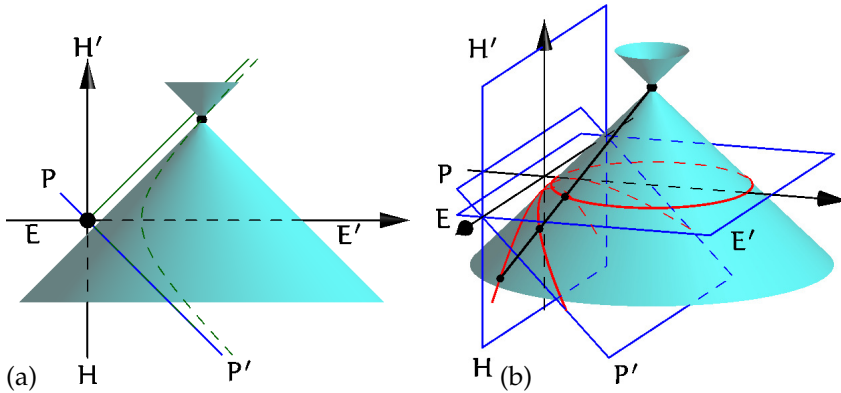


FIGURE I.1.3. K-orbits as conic sections. Circles are sections by the plane EE' , parabolas are sections by PP' and hyperbolas are sections by HH' . Points on the same generator of the cone correspond to the same value of ϕ .

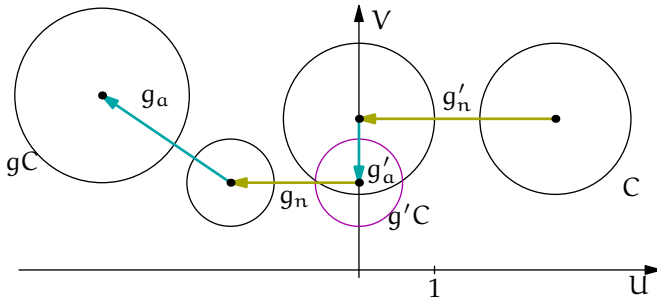


FIGURE I.1.4. Decomposition of an arbitrary Möbius transformation g into a product.

For a fixed C , there is the unique pair of transformations g'_n from the subgroup N and $g'_a \in A$ that the cycle $g'_a g'_n C$ is exactly a K-orbit. This will be shown later in Exercise I.4.7.

We make a decomposition of $g(g'_a g'_n)^{-1}$ into a product similar to (I.1.3):

$$g(g'_a g'_n)^{-1} = g_a g_n g_k.$$

Since $g'_a g'_n C$ is a K-orbit, we have $g_k(g'_a g'_n C) = g'_a g'_n C$. Then:

$$\begin{aligned} gC &= g(g'_a g'_n)^{-1} g'_a g'_n C = g_a g_n g_k g'_a g'_n C \\ &= g_a g_n g_k(g'_a g'_n C) = g_a g_n g'_a g'_n C. \end{aligned}$$

All transformations from subgroups A and N preserve the shape of any cycles in an obvious way. Therefore, the last expression $g_a g_n g'_a g'_n C$ represents a cycle and our proof is finished. \square

According to Erlangen ideology, we should now study the invariant properties of cycles.

I.1.2. Covariance of FSCc

Figure I.1.3 suggests that we may obtain a unified treatment of cycles in all EPH cases by consideration of higher-dimension spaces. The standard mathematical method is to declare objects under investigation (cycles in our case, functions in functional analysis, etc.) to be simply points of some larger space. This space should be equipped with an appropriate structure to hold information externally which previously described the inner properties of our objects.

A generic cycle is the set of points $(u, v) \in \mathbb{R}^2$ defined for all values of σ by the equation

$$(I.1.4) \quad k(u^2 - \sigma v^2) - 2lu - 2nv + m = 0.$$

This equation (and the corresponding cycle) is defined by a point (k, l, n, m) from a *projective space* \mathbb{P}^3 , since, for a scaling factor $\lambda \neq 0$, the point $(\lambda k, \lambda l, \lambda n, \lambda m)$ defines an equation equivalent to (I.1.4). We call \mathbb{P}^3 the *cycle space* and refer to the initial \mathbb{R}^2 as the *point space*.

In order to obtain a connection with the Möbius action (I.1.1), we arrange numbers (k, l, n, m) into the matrix

$$(I.1.5) \quad C_{\check{\sigma}}^s = \begin{pmatrix} l + \check{i}sn & -m \\ k & -l + \check{i}sn \end{pmatrix},$$

with a new hypercomplex unit \check{i} and an additional parameter s , usually equal to ± 1 . The values of $\check{\sigma} := \check{i}^2$ are $-1, 0$ or 1 independent of the value of σ . The matrix (I.1.5) is the cornerstone of an extended *Fillmore–Springer–Cnops construction* (FSCc) [65, 100, 300].

The significance of FSCc in the Erlangen framework is provided by the following result:

THEOREM I.1.3. [300, § 6.e] *The image $\tilde{C}_{\check{\sigma}}^s$ of a cycle $C_{\check{\sigma}}^s$ under transformation (I.1.1) with $g \in \text{SL}_2(\mathbb{R})$ is given by similarity of the matrix (I.1.5):*

$$(I.1.6) \quad \tilde{C}_{\check{\sigma}}^s = g C_{\check{\sigma}}^s g^{-1}.$$

In other words, FSCc (I.1.5) intertwines Möbius action (I.1.1) on cycles with linear map (I.1.6).

There are several ways to prove (I.1.6). Either by a brute-force calculation (which can, fortunately, be **performed by a CAS**) in Section I.4.3, or through the related orthogonality of cycles [65]—see the end of Section I.1.4.

The important observation here is that our extended version of FSCc (I.1.5) uses an imaginary unit \check{i} , which is not related to ι , that defines the appearance of cycles on the plane. In other words, any EPH type of geometry in the cycle space \mathbb{P}^3 admits drawing of cycles in the point space \mathbb{R}^2 as circles, parabolas or hyperbolas. We may think of points of \mathbb{P}^3 as ideal cycles while their depictions on \mathbb{R}^2 are only their shadows on the wall of **Plato's cave**.

Figure I.1.5(a) shows the same cycles drawn in different EPH styles. We note the first order contact between the circle, parabola and hyperbola in the intersection points

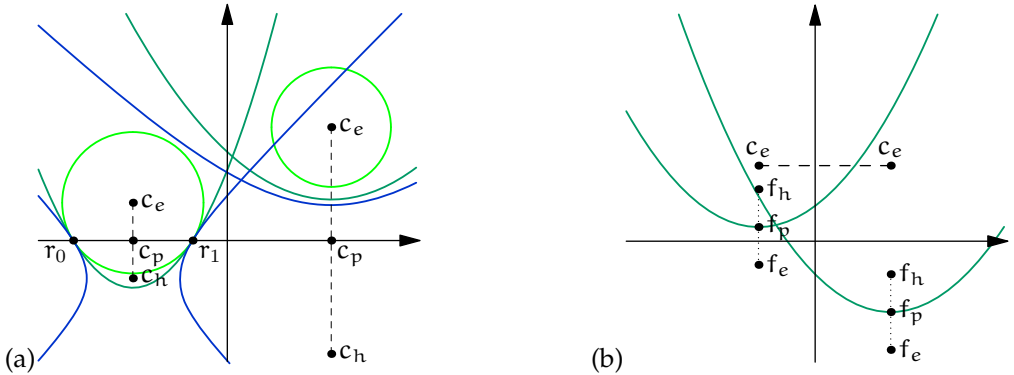


FIGURE I.1.5. Cycle implementations, centres and foci. (a) Different EPH implementations of the same cycles defined by quadruples of numbers. (b) Centres and foci of two parabolas with the same focal length.

with the real line. Informally, we can say that EPH realisations of a cycle look the same in a vicinity of the real line. It is not surprising since cycles are invariants of the hypercomplex Möbius transformations, which are extensions of $SL_2(\mathbb{R})$ -action (I.3.24) on the real line.

Points $c_{e,p,h} = (\frac{1}{k}, -\frac{\sigma}{k})$ on Fig. I.1.5(a) are the respective e/p/h-centres of drawn cycles. They are related to each other through several identities:

$$(I.1.7) \quad c_e = \bar{c}_h, \quad c_p = \frac{1}{2}(c_e + c_h).$$

Figure I.1.5(b) presents two cycles drawn as parabolas. They have the same focal length, $\frac{\sigma}{2k}$, and, thus, their e-centres are on the same level. In other words, *concentric* parabolas are obtained by a vertical shift, not by scaling, as an analogy with circles or hyperbolas may suggest.

Figure I.1.5(b) also presents points, called e/p/h-foci,

$$(I.1.8) \quad f_{e,p,h} = \left(\frac{1}{k}, \frac{\det C_{\sigma}^s}{2nk} \right),$$

which are independent of the sign of s . If a cycle is depicted as a parabola, then the h-focus, p-focus and e-focus are, correspondingly, the geometrical focus of the parabola, its vertex, and the point on the directrix nearest to the vertex.

As we will see (cf. Theorems I.1.5 and I.1.7), all three centres and three foci are useful attributes of a cycle, even if it is drawn as a circle.

I.1.3. Invariants: Algebraic and Geometric

We use known algebraic invariants of matrices to build appropriate geometric invariants of cycles. It is yet another demonstration that any division of mathematics into subjects is only illusive.

For 2×2 matrices (and, therefore, cycles), there are only two essentially different invariants under similarity (I.1.6) (and, therefore, under Möbius action (I.1.1)): the *trace* and the *determinant*. The latter was already used in (I.1.8) to define a cycle's foci. However, due to the projective nature of the cycle space \mathbb{P}^3 , the absolute values of the trace or determinant are irrelevant, unless they are zero.

Alternatively, we may have a special arrangement for the normalisation of quadruples (k, l, n, m) . For example, if $k \neq 0$, we may normalise the quadruple to $(1, \frac{1}{k}, \frac{n}{k}, \frac{m}{k})$ with the highlighted cycle's centre. Moreover, in this case, $-\det C_{\check{\sigma}}^s$ is equal to the square of cycle's radius, cf. Section I.1.6. Another normalisation, $\det C_{\check{\sigma}}^s = \pm 1$, is used in [163] to obtain a good condition for touching circles.

We still have important characterisation even with non-normalised cycles. For example, invariant classes (for different $\check{\sigma}$) of cycles are defined by the condition $\det C_{\check{\sigma}}^s = 0$. Such a class is parameterised only by two real numbers and, as such, is easily attached to a certain point of \mathbb{R}^2 . For example, the cycle $C_{\check{\sigma}}^s$ with $\det C_{\check{\sigma}}^s = 0$, $\check{\sigma} = -1$, drawn elliptically, represents just a point $(\frac{1}{k}, \frac{n}{k})$, i.e. an (elliptic) zero-radius circle. The same condition with $\check{\sigma} = 1$ in hyperbolic drawing produces a null-cone originating at point $(\frac{1}{k}, \frac{n}{k})$:

$$(u - \frac{1}{k})^2 - (v - \frac{n}{k})^2 = 0,$$

i.e. a zero-radius cycle in a hyperbolic metric.

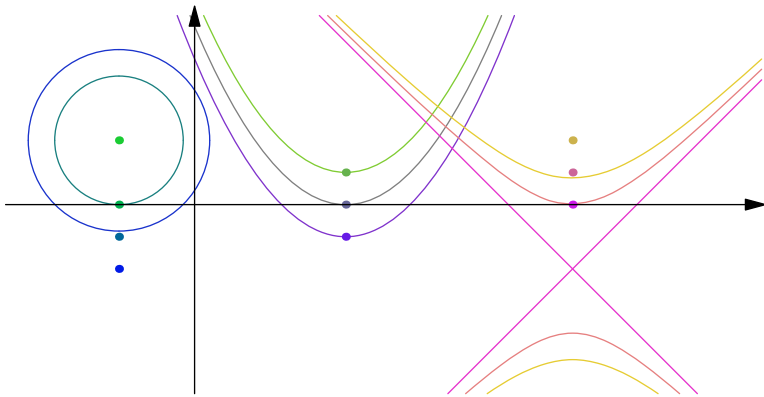


FIGURE I.1.6. Different σ -implementations of the same $\check{\sigma}$ -zero-radius cycles. The corresponding foci belong to the real axis.

In general, for every concept there are at least nine possibilities: three EPH cases in the cycle space times three EPH realisations in the point space. These nine cases for “zero-radius” cycles are shown in Fig. I.1.6. For example, p-zero-radius cycles in any implementation touch the real axis, that is they are *horocycles*.

This “touching” property is a manifestation of the *boundary effect* in the upper-half plane geometry. The famous question **about hearing a drum's shape** has a counterpart: *Can we see/feel the boundary from inside a domain?*

Both orthogonality relations described below are “boundary-aware” as well. After all, it is not surprising since $SL_2(\mathbb{R})$ action on the upper half-plane was obtained as an extension of its action (I.1.1) on the boundary.

According to the **categorycal viewpoint**, internal properties of objects are of minor importance in comparison to their relations with other objects from the same class. As an example, we may give the proof of Theorem I.1.3 described at the end of the next section. Thus, from now on, we will look for invariant relations between two or more cycles.

I.1.4. Joint Invariants: Orthogonality

The most expected relation between cycles is based on the following Möbius--invariant “inner product”, built from a trace of the product of two cycles as matrices:

$$(I.1.9) \quad \left\langle C_{\check{\sigma}}^s, \tilde{C}_{\check{\sigma}}^s \right\rangle = -\operatorname{tr}(C_{\check{\sigma}}^s \overline{\tilde{C}_{\check{\sigma}}^s}).$$

Here, $\overline{\tilde{C}_{\check{\sigma}}^s}$ means the complex conjugation of elements of the matrix $\tilde{C}_{\check{\sigma}}^s$. Notably, an inner product of this type is used, for example, in **GNS construction** to make a Hilbert space out of C^* -algebra. The next standard move is given by the following definition:

DEFINITION I.1.4. Two cycles are called $\check{\sigma}$ -orthogonal if $\left\langle C_{\check{\sigma}}^s, \tilde{C}_{\check{\sigma}}^s \right\rangle = 0$.

For the case of $\check{\sigma} = 1$, i.e. when the geometries of the cycle and point spaces are both either elliptic or hyperbolic, such an orthogonality is standard, defined in terms of angles between tangent lines in the intersection points of two cycles. However, in the remaining seven ($9 - 2$) cases, the innocent-looking Definition I.1.4 brings unexpected relations.

Elliptic (in the point space) realisations of Definition I.1.4, i.e. $\sigma = -1$, are shown in Fig. I.1.7. Figure I.1.7(a) corresponds to the elliptic cycle space, e.g. $\check{\sigma} = -1$. The orthogonality between the red circle and any circle from the blue or green families is given in the usual Euclidean sense. Figure I.1.7(b) (parabolic in the cycle space) and Fig. I.1.7(c) (hyperbolic) show the non-local nature of the orthogonality. There are analogous pictures in parabolic and hyperbolic point spaces—see Section I.6.1.

This orthogonality may still be expressed in the traditional sense if we will associate to the red circle the corresponding “ghost” circle, which is shown by the dashed lines in Fig. I.1.7. To describe the ghost cycle, we need the **Heaviside function** $\chi(\sigma)$:

$$(I.1.10) \quad \chi(t) = \begin{cases} 1, & t \geq 0; \\ -1, & t < 0. \end{cases}$$

THEOREM I.1.5. A cycle is $\check{\sigma}$ -orthogonal to cycle $C_{\check{\sigma}}^s$ if it is orthogonal in the usual sense to the σ -realisation of “ghost” cycle $\hat{C}_{\check{\sigma}}^s$, which is defined by the following two conditions:

- i. The $\chi(\sigma)$ -centre of $\hat{C}_{\check{\sigma}}^s$ coincides with the $\check{\sigma}$ -centre of $C_{\check{\sigma}}^s$.
- ii. Cycles $\hat{C}_{\check{\sigma}}^s$ and $C_{\check{\sigma}}^s$ have the same roots. Moreover, $\det \hat{C}_{\check{\sigma}}^1 = \det C_{\check{\sigma}}^{\chi(\check{\sigma})}$.

The above connection between various centres of cycles illustrates their relevance to our approach.

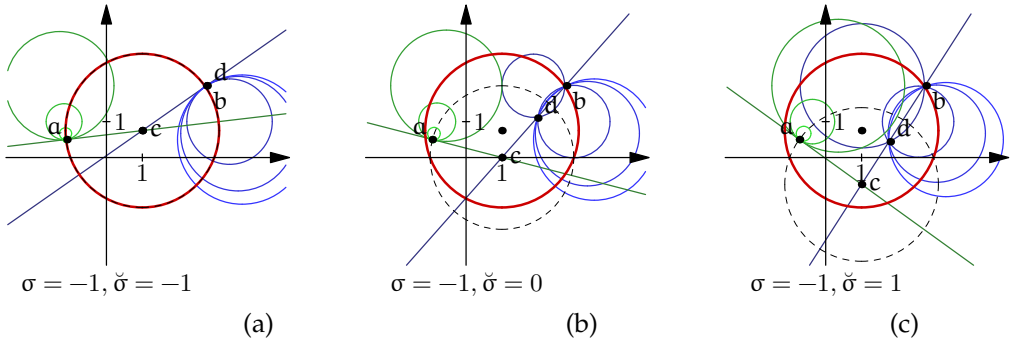


FIGURE I.1.7. Orthogonality of the first kind in the elliptic point space. Each picture presents two groups (green and blue) of cycles which are orthogonal to the red cycle $C_{\check{\sigma}}^s$. Point b belongs to $C_{\check{\sigma}}^s$ and the family of blue cycles passing through b is orthogonal to $C_{\check{\sigma}}^s$. They all also intersect at the point d which is the inverse of b in $C_{\check{\sigma}}^s$. Any orthogonality is reduced to the usual orthogonality with a new (“ghost”) cycle (shown by the dashed line), which may or may not coincide with $C_{\check{\sigma}}^s$. For any point a on the “ghost” cycle, the orthogonality is reduced to the local notion in terms of tangent lines at the intersection point. Consequently, such a point a is always the inverse of itself.

One can easily check the following orthogonality properties of the zero-radius cycles defined in the previous section:

- i. Due to the identity $\langle C_{\check{\sigma}}^s, C_{\check{\sigma}}^s \rangle = 2 \det C_{\check{\sigma}}^s$, zero-radius cycles are self-orthogonal (isotropic).
- ii. A cycle $C_{\check{\sigma}}^s$ is σ -orthogonal to a zero-radius cycle $Z_{\check{\sigma}}^s$ if and only if $C_{\check{\sigma}}^s$ passes through the σ -centre of $Z_{\check{\sigma}}^s$.

SKETCH OF PROOF OF THEOREM I.1.3. The validity of Theorem I.1.3 for a zero-radius cycle

$$Z_{\check{\sigma}}^s = \begin{pmatrix} z & -z\bar{z} \\ 1 & -\bar{z} \end{pmatrix} = \frac{1}{2} \begin{pmatrix} z & z \\ 1 & 1 \end{pmatrix} \begin{pmatrix} 1 & -\bar{z} \\ 1 & -\bar{z} \end{pmatrix}$$

with the centre $z = x + iy$ is straightforward. This implies the result for a generic cycle with the help of Möbius invariance of the product (I.1.9) (and, thus, the orthogonality) and the above relation (Theorem I.1.5.ii) between the orthogonality and the incidence. See Exercise I.6.7 for details. \square

I.1.5. Higher-order Joint Invariants: Focal Orthogonality

With our appetite already whet we may wish to build more joint invariants. Indeed, for any polynomial $p(x_1, x_2, \dots, x_n)$ of several non-commuting variables, one may define an invariant joint disposition of n cycles ${}^i C_{\check{\sigma}}^s$ by the condition

$$\text{tr } p({}^1 C_{\check{\sigma}}^s, {}^2 C_{\check{\sigma}}^s, \dots, {}^n C_{\check{\sigma}}^s) = 0.$$

However, it is preferable to keep some geometrical meaning of constructed notions.

An interesting observation is that, in the matrix similarity of cycles (I.1.6), one may replace element $g \in \mathrm{SL}_2(\mathbb{R})$ by an arbitrary matrix corresponding to another cycle. More precisely, the product $C_{\check{\sigma}}^s \tilde{C}_{\check{\sigma}}^s C_{\check{\sigma}}^s$ is again the matrix of the form (I.1.5) and, thus, may be associated with a cycle. This cycle may be considered as the reflection of $\tilde{C}_{\check{\sigma}}^s$ in $C_{\check{\sigma}}^s$.

DEFINITION I.1.6. A cycle $C_{\check{\sigma}}^s$ is f -orthogonal to a cycle $\tilde{C}_{\check{\sigma}}^s$ if the reflection of $\tilde{C}_{\check{\sigma}}^s$ in $C_{\check{\sigma}}^s$ is orthogonal (in the sense of Definition I.1.4) to the real line. Analytically, this is defined by

$$(I.1.11) \quad \mathrm{tr}(C_{\check{\sigma}}^s \tilde{C}_{\check{\sigma}}^s C_{\check{\sigma}}^s R_{\check{\sigma}}^s) = 0.$$

Due to invariance of all components in the above definition, f -orthogonality is a Möbius-invariant condition. Clearly, this is not a symmetric relation—if $C_{\check{\sigma}}^s$ is f -orthogonal to $\tilde{C}_{\check{\sigma}}^s$, then $\tilde{C}_{\check{\sigma}}^s$ is not necessarily f -orthogonal to $C_{\check{\sigma}}^s$.

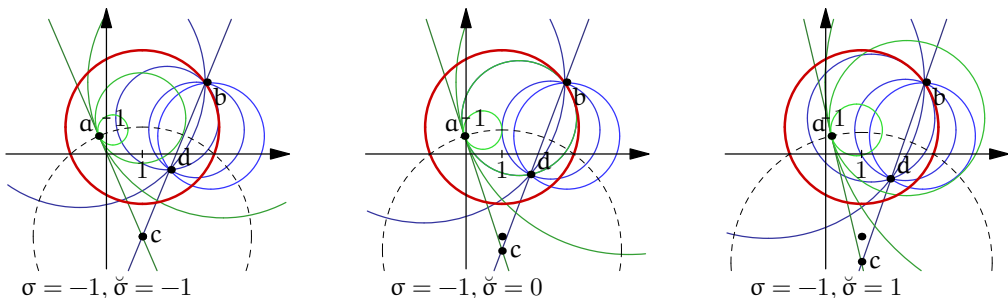


FIGURE I.1.8. Focal orthogonality for circles. To highlight both similarities and distinctions with ordinary orthogonality, we use the same notations as in Fig. I.1.7.

Figure I.1.8 illustrates f -orthogonality in the elliptic point space. In contrast to Fig. I.1.7, it is not a local notion at the intersection points of cycles for all $\check{\sigma}$. However, it may again be clarified in terms of the appropriate f -ghost cycle, cf. Theorem I.1.5.

THEOREM I.1.7. A cycle is f -orthogonal to a cycle $C_{\check{\sigma}}^s$ if it is orthogonal in the traditional sense to its f -ghost cycle $\tilde{C}_{\check{\sigma}}^{\check{\sigma}} = C_{\check{\sigma}}^{\chi(\sigma)} \mathbb{R}_{\check{\sigma}}^{\check{\sigma}} C_{\check{\sigma}}^{\chi(\sigma)}$, which is the reflection of the real line in $C_{\check{\sigma}}^{\chi(\sigma)}$ and χ is the Heaviside function (I.1.10). Moreover:

- i. The $\chi(\sigma)$ -centre of $\tilde{C}_{\check{\sigma}}^{\check{\sigma}}$ coincides with the $\check{\sigma}$ -focus of $C_{\check{\sigma}}^s$. Consequently, all lines f -orthogonal to $C_{\check{\sigma}}^s$ pass the respective focus.
- ii. Cycles $C_{\check{\sigma}}^s$ and $\tilde{C}_{\check{\sigma}}^{\check{\sigma}}$ have the same roots.

Note the above intriguing interplay between the cycle's centres and foci. Although f -orthogonality may look exotic, it will appear again at the end of next section.

Of course, it is possible to define other interesting higher-order joint invariants of two or even more cycles.

I.1.6. Distance, Length and Perpendicularity

Geometry in the plain meaning of the word deals with *distances* and *lengths*. Can we obtain them from cycles?

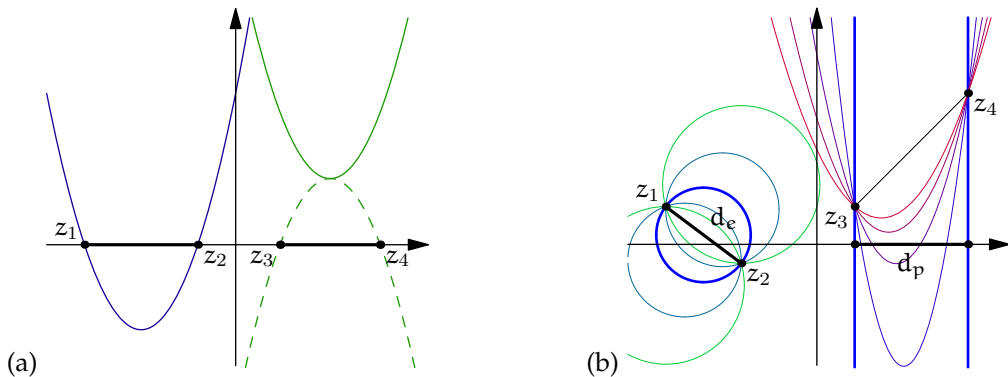


FIGURE I.1.9. Radius and distance for parabolas. (a) The square of the parabolic diameter is the square of the distance between roots if they are real (z_1 and z_2). Otherwise, it is the negative square of the distance between the adjoint roots (z_3 and z_4). (b) Distance is the extremum of diameters in elliptic (z_1 and z_2) and parabolic (z_3 and z_4) cases.

We already mentioned that, for circles normalised by the condition $k = 1$, the value $-\det C_{\check{\sigma}}^s = -\frac{1}{2} \langle C_{\check{\sigma}}^s, C_{\check{\sigma}}^s \rangle$ produces the square of the traditional circle radius. Thus, we may keep it as the definition of the $\check{\sigma}$ -radius for any cycle. However, we then need to accept that, in the parabolic case, the radius is the (Euclidean) distance between (real) roots of the parabola—see Fig. I.1.9(a).

Having already defined the radii of circles, we may use them for other measurements in several different ways. For example, the following variational definition may be used:

DEFINITION I.1.8. The *distance* between two points is the extremum of diameters of all cycles passing through both points—see Fig. I.1.9(b).

If $\check{\sigma} = \sigma$, this definition gives, in all EPH cases, the following expression for a distance $d_{e,p,h}(u, v)$ between the endpoints of any vector $w = u + iv$:

$$(I.1.12) \quad d_{e,p,h}(u, v)^2 = (u + iv)(u - iv) = u^2 - \sigma v^2.$$

The parabolic distance $d_p^2 = u^2$, see Fig. I.1.9(b), sits algebraically between d_e and d_h according to the general principle (I.1.2) and is widely accepted [339]. However, one may be unsatisfied by its degeneracy.

An alternative measurement is motivated by the fact that a circle is the set of equidistant points from its centre. However, there are now several choices for the “centre”: it may be either a point from three centres (I.1.7) or three foci (I.1.8).

DEFINITION I.1.9. The *length* of a directed interval \overrightarrow{AB} is the radius of the cycle with its *centre* (denoted by $l_c(\overrightarrow{AB})$) or *focus* (denoted by $l_f(\overrightarrow{AB})$) at the point A which passes through B.

This definition is less common and has some unusual properties like non-symmetry: $l_f(\overrightarrow{AB}) \neq l_f(\overrightarrow{BA})$. However, it comfortably fits the Erlangen programme due to its $SL_2(\mathbb{R})$ -conformal invariance:

THEOREM I.1.10 ([191]). Let l denote either the EPH distances (I.1.12) or any length from Definition I.1.9. Then, for fixed $y, y' \in \mathbb{A}$, the limit

$$\lim_{t \rightarrow 0} \frac{l(g \cdot y, g \cdot (y + ty'))}{l(y, y + ty')}$$

(where $g \in SL_2(\mathbb{R})$) exists and its value depends only on y and g and is independent of y' .

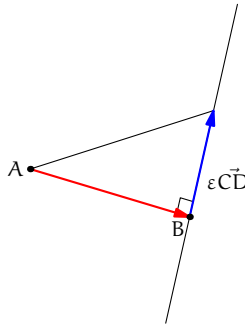


FIGURE I.1.10. The perpendicular as the shortest route to a line.

We may return from lengths to angles noting that, in the Euclidean space, a perpendicular is the shortest route from a point to a line—see Fig. I.1.10.

DEFINITION I.1.11. Let l be a length or distance. We say that a vector \overrightarrow{AB} is *l-perpendicular* to a vector \overrightarrow{CD} if function $l(\overrightarrow{AB} + \epsilon \overrightarrow{CD})$ of a variable ϵ has a local extremum at $\epsilon = 0$.

A pleasant surprise is that l_f -perpendicularity obtained using the length from focus (Definition I.1.9) coincides with f-orthogonality (already defined in Section I.1.5), as follows from Theorem I.1.7.i.

All these study are waiting to be generalised to higher-dimensions. Quaternions and Clifford algebras provide a suitable language for this [191, 273].

I.1.7. The Erlangen Programme at Large

As we already mentioned, the division of mathematics into separate areas is purely imaginary. Therefore, it is unnatural to limit the Erlangen programme only to “geometry”. We may continue to look for $SL_2(\mathbb{R})$ -invariant objects in other related fields.

For example, transform (I.1.1) generates the unitary representation on the space $L_2(\mathbb{R})$:

$$(I.1.13) \quad g : f(x) \mapsto \frac{1}{(cx + d)} f\left(\frac{ax + b}{cx + d}\right).$$

The above transformations have two invariant subspaces within $L_2(\mathbb{R})$: the Hardy space and its orthogonal complements. These spaces are of enormous importance in *harmonic analysis*. Similar transformations

$$(I.1.14) \quad g : f(z) \mapsto \frac{1}{(cz + d)^m} f\left(\frac{az + b}{cz + d}\right),$$

for $m = 2, 3, \dots$, can be defined on square-integrable functions in the upper half-plane. The respective invariant subspaces are weighted Bergman spaces of complex-valued analytic and poly-analytic functions.

Transformations (I.1.14) produce the *discrete series* representations of $SL_2(\mathbb{R})$, cf. [240, § IX.2]. Consequently, all main objects of *complex analysis* can be obtained in terms of invariants of these representations. For example:

- The Cauchy and Bergman integrals are special cases of *wavelet transform*, cf. [176, § 3]. The corresponding *mother wavelets* are eigenfunctions of operators from the representations of the subgroup K .
- The Cauchy–Riemann and Laplace operators are invariant differential operators. They annihilate the respective mother wavelet which are mentioned above, cf. [193, § 3].
- Taylor series is a decomposition over eigenfunctions of the subgroup K , cf. [170, § 3.4].

It would be an omission to limit this construction only to the discrete series, complex numbers and the subgroup K . Two other series of representations (*principal* and *complimentary*—see [240, § VI.6]) are related to important special functions [333] and differential operators [254]. These series have unitary realisations in dual and double numbers [170, 194]. Their relations with subgroups N' and A' will be shown in Section I.3.3.4.

Moving further, we may observe that transform (I.1.1) is also defined for an element x in any algebra \mathfrak{A} with a unit $\mathbf{1}$ as soon as $(cx + d\mathbf{1}) \in \mathfrak{A}$ has an inverse. If \mathfrak{A} is equipped with a topology, e.g. is a Banach algebra, then we may study a *functional calculus* for element x [168] in this way. It is defined as an intertwining operator between the representations (I.1.13) or (I.1.14) in spaces of analytic functions and similar representations in left \mathfrak{A} -modules.

In the spirit of the Erlangen programme, such functional calculus is still a geometry, since it is dealing with invariant properties under a group action. However, even for the simplest non-normal operator, e.g. a Jordan block of length k , the obtained space is not like a space of points but is, rather, a space of *k-th jets* [182]. Such non-point behaviour is often attributed to *non-commutative geometry* and the Erlangen programme provides an important insight on this popular topic [176].

Of course, there is no reason to limit the Erlangen programme to the group $SL_2(\mathbb{R})$ only—other groups may be more suitable in different situations. For example, the

Heisenberg group and its hypercomplex representations are useful in quantum mechanics [196, 199]. However, $\mathrm{SL}_2(\mathbb{R})$ still possesses large unexplored potential and is a good object to start with.

Groups and Homogeneous Spaces

Group theory and representation theory are themselves two enormous and interesting subjects. However, they are auxiliary in our presentation and we are forced to restrict our consideration to a brief overview.

Besides introduction to that areas presented in [254, 333] we recommend additionally the books [159, 321]. The representation theory intensively uses tools of functional analysis and on the other hand inspires its future development. We use the book [164] for references on functional analysis here and recommend it as a nice reading too.

I.2.1. Groups and Transformations

We start from the definition of the central object, which formalises the universal notion of symmetries [159, § 2.1].

DEFINITION I.2.1. A *transformation group* G is a non-void set of mappings of a certain set X into itself with the following properties:

- i. The identical map is included in G .
- ii. If $g_1 \in G$ and $g_2 \in G$ then $g_1 g_2 \in G$.
- iii. If $g \in G$ then g^{-1} exists and belongs to G .

EXERCISE I.2.2. List all transformation groups on a set of three elements.

EXERCISE I.2.3. Verify that the following sets are transformation groups:

- i. The group of permutations of n elements.
- ii. The group of **rotations** of the unit circle \mathbb{T} .
- iii. The groups of **shifts** of the real line \mathbb{R} and the plane \mathbb{R}^2 .
- iv. The group of one-to-one linear maps of an n -dimensional vector space over a field \mathbb{F} onto itself.
- v. The group of linear-fractional (Möbius) transformations:

$$(I.2.1) \quad \begin{pmatrix} a & b \\ c & d \end{pmatrix} : z \mapsto \frac{az + b}{cz + d},$$

of the extended complex plane such that $ad - bc \neq 0$.

It is worth (and often done) to push abstraction one level higher and to keep the group alone without the underlying space:

DEFINITION I.2.4. An *abstract group* (or simply *group*) is a non-void set G on which there is a law of *group multiplication* (i.e. mapping $G \times G \rightarrow G$) with the properties:

- i. *Associativity*: $g_1(g_2 g_3) = (g_1 g_2)g_3$.

- ii. The existence of the *identity*: $e \in G$ such that $eg = ge = g$ for all $g \in G$.
- iii. The existence of the *inverse*: for every $g \in G$ there exists $g^{-1} \in G$ such that $gg^{-1} = g^{-1}g = e$.

EXERCISE I.2.5. Check that

- i. any transformation group is an abstract group; and
- ii. any abstract group is isomorphic to a transformation group. HINT: Use the action of the abstract group on itself by *left* (or *right*the *right shift*) shifts from Exercise . \diamond

If we forget the nature of the elements of a transformation group G as transformations of a set X then we need to supply a separate “multiplication table” for elements of G . By the previous Exercise both concepts are mathematically equivalent. However, an advantage of a transition to abstract groups is that the same abstract group can act by transformations of apparently different sets.

EXERCISE I.2.6. Check that the following transformation groups (cf. Example I.2.3) have the same law of multiplication, i.e. are equivalent as abstract groups:

- i. The group of isometric mapping of an equilateral triangle onto itself.
- ii. The group of all permutations of a set of three elements.
- iii. The group of invertible matrices of order 2 with coefficients in the field of integers modulo 2.
- iv. The group of linear fractional transformations of the extended complex plane generated by the mappings $z \mapsto z^{-1}$ and $z \mapsto 1 - z$.

HINT: Recall that linear fractional transformations are represented by matrices (I.2.1). Furthermore, a linear fractional transformation is completely defined by the images of any three different points (say, 0, 1 and ∞), see Exercise I.3.1.(d)ii. What are images of 0, 1 and ∞ under the maps specified in I.2.6.iv? \diamond

EXERCISE* I.2.7. Expand the list in the above exercise.

It is much simpler to study groups with the following additional property.

DEFINITION I.2.8. A group G is *commutative* (or *abelian*) if, for all $g_1, g_2 \in G$, we have $g_1g_2 = g_2g_1$.

However, most of the interesting and important groups are non-commutative.

EXERCISE I.2.9. Which groups among those listed in Exercises I.2.2 and I.2.3 are commutative?

Groups may have some additional **analytical** structures, e.g. they can be a topological space with a corresponding notion of **limit** and respective **continuity**. We also assume that our topological groups are always *locally compact* [159, § 2.4], that is there exists a compact neighbourhood of every point. It is common to assume that the topological and group structures are in agreement:

DEFINITION I.2.10. If, for a group G , group multiplication and inversion are **continuous** mappings, then G is *continuous group*.

EXERCISE I.2.11. i. Describe topologies which make groups from Exercises I.2.2 and I.2.3 continuous.

- ii. Show that a continuous group is locally compact if there exists a compact neighbourhood of its identity.

An even better structure can be found among *Lie groups* [159, § 6], e.g. groups with a **differentiable** law of multiplication. In the investigation of such groups, we could employ the whole arsenal of analytical tools. Hereafter, most of the groups studied will be Lie groups.

EXERCISE I.2.12. Check that the following are non-commutative Lie (and, thus, continuous) groups:

- i. The $ax + b$ group (or the *affine group*) [321, Ch. 7] of the real line: the set of elements (a, b) , $a \in \mathbb{R}_+$, $b \in \mathbb{R}$ with the group law:

$$(a, b) * (a', b') = (aa', ab' + b).$$

The identity is $(1, 0)$ and $(a, b)^{-1} = (a^{-1}, -b/a)$.

- ii. The *Heisenberg group* \mathbb{H}^1 [138; 321, Ch. 1]: a set of triples of real numbers (s, x, y) with the group multiplication:

$$(I.2.2) \quad (s, x, y) * (s', x', y') = (s + s' + \frac{1}{2}(x'y - xy'), x + x', y + y').$$

The identity is $(0, 0, 0)$ and $(s, x, y)^{-1} = (-s, -x, -y)$.

- iii. The $SL_2(\mathbb{R})$ group [140, 240]: a set of 2×2 matrices $\begin{pmatrix} a & b \\ c & d \end{pmatrix}$ with real entries $a, b, c, d \in \mathbb{R}$ and the determinant $\det = ad - bc$ equal to 1 and the group law coinciding with matrix multiplication:

$$\begin{pmatrix} a & b \\ c & d \end{pmatrix} \begin{pmatrix} a' & b' \\ c' & d' \end{pmatrix} = \begin{pmatrix} aa' + bc' & ab' + bd' \\ ca' + dc' & cb' + dd' \end{pmatrix}.$$

The identity is the unit matrix and

$$\begin{pmatrix} a & b \\ c & d \end{pmatrix}^{-1} = \begin{pmatrix} d & -b \\ -c & a \end{pmatrix}.$$

The above three groups are behind many important results of real and complex analysis [138, 140, 185, 240] and we meet them many times later.

I.2.2. Subgroups and Homogeneous Spaces

A study of any mathematical object is facilitated by a decomposition into smaller or simpler blocks. In the case of groups, we need the following:

DEFINITION I.2.13. A *subgroup* of a group G is subset $H \subset G$ such that the restriction of multiplication from G to H makes H a group itself.

EXERCISE I.2.14. Show that the $ax + b$ group is a subgroup of $SL_2(\mathbb{R})$.

HINT: Consider matrices $\frac{1}{\sqrt{a}} \begin{pmatrix} a & b \\ 0 & 1 \end{pmatrix}$. \diamond

While **abstract groups** are a suitable language for investigation of their general properties, we meet groups in applications as **transformation groups** acting on a set X . We will describe the connections between those two viewpoints. It can be approached either by having a homogeneous space build the class of isotropy subgroups or by having a subgroup define respective homogeneous spaces. The next two subsections explore both directions in detail.

I.2.2.1. From a Homogeneous Space to the Isotropy Subgroup. Let X be a set and let us define, for a group G , an operation $G : X \rightarrow X$ of G on X . We say that a subset $S \subset X$ is G -invariant if $g \cdot s \in S$ for all $g \in G$ and $s \in S$.

EXERCISE I.2.15. Show that if $S \subset X$ is G -invariant then its complement $X \setminus S$ is G -invariant as well.

Thus, if X has a non-trivial invariant subset, we can split X into disjoint parts. The finest such decomposition is obtained from the following **equivalence relation** on X , say, $x_1 \sim x_2$, if and only if there exists $g \in G$ such that $gx_1 = x_2$, with respect to which X is a disjoint union of distinct *orbits* [239, § I.5], that is subsets of all gx_0 with a fixed $x_0 \in X$ and arbitrary $g \in G$.

EXERCISE I.2.16. Let the group $SL_2(\mathbb{R})$ act on \mathbb{C} by means of linear-fractional transformations (I.2.1). Show that there exist three orbits: the real axis \mathbb{R} , the *upper* \mathbb{R}_+^2 and *lower* \mathbb{R}_-^2 half-planes:

$$\mathbb{R}_+^2 = \{x \pm iy \mid x, y \in \mathbb{R}, y > 0\} \quad \text{and} \quad \mathbb{R}_-^2 = \{x \pm iy \mid x, y \in \mathbb{R}, y < 0\}.$$

Thus, from now on, without loss of generality, we assume that the action of G on X is *transitive*, i.e. for every $x \in X$ we have

$$Gx := \bigcup_{g \in G} gx = X.$$

In this case, X is *G -homogeneous space*.

EXERCISE I.2.17. Show that either of the following conditions define a transitive action of G on X :

- i. For two arbitrary points $x_1, x_2 \in X$, there exists $g \in G$ such that $gx_1 = x_2$.
- ii. There is a point $x_0 \in X$ with the property that for an arbitrary point $x \in X$, there exists $g \in G$ such that $gx_0 = x$.

EXERCISE I.2.18. Show that, for any group G , we can define its action on $X = G$ as follows:

- i. The *conjugation* $g : x \mapsto gxg^{-1}$.
- ii. The *left shift* $\Lambda(g) : x \mapsto gx$ and the *right shift* $R(g) : x \mapsto xg^{-1}$.

The above actions define group homomorphisms from G to the transformation group of G . However, the conjugation is trivial for all commutative groups.

EXERCISE I.2.19. Show that:

- i. The set of elements $G_x = \{g \in G \mid gx = x\}$ for a fixed point $x \in X$ forms a subgroup of G , which is called the *isotropy (sub)group* of x in G [239, § I.5].

- ii. For any $x_1, x_2 \in X$, isotropy subgroups G_{x_1} and G_{x_2} are *conjugated*, that is, there exists $g \in G$ such that $G_{x_1} = g^{-1}G_{x_2}g$.

This provides a transition from a G -action on a homogeneous space X to a subgroup of G , or even to an equivalence class of such subgroups under conjugation.

EXERCISE I.2.20. Find a subgroup which corresponds to the given action of G on X :

- i. Action of **ax + b group** on \mathbb{R} by the formula: $(a, b) : x \mapsto ax + b$ for the point $x = 0$.
 ii. Action of **$SL_2(\mathbb{R})$ group** on one of three orbit from Exercise I.2.16 with respective points $x = 0, i$ and $-i$.

I.2.2.2. From a Subgroup to the Homogeneous Space. We can also go in the opposite direction—given a subgroup of G , find the corresponding homogeneous space. Let G be a group and H be its subgroup. Let us define the space of *cosets* $X = G/H$ by the equivalence relation: $g_1 \sim g_2$ if there exists $h \in H$ such that $g_1 = g_2h$.

There is an important type of subgroups:

DEFINITION I.2.20(a). A subgroup H of a group G is said to be *normal* if H is invariant under conjugation, that is $g^{-1}hg \in H$ for all $g \in G, h \in H$.

The special role of normal subgroups is explained by the following property:

EXERCISE I.2.20(b). Check that, the binary operation $g_1H \cdot g_2H = (g_1g_2)H$, where $g_1, g_2 \in G$, is well-defined on $X = G/H$. Furthermore, this operation turns X into a group, called the *quotient group*.

In our studies normal subgroup will not appear and the set $X = G/H$ will not be a group. However, for any subgroup $H \subset G$ the set $X = G/H$ is a homogeneous space under the left G -action $g : g_1H \mapsto (gg_1)H$. For practical purposes it is more convenient to have a parametrisation of X and express the above G -action through those parameters, as shown below.

We define a function (*section*) [159, § 13.2] $s : X \rightarrow G$ such that it is a right inverse to the natural projection $p : G \rightarrow G/H$, i.e. $p(s(x)) = x$ for all $x \in X$. Depending on situation some additional properties of s may be required, e.g. continuity. In our work we will usually need only that the section s is a measurable function.

EXERCISE I.2.21. Check that, for any $g \in G$, we have $s(p(g)) = gh$, for some $h \in H$ depending on g .

Then, any $g \in G$ has a unique decomposition of the form $g = s(x)h$, where $x = p(g) \in X$ and $h \in H$. We define a map r associated to s through the identities:

$$x = p(g), \quad h = r(g) := s(x)^{-1}g.$$

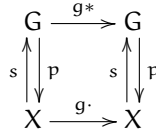
EXERCISE I.2.22. Show that:

- i. X is a left G -space with the G -action defined in terms of maps s and p as follows:

$$(I.2.3) \quad g : x \mapsto g \cdot x = p(g * s(x)),$$

where $*$ is the multiplication on G . This is illustrated by the diagram:

(I.2.4)



- ii. The above action of $G : X \rightarrow X$ is transitive on X , thus X is a G -homogeneous space.
- iii. The choice of a section s is not essential in the following sense. Let s_1 and s_2 be two maps, such that $p(s_i(x)) = x$ for all $x \in X$, $i = 1, 2$. Then, $p(g * s_1(x)) = p(g * s_2(x))$ for all $g \in G$.

Thus, starting from a subgroup H of a group G , we can define a G -homogeneous space $X = G/H$.

I.2.3. Differentiation on Lie Groups and Lie Algebras

To do some analysis on groups, we need suitably-defined basic operations: **differentiation** and **integration**.

Differentiation is naturally defined for Lie groups. If G is a Lie group and G_x is its closed subgroup, then the homogeneous space G/G_x considered above is a smooth manifold (and a *loop* as an algebraic object) for every $x \in X$ [159, Thm. 2 in § 6.1]. Therefore, the one-to-one mapping $G/G_x \rightarrow X$ from § I.2.2.2 induces a structure of C^∞ -manifold on X . Thus, the class $C_0^\infty(X)$ of smooth functions with compact supports on X has the natural definition.

For every Lie group G there is an associated *Lie algebra* \mathfrak{g} . This algebra can be realised in many different ways. We will use the following two out of four listed in [159, § 6.3].

I.2.3.1. One-parameter Subgroups and Lie Algebras. For the first realisation, we consider a *one-dimensional continuous subgroup* $\chi(t)$ of G as a group homomorphism of $\chi : (\mathbb{R}, +) \rightarrow G$. For such a homomorphism χ , we have $\chi(s + t) = \chi(s)\chi(t)$ and $\chi(0) = e$.

EXERCISE I.2.23. Check that the following subsets of elements parametrised by $t \in \mathbb{R}$ are one-parameter subgroups:

- i. For the affine group: $\mathfrak{a}(t) = (e^t, 0)$ and $\mathfrak{n}(t) = (1, t)$.
- ii. For the Heisenberg group \mathbb{H}^1 :

$$s(t) = (t, 0, 0), \quad \mathfrak{x}(t) = (0, t, 0) \quad \text{and} \quad \mathfrak{y}(t) = (0, 0, t).$$

- iii. For the group $SL_2(\mathbb{R})$:

$$(I.2.5) \quad \mathfrak{a}(t) = \begin{pmatrix} e^{-t/2} & 0 \\ 0 & e^{t/2} \end{pmatrix}, \quad \mathfrak{n}(t) = \begin{pmatrix} 1 & t \\ 0 & 1 \end{pmatrix},$$

$$(I.2.6) \quad \mathfrak{b}(t) = \begin{pmatrix} \cosh \frac{t}{2} & \sinh \frac{t}{2} \\ \sinh \frac{t}{2} & \cosh \frac{t}{2} \end{pmatrix}, \quad \mathfrak{z}(t) = \begin{pmatrix} \cos t & \sin t \\ -\sin t & \cos t \end{pmatrix}.$$

The one-parameter subgroup $x(t)$ defines a tangent vector $X = x'(0)$ belonging to the tangent space T_e of G at $e = x(0)$. The Lie algebra \mathfrak{g} can be identified with this *tangent space*. The important *exponential map* $\exp : \mathfrak{g} \rightarrow G$ works in the opposite direction and is defined by $\exp X = x(1)$ in the previous notations. For the case of a matrix group, the exponent map can be explicitly realised through the exponentiation of the matrix representing a tangent vector:

$$\exp(A) = I + A + \frac{A^2}{2} + \frac{A^3}{3!} + \frac{A^4}{4!} + \dots$$

EXERCISE I.2.24. i. Check that subgroups $a(t)$, $n(t)$, $b(t)$ and $z(t)$ from Exercise I.2.23.iii are generated by the exponent map of the following zero-trace matrices:

$$(I.2.7) \quad a(t) = \exp \begin{pmatrix} -\frac{t}{2} & 0 \\ 0 & \frac{t}{2} \end{pmatrix}, \quad n(t) = \exp \begin{pmatrix} 0 & t \\ 0 & 0 \end{pmatrix},$$

$$(I.2.8) \quad b(t) = \exp \begin{pmatrix} 0 & \frac{t}{2} \\ \frac{t}{2} & 0 \end{pmatrix}, \quad z(t) = \exp \begin{pmatrix} 0 & t \\ -t & 0 \end{pmatrix}.$$

ii. Check that for any $g \in \mathrm{SL}_2(\mathbb{R})$ there is a unique (up to a parametrisation) one-parameter subgroup passing g . Alternatively, the identity $e^{tX} = e^{sY}$ for some $X, Y \in \mathfrak{sl}_2$ and $t, s \in \mathbb{R}$ implies $X = uY$ for some $u \in \mathbb{R}$.

I.2.3.2. Invariant Vector Fields and Lie Algebras. In the second realisation of the Lie algebra, \mathfrak{g} is identified with the left (right) *invariant vector fields* on the group G , that is, first-order differential operators X defined at every point of G and invariant under the left (right) shifts: $X\lambda = \lambda X$ ($XR = RX$). This realisation is particularly usable for a Lie group with an appropriate parametrisation. The following examples describe different techniques for finding such invariant fields.

EXAMPLE I.2.25. Let us build left (right) invariant vector fields on G —the $a_x + b$ group using the plain definition. Take the basis $\{\partial_a, \partial_b\}$ ($\{-\partial_a, -\partial_b\}$) of the tangent space T_e to G at its identity. We will propagate these vectors to an arbitrary point through the invariance under shifts. That is, to find the value of the invariant field at the point $g = (a, b)$, we

- i. make the left (right) shift by g ,
- ii. apply a differential operator from the basis of T_e ,
- iii. make the inverse left (right) shift by $g^{-1} = (\frac{1}{a}, -\frac{b}{a})$.

Thus, we will obtain the following invariant vector fields:

$$(I.2.9) \quad A^l = a\partial_a, \quad N^l = a\partial_b; \quad \text{and} \quad A^r = -a\partial_a - b\partial_b, \quad N^r = -\partial_b.$$

EXAMPLE I.2.26. An alternative calculation for the same Lie algebra can be done as follows. The Jacobians at $g = (a, b)$ of the left and the right shifts

$$\Lambda(u, v) : f(a, b) \mapsto f\left(\frac{a}{u}, \frac{b-v}{u}\right), \quad \text{and} \quad R(u, v) : f(a, b) \mapsto f(ua, va+b)$$

by $h = (u, v)$ are:

$$J_\Lambda(h) = \begin{pmatrix} \frac{1}{u} & 0 \\ 0 & \frac{1}{u} \end{pmatrix}, \quad \text{and} \quad J_R(h) = \begin{pmatrix} u & 0 \\ v & 1 \end{pmatrix}.$$

Then the invariant vector fields are obtained by the transpose of Jacobians:

$$\begin{aligned} \begin{pmatrix} A^l \\ N^l \end{pmatrix} &= J_\lambda^t(g^{-1}) \begin{pmatrix} \partial_a \\ \partial_b \end{pmatrix} = \begin{pmatrix} a & 0 \\ 0 & a \end{pmatrix} \begin{pmatrix} \partial_a \\ \partial_b \end{pmatrix} = \begin{pmatrix} a\partial_a \\ a\partial_b \end{pmatrix} \\ \begin{pmatrix} A^r \\ N^r \end{pmatrix} &= J_k^t(g) \begin{pmatrix} -\partial_a \\ -\partial_b \end{pmatrix} = \begin{pmatrix} a & b \\ 0 & 1 \end{pmatrix} \begin{pmatrix} -\partial_a \\ -\partial_b \end{pmatrix} = \begin{pmatrix} -a\partial_a - b\partial_b \\ -\partial_b \end{pmatrix} \end{aligned}$$

This rule is a very special case of the general theorem on the change of variables in the calculus of *pseudo-differential operators* (PDO), cf. [136, Thm. 18.1.17; 305, § 4.2].

EXAMPLE I.2.27. Finally, we calculate the invariant vector fields on the $ax + b$ group through a connection to the above one-parameter subgroups. The left-invariant vector field corresponding to the subgroup $a(t)$ from Exercise I.2.23.i is obtained through the differentiation of the right action of this subgroup:

$$\begin{aligned} [A^l f](a, b) &= \left. \frac{d}{dt} f((a, b) * (e^t, 0)) \right|_{t=0} = \left. \frac{d}{dt} f(ae^t, b) \right|_{t=0} = af'_a(a, b), \\ [N^l f](a, b) &= \left. \frac{d}{dt} f((a, b) * (1, t)) \right|_{t=0} = \left. \frac{d}{dt} f(a, at + b) \right|_{t=0} = af'_b(a, b). \end{aligned}$$

Similarly, the right-invariant vector fields are obtained by the derivation of the left action:

$$\begin{aligned} [A^r f](a, b) &= \left. \frac{d}{dt} f((e^{-t}, 0) * (a, b)) \right|_{t=0} \\ &= \left. \frac{d}{dt} f(e^{-t}a, e^{-t}b) \right|_{t=0} = -af'_a(a, b) - bf'_b(a, b), \\ [N^r f](a, b) &= \left. \frac{d}{dt} f((1, -t) * (a, b)) \right|_{t=0} = \left. \frac{d}{dt} f(a, b - t) \right|_{t=0} = -f'_b(a, b). \end{aligned}$$

EXERCISE I.2.28. Use the above techniques to calculate the following left (right) invariant vector fields on the Heisenberg group:

$$(I.2.10) \quad S^{l(r)} = \pm\partial_s, \quad X^{l(r)} = \pm\partial_x - \frac{1}{2}y\partial_s, \quad Y^{l(r)} = \pm\partial_y + \frac{1}{2}x\partial_s.$$

I.2.3.3. Commutator in Lie Algebras. The important operation in a Lie algebra is a *commutator*. If the Lie algebra of a matrix group is realised by matrices, e.g. Exercise I.2.24, then the commutator is defined by the expression $[A, B] = AB - BA$ in terms of the respective matrix operations. If the Lie algebra is realised through left (right) invariant first-order differential operators, then the commutator $[A, B] = AB - BA$ again defines a left (right) invariant first-order operator—an element of the same Lie algebra.

Among the important properties of the commutator are its anti-commutativity ($[A, B] = -[B, A]$) and the *Jacobi identity*

$$(I.2.11) \quad [A, [B, C]] + [B, [C, A]] + [C, [A, B]] = 0.$$

EXERCISE I.2.29. Check the following commutation relations:

- i. For the Lie algebra (I.2.9) of the $a\mathfrak{x} + b$ group

$$[A^{l(r)}, N^{l(r)}] = N^{l(r)}.$$

- ii. For the Lie algebra (IV.2.11) of Heisenberg group

$$(I.2.12) \quad [X^{l(r)}, Y^{l(r)}] = S^{l(r)}, \quad [X^{l(r)}, S^{l(r)}] = [Y^{l(r)}, S^{l(r)}] = 0.$$

These are the celebrated *Heisenberg commutation relations*, which are very important in quantum mechanics.

- iii. Denote by A , B and Z the generators of the one-parameter subgroups $a(t)$, $b(t)$ and $z(t)$ in (I.2.7) and (I.2.8). The commutation relations in the Lie algebra \mathfrak{sl}_2 are

$$(I.2.13) \quad [Z, A] = 2B, \quad [Z, B] = -2A, \quad [A, B] = -\frac{1}{2}Z.$$

The procedure from Example I.2.27 can also be used to calculate the *derived action* of a G -action on a homogeneous space.

EXAMPLE I.2.30. Consider the action of the $a\mathfrak{x} + b$ group on the real line associated with group's name:

$$(a, b) : x \mapsto ax + b, \quad x \in \mathbb{R}.$$

Then, the derived action on the real line is:

$$\begin{aligned} [A^d f](x) &= \left. \frac{d}{dt} f(e^{-t}x) \right|_{t=0} = -xf'(x), \\ [N^d f](a, b) &= \left. \frac{d}{dt} f(x-t) \right|_{t=0} = -f'(x). \end{aligned}$$

I.2.4. Integration on Groups

In order to perform an integration we need a suitable *measure*. A measure $d\mu$ on X is called (left) *invariant measure* with respect to an operation of G on X if

$$(I.2.14) \quad \int_X f(x) d\mu(x) = \int_X f(g \cdot x) d\mu(x), \quad \text{for all } g \in G, f(x) \in C_0^\infty(X).$$

EXERCISE I.2.31. Show that measure $y^{-2} dy dx$ on the upper half-plane \mathbb{R}_+^2 is invariant under action from Exercise I.2.16.

Left invariant measures on $X = G$ is called the (left) *Haar measure*. It always exists and is uniquely defined up to a scalar multiplier [321, § 0.2]. An equivalent formulation of (I.2.14) is: G operates on $L_2(X, d\mu)$ by *unitary operators*. We will transfer the Haar measure $d\mu$ from G to \mathfrak{g} via the exponential map $\exp : \mathfrak{g} \rightarrow G$ and will call it as the *invariant measure on a Lie algebra* \mathfrak{g} .

EXERCISE I.2.32. Check that the following are Haar measures for corresponding groups:

- i. The *Lebesgue measure* dx on the real line \mathbb{R} .
- ii. The *Lebesgue measure* $d\phi$ on the unit circle \mathbb{T} .
- iii. dx/x is a Haar measure on the multiplicative group $\mathbb{R}_+;$

- iv. $dx dy/(x^2 + y^2)$ is a Haar measure on the multiplicative group $\mathbb{C} \setminus \{0\}$, with coordinates $z = x + iy$.
- v. $a^{-2} da db$ and $a^{-1} da db$ are the left and right invariant measure on **$ax + b$ group**.
- vi. The Lebesgue measure $ds dx dy$ of \mathbb{R}^3 for the **Heisenberg group** \mathbb{H}^1 .

In this notes we assume *all integrations on groups performed over the Haar measures*.

EXERCISE I.2.33. Show that invariant measure on a compact group G is finite and thus can be normalised to total measure 1.

The above simple result has surprisingly important consequences for representation **theory of compact groups**.

DEFINITION I.2.34. The left *convolution* $f_1 * f_2$ of two functions $f_1(g)$ and $f_2(g)$ defined on a group G is

$$f_1 * f_2(g) = \int_G f_1(h) f_2(h^{-1}g) dh$$

EXERCISE I.2.35. Let $k(g) \in L_1(G, d\mu)$ and operator K on $L_1(G, d\mu)$ is the left *convolution operator* with k , i.e. $K : f \mapsto k * f$. Show that K commutes with all **right shifts** on G .

The following Lemma characterizes *linear subspaces* of $L_1(G, d\mu)$ invariant under shifts in the term of *ideals of convolution algebra* $L_1(G, d\mu)$ and is of the separate interest.

LEMMA I.2.36. *A closed linear subspace H of $L_1(G, d\mu)$ is invariant under left (right) shifts if and only if H is a left (right) ideal of the right group convolution algebra $L_1(G, d\mu)$.*

PROOF. Of course we consider only the “right-invariance and right-convolution” case. Then the other three cases are analogous. Let H be a closed linear subspace of $L_1(G, d\mu)$ invariant under right shifts and $k(g) \in H$. We will show the inclusion

$$(I.2.15) \quad [f * k]_r(h) = \int_G f(g)k(hg) d\mu(g) \in H,$$

for any $f \in L_1(G, d\mu)$. Indeed, we can treat integral (I.2.15) as a limit of sums

$$(I.2.16) \quad \sum_{j=1}^N f(g_j)k(hg_j)\Delta_j.$$

But the last sum is simply a linear combination of vectors $k(hg_j) \in H$ (by the invariance of H) with coefficients $f(g_j)$. Therefore sum (I.2.16) belongs to H and this is true for integral (I.2.15) by the closeness of H .

Otherwise, let H be a right ideal in the group convolution algebra $L_1(G, d\mu)$ and let $\phi_j(g) \in L_1(G, d\mu)$ be an approximate unit of the algebra [84, § 13.2], i.e. for any $f \in L_1(G, d\mu)$ we have

$$[\phi_j * f]_r(h) = \int_G \phi_j(g)f(hg) d\mu(g) \rightarrow f(h), \text{ when } j \rightarrow \infty.$$

Then for $k(g) \in H$ and for any $h' \in G$ the right convolution

$$[\phi_j * k]_r(hh') = \int_G \phi_j(g)k(hh'g) d\mu(g) = \int_G \phi_j(h'^{-1}g')k(hg') d\mu(g'), \quad g' = h'g,$$

from the first expression is tensing to $k(hh')$ and from the second one belongs to H (as a right ideal). Again the closeness of H implies $k(hh') \in H$ that proves the assertion. \square

Homogeneous Spaces from the Group $SL_2(\mathbb{R})$

Now we adopt the previous theoretical constructions for the particular case of the group $SL_2(\mathbb{R})$. It is common to present $SL_2(\mathbb{R})$ solely as the transformation group of the Lobachevsky half-plane. We take a wider viewpoint considering $SL_2(\mathbb{R})$ as an abstract group and wish to classify all its realizations as a transformation group of certain sets. More specifically, we describe all homogeneous spaces $SL_2(\mathbb{R})/H$, where H is a closed continuous subgroup of $SL_2(\mathbb{R})$, see Section I.2.2.2. To begin with, we start from the two-dimensional subgroup.

I.3.1. The Affine Group and the Real Line

The affine group of the real line, also known as the $ax + b$ group, can be identified with either subgroup of lower- or upper-triangular matrices of the form:

$$F = \left\{ \frac{1}{\sqrt{a}} \begin{pmatrix} a & 0 \\ c & 1 \end{pmatrix}, a > 0 \right\}, \quad F' = \left\{ \frac{1}{\sqrt{a}} \begin{pmatrix} a & b \\ 0 & 1 \end{pmatrix}, a > 0 \right\}.$$

These subgroups are obviously conjugates of each other and we can consider only the subgroup F here. We are following the construction from Section I.2.2.2 and using its notations.

Firstly, we address the simpler case of the subgroup \tilde{F} of all lower triangular matrices in $SL_2(\mathbb{R})$, which admits both positive and negative entries on the main diagonal. The corresponding homogeneous space $X = SL_2(\mathbb{R})/\tilde{F}$ is one-dimensional and can be parametrised by real numbers. We define the natural projection p as:

$$(I.3.1) \quad p : SL_2(\mathbb{R}) \rightarrow \mathbb{R} : \begin{pmatrix} a & b \\ c & d \end{pmatrix} \mapsto \frac{b}{d}, \quad \text{for } d \neq 0,$$

since there is the following decomposition:

$$(I.3.1a) \quad \begin{pmatrix} a & b \\ c & d \end{pmatrix} = \begin{pmatrix} 1 & \frac{b}{d} \\ 0 & 1 \end{pmatrix} \begin{pmatrix} \frac{1}{d} & 0 \\ c & d \end{pmatrix}, \quad \text{where } \begin{pmatrix} \frac{1}{d} & 0 \\ c & d \end{pmatrix} \in \tilde{F}.$$

The decomposition shows that each coset in $SL_2(\mathbb{R})/\tilde{F}$ either

- contains exactly one upper-triangular matrix of the form $\begin{pmatrix} 1 & u \\ 0 & 1 \end{pmatrix}$ and, thus, can be parametrised by the real number u ; or
- is the coset of matrices $\begin{pmatrix} a & b \\ -b^{-1} & 0 \end{pmatrix}$ which represents ∞ .

Then, we define the smooth map s to be a right inverse of p :

$$(I.3.2) \quad s : \mathbb{R} \rightarrow SL_2(\mathbb{R}) : u \mapsto \begin{pmatrix} 1 & u \\ 0 & 1 \end{pmatrix}.$$

The corresponding map $r(g) = s(p(g))^{-1}g$ is calculated to be:

$$(I.3.3) \quad r : SL_2(\mathbb{R}) \rightarrow \tilde{F} : \begin{pmatrix} a & b \\ c & d \end{pmatrix} \mapsto \begin{pmatrix} d^{-1} & 0 \\ c & d \end{pmatrix}.$$

Consequently, the decomposition $g = s(p(g))r(g)$ is given by (I.3.1a).

Therefore the action of $SL_2(\mathbb{R})$ on $SL_2(\mathbb{R})/\tilde{F}$ is the Möbius (linear-fractional) transformations of the *projective real line* $\dot{\mathbb{R}} = \mathbb{R} \cup \{\infty\}$:

$$(I.3.4) \quad g : u \mapsto p(g * s(u)) = \frac{au + b}{cu + d}, \quad \text{where } g = \begin{pmatrix} a & b \\ c & d \end{pmatrix}.$$

EXERCISE I.3.1. i. Check that the derived actions, see Exercise I.2.30, associated with the one-parameter subgroups $a(t)$, $b(t)$ and $z(t)$ from Exercise I.2.24, are, respectively:

$$A_F = x \frac{d}{dx}, \quad B_F = \frac{x^2 - 1}{2} \frac{d}{dx}, \quad Z_F = -(x^2 + 1) \frac{d}{dx}.$$

ii. Verify that the above operators satisfy the commutator relations for the Lie algebra \mathfrak{sl}_2 , cf. (II.3.14):

$$(I.3.5) \quad [Z_F, A_F] = 2B_F, \quad [Z_F, B_F] = -2A_F, \quad [A_F, B_F] = -\frac{1}{2}Z_F.$$

In Section I.4.4, we will see the relevance of this action to projective spaces.

EXERCISE I.3.1(a). Formula (I.3.4) uses division by $cu + d$, how it shall be understood (or modified) if $cu + d = 0$?

HINT: A similar issue is addressed in Sec. I.8.1 and can be consistently resolved through the projective coordinates. Another common approach is to extend arithmetic of real numbers to the projective real line $\dot{\mathbb{R}}$ by the following rules involving infinity:

$$(I.3.5a) \quad \frac{a}{0} = \infty, \quad \frac{a}{\infty} = 0, \quad \frac{\infty}{\infty} = 1, \quad \text{where } a \neq 0.$$

As a consequence we also note that $a \cdot \infty + b = a \cdot \infty$ for $a \neq 0$. But we do not define (and, actually, will not need) values of $\frac{0}{0}$, $0 \cdot \infty$ or $\infty - \infty$, etc. Check, that formulae (I.3.5a) together with ordinary arithmetic define in (I.3.4) a bijection $\dot{\mathbb{R}} \rightarrow \dot{\mathbb{R}}$ for $g \in SL_2(\mathbb{R})$. \diamond

To describe the homogeneous space $SL_2(\mathbb{R})/F$ and $SL_2(\mathbb{R})$ -action on it, we rewrite the identity (I.3.1a) for $d \neq 0$ as:

$$(I.3.5b) \quad \begin{pmatrix} a & b \\ c & d \end{pmatrix} = \begin{pmatrix} 1 & \frac{b}{a} \\ 0 & 1 \end{pmatrix} \begin{pmatrix} \chi(d) & 0 \\ 0 & \chi(d) \end{pmatrix} \begin{pmatrix} \frac{1}{\chi(d)c} & 0 \\ \chi(d)c & |d| \end{pmatrix},$$

where χ is the Heaviside function (I.1.10). The last matrix in the right-hand side of (I.3.5b) belongs to F and is uniquely defined by this identity. Thus, cosets representing matrices with $d \neq 0$ are parametrised by $\mathbb{R} \times \{-1, +1\}$. The respective realisations

of maps from Section I.2.2.2 are:

$$(I.3.5c) \quad p: SL_2(\mathbb{R}) \rightarrow \mathbb{R} \times \{-1, +1\}: \begin{pmatrix} a & b \\ c & d \end{pmatrix} \mapsto \left(\frac{b}{d}, \chi(d) \right),$$

$$(I.3.5d) \quad s: \mathbb{R} \times \{-1, +1\} \rightarrow SL_2(\mathbb{R}): (u, \sigma) \mapsto \begin{pmatrix} \sigma & \sigma u \\ 0 & \sigma \end{pmatrix},$$

$$(I.3.5e) \quad r: SL_2(\mathbb{R}) \rightarrow \mathbb{F}: \begin{pmatrix} a & b \\ c & d \end{pmatrix} \mapsto \begin{pmatrix} \frac{1}{|d|} & 0 \\ \chi(d)c & |d| \end{pmatrix}.$$

EXERCISE I.3.1(b). Extend the above maps (I.3.5c)–(I.3.5e) for the matrices with $d = 0$.

HINT: Note, that all matrices $\begin{pmatrix} a & b \\ -b^{-1} & 0 \end{pmatrix} \in SL_2(\mathbb{R})$ belong to two different cosets in $SL_2(\mathbb{R})/F$ depending from the value of $\chi(b)$. These cosets can be denoted by $(\infty, +1)$ and $(\infty, -1)$. \diamond

Thus, the homogeneous space $SL_2(\mathbb{R})/F$ can be identified with the double cover of the projective real line. $SL_2(\mathbb{R})$ -action on $SL_2(\mathbb{R})/F$ in terms of the above maps (I.3.5c)–(I.3.5e) is:

$$(I.3.5f) \quad g: (u, \sigma) \mapsto p(g * s(u, \sigma)) = \left(\frac{au + b}{cu + d}, \chi(cu + d)\sigma \right), \text{ where } g = \begin{pmatrix} a & b \\ c & d \end{pmatrix}.$$

EXERCISE I.3.1(c). Extend the arithmetic rules (I.3.5a) and the Heaviside function in (I.3.5f) for the exceptional cases of either $u = \infty$ or $cu + d = 0$ to produce a bijection $SL_2(\mathbb{R})/F \rightarrow SL_2(\mathbb{R})/F$.

Here is some properties of the Möbius transformations of the real line:

EXERCISE I.3.1(d). i. For a non-constant Möbius transformation, there may exist only two, one or none fixed point(s) on the real line.

ii. Let x_1, x_2, x_3 be arbitrary pairwise distinct points of \mathbb{R} with x_2 being between x_1 and x_3 . Then there is the unique element in $SL_2(\mathbb{R})$ such that the associated Möbius transformation maps $0, 1, \infty$ to x_1, x_2, x_3 respectively. Therefore, $SL_2(\mathbb{R})$ acts simply transitively on ordered triples of pair-wise distinct elements of \mathbb{R} .

HINT: Check that the matrix $\begin{pmatrix} x_3 \frac{x_2 - x_1}{x_3 - x_2} & x_1 \\ \frac{x_2 - x_1}{x_3 - x_2} & 1 \end{pmatrix}$ provides the required map and normalize its determinant. \diamond

I.3.2. One-dimensional Subgroups of $SL_2(\mathbb{R})$

Any element X of the Lie algebra \mathfrak{sl}_2 defines a one-parameter continuous subgroup $g_X(t) = e^{tX}$, $t \in \mathbb{R}$ of $SL_2(\mathbb{R})$. Two such subgroups $g_X(t)$ and $g_Y(t)$ with $X = aY$ for a non-zero $a \in \mathbb{R}$ coincide as sets and we can easily re-parameterise them: $g_Y(t) = g_X(at)$. Therefore we will not distinguish such subgroups in the following.

We already listed four one-parameter continuous subgroups in Exercise I.2.23.iii and can provide further examples, e.g. the subgroup of lower-triangular matrices. However, there are only *three* different types of subgroups under the matrix similarity $A \mapsto MAM^{-1}$.

PROPOSITION I.3.2. *Any continuous one-parameter subgroup of $SL_2(\mathbb{R})$ is conjugate to one of the following subgroups:*

$$(I.3.6) \quad A = \left\{ \begin{pmatrix} e^{-t/2} & 0 \\ 0 & e^{t/2} \end{pmatrix} = \exp \begin{pmatrix} -t/2 & 0 \\ 0 & t/2 \end{pmatrix}, t \in \mathbb{R} \right\},$$

$$(I.3.7) \quad N = \left\{ \begin{pmatrix} 1 & t \\ 0 & 1 \end{pmatrix} = \exp \begin{pmatrix} 0 & t \\ 0 & 0 \end{pmatrix}, t \in \mathbb{R} \right\},$$

$$(I.3.8) \quad K = \left\{ \begin{pmatrix} \cos t & \sin t \\ -\sin t & \cos t \end{pmatrix} = \exp \begin{pmatrix} 0 & t \\ -t & 0 \end{pmatrix}, t \in (-\pi, \pi] \right\}.$$

PROOF. Any one-parameter subgroup is obtained through the exponential map, see Section I.2.3,

$$(I.3.9) \quad e^{tX} = \sum_{n=0}^{\infty} \frac{t^n}{n!} X^n$$

of an element X of the Lie algebra \mathfrak{sl}_2 of $SL_2(\mathbb{R})$. Such an X is a 2×2 matrix with zero trace. The behaviour of the Taylor expansion (I.3.9) depends on the properties of the powers X^n . This can be classified by a straightforward calculation:

LEMMA I.3.3. *The square X^2 of a traceless matrix $X = \begin{pmatrix} a & b \\ c & -a \end{pmatrix}$ is the identity matrix times $a^2 + bc = -\det X$. The factor can be negative, zero or positive, which corresponds to the three different types of the Taylor expansion (I.3.9) of e^{tX} .*

It is a simple exercise in characteristic polynomials to see that, through the matrix similarity, we can obtain from X a generator

- of the subgroup K if $(-\det X) < 0$,
- of the subgroup N if $(-\det X) = 0$,
- of the subgroup A if $(-\det X) > 0$.

The determinant is invariant under the similarity. Thus, these cases are distinct. \square

EXERCISE I.3.4. Find matrix conjugations of the following two subgroups to A and N respectively:

$$(I.3.10) \quad A' = \left\{ \begin{pmatrix} \cosh t & \sinh t \\ \sinh t & \cosh t \end{pmatrix} = \exp \begin{pmatrix} 0 & t \\ t & 0 \end{pmatrix}, t \in \mathbb{R} \right\},$$

$$(I.3.11) \quad N' = \left\{ \begin{pmatrix} 1 & 0 \\ t & 1 \end{pmatrix} = \exp \begin{pmatrix} 0 & 0 \\ t & 0 \end{pmatrix}, t \in \mathbb{R} \right\}.$$

EXERCISE I.3.4(a). i. Determine which $g \in SL_2(\mathbb{R})$ belongs to a one-partial-rightarrowmeter subgroup, that is find the range of the exponential map $X \mapsto e^X$, where $X \in \mathfrak{sl}_2$ and $e^X \in SL_2(\mathbb{R})$. HINT: The image excludes matrices with real, negative eigenvalues, other than $-I$ [125, Ex. 3.22]. \diamond

ii. Show that $g = e^X \in SL_2(\mathbb{R})$ belongs to a subgroup conjugated to A , N or K if and only if $|\operatorname{tr}(g)|$ is bigger, equal or less than 2 respectively. HINT: Use the invariance of trace under matrix conjugation and the values of trace for matrices in A , N and K . \diamond

- iii. Let a Möbius transformation of the real line has two, one or none fixed points as described in Exercise I.3.1.(d)i, then it is generated by a matrix which is conjugated to an element of the subgroups A , N and K respectively. Why we do not mention either the matrix belongs to the image of exponential map in this part?

We will often use subgroups A' and N' as representatives of the corresponding equivalence classes under matrix conjugation.

An interesting property of the subgroups A , N and K is their appearance in the *Iwasawa decomposition* [240, § III.1] of $SL_2(\mathbb{R}) = ANK$ in the following sense. Any element of $SL_2(\mathbb{R})$ can be represented as the product:

$$(I.3.12) \quad \begin{pmatrix} a & b \\ c & d \end{pmatrix} = \begin{pmatrix} \alpha & 0 \\ 0 & \alpha^{-1} \end{pmatrix} \begin{pmatrix} 1 & \nu \\ 0 & 1 \end{pmatrix} \begin{pmatrix} \cos \phi & -\sin \phi \\ \sin \phi & \cos \phi \end{pmatrix}.$$

EXERCISE I.3.5. Check that the values of parameters in the above decomposition are as follows:

$$\alpha = (c^2 + d^2)^{-1/2}, \quad \nu = ac + bd, \quad \phi = \arctan \frac{c}{d}.$$

Consequently, $\cos \phi = \frac{d}{\sqrt{c^2+d^2}}$ and $\sin \phi = \frac{-c}{\sqrt{c^2+d^2}}$.

The Iwasawa decomposition shows once more that $SL_2(\mathbb{R})$ is a three-dimensional manifold. A similar decomposition $G = ANK$ is possible for any semisimple Lie group G , where K is the maximal compact group, N is nilpotent and A normalises N . Although the Iwasawa decomposition will be used here on several occasions, it does not play a crucial role in the present consideration. Instead, Proposition I.3.2 will be the cornerstone of our construction.

I.3.3. Two-dimensional Homogeneous Spaces

Here, we calculate the action of $SL_2(\mathbb{R})$ (I.2.3) (see Section I.2.2.2) on $X = SL_2(\mathbb{R})/H$ for all three possible one-dimensional subgroups $H = A'$, N' or K . Counting dimensions ($3 - 1 = 2$) suggests that the corresponding homogeneous spaces are two-dimensional manifolds. In fact, we identify X in each case with a subset of \mathbb{R}^2 as follows. First, for every equivalence class of $SL_2(\mathbb{R})/H$ we chose a representative, which is an upper-triangular matrix.

EXERCISE I.3.6. Show that

- i. For any matrix $g \in SL_2(\mathbb{R})$ and for each value $\sigma = -1, 0, 1$ there is a factorisation $g = g_u \begin{pmatrix} d & \sigma c \\ c & d \end{pmatrix}$ for some upper-triangular 2×2 matrix g_u . HINT: See (I.3.14), (I.3.17) and (I.3.20). \diamond
- ii. There is at most one upper-triangular matrix in every equivalence class $SL_2(\mathbb{R})/H$, where $H = A'$, N' or K , where, in the last case, uniqueness is up to the constant factor ± 1 . For the subgroup A' , there may be not such upper triangular matrix.

HINT: The identity matrix is the only upper-triangular matrix in these three subgroups, where, again, the uniqueness for the subgroup K is understood up to the scalar factor ± 1 . \diamond

The existence of such a triangular matrix will be demonstrated in each case separately. Now, we define the projection $p : SL_2(\mathbb{R}) \rightarrow X$, assigning $p(g) = (a_1 b_1, a_1^2)$, where $\begin{pmatrix} a_1 & b_1 \\ 0 & a_1^{-1} \end{pmatrix}$ is the upper-triangular matrix¹ representing the equivalence class of g . We also choose [170, p. 108] the map $s : X \rightarrow G$ in the form:

$$(I.3.13) \quad s : (u, v) \mapsto \frac{1}{\sqrt{v}} \begin{pmatrix} v & u \\ 0 & 1 \end{pmatrix}, \quad (u, v) \in \mathbb{R}^2, v > 0.$$

This formula will be used for all three possible subgroups H .

I.3.3.1. From the Subgroup K . The homogeneous space $SL_2(\mathbb{R})/K$ is the most traditional case in representation theory. The maps p and s defined above produce the following decomposition $g = s(p(g))r(g)$:

$$(I.3.14) \quad \begin{pmatrix} a & b \\ c & d \end{pmatrix} = \frac{1}{d^2 + c^2} \begin{pmatrix} 1 & bd + ac \\ 0 & c^2 + d^2 \end{pmatrix} \begin{pmatrix} d & -c \\ c & d \end{pmatrix}.$$

Then, the $SL_2(\mathbb{R})$ -action defined by the formula $g \cdot x = p(g * s(x))$ (I.2.3) takes the form:

$$(I.3.15) \quad \begin{pmatrix} a & b \\ c & d \end{pmatrix} : (u, v) \mapsto \left(\frac{(au + b)(cu + d) + cav^2}{(cu + d)^2 + (cv)^2}, \frac{v}{(cu + d)^2 + (cv)^2} \right).$$

EXERCISE I.3.7. Use CAS to check the above formula, as well as analogous formulae (I.3.18) and (I.3.21) below. See Appendix C.3 for CAS usage.

Obviously, it preserves the upper half-plane $v > 0$. The expression (I.3.15) is very cumbersome and it can be simplified by the complex imaginary unit $i^2 = -1$, which reduces (I.3.15) to the Möbius transformation

$$(I.3.16) \quad \begin{pmatrix} a & b \\ c & d \end{pmatrix} : w \mapsto \frac{aw + b}{cw + d}, \quad \text{where } w = u + iv.$$

We need to assign a meaning to the case $cw + d = 0$ and this can be done by the addition of an infinite point ∞ to the set of complex numbers—see, for example, [26, Definition 13.1.3] for details.

In this case, *complex numbers* appeared naturally.

I.3.3.2. From the Subgroup N' . We consider the subgroup of lower-triangular matrices N' (I.3.11). For this subgroup, the representative of cosets among the upper-triangular matrices will be different. Therefore, we receive an apparently different decomposition $g = s(p(g))r(g)$, cf. (I.3.14)

$$(I.3.17) \quad \begin{pmatrix} a & b \\ c & d \end{pmatrix} = \frac{1}{d^2} \begin{pmatrix} 1 & bd \\ 0 & d^2 \end{pmatrix} \begin{pmatrix} d & 0 \\ c & d \end{pmatrix}, \quad \text{where } d \neq 0.$$

We postpone the treatment of the exceptional case $d = 0$ until Section I.8.1. The $SL_2(\mathbb{R})$ -action (I.2.3) now takes the form:

$$(I.3.18) \quad \begin{pmatrix} a & b \\ c & d \end{pmatrix} : (u, v) \mapsto \left(\frac{au + b}{cu + d}, \frac{v}{(cu + d)^2} \right).$$

¹For the subgroup A' this will be refined in the subsection I.3.3.3.

This map preserves the upper half-plane $v > 0$ just like the case of the subgroup K . The expression (I.3.18) is simpler than (I.3.15), yet we can again rewrite it as a linear-fractional transformation with the help of the **dual numbers** unit $\varepsilon^2 = 0$:

$$(I.3.19) \quad \begin{pmatrix} a & b \\ c & d \end{pmatrix} : w \mapsto \frac{aw + b}{cw + d}, \quad \text{where } w = u + \varepsilon v.$$

We briefly review the algebra of dual numbers in Appendix B.1. Since they have zero divisors, the fraction is not properly defined for all $cu + d = 0$. The proper treatment will be considered in Section I.8.1 since it is not as simple as in the case of complex numbers.

I.3.3.3. From the Subgroup A' . In the last case of the subgroup A' , we still can obtain the decomposition

$$(I.3.20) \quad \begin{pmatrix} a & b \\ c & d \end{pmatrix} = \frac{1}{d^2 - c^2} \begin{pmatrix} 1 & bd - ac \\ 0 & d^2 - c^2 \end{pmatrix} \begin{pmatrix} d & c \\ c & d \end{pmatrix}, \quad \text{where } d \neq \pm c.$$

However, the new aspect is here that (I.3.20) presents the decomposition $g = s(p(g))r(g)$ if and only if $d^2 - c^2 > 0$. Otherwise the matrix $\begin{pmatrix} d & c \\ c & d \end{pmatrix}$ is not in A' . If $d^2 - c^2 < 0$ we use the decomposition

$$(I.3.20a) \quad \begin{pmatrix} a & b \\ c & d \end{pmatrix} = \frac{1}{c^2 - d^2} \begin{pmatrix} ac - bd & -1 \\ c^2 - d^2 & 0 \end{pmatrix} \begin{pmatrix} c & d \\ d & c \end{pmatrix}, \quad \text{where } d \neq \pm c.$$

The modified maps $p(g) : G \rightarrow G/H$ is:

$$(I.3.20b) \quad p(g) = \begin{cases} (a_1 b_1, a_1^2), & \text{if } g \sim \begin{pmatrix} a_1 & b_1 \\ 0 & a_1^{-1} \end{pmatrix}; \\ (a_1 b_1, -a_1^2), & \text{if } g \sim \begin{pmatrix} b_1 & -a_1 \\ a_1^{-1} & 0 \end{pmatrix}. \end{cases}$$

The respective modification of the map $s : G/H \rightarrow G$ is:

$$(I.3.20c) \quad s(u, v) = \begin{cases} \frac{1}{\sqrt{v}} \begin{pmatrix} v & u \\ 0 & 1 \end{pmatrix}, & \text{if } v > 0; \\ \frac{1}{\sqrt{-v}} \begin{pmatrix} u & v \\ 1 & 0 \end{pmatrix}, & \text{if } v < 0. \end{cases}$$

The geometrical meaning of this modification is that the homogeneous spaces G/K and G/N are parametrised by points of the upper half-plane, while G/A' shall be parametrised by the union of the upper and lower half-planes. We will further discuss this difference Section I.8.2. The exceptional situation $d = \pm c$ will be treated in Section I.8.1.

The $SL_2(\mathbb{R})$ -action (I.2.3) takes the form

$$(I.3.21) \quad \begin{pmatrix} a & b \\ c & d \end{pmatrix} : (u, v) \mapsto \left(\frac{(au + b)(cu + d) - cav^2}{(cu + d)^2 - (cv)^2}, \frac{v}{(cu + d)^2 - (cv)^2} \right).$$

Notably, this time the map does *not* preserve the upper half-plane $v > 0$: the sign of $(cu + d)^2 - (cv)^2$ is not determined. To express this map as a Möbius transformation,

we require the **double numbers** (also known as *split-complex numbers*) unit $j^2 = 1$:

$$\begin{pmatrix} a & b \\ c & d \end{pmatrix} : w \mapsto \frac{aw + b}{cw + d}, \quad \text{where } w = u + jv.$$

The algebra of double numbers is briefly introduced in Appendix B.1.

I.3.3.4. Unifying All Three Cases. There is an obvious similarity in the formulae obtained in each of the above cases. To present them in a unified way, we introduce the parameter σ which is equal to $-1, 0$ or 1 for the subgroups K, N' or A' , respectively. Then, decompositions (I.3.14), (I.3.17) and (I.3.20) are

$$(I.3.22) \quad \begin{pmatrix} a & b \\ c & d \end{pmatrix} = \frac{1}{d^2 - \sigma c^2} \begin{pmatrix} 1 & bd - \sigma ac \\ 0 & d^2 - \sigma c^2 \end{pmatrix} \begin{pmatrix} d & \sigma c \\ c & d \end{pmatrix}, \quad \text{where } d^2 - \sigma c^2 \neq 0.$$

The respective $SL_2(\mathbb{R})$ -actions on the homogeneous space $SL_2(\mathbb{R})/H$, where $H = A', N'$ or K , are given by

$$(I.3.23) \quad \begin{pmatrix} a & b \\ c & d \end{pmatrix} : (u, v) \mapsto \left(\frac{(au + b)(cu + d) - \sigma cv^2}{(cu + d)^2 - \sigma (cv)^2}, \frac{v}{(cu + d)^2 - \sigma (cv)^2} \right).$$

Finally, this action becomes the linear-fractional (Möbius) transformation for hyper-complex numbers in two-dimensional commutative associative algebra (see Appendix B.1) spanned by 1 and ι :

$$(I.3.24) \quad \begin{pmatrix} a & b \\ c & d \end{pmatrix} : w \mapsto \frac{aw + b}{cw + d}, \quad \text{where } w = u + \iota v, \quad \iota^2 = \sigma.$$

Thus, a comprehensive study of $SL_2(\mathbb{R})$ -homogeneous spaces naturally introduces three number systems. Obviously, only one case (complex numbers) belongs to mainstream mathematics. We start to discover empty cells in our periodic table.

REMARK I.3.8. As we can now see, the dual and double numbers naturally appear in relation to the group $SL_2(\mathbb{R})$ and, thus, their introduction in [185, 190] was not “a purely generalistic attempt”, cf. the remark on quaternions of [288, p. 4].

REMARK I.3.9. A different choice of the map $s : G/H \rightarrow G$ will produce different (but isomorphic) geometric models. In this way, we will obtain three types of “unit disks” in Chapter I.10.

I.3.4. Elliptic, Parabolic and Hyperbolic Cases

As we have seen in the previous section, there is no need to be restricted to the traditional route of complex numbers only. The arithmetic of dual and double numbers is different from complex numbers mainly in the following aspects:

- i. They have zero divisors. However, we are still able to define their transforms by (I.3.24) in most cases. The proper treatment of zero divisors will be done through corresponding compactification—see Section I.8.1.
- ii. They are not algebraically closed. However, this property of complex numbers is not used very often in analysis.

We have agreed in Section I.1.1 that three possible values $-1, 0$ and 1 of $\sigma := t^2$ will be referred to here as *elliptic*, *parabolic* and *hyperbolic* cases, respectively. This separation into three cases will be referred to as the *EPH classification*. Unfortunately, there is a clash here with the already established label for the *Lobachevsky geometry*. It is often called hyperbolic geometry because it can be realised as a Riemann geometry on a two-sheet hyperboloid. However, within our framework, the Lobachevsky geometry should be called elliptic and it will have a true hyperbolic counterpart.

NOTATION I.3.10. We denote the space \mathbb{R}^2 of vectors $u + v$ by \mathbb{C} , \mathbb{D} or \mathbb{O} to highlight which number system (complex, dual or double, respectively) is used. The notation \mathbb{A} is used for a generic case. The use of E, P, H or e, p, h (for example, in labelling the different sections of an exercise) corresponds to the elliptic, parabolic, hyperbolic cases.

REMARK I.3.11. In introducing the parabolic objects on a common ground with elliptic and hyperbolic ones, we should warn against some common prejudices suggested by the diagram (I.1.2):

- i. The parabolic case is unimportant (has “zero measure”) in comparison to the elliptic and hyperbolic cases. As we shall see (e.g. Remark I.10.8 and I.7.12.ii), the parabolic case presents some richer geometrical features.
- ii. The parabolic case is a limiting situation or an intermediate position between the elliptic and hyperbolic cases. All properties of the former can be guessed or obtained as a limit or an average from the latter two. In particular, this point of view is implicitly supposed in [241].

Although there are some confirmations of this (e.g. Fig. I.10.3(E)–(H)), we shall see (e.g. Remark I.7.21) that some properties of the parabolic case cannot be guessed in a straightforward manner from a combination of elliptic and hyperbolic cases.

- iii. All three EPH cases are even less disjoint than is usually thought. For example, there are meaningful notions of the *centre of a parabola* (I.4.3) or the *focus of a circle* (I.5.2).
- iv. A (co-)invariant geometry is believed to be “coordinate-free”, which sometimes is pushed to an absolute mantra. However, our study within the Erlangen programme framework reveals two useful notions (Definition I.4.3 and (I.5.2)), mentioned above, which are defined by coordinate expressions and look very “non-invariant” at first glance.

I.3.5. Orbits of the Subgroup Actions

We start our investigation of the Möbius transformations (I.3.24)

$$\begin{pmatrix} a & b \\ c & d \end{pmatrix} : w \mapsto \frac{aw + b}{cw + d}$$

on the hypercomplex numbers $w = u + tv$ from a description of orbits produced by the subgroups A, N and K . Due to the Iwasawa decomposition (I.3.12), any Möbius transformation can be represented as a superposition of these three actions.

The actions of subgroups A and N for any kind of hypercomplex numbers on the plane are the same as on the real line: A dilates and N shifts—see Fig. I.1.1 for illustrations. Thin traversal lines in Fig. I.1.1 join points of orbits obtained from the vertical axis by the same values of t and grey arrows represent “local velocities”—vector fields of derived representations.

EXERCISE I.3.12. Check that:

- i. The matrix $\begin{pmatrix} e^{-t} & 0 \\ 0 & e^t \end{pmatrix} = \exp \begin{pmatrix} -t & 0 \\ 0 & t \end{pmatrix}$ from A makes a dilation by e^{-2t} , i.e. $z \mapsto e^{-2t}z$. The respective derived action, see Example I.2.30, is twice the Euler operator $u\partial_u + v\partial_v$.
- ii. The matrix $\begin{pmatrix} 1 & t \\ 0 & 1 \end{pmatrix} = \exp \begin{pmatrix} 0 & t \\ 0 & 0 \end{pmatrix}$ from N shifts points horizontally by t , i.e. $z \mapsto z + t = (u + t) + iv$. The respective derived action is ∂_u .
- iii. The subgroup of $SL_2(\mathbb{R})$ generated by A and N is isomorphic to the $ax + b$ group, which acts transitively on the upper half-plane.

HINT: Note that the matrix $\begin{pmatrix} \sqrt{a} & b/\sqrt{a} \\ 0 & 1/\sqrt{a} \end{pmatrix} = \begin{pmatrix} 1 & b \\ 0 & 1 \end{pmatrix} \begin{pmatrix} \sqrt{a} & 0 \\ 0 & 1/\sqrt{a} \end{pmatrix}$ maps t to $at + b$ and use Exercise I.2.17.ii. \diamond

By contrast, the action of the third matrix from the subgroup K sharply depends on $\sigma = t^2$, as illustrated by Fig. I.1.2. In elliptic, parabolic and hyperbolic cases, K -orbits are circles, parabolas and (equilateral) hyperbolas, respectively. The meaning of traversal lines and vector fields is the same as on the previous figure.

EXERCISE I.3.13. The following properties characterise K -orbits:

- i. The derived action of the subgroup K is given by:

$$(I.3.25) \quad K_\sigma^d(u, v) = (1 + u^2 + \sigma v^2)\partial_u + 2uv\partial_v, \quad \sigma = t^2.$$

HINT: Use the explicit formula for Möbius transformation of the components (I.3.23). An alternative with CAS is provided as well, see Appendix C.3 for usage. \diamond

- ii. A K -orbit in \mathbb{A} passing the point $(0, s)$ has the following equation:

$$(I.3.26) \quad (u^2 - \sigma v^2) - 2v \frac{s^{-1} - \sigma s}{2} + 1 = 0.$$

HINT: Note that the equation (I.3.26) defines *contour lines* of the function $F(u, v) = (u^2 - \sigma v^2 + 1)/v$, that is, solve the equations $F(u, v) = \text{const}$. Then, apply the operator (I.3.25) to obtain $K_\sigma^d F = 0$. \diamond

- iii. The curvature of a K -orbit at point $(0, s)$ is equal to

$$(I.3.27) \quad \kappa = \frac{2s}{1 + \sigma s^2}.$$

- iv. The transverse line obtained from the vertical axis has the equations:

$$(I.3.28) \quad (u^2 - \sigma v^2) + 2 \cot(2\phi)u - 1 = 0, \quad \text{for } g = \begin{pmatrix} \cos \phi & \sin \phi \\ -\sin \phi & \cos \phi \end{pmatrix} \in K.$$

HINT: A direct calculation for a point $(0, s)$ in the formula (I.3.23) is possible but demanding. A computer symbolic calculation is provided as well. \diamond

Much more efficient proofs will be given later (see Exercise I.4.16.ii), when suitable tools will be at our disposal. It will also explain why K-orbits, which are circles, parabolas and hyperbolas, are defined by the same equation (I.3.26). Meanwhile, these formulae allow us to produce geometric characterisation of K-orbits in terms of classical notions of conic sections, cf. Appendix B.2.

EXERCISE I.3.14. Check the following properties of K-orbits (I.3.26):

- (e) For the elliptic case, the orbits of K are circles. A circle with centre at $(0, (s + s^{-1})/2)$ passing through two points $(0, s)$ and $(0, s^{-1})$.
- (p) For the parabolic case, the orbits of K are parabolas with the vertical axis V. A parabola passing through $(0, s)$ has horizontal directrix passing through $(0, s - 1/(4s))$ and focus at $(0, s + 1/(4s))$.
- (h) For the hyperbolic case, the orbits of K are hyperbolas with asymptotes parallel to lines $u = \pm v$. A hyperbola passing the point $(0, s)$ has the second branch passing $(0, -s^{-1})$ and asymptotes crossing at the point $(0, (s - s^{-1})/2)$. Foci of this hyperbola are:

$$f_{1,2} = \left(0, \frac{1}{2} \left((1 \pm \sqrt{2})s - (1 \mp \sqrt{2})s^{-1} \right)\right).$$

The amount of similarities between orbits in the three EPH cases suggests that they should be unified one way or another. We start such attempts in the next section.

I.3.6. Unifying EPH Cases: The First Attempt

It is well known that any K-orbit above is a *conic section* and an interesting observation is that corresponding K-orbits are, in fact, sections of the same two-sided right-angle cone. More precisely, we define the family of double-sided right-angle cones to be parameterized by $s > 0$:

$$(I.3.29) \quad x^2 + \left(y - \frac{1}{2}(s + s^{-1})\right)^2 - \left(z - \frac{1}{2}(s - s^{-1})\right)^2 = 0.$$

Therefore, vertices of cones belong to the hyperbola $\{x = 0, y^2 - z^2 = 1\}$ —see Fig. I.1.3.

EXERCISE I.3.15. Derive equations for the K-orbits described in Exercise I.3.14 by calculation of intersection of a cone (I.3.29) with the following planes:

- (e) Elliptic K-orbits are sections of cones (I.3.29) by the plane $z = 0$ (EE' on Fig. I.1.3).
- (p) Parabolic K-orbits are sections of (I.3.29) by the plane $y = \pm z$ (PP' on Fig. I.1.3).
- (h) Hyperbolic K-orbits are sections of (I.3.29) by the plane $y = 0$ (HH' on Fig. I.1.3);

Moreover, each straight line generating the cone, see Fig. I.1.3(b), is crossing corresponding EPH K-orbits at points with the same value of parameter ϕ from (I.3.12). In other words, all three types of orbits are generated by the rotations of this generator along the cone.

EXERCISE I.3.16. Verify that the rotation of a cone's generator corresponds to the Möbius transformations in three planes.

HINT: I do not know a smart way to check this, so a CAS solution is provided.◊

From the above algebraic and geometric descriptions of the orbits we can make several observations.

- REMARK I.3.17.
- i. The values of all three vector fields dK_e , dK_p and dK_h coincide on the “real” U -axis ($v = 0$), i.e. they are three different extensions into the domain of the same boundary condition. Another origin of this: the axis U is the intersection of planes EE' , PP' and HH' on Fig. I.1.3.
 - ii. The hyperbola passing through the point $(0, 1)$ has the shortest focal length $\sqrt{2}$ among all other hyperbolic orbits since it is the section of the cone $x^2 + (y - 1)^2 + z^2 = 0$ closest from the family to the plane HH' .
 - iii. Two hyperbolas passing through $(0, v)$ and $(0, v^{-1})$ have the same focal length since they are sections of two cones with the same distance from HH' . Moreover, two such hyperbolas in the lower and upper half-planes passing the points $(0, v)$ and $(0, -v^{-1})$ are sections of the same double-sided cone. They are related to each other as explained in Remark I.8.4.

We make a generalisation to all EPH cases of the following notion, which is well known for circles [71, § 2.3] and parabolas [339, § 10]:

DEFINITION I.3.18. A *power* p of a point (u, v) with respect to a conic section given by the equation $x^2 - \sigma y^2 - 2lx - 2ny + c = 0$ is defined by the identity

$$(I.3.30) \quad p = u^2 - \sigma v^2 - 2lu - 2nv + c.$$

EXERCISE I.3.19. Check the following properties:

- i. A conic section is the collection of points having zero power with respect to the section.
- ii. The collection of points having the same power with respect to two given conic sections of the above type is either empty or the straight line. This line is called *radical axis* of the two sections.
- iii. All K -orbits are *coaxial* [71, § 2.3] with the real line being their joint radical axis, that is, for a given point on the real line, its power with respect to any K -orbit is the same.
- iv. All transverse lines (I.3.28) are coaxial, with the vertical line $u = 0$ being the respective radial axis.

In the case of circles the power of a point is known as *Steiner power*.

I.3.7. Isotropy Subgroups

In Section I.2.2 we described the two-sided connection between homogeneous spaces and subgroups. Section I.3.3 uses it in one direction: from subgroups to homogeneous spaces. The following exercise does it in the opposite way: from the group action on a homogeneous space to the corresponding subgroup, which fixes the certain point.

EXERCISE I.3.20. Let $SL_2(\mathbb{R})$ act by Möbius transformations (I.3.24) on the three number systems. Show that the isotropy subgroups of the point ι are:

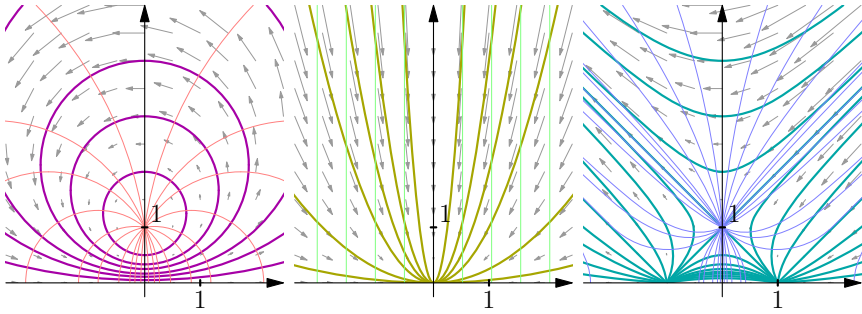


FIGURE I.3.1. Actions of isotropy subgroups K , N' and A' , which fix point ι in three EPH cases.

(e) The subgroup K in the elliptic case. Thus, the elliptic upper half-plane is a model for the homogeneous space $SL_2(\mathbb{R})/K$.

(p) The subgroup N' (I.3.11) of matrices

$$(I.3.31) \quad \begin{pmatrix} 1 & 0 \\ \nu & 1 \end{pmatrix} = \begin{pmatrix} 0 & -1 \\ 1 & 0 \end{pmatrix} \begin{pmatrix} 1 & \nu \\ 0 & 1 \end{pmatrix} \begin{pmatrix} 0 & 1 \\ -1 & 0 \end{pmatrix}$$

in the parabolic case. It also fixes any point $\epsilon\nu$ on the vertical axis, which is the set of zero divisors in dual numbers. The subgroup N' is conjugate to subgroup N , thus the *parabolic upper half-plane* is a model for the homogeneous space $SL_2(\mathbb{R})/N$.

(h) The subgroup A' (I.3.10) of matrices

$$(I.3.32) \quad \begin{pmatrix} \cosh \tau & \sinh \tau \\ \sinh \tau & \cosh \tau \end{pmatrix} = \frac{1}{2} \begin{pmatrix} 1 & -1 \\ 1 & 1 \end{pmatrix} \begin{pmatrix} e^\tau & 0 \\ 0 & e^{-\tau} \end{pmatrix} \begin{pmatrix} 1 & 1 \\ -1 & 1 \end{pmatrix}$$

in the hyperbolic case. These transformations also fix the light cone centred at j , that is, consisting of $j +$ zero divisors. The subgroup A' is conjugate to the subgroup A , thus two copies of the upper half-plane (see Section I.8.2) are a model for $SL_2(\mathbb{R})/A$.

Figure I.3.1 shows actions of the above isotropic subgroups on the respective numbers, we call them *rotations* around ι . Note, that in parabolic and hyperbolic cases they fix larger sets connected with zero divisors.

It is inspiring to compare the action of subgroups K , N' and A' on three number systems, this is presented on Fig. I.3.2. Some features are preserved if we move from top to bottom along the same column, that is, keep the subgroup and change the metric of the space. We also note the same system of a gradual transition if we compare pictures from left to right along a particular row. Note, that Fig. I.3.1 extracts diagonal images from Fig. I.3.2, this puts three images from Fig. I.3.1 into a context, which is not obvious from Fig. I.3.2. Even greater similarity in the respective analytic expressions is presented by the next exercise.

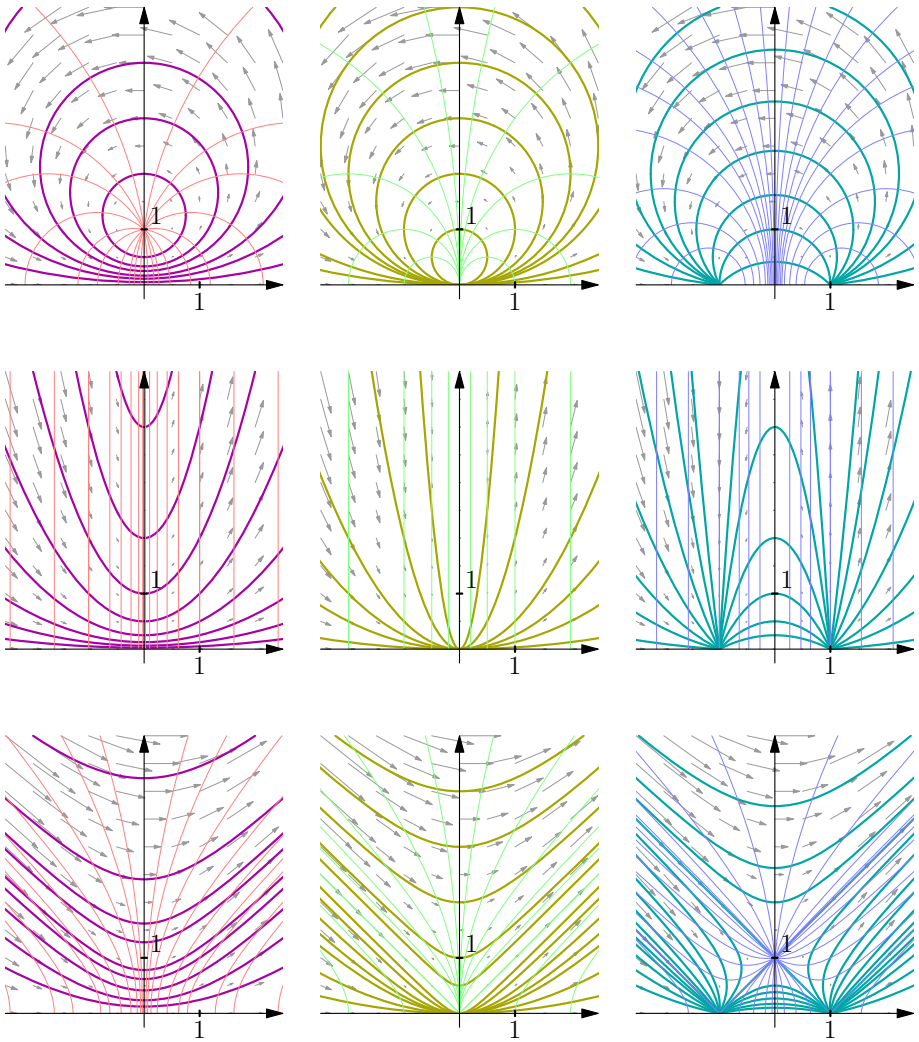


FIGURE I.3.2. Actions of the subgroups K , N' , A' are shown in the first, middle and last columns respectively. The elliptic, parabolic and hyperbolic spaces are presented in the first, middle and last rows respectively. The diagonal drawings comprise Fig. I.3.1 and the first column Fig. I.1.2.

EXERCISE I.3.21. Using the parameter $\tau = -1, 0, 1$ for the subgroups K , N' and A' respectively, check the following properties of the actions of the subgroups K , N' and A' :

- i. Vector fields of the respective actions are

$$(\mathbf{u}^2 + \sigma\mathbf{v}^2 - \tau)\partial_{\mathbf{u}} + 2\mathbf{u}\mathbf{v}\partial_{\mathbf{v}},$$

where $\sigma = \iota^2$ represent the metric of the space .

ii. Orbits of the isotropy subgroups A' , N' and K satisfy the equation

$$(I.3.33) \quad (\mathbf{u}^2 - \sigma\mathbf{v}^2) - 2\mathbf{n}\mathbf{v} - \tau = 0, \quad \text{where } \mathbf{n} \in \mathbb{R}.$$

HINT: See method used in Exercise I.3.13.ii. An alternative derivation will be available in Exercise I.5.24.◇

iii. The isotropy subgroups of ι in all EPH cases are uniformly expressed by matrices of the form

$$(I.3.33a) \quad \begin{pmatrix} \mathbf{a} & \sigma\mathbf{b} \\ \mathbf{b} & \mathbf{a} \end{pmatrix}, \quad \text{where } \mathbf{a}^2 - \sigma\mathbf{b}^2 = 1.$$

iv. The isotropy subgroup of a point $\mathbf{u} + \iota\mathbf{v}$ consists of matrices

$$\begin{pmatrix} \sqrt{1 + \sigma\mathbf{v}^2\mathbf{c}^2} + \mathbf{u}\mathbf{c} & \mathbf{c}(\sigma\mathbf{v}^2 - \mathbf{u}^2) \\ \mathbf{c} & \sqrt{1 + \sigma\mathbf{v}^2\mathbf{c}^2} - \mathbf{u}\mathbf{c} \end{pmatrix} \in \text{SL}_2(\mathbb{R})$$

and describe admissible values of the parameter \mathbf{c} .

HINT: Use the previous item and the transitive action of the $\mathbf{a}\mathbf{x} + \mathbf{b}$ from Exercise I.3.12.iii.◇

v. The transverse lines on Fig. I.3.2 in all nine cases are, cf. (I.3.33):

$$(I.3.34) \quad (\mathbf{u}^2 - \sigma\mathbf{v}^2) - \mathbf{l}\mathbf{u} + \tau = 0, \quad \text{where } \mathbf{l} \in \mathbb{R}.$$

DEFINITION I.3.22. In the hyperbolic case, we extend the subgroup A' to a subgroup A'' by the element $\begin{pmatrix} 0 & 1 \\ -1 & 0 \end{pmatrix}$.

This additional elements flips the upper and lower half-planes of double numbers—see Section I.8.2. Therefore, the subgroup A''_h fixes the set $\{\iota, -\iota\}$.

LEMMA I.3.23. *Möbius action of $\text{SL}_2(\mathbb{R})$ in each EPH case is generated by action of the corresponding isotropy subgroup (A''_h in the hyperbolic case) and actions of the $\mathbf{a}\mathbf{x} + \mathbf{b}$ group, e.g. subgroups A and N .*

PROOF. The $\mathbf{a}\mathbf{x} + \mathbf{b}$ group acts transitively on the upper or lower half-planes. Thus, for any $\mathbf{g} \in \text{SL}_2(\mathbb{R})$, there is an \mathbf{h} in the $\mathbf{a}\mathbf{x} + \mathbf{b}$ group such that $\mathbf{h}^{-1}\mathbf{g}$ either fixes ι or sends it to $-\iota$. Thus, $\mathbf{h}^{-1}\mathbf{g}$ is in the corresponding isotropy subgroup. □

I.3.7.1. Trigonometric Functions. The actions of isotropy subgroups can be viewed as “rotations around ι ”. In the Euclidean geometry rotations are transformations preserving angles. Thus, we can use isotropy subgroups to define angles in all EPH geometries as certain invariants of Möbius transformations.

DEFINITION I.3.24. The σ -tangent (denoted \tan_σ) between two vectors $P = (\mathbf{u}, \mathbf{v})$ and $P' = (\mathbf{u}', \mathbf{v}')$ in \mathbb{A}^2 is defined by:

$$(I.3.35) \quad \tan_\sigma(P, P') = \frac{\mathbf{u}\mathbf{v}' - \mathbf{u}'\mathbf{v}}{\mathbf{u}\mathbf{u}' - \sigma\mathbf{v}\mathbf{v}'}.$$

Then, the respective σ -cosine and σ -sine functions are connected to σ -tangent by:

$$(I.3.36) \quad \begin{aligned} \cos_{\sigma}^2(P, P') &= \frac{1}{1 - \sigma \tan_{\sigma}^2(P, P')} \\ &= \frac{(uu' - \sigma vv')^2}{(uu' - \sigma vv')^2 - \sigma(uv' - vu')^2} = \frac{(uu' - \sigma vv')^2}{(u^2 - \sigma v^2)(u'^2 - \sigma v'^2)}, \end{aligned}$$

$$(I.3.37) \quad \begin{aligned} \sin_{\sigma}^2(P, P') &= \frac{\tan_{\sigma}^2(P, P')}{1 - \sigma \tan_{\sigma}^2(P, P')} \\ &= \frac{(uv' - vu')^2}{(uu' - \sigma vv')^2 - \sigma(uv' - vu')^2} = \frac{(uv' - vu')^2}{(u^2 - \sigma v^2)(u'^2 - \sigma v'^2)}. \end{aligned}$$

As a consequence we have the following EPH form of the Pythagoras identity, cf. the identity at (I.3.33a):

$$(I.3.38) \quad \cos_{\sigma}^2(P, P') - \sigma \sin_{\sigma}^2(P, P') = 1.$$

EXERCISE I.3.25. Let P and P' be two vectors tangent to \mathbb{A}^2 at ι . Denote by \tilde{P} and \tilde{P}' images of P and P' under the action of the matrix $\begin{pmatrix} a & \sigma b \\ b & a \end{pmatrix}$ from the corresponding isotropy subgroup, see (I.3.33a). Then:

- i. The angle between a vector and its image is independent from the vector:

$$\tan_{\sigma}(P, \tilde{P}) = \frac{2ab}{a^2 + \sigma b^2}.$$

- ii. The angle between vectors is preserved by the transformation: $\tan_{\sigma}(P, P') = \tan_{\sigma}(\tilde{P}, \tilde{P}')$. Since cosine and sine are functions of the tangent they are preserved as well

EXERCISE I.3.26. Show that the angle between any two tangent vectors at any point of \mathbb{A}^2 is preserved by an arbitrary Möbius transformation from $SL_2(\mathbb{R})$. HINT: Use a combination of Lem. I.3.23 and Exercise I.3.25.ii. \diamond

We continue to use the standard notation \tan and \tanh for the respective elliptic \tan_e and hyperbolic \tan_h functions, similarly for sines and cosines.

The Extended Fillmore–Springer–Cnops Construction

Cycles—circles, parabolas and hyperbolas—are invariant families under their respective Möbius transformations. We will now proceed with a study of the invariant properties of cycles according to the Erlangen programme. A crucial step is to treat cycles not as subsets of \mathbb{R}^n but rather as points of some projective space of higher dimensionality, see [33, Ch. 3; 59; 276]. It is common in algebra to represent quadratic forms by square matrices, thus circles and their Möbius transformations are naturally described by 2×2 matrices, see [300, Ch. 1; 306, Ch. 9]. Yet one important component is still missing in those works: the invariant cycle product. This enhancement was independently introduced by several researchers in hypercomplex context [65, 100], see also [163]. This chapter introduces a further extension: the signature of the cycle project can vary even for the same type of point space.

I.4.1. Invariance of Cycles

K-orbits, shown in Fig. I.1.2, are K-invariant in a trivial way. Moreover, since actions of both A and N for any σ are extremely ‘shape-preserving’, see Exercise I.3.12, we meet natural invariant objects of the Möbius map:

DEFINITION I.4.1. The common name *cycle* [339] is used to denote circles, parabolas with horizontal directrices and equilateral hyperbolas with vertical axes of symmetry (as well as straight lines as the limiting cases of any from above) in the respective EPH case.

It is known, from analytic geometry, that a cycle is defined by the equation

$$(I.4.1) \quad k(u^2 - \sigma v^2) - 2lu - 2nv + m = 0,$$

where $\sigma = \iota^2$ and k, l, n, m are real parameters, such that *not all of them* are equal to zero. Using hypercomplex numbers, we can write the same equation as, cf. [339, Suppl. C(42a)],

$$(I.4.2) \quad Kw\bar{w} - Lw + \bar{L}\bar{w} + M = 0,$$

where $w = u + \iota v$, $K = \iota k$, $L = n + \iota l$, $M = \iota m$ and conjugation is defined by $\bar{w} = u - \iota v$.

EXERCISE I.4.2. Check that such cycles result in straight lines for certain k, l, n, m and, depending from the case, one of the following:

- (e) In the elliptic case: circles with centre $(\frac{l}{k}, \frac{n}{k})$ and squared radius $(l^2 + n^2 - mk)/k^2$.
- (p) In the parabolic case: parabolas with horizontal directrices and focus at $(\frac{l}{k}, \frac{m}{2n} - \frac{l}{2\tau})$.

- (h) In the hyperbolic case: rectangular hyperbolas with centre $(\frac{1}{k}, -\frac{n}{k})$ and vertical axes of symmetry.

Hereafter, the words parabola and hyperbola always assume only the above described types. Straight lines are also called *flat cycles*.

All three EPH types of cycles enjoy many common properties, sometimes even beyond those which we normally expect. For example, the following definition is quite intelligible even when extended from the above elliptic and hyperbolic cases to the parabolic one:

DEFINITION I.4.3. $\hat{\sigma}$ -Centre of the σ -cycle (I.15.3) for any EPH case is the point $(\frac{1}{k}, -\hat{\sigma}\frac{n}{k}) \in \mathbb{A}$. Notions of e-centre, p-centre, h-centre are used according the adopted EPH notations.

Centres of straight lines are at infinity, see Subsection I.8.1.

REMARK I.4.4. Here, we use a signature $\hat{\sigma} = -1, 0$ or 1 of a number system which does not coincide with the signature σ of the space \mathbb{A} . We will also need a third signature $\check{\sigma}$ to describe the geometry of cycles in Definition I.4.11.

EXERCISE I.4.5. Note that some quadruples (k, l, n, m) may correspond through the Equation (I.15.3) to the empty set on a certain point space \mathbb{A} . Give the full description of parameters (k, l, n, m) and σ which leads to the empty set. HINT: Use the coordinates of the cycle's centre and completion to full squares to show that the empty set may appear only in the elliptic point space. Such circles are usually called *imaginary*. \diamond

The usefulness of Defn. I.4.3, even in the parabolic case, will be justified, for example, by

- the uniformity of the description of relations between the centres of orthogonal cycles, see the next subsection and Fig. I.6.3,
- the appearance of *concentric parabolas* in Fig. I.10.3 ($P_e : \mathbb{N}$ and $P_h : \mathbb{N}$).

Here is one more example of the natural appearance of concentric parabolas:

EXERCISE I.4.6. Show that, in all EPH cases, the locus of points having a fixed *power* with respect to a given cycle C is a cycle concentric with C .

This property is classical for circles [71, § 2.3] and is also known for parabolas [339, § 10]. However, for parabolas, Yaglom used the word 'concentric' in quotes, since he did not define the centres of a parabola explicitly.

The family of all cycles from Definition I.4.1 is invariant under Möbius transformations (I.3.24) in all EPH cases, which was already stated in Theorem I.1.2. If a cycle does not intersect the real axis then the proof of Theorem I.1.2 has the only gap: a demonstration that we can always transform the cycle to a K-orbit.

EXERCISE I.4.7. Let C be a cycle in \mathbb{A} with its centre on the vertical axis. Show that there is the unique scaling $w \mapsto a^2 w$ which maps C into a K-orbit. HINT: Check that a cycle in \mathbb{A} with its centre belonging to the vertical axis is completely defined by the point of its intersection with the vertical axis and its curvature at this point. Then find the value of a for a scaling such that the image of C will satisfy the relation (I.3.27). \diamond

To finish the proof of Theorem I.1.2 we need to consider two more cases which are also related to the structure of the group $SL_2(\mathbb{R})$:

- EXERCISE I.4.7(a). i. An arbitrary cycle may have only two, one or none common point(s) with the real axis. This number is invariant under Möbius transformations.
- ii. If a cycle has two, one or none common point(s) with the real axis and is fixed by a Möbius transformation, then the map is generated by a matrix which is conjugated to an element of subgroup A , N or K . HINT: Use the Exercise I.3.4.(a)iii.◇

If all the above details are taking into consideration the proof of Theorem I.1.2 may not appear as simple as we may initially thought. However, it still highlights important connections between the invariance of cycles and the structure of the group $SL_2(\mathbb{R})$. Furthermore, we fully describe how cycles are transformed by Möbius transformations in Theorem I.4.13.

I.4.2. Projective Spaces of Cycles

Figure I.1.3 suggests that we may obtain a unified treatment of cycles in all EPH cases by consideration of higher-dimension spaces. The standard mathematical method is to declare objects under investigation to be simply points of some larger space.

EXAMPLE I.4.8. In functional analysis, sequences or functions are considered as points (vectors) of certain linear spaces. Linear operations (addition and multiplication by a scalar) on vectors (that is, functions) are defined point-wise.

If an object is considered as a point (in a new space) all information about its inner structure is lost, of course. Therefore, this space should be equipped with an appropriate structure to hold information externally which previously described the inner properties of our objects. In other words, the inner structure of an object is now revealed through its relations to its peers¹.

EXAMPLE I.4.9. Take the linear space of continuous real-valued functions on the interval $[0, 1]$ and introduce the *inner product* of two functions by the formula:

$$\langle f, g \rangle = \int_0^1 f(t) g(t) dt.$$

It allows us to define the *norm* of a function and the *orthogonality* of two functions. These are the building blocks of *Hilbert space* theory, which recovers much of Euclidean geometry in terms of the spaces of functions.

In the geometry, the similar ideas are known as representational geometry, see [99, 101] and references there for a discussion. We will utilise this fundamental approach for cycles. A generic cycle from Definition I.4.1 is the set of points $(u, v) \in \mathbb{A}$ defined for the respective values of σ by the equation

$$(I.4.3) \quad k(u^2 - \sigma v^2) - 2lu - 2nv + m = 0.$$

¹The same is true for human beings.

This equation (and the corresponding cycle) is completely determined by a point $(k, l, n, m) \in \mathbb{R}^4$. However, this is not a one-to-one correspondence. For a scaling factor $\lambda \neq 0$, the point $(\lambda k, \lambda l, \lambda n, \lambda m)$ defines an equivalent equation to (I.4.3). Thus, we prefer to consider the *projective space* \mathbb{P}^3 , that is, \mathbb{R}^4 factorised by the equivalence relation $(k, l, n, m) \sim (\lambda k, \lambda l, \lambda n, \lambda m)$ for any real $\lambda \neq 0$. A good introductory read on projective spaces is [296, Ch. 10], see also Ch. 13 in [311]. The chapter in the later book is titled “Projective Geometry Is All Geometry”, which is a quote from Arthur Cayley and our consideration below is a further illustration to this claim.

DEFINITION I.4.10. We call \mathbb{P}^3 the *cycle space* and refer to the initial \mathbb{A} as the *point space*. The correspondence which associates a point of the cycle space to a cycle equation (I.4.3) is called $\text{map } Q$.

EXERCISE I.4.10(a). Which cycles correspond to the quadruples $(1, 0, 0, 0)$, $(0, 1, 0, 0)$, $(0, 0, 1, 0)$ and $(0, 0, 0, 1)$?

Hint: for the last cycle see Defn. I.8.1 and the following Ex. I.8.2.

We also note that the Equation (I.4.2) of a cycle can be written as a quadratic form (I.4.4)

$$Kw_1\bar{w}_1 - Lw_1\bar{w}_2 + \bar{L}\bar{w}_1w_2 + Mw_2\bar{w}_2 = 0$$

in the homogeneous coordinates (w_1, w_2) , such that $w = \frac{w_1}{w_2}$. Since quadratic forms are related to square matrices, see Section I.4.4, we define another map on the cycle space as follows.

DEFINITION I.4.11. We arrange numbers (k, l, n, m) into the *cycle matrix*

$$(I.4.5) \quad C_{\check{\sigma}}^s = \begin{pmatrix} l + \check{i}sn & -m \\ k & -l + \check{i}sn \end{pmatrix},$$

with a new hypercomplex unit \check{i} and an additional real parameter s , which is usually equal to ± 1 . If we omit it in the cycle notation $C_{\check{\sigma}}$, then the value $s = 1$ is assumed.

The values of $\check{\sigma} := \check{i}^2$ are $-1, 0$ or 1 , independent of the value of σ . The parameter $s = \pm 1$ often (but not always) is equal to σ . Matrices which differ by a real non-zero factor are considered to be equivalent.

We denote by M such a map from \mathbb{P}^3 to the projective space of 2×2 matrices.

The matrix (I.4.5) is the cornerstone of the (extended) *Fillmore–Springer–Cnops construction (FSCc)* [65, 100] and is closely related to the technique recently used by A.A. Kirillov to study the *Apollonian gasket* [163]. A hint for the composition of this matrix is provided by the following exercise.

EXERCISE I.4.12. Let the space \mathbb{A}^2 be equipped with a product of symplectic type

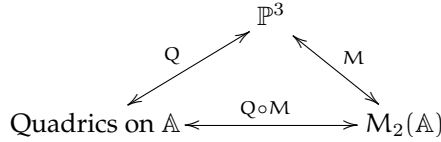
$$[w, w'] = \bar{w}_1w'_2 - \bar{w}_2w'_1,$$

where $w^{(\prime)} = (w_1^{(\prime)}, w_2^{(\prime)}) \in \mathbb{A}^2$. Letting $C = \begin{pmatrix} L & -M \\ K & \bar{L} \end{pmatrix}$, check that the equation of the cycle (I.4.4) is given by the expression $[w, Cw] = 0$.

Identifications of both Q and M are straightforward. Indeed, a point $(k, l, n, m) \in \mathbb{P}^3$ equally well represents (as soon as $\sigma, \check{\sigma}$ and s are already fixed) both the Equation (I.4.3) and the line of matrix (I.4.5). Thus, for fixed $\sigma, \check{\sigma}$ and s , one can introduce

the correspondence between quadrics and matrices shown by the horizontal arrow on the following diagram:

(I.4.6)



which combines Q and M .

I.4.3. Covariance of FSCc

At first glance, the horizontal arrow in (I.4.6) seems to be of little practical interest since it depends on too many different parameters (σ , $\check{\sigma}$ and s). However, the following result demonstrates that it is compatible with simple calculations of cycles' images under the Möbius transformations.

THEOREM I.4.13. *The image $\tilde{C}_{\check{\sigma}}^s$ of a cycle $C_{\check{\sigma}}^s$ under transformation (I.3.24) in \mathbb{A} with $g \in \text{SL}_2(\mathbb{R})$ is given by similarity of the matrix (I.4.5):*

(I.4.7)

$$\tilde{C}_{\check{\sigma}}^s = g C_{\check{\sigma}}^s g^{-1}.$$

In other word, FSCc (I.4.5) intertwines Möbius action (I.3.24) on cycles with linear map (I.4.7). Explicitly, it means:

(I.4.8)

$$\begin{pmatrix} \tilde{l} + \check{i}s\tilde{n} & -\tilde{m} \\ \tilde{k} & -\tilde{l} + \check{i}s\tilde{n} \end{pmatrix} = \begin{pmatrix} a & b \\ c & d \end{pmatrix} \begin{pmatrix} l + \check{i}sn & -m \\ k & -l + \check{i}sn \end{pmatrix} \begin{pmatrix} d & -b \\ -c & a \end{pmatrix}.$$

PROOF. There are several ways to prove (I.4.7), but for now we present a brute-force calculation, which can fortunately be performed by a CAS [191]. See Appendix C for information on how to install (Section C.2) and start (Section C.3) the software, which will be sufficient for this proof. Further use of the software would be helped by learning which methods are available from the library (Section C.4) and which predefined objects exist upon initialisation (Section C.5). Assuming the above basics are known we proceed as follows.

First, we build a cycle passing a given point $P=[u, v]$. For this, a generic cycle C with parameters (k, l, n, m) is bounded by the corresponding condition:

```
In [2]: C2=C.subject_to(C.passing(P))
```

Then, we build the conjugated cycle with a generic $g = \begin{pmatrix} a & b \\ c & d \end{pmatrix} \in \text{SL}_2(\mathbb{R})$ and a hypercomplex unit e s and parameter $s = \pm 1$:

```
In [3]: C3=C2.sl2_similarity(a, b, c, d, es, matrix([[1,0],[0,s]]))
```

We also find the image of P under the Möbius transformation with the same element of $g \in \text{SL}_2(\mathbb{R})$ but a different hypercomplex unit e :

```
In [4]: P1=clifford_moebius_map(sl2_clifford(a, b, c, d, e), P, e)
```

Finally, we check that the conjugated cycle $C3$ passes the Möbius transform $P1$. A simplification based on the determinant value 1 and $s = \pm 1$ will be helpful:

```
In [5]: print C3.val(P1).subs([a==(1+b*c)/d,pow(s,2)==1]) \
        .normal().is_zero()
```

```
Out[5]: True
```

Thus, we have confirmation that the theorem is true in the stated generality. One may wish that every mathematical calculation can be done as simply. \square

REMARK I.4.14. There is a bit of cheating in the above proof. In fact, the library does not use the hypercomplex form (I.4.5) of FSCc matrices. Instead, it operates with non-commuting Clifford algebras, which makes it usable at any dimension—see Section B.5 and [186, 191].

The above proof cannot satisfy everyone’s aesthetic feeling. For this reason, an alternative route based on orthogonality of cycles [65] will be given later—see Exercise I.6.7.

It is worth noticing that the image $\tilde{C}_{\mathfrak{g}}^{\mathfrak{s}}$ under similarity (I.4.7) is independent of the values of s and \check{s} . This, in particular, follows from the following exercise.

EXERCISE I.4.15. Check that the image $(\tilde{k}, \tilde{l}, \tilde{n}, \tilde{m})$ of the cycle (k, l, n, m) under similarity with $g = \begin{pmatrix} a & b \\ c & d \end{pmatrix} \in \mathrm{SL}_2(\mathbb{R})$ is

$$(\tilde{k}, \tilde{l}, \tilde{n}, \tilde{m}) = (kd^2 + 2lcd + mc^2, kbd + l(bc + ad) + mac, n, kb^2 + 2lab + ma^2).$$

This can also be presented through matrix multiplication:

$$\begin{pmatrix} \tilde{k} \\ \tilde{l} \\ \tilde{n} \\ \tilde{m} \end{pmatrix} = \begin{pmatrix} d^2 & 2cd & 0 & c^2 \\ bd & bc + ad & 0 & ac \\ 0 & 0 & 1 & 0 \\ b^2 & 2ab & 0 & a^2 \end{pmatrix} \begin{pmatrix} k \\ l \\ n \\ m \end{pmatrix}.$$

Now we have an efficient tool for investigating the properties of some notable cycles, which have appeared before.

EXERCISE I.4.16. Use the similarity formula (I.4.7) for the following:

- i. Show that the real axis $v = 0$ is represented by the line passing through $(0, 0, 1, 0)$ and a matrix $\begin{pmatrix} s\check{s} & 0 \\ 0 & s\check{s} \end{pmatrix}$. For any $\begin{pmatrix} a & b \\ c & d \end{pmatrix} \in \mathrm{SL}_2(\mathbb{R})$, we have

$$\begin{pmatrix} a & b \\ c & d \end{pmatrix} \begin{pmatrix} s\check{s} & 0 \\ 0 & s\check{s} \end{pmatrix} \begin{pmatrix} d & -b \\ -c & a \end{pmatrix} = \begin{pmatrix} s\check{s} & 0 \\ 0 & s\check{s} \end{pmatrix},$$

- i.e. the real line is $\mathrm{SL}_2(\mathbb{R})$ -invariant.
- ii. Write matrices which describe cycles represented by A , N and K -orbits shown in Figs. I.1.1 and I.1.2. Verify that matrices representing these cycles are invariant under the similarity with elements of the respective subgroups A , N and K .
- iii. Show that cycles $(1, 0, n, \sigma)$, which are orbits of isotropy groups as described in Exercise I.3.21.ii, are invariant under the respective matrix similarity for the respective values of $\sigma = \iota^2$ and any real n .

- iv. Find the cycles which are transverse to orbits of the isotropy subgroups, i.e. are obtained from the vertical axis by the corresponding actions.

These easy examples also show that the software is working as expected.

I.4.4. Origins of FSCc

The Fillmore–Springer–Cnops construction, in its generalised form, will play a central rôle in our subsequent investigation. Thus, it is worth looking at its roots and its origins before we begin using it. So far, it has appeared from the thin air, but can we intentionally invent it? Are there further useful generalisations of FSCc? All these are important questions and we will make an attempt to approach them here.

As is implied by its name, FSCc was developed in stages. Moreover, it appeared independently in a different form in the recent work of Kirillov [163]. This indicates the naturalness and objectivity of the construction. We are interested, for now, in the flow of ideas rather than exact history or proper credits. For the latter, the reader may consult the original works [64; 65; 100; 163; 289, Ch. 18] as well as references therein. Here, we treat the simplest two-dimensional case. In higher dimensions, non-commutative Clifford algebras are helpful with some specific adjustments.

I.4.4.1. Projective Coordinantes and Polynomials. An important old observation is that Möbius maps appear from linear transformations of homogeneous (projective) coordinates, see [269, Ch. 1] for this in a context of invariant theory. This leads to the FSCc in several steps:

- i. Take a real projective space \mathbb{P}^1 as a quotient of \mathbb{R}^2 by the equivalence relation $(x, y) \sim (tx, ty)$ for $t \neq 0$. Then, any line with $y \neq 0$ can be represented by $(x/y, 1)$. Thus, the invertible linear transformation

$$(I.4.9) \quad \begin{pmatrix} a & b \\ c & d \end{pmatrix} \begin{pmatrix} x \\ y \end{pmatrix} = \begin{pmatrix} ax + by \\ cx + dy \end{pmatrix}, \quad g = \begin{pmatrix} a & b \\ c & d \end{pmatrix} \in \mathrm{SL}_2(\mathbb{R}), \quad \begin{pmatrix} x \\ y \end{pmatrix} \in \mathbb{R}^2$$

will become the Möbius transformation (I.3.4) on the representatives $\begin{pmatrix} u \\ 1 \end{pmatrix}$.

Similarly, we can consider Möbius actions on complex numbers $w = u + iv$.

- ii. The next observation [64] is that, if we replace the vector $\begin{pmatrix} w \\ 1 \end{pmatrix}$, $w \in \mathbb{C}$ by a 2×2 matrix $\begin{pmatrix} w & w \\ 1 & 1 \end{pmatrix}$, then the matrix multiplication with $g \in \mathrm{SL}_2(\mathbb{R})$ will transform it as two separate copies of the vector in (I.4.9). The “twisted square” of this matrix is

$$(I.4.10) \quad Z = \begin{pmatrix} w & -w\bar{w} \\ 1 & -\bar{w} \end{pmatrix} = \frac{1}{2} \begin{pmatrix} w & w \\ 1 & 1 \end{pmatrix} \begin{pmatrix} 1 & -\bar{w} \\ 1 & -\bar{w} \end{pmatrix}.$$

Then, the linear action (I.4.9) on vectors is equivalent to the similarity gZg^{-1} for the respective matrix Z from (I.4.10).

- iii. Finally, one can link matrices Z in (I.4.10) with zero-radius circles, see Exercise I.5.17.i, which are also in one-to-one correspondences with their centres. Then, the above similarity $Z \mapsto gZg^{-1}$ can be generalised to the action (I.4.7).

Another route was used in a later book of Cnops [65]: a predefined geometry of spheres, specifically their orthogonality, was encoded in the respective matrices of the type (I.4.5). Similar connections between geometry of cycles and matrices lead Kirillov, see [163, § 6.3] and the end of this section. He arrived at an identification of disks with Hermitian matrices (which is similar to FSCc) through the geometry of Minkowski space-time and the intertwining property of the actions of $SL_2(\mathbb{C})$.

There is one more derivation of FSCc based on projective coordinates. We can observe that the homogeneous form (I.4.4) of cycle's equation (I.4.2) can be written using matrices as follows:

$$(I.4.11) \quad K w_1 \bar{w}_1 - L w_1 \bar{w}_2 + \bar{L} \bar{w}_1 w_2 + M w_2 \bar{w}_2 = \begin{pmatrix} -\bar{w}_2 & \bar{w}_1 \end{pmatrix} \begin{pmatrix} L & -M \\ K & \bar{L} \end{pmatrix} \begin{pmatrix} w_1 \\ w_2 \end{pmatrix} = 0.$$

Then, the linear action (I.4.9) on vectors $\begin{pmatrix} w_1 \\ w_2 \end{pmatrix}$ corresponds to conjugated action on 2×2 matrices $\begin{pmatrix} L & -M \\ K & \bar{L} \end{pmatrix}$ by the intertwining identity:

$$(I.4.12) \quad \begin{pmatrix} -\bar{w}'_2 & \bar{w}'_1 \end{pmatrix} \begin{pmatrix} L & -M \\ K & \bar{L} \end{pmatrix} \begin{pmatrix} w'_1 \\ w'_2 \end{pmatrix} = \begin{pmatrix} -\bar{w}_2 & \bar{w}_1 \end{pmatrix} \begin{pmatrix} L' & -M' \\ K' & \bar{L}' \end{pmatrix} \begin{pmatrix} w_1 \\ w_2 \end{pmatrix},$$

where the respective actions of $SL_2(\mathbb{R})$ on vectors and matrices are

$$\begin{pmatrix} w'_1 \\ w'_2 \end{pmatrix} = \begin{pmatrix} a & b \\ c & d \end{pmatrix} \begin{pmatrix} w_1 \\ w_2 \end{pmatrix}, \quad \text{and} \quad \begin{pmatrix} L' & -M' \\ K' & \bar{L}' \end{pmatrix} = \begin{pmatrix} a & b \\ c & d \end{pmatrix}^{-1} \begin{pmatrix} L & -M \\ K & \bar{L} \end{pmatrix} \begin{pmatrix} a & b \\ c & d \end{pmatrix}.$$

In other words, we obtained the usual FSCc with the intertwining property of the type (I.4.7). However, the generalised form FSCc does not result from this consideration yet.

Alternatively, we can represent the Equation (I.4.4) as:

$$K w_1 \bar{w}_1 - L w_1 \bar{w}_2 + \bar{L} \bar{w}_1 w_2 + M w_2 \bar{w}_2 = \begin{pmatrix} \bar{w}_1 & \bar{w}_2 \end{pmatrix} \begin{pmatrix} K & \bar{L} \\ -L & M \end{pmatrix} \begin{pmatrix} w_1 \\ w_2 \end{pmatrix} = 0.$$

Then, the intertwining relation similar to (I.15.5) holds if matrix similarity is replaced by the *matrix congruence*:

$$\begin{pmatrix} K' & \bar{L}' \\ -L' & M' \end{pmatrix} = \begin{pmatrix} a & b \\ c & d \end{pmatrix}^T \begin{pmatrix} K & \bar{L} \\ -L & M \end{pmatrix} \begin{pmatrix} a & b \\ c & d \end{pmatrix}.$$

This identity provides a background to the *Kirillov correspondence* between circles and matrices, see [163, § 6.3] and [306, § 9.2]. Clearly, it is essentially equivalent to FSCc and either of them may be depending on a convenience. It does not hint at the generalised form of FSCc either.

We will mainly work with the FSCc, occasionally stating equivalent forms of our results for the Kirillov correspondence.

1.4.4.2. Co-Adjoint Representation. In the above construction, the identity (I.15.4) requires the same imaginary unit to be used in the quadratic form (the left-hand side) and the FSCc matrix (the right-hand side). How can we arrive at the generalised FSCc directly without an intermediate step of the standard FSCc with the same type of EPH

geometry used in the point cycle spaces? We will consider a route originating from the representation theory.

Any group G acts on itself by the *conjugation* $g : x \mapsto gxg^{-1}$, see I.2.18.i. This map obviously fixes the group identity e . For a Lie group G , the tangent space at e can be identified with its Lie algebra \mathfrak{g} , see Subsection I.2.3.1. Then, the derived map for the conjugation at e will be a linear map $\mathfrak{g} \rightarrow \mathfrak{g}$. This is an *adjoint representation* of a Lie group G on its Lie algebra. This is the departure point for Kirillov's orbit method, which is closely connected to induced representations, see [159, 161].

EXAMPLE I.4.17. In the case of $G = \mathrm{SL}_2(\mathbb{R})$, the group operation is the multiplication of 2×2 matrices. The Lie algebra \mathfrak{g} can be identified with the set of traceless matrices, which we can write in the form $\begin{pmatrix} l & -m \\ k & -l \end{pmatrix}$ for $k, l, m \in \mathbb{R}$. Then, the coadjoint action of $\mathrm{SL}_2(\mathbb{R})$ on \mathfrak{sl}_2 is:

$$(I.4.13) \quad \begin{pmatrix} a & b \\ c & d \end{pmatrix} : \begin{pmatrix} l & -m \\ k & -l \end{pmatrix} \mapsto \begin{pmatrix} a & b \\ c & d \end{pmatrix}^{-1} \begin{pmatrix} l & -m \\ k & -l \end{pmatrix} \begin{pmatrix} a & b \\ c & d \end{pmatrix}.$$

We can also note that the above transformation fixes matrices $\begin{pmatrix} n & 0 \\ 0 & n \end{pmatrix}$ which are scalar multiples of the identity matrix. Thus, we can consider the conjugated action (I.4.13) of $\mathrm{SL}_2(\mathbb{R})$ on the pairs of matrices, or intervals in the matrix space of the type

$$\left\{ \begin{pmatrix} l & -m \\ k & -l \end{pmatrix}, \begin{pmatrix} n & 0 \\ 0 & n \end{pmatrix} \right\}, \text{ or, using hypercomplex numbers, } \begin{pmatrix} l + \imath n & -m \\ k & -l + \imath n \end{pmatrix}.$$

In other words, we obtained the generalised FSCc, cf. (I.4.5), and the respective action of $\mathrm{SL}_2(\mathbb{R})$. Furthermore, a connection of the above pairs of matrices with the cycles on a plane can be realised through the Poincaré extension, see Ch. I.14.

REMARK I.4.18. Note that scalar multiples of the identity matrix, which are invariant under similarity, correspond in FSCc to the real line, which is also Möbius invariant.

I.4.5. Projective Cross Ratio

An important invariant of Möbius transformations in complex numbers is the *cross ratio* of four distinct points, see [26, § 13.4]:

$$(I.4.14) \quad [z_1, z_2, z_3, z_4] = \frac{(z_1 - z_3)(z_2 - z_4)}{(z_1 - z_2)(z_3 - z_4)}.$$

Zero divisors make it difficult to handle a similar fraction in dual and double numbers. Projective coordinates are again helpful in this situation—see [52]. Define the *symplectic form*, cf. [11, § 41], of two vectors by

$$(I.4.15) \quad \omega(z, z') = xy' - x'y, \quad \text{where } z = (x, y), z' = (x', y') \in \mathbb{A}^2.$$

The one-dimensional projective space $\mathbb{P}^1(\mathbb{A})$ is the quotient of \mathbb{A}^2 with respect to the equivalence relation: $z \sim z'$ if their symplectic form vanishes. We also say [52] that two

points in $\mathbb{P}^1(\mathbb{A})$ are *essentially distinct* if there exist their representatives $z, z' \in \mathbb{A}^2$ such that $\omega(z, z')$ is not a zero divisor.

DEFINITION I.4.19. [52] The *projective cross ratio* of four essentially distinct points $z_i \in \mathbb{P}^1(\mathbb{A})$ represented by $(x_i, y_i) \in \mathbb{A}^2$, $i = 1, \dots, 4$, respectively, is defined by:

$$(I.4.16) \quad [z_1, z_2, z_3, z_4] = \left(\frac{(x_1 y_3 - x_3 y_1)(x_2 y_4 - x_4 y_2)}{(x_1 y_2 - x_2 y_1)(x_3 y_4 - x_4 y_3)} \right) \in \mathbb{P}^1(\mathbb{A}).$$

EXERCISE I.4.20. Check that:

- i. Let the map $S : \mathbb{A} \rightarrow \mathbb{P}^1(\mathbb{A})$ be defined by $z \mapsto (z, 1)$. Then, it intertwines the Möbius transformations on \mathbb{A} with linear maps (I.4.9).
- ii. The map S intertwines cross ratios in the following sense:

$$(I.4.17) \quad S([z_1, z_2, z_3, z_4]) = [S(z_1), S(z_2), S(z_3), S(z_4)],$$

where $z_i \in \mathbb{C}$, and the left-hand side contains the classic cross ratio (I.4.14) while the right-hand side the projective (I.4.16).

- iii. The symplectic form (IV.2.3) on \mathbb{A}^2 is invariant if vectors are multiplied by a 2×2 real matrix with the unit determinant.
- iv. The projective cross ratio (I.4.16) is invariant if points in \mathbb{A}^2 are multiplied by a matrix from $SL_2(\mathbb{R})$. Then, the classic cross ratio (I.4.14) is invariant under the Möbius transformations, cf. (I.4.17).

EXERCISE I.4.21. [52] Check further properties of the projective cross ratio.

- i. Find transformations of $[z_1, z_2, z_3, z_4]$ under all permutations of points.
- ii. Demonstrate the *cancellation formula* for cross ratio:

$$(I.4.18) \quad [z_1, z_2, z_3, z_4][z_1, z_3, z_5, z_4] = [z_1, z_2, z_5, z_4],$$

where, in the left-hand side, values in \mathbb{A}^2 are multiplied component-wise. Such a multiplication is commutative but not associative on $\mathbb{P}^1(\mathbb{A})$.

We say that a collection of points of $\mathbb{P}^1(\mathbb{A})$ is *concylic* if all their representatives in \mathbb{A}^2 satisfy to Equation (I.15.4) for some FSCc matrix $\begin{pmatrix} L & -M \\ K & \bar{L} \end{pmatrix}$.

EXERCISE I.4.22. [52] Show that:

- i. Any collection of points in \mathbb{A} belonging to some cycle is mapped by S from Exercise I.4.20.i to concyclic points in $\mathbb{P}^1(\mathbb{A})$.
- ii. For any three essentially distinct points z_1, z_2 and $z_3 \in \mathbb{P}^1(\mathbb{A})$ there is a fixed 2×2 matrix A such that $[z_1, z_2, z, z_3] = Az$ for any $z \in \mathbb{P}^1(\mathbb{A})$. Moreover, the matrix A has a determinant which is not a zero divisor.
- iii. Any four essentially distinct points in $\mathbb{P}^1(\mathbb{A})$ are concyclic if and only if their projective cross ratio is $S(r)$ for some real number r . HINT: Let $[z_1, z_2, z, z_3]$ correspond through S to a real number. We know that $[z_1, z_2, z, z_3] = Az$ for an invertible A , then $\bar{A}\bar{z} = Az$ or $\bar{z} = \bar{A}^{-1}Az$. Multiply both sides of the last identity by row vector $(-\bar{y}, \bar{x})$, where $z = \begin{pmatrix} x \\ y \end{pmatrix}$. The final step is to verify that $\bar{A}^{-1}A$ has the FSCc structure, cf. [52, § 4]. \diamond

We have seen another way to obtain FSCc—from the projective cross ratio.

Indefinite Product Space of Cycles

In the previous chapter, we represented cycles by points of the projective space \mathbb{P}^3 or by lines of 2×2 matrices. The latter is justified so far only by the similarity formula (I.4.7). Now, we will investigate connections between cycles and vector space structure. Thereafter we will use the special form of FSCc matrices to introduce very important additional structure in the cycle space. The structure is an indefinite inner product, which is particularly helpful to describe tangency of cycles, see [101; 163, Ch. 4] and Sec. I.5.5.

I.5.1. Cycles: an Appearance and the Essence

Our extension (I.4.5) of FSCc adds two new elements in comparison with the standard one [65]:

- The hypercomplex unit $\check{\iota}$, which is independent from ι .
- The additional sign-type parameter s .

Such a possibility of an extension exists because elements of $SL_2(\mathbb{R})$ are matrices with real entries. For generic Möbius transformations with hypercomplex-valued matrices considered in [65], it is impossible.

Indeed, the similarity formula (I.4.8) does not contain any squares of hypercomplex units, so their type is irrelevant for this purpose. At the moment, the hypercomplex unit $\check{\iota}$ serves only as a placeholder which keeps components l and n separated. However, the rôle of $\check{\iota}$ will be greatly extended thereafter. On the other hand, the hypercomplex unit ι defines the appearance of cycles on the plane, that is, any element (k, l, n, m) in the cycle space \mathbb{P}^3 admits its drawing as circles, parabolas or hyperbolas in the point space \mathbb{A} . We may think on points of \mathbb{P}^3 as ideal cycles while their depictions on \mathbb{A} are only their shadows on the wall of **Plato's cave**. More prosaically, we can consider cones and their (conic) sections as in Fig. I.1.3.

Of course, some elliptic shadows may be imaginary, see Exercise I.4.5, but, in most cases, we are able to correctly guess a cycle from its σ -drawing.

EXERCISE I.5.1. Describe all pairs of different cycles $C_{\check{\sigma}}^s$ and $\tilde{C}_{\check{\sigma}}^s$ such that their σ -drawing for some σ are exactly the same sets. **HINT:** Note that the vertical axis is the p -drawing of two different cycles $(1, 0, 0, 0)$ and $(0, 1, 0, 0)$ and make a proper generalisation of this observation.◊

Figure I.1.5(a) shows the same cycles drawn in different EPH styles. Points $c_{\sigma} = (\frac{1}{k}, -\sigma \frac{n}{k})$ are their respective e/p/h-centres from Definition I.4.3. They are related to

each other through several identities:

$$(I.5.1) \quad c_e = \bar{c}_h, \quad c_p = \frac{1}{2}(c_e + c_h).$$

From analytic geometry, we know that a parabola with the equation $ku^2 - 2lu - 2nv + m = 0$ has a *focal length*, the distance from its focus to the vertex, equal to $\frac{n}{2k}$. As we can see, it is half of the second coordinate in the e-centre. Figure I.1.5(b) presents two cycles drawn as parabolas. They have the same focal length $\frac{n}{2k}$ and, thus, their e-centres are on the same level. In other words, *concentric* parabolas are obtained by a vertical shift, not by scaling, as an analogy with circles or hyperbolas may suggest.

We already extended the definition of centres from circles and hyperbolas to parabolas. It is time for a courtesy payback: parabolas share with other types of cycles their focal attributes.

DEFINITION I.5.2. A $\hat{\sigma}$ -focus, where $\hat{\sigma}$ is a variable of EPH type, of a cycle $C = (k, l, n, m)$ is the point in \mathbb{A}

$$(I.5.2) \quad f_{\hat{\sigma}} = \left(\frac{l}{k}, \frac{\det C_{\hat{\sigma}}^s}{2nk} \right) \quad \text{or, explicitly,} \quad f_{\hat{\sigma}} = \left(\frac{l}{k}, \frac{mk - l^2 + \hat{\sigma}n^2}{2nk} \right).$$

We also use names *e-focus*, *p-focus*, *h-focus* and $\hat{\sigma}$ -focus, in line with previous conventions.

The *focal length* of the cycle C is $\frac{n}{2k}$.

Note that values of all centres, foci and the focal length are independent of a choice of a quadruple of real numbers (k, l, n, m) which represents a point in the projective space \mathbb{P}^3 .

Figure I.1.5(b) presents e/p/h-foci of two parabolas with the same focal length. If a cycle is depicted as a parabola, then the h-focus, p-focus and e-focus are, correspondingly, the geometrical *focus* of the parabola, the *vertex* of the parabola, and the point on the *directrix* of the parabola nearest to the vertex.

As we will see, cf. Propositions I.6.19 and I.6.40, all three centres and three foci are useful attributes of a cycle, even if it is drawn as a circle.

REMARK I.5.3. Such a variety of choices is a consequence of the usage of $SL_2(\mathbb{R})$ —a smaller group of symmetries in comparison to the all Möbius maps of \mathbb{A} . The $SL_2(\mathbb{R})$ group fixes the real line and, consequently, a decomposition of vectors into “real” (1) and “imaginary” (ι) parts is obvious. This permits us to assign an arbitrary value to the square of the hypercomplex unit ι .

The exceptional rôle of the real line can be viewed in many places. For example, geometric invariants defined below, e.g. orthogonalities in Sections I.6.1 and I.6.6, demonstrate “awareness” of the real-line invariance in one way or another. We will call this the *boundary effect* in the upper half-plane geometry. The famous question **about hearing a drum’s shape** has a counterpart:

Can we see/feel the boundary from inside a domain?

Remarks I.5.19, I.6.4, I.6.20 and I.6.35 provide hints for positive answers.

EXERCISE I.5.4. Check that different realisations of the same cycle have these properties in common:

- All implementations have the same vertical axis of symmetry.
- Intersections with the real axis (if they exist) coincide, see points r_0 and r_1 for the left triple of cycles in Fig. I.1.5(a). Moreover, all three EPH drawings of a cycle have common tangents at these intersection points.
- Centres of circle c_e and corresponding hyperbolas c_h are mirror reflections of each other in the real axis with the parabolic centre as the middle point.
- The $\check{\sigma}$ -focus of the elliptic K-orbits, see Exercise I.3.14.(e), is the reflection in the real axis of the midpoint between the $\check{\sigma}$ -centre of this orbit and the inverse of its h-centre.

Exercise I.3.14 gives another example of similarities between different implementations of the same cycles defined by the Equation (I.3.26).

I.5.2. Cycles as Vectors

Elements of the projective space \mathbb{P}^3 are lines in the linear space \mathbb{R}^4 . Would it be possible to pick a single point on each line as its “label”? We may wish to do this for the following reasons:

- To avoid ambiguity in representation of the same cycle by different quadruples (k, l, n, m) and (k', l', n', m') .
- To have explicit connections with relevant objects (see below).

However, the general scheme of projective spaces does not permit such a unique representation serving the whole space. Otherwise the cumbersome construction with lines in vector spaces would not be needed. Nevertheless, there are several partial possibilities which have certain advantages and disadvantages. We will consider two such opportunities, calling them *normalisation of a cycle*.

The first is very obvious: we try to make the coefficient k in front of the squared terms in cycle equation (I.15.3) equal to 1. The second normalises the value of the determinant of the cycle’s matrix. More formally:

DEFINITION I.5.5. A FSCc matrix representing a cycle is said to be *k-normalised* if its $(2, 1)$ -element is 1 and it is *det $\check{\sigma}$ -normalised* if its $\check{\sigma}$ -determinant is equal to ± 1 .

We will discuss cycles which do not admit either normalisation at the end of Sec. I.8.1.

EXERCISE I.5.6. Check that:

- Element $(1, 1)$ of the k -normalised $C_{\check{\sigma}}^1$ matrix is the $\check{\sigma}$ -centre of the cycle.
- Any cycle (k, l, n, m) with $k \neq 0$ has an equivalent k -normalised cycle. Cycles which do not admit k -normalisation correspond to single straight lines in any point space.
- det-normalisation is preserved by matrix similarity with $SL_2(\mathbb{R})$ elements, as in Theorem I.4.13, while k -normalisation is not.
- Any cycle with a non-zero $\check{\sigma}$ -determinant admits det $\check{\sigma}$ -normalisation. Cycles which cannot be det $\check{\sigma}$ -normalised will be studied in Section I.5.4. What are cycles which cannot be det $\check{\sigma}$ -normalised for any value of $\check{\sigma}$?

Thus, each normalisation may be preferred in particular circumstances. The det-normalisation was used, for example, in [163] to obtain a satisfactory condition for tangent cycles, cf. Exercise I.5.26.ii. On the other hand, we will see in Section I.7.1 that $\det C_{\mathbb{C}}^{\circ}$ of a k -normalised cycle is equal to the square of the *cycle radius*.

REMARK I.5.7. It is straightforward to check that there is one more cycle normalisation which is invariant under similarity (I.4.7). It is given by the condition $n = 1$. However, we will not use it at all in this work.

A cycle's normalisation is connected with scaling of vectors. Now we turn to the second linear operation: addition. Any two different lines define a unique two-dimensional plane passing through them. Vectors from the plane are linear combinations of two vectors spanning each line. If we consider circles corresponding to elements of the linear span, we will obtain a pencil of circles, see [37, § 10.10; 71, § 2.3]. As usual, there is no need to be restricted to circles only:

DEFINITION I.5.8. A *pencil of cycles* is the linear span (in the sense of \mathbb{R}^4) of two cycles.

Figure I.5.1 shows the appearance of such pencils as circles, parabolas and hyperbolas. The elliptic case is very well known in classical literature, see [71, Figs. 2.2(A,B,C); 2.3A], for example. The appearance of pencils is visually different for two cases: spanning cycles are either intersecting or disjoint. These two possibilities are represented by the left and right columns in Fig. I.5.1. We shall return to these situations in Corollary I.5.27.

EXERCISE I.5.9. Investigate the following:

- i. What happens with an elliptic pencil if one of spanning circles is imaginary? Or if both spanning circles are imaginary?
- ii. How does a pencil look if one spanning cycle is a straight line? If both cycles are straight lines?
- iii. A pair of circles is symmetric about the line joining their centres. Thus, circular pencils look similar regardless of the direction of this line of centres. Our hyperbolas and parabolas have a special orientation: their axes of symmetry are vertical. Thus, a horizontal or vertical line joining the centres of two hyperbolas/parabolas make a special arrangement, and it was used for Fig. I.5.1. How do hyperbolic pencils look if the line of centres is not horizontal?

EXERCISE I.5.10. Show the following:

- i. The image of a pencil of cycles under a Möbius transformation is again a pencil of cycles.
- ii. A pencil spanned by two concentric cycles consists of concentric cycles.
- iii. All cycles in a pencil are coaxial, see Exercise I.3.19.iii for the definition. The joint radical axis, see Exercise I.3.19.ii, is the only straight line in the pencil. This is also visible from Fig. I.5.1.
- iv. Let two pencils of cycles have no cycle in common. Then, any cycle from \mathbb{P}^3 belongs to a new pencil spanned by two cycles from two given pencils.

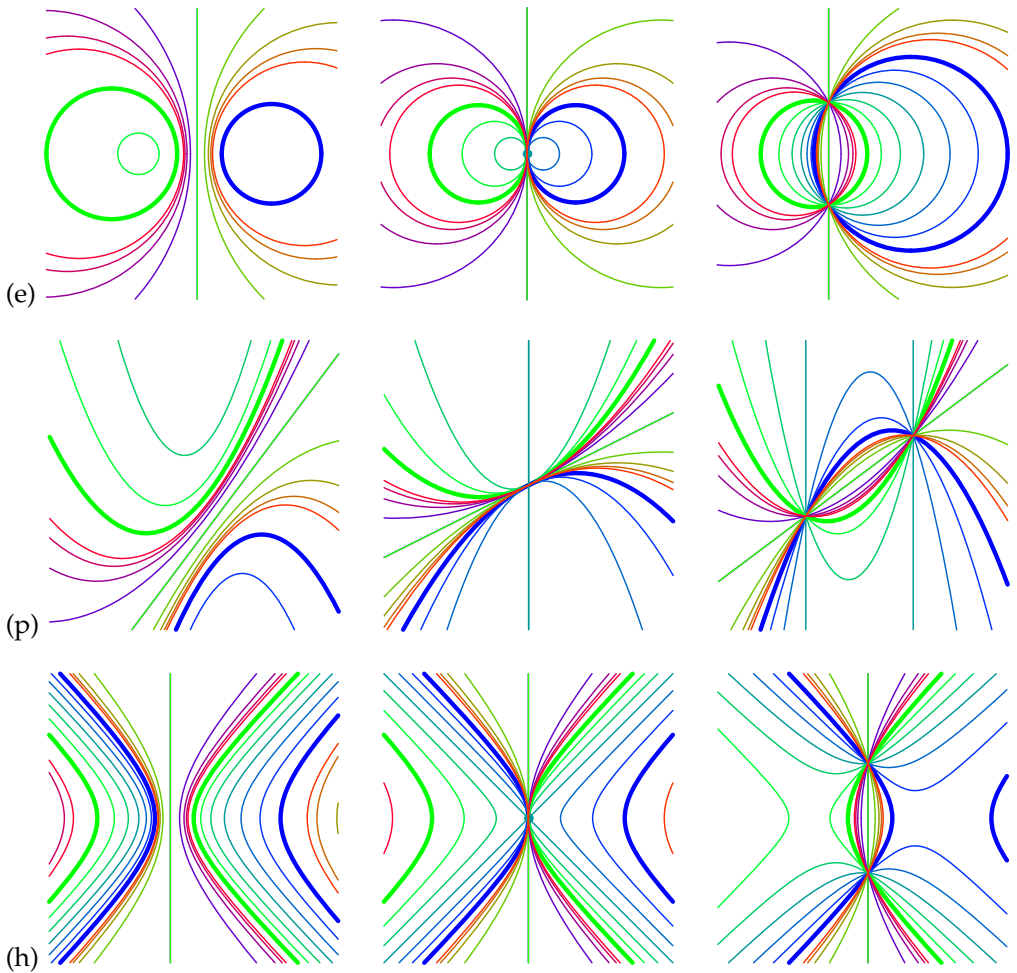


FIGURE I.5.1. Linear spans of cycle pairs in EPH cases. The initial pairs of cycles are drawn in bold (green and blue). The cycles which are between the generators are drawn in the transitional green-blue colours. The red components are used for the outer cycles. The left column shows the appearance of pencils if the generators are disjoint, the right if the generators intersect in two points, the middle—if they are touching at a point.

This section demonstrated that there are numerous connections between the linear structure of the cycle space \mathbb{P}^3 and the geometrical property of cycles in the point space \mathbb{A} .

I.5.3. Invariant Cycle Product

We are looking for a possibility to enrich the geometry of the cycle space through the FSCc matrices. Many important relations between cycles are based on the following Möbius invariant cycle product.

DEFINITION I.5.11. The *cycle $\check{\sigma}$ -product* of two cycles is given by

$$(I.5.3) \quad \langle C_{\check{\sigma}}^s, \tilde{C}_{\check{\sigma}}^s \rangle = -\operatorname{tr}(C_{\check{\sigma}}^s \overline{\tilde{C}_{\check{\sigma}}^s}),$$

that is, the negative trace of the matrix product of $C_{\check{\sigma}}^s$ and hypercomplex conjugation of $\tilde{C}_{\check{\sigma}}^s$.

In the essence the above product is **Frobenius inner product** of two matrices [137, Ch. 5]. And as we already mentioned, an inner product of type (I.5.3) is used, for example, in the **Gelfand–Naimark–Segal construction** to make a Hilbert space out of C^* -algebra. This may be more than a simple coincidence since FSCc matrices can be considered as linear operators on a two-dimensional vector space. However, a significant difference with the Hilbert space inner product is that the cycle product is indefinite, see Exercise I.5.12.iv for details. Thus, cycles form a Pontrjagin or Krein space [113] rather than Euclidean or Hilbert. A geometrical interpretation of the cycle product will be given in Exercise I.7.6.iii.

EXERCISE I.5.12. Check that:

- i. The value of cycle product (I.5.3) will remain the same if both matrices are replaced by their images under similarity (I.4.7) with the same element $g \in \operatorname{SL}_2(\mathbb{R})$.
- ii. The $\check{\sigma}$ -cycle product (I.5.3) of cycles defined by quadruples (k, l, n, m) and $(\tilde{k}, \tilde{l}, \tilde{n}, \tilde{m})$ is given by

$$(I.5.4a) \quad -2\tilde{l}l + 2\check{\sigma}s^2\tilde{n}n + \tilde{k}m + \tilde{m}k.$$

More specifically, and also taking into account the value $s = \pm 1$, it is

$$(I.5.4e) \quad -2\tilde{n}n - 2\tilde{l}l + \tilde{k}m + \tilde{m}k,$$

$$(I.5.4p) \quad -2\tilde{l}l + \tilde{k}m + \tilde{m}k,$$

$$(I.5.4h) \quad 2\tilde{n}n - 2\tilde{l}l + \tilde{k}m + \tilde{m}k$$

in the elliptic, parabolic and hyperbolic cases, respectively.

- iii. Let $C_{\check{\sigma}}$ and $\tilde{C}_{\check{\sigma}}$ be two cycles defined by e-centres (u, v) and (\tilde{u}, \tilde{v}) with σ -determinants $-r^2$ and $-\tilde{r}^2$, respectively. Then, their $\check{\sigma}$ -cycle product explicitly is

$$(I.5.5) \quad \langle C_{\check{\sigma}}, \tilde{C}_{\check{\sigma}} \rangle = (u - \tilde{u})^2 - \sigma(v - \tilde{v})^2 - 2(\sigma - \check{\sigma})v\tilde{v} - r^2 - \tilde{r}^2.$$

- iv. The cycle product is a symmetric bilinear function of two cycles. It is *indefinite* in the sense that there are two cycles $C_{\check{\sigma}}$ and $\tilde{C}_{\check{\sigma}}$ such that

$$\langle C_{\check{\sigma}}, C_{\check{\sigma}} \rangle > 0 \quad \text{and} \quad \langle \tilde{C}_{\check{\sigma}}, \tilde{C}_{\check{\sigma}} \rangle < 0.$$

HINT: It is easy to show symmetry of the cycle product from the explicit value (I.14.17). This is not so obvious from the initial definition (I.5.3) due to the presence of hyper-complex conjugation.◊

- v. Check, that the change of variables $(k, l, n, m) \mapsto (t, l, n, s)$, where $k = t + s$ and $m = t - s$, transforms the elliptic inner product (I.5.4e) to the metric of the Minkowski space [163, § 4.1]:

$$-2\tilde{n}n - 2\tilde{l}l + \tilde{k}m + \tilde{m}k \mapsto -2\tilde{n}n - 2\tilde{l}l - 2\tilde{s}s + 2\tilde{t}t.$$

A simple, but interesting, observation is that, for FSCc matrices representing cycles, we obtain the second classical invariant (determinant) under similarities (I.4.7) from the first (trace) as follows:

$$(I.5.6) \quad \langle C_{\check{\sigma}}^s, C_{\check{\sigma}}^s \rangle = -\text{tr}(C_{\check{\sigma}}^s \overline{C_{\check{\sigma}}^s}) = 2 \det C_{\check{\sigma}}^s = 2(-l^2 + \check{\sigma}s^2n^2 + mk).$$

Therefore it is not surprising that the determinant of a cycle enters Definition I.5.2 of the foci and the following definition:

DEFINITION I.5.13. We say that a $C_{\check{\sigma}}$ is $\check{\sigma}$ -zero-radius, $\check{\sigma}$ -positive or $\check{\sigma}$ -negative cycle if the value of the cycle product of $C_{\check{\sigma}}$ with itself (I.5.6) (and thus its determinant) is zero, positive or negative, respectively.

These classes of cycles fit naturally to the Erlangen programme.

EXERCISE I.5.14. Show that the zero-radius, positive and negative cycles form three non-empty disjoint Möbius-invariant families. HINT: For non-emptiness, see Exercise I.5.12.iv or use the explicit formula (I.5.6).◊

The following relations are useful for a description of these three classes of cycles.

EXERCISE I.5.15. Check that:

- i. For any cycle $C_{\check{\sigma}}^s$ there is the following relation between its determinants evaluated with elliptic, parabolic and hyperbolic unit \check{i} :

$$\det C_e^s \leq \det C_p^s \leq \det C_h^s.$$

- ii. The negative of the parabolic determinant, $-\det C_p^s$, of a cycle (k, l, n, m) coincides with the discriminant of the quadratic equation

$$(I.5.7) \quad ku^2 - 2lu + m = 0,$$

which defines intersection of the cycle with the real line (in any EPH presentation).

We already illustrated zero-radius cycles in Fig. I.1.6. This will be compared with positive and negative cycles for various values of $\check{\sigma}$ in Fig. I.5.2. The positive or negative aspect of cycles has a clear geometric manifestation for some combinations of σ and $\check{\sigma}$.

EXERCISE I.5.16. Verify the following statements:

- (e) Circles corresponding to e-positive cycles are imaginary. All regular circles are e-negative.

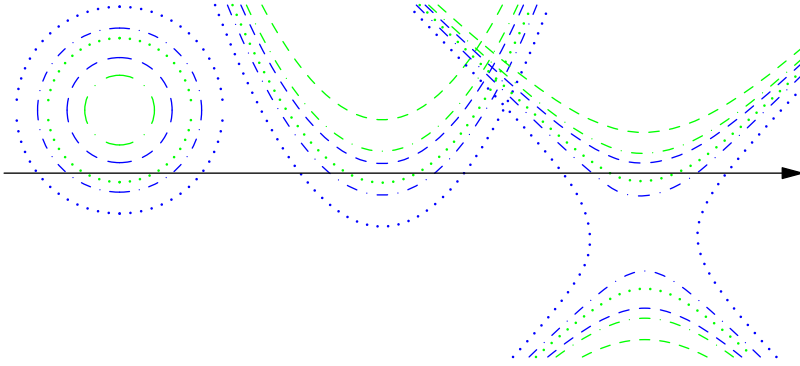


FIGURE I.5.2. Positive and negative cycles. Evaluation of determinants with elliptic value $\check{\sigma} = -1$ shown by dotted drawing, with the hyperbolic $\check{\sigma} = 1$ by dashed and with intermediate parabolic $\check{\sigma} = 0$ by dash-dotted. Blue cycles are positive for respective $\check{\sigma}$ and green cycles are negative. Cycles positive for one value of $\check{\sigma}$ can be negative for another. Compare this figure with zero-radius cycles in Fig. I.1.6.

- (p) Parabolas drawn from p- and e-negative cycles have two points of intersection with the real axis, and those drawn from p- and h-positive cycles do not intersect the real axis.
- (h) Hyperbolas representing h-negative cycles have “vertical” branches and those representing h-positive cycles have “horizontal” ones. HINT: Write the condition for a hyperbola defined by the Equation (I.15.3) to intersect the vertical line passing its centres.◊

Of course, manifestations of the indefinite nature of the cycle product (I.5.3) are not limited to the above examples and we will meet more of them on several other occasions.

I.5.4. Zero-radius Cycles

Due to the projective nature of the cycle space \mathbb{P}^3 , the absolute values of the cycle product (I.5.3) on non-normalised matrices are irrelevant, unless it is zero. There are many reasons to take a closer look at cycles with a zero-value product—zero-radius cycles, for example:

- They form a Möbius-invariant family.
- They are on the boundary between positive and negative cycles.
- They do not admit det-normalisation.

To highlight that a certain cycle is $\check{\sigma}$ -zero-radius we will denote it by $Z_{\check{\sigma}}^{\circ}$. A justification of the chosen name for such cycles is given in Exercise I.5.16.(e)—further connections will be provided in Section I.7.1.

As often happens in our study, we again have nine different possibilities—for cycles drawn in three EPH types in the point space (parametrised by σ) there are three

independent conditions $\det C_{\check{\sigma}}^s = 0$ in the cycle space (parametrised by $\check{\sigma}$). This is illustrated in Fig. I.1.6.

EXERCISE I.5.17. Show that:

- i. Any $\check{\sigma}$ -zero-radius cycle admitting k -normalisation can be represented by the matrix

$$(I.5.8) \quad Z_{\check{\sigma}}^s = \begin{pmatrix} z & -z\bar{z} \\ 1 & -\bar{z} \end{pmatrix} = \frac{1}{2} \begin{pmatrix} z & z \\ 1 & 1 \end{pmatrix} \begin{pmatrix} 1 & -\bar{z} \\ 1 & -\bar{z} \end{pmatrix} = \begin{pmatrix} u_0 + \check{\sigma}v_0 & u_0^2 - \check{\sigma}v_0^2 \\ 1 & -u_0 + \check{\sigma}v_0 \end{pmatrix},$$

for some $z = u_0 + \check{\sigma}iv_0$ being its centre and $s = \pm 1$. Compare with (I.4.10).

- ii. Describe all $\check{\sigma}$ -zero-radius cycles which cannot be k -normalised.
 iii. The $\check{\sigma}$ -focus of the $\check{\sigma}$ -zero-radius cycle belongs to the real axis—see Fig. I.1.6.
 iv. Let $Z_{\check{\sigma}}^s$ and $\tilde{Z}_{\check{\sigma}}^s$ be two k -normalised $\check{\sigma}$ -zero-radius cycles of the form (I.5.8) with e -centres (u_0, v_0) and (u_1, v_1) . Then

$$(I.5.9) \quad \langle Z_{\check{\sigma}}^s, \tilde{Z}_{\check{\sigma}}^s \rangle = (u_0 - u_1)^2 - \check{\sigma}(v_0 - v_1)^2.$$

As follows from (I.5.8), the class of $\check{\sigma}$ -zero-radius cycles is parametrised by two real numbers (u, v) only and, as such, is easily attached to the respective point of $z = u + iv \in \mathbb{A}$, at least in the elliptic and hyperbolic point spaces. In \mathbb{D} , a connection between a $\check{\sigma}$ -zero-radius cycle and its centre is obscure.

EXERCISE I.5.18. Prove the following observations from Fig. I.1.6:

- i. The cycle $Z_{\check{\sigma}}^s$ (I.5.8) with $\det Z_{\check{\sigma}}^s = 0$, $\check{\sigma} = -1$ drawn elliptically is just a single point (u_0, v_0) , i.e. an (elliptic) zero-radius circle.
 ii. The same condition $\det Z_{\check{\sigma}}^s = 0$ with $\check{\sigma} = 1$ in the hyperbolic drawing produces a *light cone* originating at point (u_0, v_0)

$$(u - u_0)^2 - (v - v_0)^2 = 0,$$

i.e. a zero-radius cycle in hyperbolic metric, see Section I.7.1.

- iii. p -zero-radius cycles in any implementation touch the real axis, see Fig. I.1.6. This property defines a *horocycle* in Lobachevsky geometry [70, § 16.6]. HINT: Note, that the parabolic determinant of a cycle (k, l, n, m) coincides with the discriminant of the quadratic equation $ku^2 - 2lu + m = 0$. See also Exercise I.5.26.iv.◇
 iv. An h -zero-radius cycle in \mathbb{A} with the e -center (a, b) intersects the real axis at points $(a \pm b, 0)$ with slopes ± 1 , see Fig. I.1.6. Furthermore, the h -centre of this cycle coincides with its e -focus. HINT: For slopes, use implicit derivation. Also, for a parabola, it follows from the Exercise I.5.17.iii and the classical reflection property of parabolas, cf. App. B.2.◇
 v. The e -centre of the transformation $gZ_{\check{\sigma}}^s g^{-1}$, $g \in \text{SL}_2(\mathbb{R})$ of the $\check{\sigma}$ -zero-radius cycle (I.5.8) coincides with the Möbius action $g \cdot z$ in $\mathbb{R}^{\check{\sigma}}$, where z is the e -centre of $Z_{\check{\sigma}}^s$. HINT: The result can be obtained along the lines from Subsection I.4.4.1.◇

REMARK I.5.19. The above “touching” property (I.5.18.iii) and intersection behaviour (I.5.18.iv) are manifestations of the already-mentioned boundary effect in the upper half-plane geometry, see Remark I.5.3.

The previous exercise shows that $\check{\sigma}$ -zero-radius cycles “encode” points into the “cycle language”. The following reformulation of Exercise I.5.18.v stresses that this encoding is Möbius-invariant as well.

LEMMA I.5.20. *The conjugate $g^{-1}Z_{\check{\sigma}}^{\check{\sigma}}(y)g$ of a $\check{\sigma}$ -zero-radius cycle $Z_{\check{\sigma}}^{\check{\sigma}}(y)$ with $g \in \text{SL}_2(\mathbb{R})$ is a $\check{\sigma}$ -zero-radius cycle $Z_{\check{\sigma}}^{\check{\sigma}}(g \cdot y)$ with centre at $g \cdot y$ —the Möbius transform of the centre of $Z_{\check{\sigma}}^{\check{\sigma}}(y)$.*

Furthermore, we can extend the relation between a zero-radius cycle $Z_{\check{\sigma}}$ and points through the following connection of $Z_{\check{\sigma}}$ with the power of its centre.

EXERCISE I.5.21. Let $Z_{\check{\sigma}}$ be the zero-radius cycle (I.5.8) defined by $z = u - i\sigma v$, that is, with the σ -centre at the point (u, v) . Show that, in the elliptic and hyperbolic (but not parabolic) cases, a power of a point, see Definition I.3.18, $(u, v) \in \mathbb{A}$ with respect to a cycle C_{σ} , is equal to the cycle product $\langle Z_{\check{\sigma}}, C_{\sigma} \rangle$, where both cycles are k -normalised.

It is noteworthy that the notion of a point’s power is not Möbius-invariant even despite its definition through the invariant cycle product. This is due to the presence of non-invariant k -normalisation. This suggests extending the notion of the power from a point (that is, a zero-radius cycle) to arbitrary cycles:

DEFINITION I.5.22. A $(\sigma, \check{\sigma})$ -power of a cycle C with respect to another cycle \tilde{C} is equal to $\langle C_{\check{\sigma}}, \tilde{C}_{\sigma} \rangle$, where both matrices are *norm-normalised* by the conditions $\langle C_{\sigma}, C_{\sigma} \rangle = \pm 1$ and $\langle \tilde{C}_{\sigma}, \tilde{C}_{\sigma} \rangle = \pm 1$.

Alternatively, $(\sigma, \check{\sigma})$ -power is equal to $\frac{1}{2} \langle C_{\check{\sigma}}, \tilde{C}_{\check{\sigma}} \rangle$ (one half their cycle product), if both matrices are *det $_{\sigma}$ -normalised*. Since both elements of this definition—the cycle product and normalisation—are Möbius-invariant, the resulting value is preserved by Möbius transformations as well. Of course, the (e,e) -variant of this notion is well known in the classical theory.

EXERCISE I.5.23. i. Show that the (e,e) -power of a circle C with respect to another circle \tilde{C} has an absolute value equal to the *inversive distance* between C and \tilde{C} , see [24, Defn. 3.2.2; 27, § 4; 71, § 5.8 and Thm. 5.91]:

$$(I.5.10) \quad d(C, \tilde{C}) = \left| \frac{|c_1 - c_2|^2 - r_1^2 - r_2^2}{2r_1 r_2} \right|.$$

Here, $c_{1,2}$ and $r_{1,2}$ are the e -centres and radii of the circles. For other two cases, Exercise I.7.8.

- ii. Check for $\sigma = \pm 1$, that the (σ, σ) -power of two intersecting σ -cycles is the σ -cosine (I.3.36) of the angle between the tangents to cycles at an intersecting point.
- iii. For $\sigma = \pm 1$, let C and \tilde{C} be two given σ -cycles and α and β be two acute angles. Consider the collection T of all σ -cycles, such that the the intersection angle with C is α and the intersection angle with \tilde{C} is β . Then, any σ -cycle from the pencil spanned by C and \tilde{C} has the same intersection angle with σ -cycles from T (see also Exercise I.5.29 and Fig. I.5.3).

As another illustration of the technique based on zero-radius cycles, we return to orbits of isotropy subgroups, cf. Exercise I.3.21.ii.

EXERCISE I.5.24. Fulfil the following steps:

- i. Write the coefficients of the σ -zero-radius cycle $Z_\sigma(\iota)$ in \mathbb{A} with e-centre at the hypercomplex unit $\iota = (0, 1)$.
- ii. According to Exercise I.5.18.v, $Z_\sigma(\iota)$ is invariant under the similarity $Z_\sigma(\iota) \mapsto hZ_\sigma(\iota)h^{-1}$ with h in the respective isotropy subgroups K , N' and A' of ι . Check this directly.
- iii. Write the coefficients of a generic cycle in the pencil spanned by $Z_\sigma(\iota)$ and the real line. Note that the real line is also invariant under the action of the isotropy subgroups (as any other Möbius transformations) and conclude that any cycle from the pencil will also be invariant under the action of the isotropy subgroups. In other words, those cycles are orbits of the isotropy subgroups. Check that you obtained their equation (I.3.33).

We halt our study of zero-radius cycles on their own, but they will appear repeatedly in the following text in relation to other objects.

I.5.5. Cauchy–Schwarz Inequality and Tangent Cycles

We already noted that the invariant cycle product is a special (and remarkable!) example of an indefinite product in a vector space. Continuing this comparison, it will be interesting to look for a role of a Cauchy–Schwarz–type inequality

$$(I.5.11) \quad \langle x, y \rangle \langle y, x \rangle \leq \langle x, x \rangle \langle y, y \rangle,$$

which is a cornerstone of the theory of inner product spaces, cf. [164, § 5.1].

First of all, the classical form (I.5.11) of this inequality failed in any indefinite product space. This can be seen from examples or an observation that all classical proofs start from the assumption that $\langle x + ty, x + ty \rangle \geq 0$ in an inner product space. In an indefinite product space, there are always pairs of vectors which realise any of three possible relations:

$$\langle x, y \rangle \langle y, x \rangle \begin{matrix} \leq \\ = \\ \geq \end{matrix} \langle x, x \rangle \langle y, y \rangle.$$

Some regularity appears from the fact that the type of inequality is inherited by linear spans.

EXERCISE I.5.25. Let two vectors x and y in an indefinite product space satisfy either of the inequalities:

$$\langle x, y \rangle \langle y, x \rangle < \langle x, x \rangle \langle y, y \rangle \quad \text{or} \quad \langle x, y \rangle \langle y, x \rangle > \langle x, x \rangle \langle y, y \rangle.$$

Then, any two non-collinear vectors z and w from the real linear span of x and y satisfy the corresponding inequality:

$$\langle z, w \rangle \langle w, z \rangle < \langle z, z \rangle \langle w, w \rangle \quad \text{or} \quad \langle z, w \rangle \langle w, z \rangle > \langle z, z \rangle \langle w, w \rangle.$$

The equality $\langle x, y \rangle \langle y, x \rangle = \langle x, x \rangle \langle y, y \rangle$ always implies $\langle z, w \rangle \langle w, z \rangle = \langle z, z \rangle \langle w, w \rangle$.

The above Cauchy–Schwarz relations have a clear geometric meaning.

EXERCISE I.5.26. Check the following:

- i. Let C_σ and \tilde{C}_σ be two cycles defined by e-centres (u, v) and (\tilde{u}, \tilde{v}) with σ -determinants $-r^2$ and $-\tilde{r}^2$. The relations

$$\left\langle C_\sigma^s, \tilde{C}_\sigma^s \right\rangle^2 \begin{matrix} \leq \\ \geq \end{matrix} \langle C_\sigma^s, C_\sigma^s \rangle \langle \tilde{C}_\sigma^s, \tilde{C}_\sigma^s \rangle$$

guarantee that σ -implementations of C_σ and \tilde{C}_σ for $\sigma = \pm 1$ are intersecting, *tangent* or disjoint, respectively. What happens for the parabolic value $\sigma = 0$?

HINT: Determine the sign of the expression $\langle C_\sigma^s, \tilde{C}_\sigma^s \rangle - \sqrt{\langle C_\sigma^s, C_\sigma^s \rangle \langle \tilde{C}_\sigma^s, \tilde{C}_\sigma^s \rangle}$ using the formula (1.5.5). For the parabolic case, Exercise 1.7.2.p will be useful. \diamond

- ii. Let two cycles C_σ and \tilde{C}_σ be in \det_σ -normalised form. Deduce from the previous item the following Descartes–Kirillov condition [163, Lem. 4.1] for C_σ and \tilde{C}_σ to be externally σ -tangent (that is externally tangent in σ -implementation):

$$(1.5.12) \quad \left\langle C_\sigma + \tilde{C}_\sigma, C_\sigma + \tilde{C}_\sigma \right\rangle = 0 \quad \text{and} \quad \left\langle C_\sigma, \tilde{C}_\sigma \right\rangle > 0.$$

Since the first identity is equivalent to $\det(C_\sigma + \tilde{C}_\sigma) = 0$, $C_\sigma + \tilde{C}_\sigma$ is a σ -zero-radius cycle. Show that the centre of $C_\sigma + \tilde{C}_\sigma$ is the tangent point of C_σ and \tilde{C}_σ . HINT: The identity in (1.5.12) follows from the inequality there and the relation

$\left| \left\langle C_\sigma, \tilde{C}_\sigma \right\rangle \right| = \sqrt{\langle C_\sigma^s, C_\sigma^s \rangle \langle \tilde{C}_\sigma^s, \tilde{C}_\sigma^s \rangle} = 1$ for tangent cycles from the first item. For the last statement, use Exercise 1.5.21. \diamond

- iii. How shall we modify Descartes–Kirillov condition (1.5.12) for two cycles internally σ -tangent?
- iv. Show the following. If $\det_p C_\sigma^s = 0$ then $\det_\sigma(C_\sigma^s - R_\sigma^s) = 0$, where C_σ^s is \det_σ -normalized and R_σ^s is the \det -normalized cycle $(0, 0, 1, 0)$ representing the real line. Thus, C_σ^s is σ -tangent to the real line, i.e. is σ -horocycle, cf. Exercise 1.5.18.iii. How to interpret the external/internal touching in this case? HINT: The condition $\det_p C_\sigma^s = 0$ defines a cycle $C_\sigma^s = (1, u, v, u^2)$ with $\det_\sigma C_\sigma^s = -\sigma v^2$. \diamond

Exercises 1.5.25 and 1.5.26.i imply (see also Exercise 1.6.10.iii):

COROLLARY 1.5.27. *For a given pencil of cycles, see Definition 1.5.8, either all cycles are pair-wise disjoint, or every pair of cycles are tangent, or all of them pass the same pair of points.*

Zero-radius cycles form a two-parameter family (in fact, a manifold) in the three-dimensional projective cycle space \mathbb{P}^3 . It is not flat, as can be seen from its intersection with projective lines—cycle pencils. The Cauchy–Schwarz inequality turns out to be relevant here as well.

EXERCISE 1.5.28. A pencil of cycles either contains at most two $\check{\sigma}$ -zero-radius cycles or consists entirely of $\check{\sigma}$ -zero-radius cycles. Moreover:

- i. A pencil spanned by two different cycles cannot consist only of e-zero-radius cycles. Describe all pencils consisting only of p- and h-zero-radius cycles. HINT: Formula (1.5.9) will be useful for describing pencils consisting of (and thus spanned by) $\check{\sigma}$ -zero-radius cycles. Orbits of subgroup N' shown on the central drawing of Fig. 1.3.1 are an example of pencils of p-zero-radius cycles drawn as parabolas. You can experiment with σ -drawing of certain $\check{\sigma}$ -zero-radius pencils. \diamond

- ii. A pencil spanned by two different cycles C_σ^s and \tilde{C}_σ^s , which does not consist only of $\check{\sigma}$ -zero-radius cycles, has exactly two, one or zero $\check{\sigma}$ -zero-radius cycles depending on which of three possible Cauchy–Schwarz-type relations holds:

$$\left\langle C_\sigma^s, \tilde{C}_\sigma^s \right\rangle^2 \begin{matrix} \leq \\ \geq \\ = \end{matrix} \left\langle C_\sigma^s, C_\sigma^s \right\rangle \left\langle \tilde{C}_\sigma^s, \tilde{C}_\sigma^s \right\rangle.$$

HINT: Write the expression for the cycle product of the span $tC_\sigma^s + \tilde{C}_\sigma^s$, $t \in \mathbb{R}$ with itself in terms of products $\left\langle C_\sigma^s, \tilde{C}_\sigma^s \right\rangle$, $\left\langle C_\sigma^s, C_\sigma^s \right\rangle$ and $\left\langle \tilde{C}_\sigma^s, \tilde{C}_\sigma^s \right\rangle$. \diamond

Tangent circles may be treated as having zero intersection angle, thus we continue theme from Exercise I.5.23.iii.

EXERCISE I.5.29. For $\sigma = \pm 1$, let C and \tilde{C} be two given σ -cycles and α and β be two acute angles. Consider the collection T of all σ -cycles, such that the the intersection angle with C is α and the intersection angle with \tilde{C} is β . Let

$$a = \cos_\sigma \alpha, \quad b = \cos_\sigma \beta, \quad c = \langle C, C \rangle, \quad d = \langle \tilde{C}, \tilde{C} \rangle, \quad p = \langle C, \tilde{C} \rangle.$$

Assume $(ab + p)^2 - (a^2 + c)(b^2 + d) \geq 0$, then, any σ -cycle from the family T is tangent to cycles $C_{1,2} = x_{1,2}C + \tilde{C}$ from the pencil spanned by C and \tilde{C} , where:

$$(I.5.13) \quad x_{1,2} = \frac{-ab - p \pm \sqrt{(ab + p)^2 - (a^2 + c)(b^2 + d)}}{a^2 + c}.$$

See Fig. I.5.3 for an illustration. HINT: Let $C_t \in T$ and $C_x = xC + \tilde{C}$ be a σ -cycle from the pencil spanned by C and \tilde{C} . Then, the tangency condition $\langle C_x, C_t \rangle^2 = \langle C_x, C_x \rangle \langle C_t, C_t \rangle$ and Exercise I.5.23.ii lead to a quadratic equation with roots (I.5.13). \diamond

The statement has counterparts in the parabolic case, see Exercise I.9.22.

REMARK I.5.30. Note that the tangency condition (I.5.12) is quadratic in parameters of a cycle C_σ . However, n such conditions with a single unknown cycle C can be reduced to the single quadratic condition $\langle C, C \rangle = 1$ and n linear conditions like $\langle C, \tilde{C}_{(i)} \rangle = \lambda_i$. This observation was implemented in the C++ library figure [211]. A similar technique was also used in [101].

Recall that straight lines are cycles which pass the infinity, that is orthogonal to the zero-radius cycle at infinity. Here is tangency property for lines:

EXERCISE I.5.31. Check that:

- i. Straight lines touching the zero-radius cycle at infinity.
- ii. Two straight lines are parallel if and only if they are touching (at infinity).

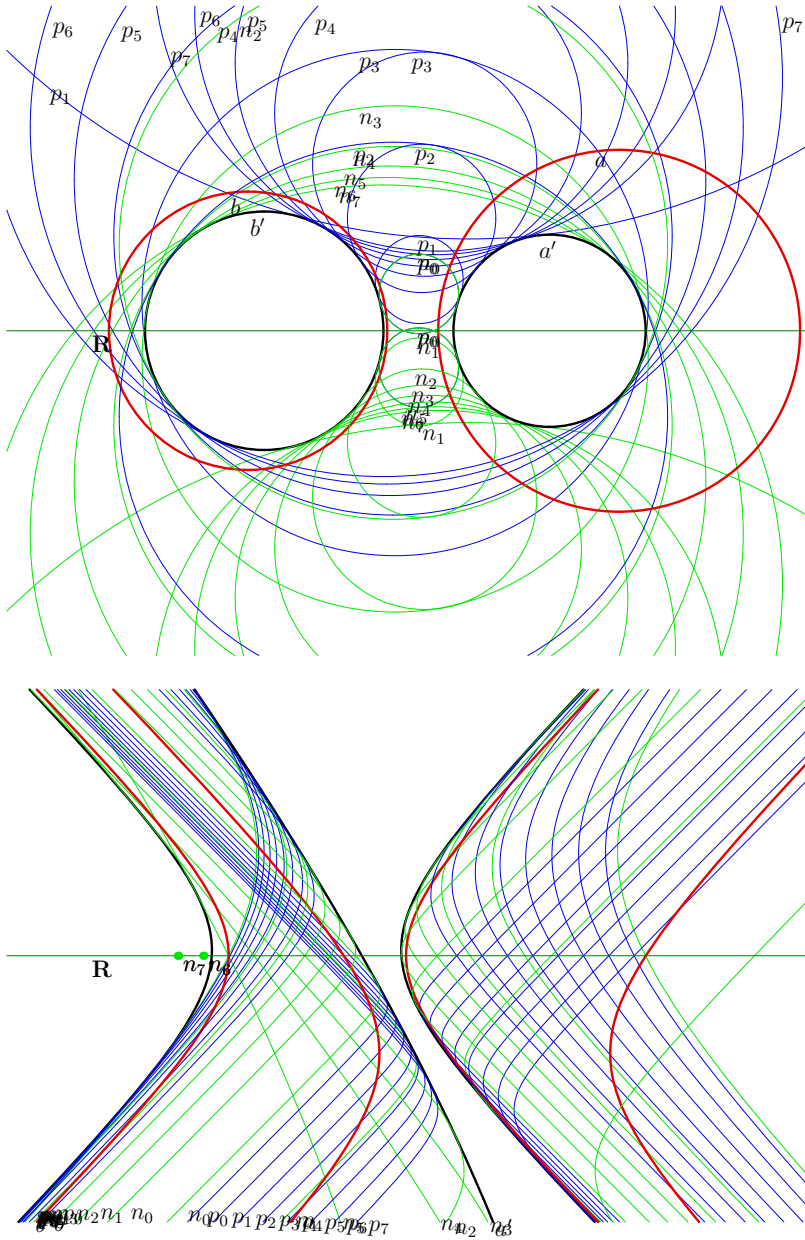


FIGURE I.5.3. Intersection and tangency: the family of blue and green σ -cycles ($\sigma = \pm 1$), which make the intersection angles with σ -cosines $(\frac{1}{2})^{-\sigma}$ and $(\frac{\sqrt{3}}{2})^{-\sigma}$ to two red σ -cycles a and b . All green and blue cycles touch two black cycles a' and b' , which belong to the pencil spanned by a and b .

Joint Invariants of Cycles: Orthogonality

The invariant cycle product, defined in the previous chapter, allows us to define joint invariants of two or more cycles. Being initially defined in an algebraic fashion, they also reveal their rich geometrical content. We will also see that FSCc matrices define reflections and inversions in cycles, which extend Möbius maps.

I.6.1. Orthogonality of Cycles

According to the **categoryical viewpoint**, the internal properties of objects are of minor importance in comparison with their relations to other objects from the same class. Such a projection of internal properties into external relations was also discussed at the beginning of Section I.4.2. As a further illustration, we may give the proof of Theorem I.4.13, outlined below. Thus, we will now look for invariant relations between two or more cycles.

After we defined the invariant cycle product (I.5.3), the next standard move is to use the analogy with Euclidean and Hilbert spaces and give the following definition:

DEFINITION I.6.1. Two cycles $C_{\check{\sigma}}^s$ and $\tilde{C}_{\check{\sigma}}^s$ are called $\check{\sigma}$ -orthogonal if their $\check{\sigma}$ -cycle product vanishes:

$$(I.6.1) \quad \langle C_{\check{\sigma}}^s, \tilde{C}_{\check{\sigma}}^s \rangle = 0.$$

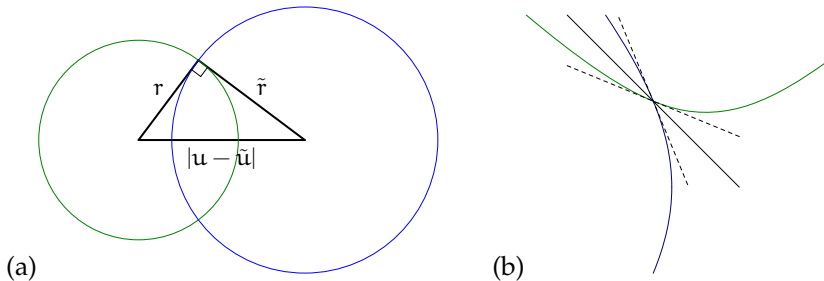


FIGURE I.6.1. Relation between centres and radii of orthogonal circles

Here are the most fundamental properties of cycle orthogonality:

EXERCISE I.6.2. Use Exercise I.5.12 to check the following:

- i. The $\check{\sigma}$ -orthogonality condition (I.6.1) is invariant under Möbius transformations.
- ii. The explicit expression for $\check{\sigma}$ -orthogonality of cycles in terms of their coefficients is

$$(I.6.2) \quad 2\check{\sigma}\check{n}\check{n} - 2\check{l}\check{l} + \check{k}\check{m} + \check{m}\check{k} = 0.$$

- iii. The $\check{\sigma}$ -orthogonality of cycles defined by their e-centres (u, v) and (\tilde{u}, \tilde{v}) with σ -determinants $-r^2$ and $-\tilde{r}^2$, respectively, is:

$$(I.6.3) \quad (u - \tilde{u})^2 - \sigma(v - \tilde{v})^2 - 2(\sigma - \check{\sigma})v\tilde{v} - r^2 - \tilde{r}^2 = 0.$$

- iv. Two circles are e-orthogonal if their tangents at an intersection point form a right angle. HINT: Use the previous formula (I.6.3), the inverse of Pythagoras' theorem and Fig. I.6.1(a) for this. \diamond

The last item can be reformulated as follows: For circles, their e-orthogonality as vectors in the cycle spaces \mathbb{P}^3 with the cycle product (I.5.3) coincides with their orthogonality as geometrical sets in the point space \mathbb{C} . This is very strong support for FSCc and the cycle product (I.5.3) defined from it. Thereafter, it is tempting to find similar interpretations for other types of orthogonality. The next exercise performs the first step for the case of σ -orthogonality in the matching point space \mathbb{A} .



EXERCISE I.6.3. Check the following geometrical meaning for σ -orthogonality of σ -cycles.

- (e,h):** Let $\sigma = \pm 1$. Then, two cycles in \mathbb{A} (that is, circles or hyperbolas) are σ -orthogonal if slopes S_1 and S_2 of their tangents at the intersection point satisfy the condition

$$(I.6.4) \quad S_1 S_2 = \sigma.$$

The geometrical meaning of this condition can be given either in terms of angles (A) or centres (C):

- (A) For the case $\sigma = -1$ (circles), equation (I.6.4) implies orthogonality of the tangents, cf. Exercise I.6.2.iv. For $\sigma = 1$, two hyperbolas are h-orthogonal if lines with the slopes ± 1 bisect the angle of intersection of the hyperbolas, see Fig. I.6.1(b). HINT: Define a cycle C_σ by the condition that it passes a point $(u, v) \in \mathbb{A}$. Define a second cycle \tilde{C}_σ by both conditions: it passes the same point (u, v) and is orthogonal to C_σ . Then use the implicit derivative formula to find the slopes of tangents to C_σ and \tilde{C}_σ at (u, v) . A script calculating this in CAS is also provided. \diamond
- (C) In the cases $\sigma = \pm 1$, the tangent to one cycle at the intersection point passes the centre of another cycle. HINT: This fact is clear for circles from inspection of, say, Fig. I.6.1(a). For hyperbolas, it is enough to observe that the slope of the tangent to a hyperbola $y = 1/x$ at a point $(x, 1/x)$ is $-1/x^2$ and the slope of the line from the centre $(0, 0)$ to the point $(x, 1/x)$ is $1/x^2$, so the angle between two lines is bisected by a vertical/horizontal line. All our hyperbolas are obtained from $y = 1/x$ by rotation of $\pm 45^\circ$ and scaling. \diamond

(p): Let $\sigma = 0$ and a parabola C_p have two real roots u_1 and u_2 . If a parabola \tilde{C}_p is p -orthogonal to C_p , then the tangent to \tilde{C}_p at a point above one of the roots $u_{1,2}$ passes the p -centre $(\frac{u_1+u_2}{2}, 0)$ of C_p .

REMARK I.6.4. Note that the geometric p -orthogonality condition for parabolas is non-local in the sense that it does not direct behaviour of tangents at the intersection points. Moreover, orthogonal parabolas need not intersect at all. We shall see more examples of such non-locality later. The relation I.6.3(p) is also another example of boundary awareness, cf. Remark I.5.3—we are taking a tangent of one parabola above the point of intersection of the other parabola with the boundary of the upper half-plane.

The stated geometrical conditions for orthogonality of cycles are not only necessary but are sufficient as well.

EXERCISE I.6.5. i. Prove the converses of the two statements in Exercise I.6.3.

HINT: To avoid irrationalities in the parabolic case and make the calculations accessible for CAS, you may proceed as follows. Define a generic parabola passing (u, v) and use implicit derivation to find its tangent at this point. Define the second parabola passing $(u, 0)$ and its centre at the intersection of the tangent of the first parabola at (u, v) and the horizontal axis. Then, check the p -orthogonality of the two parabolas. \diamond

ii. Let a parabola have two tangents touching it at (u_1, v_1) and (u_2, v_2) and these tangents intersect at a point (u, v) . Then, $u = \frac{u_1+u_2}{2}$. HINT: Use the geometric description of p -orthogonality and note that the two roots of a parabola are interchangeable in the necessary condition for p -orthogonality. \diamond

We found geometrically necessary and sufficient conditions for σ -orthogonality in the matching point space \mathbb{A} . The remaining six non-matching cases will be reduced to this in Section I.6.3 using an auxiliary ghost cycle. However, it will be useful to study some more properties of orthogonality.

I.6.2. Orthogonality Miscellanea

The explicit formulae (I.16.11) and (I.6.3) allow us to obtain several simple and yet useful conclusions.

EXERCISE I.6.6. Show that:

- i. A cycle is $\check{\sigma}$ -self-orthogonal (isotropic) if and only if it is $\check{\sigma}$ -zero-radius cycle (I.5.8).
- ii. For $\check{\sigma} = \pm 1$, there is no non-trivial cycle orthogonal to all other non-trivial cycles. For $\check{\sigma} = 0$, only the horizontal axis $v = 0$ is orthogonal to all other non-trivial cycles.
- iii. If two real (e-negative) circles are e-orthogonal, then they intersect. Give an example of h-orthogonal hyperbolas which do not intersect in \mathbb{O} . HINT: Use properties of the Cauchy–Schwarz inequality from Exercise I.5.26.i. \diamond
- iv. A cycle C_σ^s is σ -orthogonal to a zero-radius cycle Z_σ^s (I.5.8) if and only if σ -implementation of C_σ^s passes through the σ -centre of Z_σ^s , or, analytically,

$$(I.6.5) \quad k(u^2 - \sigma v^2) - 2 \langle (l, n), (u, \check{\sigma}v) \rangle + m = 0.$$

- v. For $\check{\sigma} = \pm 1$, any cycle is uniquely defined by the family of cycles orthogonal to it, i.e. $(C_{\check{\sigma}}^s)^\perp = \{C_{\check{\sigma}}^s\}$.

For $\check{\sigma} = 0$, the set $(C_{\check{\sigma}}^s)^\perp$ is the pencil spanned by $C_{\check{\sigma}}^s$ and the real line.

In particular, if $C_{\check{\sigma}}^s$ has real roots, then all cycles in $(C_{\check{\sigma}}^s)^\perp$ have these roots.

- vi. Two $\check{\sigma}$ -zero-radius cycles are $\check{\sigma}$ -orthogonal if:

(e) for $\check{\sigma} = -1$ and $\sigma = \pm 1$, cycles' σ -centres coincide.

(p) for $\check{\sigma} = 0$ and $\sigma = \pm 1$, cycles' σ -centres belong to the same vertical line.

(h) for $\check{\sigma} = 1$ and $\sigma = \pm 1$, each cycle's σ -centre belongs to the light cone defined by the other cycle.

(Note, that in the Benz axiomatisation [315, § 1] these relations between cycles' centres are called parallelism.)

HINT: Use the explicit expression for the cycle product (I.5.9).◊

The connection between orthogonality and incidence from Exercise I.6.6.iv allows us to combine the techniques of zero-radius cycles and orthogonality in an efficient tool.

EXERCISE I.6.7. Fill all gaps in the following proof:

SKETCH OF AN ALTERNATIVE PROOF OF THEOREM I.4.13. We already mentioned in Subsection I.4.4.1 that the validity of Theorem I.4.13 for a zero-radius cycle (I.5.8)

$$Z_{\check{\sigma}}^s = \begin{pmatrix} z & -z\bar{z} \\ 1 & -\bar{z} \end{pmatrix} = \frac{1}{2} \begin{pmatrix} z & z \\ 1 & 1 \end{pmatrix} \begin{pmatrix} 1 & -\bar{z} \\ 1 & -\bar{z} \end{pmatrix}$$

with the centre $z = x + iy$ is a straightforward calculation—see also Exercise I.5.18.v. This implies the result for a generic cycle with the help of

- Möbius invariance of the product (I.5.3) (and thus orthogonality) and
- the above relation I.6.6.iv between the orthogonality and the incidence.

The idea of such a proof is borrowed from [65] and details can be found therein. ◻

The above demonstration suggests a generic technique for extrapolation of results from zero-radius cycles to the entire cycle space. We will formulate it with the help of a map Q from the cycle space to conics in the point space from Definition I.4.10.

PROPOSITION I.6.8. Let $T : \mathbb{P}^3 \rightarrow \mathbb{P}^3$ be an orthogonality-preserving map of the cycle space, i.e. $\langle C_{\check{\sigma}}^s, \tilde{C}_{\check{\sigma}}^s \rangle = 0 \Leftrightarrow \langle TC_{\check{\sigma}}^s, T\tilde{C}_{\check{\sigma}}^s \rangle = 0$. Then, for $\sigma \neq 0$, there is a map $T_\sigma : \mathbb{A} \rightarrow \mathbb{A}$, such that Q intertwines T and T_σ :

$$(I.6.6) \quad QT_\sigma = TQ.$$

PROOF. If T preserves orthogonality (i.e. the cycle product (I.5.3) and, consequently, the determinant, see (I.5.6)) then the image $TZ_{\check{\sigma}}^s(u, v)$ of a zero-radius cycle $Z_{\check{\sigma}}^s(u, v)$ is again a zero-radius cycle $Z_{\check{\sigma}}^s(u_1, v_1)$. Thus we can define T_σ by the identity $T_\sigma : (u, v) \mapsto (u_1, v_1)$.

To prove the intertwining property (I.6.6) we need to show that, if a cycle $C_{\check{\sigma}}^s$ passes through (u, v) , then the image $TC_{\check{\sigma}}^s$ passes through $T_\sigma(u, v)$. However, for $\sigma \neq 0$, this is a consequence of the T -invariance of orthogonality and the expression of the point-to-cycle incidence through orthogonality from Exercise I.6.6.iv. ◻

EXERCISE I.6.9. Let $T_i : \mathbb{P}^3 \rightarrow \mathbb{P}^3$, $i = 1, 2$ be two orthogonality-preserving maps of the cycle space. Show that, if they coincide on the subspace of $\check{\sigma}$ -zero-radius cycles, $\check{\sigma} \neq 0$, then they are identical in the whole \mathbb{P}^3 .

We defined orthogonality from an inner product, which is linear in each component. Thus, orthogonality also respects linearity.

EXERCISE I.6.10. Check the following relations between orthogonality and pencils:

- i. Let a cycle $C_{\check{\sigma}}$ be $\check{\sigma}$ -orthogonal to two different cycles $\tilde{C}_{\check{\sigma}}$ and $\hat{C}_{\check{\sigma}}$. Then $C_{\check{\sigma}}$ is $\check{\sigma}$ -orthogonal to every cycle in the pencil spanned by $\tilde{C}_{\check{\sigma}}$ and $\hat{C}_{\check{\sigma}}$.
- ii. Check that all cycles $\check{\sigma}$ -orthogonal with $\check{\sigma} = \pm 1$ to two different cycles $\tilde{C}_{\check{\sigma}}$ and $\hat{C}_{\check{\sigma}}$ belong to a single pencil. Describe such a family for $\check{\sigma} = 0$. HINT: For the case $\check{\sigma} = 0$, the family is spanned by an additional cycle, which was mentioned in Exercise I.6.6.ii.◊
- iii. If two circles are non-intersecting, then the orthogonal pencil passes through two points, which are the only two e-zero-radius cycles in the pencil, see the first row of Fig. I.6.2. And *vice versa*: a pencil orthogonal to two intersecting circles consists of disjoint circles. Tangent circles have the orthogonal pencils of circles which are all tangent at the same point, cf. Corollary I.5.27.
- iv. The above relations do hold for parabolas and hyperbolas only for tangent pencils (the middle column of Fig. I.6.2). What are correct statements in other cases?

Exercise I.6.10.ii describes two *orthogonal pencils* such that each cycle in one pencil is orthogonal to every cycle in the second. In terms of indefinite linear algebra, see [113, § 2.2], we are speaking about the orthogonal complement of a two-dimensional subspace in a four-dimensional space and it turns out to be two-dimensional as well. For circles, this construction is well known, see [37, § 10.10; 71, § 5.7]. An illustration for three cases is provided by Fig. I.6.2. The reader may wish to experiment more with orthogonal complements to various parabolic and hyperbolic pencils—see Fig. I.5.1 and Exercise I.5.9.

Such orthogonal pencils naturally appear in many circumstances and we already met them on several occasions. We know from Exercise I.3.19.iii and I.3.19.iv that K-orbits and transverse lines make coaxial pencils which turn to be in a relation:

EXERCISE I.6.11. Check that:

- i. Any K-orbit (I.3.26) in \mathbb{A} is σ -orthogonal to any transverse line (I.3.28). Figure I.1.2 provides an illustration. HINT: There are several ways to check this. A direct calculation based on the explicit expressions for cycles is not difficult. Alternatively, we can observe that the pencil of transverse lines is generated by K-action from the vertical axis and orthogonality is Möbius-invariant.◊
- ii. Any orbit (I.3.33) is σ -orthogonal to any transverse line (I.3.34) for the same subgroup K , N' or A' , that is for the same value τ . Figure I.3.2 provides an illustration.

The following general statement about pencils and orthogonality is an abstract generalisation of the well-known result on a triangle's orthocenter.

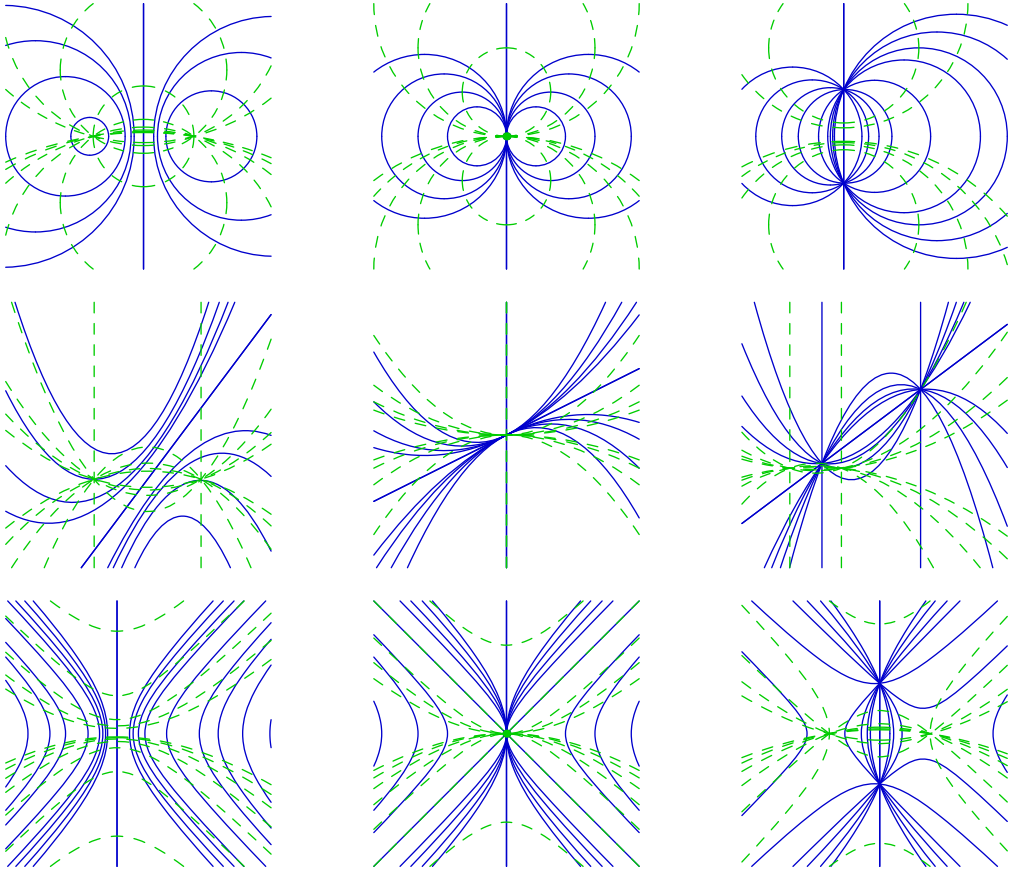


FIGURE I.6.2. σ -orthogonal pencils of σ -cycles. One pencil is drawn in solid blue, the others in dashed green styles.

EXERCISE I.6.11(a). Let C_a, C_b, C_c be three pair-wise distinct cycles with at most two of them being orthogonal to each other. We define \tilde{C}_a as the cycle

- from the pencil spanned by C_b and C_c ;
- orthogonal to C_a .

Cycles \tilde{C}_b and \tilde{C}_c are similarly defined. Then, \tilde{C}_a belongs to the pencil spanned by \tilde{C}_b and \tilde{C}_c . In particular, altitudes of a triangle are *concurrent*, that is meet at the same point, which is called the *orthocenter* of a triangle.

HINT: Note that $\tilde{C}_a = \langle C_c, C_a \rangle C_b - \langle C_b, C_a \rangle C_c$. \diamond

We may describe a finer structure of the cycle space through Möbius-invariant subclasses of cycles. Three such families—zero-radius, positive and negative cycles—were already considered in Sections I.5.3 and I.5.4. They were defined using the properties

of the cycle product with itself. Another important class of cycles is given by the value of its cycle product with the real line.

DEFINITION I.6.12. A cycle $C_{\check{\sigma}}^s$ is called *selfadjoint* if it is $\check{\sigma}$ -orthogonal with $\check{\sigma} \neq 0$ to the real line, i.e. it is defined by the condition $\langle C_{\check{\sigma}}^s, R_{\check{\sigma}}^s \rangle = 0$, where $R_{\check{\sigma}}^s = (0, 0, 1, 0)$ corresponds to the horizontal axis $v = 0$.

The following algebraic properties of selfadjoint cycles easily follow from the definition.

EXERCISE I.6.13. Show that:

- i. Selfadjoint cycles make a Möbius-invariant family.
- ii. A selfadjoint cycle $C_{\check{\sigma}}^s$ is defined explicitly by $n = 0$ in (I.15.3) for both values $\check{\sigma} = \pm 1$.
- iii. Any of the following conditions are necessary and sufficient for a cycle to be selfadjoint:
 - All three centres of the cycle coincide.
 - At least two centres of the cycle belong to the real line.

From these analytic conditions, we can derive a geometric characterisation of selfadjoint cycles.

EXERCISE I.6.14. Show that selfadjoint cycles have the following implementations in the point space \mathbb{A} :

(e,h): Circles or hyperbolas with their geometric centres on the real line.

(p): Vertical lines, consisting of points (u, v) such that $|u - u_0| = r$ for some $u_0 \in \mathbb{R}$, $r \in \mathbb{R}_+$. The cycles are also given by the $\|x - y\| = r^2$ in the parabolic metric defined below in (I.7.3).

Notably, selfadjoint cycles in the parabolic point space were labelled as “parabolic circles” by Yaglom—see [339, § 7]. On the other hand, Yaglom used the term “parabolic cycle” for our p-cycle with non-zero k and n .

EXERCISE I.6.15. Show that:

- i. Any cycle $C_{\check{\sigma}}^s = (k, l, n, m)$ belongs to a pencil spanned by a selfadjoint cycle $HC_{\check{\sigma}}^s$ and the real line

$$(I.6.7) \quad C_{\check{\sigma}}^s = HC_{\check{\sigma}}^s + nR_{\check{\sigma}}^s, \quad \text{where } HC_{\check{\sigma}}^s = (k, l, 0, m).$$

This identity is a definition of linear orthogonal projection H from the cycle space to its subspace of selfadjoint cycles. When does $HC_{\check{\sigma}}^s$ is a real cycle?

- ii. The decomposition of a cycle into the linear combination of a selfadjoint cycle and the real line is Möbius-invariant:

$$g \cdot C_{\check{\sigma}}^s = g \cdot HC_{\check{\sigma}}^s + nR_{\check{\sigma}}^s.$$

HINT: The first two items are small pieces of linear algebra in an indefinite product space, see [113, § 2.2]. \diamond

- iii. Cycles $C_{\check{\sigma}}^s$ and $HC_{\check{\sigma}}^s$ have the same real roots.

We are now equipped to consider the geometrical meaning of all nine types of cycle orthogonality.

I.6.3. Ghost Cycles and Orthogonality

For the case of $\check{\sigma} = 1$, i.e. when geometries of the cycle and point spaces are both either elliptic or hyperbolic, $\check{\sigma}$ -orthogonality can be expressed locally through tangents to cycles at the intersection points—see Exercise I.6.3(A). A semi-local condition also exists: the tangent to one cycle at the intersection point passes the centre of the second cycle—see Exercise I.6.3(C). We may note that, in the pure parabolic case $\sigma = \check{\sigma} = 0$, the geometric orthogonality condition from Exercise I.6.3(p) can be restated with help from Exercise I.6.15.i as follows:

COROLLARY I.6.16. *Two p -cycles C_p and \tilde{C}_p are p -orthogonal if the tangent to C_p at its intersection point with the projection $H\tilde{C}_p$ (I.6.7) of \tilde{C}_p to selfadjoint cycles passes the p -centre of \tilde{C}_p .*

HINT: In order to reformulate Exercise I.6.3(p) to the present form, it is enough to use Exercises I.6.14(p) and I.6.15.iii.◇

The three cases with matching geometries in point and cycle spaces are now quite well unified. Would it be possible to extend such a geometric interpretation of orthogonality to the remaining six ($= 9 - 3$) cases?

Elliptic realisations (in the point space) of Definition I.6.1, i.e. $\sigma = -1$, were shown in Fig. I.1.7 and form the first row in Fig. I.6.3. The left picture in this row corresponds to the elliptic cycle space, e.g. $\check{\sigma} = -1$. The orthogonality between the red circle and any circle from the blue or green families is given in the usual Euclidean sense described in Exercise I.6.3(e,h). In other words, we can decide on the orthogonality of circles by observing the angles between their tangents at the arbitrary small neighbourhood of the intersection point. Therefore, all circles from either the green or blue families, which are orthogonal to the red circle, have common tangents at points a and b respectively.

The central (parabolic in the cycle space) and the right (hyperbolic) pictures show the non-local nature of orthogonality if $\sigma \neq \check{\sigma}$. The blue family has the intersection point b with the red circle, and tangents to blue circles at b are different. However, we may observe that all of them pass the second point d. This property will be used in Section I.6.5 to define the inversion in a cycle. A further investigation of Fig. I.6.3 reveals that circles from the green family have a common tangent at point a, however this point does not belong to the red circle. Moreover, in line with the geometric interpretation from Exercise I.6.3(C), the common tangent to the green family at a passes the p -centre (on the central parabolic drawing) or h -centre (on the right hyperbolic drawing).

There are analogous pictures in parabolic and hyperbolic point spaces as well and they are presented in the second and third rows of Fig. I.6.3. The behaviour of green and blue families of cycles at point a, b and d is similar up to the obvious modification: the EPH case of the point space coincides with EPH case of the cycle spaces in the central drawing of the second row and the right drawing of the third row.

Therefore, we will clarify the nature of orthogonality if the locus of such points a with tangents passing the other cycle's $\check{\sigma}$ -centre are described. We are going to demonstrate that this locus is a cycle, which we shall call a "ghost". The ghost cycle is shown

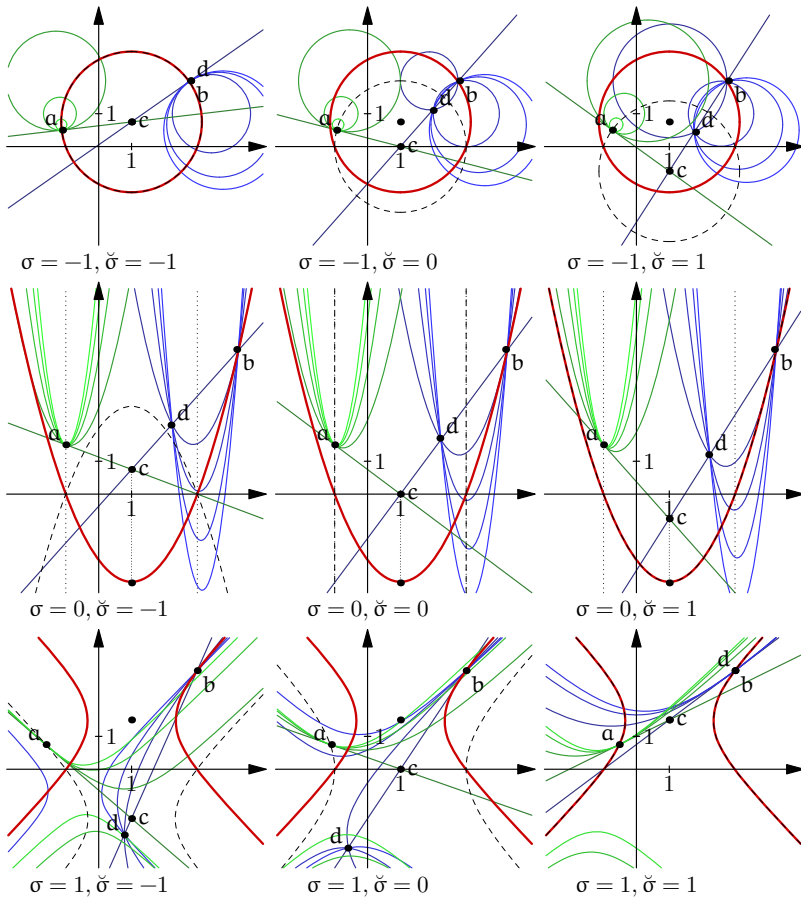


FIGURE I.6.3. Three types of orthogonality in the three types of the point space.

Each picture presents two groups (green and blue) of cycles which are orthogonal to the red cycle C_0^s . Point b belongs to C_0^s and the family of blue cycles passing through b also intersects at the point d , which is the inverse of b in C_0^s . Any orthogonality is reduced to the usual orthogonality with a new ("ghost") cycle (shown by the dashed line), which may or may not coincide with C_0^s . For any point a on the "ghost" cycle, the orthogonality is reduced to the semi-local notion in the terms of tangent lines at the intersection point. Consequently, such a point a is always the inverse of itself.

by the dashed lines in Fig. I.6.3. To give an analytic description, we need the Heaviside

function $\chi(\sigma)$:

$$(I.6.8) \quad \chi(t) = \begin{cases} 1, & t \geq 0; \\ -1, & t < 0. \end{cases}$$

More specifically, we note the relations $\chi(\sigma) = \sigma$ if $\sigma = \pm 1$ and $\chi(\sigma) = 1$ if $\sigma = 0$. Thus, the Heaviside function will be used to avoid the degeneracy of the parabolic case.

DEFINITION I.6.17. For a cycle $C_{\check{\sigma}}$ in the σ -implementation, we define the associated ($\check{\sigma}$ -)ghost cycle $\check{C}_{\check{\sigma}}$ by the following two conditions:

- i. The $\chi(\sigma)$ -centre of $\check{C}_{\check{\sigma}}$ coincides with the $\check{\sigma}$ -centre of $C_{\check{\sigma}}$.
- ii. The determinant of $\check{C}_{\check{\sigma}}^1$ is equal to the determinant of $C_{\check{\sigma}}^{\check{\sigma}}$.



EXERCISE I.6.18. Verify the following properties of a ghost cycle:

- i. \check{C}_{σ} coincides with C_{σ} if $\sigma\check{\sigma} = 1$.
- ii. \check{C}_{σ} has common roots (real or imaginary) with C_{σ} .
- iii. For a cycle $C_{\check{\sigma}}$, its p-ghost cycle $\check{C}_{\check{\sigma}}$ and the non-selfadjoint part $HC_{\check{\sigma}}$ (I.6.7) coincide.
- iv. All straight lines $\check{\sigma}$ -orthogonal to a cycle pass its $\check{\sigma}$ -centre.

The significance of the ghost cycle is that the $\check{\sigma}$ -orthogonality between two cycles in \mathbb{A} is reduced to σ -orthogonality to the ghost cycle.



PROPOSITION I.6.19. Let cycles $C_{\check{\sigma}}$ and $\tilde{C}_{\check{\sigma}}$ be $\check{\sigma}$ -orthogonal in \mathbb{A} and let $\check{C}_{\check{\sigma}}$ be the ghost cycle of $C_{\check{\sigma}}$. Then:

- i. $\check{C}_{\check{\sigma}}$ and $\tilde{C}_{\check{\sigma}}$ are σ -orthogonal in \mathbb{A} for seven cases except two cases $\sigma = 0$ and $\check{\sigma} = \pm 1$.
- ii. In the σ -implementation, the tangent line to $\tilde{C}_{\check{\sigma}}$ at its intersection point with
 - (a) the ghost cycle $\check{C}_{\check{\sigma}}$, if $\sigma = \pm 1$, or
 - (b) the non-selfadjoint part $HC_{\check{\sigma}}$ (I.6.7) of the cycle $C_{\check{\sigma}}$, if $\sigma = 0$,
 passes the $\check{\sigma}$ -centre of $C_{\check{\sigma}}$, which coincides with the σ -centre of $\check{C}_{\check{\sigma}}$.

PROOF. The statement I.6.19.i can be shown by algebraic manipulation, possibly in CAS. Then, the non-parabolic case I.6.19.ii(a) follows from the first part I.6.19.i, which reduces non-matching orthogonality to a matching one with the ghost cycle, and the geometric description of matching orthogonality from Exercise I.6.3. Therefore, we only need to provide a new calculation for the parabolic case I.6.19.ii(b). Note that, in the case $\sigma = \check{\sigma} = 0$, there is no disagreement between the first and second parts of the proposition since $HC_{\check{\sigma}} = \tilde{C}_{\check{\sigma}}$ due to I.6.18.iii. \square

Consideration of ghost cycles does present orthogonality in geometric term, but it hides the symmetry of this relation. Indeed, it is not obvious that $\tilde{C}_{\check{\sigma}}^{\check{\sigma}}$ relates to the ghost of $C_{\check{\sigma}}^{\check{\sigma}}$ in the same way as $C_{\check{\sigma}}^{\check{\sigma}}$ relates to the ghost of $\tilde{C}_{\check{\sigma}}^{\check{\sigma}}$.

REMARK I.6.20. Elliptic and hyperbolic ghost cycles are symmetric in the real line and the parabolic ghost cycle has its centre on it—see Fig. I.6.3. This is an illustration of the boundary effect from Remarks I.5.3.

Finally, we note that Proposition I.6.19 expresses $\check{\sigma}$ -orthogonality through the $\check{\sigma}$ -centre of cycles. It illustrates the meaningfulness of various centres within our approach which may not be so obvious at the beginning.

I.6.4. Actions of FSCc Matrices

Definition I.4.11 associates a 2×2 -matrix to any cycle. These matrices can be treated analogously to elements of $SL_2(\mathbb{R})$ in many respects. Similar to the $SL_2(\mathbb{R})$ action (I.3.24), we can consider a fraction-linear transformation on the point space \mathbb{A} defined by a cycle and its FSCc matrix

$$(I.6.9) \quad C_{\sigma}^s : w \mapsto C_{\sigma}^s(w) = \frac{(l + \iota sn)\bar{w} - m}{k\bar{w} + (-l + \iota sn)},$$

where C_{σ}^s is, as usual (I.4.5),

$$C_{\sigma}^s = \begin{pmatrix} l + \iota sn & -m \\ k & -l + \iota sn \end{pmatrix} \quad \text{and} \quad w = u + \iota v, \quad \sigma = \iota^2.$$

EXERCISE I.6.21. Check that $w = u + \iota v \in \mathbb{A}$ is a fixed point of the map $C_{\sigma}^{-\sigma}$ (I.6.9) if and only if the σ -implementation of $C_{\sigma}^{-\sigma}$ passes w . If $\det \tilde{C}_{\sigma}^s \neq 0$ then the second iteration of the map is the identity.

We can also extend the conjugated action (I.4.7) on the cycle space from $SL_2(\mathbb{R})$ to cycles. Indeed, a cycle \tilde{C}_{σ}^s in the matrix form acts on another cycle C_{σ}^s by the $\check{\sigma}$ -similarity

$$(I.6.10) \quad \tilde{C}_{\sigma}^{s_1} : C_{\sigma}^s \mapsto -\tilde{C}_{\sigma}^{s_1} \overline{C_{\sigma}^s} \tilde{C}_{\sigma}^{s_1}.$$

The similarity can be considered as a transformation of the cycle space \mathbb{P}^3 to itself due to the following result.

EXERCISE I.6.22. Check that:

- i. The cycle $\check{\sigma}$ -similarity (I.6.10) with a cycle \tilde{C}_{σ}^s , where $\det \tilde{C}_{\sigma}^s \neq 0$, preserves the structure of FSCc matrices and $\tilde{C}_{\sigma}^{s_1}$ is its fixed point. In a non-singular case, $\det \tilde{C}_{\sigma}^s \neq 0$, the second iteration of similarity is the identity map.
- ii. The $\check{\sigma}$ -similarity with a $\check{\sigma}$ -zero-radius cycle Z_{σ}^s always produces this cycle.
- iii. The $\check{\sigma}$ -similarity with a cycle (k, l, n, m) is a linear transformation of the cycle space \mathbb{R}^4 with the matrix

$$\begin{pmatrix} km - \det C_{\sigma} & -2kl & 2\check{\sigma}kn & k^2 \\ lm & -2l^2 - \det C_{\sigma} & 2\check{\sigma}ln & kl \\ nm & -2nl & 2\check{\sigma}n^2 - \det C_{\sigma} & kn \\ m^2 & -2ml & 2\check{\sigma}mn & km - \det C_{\sigma} \end{pmatrix} \\ = \begin{pmatrix} k \\ l \\ n \\ m \end{pmatrix} \cdot (m \quad -2l \quad 2\check{\sigma}n \quad k) - \det(C_{\sigma}) \cdot I_{4 \times 4}.$$

Note the apparent regularity of its entries.

REMARK I.6.23. Here is another example where usage of complex (dual or double) numbers is different from Clifford algebras. In order to use commutative hypercomplex numbers, we require the complex conjugation for the cycle product (I.5.3), linear-fractional transformation (I.6.9) and cycle similarity (I.6.10). Non-commutativity of Clifford algebras allows us to avoid complex conjugation in all these formulae—see Appendix B.5. For example, the reflection in the real line (complex conjugation) is given by matrix similarity with the corresponding matrix $\begin{pmatrix} e_1 & 0 \\ 0 & -e_1 \end{pmatrix}$.

A comparison of Exercises I.6.21 and I.6.22 suggests that there is a connection between two actions (I.6.9) and (I.6.10) of cycles, which is similar to the relation $SL_2(\mathbb{R})$ actions on points and cycles from Lemma I.5.20.

EXERCISE I.6.24. Letting $\det \tilde{C}_\sigma^s \neq 0$, show that:

- i. The $\check{\sigma}$ -similarity (I.6.10) $\check{\sigma}$ -preserves the orthogonality relation (I.6.1). More specifically, if \check{C}_σ^s and $\check{\check{C}}_\sigma^s$ are matrix similarity (I.6.10) of cycles C_σ^s and \hat{C}_σ^s , respectively, with the cycle $\tilde{C}_\sigma^{s_1}$, then

$$\left\langle \check{C}_\sigma^s, \check{\check{C}}_\sigma^s \right\rangle = \left\langle C_\sigma^s, \hat{C}_\sigma^s \right\rangle (\det \tilde{C}_\sigma^s)^2.$$

HINT: Note that $\tilde{C}_\sigma^s \overline{\tilde{C}_\sigma^s} = -\det(\tilde{C}_\sigma^s)I$, where I is the identity matrix. This is a particular case of the *Vahlen condition*, see [100, Prop. 2]. Thus, we have

$$\check{C}_\sigma^s \overline{\check{C}_\sigma^s} = -\tilde{C}_\sigma^{s_1} C_\sigma^s \overline{\hat{C}_\sigma^s \tilde{C}_\sigma^{s_1}} \cdot \det \tilde{C}_\sigma^s.$$

The final step uses the invariance of the trace under the matrix similarity. A CAS calculation is also provided.◊

- ii. The image $\tilde{Z}_\sigma^s = C_\sigma^{s_2} \overline{Z_\sigma^{s_1}} C_\sigma^{s_2}$ of a σ -zero-radius cycle $\tilde{Z}_\sigma^{s_1}$ under the similarity (I.6.10) is a σ -zero-radius cycle $\tilde{Z}_\sigma^{s_1}$. The $(s_1 s_2)$ -centre of \tilde{Z}_σ^s is the linear-fractional transformation (I.6.9) of the (s_2/s_1) -centre of Z_σ^s .
- iii. Both formulae (I.6.9) and (I.6.10) define the same transformation of the point space \mathbb{A} , with $\sigma = \check{\sigma} \neq 0$. Consequently, the linear-fractional transformation (I.6.9) maps cycles to cycles in these cases. HINT: This part follows from the first two items and Proposition I.6.8.◊
- iv. There is a cycle C_σ^s such that neither map of the parabolic point space \mathbb{D} represents similarity with C_σ^s . HINT: Consider $\tilde{C}_\sigma^s = (1, 0, \frac{1}{2}, -1)$ and a cycle C_σ^s passing point (u, v) . Then the similarity of C_σ^s with \tilde{C}_σ^s passes the point $T(u, v) = (\frac{1+v}{u}, \frac{v+y^2}{u^2})$ if and only if either
- C_σ^s is a straight line, or
 - (u, v) belongs to \check{C}_σ^s and is fixed by the above map T .

That is, the map T of the point space \mathbb{D} serves flat cycles and \check{C}_σ^s but no others. Thus, there is no map of the point space which is compatible with the cycle similarity for an arbitrary cycle.◊

Several demonstrations of inversion are provided in Fig. I.6.4. The initial setup is shown in Fig. I.6.4(a)—the red unit circle and the grid of horizontal (green) and vertical (blue) straight lines. It is very convenient in this case that the grid is formed by two orthogonal pencils of cycles, which can be considered to be of any EPH type.

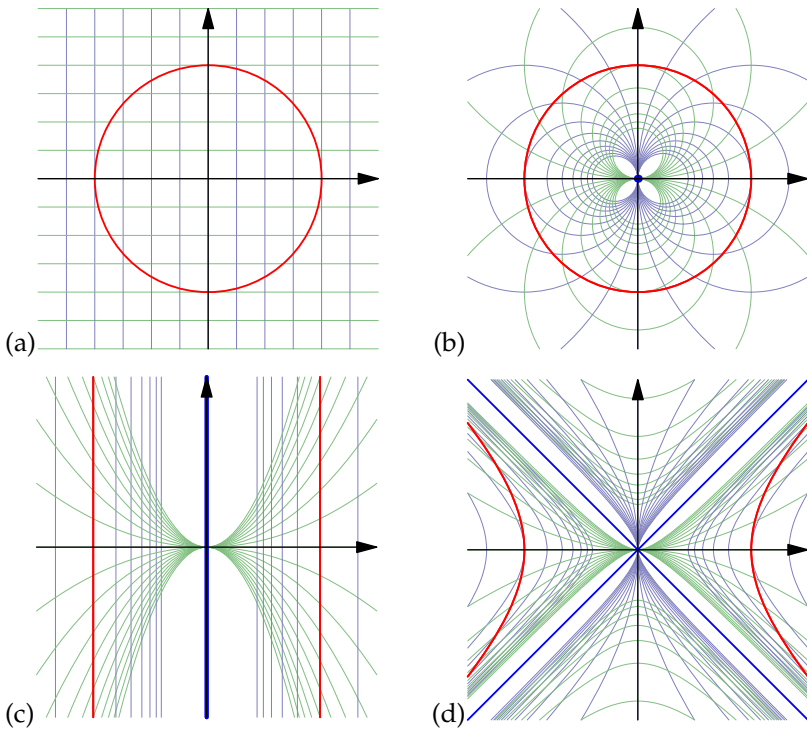


FIGURE I.6.4. Three types of inversions of the rectangular grid. The initial rectangular grid (a) is inverted elliptically in the unit circle (shown in red) in (b), parabolically in (c) and hyperbolically in (d). The blue cycle (collapsed to a point at the origin in (b)) represent the image of the cycle at infinity under inversion.

Figure I.6.4(b) shows e-inversion of the grid in the unit circle, which is, of course, the locus of fixed points. Straight lines of the rectangular grid are transformed to circles, but orthogonality between them is preserved—see Exercise I.6.24.i.

Similarly, Fig. I.6.4(c) presents the result of p-inversion in the degenerated parabolic cycle $u^2 - 1 = 0$. This time the grid is mapped to two orthogonal pencils of parabolas and vertical lines. Incidentally, due to the known optical illusion, we perceive these vertical straight lines as being bent.

Finally, Fig. I.6.4(d) demonstrates h-inversion in the unit hyperbola $u^2 - v^2 - 1 = 0$. We again obtained two pencils of orthogonal hyperbolas. The bold blue cycles—the dot at the origin in (b), vertical line in (c) and two lines (the light cone) in (d)—will be explained in Section I.8.1. Further details are provided by the following exercise.

EXERCISE I.6.25. Check that the rectangular grid in Fig. I.6.4(a) is produced by horizontal and vertical lines given by quadruples $(0, 0, 1, m)$ and $(0, 1, 0, m)$, respectively. The similarity with the cycle $(1, 0, 0, -1)$ sends a cycle (k, l, n, m) to (m, l, n, k) . In particular, the image of the grid are cycles $(m, 0, 1, 0)$ and $(m, 1, 0, 0)$.

We conclude this section by an observation that cycle similarity is similar to a mirror reflection, which preserves the directions of vectors parallel to the mirror and reverses vectors which are orthogonal.

EXERCISE I.6.26. Let $\det \tilde{C}_\sigma^s \neq 0$. Then, for similarity (I.6.10) with \tilde{C}_σ^s :

i. Verify the identities

$$\begin{aligned} -\tilde{C}_\sigma^{s_1} \overline{\tilde{C}_\sigma^s} \tilde{C}_\sigma^{s_1} &= \det_{\check{\sigma}}(\tilde{C}_\sigma^{s_1}) \cdot \tilde{C}_\sigma^{s_1} && \text{and} \\ -\tilde{C}_\sigma \overline{\tilde{C}_\sigma} \tilde{C}_\sigma &= -\det_{\check{\sigma}}(\tilde{C}_\sigma) \cdot C_\sigma, \end{aligned}$$

where C_σ^s is a cycle $\check{\sigma}$ -orthogonal to \tilde{C}_σ^s . Note the difference in the signs in the right-hand sides of both identities.

ii. Describe all cycles which are fixed (as points in the projective space \mathbb{P}^3) by the similarity with the given cycle \tilde{C}_σ^s . HINT: Use a decomposition of a generic cycle into a sum \tilde{C}_σ^s and a cycle orthogonal to \tilde{C}_σ^s similar to (I.6.7). \diamond

As we will see in the next section, these orthogonal reflections in the cycle space correspond to “bent” reflections in the point space.

I.6.5. Inversions and Reflections in Cycles

The maps in point and cycle spaces considered in the previous section were introduced from the action of FSCc matrices of cycles. They can also be approached from the more geometrical viewpoint. There are at least two natural ways to define an inversion in a cycle:

- One possibility uses orthogonality from Section I.6.1. As we can observe from Fig. I.6.3, all cycles from the blue family passing the point b also meet again at the point d . This defines a correspondence $b \leftrightarrow d$ on the point space.
- Another option defines “reflections in cycles”. The mirror reflection $z \rightarrow \bar{z}$ in the horizontal axis is a fundamental operation. If we transform a generic cycle to the real line, then we can extend the notion of reflection to the cycle.

We can formalise the above observations as follows.

DEFINITION I.6.27. For a given cycle C_σ^s , we define two maps of the point space \mathbb{A} associated to it:

- A $\check{\sigma}$ -inversion in a σ -cycle C_σ^s sends a point $b \in \mathbb{A}$ to the second point d of the intersection of all σ -cycles $\check{\sigma}$ -orthogonal to C_σ^s and passing through b —see Fig. I.6.3.
- A $\check{\sigma}$ -reflection in a σ -cycle C_σ^s is given by $M^{-1}RM$, where M is a $\check{\sigma}$ -similarity (I.6.10) which sends the σ -cycle C_σ^s into the horizontal axis and R is the mirror reflection of \mathbb{A} in that axis.

We are going to see that inversions are given by (I.6.9) and reflections are expressed through (I.6.10), thus they are essentially the same for EH cases in light of Exercise I.6.24.i. However, some facts are easier to establish using the inversion and others in terms of reflection. Thus, it is advantageous to keep both notions. Since we have three different EPH orthogonalities between cycles for every type of point space, there are also three different inversions in each of them.

EXERCISE I.6.28. Prove the following properties of inversion:

- i. Let a cycle \tilde{C}_σ^s be $\check{\sigma}$ -orthogonal to a cycle $C_\sigma^s = (k, l, n, m)$. Then, for any point $u_1 + \iota v_1 \in \mathbb{A} (\iota^2 = \sigma)$ belonging to σ -implementation of \tilde{C}_σ^s , this implementation also passes through the image of $u_1 + \iota v_1$ under the Möbius transform (I.6.9) defined by the matrix $C_\sigma^{\check{\sigma}}$:

$$(I.6.11) \quad u_2 + \iota v_2 = C_\sigma^{\check{\sigma}}(u_1 - \iota v_1) = \begin{pmatrix} l + \iota \check{\sigma} n & -m \\ k & -l + \iota \check{\sigma} n \end{pmatrix} (u_1 - \iota v_1).$$

Thus, the point $u_2 + \iota v_2$ is the *inversion* of $u_1 + \iota v_1$ in C_σ^s .

- ii. Conversely, if a cycle \tilde{C}_σ^s passes two different points $u_1 + \iota v_1$ and $u_2 + \iota v_2$ related through (I.6.11), then \tilde{C}_σ^s is $\check{\sigma}$ -orthogonal to C_σ^s .
- iii. If a cycle \tilde{C}_σ^s is $\check{\sigma}$ -orthogonal to a cycle C_σ^s , then the $\check{\sigma}$ -inversion in C_σ^s sends \tilde{C}_σ^s to itself.
- iv. $\check{\sigma}$ -inversion in the σ -implementation of a cycle C_σ^s coincides with σ -inversion in its $\check{\sigma}$ -ghost cycle \tilde{C}_σ^s .

Note the interplay between parameters σ and $\check{\sigma}$ in the above statement I.6.28.i. Although we are speaking about $\check{\sigma}$ -orthogonality, we take the Möbius transformation (I.6.11) with the imaginary unit ι such that $\iota^2 = \sigma$ (as the signature of the point space). On the other hand, the value $\check{\sigma}$ is used there as the s -parameter for the cycle $C_\sigma^{\check{\sigma}}$.

PROPOSITION I.6.29. *The reflection I.6.27.ii of a zero-radius cycle Z_σ^s in a cycle C_σ^s is given by the similarity $C_\sigma^s \overline{Z_\sigma^s} C_\sigma^s$.*

PROOF. Let a cycle \tilde{C}_σ^s have the property $\tilde{C}_\sigma^s \overline{C_\sigma^s} \tilde{C}_\sigma^s = R_\sigma^s$, where R_σ^s is the cycle representing the real line. Then, $\tilde{C}_\sigma^s R_\sigma^s \tilde{C}_\sigma^s = C_\sigma^s$, since $\overline{\tilde{C}_\sigma^s} \tilde{C}_\sigma^s = \tilde{C}_\sigma^s \overline{\tilde{C}_\sigma^s} = -\det \tilde{C}_\sigma^s I$. The mirror reflection in the real line is given by the similarity with R_σ^s , therefore the transformation described in I.6.27.ii is a similarity with the cycle $\tilde{C}_\sigma^s R_\sigma^s \tilde{C}_\sigma^s = C_\sigma^s$ and, thus, coincides with (I.6.11). \square

COROLLARY I.6.30. *The $\check{\sigma}$ -inversion with a cycle C_σ^s in the point space \mathbb{A} coincides with $\check{\sigma}$ -reflection in C_σ^s .*


The auxiliary cycle \tilde{C}_σ^s from the above proof of Prop. I.6.29 is of separate interest and can be characterised in the elliptic and hyperbolic cases as follows.

EXERCISE I.6.31. Let $C_\sigma^s = (k, l, n, m)$ be a cycle such that $\check{\sigma} \det C_\sigma^s > 0$ for $\check{\sigma} \neq 0$. Let us define the cycle \tilde{C}_σ^s by the quadruple $(k, l, n \pm \sqrt{\check{\sigma} \det C_\sigma^s}, m)$. Then:

- i. $\tilde{C}_\sigma^s C_\sigma^s \tilde{C}_\sigma^s = \mathbb{R}$ and $\tilde{C}_\sigma^s \mathbb{R} \tilde{C}_\sigma^s = C_\sigma^s$.
- ii. \tilde{C}_σ^s and C_σ^s have common roots.
- iii. In the $\check{\sigma}$ -implementation, the cycle C_σ^s passes the centre of \tilde{C}_σ^s .

HINT: One can directly observe I.6.31.ii for real roots, since they are fixed points of the inversion. Also, the transformation of C_σ^s to a flat cycle implies that C_σ^s passes the centre of inversion, hence I.6.31.iii. There is also a CAS calculation for this. \diamond

Inversions are helpful for transforming pencils of cycles to the simplest possible form.

 EXERCISE I.6.32. Check the following:


- i. Let the σ -implementation of a cycle C_σ^s pass the σ -centre of a cycle \tilde{C}_σ^s . Then, the σ -reflection of C_σ^s in \tilde{C}_σ^s is a straight line.
- ii. Let two cycles C_σ^s and \tilde{C}_σ^s intersect in two points $P, P' \in \mathbb{A}$ such that $P - P'$ is not a divisor of zero in the respective number system. Then, there is an inversion which maps the pencil of cycles orthogonal to C_σ^s and \tilde{C}_σ^s (see Exercise I.6.10.ii) into a pencil of concentric cycles. HINT: Make an inversion into a cycle with σ -centre P , then C_σ^s and \tilde{C}_σ^s will be transformed into straight lines due to the previous item. These straight lines will intersect in a finite point P'' which is the image of P' under the inversion. The pencil orthogonal to C_σ^s and \tilde{C}_σ^s will be transformed to a pencil orthogonal to these two straight lines. A CAS calculations shows that all cycles from the pencil have σ -centre at P'' . \diamond

A classical source of the above result in inversive geometry [71, Thm. 5.71] tells that an inversion can convert any pair of non-intersecting circles to concentric ones. This is due to the fact that an orthogonal pencil to the pencil generated by two non-intersecting circles always passes two special points—see Exercise I.6.10.iii for further development.

Finally, we compare our consideration for the parabolic point space with Yaglom's book. The Möbius transformation (I.6.9) and the respective inversion illustrated by Fig. I.6.4(c) essentially coincide with the *inversion of the first kind* from [339, § 10]. Yaglom also introduces the *inversion of the second kind*, see [339, § 10]. For a parabola $v = k(u - l)^2 + m$, he defined the map of the parabolic point space to be

$$(I.6.12) \quad (u, v) \mapsto (u, 2(k(u - l)^2 + m) - v),$$

i.e. the parabola bisects the vertical line joining a point and its image. There are also other geometric characterisations of this map in [339], which make it very similar to the Euclidean inversion in a circle. Here is the resulting expression of this transformation through the usual inversion in parabolas:

 EXERCISE I.6.33. The inversion of the second kind (I.6.12) is a composition of three Möbius transformations (I.6.9) defined by cycles $(1, l, 2m, l^2 + m/k)$, $(1, l, 0, l^2 + m/k)$ and the real line in the parabolic point space \mathbb{D} .

Möbius transformations (I.6.9) and similarity (I.6.12) with FSCc matrices map cycles to cycles just like matrices from $SL_2(\mathbb{R})$ do. It is natural to ask for a general type of matrices sharing this property. For this, see works [65, 100, 289] which deal with more general elliptic and hyperbolic (but not parabolic) cases. It is beyond the scope of our consideration since it derails from the geometry of $SL_2(\mathbb{R})$. We only mention the rôle of the Vahlen condition, $C_\sigma^s C_\sigma^s = -\det(C_\sigma^s)I$, used in Exercise I.6.24.i.

I.6.6. Higher-order Joint Invariants: Focal Orthogonality

Considering Möbius action (I.1.1), there is no need to be restricted to joint invariants of two cycles and a bilinear form. Indeed, for any polynomial $p(x_1, x_2, \dots, x_n)$ of

several non-commuting variables, one may define an invariant joint disposition of n cycles ${}^jC_{\check{\sigma}}^s$ by the condition

$$(I.6.13) \quad \text{tr } p({}^1C_{\check{\sigma}}^s, {}^2C_{\check{\sigma}}^s, \dots, {}^nC_{\check{\sigma}}^s) = 0,$$

where the polynomial of FSCc matrices is defined through standard matrix algebra. To create a Möbius invariant which is not affected by the projectivity in the cycle space we can either

- use a polynomial p which is homogeneous in every variable x_i , or
- substitute variables x_i with the cycles' det-normalised FSCc matrices.

Furthermore, for any two polynomials $p(x_1, x_2, \dots, x_n)$ and $q(x_1, x_2, \dots, x_n)$ such that for each variable x_i the orders of homogeneity of p and q are equal, the value

$$\frac{\text{tr } p({}^1C_{\check{\sigma}}^s, {}^2C_{\check{\sigma}}^s, \dots, {}^nC_{\check{\sigma}}^s)}{\text{tr } q({}^1C_{\check{\sigma}}^s, {}^2C_{\check{\sigma}}^s, \dots, {}^nC_{\check{\sigma}}^s)}$$

is a Möbius invariant. The simplest and yet most important realisation of this concept is the cycles cross ratio in § I.12.3

Let us construct some lower-order realisations of (I.6.13). In order to be essentially different from the previously considered orthogonality, such invariants may either contain non-linear powers of the same cycle, or accommodate more than two cycles. In this respect, consideration of higher-order invariants is similar to a transition from Riemannian to Finsler geometry [62, 107]. The latter is based on the replacement of the quadratic line element $g^{ij} dx_i dx_j$ in the tangent space by a more complicated function.

A further observation is that we can simultaneously study several invariants of various orders and link one to another by some operations. There are some standard procedures changing orders of invariants working in both directions:

- i. Higher-order invariants can be built on top of those already defined;
- ii. Lower-order invariants can be derived from higher ones.

Consider both operations as an example. We already know that a similarity of a cycle with another cycle produces a new cycle. The cycle product of the latter with a third cycle creates a joint invariant of these three cycles

$$(I.6.14) \quad \langle {}^1C_{\check{\sigma}}^s, {}^2C_{\check{\sigma}}^s, {}^1C_{\check{\sigma}}^s, {}^3C_{\check{\sigma}}^s \rangle,$$

which is built from the second-order invariant $\langle \cdot, \cdot \rangle$. Now we can reduce the order of this invariant by fixing ${}^3C_{\check{\sigma}}^s$ to be the real line, since it is $SL_2(\mathbb{R})$ -invariant. This invariant deserves special consideration. Its geometrical meaning is connected to the matrix similarity of cycles (I.6.10) (inversion in cycles) and orthogonality.

DEFINITION I.6.34. A cycle $\tilde{C}_{\check{\sigma}}^s$ is $\check{\sigma}$ -focal orthogonal (or $f_{\check{\sigma}}$ -orthogonal) to a cycle $C_{\check{\sigma}}^s$ if the $\check{\sigma}$ -reflection of $C_{\check{\sigma}}^s$ in $\tilde{C}_{\check{\sigma}}^s$ is $\check{\sigma}$ -orthogonal (in the sense of Definition I.6.1) to the real line. We denote it by $\tilde{C}_{\check{\sigma}}^s \dashv C_{\check{\sigma}}^s$.

REMARK I.6.35. This definition is explicitly based on the invariance of the real line and is an illustration to the boundary value effect from Remark I.5.3.

EXERCISE I.6.36. f -orthogonality is equivalent to either of the following

- i. The cycle $\tilde{C}_{\check{\sigma}}^s \overline{C_{\check{\sigma}}^s} \tilde{C}_{\check{\sigma}}^s$ is a *selfadjoint cycle*, see Definition I.6.12.

ii. Analytical condition:

$$(I.6.15) \quad \left\langle \tilde{C}_\sigma^s \overline{C}_\sigma^s \tilde{C}_\sigma^s, R_\sigma^s \right\rangle = \text{tr}(\tilde{C}_\sigma^s \overline{C}_\sigma^s \tilde{C}_\sigma^s R_\sigma^s) = 0.$$

REMARK I.6.37. It is easy to observe the following:

- i. f-orthogonality is not symmetric: $C_\sigma^s \dashv \tilde{C}_\sigma^s$ does not imply $\tilde{C}_\sigma^s \dashv C_\sigma^s$.
- ii. Since the horizontal axis R_σ^s and orthogonality (I.6.1) are $\text{SL}_2(\mathbb{R})$ -invariant objects, f-orthogonality is also $\text{SL}_2(\mathbb{R})$ -invariant.

However, an invariance of f-orthogonality under inversion of cycles required some study since, in general, the real line is not invariant under such transformations.

EXERCISE I.6.38. The image $\hat{C}_\sigma^{s_1} R_\sigma^s \hat{C}_\sigma^{s_1}$ of the real line under inversion in $\hat{C}_\sigma^{s_1} = (k, l, n, m)$ with $s \neq 0$ is the cycle

$$(2ss_1\check{\sigma}kn, 2ss_1\check{\sigma}ln, -\det(C_\sigma^{s_1}), 2ss_1\check{\sigma}mn).$$

It is the real line again if $\det(C_\sigma^{s_1}) \neq 0$ and either

- i. $s_1 n = 0$, in which case it is a composition of $\text{SL}_2(\mathbb{R})$ -action by $\begin{pmatrix} l & -m \\ k & -l \end{pmatrix}$ and the reflection in the real line, or
- ii. $\check{\sigma} = 0$, i.e. the parabolic case of the cycle space.

If either of two conditions is satisfied then f-orthogonality $\tilde{C}_\sigma^s \dashv C_\sigma^s$ is preserved by the $\check{\sigma}$ -similarity with $\hat{C}_\sigma^{s_1}$.

The following explicit expressions of f-orthogonality reveal further connections with cycles' invariants.

EXERCISE I.6.39. f-orthogonality of \tilde{C}_σ^s to $C_\sigma^{s_1}$ is given by either of the equivalent identities

$$\begin{aligned} sn(\tilde{l}^2 + \check{\sigma}s_1^2\tilde{n}^2 - \tilde{m}\tilde{k}) + s_1\tilde{n}(m\tilde{k} - 2\tilde{l}l + k\tilde{m}) &= 0 \quad \text{or} \\ n \det(\tilde{C}_\sigma^1) + \tilde{n} \left\langle C_\sigma^1, \tilde{C}_\sigma^1 \right\rangle &= 0, \quad \text{if } s = s_1 = 1. \end{aligned}$$

The f-orthogonality may again be related to the usual orthogonality through an appropriately chosen *f-ghost cycle*, cf. Proposition I.6.19:

PROPOSITION I.6.40. Let C_σ^s be a cycle. Then, its f-ghost cycle $\check{C}_\sigma^{\check{\sigma}} = C_\sigma^{\chi(\sigma)} \mathbb{R}_\sigma^{\check{\sigma}} C_\sigma^{\chi(\sigma)}$ is the reflection of the real line in $C_\sigma^{\chi(\sigma)}$, where $\chi(\sigma)$ is the Heaviside function (I.6.8). Then:

- i. Cycles C_σ^1 and $\check{C}_\sigma^{\check{\sigma}}$ have the same roots.
- ii. The $\chi(\sigma)$ -centre of $\check{C}_\sigma^{\check{\sigma}}$ coincides with the $(-\check{\sigma})$ -focus of C_σ^s , consequently all straight lines $\check{\sigma}$ -f-orthogonal to C_σ^s pass its $(-\check{\sigma})$ -focus.
- iii. f-inversion in C_σ^s defined from f-orthogonality (see Definition I.6.27.i) coincides with the usual inversion in $\check{C}_\sigma^{\check{\sigma}}$.

Note the above intriguing interplay between the cycle's centres and foci. It also explains our choice of name for focal orthogonality, cf. Definition I.6.17.i. f-Orthogonality and the respective f-ghost cycles are presented in Fig. I.6.5, which uses the same outline and legend as Fig. I.6.3.

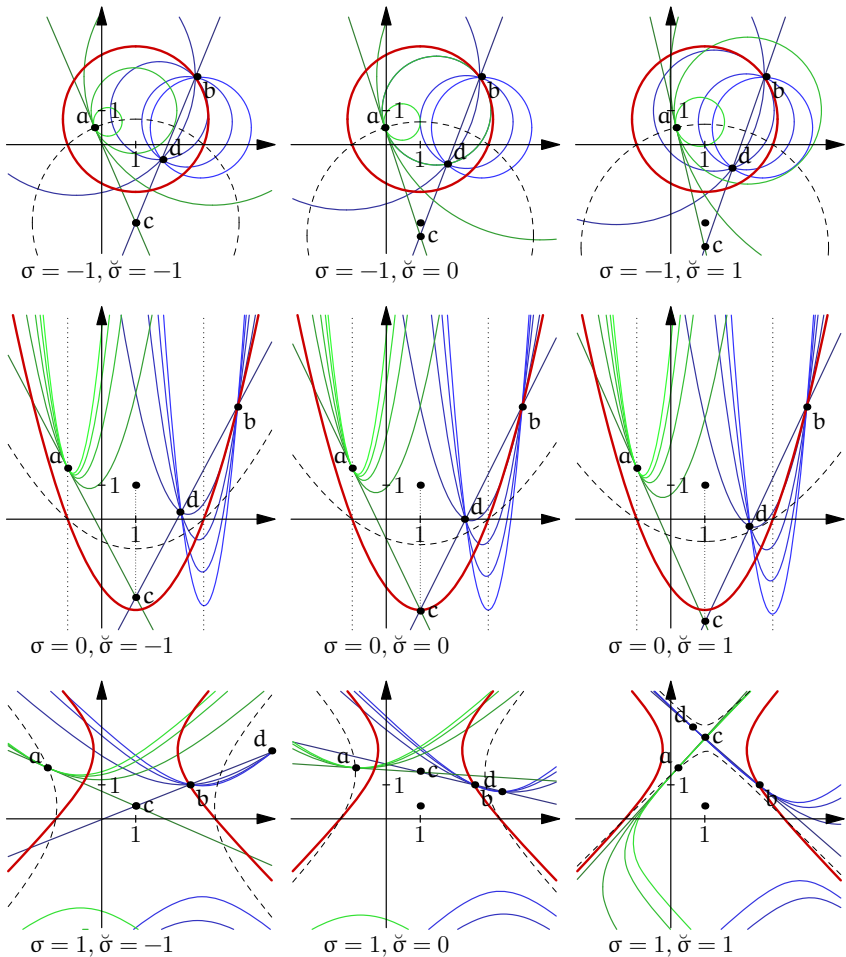


FIGURE I.6.5. Focal orthogonality of cycles. In order to highlight both the similarities and distinctions with the ordinary orthogonality, we use the same notations as in Fig. I.6.3.

The definition of f-orthogonality may look rather extravagant at first glance. However, it will find new support when we again consider lengths and distances in the next chapter. It will also be useful for infinitesimal cycles, cf. Section I.7.5.

Of course, it is possible and meaningful to define other interesting higher-order joint invariants of two or even more cycles.

Metric Invariants in Upper Half-Planes

So far, we have discussed only invariants like orthogonality, which are related to angles. However, *geometry*, in the plain meaning of the word, deals with measurements of *distances* and *lengths*. We will derive metrical quantities from cycles in a way which shall be Möbius-invariant.

I.7.1. Distances

Cycles are covariant objects performing as “circles” in our three EPH geometries. Now we play *the traditional mathematical game*: turn some properties of classical objects into definitions of new ones.

DEFINITION I.7.1. The $\check{\sigma}$ -radius $r_{\check{\sigma}}$ of a cycle $C_{\check{\sigma}}^s$, if squared, is equal to the minus $\check{\sigma}$ -determinant of the cycle’s k -normalised (see Definition I.5.5) matrix, i.e.

$$(I.7.1) \quad r_{\check{\sigma}}^2 = -\frac{\langle C_{\check{\sigma}}^s, C_{\check{\sigma}}^s \rangle}{2k^2} = -\frac{\det C_{\check{\sigma}}^s}{k^2} = \frac{l^2 - \check{\sigma}s^2n^2 - km}{k^2}.$$

As usual, the $\check{\sigma}$ -diameter of a cycle is two times its radius.

The expression (I.7.1) for radius through the invariant cycle product resembles the definition of the norm of a vector in an inner product space [164, § 5.1].

EXERCISE I.7.2. Check the following geometrical content of the formula (I.7.1):

- (e,h): The value of (I.7.1) is the usual radius of a circle or hyperbola given by the equation $k(u^2 - \sigma v^2) - 2lu - 2nv + m = 0$.
- (p): The diameter of a parabola is the (Euclidean) distance between its (real) roots, i.e. solutions of $ku^2 - 2lu + m = 0$, or roots of its “adjoint” parabola $-ku^2 + 2lu + m - \frac{2l^2}{k} = 0$ (see Fig. I.1.9(a)).

EXERCISE I.7.3. Check the following relations:

- i. The $\check{\sigma}$ -radius of a cycle $C_{\check{\sigma}}^s$ is equal to $1/k$, where k is the $(2, 1)$ -entry of the det-normalised FSCc matrix (see Definition I.5.5) of the cycle.
- ii. Let $u_{\check{\sigma}}$ be the second coordinate of a cycle’s $\check{\sigma}$ -focus and f be its focal length. Then, the square of the cycle’s $\check{\sigma}$ -radius is

$$r_{\check{\sigma}}^2 = -4fu_{\check{\sigma}}.$$

- iii. Cycles (I.5.8) have zero $\check{\sigma}$ -radius, thus Definitions I.5.13 and I.7.1 agree.

An intuitive notion of a distance in both mathematics and everyday life is usually of a variational nature. We naturally perceive a straight line as the route of the shortest distance between two points. Then, we can define the distance along a curved path through an approximation. This variational nature is also echoed in the following definition:

DEFINITION I.7.4. The $(\sigma, \check{\sigma})$ -distance $d_{\sigma, \check{\sigma}}(P, P')$ between two points P and P' is the extremum of $\check{\sigma}$ -diameters for all σ -implementations of cycles passing P and P' .

It is easy to see that the distance is a symmetric function of two points. □

LEMMA I.7.5. *The distance between two points $P = u + v$ and $P' = u' + v'$ in the elliptic or hyperbolic spaces is*

$$(I.7.2) \quad d_{\sigma, \check{\sigma}}^2(P, P') = \frac{\check{\sigma}((u - u')^2 - \sigma(v - v')^2) + 4(1 - \sigma\check{\sigma})vv'}{(u - u')^2\check{\sigma} - (v - v')^2}((u - u')^2 - \sigma(v - v')^2),$$

and, in parabolic space, it is (see Fig. I.1.9(b) and also [339, (5), p. 38])

$$(I.7.3) \quad d_{p, \check{\sigma}}^2(y, y') = (u - u')^2.$$

PROOF. Let $C_s^\sigma(l)$ be the family of cycles passing through both points (u, v) and (u', v') (under the assumption $v \neq v'$) and parametrised by its coefficient l , which is the first coordinate of the cycle's centre. By a symbolic calculation in CAS, we found that the only critical point of $\det(C_s^\sigma(l))$ is

$$(I.7.4) \quad l_0 = \frac{1}{2} \left((u' + u) + (\check{\sigma}\sigma - 1) \frac{(u' - u)(v^2 - v'^2)}{(u' - u)^2\check{\sigma} - (v - v')^2} \right).$$

Note that, for the case $\sigma\check{\sigma} = 1$, i.e. when both point and cycle spaces are simultaneously either elliptic or hyperbolic, this expression reduces to the expected midpoint $l_0 = \frac{1}{2}(u + u')$. Since, in the elliptic or hyperbolic case, the parameter l can take any real value, the extremum of $\det(C_s^\sigma(l))$ is reached in l_0 and is equal to (I.7.2), again calculated by CAS. A separate calculation for the case $v = v'$ gives the same answer.

In the parabolic case, possible values of l are either in the ranges $(-\infty, \frac{1}{2}(u + u'))$ or $(\frac{1}{2}(u + u'), \infty)$, or only $l = \frac{1}{2}(u + u')$ since, for that value, a parabola should flip between the upward and downward directions of its branches. In any of these cases, the extreme value corresponds to the boundary point $l = \frac{1}{2}(u + u')$ and is equal to (I.7.3). □

To help understand the complicated identity (I.7.2), we may observe that

$$\begin{aligned} d_{e,e}^2(P, P') &= (u - u')^2 + (v - v')^2, & \text{for elliptic values } \sigma = \check{\sigma} = -1, \\ d_{h,h}^2(P, P') &= (u - u')^2 - (v - v')^2, & \text{for hyperbolic values } \sigma = \check{\sigma} = 1. \end{aligned}$$

These are familiar expressions for distances in the elliptic and hyperbolic spaces. However, for other cases (such that $\sigma\check{\sigma} = -1$ or 0) quite different results are obtained. For example, $d_{\sigma, \check{\sigma}}^2(P, P')$ does not tend to 0 if $P \rightarrow P'$ in the usual sense.

EXERCISE I.7.6. Show that:

- i. In the three cases $\sigma = \check{\sigma} = -1, 0$ or 1 , which were typically studied in the literature, the above distances are conveniently defined through the arithmetic of corresponding numbers:

$$(I.7.5) \quad d_{\sigma, \sigma}^2(u + \iota v) = (u + \iota v)(u - \iota v) = w\bar{w}.$$

- ii. Unless $\sigma = \check{\sigma}$, the parabolic distance $d_{p, \check{\sigma}}$ (I.7.3) is not obtained from (I.7.2) by the substitution $\sigma = 0$.
 iii. If cycles $C_{\check{\sigma}}^s$ and $\tilde{C}_{\check{\sigma}}^s$ are k -normalised, then

$$\langle C_{\check{\sigma}}^s - \tilde{C}_{\check{\sigma}}^s, C_{\check{\sigma}}^s - \tilde{C}_{\check{\sigma}}^s \rangle = 2 \det(C_{\check{\sigma}}^s - \tilde{C}_{\check{\sigma}}^s) = -2d_{\check{\sigma}, \check{\sigma}}^2(P, \tilde{P}),$$

where P and \tilde{P} are e - or h -centres of $C_{\check{\sigma}}^s$ and $\tilde{C}_{\check{\sigma}}^s$. Therefore, we can rewrite the relation (I.5.5) for the cycle product

$$\langle C_{\check{\sigma}}^s, \tilde{C}_{\check{\sigma}}^s \rangle = d_{\check{\sigma}, \check{\sigma}}^2(P, \tilde{P}) - r_{\check{\sigma}}^2 - \tilde{r}_{\check{\sigma}}^2,$$

using $r_{\check{\sigma}}$ and $\tilde{r}_{\check{\sigma}}$ —the $\check{\sigma}$ -radii of the respective cycles. In particular, cf. (I.5.9),

$$\langle Z_{\check{\sigma}}^s, \tilde{Z}_{\check{\sigma}}^s \rangle = d_{\check{\sigma}, \check{\sigma}}^2(P, \tilde{P}),$$

for k -normalised $\check{\sigma}$ -zero-radius cycles $Z_{\check{\sigma}}^s$ and $\tilde{Z}_{\check{\sigma}}^s$ with centres P and \tilde{P} . From Exercise I.5.21 we can also derive that $d_{\check{\sigma}, \check{\sigma}}^2(P, \tilde{P})$ is equal to the power of the point P (\tilde{P}) with respect to the cycle $\tilde{Z}_{\check{\sigma}}^s$ ($Z_{\check{\sigma}}^s$).

Using the notation $d_{\sigma, \sigma}^2(P) = d_{\sigma, \sigma}^2(0, P)$, we can now rewrite the identities (I.3.36)–(I.3.37) as:

$$\begin{aligned} (uu' - \sigma vv')^2 &= \cos_{\sigma}^2(P, P') d_{\sigma, \sigma}^2(P) d_{\sigma, \sigma}^2(P'), \\ (uv' - \iota vu')^2 &= \sin_{\sigma}^2(P, P') d_{\sigma, \sigma}^2(P) d_{\sigma, \sigma}^2(P'). \end{aligned}$$

The distance allows us to expand the result for all EPH cases, which is well known in the cases of circles [71, § 2.1] and parabolas [339, § 10].

EXERCISE I.7.7. Show that the power of a point W with respect to a cycle (see Definition I.3.18) is the product $d_{\sigma}(W, P) \cdot d_{\sigma}(W, P')$ of (σ, σ) -distances (I.7.5), where P and P' are any two points of the cycle which are collinear with W . **HINT:** Take $P = (u, v)$ and $P' = (u', v')$. Then, any collinear W is $(tu + (1-t)u', tv + (1-t)v')$ for some $t \in \mathbb{R}$. Furthermore, a simple calculation shows that $d_{\sigma}(y, z) \cdot d_{\sigma}(z, y') = t(t-1)d_{\sigma}^2(y, y')$. The last expression is equal to the power of W with respect to the cycle—this step can be done by CAS. ◊

EXERCISE I.7.8. Let two cycles have e -centres P and P' with $\check{\sigma}$ -radii $r_{\check{\sigma}}$ and $r'_{\check{\sigma}}$. Then, the $(\check{\sigma}, \check{\sigma})$ -power of one cycle with respect to another from Definition I.5.22 is, cf. the elliptic case in (I.5.10),

$$\frac{d_{\check{\sigma}, \check{\sigma}}^2(P, P') - r_{\check{\sigma}}^2 - r'_{\check{\sigma}}^2}{2r_{\check{\sigma}} r'_{\check{\sigma}}}.$$

I.7.2. Lengths

During geometry classes, we often make measurements with a compass, which is based on the idea that a *circle is a locus of points equidistant from its centre*. We can expand it for all cycles with the following definition:

DEFINITION I.7.9. The $(\sigma, \check{\sigma}, \hat{\sigma})$ -length from the $\hat{\sigma}$ -centre (from the $\hat{\sigma}$ -focus) of a directed interval \overrightarrow{AB} is the $\check{\sigma}$ -radius of the σ -cycle with its $\hat{\sigma}$ -centre ($\hat{\sigma}$ -focus) at the point A which passes through B. These lengths are denoted by $l_c(\overrightarrow{AB})$ and $l_f(\overrightarrow{AB})$, respectively.

It is easy to be confused by the triple of parameters σ , $\check{\sigma}$ and $\hat{\sigma}$ in this definition. However, we will rarely operate in such a generality, and some special relations between the different sigmas will often be assumed. We also do not attach the triple $(\sigma, \check{\sigma}, \hat{\sigma})$ to $l_c(\overrightarrow{AB})$ and $l_f(\overrightarrow{AB})$ in formulae, since their values will be clear from the surrounding text.

EXERCISE I.7.10. Check the following properties of the lengths:

- i. The length is *not* a symmetric function of two points (unlike the distance).
- ii. A cycle is uniquely defined by its elliptic or hyperbolic centre and a point which it passes. However, the parabolic centre is not as useful. Consequently, lengths from the parabolic centre are not properly defined, therefore we always assume $\hat{\sigma} = \pm 1$ for lengths from a centre.
- iii. A cycle is uniquely defined by any focus and a point which it passes.

We now turn to calculations of the lengths.

LEMMA I.7.11. For two points $P = u + iv$, $P' = u' + iv' \in \mathbb{A}$:

- i. The $\check{\sigma}$ -length from the $\hat{\sigma}$ -centre for $\hat{\sigma} = \pm 1$ between P and P' is

$$(I.7.6) \quad l_{c_{\hat{\sigma}}}^2(\overrightarrow{PP'}) = (u - u')^2 - \sigma v'^2 + 2\hat{\sigma}vv' - \check{\sigma}v^2.$$

- ii. The $\check{\sigma}$ -length from the $\hat{\sigma}$ -focus between P and P' is

$$(I.7.7) \quad l_{f_{\hat{\sigma}}}^2(\overrightarrow{PP'}) = (\hat{\sigma} - \check{\sigma})p^2 - 2vp,$$

where:

$$(I.7.8) \quad p = \hat{\sigma} \left(-(v' - v) \pm \sqrt{\hat{\sigma}(u' - u)^2 + (v' - v)^2 - \sigma\hat{\sigma}v'^2} \right), \quad \text{if } \hat{\sigma} \neq 0$$

$$(I.7.9) \quad p = \frac{(u' - u)^2 - \sigma v'^2}{2(v' - v)}, \quad \text{if } \hat{\sigma} = 0.$$

PROOF. Identity (I.7.6) is verified with CAS. For the second part, we observe that a cycle with the $\hat{\sigma}$ -focus (u, v) passing through $(u', v') \in \mathbb{A}$ has the parameters:

$$k = 1, \quad l = u, \quad n = p, \quad m = 2\hat{\sigma}pv' - u'^2 + 2uu' + \sigma v'^2.$$

Then, the formula (I.7.7) is verified by the CAS calculation. □

EXERCISE I.7.12. Check that:

- i. The value of p in (I.7.8) is the focal length of either of the two cycles, which are, in the parabolic case, upward or downward parabolas (corresponding to the plus or minus signs) with focus at (u, v) and passing (u', v') .
- ii. In the case $\sigma\check{\sigma} = 1$, the length from the centre (I.7.6) becomes the standard elliptic or hyperbolic distance $(u-u')^2 - \sigma(v-v')^2$ obtained in (I.7.2). Since these expressions appeared both as distances and lengths they are widely used.

On the other hand, in the parabolic point space, we obtain three additional lengths besides distance (I.7.3):

$$l_{c_{\check{\sigma}}}^2(y, y') = (u - u')^2 + 2vv' - \check{\sigma}v^2$$

parametrised by three values $-1, 0$ or -1 of $\check{\sigma}$ (cf. Remark I.3.11.i).

- iii. The parabolic distance (I.7.3) can be expressed in terms of the focal length p (I.7.8) as

$$d^2(y, y') = p^2 + 2(v - v')p,$$

an expression similar to (I.7.7).

I.7.3. Conformal Properties of Möbius Maps

All lengths $l(\overrightarrow{AB})$ in \mathbb{A} from Definition I.7.9 are such that, for a fixed point A , every contour line $l(\overrightarrow{AB}) = c$ is a corresponding σ -cycle, which is a covariant object in the appropriate geometry. This is also true for distances if $\sigma = \check{\sigma}$. Thus, we can expect some covariant properties of distances and lengths.

DEFINITION I.7.13. We say that a distance or a length d is $SL_2(\mathbb{R})$ -conformal if, for fixed $y, y' \in \mathbb{A}$, the limit

$$(I.7.10) \quad \lim_{t \rightarrow 0} \frac{d(g \cdot y, g \cdot (y + ty'))}{d(y, y + ty')}, \quad \text{where } g \in SL_2(\mathbb{R}),$$

exists and its value depends only on y and g and is independent of y' .

Informally rephrasing this definition, we can say that a distance or length is $SL_2(\mathbb{R})$ -conformal if a Möbius map scales all small intervals originating at a point by the same factor. Also, since a scaling preserves the shape of cycles, we can restate the $SL_2(\mathbb{R})$ -conformality once more in familiar terms: small cycles are mapped to small cycles. To complete the analogy with conformality in the complex plane we note that preservation of angles (at least orthogonality) by Möbius transformations is automatic.

EXERCISE I.7.14. Show $SL_2(\mathbb{R})$ -conformality in the following cases:

- i. The distance (I.7.2) is conformal if and only if the type of point and cycle spaces are the same, i.e. $\sigma\check{\sigma} = 1$. The parabolic distance (I.7.3) is conformal only in the parabolic point space.
- ii. The lengths from centres (I.7.6) are conformal for any combination of values of $\sigma, \check{\sigma}$ and $\check{\sigma}$.
- iii. The lengths from foci (I.7.7) are conformal for $\check{\sigma} \neq 0$ and any combination of values of σ and $\check{\sigma}$.

The conformal property of the distance (I.7.2) and (I.7.3) from Proposition I.7.14.i is, of course, well known (see [65, 339]). However, the same property of non-symmetric lengths from Proposition I.7.14.ii and I.7.14.iii could hardly be expected. As a possible reason, one remarks that the smaller group $SL_2(\mathbb{R})$ (in comparison to all linear-fractional transforms of the whole \mathbb{R}^2) admits a larger number of conformal metrics, cf. Remark I.5.3.

The exception of the case $\mathring{\sigma} = 0$ from the conformality in I.7.14.iii looks disappointing at first glance, especially in the light of the parabolic Cayley transform considered later in Section I.10.3. However, a detailed study of algebraic structure invariant under parabolic rotations, see Chapter I.11, will remove obscurity from this case. Indeed, our Definition I.7.13 of conformality heavily depends on the underlying linear structure in \mathbb{A} —we measure a distance between points y and $y + ty'$ and intuitively expect that it is always small for small t . As explained in Section I.11.4, the standard linear structure is incompatible with the parabolic rotations and thus should be replaced by a more relevant one. More precisely, instead of limits $y' \rightarrow y$ along the straight lines towards y , we need to consider limits along vertical lines, as illustrated in Fig. I.10.1 and Definition I.11.23.

We will return to the parabolic case of conformality in Proposition I.11.24. An approach to the parabolic point space and a related conformality based on infinitesimal cycles will be considered in Section I.7.6.

REMARK I.7.15. The expressions of lengths (I.7.6) and (I.7.7) are generally non-symmetric and this is a price one should pay for their non-triviality. All symmetric distances lead only to nine two-dimensional Cayley–Klein geometries, see [116; 130; 131; 284; 339, App. B]. In the parabolic case, a symmetric distance of a vector (u, v) is always a function of u alone, cf. Remark I.7.21. For such a distance, a parabolic unit circle consists of two vertical lines (see dotted vertical lines in the second rows in Figs I.6.3 and I.6.5), which is not aesthetically attractive. On the other hand, the parabolic “unit cycles” defined by lengths (I.7.6) and (I.7.7) are parabolas, which makes the parabolic Cayley transform (see Section I.10.3) very natural.

We can also consider a distance between points in the upper half-plane which has a stronger property than $SL_2(\mathbb{R})$ -conformality. Namely, the metric shall be preserved by $SL_2(\mathbb{R})$ action or, in other words, Möbius transformations are isometries for it. We will study such a metric in Chapter I.9.

I.7.4. Perpendicularity and Orthogonality

In a Euclidean space, the shortest distance from a point to a straight line is provided by the corresponding perpendicular. Since we have already defined various distances and lengths, we may use them for a definition of the respective notions of perpendicularity¹.

DEFINITION I.7.16. Let l be a length or a distance. We say that a vector \overrightarrow{AB} is l -perpendicular to a vector \overrightarrow{CD} if function $l(\overrightarrow{AB} + t\overrightarrow{CD})$ of a variable t has a local

¹This concept is also known as Birkhoff orthogonality [39].

extremum at $t = 0$, cf. Fig. I.1.10. This is denoted by $\overrightarrow{AB} \lambda_l \overrightarrow{CD}$ or, simply, $\overrightarrow{AB} \lambda \overrightarrow{CD}$ if the meaning of l is clear from the context.

EXERCISE I.7.17. Check that:

- i. l -perpendicularity is not a symmetric notion (i.e. $\overrightarrow{AB} \lambda \overrightarrow{CD}$ does not imply $\overrightarrow{CD} \lambda \overrightarrow{AB}$), similar to f -orthogonality—see Section I.6.6.
- ii. l -perpendicularity is linear in \overrightarrow{CD} , i.e. $\overrightarrow{AB} \lambda \overrightarrow{CD}$ implies $\overrightarrow{AB} \lambda r\overrightarrow{CD}$ for any real non-zero r . However, l -perpendicularity is not generally linear in \overrightarrow{AB} , i.e. $\overrightarrow{AB} \lambda \overrightarrow{CD}$ does not necessarily imply $r\overrightarrow{AB} \lambda \overrightarrow{CD}$.

There is a connection between l -perpendicularity and f -orthogonality.

LEMMA I.7.18. Let \overrightarrow{AB} be l_c -perpendicular (l_f -perpendicular) to a vector \overrightarrow{CD} for a length from the centre (from the focus) defined by the triple $(\sigma, \check{\sigma}, \hat{\sigma})$. Then, the flat cycle (straight line) AB is $\hat{\sigma}$ -(f -)orthogonal to the σ -cycle C_σ^s with $\check{\sigma}$ -centre ($(-\hat{\sigma})$ -focus) at A passing through B . The vector \overrightarrow{CD} is tangent at B to the σ -implementation of C_σ^s .

PROOF. Consider the cycle C_σ^s with its $\check{\sigma}$ -centre at A and passing B in its σ -implementation. This cycle C_σ^s is a contour line for a function $l(X) = l_c(\overrightarrow{AX})$ with the triple $(\sigma, \check{\sigma}, \hat{\sigma})$. Therefore, the cycle separates regions where $l(X) < l_c(\overrightarrow{AB})$ and $l(X) > l_c(\overrightarrow{AB})$. The tangent line to C_σ^s at B (or, at least, its portion in the vicinity of B) belongs to one of these two regions, thus $l(X)$ has a local extremum at B . Therefore, \overrightarrow{AB} is l_c -perpendicular to the tangent line. The line AB is also $\hat{\sigma}$ -orthogonal to the cycle C_σ^s since it passes its $\check{\sigma}$ -centre A , cf. Exercise I.6.18.iv.

The second case of $l_f(\overrightarrow{AB})$ and f -orthogonality can be considered similarly with the obvious change of centre to focus, cf. Proposition I.6.40.ii. \square

Obviously, perpendicularity turns out to be familiar in the elliptic case, cf. Lemma I.7.20 below. For the two other cases, the description is given as follows:

EXERCISE I.7.19. Let $A = (u, v)$ and $B = (u', v')$. Then

- i. d -perpendicular (in the sense of (I.7.2)) to \overrightarrow{AB} in the elliptic or hyperbolic cases is a multiple of the vector

$$\left(\begin{array}{c} \sigma(v - v')^3 - (u - u')^2(v + v'(1 - 2\sigma\check{\sigma})) \\ \check{\sigma}(u - u')^3 - (u - u')(v - v')(-2v' + (v + v')\check{\sigma}\sigma) \end{array} \right),$$

which, for $\sigma\check{\sigma} = 1$, reduces to the expected value $(v - v', \sigma(u - u'))$.

- ii. d -perpendicular (in the sense of (I.7.3)) to \overrightarrow{AB} in the parabolic case is $(0, t)$, $t \in \mathbb{R}$ which coincides with the Galilean orthogonality defined in [339, § 3].
- iii. $l_{c_{\check{\sigma}}}$ -perpendicular (in the sense of (I.7.6)) to \overrightarrow{AB} is a multiple of $(\sigma v' - \hat{\sigma}v, u - u')$.
- iv. $l_{f_{\hat{\sigma}}}$ -perpendicular (in the sense of (I.7.7)) to \overrightarrow{AB} is a multiple of $(\sigma v' + p, u - u')$, where p is defined either by (I.7.8) or (I.7.9) for corresponding values of $\hat{\sigma}$.

HINT: Contour lines for all distances and lengths are cycles. Use implicit derivation of (I.15.3) to determine the tangent vector to a cycle at a point. Then apply the formula to a cycle which passes (u', v') and is a contour line for a distance or length from (u, v) . \diamond

It is worth having an idea about different types of perpendicularity in terms of the standard Euclidean geometry. Here are some examples.

EXERCISE I.7.20. Let $\overrightarrow{AB} = u + tv$ and $\overrightarrow{CD} = u' + tv'$. Then:

- (e) In the elliptic case, d-perpendicularity for $\check{\sigma} = -1$ means that \overrightarrow{AB} and \overrightarrow{CD} form a right angle, or, analytically, $uu' + vv' = 0$.
- (p) In the parabolic case, l_{f_σ} -perpendicularity for $\check{\sigma} = 1$ means that \overrightarrow{AB} bisects the angle between \overrightarrow{CD} and the vertical direction, or, analytically,

$$(I.7.11) \quad u'u - v'p = u'u - v'(\sqrt{u^2 + v^2} - v) = 0,$$

where p is the focal length (I.7.8).

- (h) In the hyperbolic case, d-perpendicularity for $\check{\sigma} = -1$ means that the angles between \overrightarrow{AB} and \overrightarrow{CD} are bisected by lines parallel to $u = \pm v$, or, analytically, $u'u - v'v = 0$. Compare with Exercise I.6.3(A).

REMARK I.7.21. If one attempts to devise a parabolic length as a limit or an intermediate case for the elliptic $l_e = u^2 + v^2$ and hyperbolic $l_p = u^2 - v^2$ lengths, then the only possible guess is $l'_p = u^2$ (I.7.3), which is too trivial for an interesting geometry.

Similarly, the only orthogonality condition linking the elliptic $u_1u_2 + v_1v_2 = 0$ and the hyperbolic $u_1u_2 - v_1v_2 = 0$ cases from the above exercise seems to be $u_1u_2 = 0$ (see [339, § 3] and I.7.19.ii), which is again too trivial. This supports Remark I.3.11.ii.

I.7.5. Infinitesimal-radius Cycles

Although parabolic zero-radius cycles defined in I.5.13 do not satisfy our expectations for “smallness”, they are often technically suitable for the same purposes as elliptic and hyperbolic ones. However, we may want to find something which fits our intuition about “zero-sized” objects better. Here, we present an approach based on non-Archimedean (non-standard) analysis—see, for example, [73, 328] for a detailed exposition.

Following Archimedes, a (positive) *infinitesimal number* x satisfies

$$(I.7.12) \quad 0 < nx < 1, \quad \text{for any } n \in \mathbb{N}.$$

Apart from this inequality infinitesimals obey all other properties of real numbers. In particular, in our CAS computations, an infinitesimal will be represented by a positive real symbol and we replace some of its powers by zero if their order of infinitesimality will admit this. The existence of infinitesimals in the standard real analysis is explicitly excluded by the Archimedean axiom, therefore the theory operating with infinitesimals is known as non-standard or non-Archimedean analysis. We assume from now on that there exists an infinitesimal number ϵ .

DEFINITION I.7.22. A cycle $C_{\check{\sigma}}^\epsilon$, such that $\det C_{\check{\sigma}}^\epsilon$ is an infinitesimal number, is called an *infinitesimal radius cycle*.



EXERCISE I.7.23. Let $\check{\sigma}$ and $\check{\sigma}$ be two metric signs and let a point $(u_0, v_0) \in \mathbb{D}$ with $v_0 > 0$. Consider a cycle $C_{\check{\sigma}}^\epsilon$ defined by

$$(I.7.13) \quad C_{\check{\sigma}}^\epsilon = (1, u_0, n, u_0^2 - \check{\sigma}n^2 + \epsilon^2),$$

where

$$(I.7.14) \quad n = \begin{cases} \frac{v_0 - \sqrt{v_0^2 - (\check{\sigma} - \check{\sigma}')\epsilon^2}}{\check{\sigma} - \check{\sigma}'}, & \text{if } \check{\sigma} \neq \check{\sigma}', \\ \frac{\epsilon^2}{2v_0}, & \text{if } \check{\sigma} = \check{\sigma}'. \end{cases}$$

Then,

- i. The point (u_0, v_0) is $\check{\sigma}$ -focus of the cycle.
- ii. The square of the $\check{\sigma}'$ -radius is exactly $-\epsilon^2$, i.e. (I.7.13) defines an infinitesimal-radius cycle.
- iii. The focal length of the cycle is an infinitesimal number of order ϵ^2 .

HINT: Combining two quadratic equations (one defines the squared $\check{\sigma}$ -radius, another— v -coordinate of the focus), we found that n satisfies the equation:

$$(\check{\sigma} - \check{\sigma}')n^2 - 2v_0n + \epsilon^2 = 0.$$

Moreover, only the root from (I.7.14) of the quadratic case $\check{\sigma} - \check{\sigma}' \neq 0$ gives an infinitesimal focal length. Then, we can find the m component of the cycle. The answer is also supported by CAS calculations.◊

The graph of cycle (I.7.13) in the parabolic space drawn at the scale of real numbers looks like a vertical ray starting at its focus, see Fig. I.7.1(a), due to the following result.

EXERCISE I.7.24. The infinitesimal cycle (I.7.13) consists of points which are infinitesimally close (in the sense of length from focus (I.7.7)) to its focus $F = (u_0, v_0)$:

$$(I.7.15) \quad (u_0 + \epsilon u, v_0 + v_0 u^2 + ((\check{\sigma}' - \check{\sigma})u^2 - \check{\sigma}')\frac{\epsilon^2}{4v_0} + O(\epsilon^3)).$$

Note that points below F (in the ordinary scale) are not infinitesimally close to F in the sense of length (I.7.7), but are in the sense of distance (I.7.3). Thus, having the set of points on the infinitesimal distance from an unknown point F we are not able to identify F . However, this is possible from the set of points on the infinitesimal length from F . Figure I.7.1(a) shows elliptic, hyperbolic *concentric* and parabolic *confocal* cycles of decreasing radii which shrink to the corresponding infinitesimal-radius cycles.

It is easy to see that infinitesimal-radius cycles have properties similar to zero-radius ones, cf. Lemma I.5.20.

EXERCISE I.7.25. The image of $SL_2(\mathbb{R})$ -action on an infinitesimal-radius cycle (I.7.13) by conjugation (I.4.7) is an infinitesimal-radius cycle of the same order. The image of an infinitesimal cycle under *cycle conjugation* is an infinitesimal cycle of the same or lesser order.

Consideration of infinitesimal numbers in the elliptic and hyperbolic cases should not bring any advantages since the (leading) quadratic terms in these cases are non-zero. However, non-Archimedean numbers in the parabolic case provide a more intuitive and efficient presentation. For example, zero-radius cycles are not helpful for the parabolic Cayley transform (see Section I.10.3), but infinitesimal cycles are their successful replacements. Another illustration is the second part of the following result as a useful substitution for Exercise I.6.6.iv.

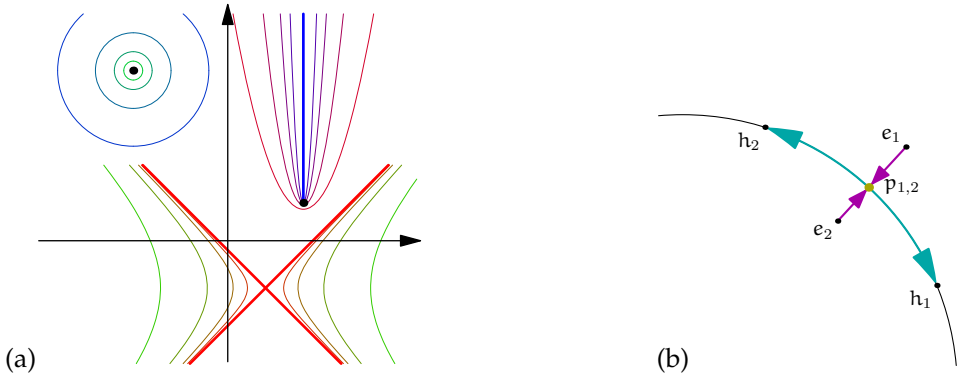


FIGURE I.7.1. Zero-radius cycles and the “phase” transition. (a) Zero-radius cycles in elliptic (black point) and hyperbolic (the red light cone) cases. The infinitesimal-radius parabolic cycle is the blue vertical ray starting at the focus. (b) Elliptic-parabolic-hyperbolic phase transition between fixed points of a subgroup. Two fixed points of an elliptic subgroup collide to a parabolic double point on the boundary and then decouple into two hyperbolic fixed points on the unit disk.

EXERCISE I.7.26. Let C_σ^s be the infinitesimal cycle (I.7.13) and $\check{C}_\sigma^s = (k, l, n, m)$ be a generic cycle. Then:

- i. Both the orthogonality condition $C_\sigma^s \perp \check{C}_\sigma^s$ (I.6.1) and the f-orthogonality $\check{C}_\sigma^s \dashv C_\sigma^s$ (I.6.15) are given by

$$ku_0^2 - 2lu_0 + m = O(\epsilon).$$

In other words, the cycle \check{C}_σ^s has the real root u_0 .

- ii. The f-orthogonality (I.6.15) $C_\sigma^s \dashv \check{C}_\sigma^s$ is given by

$$(I.7.16) \quad ku_0^2 - 2lu_0 - 2nv_0 + m = O(\epsilon).$$

In other words, the cycle \check{C}_σ^s passes the focus (u_0, v_0) of the infinitesimal cycle in the p-implementation.

It is interesting to note that the exotic f-orthogonality became a matching replacement for the usual one for infinitesimal cycles. Unfortunately, f-orthogonality is more fragile. For example, it is not invariant under a generic cycle conjugation (Exercise I.6.38) and, consequently, we cannot use an infinitesimal-radius cycle to define a new parabolic inversion besides those shown in Fig. I.6.4(c).

I.7.6. Infinitesimal Conformality

An intuitive idea of conformal maps, which is often provided in complex analysis textbooks for illustration purposes, is that they “send small circles into small circles

with respective centres". Using infinitesimal cycles, one can turn it into a precise definition.

DEFINITION I.7.27. A map of a region of \mathbb{A} to another region is *l-infinitesimally conformal* for a length l (in the sense of Definition I.7.9) if, for any l -infinitesimal cycle,

- i. its image is an l -infinitesimal cycle of the same order and
- ii. the image of its centre or focus is displaced from the centre or focus of its image by an infinitesimal number of a greater order than its radius.

REMARK I.7.28. Note that, in comparison with Definition I.7.13, we now work "in the opposite direction". Formerly, we had the fixed group of motions and looked for corresponding conformal lengths and distances. Now, we take a distance or length (encoded in the infinitesimally-equidistant cycle) and check which motions respect it.

Natural conformalities for lengths from the centre in the elliptic and parabolic cases are already well studied. Thus, we are mostly interested here in conformality in the parabolic case, where lengths from the focus are more relevant. The image of an infinitesimal cycle (I.7.13) under $SL_2(\mathbb{R})$ -action is a cycle. Moreover, it is again an infinitesimal cycle of the same order by Exercise I.7.25. This provides the first condition of Definition I.7.27. The second part fulfils as well.

EXERCISE I.7.29. Let \check{C}_σ^δ be the image under $g \in SL_2(\mathbb{R})$ of an infinitesimal cycle C_σ^δ from (I.7.13). Then, the δ -focus of \check{C}_σ^δ is displaced from $g(u_0, v_0)$ by infinitesimals of order ϵ^2 , while both cycles have δ -radius of order ϵ .

Consequently, $SL_2(\mathbb{R})$ -action is infinitesimally-conformal in the sense of Definition I.7.27 with respect to the length from the focus (Definition I.7.9) for all combinations of σ , δ and $\check{\delta}$.

Infinitesimal conformality seems to be intuitively close to Definition I.7.13. Thus, it is desirable to understand a reason for the absence of exclusion clauses in Exercise I.7.29 in comparison with Exercise I.7.14.iii.

EXERCISE I.7.30. Show that, for lengths from foci (I.7.7) and $\check{\delta} = 0$, the limit (I.7.10) at point $y_0 = u_0 + \iota v_0$ does exist but depends on the direction $y = u + \iota v$:

$$(I.7.17) \quad \lim_{t \rightarrow 0} \frac{d(g \cdot y_0, g \cdot (y_0 + ty))}{d(y_0, y_0 + ty)} = \frac{1}{(d + cu_0)^2 + \sigma c^2 v_0^2 - 2Kcv_0(d + cu_0)},$$

where $K = \frac{u}{v}$ and $g = \begin{pmatrix} a & b \\ c & d \end{pmatrix}$. Thus, the length is not conformal.

However, if we consider points (I.7.15) of the infinitesimal cycle, then $K = \frac{\epsilon u}{v_0 u^2} = \frac{\epsilon}{v_0 u}$. Thus, the value of the limit (I.7.17) at the infinitesimal scale is independent of $y = u + \iota v$. It also coincides (up to an infinitesimal number) with the value in (I.11.27), which is defined through a different conformal condition.

Infinitesimal cycles are also a convenient tool for calculations of invariant measures, Jacobians, etc.

REMARK I.7.31. There are further connections between the infinitesimal number ϵ and the dual unit ε . Indeed, in non-standard analysis, ϵ^2 is a higher-order infinitesimal than ϵ and can effectively be treated as 0 at the infinitesimal scale of ϵ . Thus, it is simply a more relaxed version of the defining property of the dual unit $\varepsilon^2 = 0$. This explains why many results of differential calculus can be deduced naturally within a dual numbers framework [58], which naturally absorbs many proofs from non-standard analysis.

Using this analogy between ϵ and ε , we can think about the parabolic point space \mathbb{D} as a model for a subset of *hyperreal numbers* \mathbb{R}^* having the representation $x + \epsilon y$, with x and y being real. Then, a vertical line in \mathbb{D} (a special line, in Yaglom's terms [339]) represents a *monad*, that is, the equivalence class of hyperreals, which are different by an infinitesimal number. Then, a Möbius transformation of \mathbb{D} is an analytic extension of the Möbius map from the real line to the subset of hyperreals.

The graph of a parabola is a section, that is, a “smooth” choice of a hyperreal representative from each monad. Geometric properties of parabolas studied in this work correspond to results about such choices of representatives and their invariants under Möbius transformations. It will be interesting to push this analogy further and look for a flow of ideas in the opposite direction: from non-standard analysis to parabolic geometry.

Global Geometry of Upper Half-Planes

So far, we have been interested in the individual properties of cycles and (relatively) localised properties of the point space. We now describe some global properties which are related to the set of cycles as a whole.

I.8.1. Compactification of the Point Space

In giving Definitions I.4.10 and I.4.11 of the maps Q and M on the *cycle space*, we did not properly consider their domains and ranges. For example, the point $(0, 0, 0, 1) \in \mathbb{P}^3$ is transformed by Q to the equation $1 = 0$, which is not a valid equation of a conic section in any point space \mathbb{A} . We have also not yet accurately investigated singular points of the Möbius map (I.3.24). It turns out that both questions are connected.

One of the standard approaches [269, § 1] for dealing with singularities of Möbius maps is to consider projective coordinates on the real line. More specifically, we assign, cf. Section I.4.4.1, a point $x \in \mathbb{R}$ to a vector $(x, 1)$, then linear-fractional transformations of the real line correspond to linear transformations of two-dimensional vectors, cf. (I.1.1) and (I.4.9). All vectors with a non-zero second component can be mapped back to the real line. However, vectors $(x, 0)$ do not correspond to real numbers and represent the *ideal element*, see [296, Ch. 10] for a pedagogical introduction. The union of the real line with the ideal element produces the *compactified* real line. A similar construction is known for Möbius transformations of the complex plain and its compactification.

Since we already have a projective space of cycles, we may use it as a model for compactification of point spaces as well, as it turns out to be even more appropriate and uniform in all EPH cases. The identification of points with zero-radius cycles, cf. Exercise I.5.18, plays an important rôle here.

DEFINITION I.8.1. The only irregular point $(0, 0, 0, 1) \in \mathbb{P}^3$ of the map Q is called the *zero-radius cycle at infinity* and is denoted by Z_∞ .

EXERCISE I.8.2. Check the following:

- i. Z_∞ is the image of the zero-radius cycle $Z_{(0,0)} = (1, 0, 0, 0)$ at the origin under reflection (inversion) into the unit cycle $(1, 0, 0, -1)$ —see blue cycles in Fig. I.6.4(b)–(d).
- ii. The following statements are equivalent:
 - (a) A point $(u, v) \in \mathbb{A}$ belongs to the *zero-radius cycle* $Z_{(0,0)}$ centred at the origin.
 - (b) The zero-radius cycle $Z_{(u,v)}$ is σ -orthogonal to the zero-radius cycle $Z_{(0,0)}$.

- (c) The inversion $z \mapsto \frac{1}{z}$ in the unit cycle is singular in the point (u, v) .
 (d) The image of $Z_{(u,v)}$ under inversion in the unit cycle is orthogonal to Z_∞ .
 If any one of the above statements is true, we also say that the image of (u, v) under inversion in the unit cycle belongs to the zero-radius cycle at infinity.

HINT: These can be easily obtained by direct calculations, even without a CAS.◊

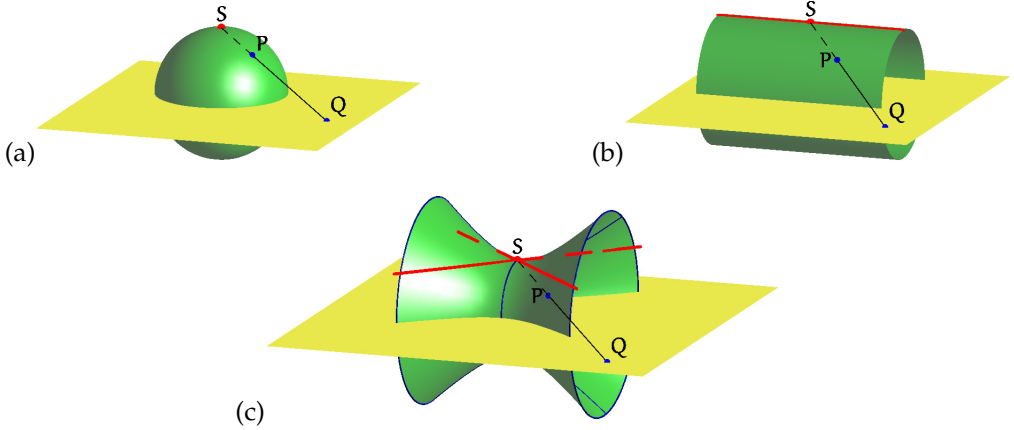


FIGURE I.8.1. Compactification of \mathbb{A} and stereographic projections in (a) elliptic (b) parabolic and (c) hyperbolic point spaces. The stereographic projection from the point S defines the one-to-one map $P \leftrightarrow Q$ between points of the plane (point space) and the model—surfaces of constant curvature. The red point and lines correspond to the light cone at infinity—the ideal elements of the model.

In the elliptic case, the compactification is done by adding to \mathbb{C} a single point ∞ (infinity), which is, of course, the elliptic zero-radius cycle. However, in the parabolic and hyperbolic cases, singularities of the inversion $z \mapsto \frac{1}{z}$ are not localised in a single point. Indeed, the denominator is a zero divisor for the whole zero-radius cycle. Thus, in each EPH case, the correct compactification is made by the union $\mathbb{A} \cup Z_\infty$.

It is common to identify the compactification $\mathring{\mathbb{C}}$ of the space \mathbb{C} with a *Riemann sphere*. This model can be visualised by the *stereographic projection* (or polar projection) as follows—see Fig. I.8.1(a) and [36, § 18.1.4] for further details. Consider a unit sphere with a centre at the origin of \mathbb{R}^3 and the horizontal plane passing the centre. Any non-tangential line passing the north pole S will intersect the sphere at another point P and meet the plane at a point Q . This defines a one-to-one correspondence of the plane and the sphere within point S . If point Q moves far from the origin the point P shall approach S . Thus it is natural to associate S with infinity.

A similar model can also be provided for the parabolic and hyperbolic spaces—see Fig. I.8.1(b),(c) and further discussion in [130; 339, § 10]. Indeed, the space \mathbb{A} can be identified with a corresponding surface of *constant curvature*: the sphere ($\sigma = -1$), the cylinder (Fig. I.8.1(b), $\sigma = 0$), or the one-sheet hyperboloid (Fig. I.8.1(c), $\sigma = 1$).

The map of a surface to \mathbb{A} is given by the polar projection—see Fig. I.8.1(a–c) as well as [130, Fig. 1; 339, Figs 129, 135, 179]. The ideal elements which do not correspond to any point of the plane are shown in red in Fig. I.8.1. As we may observe, these correspond exactly to the zero-radius cycles in each case: the point (elliptic), the line (parabolic) and two lines, that is, the light cone (hyperbolic) at infinity. These surfaces provide “compact” models of the corresponding \mathbb{A} in the sense that Möbius transformations which are lifted from \mathbb{A} to the constant curvature surface by the polar projection are not singular on these surfaces. A modern presentation of the hyperbolic case and its quantum field interpretation can be found in [298].

A more accurate realisation of compact models can be achieved through zero-radius cycles. Exercise I.5.18 tells that a point $u + v$ of \mathbb{C} (\mathbb{D} , \mathbb{O}) can be identified with the elliptic (elliptic, hyperbolic) centre of the zero-radius cycle $(1, u, v, u^2 - \sigma v^2)$. Then, ideal elements at infinity can be associated with zero-radius cycles which do not have finite centres, that is a cycle $C = (k, l, m, n)$ such that:

$$(I.8.0a) \quad \det_{\sigma} C = 0 \quad \text{and} \quad k = 0.$$

Note that those cycles admit neither k -normalisation nor \det_{σ} -normalisation.

EXERCISE I.8.2(a). Check the following:

- (e) For $\sigma = -1$, there is the unique cycle $(0, 0, 0, 1)$ satisfying (I.8.0a), which represents the point at infinity Z_{∞} of \mathbb{C} .
- (p) For $\sigma = 0$, all cycles satisfying (I.8.0a) are
 - (a) The straight line at infinity $Z_{\infty} = (0, 0, 0, 1)$ representing the pole S .
 - (b) Cycles $(0, 0, n, 1)$ parametrised by a real number $n \neq 0$ representing ideal elements different from the pole S .
 - (c) The cycle $(0, 0, 1, 0)$ representing the point, which compactifies the line at infinity.
- (h) For $\sigma = 1$, all cycles satisfying (I.8.0a) are:
 - (a) The light cone at infinity $Z_{\infty} = (0, 0, 0, 1)$, representing its vertex.
 - (b) Cycles $(0, l, l, 1)$ and $(0, l, -l, 1)$ parametrised by a real $l \neq 0$ and representing points of Z_{∞} different from its vertex.
 - (c) Cycles $(0, 1, 1, 0)$ and $(0, 1, -1, 0)$, which compactify the above lines forming the light cone at infinity.

The following observations justify our above classification in the parabolic and hyperbolic cases:

- i. Cycles listed in clauses (b) and (c) represent ideal elements, but have non-empty footprint at the finite part of the point space. In contrast, no finite points belong to cycles from clauses (a).
- ii. Consider the inversion in the unit cycle $(1, 0, 0, -1)$ which maps a cycle (k, l, n, m) to (m, l, n, k) . Cycles listed in clauses (a) and (b) are mapped by the inversion to cycles representing finite points, that is cycles having finite centres. In contrast, the cycles from the clauses (c) are invariant under the inversion, thus represent the same ideal objects after the inversion. As a consequence the later ideal elements are often missed, see the discussion of this in [147] for the hyperbolic case.

Furthermore, the hyperbolic case has its own caveats which may be easily overlooked as in [130, 298], for example. A compactification of the hyperbolic space \mathbb{O} by a *light cone*—the hyperbolic zero-radius cycle—at infinity will, indeed, produce a closed Möbius-invariant object or a model of two-dimensional conformal *space-time*. However, it will not be satisfactory for reasons explained in the next section.

I.8.2. (Non)-Invariance of The Upper Half-Plane

There is an important difference between the hyperbolic case and the others.

EXERCISE I.8.3. In the elliptic and parabolic cases, the upper half-plane in \mathbb{A} is preserved by Möbius transformations from $SL_2(\mathbb{R})$. However, in the hyperbolic case, any point (u, v) with $v > 0$ can be mapped to an arbitrary point (u', v') with $v' \neq 0$.

This is illustrated in Fig. I.1.3. Any cone from the family (I.3.29) intersect both planes EE' and PP' over a connected curve (K-orbit—a circle and parabola, respectively) belonging to a half-plane. However, the intersection of a two-sided cone with the plane HH' is two branches of a hyperbola in different half-planes (only one of them is shown in Fig. I.1.3). Thus, a rotation of the cone produces a transition of the intersection point from one half-plane to another and back again.

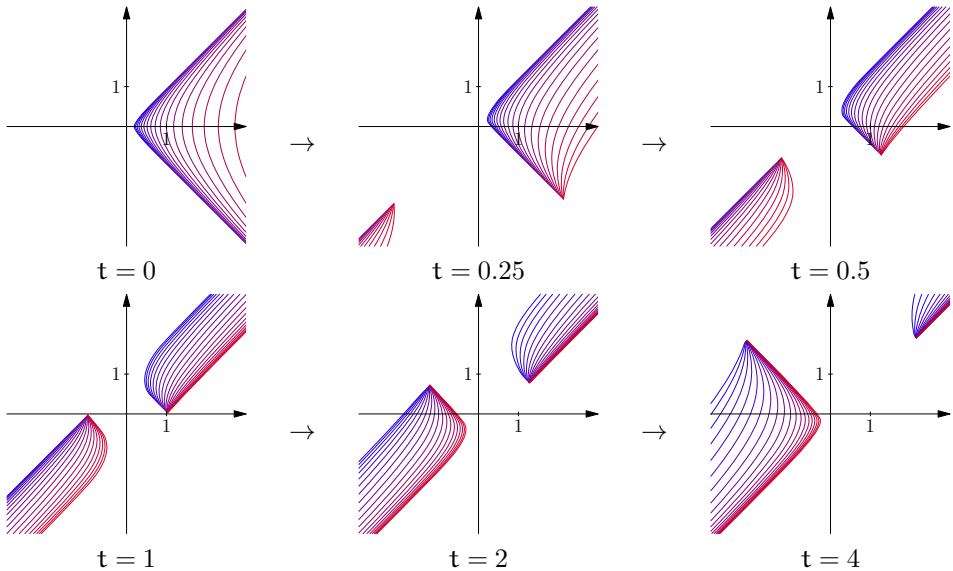


FIGURE I.8.2. Six frames from a continuous transformation from the future to the past parts of the light cone. Animations as [GIF](#) and [PDF](#) (requires Acroreader) are provided on the accompanying DVD.

The lack of invariance of the half-planes in the hyperbolic case has many important consequences in seemingly different areas, for example:

Geometry: \mathbb{O} is not split by the real axis into two disjoint pieces: there are continuous paths (through the light cone at infinity) from the upper half-plane to the lower one which do not cross the real axis, cf. a sine-like curve consisting of two branches of a hyperbola in Fig. I.8.3(a).

Physics: There is no Möbius-invariant way to separate the “past” and “future” parts of the light cone [302, Ch. II], i.e. there is a continuous family of Möbius transformations reversing the arrow of time and breaking causal orientation.

For example, the family of matrices $\begin{pmatrix} 1 & -te_1 \\ te_1 & 1 \end{pmatrix}$, $t \in [0, \infty)$ provides such a transformation. Figure I.8.2 illustrates this by the corresponding images for six subsequent values of t .

Analysis: There is no possibility of splitting the $L_2(\mathbb{R})$ space of functions into a direct sum of the Hardy-type space of functions having an analytic extension into the upper half-plane and its non-trivial complement, i.e. any function from $L_2(\mathbb{R})$ has an “analytic extension” into the upper half-plane in the sense of hyperbolic function theory—see [170].

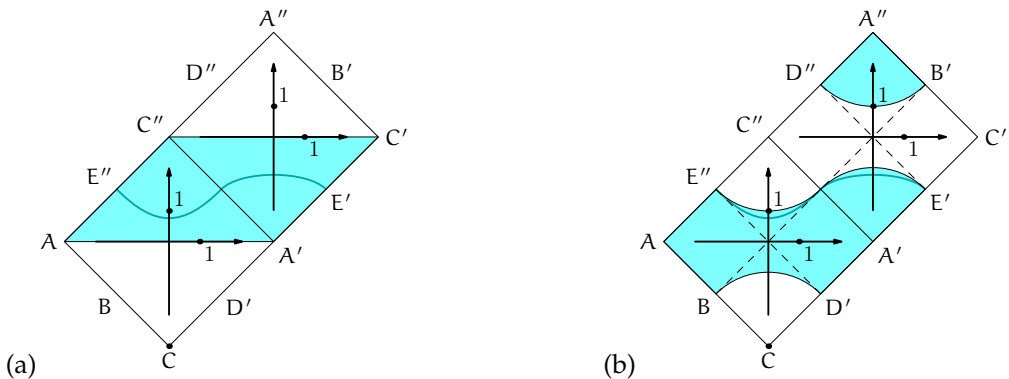


FIGURE I.8.3. Hyperbolic objects in the double cover of \mathbb{O} . If we cross the light cone at infinity from one sheet, then we will appear on the other. The shaded region is the two-fold cover of the upper half-plane on (a) and the unit disk on (b). These regions are Möbius-invariant.

All of the above problems can be resolved in the following way—see [170, § A.3; 302, § III.4]. We take two copies \mathbb{O}^+ and \mathbb{O}^- of the hyperbolic point space \mathbb{O} , depicted by the squares $ACA'C''$ and $A'C'A''C''$ in Fig. I.8.3, respectively. The boundaries of these squares are light cones at infinity and we glue \mathbb{O}^+ and \mathbb{O}^- in such a way that the construction is invariant under the natural action of the Möbius transformation. This is achieved if the letters A, B, C, D, E in Fig. I.8.3 are identified regardless of the number of primes attached to them.

This aggregate, denoted by $\tilde{\mathbb{O}}$, is a two-fold cover of \mathbb{O} . The *hyperbolic “upper” half-plane* $\tilde{\mathbb{O}}^+$ in $\tilde{\mathbb{O}}$ consists of the upper half-plane in \mathbb{O}^+ and the lower one in \mathbb{O}^- , shown as a shaded region in Fig. I.8.3(a). It is Möbius-invariant and has a matching

complement in $\tilde{\mathbb{O}}$. More formally,

$$(I.8.1) \quad \tilde{\mathbb{O}}^+ = \{(u, v) \in \mathbb{O}^+ \mid u > 0\} \cup \{(u, v) \in \mathbb{O}^- \mid u < 0\}.$$

The hyperbolic “upper” half-plane is bounded by two disjoint “real” axes denoted by AA' and $C'C''$ in Fig. I.8.3(a).

REMARK I.8.4. The hyperbolic orbit of the subgroup K in $\tilde{\mathbb{O}}$ consists of two branches of the hyperbola passing through $(0, v)$ in \mathbb{O}^+ and $(0, -v^{-1})$ in \mathbb{O}^- —see the sine-like curve in Fig. I.8.3(a). If we watch the continuous rotation of a straight line generating a cone (I.3.29) then its intersection with the plane HH' in Fig. I.1.3(b) will draw both branches. As mentioned in Remark I.3.17.ii, they have the same focal length and form a single K -orbit.

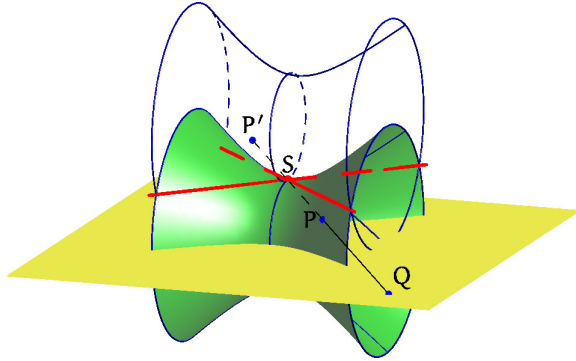


FIGURE I.8.4. Double cover of the hyperbolic space, cf. Fig. I.8.1(c). The second hyperboloid is shown as a blue skeleton. It is attached to the first one along the light cone at infinity, which is represented by two red lines. A crossing of the light cone implies a transition from one hyperboloid to another.

The corresponding model through a stereographic projection is presented in Fig. I.8.4. In comparison with the single hyperboloid in Fig. I.8.1(c), we add the second hyperboloid intersecting the first one over the light cone at infinity. A crossing of the light cone in any direction implies a swap of hyperboloids, cf. the flat map in Fig. I.8.3. A similar conformally-invariant two-fold cover of the Minkowski space-time was constructed in [302, § III.4] in connection with the red shift problem in *extragalactic astronomy*—see Section I.8.4 for further information.

I.8.3. Optics and Mechanics

We have already used many physical terms (light cone, space-time, etc.) to describe the hyperbolic point space. It will be useful to outline more physical connections for all EPH cases. Our list may not be exhaustive, but it illustrates that $SL_2(\mathbb{R})$ not only presents some distinct areas but also links them in a useful way.

I.8.3.1. Optics. Consider an optical system consisting of centred lenses. The propagation of rays close to the symmetry axis through such a device is the subject of *paraxial optics*. See [110, Ch. 2] for a pedagogical presentation of matrix methods in this area—we give only a briefly outline here. A ray at a certain point can be described by a pair of numbers $P = (y, V)$ in respect to the symmetry axis A —see Fig. I.8.5. Here, y is the height (positive or negative) of the ray above the axis A and $V = n \cos v$, where v is the angle of the ray with the axis and n is the *refractive index* of the medium.

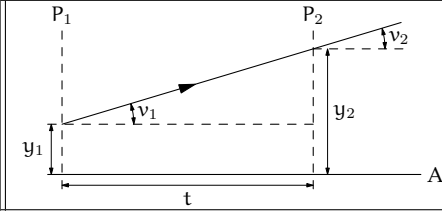
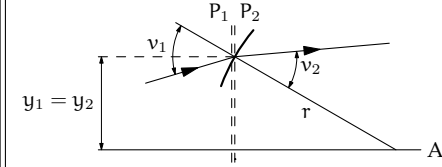
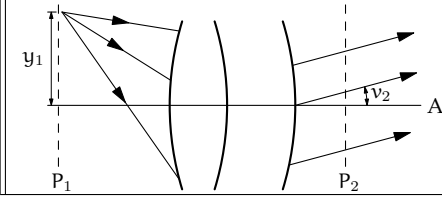
System	Transfer matrices
	Propagation in a homogeneous and isotropic medium with refractive index n : $\begin{pmatrix} y_2 \\ V_2 \end{pmatrix} = \begin{pmatrix} 1 & t/n \\ 0 & 1 \end{pmatrix} \begin{pmatrix} y_1 \\ V_1 \end{pmatrix}$
	A circular boundary between two regions with refractive indices n_1 and n_2 : $\begin{pmatrix} y_2 \\ V_2 \end{pmatrix} = \begin{pmatrix} 1 & 0 \\ \frac{n_1 - n_2}{r} & 1 \end{pmatrix} \begin{pmatrix} y_1 \\ V_1 \end{pmatrix}$
	A ray emitted from the focal plane. The output direction v_2 depends only on y_1 : $\begin{pmatrix} y_2 \\ V_2 \end{pmatrix} = \begin{pmatrix} a & b \\ c & 0 \end{pmatrix} \begin{pmatrix} y_1 \\ V_1 \end{pmatrix}$

FIGURE I.8.5. Some elementary optical systems and their transfer matrices

The paraxial approximation to geometric optics provides a straightforward recipe for evaluating the output components from the given data:

$$(I.8.2) \quad \begin{pmatrix} y_2 \\ V_2 \end{pmatrix} = \begin{pmatrix} a & b \\ c & d \end{pmatrix} \begin{pmatrix} y_1 \\ V_1 \end{pmatrix}, \quad \text{for some } \begin{pmatrix} a & b \\ c & d \end{pmatrix} \in \text{SL}_2(\mathbb{R}).$$

If two paraxial systems are aggregated one after another, then the composite is described by the product of the respective transfer matrices of the subsystems. In other words, we obtained an action of the group $\text{SL}_2(\mathbb{R})$ on the space of rays. More complicated optical systems can be approximated locally by paraxial models.

There is a covariance of the theory generated by the conjugation automorphism $g : g' \mapsto gg'g^{-1}$ of $\text{SL}_2(\mathbb{R})$. Indeed, we can simultaneously replace rays by gP and a system's matrices by gAg^{-1} for any fixed $g \in \text{SL}_2(\mathbb{R})$. Another important invariant can be constructed as follows. For matrices from $\text{SL}_2(\mathbb{R})$, we note the remarkable relation

$$(I.8.3) \quad J^{-1}AJ = (A^{-1})^T, \quad \text{where } A \in \text{SL}_2(\mathbb{R}) \text{ and } J = \begin{pmatrix} 0 & -1 \\ 1 & 0 \end{pmatrix}.$$

Subsequently, we define a *symplectic form* on \mathbb{R}^2 using the matrix J :

$$(I.8.4) \quad y\tilde{V} - \tilde{y}V = \tilde{P}^T J P, \quad \text{where } P = \begin{pmatrix} y \\ V \end{pmatrix}, \quad \tilde{P} = \begin{pmatrix} \tilde{y} \\ \tilde{V} \end{pmatrix} \in \mathbb{R}^2.$$

Then, this form is invariant under the $SL_2(\mathbb{R})$ -action (I.8.2), due to (I.8.3):

$$\begin{aligned} \tilde{P}_1^T J P_1 &= (A\tilde{P})^T J A P = \tilde{P}^T A^T J A P = \tilde{P}^T J (J^{-1} A^T J) A P \\ &= \tilde{P}^T J A^{-1} A P = \tilde{P}^T J P, \end{aligned}$$

where $P_1 = AP$ and $\tilde{P}_1 = A\tilde{P}$. In other words, the symplectic form is an invariant of the covariant action of $SL_2(\mathbb{R})$ on the optical system, cf. Exercise I.4.20.iii.

EXAMPLE I.8.5. The matrix J (I.8.3) belongs to the subgroup K . It is a transfer matrix between two focal planes of a system, cf. [110, § II.8.2]. It swaps components of the vector (y, V) , therefore the ray height y_2 at the second focal plane depends only on the ray angle V_1 in the first, and *vice versa*.

I.8.3.2. Classical Mechanics. A Hamiltonian formalism in classical mechanics was motivated by an analogy between optics and mechanics—see [11, § 46]. For a one-dimensional system, it replaces the description of rays through (y, V) by a point (q, p) in the *phase space* \mathbb{R}^2 . The component q gives the coordinate of a particle and p is its momentum.

Paraxial optics corresponds to transformations of the phase space over a fixed period of time t under quadratic Hamiltonians. They are also represented by linear transformations of \mathbb{R}^2 with matrices from $SL_2(\mathbb{R})$, preserve the symplectic form (I.8.3) and are covariant under the linear changes of coordinates in the phase space with matrices from $SL_2(\mathbb{R})$.

For a generic Hamiltonian, we can approximate it by a quadratic one at the infinitesimal scale of phase space and time interval t . Thus, the symplectic form becomes an invariant object in the tangent space of the phase space. There is a wide and important class of non-linear transformations of the phase space whose derived form preserves the symplectic form on the tangent space to every point. They are called *canonical transformations*. In particular, Hamiltonian dynamics is a one-parameter group of canonical transformations.

EXAMPLE I.8.6. The transformation of the phase space defined by the matrix J (I.8.3) is provided by the quadratic Hamiltonian $q^2 + p^2$ of the *harmonic oscillator*. Similarly to the optical Example I.8.5, it swaps the coordinates and momenta of the system, rotating the phase space by 90 degrees.

I.8.3.3. Quantum Mechanics. Having a transformation ϕ of a set X we can always extend it to a linear transformation ϕ^* in a function space defined on X through the “change of variables”: $[\phi^* f](x) = f(\phi(x))$. Using this for transformations of the phase space, we obtain a language for working with statistical ensembles: functions on X can describe the probability distribution on the set.

However, there is an important development of this scheme for the case of a homogeneous space $X = G/H$. We use maps $p : G \rightarrow G/H$, $s : X \rightarrow G$ and $r : G \rightarrow H$ defined in Subsection I.2.2.2. Let $\chi : H \rightarrow B(V)$ be a linear representation of H in a

vector space V . Then, χ induces a linear representation of G in a space of V -valued functions on X given by the formula (cf. [159, § 13.2.(7)–(9)])

$$(I.8.5) \quad [\rho_\chi(g)f](x) = \chi(r(g^{-1} * s(x))) f(g^{-1} \cdot x),$$

where $g \in G$, $x \in X$ and $h \in H$. “ $*$ ” denotes multiplication on G and “ \cdot ” denotes the action (I.2.3) of G on X from the left.

One can build induced representations for the action $SL_2(\mathbb{R})$ on the classical phase space and, as a result, quantum mechanics emerges from classical mechanics [196, 199]. The main distinction between the two mechanics is encoded in the factor $\chi(r(g^{-1} * s(x)))$ in (II.3.6). If this term takes complex values then there is self-interaction of functions in linear combinations. Such an effect is natural for *wave packets* rather than the classical statistical distributions. It is commonly believed that non-commutativity of observables is the characteristic feature of quantum mechanics, however a closer consideration [200] reveals the key role of complex numbers instead.

EXAMPLE I.8.7. Let us return to the matrix J (I.8.3) and its action on the phase space from Example I.8.6. In standard quantum mechanics, the representation (II.3.6) is induced by a complex-valued character of the subgroup K . Consequently, the action of J is $[\rho_\chi(J)f](p, q) = if(-p, q)$. There are eigenfunctions $w_n(q, p) = (q + ip)^n$ of this action and the respective eigenvalues compose the energy spectrum of a quantum harmonic oscillator. A similar discreteness is responsible for the appearance of spectral lines in the light emission by the atoms of chemical elements.

I.8.4. Relativity of Space-Time

Relativity describes an invariance of a kinematics with respect to a group of transformations, generated by transitions from one admissible reference system to another. Obviously, it is a counterpart of the Erlangen programme in physics and can be equivalently stated: a physical theory studies invariants under a group of transformations, acting transitively on the set of admissible observers. One will admit that group invariance is much more respected in physics than in mathematics.

We saw an example of $SL_2(\mathbb{R})$ (symplectic) invariance in the previous section. The main distinction is that the transformations in kinematic relativity involve time components of space-time, while mechanical covariance was formulated for the phase space.

There are many good sources with a comprehensive discussion of relativity—see, for example, [42, 339]. We will briefly outline the main principles, only restricting ourselves to two-dimensional space-time with a one-dimensional spatial component. We also highlight the role of subgroups N' and A' in the relativity formulation to make a closer connection to the origin of our development—cf. Section I.3.3.

EXAMPLE I.8.8 (Galilean relativity of classical mechanics). Denote by (t, x) coordinates in \mathbb{R}^2 , which is identified with space-time. Specifically, t denotes time and x the spatial component. Then, the Galilean relativity principle tells us that the laws of mechanics will be invariant under the shifts of the reference point and the following

linear transformations:

$$(I.8.6) \quad \begin{pmatrix} t' \\ x' \end{pmatrix} = \begin{pmatrix} t \\ x + vt \end{pmatrix} = G_v \begin{pmatrix} t \\ x \end{pmatrix}, \quad \text{where } G = \begin{pmatrix} 1 & 0 \\ v & 1 \end{pmatrix} \in \text{SL}_2(\mathbb{R}).$$

This map translates events to another reference system, which is moving with a constant speed v with respect to the first one. The matrix G_v in (I.8.6) belongs to the subgroup N' (I.3.11).

It is easy to see directly that parabolic cycles make an invariant family under the transformations (I.8.6). These parabolas are graphs of particles moving with a constant acceleration; the acceleration is the reciprocal of the focal length of this parabola (up to a factor). Thus, movements with a constant acceleration a form an invariant class in Galilean mechanics. A particular case is $a = 0$, that is, a uniform motion, which is represented by non-vertical straight lines. Each such line can be mapped to another by a Galilean transformation.

The class of vertical lines, representing sets of simultaneous events, is also invariant under Galilean transformations. In other words, Galilean mechanics possesses the absolute time which is independent from spatial coordinates and their transformations. See [339, § 2] for a detailed examination of Galilean relativity.

A different type class of transformations, discovered by Lorentz and Poincare, is admitted in Minkowski space-time.

EXAMPLE I.8.9 (Lorentz–Poincare). We again take the space-time \mathbb{R}^2 with coordinates (t, x) , but consider linear transformations associated to elements of subgroup A' :

$$(I.8.7) \quad \begin{pmatrix} t' \\ x' \end{pmatrix} = \begin{pmatrix} \frac{t-vx}{\sqrt{1-v^2}} \\ -vt+x \\ \frac{-vt+x}{\sqrt{1-v^2}} \end{pmatrix} = L_v \begin{pmatrix} t \\ x \end{pmatrix} \quad \text{where } L_x = \frac{1}{\sqrt{1-v^2}} \begin{pmatrix} 1 & -v \\ -v & 1 \end{pmatrix}.$$

The physical meaning of the transformation is the same: they provide a transition from a given reference system to a new one moving with a velocity v with respect to the first. The relativity principle again requires the laws of mechanics to be invariant under Lorentz–Poincare transformations generated by (I.8.7) and shifts of the reference point.

The admissible values $v \in (-1, 1)$ for transformations (I.8.7) are bounded by 1, which serves as the *speed of light*. Velocities greater than the speed of light are not considered in this theory. The fundamental object preserved by (I.8.7) is the *light cone*:

$$(I.8.8) \quad C_0 = \{(t, x) \in \mathbb{R}^2 \mid t = \pm x\}.$$

More generally, the following quadratic form is also preserved:

$$d_h(t, x) = t^2 - x^2.$$

The light cone C_0 is obviously the collection of points $d_h(t, x) = 0$. For other values, we obtain hyperbolas with asymptotes formed by C_0 . The light cone separates areas of space-time where $d_h(t, x) > 0$ or $d_h(t, x) < 0$. The first consists of *time-like intervals* and the second of *space-like* ones. They can be transformed by (I.8.7) to pure time $(t, 0)$ or pure space $(0, x)$ intervals, respectively. However, no mixing between intervals of different kinds is admitted by Lorentz–Poincare transformations.

Furthermore, for time-like intervals, there is a preferred direction which assigns the meaning of the future (also known as the arrow of time) to one half of the cone consisting of time-like intervals, e.g. if the t -component is positive. This *causal orientation* [302, § II.1] is required by the real-world observation that we cannot remember the future states of a physical system but may affect them. Conversely, we may have a record of the system's past but cannot change it in the present.

EXERCISE I.8.10. Check that such a separation of the time-like cone $d_h(t, x) > 0$ into future ($t > 0$) and past ($t < 0$) halves is compatible with the group of Lorentz–Poincare transformations generated by the hyperbolic rotations (I.8.7).

However, the causal orientation is not preserved if the group of admissible transformations is extended to conformal maps by an addition of inversions—see Fig. I.8.2. Such an extension is motivated by a study of the red shift in astronomy. Namely, spectral lines of chemical elements (cf. Example I.8.7) observed from remote stars are shifted toward the red part of the spectrum in comparison to values known from laboratory measurements. Conformal (rather than Lorentz–Poincare) invariance produces much better correlation to experimental data [302] than the school textbook explanation of a red shift based on the Doppler principle and an expanding universe.

Further discussion of relativity can be found in [42; 339, § 11].

Invariant Metric and Geodesics

The Euclidean metric is not preserved by automorphisms of the Lobachevsky half-plane. Instead, one has only a weaker property of conformality. However, it is possible to find such a metric on the Lobachevsky half-plane that Möbius transformations will be isometries. Similarly, in Chapter I.7, we described a variety of distances and lengths and many of them had conformal properties with respect to $SL_2(\mathbb{R})$ action. However, it is worth finding a metric which is preserved by Möbius transformations. We will now proceed to do this, closely following [165].

Our consideration will be based on equidistant orbits, which physically correspond to wavefronts with a constant velocity. For example, if a stone is dropped into a pond, the resulting ripples are waves which travel the same distance from the drop point, assuming a constant wave velocity. An alternative description to wavefronts uses rays—the paths along which waves travel, i.e. the geodesics in the case of a constant velocity. The duality between wavefronts and rays is provided by Huygens' principle—see [11, § 46].

Geodesics also play a central role in differential geometry, generalising the notion of a straight line. They are closely related to metrics: a geodesic is often defined as a curve between two points with an extremum of length. As a consequence, the metric is additive along geodesics.

I.9.1. Metrics, Curves' Lengths and Extrema

We start by recalling the standard definition—see [164, § I.2].

DEFINITION I.9.1. A *metric* on a set X is a function $d : X \times X \rightarrow \mathbb{R}^+$ such that

- i. $d(x, y) \geq 0$ (positivity),
- ii. $d(x, y) = 0$ if and only if $x = y$ (non-degeneracy),
- iii. $d(x, y) = d(y, x)$ (symmetry) and
- iv. $d(x, y) \leq d(x, z) + d(z, y)$ (the triangle inequality),

for all $x, y, z \in X$.

Although adequate in many cases, the definition does not cover all metrics of interest. Examples include the non-symmetric lengths from Section I.7.2 or distances (I.7.5) in the Minkowski space with the reverse triangle inequality $d(x, y) \geq d(x, z) + d(z, y)$.

Recall the established procedure of constructing geodesics in Riemannian geometry (two-dimensional case) from [337, § 7]:

- i. Define the (pseudo-)Riemannian metric on the tangent space:

$$(I.9.1) \quad g(du, dv) = Edu^2 + Fdudv + Gdv^2.$$

ii. Define the *length* for a curve Γ as:

$$(I.9.2) \quad \text{length}(\Gamma) = \int_{\Gamma} (\mathbb{E}du^2 + \mathbb{F}dudv + \mathbb{G}dv^2)^{\frac{1}{2}}.$$

iii. Then, geodesics will be defined as the curves which give a stationary point for the length.

iv. Lastly, the metric between two points is the length of a geodesic joining those two points.

EXERCISE I.9.2. Let the quadratic form (I.9.1) be $\text{SL}_2(\mathbb{R})$ -invariant. Show that the above procedure leads to an $\text{SL}_2(\mathbb{R})$ -invariant metric.

We recall from Section I.3.7 that an isotropy subgroup H fixing the hypercomplex unit ι under the action of (I.3.24) is K (I.3.8), N' (I.3.11) and A' (I.3.10) in the corresponding EPH cases. We will refer to H -action as *EPH rotation* around ι . For an $\text{SL}_2(\mathbb{R})$ invariant metric, the orbits of H will be equidistant points from ι , giving some indication what the metric should be. However, this does not determine the metric entirely since there is freedom in assigning values to the orbits.

LEMMA I.9.3. *The invariant infinitesimal metric in EPH cases is*

$$(I.9.3) \quad ds^2 = \frac{du^2 - \sigma dv^2}{v^2},$$

where $\sigma = -1, 0, 1$ respectively.

In the proof below, we will follow the procedure from [56, § 10].

PROOF. In order to calculate the infinitesimal metric, consider the subgroups H of Möbius transformations which fix ι . Denote an element of these rotations by E_{σ} . We require an isometry, so

$$d(\iota, \iota + \delta v) = d(\iota, E_{\sigma}(\iota + \delta v)).$$

Using the Taylor series, we obtain

$$E_{\sigma}(\iota + \delta v) = \iota + J_{\sigma}(\iota)\delta v + o(\delta v),$$

where the Jacobian denoted J_{σ} is, respectively,

$$\begin{pmatrix} \cos 2\theta & -\sin 2\theta \\ \sin 2\theta & \cos 2\theta \end{pmatrix}, \quad \begin{pmatrix} 1 & 0 \\ 2t & 1 \end{pmatrix} \quad \text{or} \quad \begin{pmatrix} \cosh 2\alpha & \sinh 2\alpha \\ \sinh 2\alpha & \cosh 2\alpha \end{pmatrix}.$$

A metric is invariant under the above rotations if it is preserved under the linear transformation

$$\begin{pmatrix} dU \\ dV \end{pmatrix} = J_{\sigma} \begin{pmatrix} du \\ dv \end{pmatrix},$$

which turns out to be $du^2 - \sigma dv^2$ in the three cases.

To calculate the metric at an arbitrary point $w = u + iv$, we map w to ι by an affine Möbius transformation, which acts transitively on the upper half-plane

$$(I.9.4) \quad r^{-1} : w \rightarrow \frac{w - u}{v}.$$

Hence, there is a factor of $\frac{1}{v^2}$, so the resulting metric is $ds^2 = \frac{du^2 - \sigma dv^2}{v^2}$. \square

COROLLARY I.9.4. *With the above notation, for an arbitrary curve Γ ,*

$$(I.9.5) \quad \text{length}(\Gamma) = \int_{\Gamma} \frac{(\mathrm{d}u^2 - \sigma \mathrm{d}v^2)^{\frac{1}{2}}}{v}.$$

It is invariant under Möbius transformations of the upper half-plane.

The standard tools for finding geodesics for a given Riemannian metric are the Euler–Lagrange equations—see [337, § 7.1]. For the metric (I.9.3), they take the form

$$(I.9.6) \quad \frac{\mathrm{d}}{\mathrm{d}t} \left(\frac{\dot{\gamma}_1}{y^2} \right) = 0 \quad \text{and} \quad \frac{\mathrm{d}}{\mathrm{d}t} \left(\frac{\sigma \dot{\gamma}_2}{y^2} \right) = \frac{\dot{\gamma}_1^2 - \sigma \dot{\gamma}_2^2}{y^3},$$

where γ is a smooth curve $\gamma(t) = (\gamma_1(t), \gamma_2(t))$ and $t \in (a, b)$. This general approach can be used in the two non-degenerate cases (elliptic and hyperbolic) and produces curves with the minimum or maximum lengths, respectively. However, the $\mathrm{SL}_2(\mathbb{R})$ -invariance of the metric allows us to use more elegant methods in this case. For example, in the Lobachevsky half-plane, the solutions are well known—semicircles orthogonal to the real axes or vertical lines, cf. Fig. I.9.1(a) and [26, Ch. 15].

EXERCISE I.9.5. For the elliptic space ($\sigma = -1$):

- i. Write a parametric equation of a circle orthogonal to the real line and check that the curve satisfies the Euler–Lagrange equations (I.9.6).
- ii. Geodesics passing the imaginary unit i are transverse circles to K -orbits from Fig. I.1.2 and Exercise I.4.16.iv with the equation, cf. Fig. I.9.3(E)

$$(I.9.7) \quad (u^2 + v^2) - 2tu - 1 = 0, \quad \text{where } t \in \mathbb{R}.$$

- iii. The Möbius invariant metric is

$$(I.9.8) \quad m(z, w) = \sinh^{-1} \frac{|z - w|_e}{2\sqrt{\Im[z]\Im[w]}},$$

where $\Im[z]$ is the imaginary part of a complex number z and $|z|_e^2 = u^2 + v^2$. HINT: One can directly or, by using CAS, verify that this is a Möbius-invariant expression. Thus, we can transform z and w to i and a point on the imaginary axis by a suitable Möbius transformation without changing the metric. The shortest curve in the Riemannian metric (I.9.3) is the vertical line, that is, $\mathrm{d}u = 0$. For a segment of the vertical line, the expression (I.9.8) can easily be evaluated. See also [24, Thm. 7.2.1] for detailed proof and a number of alternative expressions.◊

EXERCISE I.9.6. Show, similarly, that, in the hyperbolic case ($\sigma = 1$):

- i. There are two families of solutions passing the double unit j , one space-like (Fig. I.9.3(H_S)) and one time-like (Fig. I.9.3(H_T)), cf. Section I.8.4:

$$(I.9.9) \quad (u^2 - v^2) - 2tu + 1 = 0, \quad \text{where } |t| > 1 \text{ or } |t| < 1.$$

The space-like solutions are obtained by A' rotation of the vertical axis and the time-like solution is the A' -image of the cycle $(1, 0, 0, 1)$ —cf. Fig. I.3.1. They also consist of positive and negative cycles, respectively, which are orthogonal to the real axis.

ii. The respective metric in these two cases is:

$$(I.9.10) \quad d(z, w) = \begin{cases} 2 \sin^{-1} \frac{|z - w|_h}{2\sqrt{\Im[z]\Im[w]}}, & \text{when } z - w \text{ is time-like} \\ 2 \sinh^{-1} \frac{|z - w|_h}{2\sqrt{\Im[z]\Im[w]}}, & \text{when } z - w \text{ is space-like,} \end{cases}$$

where $\Im[z]$ is the imaginary part of a double number z and $|z|_h^2 = u^2 - v^2$. HINT: The hint from the previous exercise can be used again here with some modification to space-/time-like curves and by replacing the minimum of the possible curves' lengths by the maximum. \diamond

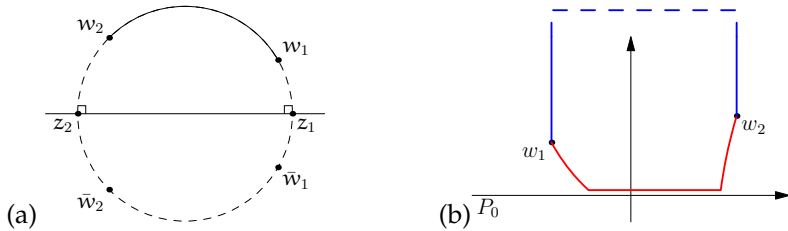


FIGURE I.9.1. Lobachevsky geodesics and extrema of curves' lengths. (a) The geodesic between w_1 and w_2 in the Lobachevsky half-plane is the circle orthogonal to the real line. The invariant metric is expressed through the cross-ratios $[z_1, w_1, w_2, z_2] = [\bar{w}_1, w_1, w_2, \bar{w}_2]$. (b) Extrema of curves' lengths in the parabolic point space. The length of the blue curve (going up) can be arbitrarily close to 0 and can be arbitrarily large for the red one (going down).

The same geodesic equations can be obtained by Beltrami's method—see [42, § 8.1]. However, the parabolic case presents yet another disappointment.

EXERCISE I.9.7. Show that, for the parabolic case ($\sigma = 0$):

- i. The only solution of the Euler–Lagrange equations (I.9.6) are vertical lines, as in [339, § 3], which are again orthogonal to the real axes.
- ii. Vertical lines minimise the curves' length between two points w_1 and w_2 . See Fig. I.9.1(b) for an example of a blue curve with its length tending to zero value of the infimum. The respective “geodesics” passing the dual unit ε are

$$(I.9.11) \quad u^2 - 2tu = 0.$$

Similarly, a length of the red curve can be arbitrarily large if the horizontal path is close enough to the real axis.

- iii. The only $SL_2(\mathbb{R})$ -invariant metric obtained from the above extremal consideration is either identically equal to 0 or infinity.

There is a similarity between all three cases. For example, we can uniformly write equations (I.9.7), (I.9.9) and (I.9.11) of geodesics through ι as

$$(u^2 - \sigma v^2) - 2tu + \sigma = 0, \quad \text{where } t \in \mathbb{R}.$$

However, the triviality of the parabolic invariant metric is awkward and we go on to study further the algebraic and geometric invariants to find a more adequate answer.

I.9.2. Invariant Metric

We seek all real-valued functions f of two points on the half-plane which are invariant under the Möbius action

$$f(g(z), g(w)) = f(z, w) \quad \text{for all } z, w \in \mathbb{A} \quad \text{and} \quad g \in \text{SL}_2(\mathbb{R}).$$

We have already seen one like this in (I.9.8) and (I.9.10):

$$(I.9.12) \quad F(z, w) = \frac{|z - w|_\sigma}{\sqrt{\mathcal{J}[z]\mathcal{J}[w]}},$$

which can be shown by a simple direct calculation (for CAS, see Exercise I.9.5.iii). Recall that $|z|_\sigma^2 = u^2 - \sigma v^2$ by analogy with the distance $d_{\sigma, \sigma}$ (I.7.5) in EPH geometries and [339, App. C]. In order to describe other invariant functions we will need the following definition.

DEFINITION I.9.8. A function $f : X \times X \rightarrow \mathbb{R}^+$ is called a *monotonous* metric if $f(\Gamma(0), \Gamma(t))$ is a continuous monotonically-increasing function of t , where $\Gamma : [0, 1) \rightarrow X$ is a smooth curve with $\Gamma(0) = z_0$ that intersects all equidistant orbits of z_0 exactly once.

EXERCISE I.9.9. Check the following:

- i. The function $F(z, w)$ (I.9.12) is monotonous.
- ii. If h is a monotonically-increasing, continuous, real function, then $f(z, w) = h \circ F(z, w)$ is a monotonous $\text{SL}_2(\mathbb{R})$ -invariant function.

In fact, the last example provides all such functions.

THEOREM I.9.10. A monotonous function $f(z, w)$ is invariant under $g \in \text{SL}_2(\mathbb{R})$ if and only if there exists a monotonically-increasing, continuous, real function h such that $f(z, w) = h \circ F(z, w)$.

PROOF. Because of the Exercise I.9.9.ii, we show the necessity only. Suppose there exists another function with such a property, say, $H(z, w)$. Due to invariance under $\text{SL}_2(\mathbb{R})$, this can be viewed as a function in one variable if we apply r^{-1} (cf. (I.9.4)) which sends z to ι and w to $r^{-1}(w)$. Now, by considering a fixed smooth curve Γ from Definition I.9.8, we can completely define $H(z, w)$ as a function of a single real variable $h(t) = H(\iota, \Gamma(t))$ and, similarly for $F(z, w)$,

$$H(z, w) = H(\iota, r^{-1}(w)) = h(t) \quad \text{and} \quad F(z, w) = F(\iota, r^{-1}(w)) = f(t),$$

where h and f are both continuous and monotonically-increasing since they represent metrics. Hence, the inverse f^{-1} exists everywhere by the inverse function theorem. So,

$$H(\iota, r^{-1}(w)) = h \circ f^{-1} \circ F(\iota, r^{-1}(w)).$$

Note that hf^{-1} is monotonic, since it is the composition of two monotonically-increasing functions, and this ends the proof. \square

REMARK I.9.11. The above proof carries over to a more general theorem which states: If there exist two monotonous functions $F(u, v)$ and $H(u, v)$ which are invariant under a transitive action of a group G , then there exists a monotonically-increasing real function h such that $H(z, w) = h \circ F(z, w)$.

As discussed in the previous section, in elliptic and hyperbolic geometries the function h from above is either $\sinh^{-1} t$ or $\sin^{-1} t$ (I.9.8) (I.9.10). Hence, it is reasonable to try inverse trigonometric and hyperbolic functions in the intermediate parabolic case as well.

REMARK I.9.12. The above result sheds light on the possibilities we have—we can either

- i. “label” the equidistant orbits with numbers, i.e choose a function h which will then determine the geodesic, or
- ii. choose a geodesic which will then determine h .

These two approaches are reflected in the next two sections.

I.9.3. Geodesics: Additivity of Metric

As pointed out earlier, there might not be a metric function which satisfies all the traditional properties. However, we still need the key ones, and we therefore make the following definition:

DEFINITION I.9.13. *Geodesics* for a metric d are smooth curves along which d is additive, that is $d(x, y) + d(y, z) = d(x, z)$, for any three point, of the curve, such that y is between x and z .

This definition is almost identical to the Menger line—see [32, § 2.3].

REMARK I.9.14. It is important that this definition is relevant in all EPH cases, i.e. in the elliptic and hyperbolic cases it would produce the well-known geodesics defined by the extremality condition.

Schematically, the proposed approach is:

$$(I.9.13) \quad \text{invariant metric} \xrightarrow{\text{additivity}} \text{invariant geodesic.}$$

Compare this with the Riemannian described in Section I.9.1:

$$(I.9.14) \quad \text{local metric} \xrightarrow{\text{extrema}} \text{geodesic} \xrightarrow{\text{integration}} \text{metric.}$$

Let us now proceed with finding geodesics from a metric function.

EXERCISE I.9.15. Let γ be a geodesic for a metric d . Write the differential equation for γ in term of d . HINT: Consider $d(w, w')$ as a real function in four variables, say $f(u, v, u', v')$. Then write the infinitesimal version of the additivity condition and obtain the equation

$$(I.9.15) \quad \frac{\delta v}{\delta u} = \frac{-f'_3(u, v, u', v') + f'_3(u', v', u', v')}{f'_4(u, v, u', v') - f'_4(u', v', u', v')},$$

where f'_n stands for the partial derivative of f with respect to the n -th variable. ◊

A natural choice for a metric is, cf. Exercises I.9.5.iii and I.9.6.ii,

$$(I.9.16) \quad d_{\sigma, \mathring{\sigma}}(w, w') = \sin_{\mathring{\sigma}}^{-1} \frac{|w - w'|_{\sigma}}{2\sqrt{\mathcal{J}[w]\mathcal{J}[w']}},$$

where the elliptic, parabolic and hyperbolic inverse sine functions are (see [129, 190])

$$(I.9.17) \quad \sin_{\mathring{\sigma}}^{-1} t = \begin{cases} \sinh^{-1} t, & \text{if } \mathring{\sigma} = -1, \\ 2t, & \text{if } \mathring{\sigma} = 0, \\ \sin^{-1} t, & \text{if } \mathring{\sigma} = 1. \end{cases}$$

Note that $\mathring{\sigma}$ is independent of σ although it takes the same three values, similar to the different signatures of point and cycle spaces introduced in Chapter I.4. It is used to denote the possible sub-cases within the parabolic geometry alone.

EXERCISE I.9.16. Check that:

- i. For $u = 0, v = 1$ and the metric $d_{p, \mathring{\sigma}}$ (I.9.16), Equation (I.9.15) is:

$$\frac{\delta v}{\delta u} = \frac{2v}{u} - \frac{\sqrt{|\mathring{\sigma}u^2 + 4v|}}{u}.$$

- ii. The geodesics through t for the metric $d_{p, \mathring{\sigma}}$ (I.9.16) are parabolas:

$$(I.9.18) \quad (\mathring{\sigma} + 4t^2)u^2 - 8tu - 4v + 4 = 0.$$

Let us verify which properties from Definition I.9.1 are satisfied by the invariant metric derived from (I.9.16). Two of the four properties hold—it is clearly symmetric and positive for every two points. However, the metric of any point to a point on the same vertical line is zero, so $d(z, w) = 0$ does not imply $z = w$. This can be overcome by introducing a different metric function just for the points on the vertical lines—see [339, § 3]. Note that we still have $d(z, z) = 0$ for all z .

The triangle inequality holds only in the elliptic point space, whereas, in the hyperbolic point space, we have the reverse situation: $d(w_1, w_2) \geq d(w_1, z) + d(z, w_2)$. There is an intermediate situation in the parabolic point space:

LEMMA I.9.17. *Take any $SL_2(\mathbb{R})$ -invariant metric function and take two points w_1, w_2 and the geodesic (in the sense of Definition I.9.13) through the points. Consider the strip $\Re[w_1] < u < \Re[w_2]$ and take a point z in it. Then, the geodesic divides the strip into two regions where $d(w_1, w_2) \leq d(w_1, z) + d(z, w_2)$ and where $d(w_1, w_2) \geq d(w_1, z) + d(z, w_2)$.*

PROOF. The only possible invariant metric function in parabolic geometry is of the form $d(z, w) = h \circ \frac{|\Re[z-w]|}{2\sqrt{\mathcal{J}[z]\mathcal{J}[w]}}$, where h is a monotonically-increasing, continuous, real function by Theorem I.9.10. Fix two points w_1, w_2 and the geodesic through them. Now consider some point $z = a + ib$ in the strip. The metric function is additive along a geodesic, so $d(w_1, w_2) = d(w_1, w(a)) + d(w(a), w_2)$, where $w(a)$ is a point on the geodesic with real part equal to a . However, if $\mathcal{J}[w(a)] < b$, then $d(w_1, w(a)) > d(w_1, z)$ and $d(w(a), w_2) > d(z, w_2)$, which implies $d(w_1, w_2) > d(w_1, z) + d(z, w_2)$. Similarly, if $\mathcal{J}[w(a)] > b$, then $d(w_1, w_2) < d(w_1, z) + d(z, w_2)$. ◻

REMARK I.9.18. The reason for the ease with which the result is obtained is the fact that the metric function is additive along the geodesics. This justifies the Definition I.9.13 of geodesics, in terms of additivity.

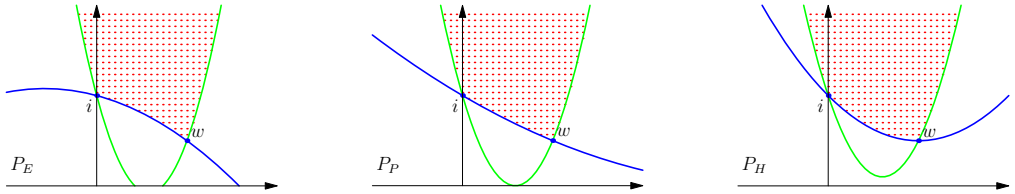


FIGURE I.9.2. Showing the region where the triangular inequality fails (shaded red).

To illustrate these ideas, look at the region where the converse of the triangular inequality holds for $d(z, w)_{\hat{\sigma}} = \sin_{\hat{\sigma}}^{-1} \frac{|\Re[z-w]|}{2\sqrt{\Im[z]\Im[w]}}$, shaded red in Fig. I.9.2. It is enclosed by two parabolas both of the form $(\hat{\sigma} + 4t^2)u^2 - 8tu - 4v + 4 = 0$ (which is the general equation of geodesics) and both passing through the two fixed points. The parabolas arise from taking both signs of the root, when solving the quadratic equation to find t . Segments of these parabolas, which bound the red region, are of different types—one of them is between points w_1 and w_2 , the second joins these points with infinity.

I.9.4. Geometric Invariants

In the previous section, we defined an invariant metric and derived the respective geodesics. Now, we will proceed in the opposite direction. As we discussed in Exercise I.9.7, the parabolic invariant metric obtained from the extremality condition is trivial. We work out an invariant metric from the Riemannian metric and predefined geodesics. It is schematically depicted, cf. (I.9.14), by

$$(I.9.19) \quad \text{Riemann metric} + \text{invariant geodesics} \xrightarrow{\text{integration}} \text{metric}.$$

A minimal requirement for the family of geodesics is that they should form an invariant subset of an invariant class of curves with no more than one curve joining every two points. Thus, if we are looking for $SL_2(\mathbb{R})$ -invariant metrics it is natural to ask whether geodesics are cycles. An invariant subset of cycles may be characterised by an invariant algebraic condition, e.g. orthogonality. However, the ordinary orthogonality is already fulfilled for the trivial geodesics from Exercise I.9.7, so, instead, we will try f -orthogonality to the real axes, Definition I.6.34. Recall that a cycle is f -orthogonal to the real axes if the real axes inverted in a cycle are orthogonal (in the usual sense) to the real axes.

EXERCISE I.9.19. Check that a parabola $ku^2 - 2lu - 2nv + m = 0$ is $\hat{\sigma}$ - f -orthogonal to the real line if $l^2 + \hat{\sigma}n^2 - mk = 0$, i.e. it is a $(-\hat{\sigma})$ -zero radius cycle.

As a starting point, consider the cycles that pass through ι . It is enough to specify only one such f -orthogonal cycle—the rest will be obtained by Möbius transformations fixing ι , i.e. parabolic rotations. Within these constraints there are three different families of parabolas determined by the value $\tilde{\sigma}$.

EXERCISE I.9.20. Check that the main parabolas passing ε

$$(I.9.20) \quad \tilde{\sigma}u^2 - 4v + 4 = 0,$$

where $\tilde{\sigma} = -1, 0, 1$, are f -orthogonal to the real line. Their rotations by an element of N' are parabolas (I.9.18).

Note that these are exactly the same geodesics obtained in (I.9.18). Hence, we already know what the metric function has to be. However, it is instructive to make the calculation from scratch since it does not involve anything from the previous section and is, in a way, more elementary and intuitive.

EXERCISE I.9.21. Follow these steps to calculate the invariant metric:

- i. Calculate the metric from ε to a point on the main parabola (I.9.20). HINT: Depending on whether the discriminant of the denominator in the integral (I.9.2) is positive, zero or negative, the results are trigonometric, rationals or hyperbolic, respectively:

$$\int_0^u \frac{dt}{\frac{1}{4}\tilde{\sigma}t^2 + 1} = \begin{cases} 4 \log \frac{2+u}{2-u}, & \text{if } \tilde{\sigma} = -1, \\ u, & \text{if } \tilde{\sigma} = 0, \\ \tan^{-1} \frac{u}{2}, & \text{if } \tilde{\sigma} = 1. \end{cases}$$

This is another example of EPH classification.◊

- ii. For a generic point (u, v) , find the N' rotation which puts the point on the main parabola (I.9.20).
- iii. For two given points w and w' , combine the Möbius transformation g such that $g : w \mapsto \varepsilon$ with the N' -rotation which puts $g(w')$ on the main parabola.
- iv. Deduce from the previous items the invariant metric from ε to (u, v) and check that it is a multiple of (I.9.16).
- v. The invariant parabolic metric for $\tilde{\sigma} = 1$ is equal to the angle between the tangents to the geodesic at its endpoints.

We meet an example of the splitting of the parabolic geometry into three different sub-cases, this will be followed by three types of Cayley transform in Section I.10.3 and Fig. I.10.3. The respective geodesics and equidistant orbits have been drawn in Fig. I.9.3. There is one more gradual transformation between the different geometries. We can see the transitions from the elliptic case to P_e , then to P_p , to P_h , to hyperbolic light-like and, finally, to space-like. To link it back, we observe a similarity between the final space-like case and the initial elliptic one.

EXERCISE I.9.22. Show that all parabolic geodesics from ε for a given value of $\tilde{\sigma}$ touch a certain parabola. This parabola can be called the *horizon* because geodesic rays will never reach points outside it. Note the similar effect for space-like and time-like geodesics in the hyperbolic case. HINT: This fact is a parabolic counterpart of Exercise I.5.29.◊

There is one more useful parallel between all the geometries. In Lobachevsky and Minkowski geometries, the *centres* of geodesics lie on the real axes. In parabolic geometry, the respective *ȯ-foci* (see Definition I.5.2) of *ȯ*-geodesic parabolas lie on the real axes. This fact is due to the relations between *f*-orthogonality and foci, cf. Proposition I.6.40.

I.9.5. Invariant Metric and Cross-Ratio

A very elegant presentation of the Möbius-invariant metric in the Lobachevsky half-plane is based on the cross-ratio (I.4.14)—see [26, § 15.2].

Let w_1 and w_2 be two different points of the Lobachevsky half-plane. Draw a selfadjoint circle (i.e. orthogonal to the real line) which passes through w_1 and w_2 . Let z_1 and z_2 be the points of intersection of the circle and the real line, cf. Fig. I.9.1(a). From Exercise I.4.22.iii, a cross-ratio of four concyclic points is real, thus we define the function of two points

$$\rho(w_1, w_2) = \log[z_1, w_1, w_2, z_2].$$

Surprisingly, this simple formula produces the Lobachevsky metric.

EXERCISE I.9.23. Show the following properties of ρ :

- i. It is Möbius-invariant, i.e. $\rho(w_1, w_2) = \rho(g \cdot w_1, g \cdot w_2)$ for any $g \in \text{SL}_2(\mathbb{R})$.
HINT: Use the fact that selfadjoint cycles form an invariant family and the Möbius-invariance of the cross-ratio, cf. Exercise I.4.20.iv.◊
- ii. It is additive, that is, for any three different points w_1, w_2, w_3 on the arc of a selfadjoint circle we have $\rho(w_1, w_3) = \rho(w_1, w_2) + \rho(w_2, w_3)$. HINT: Use the cancellation formula (I.4.18).◊
- iii. It coincides with the Lobachevsky metric (I.9.8). HINT: Evaluate that $\rho(i, ia) = \log a$ for any real $a > 1$. Thus, $\rho(i, ia)$ is the Lobachevsky metric between i and ia . Then, apply the Möbius-invariance of ρ and the Lobachevsky metric to extend the identity for any pair of points.◊

This approach to the invariant metric cannot be transferred to the parabolic and hyperbolic cases in a straightforward manner for geometric reasons. As we can see from Fig. I.9.3, there are certain types of geodesics which do not meet the real line. However, the case of *e*-geodesics in \mathbb{D} , which is the closest relative of the Lobachevsky half-plane, offers such a possibility.

EXERCISE I.9.24. Check that:

- i. $[-2, \varepsilon, w, 2] = (u + 2)/(2 - u)$, where $w = u + \varepsilon(1 - u^2/4)$, $u > 0$ is the point of the *e*-geodesics (main parabola) (I.9.20) passing ε and 2.
- ii. Let z_1 and z_2 be the intersections of the real line and the *e*-geodesic (I.9.18) passing two different points w_1 and w_2 in the upper half-plane, then $\rho(w_1, w_2) = 4 \log[z_1, w_1, w_2, z_2]$ is the invariant metric. HINT: Note that $\rho(\varepsilon, z) = 4 \log[-2, \varepsilon, z, 2]$ gives the metric calculated in Exercise I.9.21.i and use the Möbius-invariance of the cross-ratio.◊
- iii. In the case of *p*-geodesics in \mathbb{D} , find a fixed parabola C in the upper half-plane which replaces the real line in the following sense. The cross-ratio of two points and two intersections of C with *p*-geodesics though the points

produces an invariant metric. Find also the corresponding parabola for h-geodesics.

This is only a partial success in transferring of the elliptic theory to dual numbers. A more unified treatment for all EPH cases can be obtained from the projective cross-ratio [52]—see Section I.4.5 for corresponding definitions and results. In addition, we define the map $P(x, y) = \frac{x}{y}$ on the subset of $\mathbb{P}^1(\mathbb{A})$ consisting of vectors $(x, y) \in \mathbb{A}^2$ such that y is not a zero divisor. It is a left inverse of the map $S(z) = (z, 1)$ from Section I.4.5.

EXERCISE I.9.25. [52] Let $w_1, w_2 \in \mathbb{P}^1(\mathbb{A})$ be two essentially distinct points.

- i. Let w_1 and \bar{w}_2 be essentially distinct, express a generic invariant metric in $\mathbb{P}^1(\mathbb{A})$ through $[w_1, \bar{w}_2, w_2, \bar{w}_1]$ using the Möbius-invariance of the projective cross-ratio and the method from Section I.9.2.
- ii. For \mathbb{A} being complex or double numbers, let w_1 and w_2 be in the domain of P and $z_i = P(w_i)$, $i = 1, 2$. Show that, cf. Fig. I.9.1(a),

$$(I.9.21) \quad [w_1, \bar{w}_1, w_2, \bar{w}_2] = S \left(\frac{|z_1 - z_2|_\sigma^2}{4\Im[z_1]\Im[z_2]} \right).$$

Deduce a generic Möbius-invariant metric on \mathbb{A} based on (I.9.12).

To obtain the respective notion of geodesics in $\mathbb{P}^1(\mathbb{A})$ from the above Möbius-invariant metric we can again use the route from Section I.9.3.

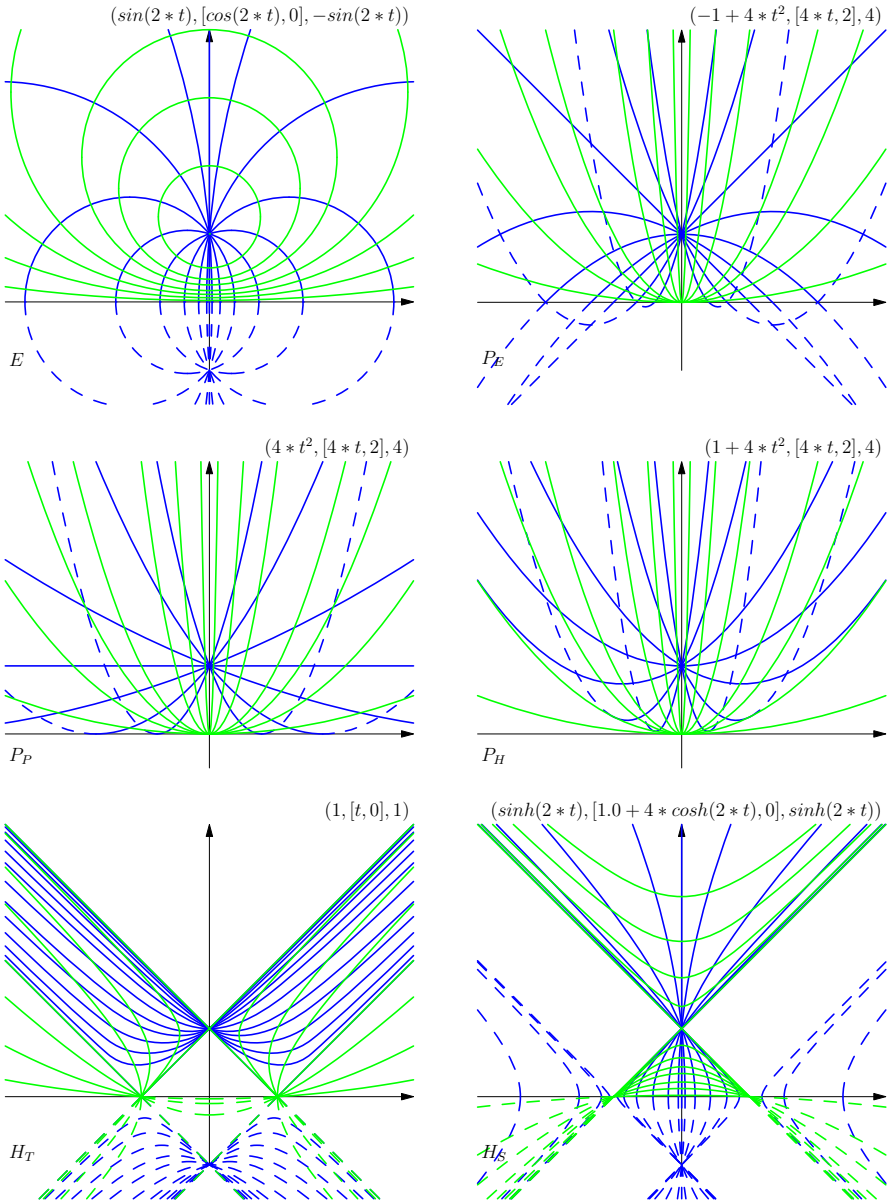


FIGURE I.9.3. Showing geodesics (blue) and equidistant orbits (green) in EPH geometries. Above are written $(k, [l, n], m)$ in $ku^2 - 2lu - 2nv + m = 0$, giving the equation of geodesics.

Conformal Unit Disk

The upper half-plane is a universal object for all three EPH cases, which was obtained in a uniform fashion considering two-dimensional homogeneous spaces of $SL_2(\mathbb{R})$. However, universal models are rarely well-suited to all circumstances. For example, it is more convenient, for many reasons, to consider the compact *unit disk* in \mathbb{C} rather than the unbounded upper half-plane:

“... the reader must become adept at frequently changing from one model to the other as each has its own particular advantage.” [24, § 7.1]

Of course, both models are conformally-isomorphic through the *Cayley transform*.

We derive similar constructions for parabolic and hyperbolic cases in this chapter. However, we shall see that there is not a “universal unit disk”. Instead, we obtain something specific in each EPH case from the same upper half-plane. As has already happened on several occasions, the elliptic and hyperbolic cases are rather similar and, thus, it is the parabolic case which requires special treatment.

I.10.1. Elliptic Cayley Transforms

In the elliptic and hyperbolic cases, the Cayley transform is given by the matrix $Y_\sigma = \begin{pmatrix} 1 & -\iota \\ \sigma\iota & 1 \end{pmatrix}$, where $\sigma = \iota^2$ and $\det Y_\sigma = 2$. The matrix Y_σ produces the respective Möbius transform $\mathbb{A} \rightarrow \mathbb{A}$:

$$(I.10.1) \quad \begin{pmatrix} 1 & -\iota \\ \sigma\iota & 1 \end{pmatrix} : w = (u + \iota v) \mapsto Y_\sigma w = \frac{(u + \iota v) - \iota}{\sigma\iota(u + \iota v) + 1}.$$

The same matrix Y_σ acts by conjugation $g_Y = \frac{1}{2}Y_\sigma g Y_\sigma^{-1}$ on an element $g \in SL_2(\mathbb{R})$:

$$(I.10.2) \quad g_Y = \frac{1}{2} \begin{pmatrix} 1 & -\iota \\ \sigma\iota & 1 \end{pmatrix} \begin{pmatrix} a & b \\ c & d \end{pmatrix} \begin{pmatrix} 1 & \iota \\ -\sigma\iota & 1 \end{pmatrix}.$$

The connection between the two forms (I.10.1) and (I.10.2) of the Cayley transform is $g_Y Y_\sigma w = Y_\sigma(gw)$, i.e. Y_σ intertwines the actions of g and g_Y .

The Cayley transform in the elliptic case is very important [240, § IX.3; 321, Ch. 8, (1.12)], both for complex analysis and representation theory of $SL_2(\mathbb{R})$. The transformation $g \mapsto g_Y$ (I.10.2) is an isomorphism of the groups $SL_2(\mathbb{R})$ and $SU(1, 1)$. Namely, in complex numbers, we have

$$(I.10.3) \quad g_Y = \frac{1}{2} \begin{pmatrix} \alpha & \beta \\ \bar{\beta} & \bar{\alpha} \end{pmatrix}, \text{ with } \alpha = (a + d) + (b - c)i \text{ and } \beta = (b + c) + (a - d)i.$$

The group $SU(1, 1)$ acts transitively on the *elliptic unit disk*. The images of the elliptic actions of subgroups A , N , K are given in Fig. I.10.3(E). Any other subgroup is conjugated to one of them and its class can be easily distinguished in this model by the number of *fixed points on the boundary*—two, one and zero, respectively. A closer inspection demonstrates that there are always *two* fixed points on the whole plane. They are either

- one strictly inside and one strictly outside of the unit circle,
- one *double* fixed point on the unit circle, or
- two different fixed points exactly on the circle.

Consideration of Fig. I.7.1(b) shows that the parabolic subgroup N is like a phase transition between the elliptic subgroup K and hyperbolic A , cf. (I.1.2). Indeed, if a fixed point of a subgroup conjugated to K approaches a place on the boundary, then the other fixed point moves to the same place on the unit disk from the opposite side. After they collide to a parabolic double point on the boundary, they may decouple into two distinct fixed points on the unit disk representing a subgroup conjugated to A .

In some sense the elliptic Cayley transform swaps complexities. In contrast to the upper half-plane, the K -action is now simple but A and N are not. The simplicity of K orbits is explained by diagonalisation of the corresponding matrices:

$$(I.10.4) \quad \frac{1}{2} \begin{pmatrix} 1 & -i \\ -i & 1 \end{pmatrix} \begin{pmatrix} \cos \phi & \sin \phi \\ -\sin \phi & \cos \phi \end{pmatrix} \begin{pmatrix} 1 & i \\ i & 1 \end{pmatrix} = \begin{pmatrix} e^{i\phi} & 0 \\ 0 & e^{-i\phi} \end{pmatrix}.$$

These diagonal matrices generate Möbius transformations which correspond to multiplication by the unimodular scalar $e^{2i\phi}$. Geometrically, they are isometric rotations, i.e. they preserve distances $d_{e,e}$ (I.7.2) and length l_{c_e} .

EXERCISE I.10.1. Check, in the elliptic case, that the real axis is transformed to the *unit circle* and the upper half-plane is mapped to the *elliptic unit disk*

$$(I.10.5) \quad \mathbb{R} = \{(u, v) \mid v = 0\} \rightarrow \mathbb{T}_e = \{(u, v) \mid l_{c_e}^2(u, v) = u^2 + v^2 = 1\},$$

$$(I.10.6) \quad \mathbb{R}_+^c = \{(u, v) \mid v > 0\} \rightarrow \mathbb{D}_e = \{(u, v) \mid l_{c_e}^2(u, v) = u^2 + v^2 < 1\},$$

where the length from centre $l_{c_e}^2$ is given by (I.7.6) for $\sigma = \check{\sigma} = -1$ and coincides with the distance $d_{e,e}$ (I.7.2).

$SL_2(\mathbb{R})$ acts transitively on both sets and the unit circle is generated, for example, by the point $(0, 1)$, and the unit disk by $(0, 0)$.

I.10.2. Hyperbolic Cayley Transform

A hyperbolic version of the Cayley transform was used in [170]. The above formula (I.10.2) in \mathbb{O} becomes

$$(I.10.7) \quad g_V = \frac{1}{2} \begin{pmatrix} \alpha & \beta \\ -\bar{\beta} & \bar{\alpha} \end{pmatrix}, \text{ with } \alpha = a + d - (b + c)j \text{ and } h = (a - d)j + (b - c),$$

with some subtle differences in comparison to (I.10.3). The corresponding A , N and K orbits are given in Fig. I.10.3(H). However, there is an important distinction between the elliptic and hyperbolic cases similar to the one discussed in Section I.8.2.

EXERCISE I.10.2. Check, in the hyperbolic case, that the real axis is transformed to the cycle

$$(I.10.8) \quad \mathbb{R} = \{(u, v) \mid v = 0\} \rightarrow \mathbb{T}_h = \{(u, v) \mid l_{c_h}^2(u, v) = u^2 - v^2 = -1\},$$

where the length from the centre $l_{c_h}^2$ is given by (I.7.6) for $\sigma = \check{\sigma} = 1$ and coincides with the distance $d_{h,h}$ (I.7.2). On the hyperbolic unit circle, $SL_2(\mathbb{R})$ acts transitively and it is generated, for example, by point $(0, 1)$.

$SL_2(\mathbb{R})$ acts also *transitively on the whole complement*

$$\{(u, v) \mid l_{c_h}^2(u, v) \neq -1\}$$

to the unit circle, i.e. on its “inner” and “outer” parts together.

Recall from Section I.8.2 that we defined $\tilde{\mathbb{O}}$ to be the two-fold cover of the hyperbolic point space \mathbb{O} consisting of two isomorphic copies \mathbb{O}^+ and \mathbb{O}^- glued together, cf. Fig. I.8.3. The conformal version of the *hyperbolic unit disk* in $\tilde{\mathbb{O}}$ is, cf. the upper half-plane from (I.8.1),

$$(I.10.9) \quad \tilde{\mathbb{D}}_h = \{(u, v) \in \mathbb{O}^+ \mid u^2 - v^2 > -1\} \cup \{(u, v) \in \mathbb{O}^- \mid u^2 - v^2 < -1\}.$$

EXERCISE I.10.3. Verify that:

- i. $\tilde{\mathbb{D}}_h$ is conformally-invariant and has a boundary $\tilde{\mathbb{T}}_h$ —two copies of the unit hyperbolas in \mathbb{O}^+ and \mathbb{O}^- .
- ii. The hyperbolic Cayley transform is a one-to-one map between the hyperbolic upper half-plane $\tilde{\mathbb{O}}^+$ and hyperbolic unit disk $\tilde{\mathbb{D}}_h$.

We call $\tilde{\mathbb{T}}_h$ the *hyperbolic unit cycle* in \mathbb{O} . Figure I.8.3(b) illustrates the geometry of the hyperbolic unit disk in $\tilde{\mathbb{O}}$ compared to the upper half-plane. We can also say, rather informally, that the hyperbolic Cayley transform maps the “upper” half-plane onto the “inner” part of the unit disk.

One may wish that the hyperbolic Cayley transform diagonalises the action of subgroup A , or some conjugate of it, in a fashion similar to the elliptic case (I.10.4) for K . Geometrically, it corresponds to hyperbolic rotations of the hyperbolic unit disk around the origin. Since the origin is the image of the point ι in the upper half-plane under the Cayley transform, we will use the isotropy subgroup A' . Under the Cayley map (I.10.7), an element of the subgroup A' becomes

$$(I.10.10) \quad \frac{1}{2} \begin{pmatrix} 1 & -j \\ j & 1 \end{pmatrix} \begin{pmatrix} \cosh t & -\sinh t \\ -\sinh t & \cosh t \end{pmatrix} \begin{pmatrix} 1 & j \\ -j & 1 \end{pmatrix} = \begin{pmatrix} e^{jt} & 0 \\ 0 & e^{-jt} \end{pmatrix},$$

where $e^{jt} = \cosh t + j \sinh t$. The corresponding Möbius transformation is a multiplication by e^{2jt} , which obviously corresponds to isometric hyperbolic rotations of \mathbb{O} for distance $d_{h,h}$ and length l_{c_h} . This is illustrated in Fig. I.10.1(H:A').

I.10.3. Parabolic Cayley Transforms

The parabolic case benefits from a larger variety of choices. The first, natural, attempt is to define a Cayley transform from the same formula (I.10.1) with the parabolic

value $\sigma = 0$. The corresponding transformation is defined by the matrix $\begin{pmatrix} 1 & -\varepsilon \\ 0 & 1 \end{pmatrix}$ and, geometrically, produces a shift one unit down.

However, within the extended FSCc, a more general version of the parabolic Cayley transform is also possible. It is given by the matrix

$$(I.10.11) \quad Y_{\check{\sigma}} = \begin{pmatrix} 1 & -\varepsilon \\ \check{\sigma}\varepsilon & 1 \end{pmatrix}, \quad \text{where } \check{\sigma} = -1, 0, 1 \text{ and } \det Y_{\check{\sigma}} = 1 \text{ for all } \check{\sigma}.$$

Here, $\check{\sigma} = -1$ corresponds to the parabolic Cayley transform P_e with an elliptic flavour, and $\check{\sigma} = 1$ to the parabolic Cayley transform P_h with a hyperbolic flavour. Finally, the parabolic-parabolic transform P_p is given by the upper-triangular matrix mentioned at the beginning of this section.

Figure I.10.3 presents these transforms in rows P_e , P_p and P_h , respectively. The row P_p almost coincides with Fig. I.1.1 and the parabolic case in Fig. I.1.2. Consideration of Fig. I.10.3 by following the columns from top to bottom gives an impressive mixture of many common properties (e.g. the number of fixed points on the boundary for each subgroup) with several gradual mutations.

The description of the parabolic unit disk admits several different interpretations in terms of lengths from Definition I.7.9.

EXERCISE I.10.4. The parabolic Cayley transform $P_{\check{\sigma}}$, as defined by the matrix $Y_{\check{\sigma}}$ (I.10.11), always acts on the V -axis as a shift one unit down.

If $\check{\sigma} \neq 0$, then $P_{\check{\sigma}}$ transforms the real axis to the *parabolic unit cycle* such that

$$(I.10.12) \quad \mathbb{T}^{P_{\check{\sigma}}} = \{(u, v) \in \mathbb{D} \mid l^2(B, (u, v)) \cdot (-\check{\sigma}) = 1\},$$

and the image of upper half-plane is

$$(I.10.13) \quad \mathbb{D}^{P_{\check{\sigma}}} = \{(u, v) \in \mathbb{D} \mid l^2(B, (u, v)) \cdot (-\check{\sigma}) < 1\},$$

where the length l and the point B can be any of the following:

- i. $l^2 = l_{c_e}^2(B, (u, v)) = u^2 + \check{\sigma}v$ is the (p,p,e) -length (I.7.6) from the e -centre $B_e = (0, -\frac{\check{\sigma}}{2})$.
- ii. $l^2 = l_{f_h}^2(B, (u, v))$ is the (p,p,h) -length (I.7.8) from the h -focus $B = (0, -1 - \frac{\check{\sigma}}{4})$.
- iii. $l^2 = l_{f_p}^2(B, (u, v)) = \frac{u^2}{v+1}$ is the (p,p,p) -length (I.7.9) from the p -focus $B = (0, -1)$.

HINT: The statements are slightly tautological, since, by definition, p -cycles are the loci of points with certain defined lengths from their respective centres or foci.◊

REMARK I.10.5. Note that both the elliptic (I.10.5) and hyperbolic (I.10.8) unit cycles can be also presented in the form similar to (I.10.12),

$$\mathbb{D}_{\sigma} = \{(u', v') \mid l_{c_{\sigma}}^2(B, (u, v)) \cdot (-\sigma) = 1\},$$

in terms of the (σ, σ) -length from the σ -centre $B = (0, 0)$ as in Exercise I.10.4.i.

The above descriptions (I.10.4.i and I.10.4.iii) are attractive for reasons given in the following two exercises. Firstly, we note that K -orbits in the elliptic case (Fig. I.10.1(E:K)) and A' -orbits in the hyperbolic case (Fig. I.10.1(H:A')) of the Cayley transform are concentric.

EXERCISE I.10.6. N-orbits in the parabolic cases (Fig. I.10.3($P_e : N$, $P_p : N$, $P_h : N$)) are *concentric parabolas* (or straight lines) in the sense of Definition I.4.3 with e-centres at $(0, \frac{1}{2})$, $(0, \infty)$ and $(0, -\frac{1}{2})$, respectively. Consequently, the N-orbits are loci of equidistant points in terms of the (p,p,e) -length from the respective centres.

Secondly, we observe that Cayley images of the isotropy subgroups' orbits in elliptic and hyperbolic spaces in Fig. I.10.1(E:K) and (H:A) are equidistant from the origin in the corresponding metrics.

EXERCISE I.10.7. The Cayley transform of orbits of the parabolic isotropy subgroup in Fig. I.10.1($P_e : N'$) comprises confocal parabolas consisting of points on the same l_p -length (I.7.7) from the point $(0, -1)$ —cf. I.10.4.iii.

We will introduce linear structures preserved by actions of the subgroups N and N' on the parabolic unit disk in Chapter I.11.

REMARK I.10.8. We see that the variety of possible Cayley transforms in the parabolic case is larger than in the other two cases. It is interesting that this variety is a consequence of the parabolic degeneracy of the generator $\varepsilon^2 = 0$. Indeed, for both the elliptic and the hyperbolic signs in $t^2 = \pm 1$, only one matrix (I.10.1) out of two possible $\begin{pmatrix} 1 & t \\ \pm\sigma t & 1 \end{pmatrix}$ has a non-zero determinant. Also, all these matrices are non-singular only for the degenerate parabolic value $t^2 = 0$.

Orbits of the isotropy subgroups A' , N' and K from Exercise I.3.20 under the Cayley transform are shown in Fig. I.10.1, which should be compared with the action of the same subgroup on the upper half-plane in Fig. I.3.1.

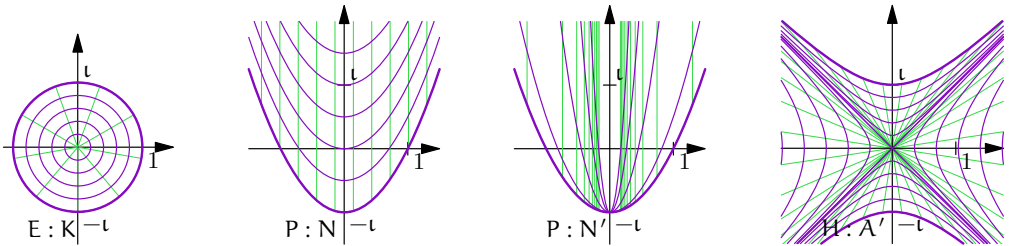


FIGURE I.10.1. Action of the isotropy subgroups of t under the Cayley transform—subgroup K in the elliptic case, N' in the parabolic and A' in the hyperbolic. Orbits of K and A' are concentric while orbits of N' are confocal. We also provide orbits of N which are concentric in the parabolic case. The action of K, N' and A' on the upper half-plane are presented in Fig. I.3.1.

I.10.4. Cayley Transforms of Cycles

The next natural step within the FSCc is to expand the Cayley transform to the space of cycles.

I.10.4.1. Cayley Transform and FSSc. The effect of the Cayley transform on cycles turns out to be a cycle similarity in the elliptic and hyperbolic cases only, the degeneracy of the parabolic case requires a special treatment.

EXERCISE I.10.9. Let C_σ^s be a cycle in \mathbb{A} . Check that:

- (e, h) In the elliptic or hyperbolic cases, the Cayley transform of the cycle C_σ is $R_\sigma \hat{C}_\sigma C_\sigma \hat{C}_\sigma R_\sigma$, i.e. the composition of the similarity (I.6.10) by the cycle $\hat{C}_\sigma^s = (\sigma, 0, 1, 1)$ and the similarity by the real line (see the first and last drawings in Fig. I.10.2).
- (p) In the parabolic case, the Cayley transform maps a cycle (k, l, n, m) to the cycle $(k - 2\check{\sigma}n, l, n, m - 2n)$.

HINT: We can follow a similar path to the proof of Theorem I.4.13. Alternatively, for the first part, we notice that the matrix Y_σ of the Cayley transform and the FSSc matrix of the cycle \hat{C}_σ^s are different by a constant factor. The reflection in the real line compensates the effect of complex conjugation in the similarity (I.6.10). \diamond

EXERCISE I.10.10. Investigate what are images under the Cayley transform of zero-radius cycles, selfadjoint cycles, orthogonal cycles and f-orthogonal cycles.

The above extension of the Cayley transform to the cycle space is linear, but in the parabolic case it is not expressed as a similarity of matrices (*reflections in a cycle*). This can be seen, for example, from the fact that the parabolic Cayley transform does not preserve the zero-radius cycles represented by matrices with zero p-determinant. Since orbits of all subgroups in $SL_2(\mathbb{R})$, as well as their Cayley images, are cycles in

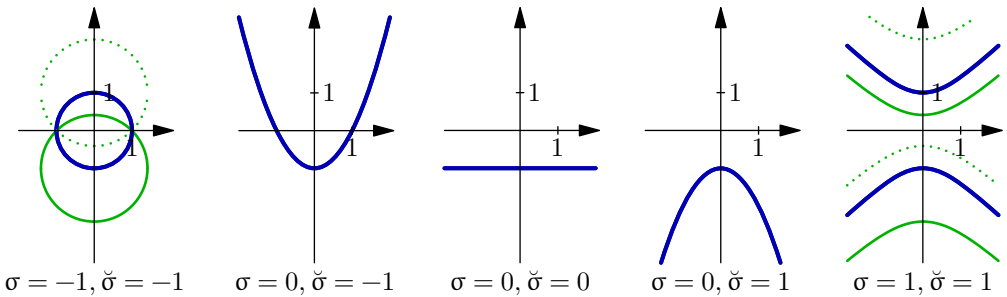


FIGURE I.10.2. Cayley transforms in elliptic ($\sigma = -1$), parabolic ($\sigma = 0$) and hyperbolic ($\sigma = 1$) spaces. In each picture, the reflection of the real line in the green cycles (drawn continuously or dotted) is the blue “unit cycle”. Reflections in the solidly-drawn cycles send the upper half-plane to the unit disk and reflections in the dashed cycles send it to its complement. Three Cayley transforms in the parabolic space ($\sigma = 0$) are themselves elliptic ($\check{\sigma} = -1$), parabolic ($\check{\sigma} = 0$) and hyperbolic ($\check{\sigma} = 1$), giving a gradual transition between proper elliptic and hyperbolic cases.

the corresponding metrics, we may use Exercises I.10.9(p) and I.4.16.ii to prove the following statements (in addition to Exercise I.10.6).

EXERCISE I.10.11. Verify that:

- i. A-orbits in transforms P_e and P_h are segments of parabolas with focal length $\frac{1}{4}$ and passing through $(0, -1)$. Their p-foci (i.e. vertices) belong to two parabolas $v = (-u^2 - 1)$ and $v = (u^2 - 1)$ respectively, which are the boundaries of parabolic circles in P_h and P_e (note the swap!).
- ii. K-orbits in transform P_e are parabolas with focal length less than $\frac{1}{4}$. In transform P_h , they are parabolas where the reciprocal of the focal length is larger than -4 .

Since the action of the parabolic Cayley transform on cycles does not preserve zero-radius cycles, one would be better using infinitesimal-radius cycles from Section I.7.5 instead. Indeed, the Cayley transform preserves infinitesimality.

EXERCISE I.10.12. Show that images of infinitesimal cycles under the parabolic Cayley transform are, themselves, infinitesimal cycles.

We recall a useful expression of concurrence with an infinitesimal cycle's focus through f -orthogonality from Exercise I.7.26.ii. Some caution is required since f -orthogonality of generic cycles is not preserved by the parabolic Cayley transform, just like it is not preserved by cycle similarity in Exercise I.10.9(p). A remarkable exclusion happens for infinitesimal cycles.

EXERCISE I.10.13. An infinitesimal cycle $C_{\tilde{\sigma}}^{\alpha}$ (I.7.13) is f -orthogonal (in the sense of Exercise I.7.26.ii) to a cycle $\tilde{C}_{\tilde{\sigma}}^{\alpha}$ if and only if the Cayley transform I.10.9(p) of $C_{\tilde{\sigma}}^{\alpha}$ is f -orthogonal to the Cayley transform of $\tilde{C}_{\tilde{\sigma}}^{\alpha}$.

I.10.4.2. Geodesics on the Disks. We apply the advise quoted at the beginning of this chapter to the invariant distance discussed in Chapter I.9. The equidistant curves and respective geodesics in \mathbb{A} are cycles, they correspond to certain cycles on the unit disks. As on many previous occasions we need to distinguish the elliptic and hyperbolic cases from the parabolic one.

EXERCISE I.10.14. [165] Check that:

(e,h): Elliptic and hyperbolic Cayley transforms (I.10.1) send the respective geodesics and (I.9.9) passing ι to the straight line passing the origin. Consequently, any geodesics is a cycle orthogonal to the boundary of the unit disk. The respective invariant metrics on the unit disks are, cf. [339, Table VI],

$$(I.10.14) \quad \sin_{\tilde{\sigma}}^{-1} \frac{|w - w'|_{\tilde{\sigma}}}{2\sqrt{(1 + \sigma w \bar{w})(1 + \sigma w' \bar{w}')}} ,$$

where $\tilde{\sigma} = 1$ in the elliptic case and has a value depending on the degree of space- or light-likeness in the hyperbolic case.

(p): The $\tilde{\sigma}$ -parabolic Cayley transform (I.10.11) maps the $\tilde{\sigma}$ -geodesics (I.9.18) passing ε to the parabolas passing the origin:

$$(\tilde{\sigma} - 4\check{\sigma} + 4t^2)u^2 - 8tu - 4v = 0.$$

The invariant $\check{\sigma}$ -metric on the $\check{\sigma}$ -parabolic unit circle is

$$(I.10.15) \quad \sin_{\check{\sigma}}^{-1} \frac{|u - u'|}{\sqrt{(1 + v + \check{\sigma}u^2)(1 + v' + \check{\sigma}u'^2)}} .$$

The appearance of straight lines as geodesics in the elliptic and hyperbolic disks is an illustration of its “own particular advantage” mentioned in the opening quote to this chapter.

We will look closer on isometric transformations the unit disks in the next chapter.

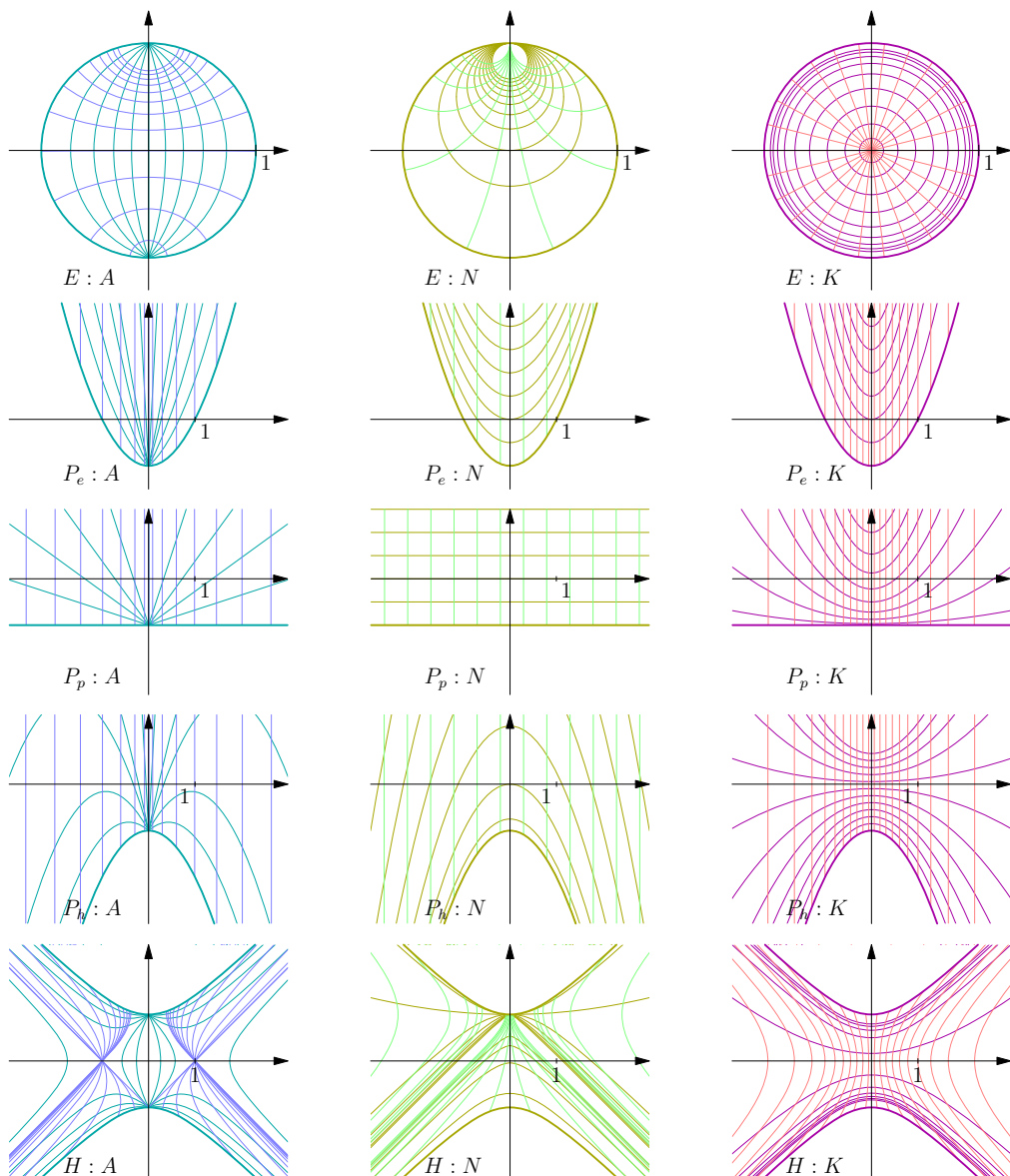


FIGURE I.10.3. EPH unit disks and actions of one-parameter subgroups A , N and K .

(E): The elliptic unit disk.

(P_e), (P_p), (P_h): The elliptic, parabolic and hyperbolic flavours of the parabolic unit disk.

(H): The hyperbolic unit disk.

Unitary Rotations

One of the important advantages of the elliptic and hyperbolic unit disks introduced in Sections I.10.1–I.10.2 is a simplification of isotropy subgroup actions. Indeed, images of the subgroups K and A' , which fix the origin in the elliptic and hyperbolic disks, respectively, consist of diagonal matrices—see (I.10.4) and (I.10.10). These diagonal matrices produce Möbius transformations, which are multiplications by hypercomplex unimodular numbers and, thus, are linear. In this chapter, we discuss the possibility of similar results in the parabolic unit disks from Section I.10.3.

I.11.1. Unitary Rotations—an Algebraic Approach

Consider the elliptic unit disk $z\bar{z} < 1$ (I.10.6) with the Möbius transformations transferred by the Cayley transform (I.10.1) from the upper half-plane. The isotropy subgroup of the origin is conjugated to K and consists of the diagonal matrices $\begin{pmatrix} e^{i\phi} & 0 \\ 0 & e^{-i\phi} \end{pmatrix}$. The corresponding Möbius transformations are linear and are represented geometrically by rotation of \mathbb{R}^2 by the angle 2ϕ . After making the identification $\mathbb{R}^2 = \mathbb{C}$, this action is given by the multiplication $e^{2i\phi}$. The rotation preserves the (elliptic) distance (I.7.5) given by

$$(I.11.1) \quad x^2 + y^2 = (x + iy)(x - iy).$$

Therefore, the orbits of rotations are circles and any line passing the origin (a “spoke”) is rotated by an angle 2ϕ —see Fig. II.3.1(E). We can also see that those rotations are isometries for the conformally-invariant metric (I.10.14) on the elliptic unit disk. Moreover, the rotated “spokes”—the straight lines through the origin—are geodesics for this invariant metric.

A natural attempt is to employ the algebraic aspect of this construction and translate to two other cases (parabolic and hyperbolic) through the respective hypercomplex numbers.

EXERCISE I.11.1. Use the algebraic similarity between the three number systems from Fig. B.2 and its geometric depiction from Fig. II.3.1 to check the following for each EPH case:

- i. The algebraic EPH disks are defined by the condition $d_{\sigma,\sigma}(0, z) < 1$, where $d_{\sigma,\sigma}^2(0, z) = z\bar{z}$.
- ii. There is the one-parameter group of automorphisms provided by multiplication by $e^{t\mathfrak{t}}$, $t \in \mathbb{R}$. Orbits of these transformations are “rims” $d_{\sigma,\sigma}(0, z) = r$, where $r < 1$.

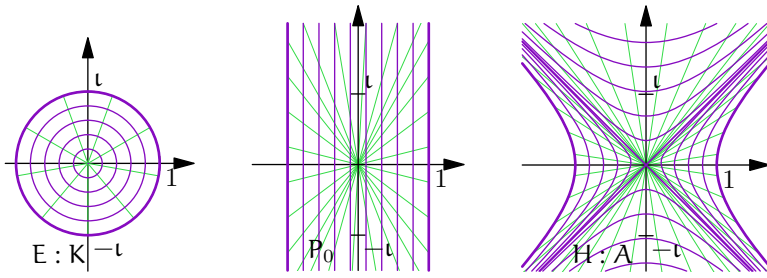


FIGURE I.11.1. Rotations of algebraic wheels, i.e. multiplication by $e^{t\epsilon}$: elliptic (E), trivial parabolic (P_0) and hyperbolic (H). All blue orbits are defined by the identity $x^2 - t^2 y^2 = r^2$. Green “spokes” (straight lines from the origin to a point on the orbit) are “rotated” from the real axis.

- iii. The “spokes”, that is, the straight lines through the origin, are rotated. In other words, the image of one spoke is another spoke.

The value of $e^{t\epsilon}$ can be defined, e.g. from the Taylor expansion of the exponent. In particular, for the parabolic case, $\epsilon^k = 0$ for all $k \geq 2$, so $e^{\epsilon t} = 1 + \epsilon t$. Then, the parabolic rotations explicitly act on dual numbers as follows:

$$(I.11.2) \quad e^{\epsilon x} : a + \epsilon b \mapsto a + \epsilon(\alpha x + b).$$

In other words, the value of the imaginary part does not affect transformation of the real one, but not *vice versa*. This links the parabolic rotations with the Galilean group [339] of symmetries of classical mechanics, with the absolute time disconnected from space, cf. Section I.8.4.

The obvious algebraic similarity from Exercise II.3.1 and the connection to classical kinematics is a widespread justification for the following viewpoint on the parabolic case, cf. [129, 339]:

- The parabolic trigonometric functions cosp and sinp are trivial:

$$(I.11.3) \quad \text{cosp } t = \pm 1, \quad \text{sinp } t = t.$$

- The parabolic distance is independent from v if $u \neq 0$:

$$(I.11.4) \quad u^2 = (u + \epsilon v)(u - \epsilon v).$$

- The polar decomposition of a dual number is defined by, cf. [339, App. C(30')]:

$$(I.11.5) \quad u + \epsilon v = u(1 + \epsilon \frac{v}{u}), \quad \text{thus} \quad |u + \epsilon v| = u, \quad \arg(u + \epsilon v) = \frac{v}{u}.$$

- The parabolic wheel looks rectangular, see Fig. II.3.1(P_0).

These algebraic analogies are quite explicit and are widely accepted as an ultimate source for parabolic trigonometry [129, 241, 339]. However, we will see shortly that there exist geometric motivation and a connection with the parabolic equation of mathematical physics.

I.11.2. Unitary Rotations—a Geometrical Viewpoint

We make another attempt at describing parabolic rotations. The algebraic attempt exploited the representation of rotation by hypercomplex multiplication. However, in the case of dual numbers this leads to a degenerate picture. If multiplication (a linear transformation) is not sophisticated enough for this, we can advance to the next level of complexity: linear-fractional.

In brief, we change our viewpoint from algebraic to geometric. Elliptic and hypercomplex rotations of the respective unit disks are also Möbius transformations from the one-parameter subgroups K and A' in the respective Cayley transform. Therefore, the parabolic counterpart corresponds to Möbius transformations from the subgroup N' .

For the sake of brevity, we will only treat the elliptic version P_e of the parabolic Cayley transform from Section I.10.3. We use the Cayley transform defined by the matrix

$$C_\varepsilon = \begin{pmatrix} 1 & -\varepsilon \\ -\varepsilon & 1 \end{pmatrix}.$$

The Cayley transform of matrices (I.3.7) from the subgroup N is

$$(I.11.6) \quad \begin{pmatrix} 1 & -\varepsilon \\ -\varepsilon & 1 \end{pmatrix} \begin{pmatrix} 1 & t \\ 0 & 1 \end{pmatrix} \begin{pmatrix} 1 & \varepsilon \\ \varepsilon & 1 \end{pmatrix} = \begin{pmatrix} 1 + \varepsilon t & t \\ 0 & 1 - \varepsilon t \end{pmatrix} = \begin{pmatrix} e^{\varepsilon t} & t \\ 0 & e^{-\varepsilon t} \end{pmatrix}.$$

This is not too different from the diagonal forms in the elliptic (I.10.4) and hyperbolic (I.10.10). However, the off-diagonal $(1, 2)$ -term destroys harmony. Nevertheless, we will continue defining a unitary parabolic rotation to be the Möbius transformation with the matrix (I.11.6), which is no longer multiplication by a scalar. For the subgroup N' , the matrix is obtained by transposition of (I.11.6).

In the elliptic and hyperbolic cases, the image of reference point $(-i)$ is:

$$(I.11.7) \quad \begin{pmatrix} e^{it} & 0 \\ 0 & e^{-it} \end{pmatrix} : -i \mapsto \sin 2t - i \cos 2t,$$

$$(I.11.8) \quad \begin{pmatrix} e^{jt} & 0 \\ 0 & e^{-jt} \end{pmatrix} : -j \mapsto -\sinh 2t - j \cosh 2t,$$

EXERCISE I.11.2. Check that parabolic rotations with the upper-triangular matrices from the subgroup N become:

$$(I.11.9) \quad \begin{pmatrix} e^{\varepsilon t} & t \\ 0 & e^{-\varepsilon t} \end{pmatrix} : -\varepsilon \mapsto t - \varepsilon(1 - t^2).$$

This coincides with the *cyclic rotations* defined in [339, § 8]. A comparison with the Euler formula seemingly confirms that $\sinp t = t$, but suggests a new expression for $\cosp t$:

$$\cosp t = 1 - t^2, \quad \sinp t = t.$$

Therefore, the parabolic Pythagoras' identity would be

$$(I.11.10) \quad \sinp^2 t + \cosp t = 1,$$

which fits well between the elliptic and hyperbolic versions:

$$\sin^2 t + \cos^2 t = 1, \quad \sinh^2 t - \cosh^2 t = -1.$$

The identity (I.11.10) is also less trivial than the version $\cosh^2 t = 1$ from (II.3.3)–(II.3.4)—see also [129]. The possible ranges of the cosine and sine functions are given by the table:

	elliptic	parabolic	hyperbolic
cosine	$[-1, 1]$	$(-\infty, 1]$	$[1, \infty)$
sine	$[-1, 1]$	$(-\infty, \infty)$	$(-\infty, \infty)$

There is a second option for defining parabolic rotations for the lower-triangular matrices from the subgroup N' . The important difference is now that the reference point cannot be $-\varepsilon$ since it is a fixed point (as well as any point on the vertical axis). Instead, we take ε^{-1} , which is an ideal element (a point at infinity), since ε is a divisor of zero. The proper treatment is based on the projective coordinates, where point ε^{-1} is represented by a vector $(1, \varepsilon)$ —see Section I.8.1.

EXERCISE I.11.3. Check the map of reference point ε^{-1} for the subgroup N' :

$$(I.11.11) \quad \begin{pmatrix} e^{-\varepsilon t} & 0 \\ t & e^{\varepsilon t} \end{pmatrix} : \frac{1}{\varepsilon} \mapsto \frac{1}{t} + \varepsilon \left(1 - \frac{1}{t^2}\right).$$

A comparison with (I.11.9) shows that this form is obtained by the substitution $t \mapsto t^{-1}$. The same transformation gives new expressions for parabolic trigonometric functions. The parabolic “unit cycle” is defined by the equation $u^2 - v = 1$ for both subgroups—see Fig. I.10.1(P) and (P') and Exercise I.10.4. However, other orbits are different and we will give their description in the next section. Figure I.10.1 illustrates Möbius actions of matrices (I.11.7), (I.11.8) and (I.11.6) on the respective “unit disks”, which are images of the upper half-planes under the respective Cayley transforms from Sections I.10.1 and I.10.3.

At this point, the reader may suspect that the structural analogy mentioned at the beginning of the section is insufficient motivation to call transformations (I.11.9) and (I.11.11) “parabolic rotation” and the rest of the chapter is a kind of post-modern deconstruction. To dispel any doubts, we present the following example:

EXAMPLE I.11.4 (The heat equation and kernel). The dynamics of heat distribution $f(x, t)$ over a one-dimensional infinite string is modelled by the partial differential equation

$$(I.11.12) \quad (\partial_t - k\partial_x^2)f(x, t) = 0, \quad \text{where } x \in \mathbb{R}, t \in \mathbb{R}_+.$$

For the initial-value problem with the data $f(x, 0) = g(x)$, the solution is given by the convolution (Poisson’s integral) [335, § 14.2]:

$$(I.11.13) \quad u(x, t) = \frac{1}{\sqrt{4\pi kt}} \int_{-\infty}^{\infty} \exp\left(-\frac{(x-y)^2}{4kt}\right) g(y) dy,$$

with the function $\exp(-\frac{x^2}{4kt})$, which is called the *heat kernel*.

EXERCISE I.11.5. Check that the Möbius transformations

$$\begin{pmatrix} 1 & 0 \\ c & 1 \end{pmatrix} : x + \varepsilon t \mapsto \frac{x + \varepsilon t}{c(x + \varepsilon t) + 1}$$

from the subgroup N' do not change the heat kernel. HINT: N' -orbits from Fig. I.3.1 are contour lines of the function $\exp(-\frac{u^2}{t})$. \diamond

The last example hints at further works linking the parabolic geometry with parabolic partial differential equations.

I.11.3. Rebuilding Algebraic Structures from Geometry

Rotations in elliptic and hyperbolic cases are given by products of complex or double numbers, respectively, and, thus, are linear. However, non-trivial parabolic rotations (I.11.9) and (I.11.11) (Fig. I.10.1(P) and (P')) are not linear.

Can we find algebraic operations for dual numbers which linearise these Möbius transformations? To this end, we will “revert a theorem into a definition” and use this systematically to recover a compatible algebraic structure.

I.11.3.1. Modulus and Argument. In the elliptic and hyperbolic cases, orbits of rotations are points with a constant norm (modulus), either $x^2 + y^2$ or $x^2 - y^2$. In the parabolic case, we already employed this point of view in Chapter I.9 to treat orbits of the subgroup N' as equidistant points for certain Möbius-invariant metrics, and we will do this again.

DEFINITION I.11.6. Orbits of actions (I.11.9) and (I.11.11) are contour lines for the following functions which we call the respective moduli (norms):

$$(I.11.14) \quad \text{for } N : |u + \varepsilon v| = u^2 - v, \quad \text{for } N' : |u + \varepsilon v|' = \frac{u^2}{v + 1}.$$

REMARK I.11.7. The definitions are supported by the following observations:

- i. The expression $|(u, v)| = u^2 - v$ represents a parabolic distance from $(0, \frac{1}{2})$ to (u, v) —see Exercise I.10.6—which is in line with the parabolic Pythagoras' identity (I.11.10).
- ii. The modulus for N' expresses the parabolic focal length from $(0, -1)$ to (u, v) as described in Exercise I.10.7.

The only straight lines preserved by both parabolic rotations N and N' are vertical lines, so we will treat them as “spokes” for parabolic “wheels”. Elliptic spokes, in mathematical terms, are “points on the complex plane with the same argument”. Therefore we again use this for the parabolic definition.

DEFINITION I.11.8. Parabolic arguments are defined as follows:

$$(I.11.15) \quad \text{for } N : \arg(u + \varepsilon v) = u, \quad \text{for } N' : \arg'(u + \varepsilon v) = \frac{1}{u}.$$

Both Definitions I.11.6 and I.11.8 possess natural properties with respect to parabolic rotations.

EXERCISE I.11.9. Let w_t be a parabolic rotation of w by an angle t in (I.11.9) or in (I.11.11). Then

$$|w_t|^{(\prime)} = |w|^{(\prime)}, \quad \arg^{(\prime)} w_t = \arg^{(\prime)} w + t,$$

where the primed versions are used for subgroup N' .

REMARK I.11.10. Note that, in the commonly-accepted approach, cf. [339, App. C(30')], the parabolic modulus and argument are given by expressions (II.3.5), which are, in a sense, opposite to our present agreements.

I.11.3.2. Rotation as Multiplication. We revert again theorems into definitions to assign multiplication. In fact, we consider parabolic rotations as multiplications by unimodular numbers, thus we define multiplication through an extension of properties from Exercise I.11.9:

DEFINITION I.11.11. The product of vectors w_1 and w_2 is defined by the following two conditions:

- i. $\arg^{(\prime)}(w_1 w_2) = \arg^{(\prime)} w_1 + \arg^{(\prime)} w_2$ and
- ii. $|w_1 w_2|^{(\prime)} = |w_1|^{(\prime)} \cdot |w_2|^{(\prime)}$.

Hereafter, primed versions of formulae correspond to the case of subgroup N' and unprimed to the subgroup N .

We also need a special form of parabolic conjugation which coincides with sign reversion of the argument:

DEFINITION I.11.12. Parabolic conjugation is given by
(I.11.16)
$$\overline{u + \varepsilon v} = -u + \varepsilon v.$$

Obviously, we have the properties $|\overline{w}|^{(\prime)} = |w|^{(\prime)}$ and $\arg^{(\prime)} \overline{w} = -\arg^{(\prime)} w$. A combination of Definitions I.11.6, I.11.8 and I.11.11 uniquely determines expressions for products.

EXERCISE I.11.13. Check the explicit expressions for the parabolic products:

$$(I.11.17) \quad \text{For } N: \quad (u, v) * (u', v') = (u + u', (u + u')^2 - (u^2 - v)(u'^2 - v')).$$

$$(I.11.18) \quad \text{For } N': \quad (u, v) * (u', v') = \left(\frac{uu'}{u + u'}, \frac{(v + 1)(v' + 1)}{(u + u')^2} - 1 \right).$$

Although both the above expressions look unusual, they have many familiar properties, which are easier to demonstrate from the implicit definition rather than the explicit formulae.

EXERCISE I.11.14. Check that both the products (I.11.17) and (I.11.18) satisfy the following conditions:

- i. They are commutative and associative.
- ii. The respective rotations (I.11.9) and (I.11.11) are given by multiplications of a dual number with the unit norm.
- iii. The product $w_1 w_2$ is invariant under the respective rotations (I.11.9) and (I.11.11).

iv. For any dual number w , the following identity holds:

$$|w\bar{w}| = |w|^2.$$

In particular, the property (I.11.14.iii) will be crucial below for an inner product.

We defined multiplication through the modulus and argument described in the previous subsection. Our notion of the norm is rotational-invariant and unique up to composition with a monotonic function of a real argument—see the discussion in Section I.9.2. However, the argument can be defined with greater freedom—see Section I.11.6.2.

I.11.4. Invariant Linear Algebra

Now, we wish to define a linear structure on \mathbb{R}^2 which is invariant under point multiplication from the previous subsection (and, thus, under the parabolic rotations, cf. Exercise I.11.14.ii). Multiplication by a real scalar is straightforward (at least for a positive scalar)—it should preserve the argument and scale the norm of a vector. Thus, we have formulae, for $\alpha > 0$,

$$(I.11.19) \quad \alpha \cdot (u, v) = (u, \alpha v + u^2(1 - \alpha)) \quad \text{for } N \text{ and}$$

$$(I.11.20) \quad \alpha \cdot (u, v) = \left(u, \frac{v+1}{\alpha} - 1 \right) \quad \text{for } N'.$$

On the other hand, the addition of vectors can be done in several different ways. We present two possibilities—one is tropical and the other, exotic.

I.11.4.1. Tropical form.

EXERCISE I.11.15 (Tropical mathematics). Consider the so-called max-plus algebra \mathbb{R}_{\max} , namely the field of real numbers together with minus infinity: $\mathbb{R}_{\max} = \mathbb{R} \cup \{-\infty\}$. Define operations $x \oplus y = \max(x, y)$ and $x \odot y = x + y$. Check that:

- i. The addition \oplus and the multiplication \odot are associative.
- ii. The addition \oplus is commutative.
- iii. The multiplication \odot is distributive with respect to the addition \oplus ;
- iv. $-\infty$ is the neutral element for \oplus .

Similarly, define $\mathbb{R}_{\min} = \mathbb{R} \cup \{+\infty\}$ with the operations $x \oplus y = \min(x, y)$, $x \odot y = x + y$ and verify the above properties.

The above example is fundamental in the broad area of *tropical mathematics* or idempotent mathematics, also known as Maslov dequantisation algebras—see [246] for a comprehensive survey.

Let us introduce the lexicographic order on \mathbb{R}^2 :

$$(u, v) \prec (u', v') \quad \text{if and only if} \quad \begin{cases} \text{either} & u < u', \\ \text{or} & u = u', v < v'. \end{cases}$$

EXERCISE I.11.16. Check that above relation is transitive.

One can define functions \min and \max of a pair of points on \mathbb{R}^2 , respectively. Then, an addition of two vectors can be defined either as their minimum or maximum.

EXERCISE I.11.17. Check that such an addition is commutative, associative and distributive with respect to scalar multiplications (I.11.19) and (I.11.20) and, consequently, is invariant under parabolic rotations.

Although an investigation of this framework looks promising, we do not study it further for now.

I.11.4.2. Exotic form. Addition of vectors for both subgroups N and N' can be defined by the following common rules, where subtle differences are hidden within the corresponding Definitions I.11.6 (norms) and I.11.8 (arguments).

DEFINITION I.11.18. Parabolic addition of vectors is defined by the formulae:

$$(I.11.21) \quad \arg^{(\prime)}(w_1 + w_2) = \frac{\arg^{(\prime)} w_1 \cdot |w_1|^{(\prime)} + \arg^{(\prime)} w_2 \cdot |w_2|^{(\prime)}}{|w_1 + w_2|^{(\prime)}} \text{ and}$$

$$(I.11.22) \quad |w_1 + w_2|^{(\prime)} = |w_1|^{(\prime)} \pm |w_2|^{(\prime)},$$

where primed versions are used for the subgroup N' .

The rule for the norm of sum (I.11.22) may look too trivial at first glance. We should say, in its defence, that it fits well between the elliptic $|w + w'| \leq |w| + |w'|$ and hyperbolic $|w + w'| \geq |w| + |w'|$ triangle inequalities for norms—see Section I.9.3 for their discussion.

The rule (I.11.21) for the argument of the sum is also not arbitrary. From the law of sines in Euclidean geometry, we can deduce that

$$\sin(\phi - \psi') = \frac{|w| \cdot \sin(\psi - \psi')}{|w + w'|} \text{ and } \sin(\psi' - \phi) = \frac{|w'| \cdot \sin(\psi - \psi')}{|w + w'|},$$

where $\psi^{(\prime)} = \arg w^{(\prime)}$ and $\phi = \arg(w + w^{(\prime)})$. Using parabolic expression (II.3.3) for the sine, $\sin \theta = \theta$, we obtain the arguments addition formula (I.11.21).

A proper treatment of zeros in the denominator of (I.11.21) can be achieved through a representation of a dual number $w = u + \varepsilon v$ as a pair of homogeneous polar (projective) coordinates $[a, r] = [|w|^{(\prime)} \cdot \arg^{(\prime)} w, |w|^{(\prime)}]$ (primed version for the subgroup N'). Then, the above addition is defined component-wise in the homogeneous coordinates

$$w_1 + w_2 = [a_1 + a_2, r_1 + r_2], \quad \text{where } w_i = [a_i, r_i].$$

The multiplication from Definition I.11.11 is given in the homogeneous polar coordinates by

$$w_1 \cdot w_2 = [a_1 r_2 + a_2 r_1, r_1 r_2], \quad \text{where } w_i = [a_i, r_i].$$

Thus, homogeneous coordinates linearise the addition (I.11.21) and (I.11.22) and multiplication by a scalar (I.11.19).

Both formulae (I.11.21) and (I.11.22) together uniquely define explicit expressions for the addition of vectors. However, these expressions are rather cumbersome and not really much needed. Instead, we list the properties of these operations.

EXERCISE I.11.19. Verify that the vector additions for subgroups N and N' defined by (I.11.21) and (I.11.22) satisfy the following conditions:

- i. they are commutative and associative;

- ii. they are distributive for multiplications (I.11.17) and (I.11.18). Consequently:
- iii. they are parabolic rotationally-invariant;
- iv. they are distributive in both ways for the scalar multiplications (I.11.19) and (I.11.20) respectively:

$$a \cdot (w_1 + w_2) = a \cdot w_1 + a \cdot w_2, \quad (a + b) \cdot w = a \cdot w + b \cdot w.$$

To complete the construction, we need to define the zero vector and the inverse. The inverse of w has the same argument as w and the opposite norm.

EXERCISE I.11.20. Check that, for corresponding subgroups, we have:

(N): The zero vector is $(0, 0)$ and, consequently, the inverse of (u, v) is $(u, 2u^2 - v)$.

(N'): The zero vector is $(\infty, -1)$ and, consequently, the inverse of (u, v) is $(u, -v - 2)$.

Thereafter, we can check that scalar multiplications by negative reals are given by the same identities (I.11.19) and (I.11.20) as for positive ones.

I.11.5. Linearisation of the Exotic Form

Some useful information can be obtained from the transformation between the parabolic unit disk and its linearised model. In such linearised coordinates (a, b) , the addition (I.11.21) and (I.11.22) is done in the usual coordinate-wise manner: $(a, b) + (a', b') = (a + a', b + b')$.

EXERCISE I.11.21. Calculate values of a and b in the linear combination $(u, v) = a \cdot (1, 0) + b \cdot (-1, 0)$ and check the following:

- i. For the subgroup N , the relations are:

$$(I.11.23) \quad u = \frac{a - b}{a + b}, \quad v = \frac{(a - b)^2}{(a + b)^2} - (a + b),$$

$$(I.11.24) \quad a = \frac{u^2 - v}{2}(1 + u), \quad b = \frac{u^2 - v}{2}(1 - u).$$

- ii. For the subgroup N' , the relations are:

$$u = \frac{a + b}{a - b}, \quad v = \frac{(a + b)}{(a - b)^2} - 1, \quad a = \frac{u(u + 1)}{2(v + 1)}, \quad b = \frac{u(u - 1)}{2(v + 1)}.$$

We also note that both norms (I.11.14) have exactly the same value $a + b$ in the respective (a, b) -coordinates. It is not difficult to transfer parabolic rotations from the (u, v) -plane to (a, b) -coordinates.

EXERCISE I.11.22. Show that:

- i. The expression for N action (I.11.9) in (a, b) coordinates is:

$$(I.11.25) \quad \begin{pmatrix} e^{\varepsilon t} & t \\ 0 & e^{-\varepsilon t} \end{pmatrix} : (a, b) \mapsto \left(a + \frac{t}{2}(a + b), b - \frac{t}{2}(a + b) \right).$$

HINT: Use identities (I.11.23). \diamond

ii. After (Euclidean) rotation by 45° given by

$$(I.11.26) \quad (a, b) \mapsto (a + b, a - b),$$

formula (I.11.25) coincides with the initial parabolic rotation (II.3.2) shown in Fig. II.3.1(P₀).

iii. The composition of transformations (I.11.23) and (I.11.26) maps algebraic operations from Definitions I.11.11 and I.11.18 to the corresponding operations on dual numbers.

This should not be surprising, since any associative and commutative two-dimensional algebra is formed either by complex, dual or double numbers [241]. However, it does not trivialise our construction, since the above transition is essentially singular and shall be treated within the birational geometry framework [224]. Similar singular transformations of time variable in the hyperbolic setup allow us to linearise many non-linear problems of mechanics [281, 282].

Another application of the exotic linear algebra is the construction of linear representations of $SL_2(\mathbb{R})$ induced by characters of subgroup N' which are realised as parabolic rotations [194].

I.11.6. Conformality and Geodesics

We conclude our consideration of the parabolic rotations with a couple of links to other notions considered earlier.

I.11.6.1. Retrospective: Parabolic Conformality. The irrelevance of the standard linear structure for parabolic rotations manifests itself in many different ways, e.g. in an apparent “non-conformality” of lengths from parabolic foci, that is, with the parameter $\delta = 0$ in Proposition I.7.14.iii. Adapting our notions to the proper framework restores a clear picture.

The initial Definition I.7.13 of conformality considers the usual limit $y' \rightarrow y$ along a straight line, i.e. a “spoke” in terms of Fig. II.3.1. This is justified in the elliptic and hyperbolic cases. However, in the parabolic setting the proper “spokes” are vertical lines—see Definition I.11.8 of the argument and the illustration in Fig. I.10.1(P) and (P'). Therefore, the parabolic limit should be taken along the vertical lines.

DEFINITION I.11.23. We say that a length l is *p-conformal* if, for any given $P = u + \nu v$ and another point $P' = u' + \nu' v'$, the following limit exists and is independent from u' :

$$\lim_{\nu' \rightarrow \infty} \frac{l(\overrightarrow{QQ'})}{l(\overrightarrow{PP'})}, \quad \text{where } g \in SL_2(\mathbb{R}), Q = g \cdot P, Q' = g \cdot P'.$$

EXERCISE I.11.24. Let the focal length be given by the identity (I.7.7) with $\sigma = \delta = 0$:

$$l_{f_\delta}^2(\overrightarrow{PP'}) = -\delta p^2 - 2vp, \quad \text{where } p = \frac{(u' - u)^2}{2(\nu' - \nu)}.$$

Check that l_{f_δ} is *p-conformal* and, moreover,

$$(I.11.27) \quad \lim_{\nu' \rightarrow \infty} \frac{l_{f_\delta}(\overrightarrow{QQ'})}{l_{f_\delta}(\overrightarrow{PP'})} = \frac{1}{(cu + d)^2}, \quad \text{where } g = \begin{pmatrix} a & b \\ c & d \end{pmatrix}$$

and $Q = g \cdot P$, $Q' = g \cdot P'$.

I.11.6.2. Perspective: Parabolic Geodesics. We illustrated unitary rotations of the unit disk by an analogy with a wheel. Unitarity of rotations is reflected in the rigid structure of transverse “rims” and “spokes”. The shape of “rims” is always predefined—they are orbits of rotations. They also define the loci of points with the constant norm. However, there is some flexibility in our choice of parabolic “spokes”, i.e. points with the same value of argument. This is not determined even under the strict guidance of the elliptic and hyperbolic cases.

In this chapter, we take the simplest possible assumption: elliptic and hyperbolic “spokes” are straight lines passing through the origin. Consequently, we have looked for parabolic “spokes” which are straight lines as well. The only family of straight lines invariant under the parabolic rotations (I.11.9) and (I.11.11) are vertical lines, thus we obtained the situation depicted in Fig. I.10.1.

However, the above path is not the only possibility. We can view straight lines in the elliptic and hyperbolic cases as geodesics for the invariant distance on the respective unit disks, see Exercise I.10.14(e,p). This is perfectly consistent with unitary rotations and suggests that parabolic “rims” for rotations (I.11.11) shall be respective parabolic geodesics on the parabolic unit disk, see Fig. I.11.2.

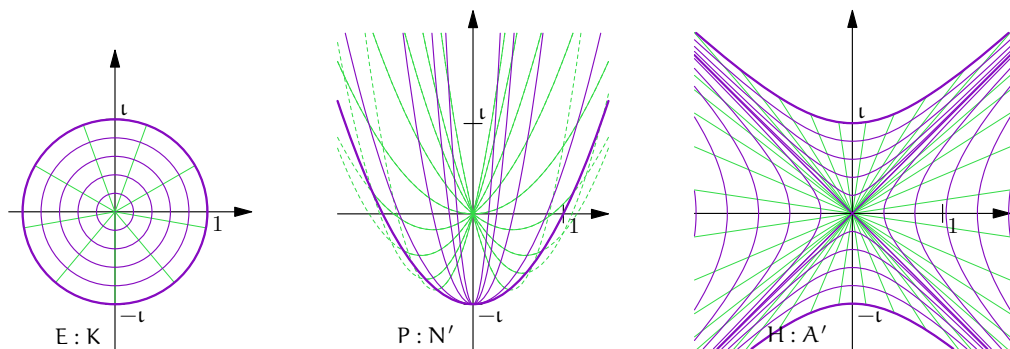


FIGURE I.11.2. Geodesics as spokes. In each case “rims” are points equidistant from the origin, “spokes” are geodesics between the origin and any point on the rims.

There are three flavours of parabolic geodesics, cf. Fig. I.9.3(P_E – P_H) and Exercise I.10.14(p). All of them can be used as “spokes” of parabolic unit disk, but we show only the elliptic flavour in Fig. I.11.2.

EXERCISE I.11.25. Define the parabolic argument to be constant along geodesics from Exercise I.10.14(p) drawn by blue lines in Fig. I.9.3. What is the respective multiplication formula? Is there a rotation-invariant linear algebra?

Cycles Cross Ratio: an Invitation

In this chapter we review the cycles cross ratio introduced in [217]. This is an invariant with applications in Möbius and Lie sphere geometry [32, Ch. 3; 59; 148] which is analogous to the cross-ratio of four points in projective [255; 303, § 9.3; 339, App. A] and hyperbolic geometries [24, § 4.4; 276, III.5; 300, § I.5]. To avoid technicalities and stay visual we will work in two dimensions, luckily all main features are already illuminated in this case. Our purpose is not to give an exhausting presentation (in fact, we are hoping it is far from being possible now), but rather to draw attention to the new invariant and its benefits to the various geometrical settings. There are several far-reaching generalisations in higher dimensions and non-Euclidean metrics, see Sect. I.12.4 for a discussion. In abstract framework the new invariant can be considered in any projective space with a bilinear pairing.

There is an [interactive version of this chapter](#) implemented as a Jupyter notebook [216] based on the MoebInv software package [215].

I.12.1. Preliminaries: Projective space of cycles

We introduce our topic following its historic development. This conforms to our hands-on approach as an opposition to a start from the most general abstract construction.

Circles are the traditional subject of geometrical studies and their numerous properties were already widely presented in Euclid's *Elements*. However, advances in their analytical presentations is not a so distant history.

A straightforward parametrisation of a circle equation:

$$(I.12.1) \quad x^2 + y^2 + 2gx + 2fy + c = 0$$

by a point (g, f, c) in some subset of the three-dimensional Euclidean space \mathbb{R}^3 was used in [276, Ch. II]. Abstractly, we can treat a *point* (x_0, y_0) of a plane as the zero radius circle with coefficients $(g, f, c) = (-x_0, -y_0, x_0^2 + y_0^2)$.

It is more advantageous to use the equation

$$(I.12.2) \quad k(x^2 + y^2) - 2lx - 2ny + m = 0,$$

which also includes *straight lines* for $k = 0$. This extension comes at a price: parameters (k, l, n, m) shall be treated as elements of the three dimensional projective space $\mathbb{P}\mathbb{R}^3$ rather than the Euclidean space \mathbb{R}^4 since equations (I.12.2) with (k, l, n, m) and $(k_1, l_1, n_1, m_1) = (\lambda k, \lambda l, \lambda n, \lambda m)$ defines the same set of points for any $\lambda \neq 0$. This parametrisation is known as tetracyclic/polyspheric coordinates, cf. [36, § 20.7; 150, § 2.4.1].

The next observation is that the linear structure of $\mathbb{P}\mathbb{R}^3$ is relevant for circles geometry. For example, the traditional concept of *pencil of circles* [71, § 2.3] is nothing else but the linear span in $\mathbb{P}\mathbb{R}^3$ [300, § I.1.c]. Therefore, it will be convenient to accept all points $(k, l, n, m) \in \mathbb{P}\mathbb{R}^3$ on equal ground even if they correspond to an empty set of solutions (x, y) in (I.12.2). The latter can be thought as “circles with imaginary radii”.

It is also appropriate to consider $(0, 0, 0, 1)$ as a representative of the point C_∞ at infinity, which complements \mathbb{R}^2 to the Riemann sphere. Following [339], we call circles (with real and imaginary radii), straight lines and points (including C_∞) on a plane by joint name *cycles*. Correspondingly, the space $\mathbb{P}\mathbb{R}^3$ representing them—the *cycles space*.

Sometimes, we need to consider cycles with an *orientation*. This can be used, for example, to distinguish “inner” and “outer” tangency of cycles [101, 211, 215]. Furthermore, oriented cycles and their tangency relations are the starting point for the Lie sphere geometry. It is easy to encode cycles’ orientations through polyspheric coordinates: cycles (k, l, n, m) and (k', l', n', m') have the opposite orientations if $(k, l, n, m) = (\lambda k', \lambda l', \lambda n', \lambda m')$ for some negative λ and two points (k, l, n, m) and (k', l', n', m') are considered as representatives of the same oriented cycle if $(k, l, n, m) = (\lambda k', \lambda l', \lambda n', \lambda m')$ for a positive λ .

An algebraic consideration often benefits from the introduction of complex numbers. For example, we can re-write (I.12.2) as:

$$(I.12.3) \quad (-1 \quad \bar{z}) \begin{pmatrix} \bar{L} & -m \\ k & -L \end{pmatrix} \begin{pmatrix} z \\ 1 \end{pmatrix} = kz\bar{z} - L\bar{z} - \bar{L}z + m \\ = k(x^2 + y^2) - 2lx - 2ny + m.$$

where $z = x + iy$ and $L = l + in$. We call *Fillmore–Springer–Cnops construction* (or *FSCc* for short) the association of the matrix $C = \begin{pmatrix} \bar{L} & -m \\ k & -L \end{pmatrix}$ to a cycle with coefficients (k, l, n, m) [64; 65, § 4.1; 100].

A reader may expect a more straightforward realisation of the quadratic form (I.12.2), cf. [300, § I.1; 306, Thm. 9.2.11]:

$$(I.12.4) \quad (\bar{z} \quad 1) \begin{pmatrix} k & -L \\ -\bar{L} & m \end{pmatrix} \begin{pmatrix} z \\ 1 \end{pmatrix} = kz\bar{z} - L\bar{z} - \bar{L}z + m.$$

However, FSCc will show its benefits in the next section. Meanwhile, we note that a point z corresponding to the zero radius cycle with the centre z is represented by the matrix

$$(I.12.5) \quad Z = \begin{pmatrix} \bar{z} & -z\bar{z} \\ 1 & -z \end{pmatrix} = \frac{1}{2} \begin{pmatrix} \bar{z} & \bar{z} \\ 1 & 1 \end{pmatrix} \begin{pmatrix} 1 & -z \\ 1 & -z \end{pmatrix} \quad \text{for } (k, l, n, m) = (1, x, y, x^2 + y^2)$$

where $\det Z = 0$. Also, the point at infinity can be represented by a zero radius cycle:

$$(I.12.6) \quad C_\infty = \begin{pmatrix} 0 & -1 \\ 0 & 0 \end{pmatrix} \quad \text{for } (k, l, n, m) = (0, 0, 0, 1).$$

More generally, $\det \begin{pmatrix} \bar{L} & -m \\ k & -L \end{pmatrix} = -k^2r^2$ for $k \neq 0$ and the cycle’s radius r .

I.12.2. Fractional linear transformations and the invariant product

In the spirit of the **Erlangen programme** of Felix Klein (greatly influenced by Sophus Lie), a consideration of cycle geometry is based on a group of transformations preserving this family [185, 198]. Let $M = \begin{pmatrix} \alpha & \beta \\ \gamma & \delta \end{pmatrix}$ be an invertible 2×2 complex matrix. Then the *fractional linear transformation* (FLT for short) of the extended complex plane $\hat{\mathbb{C}} = \mathbb{C} \cup \{\infty\}$ is defined by:

$$(I.12.7) \quad \begin{pmatrix} \alpha & \beta \\ \gamma & \delta \end{pmatrix} : z \mapsto \frac{\alpha z + \beta}{\gamma z + \delta}.$$

It will be convenient to introduce the notation \overline{M} for the matrix $\begin{pmatrix} \overline{\alpha} & \overline{\beta} \\ \overline{\gamma} & \overline{\delta} \end{pmatrix}$ with complex conjugated entries of M . For a cycle C the matrix \overline{C} corresponds to the reflection of C in the real axis $y = 0$. Also, due to special structure of FSCc matrix we easily check that

$$(I.12.8) \quad \overline{C}C = C\overline{C} = -\det(C)I \quad \text{or} \quad \overline{C} \sim C^{-1} \text{ projectively if } \det(C) \neq 0.$$

If a cycle C is composed from a non-empty set of points in $(x, y) \in \mathbb{R}^2$ satisfying (I.12.2), then their images under transformation (I.15.1) form again a cycle C_1 with notable link to FSCc:

LEMMA I.12.1. Transformation (I.15.1) maps a cycle $C = \begin{pmatrix} \overline{L} & -m \\ k & -L \end{pmatrix}$ into a cycle $C_1 = \begin{pmatrix} \overline{L}_1 & -m_1 \\ k_1 & -L_1 \end{pmatrix}$ such that $C_1 = \overline{M}CM^{-1}$.

Clearly, the map $C \rightarrow \overline{M}CM^{-1}$ is meaningful for any cycle, including imaginary ones, thus we regard it as FLT action on the cycle space. For the matrix form (I.12.4) the above identity $C_1 = \overline{M}CM^{-1}$ needs to be replaced by the matrix congruence $C_1 = M^*CM$ [300, § II.6.e; 306, Thm. 9.2.13]. This difference is significant in view of the following definition.

DEFINITION I.12.2. For two cycles C and C_1 define the *cycles product* by:

$$(I.12.9) \quad \langle C, C_1 \rangle = -\text{tr}(C\overline{C}_1),$$

where tr denotes the trace of a matrix.

We call two cycles C and C_1 *orthogonal* if $\langle C, C_1 \rangle = 0$.

It is easy to find the explicit expression of the cycle product (I.12.9):

$$(I.12.10) \quad \langle C, C_1 \rangle = km_1 + k_1m - 2ll_1 - 2nn_1,$$

and observe that it is linear in coefficients of the cycle C (and C_1 as well). On the other hand, it is the initial definition (I.12.9), which allows us to use the invariance of trace under matrix similarity to conclude the following.

COROLLARY I.12.3. The cycles product is invariant under the transformation $C \mapsto \overline{M}CM^{-1}$. Therefore FLT (I.15.1) preserves orthogonality of cycles.

The cycle product is a rather recent addition to the cycle geometry, see independent works [64; 65, § 4.1; 100; 163, § 4.2]. Interestingly, expression (I.12.9) essentially repeats the GNS-construction in C^* -algebras [14] which is older by half of century at least.

EXAMPLE I.12.4. [198, Ch. 6; 211; 212] The cycles product and cycles orthogonality encode a great amount of geometrical characteristics. For example, for cycles represented by non-empty sets of points in \mathbb{R}^2 we note the following:

- i. A cycle is a straight line if it is orthogonal $\langle C, C_\infty \rangle = 0$ to the zero radius cycle at infinity C_∞ (I.12.6).
- ii. A cycle Z represents a point if Z is self-orthogonal (*isotropic*): $\langle Z, Z \rangle = 0$. More generally, (I.12.8) implies:

$$(I.12.11) \quad \langle C, C \rangle = 2 \det(C).$$

- iii. A cycle C passes a point Z if they are orthogonal $\langle C, Z \rangle = 0$.
- iv. A cycle C represents a line in Lobachevsky geometry [303, Ch. 12] if it is orthogonal $\langle C, C_{\mathbb{R}} \rangle = 0$ to the real line cycle $C_{\mathbb{R}} = \begin{pmatrix} i & 0 \\ 0 & i \end{pmatrix}$.
- v. Two cycles are orthogonal as subsets of a plane (i.e. they have perpendicular tangents at an intersection point) if they are orthogonal in the sense of Defn. I.12.2.
- vi. Two cycles C and C_1 are *tangent* (i.e. have a unique point in common) if

$$\langle C, C_1 \rangle^2 = \langle C, C \rangle \langle C_1, C_1 \rangle.$$

- vii. *Inversive distance* [71, § 5.8] θ of two (non-isotropic) cycles is defined by the formula:

$$(I.12.12) \quad \theta = \frac{\langle C, C_1 \rangle}{\sqrt{\langle C, C \rangle \langle C_1, C_1 \rangle}}.$$

In particular, the above discussed orthogonality corresponds to $\theta = 0$ and the tangency to $\theta = \pm 1$. For intersecting cycles θ is the cosine of the intersecting angle.

- viii. A generalisation of *Steiner power* $d(C, C_1)$ of two cycles is defined as, cf. [101, § 1.1]:

$$(I.12.13) \quad d(C, C_1) = \langle C, C_1 \rangle + \sqrt{\langle C, C \rangle \langle C_1, C_1 \rangle},$$

where both cycles C and C_1 are scaled to have $k = 1$ and $k_1 = 1$. Geometrically, the generalised Steiner power for spheres provides the square of *tangential distance*.

REMARK I.12.5. The cycles product is *indefinite*, see [113] for an account of the theory with some refreshing differences to the more familiar situation of inner product spaces. One illustration is the presence of self-orthogonal non-zero vectors, see Ex. I.13.2.iii above. Another noteworthy observation is that the product (I.12.10) has the Lorentzian signature $(1, 3)$ and \mathbb{R}^4 with this product is isomorphic to Minkowski space-time [163, § 4.2].

I.12.3. Cycles cross ratio

Due to the projective nature of the cycles space (i.e. matrices C and λC correspond to the same cycle) a *non-zero* value of the cycle product (I.12.9) is not directly meaningful. Of course, this does not affect the cycles orthogonality. A partial remedy in other cases is possible through various *normalisations* [198, § 5.2]. Usually they are specified by either of the following conditions

- i. $k = 1$, which is convenient for metric properties of cycles. It brings us back to the initial equation (I.12.1) and is not possible for straight lines; or
- ii. $\langle C, C \rangle = \pm 1$ which was suggested in [163, § 4.2] and is useful, say, for tangency but is not possible for points.

Recall, that the projective ambiguity is elegantly balanced in the *cross ratio* of four points [24, § 4.4; 276, III.5; 300, § I.5]:

$$(I.12.14) \quad (z_1, z_2; z_3, z_4) = \frac{z_1 - z_3}{z_1 - z_4} : \frac{z_2 - z_3}{z_2 - z_4}.$$

We use this classical pattern in the following definition.

DEFINITION I.12.6. A *cycles cross ratio* of four cycles C_1, C_2, C_3 and C_4 is:

$$(I.12.15) \quad \langle C_1, C_2; C_3, C_4 \rangle = \frac{\langle C_1, C_3 \rangle}{\langle C_1, C_4 \rangle} : \frac{\langle C_2, C_3 \rangle}{\langle C_2, C_4 \rangle}$$

assuming $\langle C_1, C_4 \rangle \langle C_2, C_3 \rangle \neq 0$. If $\langle C_1, C_4 \rangle \langle C_2, C_3 \rangle = 0$ but $\langle C_1, C_3 \rangle \langle C_2, C_4 \rangle \neq 0$ we put $\langle C_1, C_2; C_3, C_4 \rangle = \infty$. The cycles cross ratio is generally undefined in the remaining case of an indeterminacy $\frac{0}{0}$.

Note that some additional geometrical reasons may help to resolve the last situation, see the consideration of orthogonality/tangency with zero radius cycle in Ex. I.12.9. As an initial justification of the definition we list the following properties.

- PROPOSITION I.12.7.
- i. *The cycles cross ratio is a well-defined FLT-invariant of quadruples of cycles.*
 - ii. *The cycles cross ratio of four zero radius cycles is the squared modulus of the cross ratio for the respective points:*

$$(I.12.16) \quad \langle Z_1, Z_2; Z_3, Z_4 \rangle = |(z_1, z_2; z_3, z_4)|^2.$$

- iii. *There is the cancellation formula:*

$$(I.12.17) \quad \langle C_1, C; C_3, C_4 \rangle \langle C, C_2; C_3, C_4 \rangle = \langle C_1, C_2; C_3, C_4 \rangle.$$

PROOF. The first statement follows from Cor. I.12.3 and the construction of the cycles cross ratio. To show the second statement we derive from (I.12.5) and (I.12.10) that:

$$\langle Z_i, Z_j \rangle = |z_i - z_j|^2,$$

if we use representations of zero radius cycles Z_i and Z_j by coefficients with $k_i = k_j = 1$. This implies (I.12.16). A demonstration of (I.12.17) is straightforward. \square

To demonstrate that there is more than just a formal similarity between the two we briefly list some applications. First, we rephrase Ex. I.12.4.vii in new terms.

EXAMPLE I.12.8. The *capacitance* $\text{cap}(C, C_1)$ of two cycles [144, § 5.1; 145, Defn. 3] coincides with the following cycles cross product:

$$\text{cap}(C, C_1) = \langle C, C_1; C_1, C \rangle = \theta^2,$$

where θ is the inversive distance (I.13.11). Thereafter, FLT-invariance of the cycles cross ratio implies that the intersection angle of cycles is FLT-invariant. In particular cycles are

- i. orthogonal if $\langle C, C_1; C_1, C \rangle = 0$;
- ii. tangent if $\langle C, C_1; C_1, C \rangle = \pm 1$; and
- iii. disjoint if $|\langle C, C_1; C_1, C \rangle| > 1$.

Relation I.12.8.i is merely a consequence of the first-order orthogonality relation $\langle C, C_1 \rangle = 0$, which is fundamental to conformal and incidence geometries, cf. Ex. I.12.4(i)–(v). Meanwhile, the tangency condition (ii) is genuinely quadratic and shall be equally significant in Lie spheres geometry, the Steiner’s porism [144, 145], and other questions formulated purely in terms of cycles’ tangency.

EXAMPLE I.12.9. If a non-zero radius cycle passes a zero radius cycle (point) their cross ratio has an indeterminacy $\frac{0}{0}$. Geometrically their relation can be seen in either ways: as orthogonality or tangency. Therefore, the indeterminacy of the cycle cross ratio can be geometrically resolved differently either to 0 (indicates orthogonality) or 1 (corresponds to tangency). More specifically (see the supporting symbolic computations in the notebook [216]):

- *Orthogonality.* Consider a cycle Z_t with a fixed centre and a variable squared radius t . Take a generic cycle C orthogonal to Z_t . To resolve an indeterminacy $\frac{0}{0}$ we use l’Hospitals’ rule at the point $t = 0$, which corresponds to Z_t becoming a zero radius cycle. This produces $\langle C, Z_t; Z_t, C \rangle|_{t=0} = 0$.
- *Tangency.* For a zero radius cycle Z and passing it cycle C , consider a generic cycle $C_t = (1 - t) \cdot Z + t \cdot C$, $t \in [0, 1]$ from the pencil (linearly) spanned by Z and C . Since C_t touches C Ex. I.12.8.ii implies that $\langle C_t, C; C, C_t \rangle = 1$ for $t > 0$ and C_t coincides with Z for $t = 0$. Thus, we can extend the value 1 to $[Z, C; C, Z]$ by continuity.

The last technique makes the cycles cross ratio meaningful for Lie spheres geometry, which extends FLT by non-point Lie transformations, when a non-zero radius cycle is sent to a zero radius one.

EXAMPLE I.12.10. The Steiner power (I.13.12) can be written as:

$$(I.12.18) \quad d(C, C_1) = \langle C, C_{\mathbb{R}}; C_1, C_{\mathbb{R}} \rangle + \sqrt{\langle C, C_{\mathbb{R}}; C, C_{\mathbb{R}} \rangle} \cdot \sqrt{\langle C_1, C_{\mathbb{R}}; C_1, C_{\mathbb{R}} \rangle},$$

where $C_{\mathbb{R}}$ is the real line and cycles C and C_1 do not need to be normalised in any particular way. Thereafter, the Steiner power is an invariant of two cycles C and C_1 under Möbius transformations, since they fix the real line $C_{\mathbb{R}}$. The Möbius invariance is not so obvious from expression (I.13.12).

The next two applications will generalise the main features of the traditional cross ratio. Recall the other name of the cross ratio—the anharmonic ratio. The origin of the latter is as follows. Two points z_1 and z_2 on a line define a one-dimensional sphere

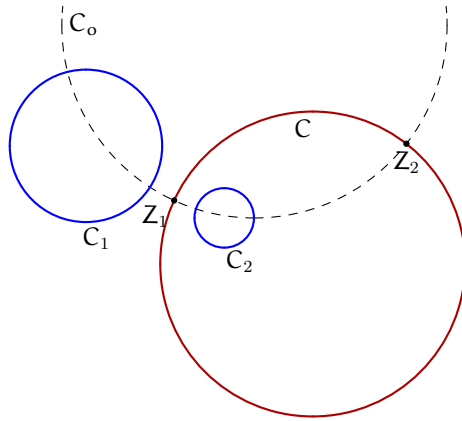


FIGURE I.12.1. Cycles cross ratio for two conjugated cycles

with the centre $O = \frac{1}{2}(z_1 + z_2)$, which can be taken as the origin. Two points c_1 and c_2 are called *harmonically conjugated* (with respect to z_1 and z_2) if:

$$c_1 \cdot c_2 = -z_1 \cdot z_2, \quad \text{cf.} \quad \begin{array}{ccccccc} & \bullet & & \bullet & & \bullet & \\ & z_1 & & O & & c_1 & z_2 & c_2 \end{array}$$

It is easy to check that in this case

$$(I.12.19) \quad (c_1, c_2; z_1, z_2) = -1.$$

Thus, the cross ratio can be viewed as a measure how far four points are from harmonic conjugation, i.e. a measure of anharmonicity of a quadruple. To make a similar interpretation of the cycles cross ratio recall that for FSCc matrices of a cycle C_1 and its reflection C_2 in a cycle C we have: $C_2 = C\bar{C}_1C$, cf. [198, § 6.5]. That is, the reflection in a cycle C is the composition of FLT transform with FSCc matrix C and complex conjugation of matrix entries. It is easy to obtain the following:

PROPOSITION I.12.11. *If a cycle C_1 is a reflection of C_2 in a cycle C then:*

$$\langle C_1, C; C, C_1 \rangle = \langle C_2, C; C, C_2 \rangle.$$

More generally, the reflection in a cycle preserves the inversive distance, cf. Ex. I.12.8.

The above condition is necessary, we describe a sufficient one as a *figure* in the sense of [211, 212, 215]. In short, a figure is an ensemble of cycles interrelated by cycles' relations. For the purpose of this chapter an FLT-invariant relation "to be orthogonal" between two cycles is enough. Software implementations of these figures can be found in [216].

- CONSTRUCTION I.12.12.
- i. For two given cycles C and C_1 construct the reflection $C_2 = C\bar{C}_1C$ of C_1 in C .
 - ii. Take any cycle C_0 orthogonal to C and C_1 , see Ill. I.12.1. All such cycles make a *pencil*—one dimensional subspace of the projective space of cycles. That is because there are only two linear equations for orthogonality (I.12.10) to

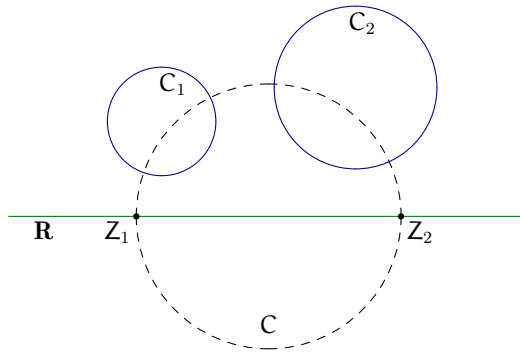


FIGURE I.12.2. Construction for Möbius invariant distance between two cycles

determine four projective coordinates (k_o, l_o, n_o, m_o) . By Prop. I.12.11 C_o is also orthogonal to C_2 .

iii. Define cycles by orthogonality to C, C_o and itself (zero radius condition), that is the intersection points of C and C_o . Since self-orthogonality is a quadratic condition there are two solutions: Z_1 and Z_2 .

iv. The harmonic conjugation of C_1 and C_2 (their reflection in C) implies, cf. (I.12.19):

$$(I.12.20) \quad \langle C_1, C_2; Z_1, Z_2 \rangle = 1.$$

This is demonstrated by symbolic computation in [216].

As the final illustration, we introduce Möbius-invariant distance between cycles. Recall that FLT with an $SL_2(\mathbb{R})$ matrix fixes the real line and it is called a *Möbius transformation* [185; 198, Ch. 1; 306, § 9.3]. The corresponding figure is as follows, see Ill. I.12.2:

CONSTRUCTION I.12.13. i. Let two distinct cycles C_1 and C_2 be given and they are different from the real line $C_{\mathbb{R}}$.

ii. Define a cycle C to be orthogonal to C_1, C_2 , and $C_{\mathbb{R}}$. It is specified by three linear equations for homogeneous coordinates (k, l, n, m) . In generic position a solution is unique, however it can be an imaginary cycle (with a negative square of the radius).

iii. Define cycles by orthogonality to $C, C_{\mathbb{R}}$ and itself, that is the intersection points of C and $C_{\mathbb{R}}$. In general position there are two solutions which we denote by Z_1 and Z_2 . For an imaginary cycle C first coordinates of Z_1 and Z_2 are conjugated complex numbers.

iv. Since the entire construction is completely determined by the given cycles C_1 and C_2 we define the *distance between two cycles* by:

$$(I.12.21) \quad d(C_1, C_2) = \frac{1}{2} \log \langle C_1, C_2; Z_1, Z_2 \rangle.$$

From Möbius invariance of the real line and cycles cross ratio our construction implies the following:

- PROPOSITION I.12.14. i. Distance (I.12.21) is Möbius invariant;
 ii. For zero radius cycles C_1, C_2 formula (I.12.21) coincides with the Lobachevsky metric on the upper-half plane.
 iii. For any cycle C_3 orthogonal to C the (signed) distance is additive: $d(C_1, C_3) = d(C_1, C_2) + d(C_2, C_3)$.
 iv. If centres of C_1 and C_2 are on the imaginary axis (therefore Z_1 and Z_2 are zero and infinity) then $d(C_1, C_2) = \log(m_1/k_1) - \log(k_2/m_2)$.

Obviously, Prop. I.12.14.ii is the consequence of (I.12.16) and I.12.14.iii follows from the cancellation rule (I.12.17). On the other hand, the expression in I.12.14.iv can be obtained by a direct computation, see [216]. Note, that in this case m_i/k_i is the square *tangential distance* (also known as the generalised Steiner power (I.13.12), (I.12.18)) from Z_1 (the origin) to the cycle C_i . Thus, for a zero radius C_i it coincides with the usual distance between centres of Z_1 and C_i and Prop. I.12.14.iv recreates the classical result [24, (7.2.6)].

Comparing constructions on III. I.12.1–I.12.2 and formulae (I.12.20)–(I.12.21) we can say that the invariant distance measures how far two cycles are from being reflections of each other in the real line.

There is an alternative way to define a distance between spheres using cross ratio. Recall the formula [26, (15.2.1)]

$$(I.12.22) \quad \sinh^2 \frac{1}{2} d(z, w) = \frac{|z - w|^2}{4\Im z \Im w}.$$

The alternative distance is defined again via the cross ratio although of the different form:

$$(I.12.23) \quad \sinh^2 \frac{1}{2} d_a(z, w) = -\frac{1}{2} (C_1, \mathbb{R}; C_2, \mathbb{R}).$$

Note, that this time we do not use additional cycles besides the Möbius-invariant real line.

The connection between the definition (I.12.21) of the distance and the new one is given by the formula

$$\sinh^2 \frac{t}{2} = \frac{e^t + e^{-t} - 2}{4}.$$

To see the distinction of two definitions we compare them for two cycles

$$C = (1, 0, v, d^2) \quad \text{and} \quad C_1 = (1, 0, v_1, d_1^2),$$

which are vertically aligned. Without loss of generality this can be always achieved by a suitable Möbius transformation. Another technical assumption is that cycles do not intersect the real axis, which simplifies the symbolic computations. With all of these we get:

$$(I.12.24) \quad \sinh^2 \frac{1}{2} d(C, C_1) = \frac{1}{4} \frac{d^2 - 2dd_1 + d_1^2}{dd_1} \quad \text{and} \quad \sinh^2 \frac{1}{2} d_a(C, C_1) = \frac{1}{2} \frac{d^2 - 2vv_1 + d_1^2}{vv_1}.$$

There is the clear inconsistency of two expressions by the presence of parameters v and v_1 in the second one. Yet, both formulae give the same distances for points,

which correspond to the case $d = v$ and $d_1 = v_1$ in (??). Obviously, we get the value $\sinh^2 \frac{1}{2} d_a(C, C_1) = \frac{1}{4} \frac{(v-v_1)^2}{vv_1}$ agreeing with (I.12.22).

Further example with geometric significance is the cycle distance from a point $(0, v)$ to a cycle $(1, 0, v_1, v_1^2 - r^2)$ with a radius r . The answer is

$$\sinh^2 \frac{1}{2} d_a(C, C_1) = \frac{1}{4} \frac{(v - v_1)^2 - r^2}{vv_1}.$$

That is the tangential distance $(v - v_1)^2 - r^2$ to the cycle modified by the same "hyperbolic factor" $1/(vv_1)$. as in the point case (I.12.22).

I.12.4. Discussion and generalisations

We presented some evidence that the cycles cross ratio extends to Lie spheres geometry the concept of the cross ratio of four points. It is natural to expect that a majority of the classic theory [24, § 4.4; 255; 276, III.5; 300, § I.5; 303, § 9.3; 339, App. A] admits similar adaptation as well. However, we can expect even more than that.

One can lay down a general framework for the introduced invariant (I.12.15) in generic projective spaces as follows¹. Let V be a vector space over an arbitrary field \mathbb{F} with a bilinear pairing $\langle \cdot, \cdot \rangle : V \times V \rightarrow \mathbb{F}$. Upon choosing any four points of the projective space on V one may select arbitrary non-zero vectors, say c_1, c_2, c_3, c_4 , representing these points. Then the quotient

$$(I.12.25) \quad \frac{\langle c_1, c_3 \rangle}{\langle c_1, c_4 \rangle} : \frac{\langle c_2, c_3 \rangle}{\langle c_2, c_4 \rangle}$$

will in general be an element of \mathbb{F} . Whenever this scalar is well defined it obviously will be an invariant under the natural action of the general orthogonal group $GO(V, \langle \cdot, \cdot \rangle)$ on the point set of the underlying projective space. More generally, a sort of projective space can be defined on a module V for a weaker structure than a field, say, algebras of dual and double numbers [261]. In such cases numerous divisors of zero prompt a projective treatment [52; 198, § 4.5] of the new cross ratio (I.12.25). Another perspective direction to research are discrete Möbius geometries [144, 145].

The geometric applications of the new invariant (I.12.15), (I.12.25) are expected much beyond the currently presented situation of circles on a plane. Indeed, FSCc and cycles product based on Clifford algebras works in spaces of higher dimensions and with non-degenerate metrics of arbitrary signatures [64; 65, § 4.1; 100; 198]. In a straightforward fashion cycles cross ratio (I.12.15) remains a geometric FLT-invariant in higher dimensions as well.

A more challenging situation occurs if we have a degenerate metric and cycles are represented by parabolas [339] and respective FLT are based on dual numbers [44]. Besides theoretical interest such spaces are meaningful physical models [117, 118, 150, 339]. The differential geometry loses its ground in the degenerate case and non-commutative local effects appear [198, § 7.2]. The presence of zero divisors among dual numbers

¹I am grateful to an anonymous referee for pointing this out in his/her report.

prompts a projective approach [52; 198, § 4.5] to the cross ratio of four dual numbers, which replaces (I.12.14). Variational methods do not produce FLT-invariant family of geodesics in the degenerate case, instead geometry of cycles needs to be employed [165]. Our construction from Figure I.12.13 shall be usable to define Möbius invariant distance between parabolic cycles as well, cf. [198, § 9.5].

Last but not least, if we restrict the group of transformations from FLT to Möbius maps (or any other subgroup of FLT which fixes a particular cycle) we will get a larger set of invariants. In particular, the FSCc matrix (I.12.3) and the corresponding cycles product (I.12.9) can use different number systems (complex, dual or double) independently from the geometry of the plane [185; 198, § 5.3; 209]. Therefore, there will be three different cycles cross ratios (I.12.15) for each geometry of circles, parabolas and hyperbolas. This echoes the existence of nine Cayley–Klein geometries [115; 284; 339, App. A].

Various aspects of the cycles cross ratio appear to be a wide and fruitful field for further research.

An Extension of Möbius–Lie Geometry with Conformal Ensembles of Cycles

We propose to consider ensembles of cycles (quadrics), which are interconnected through conformal-invariant geometric relations (e.g. “to be orthogonal”, “to be tangent”, etc.), as new objects in an extended Möbius–Lie geometry. It was recently demonstrated in several related papers, that such ensembles of cycles naturally parameterise many other conformally-invariant families of objects, e.g. loxodromes or continued fractions.

The paper describes a method, which reduces a collection of conformally invariant geometric relations to a system of linear equations, which may be accompanied by one fixed quadratic relation. To show its usefulness, the method is implemented as a C++ library. It operates with numeric and symbolic data of cycles in spaces of arbitrary dimensionality and metrics with any signatures. Numeric calculations can be done in exact or approximate arithmetic. In the two- and three-dimensional cases illustrations and animations can be produced. An interactive Python wrapper of the library is provided as well.

I.13.1. Introduction

Lie sphere geometry [32, Ch. 3; 59; 148] in the simplest planar setup unifies circles, lines and points—all together called *cycles* in this setup. Symmetries of Lie spheres geometry include (but are not limited to) fractional linear transformations (FLT) of the form:

$$(I.13.1) \quad \begin{pmatrix} a & b \\ c & d \end{pmatrix} : x \mapsto \frac{ax + b}{cx + d}, \quad \text{where } \det \begin{pmatrix} a & b \\ c & d \end{pmatrix} \neq 0.$$

Following other sources, e.g. [306, § 9.2], we call (I.13.1) by FLT and reserve the name “Möbius maps” for the subgroup of FLT which fixes a particular cycle. For example, on the complex plane FLT are generated by elements of $SL_2(\mathbb{C})$ and Möbius maps fixing the real line are produced by $SL_2(\mathbb{R})$ [198, Ch. 1].

There is a natural set of FLT-invariant geometric relations between cycles (to be orthogonal, to be tangent, etc.) and the restriction of Lie sphere geometry to invariants of FLT is called *Möbius–Lie geometry*. Thus, an ensemble of cycles, structured by a set of such relations, will be mapped by FLT to another ensemble with the same structure.

It was shown recently that ensembles of cycles with certain FLT-invariant relations provide helpful parametrisations of new objects, e.g. points of the Poincaré extended

space [209], loxodromes [218] or continued fractions [28, 208], see Example I.13.3 below for further details. Thus, we propose to *extend Möbius–Lie geometry and consider ensembles of cycles as its new objects*, cf. formal Defn. I.13.5. Naturally, “old” objects—cycles—are represented by simplest one-element ensembles without any relation. This paper provides conceptual foundations of such extension and demonstrates its practical implementation as a C++ library figure¹. Interestingly, the development of this library shaped the general approach, which leads to specific realisations in [208, 209, 218].

More specifically, the library figure manipulates ensembles of cycles (quadrics) interrelated by certain FLT-invariant geometric conditions. The code is build on top of the previous library cycle [185, 186, 198], which manipulates individual cycles within the GiNaC [21] computer algebra system. Thinking an ensemble as a graph, one can say that the library cycle deals with individual vertices (cycles), while figure considers edges (relations between pairs of cycles) and the whole graph. Intuitively, an interaction with the library figure reminds compass-and-straightedge constructions, where new lines or circles are added to a drawing one-by-one through relations to already presented objects (the line through two points, the intersection point or the circle with given centre and a point). See Example I.13.6 of such interactive construction from the Python wrapper, which provides an analytic proof of a simple geometric statement.

It is important that both libraries are capable to work in spaces of any dimensionality and metrics with an arbitrary signatures: Euclidean, Minkowski and even degenerate. Parameters of objects can be symbolic or numeric, the latter admit calculations with exact or approximate arithmetic. Drawing routines work with any (elliptic, parabolic or hyperbolic) metric in two dimensions and the euclidean metric in three dimensions.

The mathematical formalism employed in the library cycle is based on Clifford algebras, which are intimately connected to fundamental geometrical and physical objects [132, 133]. Thus, it is not surprising that Clifford algebras have been already used in various geometric algorithms for a long time, for example see [86, 134, 334] and further references there. Our package deals with cycles through Fillmore–Springer–Cnops construction (FSCc) which also has a long history, see [65, § 4.1; 100; 163, § 4.2; 191; 198, § 4.2; 300, § 1.1] and section I.13.2.1 below. Compared to a plain analytical treatment [32, Ch. 3; 276, Ch. 2], FSCc is much more efficient and conceptually coherent in dealing with FLT-invariant properties of cycles. Correspondingly, the computer code based on FSCc is easy to write and maintain.

The paper outline is as follows. In Section I.13.2 we sketch the mathematical theory (Möbius–Lie geometry) covered by the package of the previous library cycle [186] and the present library figure. We expose the subject with some references to its history since this can facilitate further development.

Sec. I.13.3.1 describes the principal mathematical tool used by the library figure. It allows to reduce a collection of various linear and quadratic equations (expressing geometrical relations like orthogonality and tangency) to a set of linear equations and *at most one* quadratic relation (I.13.8). Notably, the quadratic relation is the same in all cases, which greatly simplifies its handling. This approach is the cornerstone of

¹All described software is licensed under GNU GPLv3 [112].

the library effectiveness both in symbolic and numerical computations. In Sec. I.13.3.2 we present several examples of ensembles, which were already used in mathematical theories [208, 209, 218], then we describe how ensembles are encoded in the present library figure through the functional programming framework.

Sec. I.13.4 outlines several typical usages of the package. An example of a new statement discovered and demonstrated by the package is given in Thm. I.13.7. In Sec. I.13.5 we list of some further tasks, which will extend capacities and usability of the package.

All coding-related material is enclosed as appendices in the full documentation on the project page [186]. They contain:

- i. Numerous examples of the library usage starting from the very simple ones.
- ii. A systematic list of callable methods.
- iii. Actual code of the library.

Sec. I.13.2, Example I.13.6 below or the above-mentioned first two appendices of the full documentation can serve as an entry point for a reader with respective preferences and background.

I.13.2. Möbius–Lie Geometry and the cycle Library

We briefly outline mathematical formalism of the extend Möbius–Lie geometry, which is implemented in the present package. We do not aim to present the complete theory here, instead we provide a minimal description with a sufficient amount of references to further sources. The hierarchical structure of the theory naturally splits the package into two components: the routines handling individual cycles (the library cycle briefly reviewed in this section), which were already introduced elsewhere [186], and the new component implemented in this work, which handles families of interrelated cycles (the library figure introduced in the next section).

I.13.2.1. Möbius–Lie geometry and FSC construction. Möbius–Lie geometry in \mathbb{R}^n starts from an observation that points can be treated as spheres of zero radius and planes are the limiting case of spheres with radii diverging to infinity. Oriented spheres, planes and points are called together *cycles*. Then, the second crucial step is to treat cycles not as subsets of \mathbb{R}^n but rather as points of some projective space of higher dimensionality, see [33, Ch. 3; 59; 276; 300].

To distinguish two spaces we will call \mathbb{R}^n as the *point space* and the higher dimension space, where cycles are represented by points—the *cycle space*. Next important observation is that geometrical relations between cycles as subsets of the point space can be expressed in term of some indefinite metric on the cycle space. Therefore, if an indefinite metric shall be considered anyway, there is no reason to be limited to spheres in Euclidean space \mathbb{R}^n only. The same approach shall be adopted for quadrics in spaces \mathbb{R}^{p+q+r} of an arbitrary signature $p + q + r = n$, including r nilpotent elements, cf. (I.13.2) below.

A useful addition to Möbius–Lie geometry is provided by the Fillmore–Springer–Cnops construction (FSCc) [65, § 4.1; 100; 163, § 4.2; 191; 198, § 4.2; 289, § 18; 300, § 1.1]. It is a correspondence between the cycles (as points of the cycle space) and certain 2×2 -matrices defined in (I.16.14) below. The main advantages of FSCc are:

- i. The correspondence between cycles and matrices respects the projective structure of the cycle space.
- ii. The correspondence is FLT covariant.
- iii. The indefinite metric on the cycle space can be expressed through natural operations on the respective matrices.

The last observation is that for restricted groups of Möbius transformations the metric of the cycle space may not be completely determined by the metric of the point space, see [185; 191; 198, § 4.2] for an example in two-dimensional space.

FSCc is useful in consideration of the Poincaré extension of Möbius maps [209], loxodromes [218] and continued fractions [208]. In theoretical physics FSCc nicely describes conformal compactifications of various space-time models [130; 187; 198, § 8.1]. Regretfully, FSCc have not yet propagated back to the most fundamental case of complex numbers, cf. [306, § 9.2] or somewhat cumbersome techniques used in [32, Ch. 3]. Interestingly, even the founding fathers were not always strict followers of their own techniques, see [101].

We turn now to the explicit definitions.

I.13.2.2. Clifford algebras, FLT transformations, and Cycles. We describe here the mathematics behind the the first library called *cycle*, which implements fundamental geometrical relations between quadrics in the space \mathbb{R}^{p+q+r} with the dimensionality $n = p + q + r$ and metric $x_1^2 + \dots + x_p^2 - x_{p+1}^2 - \dots - x_{p+q}^2$. A version simplified for complex numbers only can be found in [208, 209, 218].

The Clifford algebra $\mathcal{C}(p, q, r)$ is the associative unital algebra over \mathbb{R} generated by the elements e_1, \dots, e_n satisfying the following relation:

$$(I.13.2) \quad e_i e_j = -e_j e_i, \quad \text{and} \quad e_i^2 = \begin{cases} -1, & \text{if } 1 \leq i \leq p; \\ 1, & \text{if } p+1 \leq i \leq p+q; \\ 0, & \text{if } p+q+1 \leq i \leq p+q+r. \end{cases}$$

It is common [65, 75, 132, 133, 289] to consider mainly Clifford algebras $\mathcal{C}(n) = \mathcal{C}(n, 0, 0)$ of the Euclidean space or the algebra $\mathcal{C}(p, q) = \mathcal{C}(p, q, 0)$ of the pseudo-Euclidean (Minkowski) spaces. However, Clifford algebras $\mathcal{C}(p, q, r)$, $r > 0$ with nilpotent generators $e_i^2 = 0$ correspond to interesting geometry [191, 198, 261, 339] and physics [117, 118, 120, 200, 203, 210] as well. Yet, the geometry with idempotent units in spaces with dimensionality $n > 2$ is still not sufficiently elaborated.

An element of $\mathcal{C}(p, q, r)$ having the form $x = x_1 e_1 + \dots + x_n e_n$ can be associated with the vector $(x_1, \dots, x_n) \in \mathbb{R}^{p+q+r}$. The *reversion* $a \mapsto a^*$ in $\mathcal{C}(p, q, r)$ [65, (1.19(ii))] is defined on vectors by $x^* = x$ and extended to other elements by the relation $(ab)^* = b^* a^*$. Similarly the *conjugation* is defined on vectors by $\bar{x} = -x$ and the relation $\overline{ab} = \bar{b} \bar{a}$. We also use the notation $|a|^2 = a \bar{a}$ for any product a of vectors. An important observation is that any non-zero $x \in \mathbb{R}^{n00}$ has a multiplicative inverse: $x^{-1} = \frac{\bar{x}}{|x|^2}$. For

a 2×2 -matrix $M = \begin{pmatrix} a & b \\ c & d \end{pmatrix}$ with Clifford entries we define, cf. [65, (4.7)]

$$(I.13.3) \quad \bar{M} = \begin{pmatrix} \bar{d}^* & -\bar{b}^* \\ -\bar{c}^* & \bar{a}^* \end{pmatrix} \quad \text{and} \quad M^* = \begin{pmatrix} \bar{d} & \bar{b} \\ \bar{c} & \bar{a} \end{pmatrix}.$$

Then $M\bar{M} = \delta I$ for the *pseudodeterminant* $\delta := ad^* - bc^*$.

Quadrics in $\mathbb{R}^{p,q}$ —which we continue to call *cycles*—can be associated to 2×2 matrices through the FSC construction [65, (4.12); 100; 198, § 4.4]:

$$(I.13.4) \quad k\bar{x}x - l\bar{x} - x\bar{l} + m = 0 \quad \leftrightarrow \quad C = \begin{pmatrix} l & m \\ k & \bar{l} \end{pmatrix},$$

where $k, m \in \mathbb{R}$ and $l \in \mathbb{R}^{p,q}$. For brevity we also encode a cycle by its coefficients (k, l, m) . A justification of (I.16.14) is provided by the identity:

$$(1 \quad \bar{x}) \begin{pmatrix} l & m \\ k & \bar{l} \end{pmatrix} \begin{pmatrix} x \\ 1 \end{pmatrix} = kx\bar{x} - l\bar{x} - x\bar{l} + m, \quad \text{since } \bar{x} = -x \text{ for } x \in \mathbb{R}^{p,q}.$$

The identification is also FLT-covariant in the sense that the transformation (I.13.1) associated with the matrix $M = \begin{pmatrix} a & b \\ c & d \end{pmatrix}$ sends a cycle C to the cycle MCM^* [65, (4.16)]. We define the FLT-invariant inner product of cycles C_1 and C_2 by the identity

$$(I.13.5) \quad \langle C_1, C_2 \rangle = \Re \operatorname{tr}(C_1 C_2),$$

where \Re denotes the scalar part of a Clifford number. This definition in term of matrices immediately implies that the inner product is FLT-invariant. The explicit expression in terms of components of cycles $C_1 = (k_1, l_1, m_1)$ and $C_2 = (k_2, l_2, m_2)$ is also useful sometimes:

$$(I.13.6) \quad \langle C_1, C_2 \rangle = l_1 l_2 + \bar{l}_1 \bar{l}_2 + m_1 k_2 + m_2 k_1.$$

As usual, the relation $\langle C_1, C_2 \rangle = 0$ is called the *orthogonality* of cycles C_1 and C_2 . In most cases it corresponds to orthogonality of quadrics in the point space. More generally, most of FLT-invariant relations between quadrics may be expressed in terms FLT-invariant inner product (I.13.5). For the full description of methods on individual cycles, which are implemented in the library cycle, see the respective documentation [186].

REMARK I.13.1. Since cycles are elements of the projective space, the following *normalised cycle product*:

$$(I.13.7) \quad [C_1, C_2] := \frac{\langle C_1, C_2 \rangle}{\sqrt{\langle C_1, C_1 \rangle \langle C_2, C_2 \rangle}}$$

is more meaningful than the cycle product (I.13.5) itself. Note that, $[C_1, C_2]$ is defined only if neither C_1 nor C_2 is a zero-radius cycle (i.e. a point). Also, the normalised cycle product is $GL_2(\mathbb{C})$ -invariant in comparison to $SL_2(\mathbb{C})$ -invariance of (I.13.5).

We finish this brief review of the library cycle by pointing to its light version written in Asymptote language [126] and distributed together with the paper [218]. Although the light version mostly inherited API of the library cycle, there are some significant limitations caused by the absence of GiNaC support:

- i. there is no symbolic computations of any sort;
- ii. the light version works in two dimensions only;
- iii. only elliptic metrics in the point and cycle spaces are supported.

On the other hand, being integrated with Asymptote the light version simplifies production of illustrations, which are its main target.

I.13.3. Ensembles of Interrelated Cycles and the figure Library

The library figure has an ability to store and resolve the system of geometric relations between cycles. We explain below some mathematical foundations, which greatly simplify this task.

I.13.3.1. Connecting quadrics and cycles. We need a vocabulary, which translates geometric properties of quadrics on the point space to corresponding relations in the cycle space. The key ingredient is the cycle product (I.13.5)–(I.14.17), which is linear in each cycles' parameters. However, certain conditions, e.g. tangency of cycles, involve polynomials of cycle products and thus are non-linear. For a successful algorithmic implementation, the following observation is important: *all non-linear conditions below can be linearised if the additional quadratic condition of normalisation type is imposed:*

$$(I.13.8) \quad \langle C, C \rangle = \pm 1.$$

This observation in the context of the Apollonius problem was already made in [101]. Conceptually the present work has a lot in common with the above mentioned paper of Fillmore and Springer, however a reader need to be warned that our implementation is totally different (and, interestingly, is more closer to another paper [100] of Fillmore and Springer).

REMARK I.13.2. Interestingly, the method of order reduction for algebraic equations is conceptually similar to the method of order reduction of differential equations used to build a geometric dynamics of quantum states in [7].

Here is the list of relations between cycles implemented in the current version of the library figure.

- i. A quadric is flat (i.e. is a hyperplane), that is, its equation is linear. Then, either of two equivalent conditions can be used:
 - (a) k component of the cycle vector is zero;
 - (b) the cycle is orthogonal $\langle C_1, C_\infty \rangle = 0$ to the “zero-radius cycle at infinity” $C_\infty = (0, 0, 1)$.
- ii. A quadric on the plane represents a line in Lobachevsky-type geometry if it is orthogonal $\langle C_1, C_{\mathbb{R}} \rangle = 0$ to the real line cycle $C_{\mathbb{R}}$. A similar condition is meaningful in higher dimensions as well.
- iii. A quadric C represents a point, that is, it has zero radius at given metric of the point space. Then, the determinant of the corresponding FSC matrix is zero or, equivalently, the cycle is self-orthogonal (isotropic): $\langle C, C \rangle = 0$. Naturally, such a cycle cannot be normalised to the form (I.13.8).
- iv. Two quadrics are orthogonal in the point space $\mathbb{R}P^q$. Then, the matrices representing cycles are orthogonal in the sense of the inner product (I.13.5).

- v. Two cycles C and \tilde{C} are tangent. Then we have the following quadratic condition:

$$(I.13.9) \quad \langle C, \tilde{C} \rangle^2 = \langle C, C \rangle \langle \tilde{C}, \tilde{C} \rangle \quad \left(\text{or } [C, \tilde{C}] = \pm 1 \right).$$

With the assumption, that the cycle C is normalised by the condition (I.13.8), we may re-state this condition in the relation, which is linear to components of the cycle C :

$$(I.13.10) \quad \langle C, \tilde{C} \rangle = \pm \sqrt{\langle \tilde{C}, \tilde{C} \rangle}.$$

Different signs here represent internal and outer touch.

- vi. Inversive distance θ of two (non-isotropic) cycles is defined by the formula:

$$(I.13.11) \quad \langle C, \tilde{C} \rangle = \theta \sqrt{\langle C, C \rangle} \sqrt{\langle \tilde{C}, \tilde{C} \rangle}$$

In particular, the above discussed orthogonality corresponds to $\theta = 0$ and the tangency to $\theta = \pm 1$. For intersecting spheres θ provides the cosine of the intersecting angle. For other metrics, the geometric interpretation of inversive distance shall be modified accordingly.

If we are looking for a cycle C with a given inversive distance θ to a given cycle \tilde{C} , then the normalisation (I.13.8) again turns the defining relation (I.13.11) into a linear with respect to parameters of the unknown cycle C .

- vii. A generalisation of Steiner power d of two cycles is defined as, cf. [101, § 1.1]:

$$(I.13.12) \quad d = \langle C, \tilde{C} \rangle + \sqrt{\langle C, C \rangle} \sqrt{\langle \tilde{C}, \tilde{C} \rangle},$$

where both cycles C and \tilde{C} are k -normalised, that is the coefficient in front the quadratic term in (I.16.14) is 1. Geometrically, the generalised Steiner power for spheres provides the square of tangential distance. However, this relation is again non-linear for the cycle C .

If we replace C by the cycle $C_1 = \frac{1}{\sqrt{\langle C, C \rangle}} C$ satisfying (I.13.8), the identity (I.13.12) becomes:

$$(I.13.13) \quad d \cdot k = \langle C_1, \tilde{C} \rangle + \sqrt{\langle \tilde{C}, \tilde{C} \rangle},$$

where $k = \frac{1}{\sqrt{\langle C, C \rangle}}$ is the coefficient in front of the quadratic term of C_1 . The last identity is linear in terms of the coefficients of C_1 .

Summing up: if an unknown cycle is connected to already given cycles by any combination of the above relations, then all conditions can be expressed as a *system of linear equations for coefficients of the unknown cycle and at most one quadratic equation* (I.13.8).

I.13.3.2. Figures as families of cycles—functional approach. We start from some examples of ensembles of cycles, which conveniently describe FLT-invariant families of objects.

EXAMPLE I.13.3.

- i. The Poincaré extension of Möbius transformations from the real line to the upper half-plane of complex numbers is described by a triple of cycles $\{C_1, C_2, C_3\}$ such that:
 - (a) C_1 and C_2 are orthogonal to the real line;
 - (b) $\langle C_1, C_2 \rangle^2 \leq \langle C_1, C_1 \rangle \langle C_2, C_2 \rangle$;
 - (c) C_3 is orthogonal to any cycle in the triple including itself.
 A modification [208] with ensembles of four cycles describes an extension from the real line to the upper half-plane of complex, dual or double numbers. The construction can be generalised to arbitrary dimensions [24].
- ii. A parametrisation of loxodromes is provided by a triple of cycles $\{C_1, C_2, C_3\}$ such that, cf. [218] and Fig. I.13.1:
 - (a) C_1 is orthogonal to C_2 and C_3 ;
 - (b) $\langle C_2, C_3 \rangle^2 \geq \langle C_2, C_2 \rangle \langle C_3, C_3 \rangle$.

Then, main invariant properties of Möbius–Lie geometry, e.g. tangency of loxodromes, can be expressed in terms of this parametrisation [218].

- iii. A continued fraction is described by an infinite ensemble of cycles (C_k) such that [28]:
 - (a) All C_k are touching the real line (i.e. are *horocycles*);
 - (b) (C_1) is a horizontal line passing through $(0, 1)$;
 - (c) C_{k+1} is tangent to C_k for all $k > 1$.

This setup was extended in [208] to several similar ensembles. The key analytic properties of continued fractions—their convergence—can be linked to asymptotic behaviour of such an infinite ensemble [28].

- iv. A remarkable relation exists between discrete integrable systems and Möbius geometry of finite configurations of cycles [41, 226–228, 297]. It comes from “reciprocal force diagrams” used in 19th-century statics, starting with J.C. Maxwell. It is demonstrated in that the geometric compatibility of reciprocal figures corresponds to the algebraic compatibility of linear systems defining these configurations. On the other hand, the algebraic compatibility of linear systems lies in the basis of integrable systems. In particular [226, 227], important integrability conditions encapsulate nothing but a fundamental theorem of ancient Greek geometry.
- v. An important example of an infinite ensemble is provided by the representation of an arbitrary wave as the envelope of a continuous family of spherical waves. A finite subset of spheres can be used as an approximation to the infinite family. Then, discrete snapshots of time evolution of sphere wave packets represent a FLT-covariant ensemble of cycles [20]. Further physical applications of FLT-invariant ensembles may be looked at [150].

One can easily note that the above parametrisations of some objects by ensembles of cycles are not necessary unique. Naturally, two ensembles parametrisating the same

object are again connected by FLT-invariant conditions. We presented only one example here, cf. [218].

FIGURE I.13.1. Animated graphics of equivalent three-cycle parametrisations of a loxodrome. The green cycle is C_1 , two red circles are C_2 and C_3 .

EXAMPLE I.13.4. Two non-degenerate triples $\{C_1, C_2, C_3\}$ and $\{\tilde{C}_1, \tilde{C}_2, \tilde{C}_3\}$ parameterise the same loxodrome as in Ex. I.13.3I.13.3.ii if and only if all the following conditions are satisfied:

- i. Pairs $\{C_2, C_3\}$ and $\{\tilde{C}_2, \tilde{C}_3\}$ span the same hyperbolic pencil. That is cycles \tilde{C}_2 and \tilde{C}_3 are linear combinations of C_2 and C_3 and vice versa.
- ii. Pairs $\{C_2, C_3\}$ and $\{\tilde{C}_2, \tilde{C}_3\}$ have the same normalised cycle product (I.15.12):

$$(I.13.14) \quad [C_2, C_3] = [\tilde{C}_2, \tilde{C}_3].$$

iii. The elliptic-hyperbolic identity holds:

$$(I.13.15) \quad \frac{\operatorname{arccosh} [C_j, \tilde{C}_j]}{\operatorname{arccosh} [C_2, C_3]} \equiv \frac{1}{2\pi} \operatorname{arccos} [C_1, \tilde{C}_1] \pmod{1},$$

where j is either 2 or 3.

Equivalent triples of cycles parametrising the same loxodrome are shown on Fig. I.13.1 (an animation is available with the electronic version of this paper).

The respective equivalence relation for parametrisation of Poincaré extension from Ex. I.13.3I.13.3.i is provided in [209, Prop. 12]. These examples suggest that one can expand the subject and applicability of Möbius–Lie geometry through the following formal definition.

DEFINITION I.13.5. Let X be a set, $R \subset X \times X$ be an oriented graph on X and f be a function on R with values in FLT-invariant relations from § I.13.3.1. Then (R, f) -ensemble is a collection of cycles $\{C_j\}_{j \in X}$ such that

$$C_i \text{ and } C_j \text{ are in the relation } f(i, j) \text{ for all } (i, j) \in R.$$

For a fixed FLT-invariant equivalence relations \sim on the set \mathcal{E} of all (R, f) -ensembles, the extended Möbius–Lie geometry studies properties of cosets \mathcal{E}/\sim .

This definition can be suitably modified for

- i. ensembles with relations of more than two cycles; and/or
- ii. ensembles parametrised by continuous sets X , cf. wave envelopes in Ex. I.13.3I.13.3.

The above extension was developed along with the realisation the library figure within the *functional programming* framework—in contrast to *procedural approach* used in popular software packages like GeoGebra [135], CaRMetal [124], Kig [77], Dr. Geo [96] etc. The later provides a fixed set of geometric construction procedures, e.g. “find the midpoint of an interval”, “drop the perpendicular from a point to a line”, etc. In contrast, all new cycles in class figure are added through a list of defining relations, which links the new cycle to already existing ones². So other geometric packages are designed in the same paradigm as FORTRAN programming language while class figure is similar to Lisp.

It is well-known that both procedural and functional approaches to programme languages realises Turing computability paradigm. Similarly, the above mentioned interactive geometry packages and the present figure library may be treated as an extension of the classical geometric compass-and-straightedge constructions, where new lines or circles are drawn through already existing elements. If requested, an explicit evaluation of cycles’ parameters from this data may be attempted.

To avoid “chicken or the egg” dilemma all cycles are stored in a hierarchical structure of generations, numbered by integers. The basic principles are:

- i. Any explicitly defined cycle (i.e., a cycle which is not related to any previously known cycle) is placed into generation-0;

²In fact, it is possible (and useful!) to include relations of a new cycle to itself as well. For example, points are defined by the condition to be self-orthogonal.

- ii. Any new cycle defined by relations to *previous* cycles from generations k_1, k_2, \dots, k_n is placed to the generation k calculated as:

$$(I.13.16) \quad k = \max(k_1, k_2, \dots, k_n) + 1.$$

This rule does not forbid a cycle to have a relation to itself, e.g. isotropy (self-orthogonality) condition $\langle C, C \rangle = 0$, which specifies point-like cycles, cf. relation I.13.2.iii in § I.13.3.1. In fact, this is the only allowed type of relations to cycles in the same (not even speaking about younger) generations.

There are the following alterations of the above rules:

- i. From the beginning, every figure has two pre-defined cycles: the real line (hyperplane) $C_{\mathbb{R}}$ and the zero radius cycle at infinity $C_{\infty} = (0, 0, 1)$. These cycles are required for relations I.13.2.i and I.13.2.ii from the previous subsection. As predefined cycles, $C_{\mathbb{R}}$ and C_{∞} are placed in negative-numbered generations defined by the macros *REAL_LINE_GEN* and *INFINITY_GEN*.
- ii. If a point is added to generation-0 of a figure, then it is represented by a zero-radius cycle with its centre at the given point. Particular parameter of such cycle dependent on the used metric, thus this cycle is not considered as explicitly defined. Thereafter, the cycle shall have some parents at a negative-numbered generation defined by the macro *GHOST_GEN*.

A figure can be in two different modes: *freeze* or *unfreeze*, the second is default. In the *unfreeze* mode an addition of a new cycle by its relation prompts an evaluation of its parameters. If the evaluation was successful then the obtained parameters are stored and will be used in further calculations for all children of the cycle. Since many relations (see the previous Subsection) are connected to quadratic equation (I.13.8), the solutions may come in pairs. Furthermore, if the number or nature of conditions is not sufficient to define the cycle uniquely (up to natural quadratic multiplicity), then the cycle will depend on a number of free (symbolic) variable.

There is a macro-like tool, which is called subfigure. Such a subfigure is a figure itself, such that its inner hierarchy of generations and relations is not visible from the current figure. Instead, some cycles (of any generations) of the current figure are used as pre-defined cycles of generation-0 of subfigure. Then only one dependent cycle of subfigure, which is known as result, is returned back to the current figure. The generation of the result is calculated from generations of input cycles by the same formula (I.13.16).

There is a possibility to test certain conditions (“are two cycles orthogonal?”) or measure certain quantities (“what is their intersection angle?”) for already defined cycles. In particular, such methods can be used to prove geometrical statements according to the Cartesian programme, that is replacing the synthetic geometry by purely algebraic manipulations.

EXAMPLE I.13.6. As an elementary demonstration, let us prove that if a cycle r is orthogonal to a circle a at the point C of its contact with a tangent line l , then r is also orthogonal to the line l . To simplify setup we assume that a is the unit circle. Here is the Python code:

```
1 F=figure()
2 a=F.add_cycle(cycle2D(1,[0,0],-1),"a")
```

```

3 l=symbol("l")
4 C=symbol("C")
5 F.add_cycle_rel([is_tangent_i(a),is_orthogonal(F.get_infinity()),only_reals(1)
  ],l)
6 F.add_cycle_rel([is_orthogonal(C),is_orthogonal(a),is_orthogonal(l),only_reals
  (C)],C)
7 r=F.add_cycle_rel([is_orthogonal(C),is_orthogonal(a)],"r")
8 Res=F.check_rel(l,r,"orthogonal")
9 for i in range(len(Res)):
10     print "Tangent and radius are orthogonal: %s" %\
11     bool(Res[i].subs(pow(cos(wild(0)),2)==1-pow(sin(wild(0)),2)).normal())

```

The first line creates an empty figure F with the default euclidean metric. The next line explicitly uses parameters $(1, 0, 0, -1)$ of a to add it to F . Lines 3–4 define symbols l and C , which are needed because cycles with these labels are defined in lines 5–6 through some relations to themselves and the cycle a . In both cases we want to have cycles with real coefficients only and C is additionally self-orthogonal (i.e. is a zero-radius). Also, l is orthogonal to infinity (i.e. is a line) and C is orthogonal to a and l (i.e. is their common point). The tangency condition for l and self-orthogonality of C are both quadratic relations. The former has two solutions each depending on one real parameter, thus line l has two instances. Correspondingly, the point of contact C and the orthogonal cycle r through C (defined in line 7) each have two instances as well. Finally, lines 8–11 verify that every instance of l is orthogonal to the respective instance of r , this is assisted by the trigonometric substitution $\cos^2(*) = 1 - \sin^2(*)$ used for parameters of l in line 11. The output predictably is:

```

Tangent and circle r are orthogonal: True
Tangent and circle r are orthogonal: True

```

An original statement proved by the library figure for the first time will be considered in the next Section.

I.13.4. Mathematical Usage of the Library

The developed library figure has several different uses:

- It is easy to produce high-quality illustrations, which are fully-accurate in mathematical sense. The user is not responsible for evaluation of cycles' parameters, all computations are done by the library as soon as the figure is defined in terms of few geometrical relations. This is especially helpful for complicated images which may contain thousands of interrelated cycles. See Escher-like Fig. I.13.2 which shows images of two circles under the modular group action [316, § 14.4].
- The package can be used for computer experiments in Möbius–Lie geometry. There is a possibility to create an arrangement of cycles depending on one or several parameters. Then, for particular values of those parameters certain conditions, e.g. concurrency of cycles, may be numerically tested or graphically visualised. It is possible to create animations with gradual change of the

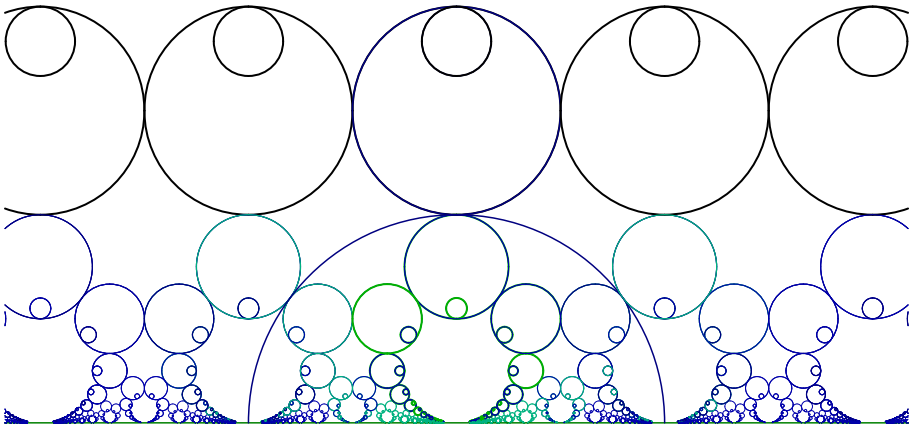


FIGURE I.13.2. Action of the modular group on the upper half-plane.

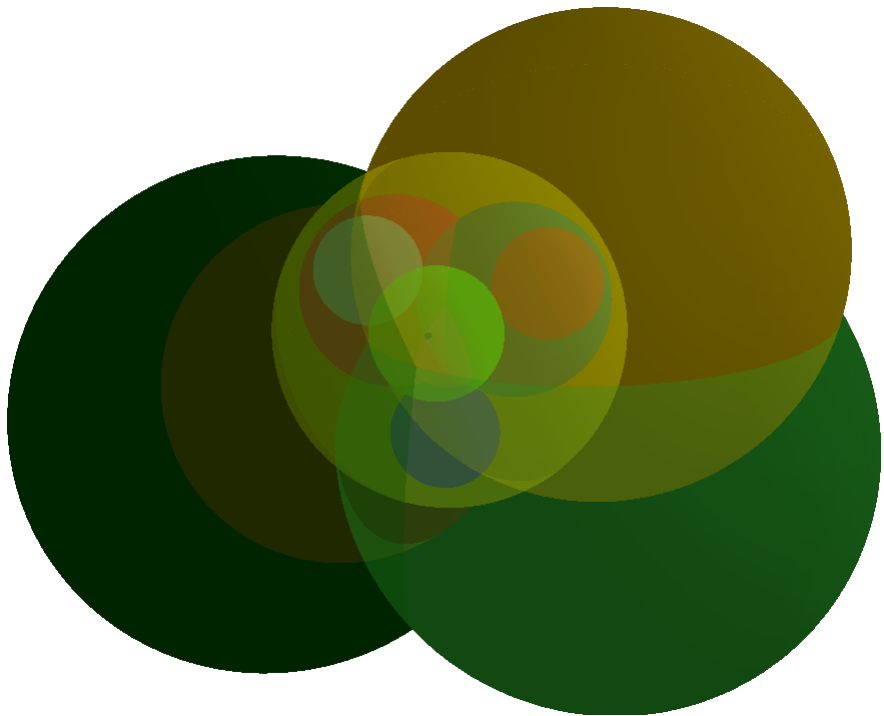


FIGURE I.13.3. An example of Apollonius problem in three dimensions.

parameters, which are especially convenient for illustrations, see Fig. I.13.5 in the electronic version of this paper and [207].

- Since the library is based on the GiNaC system, which provides a symbolic computation engine, there is a possibility to make fully automatic proofs of various statements in Möbius–Lie geometry. Usage of computer-supported proofs in geometry is already an established practice [198, 275] and it is naturally to expect its further rapid growth.
- Last but not least, the combination of classical beauty of Lie sphere geometry and modern computer technologies is a useful pedagogical tool to widen interest in mathematics through visual and hands-on experience.

Computer experiments are especially valuable for Lie geometry of indefinite or nilpotent metrics since our intuition is not elaborated there in contrast to the Euclidean space [185, 190, 191]. Some advances in the two-dimensional space were achieved recently [198, 261], however further developments in higher dimensions are still awaiting their researchers.

As a non-trivial example of automated proof accomplished by the figure library for the first time, we present a FLT-invariant version of the classical nine-point theorem [71, § 1.8; 276, § I.1], cf. Fig. I.13.4(a):

THEOREM I.13.7 (Nine-point cycle). *Let ABC be an arbitrary triangle with the orthocenter (the points of intersection of three altitudes) H, then the following nine points belongs to the same cycle, which may be a circle or a hyperbola:*

- Foots of three altitudes, that is points of pair-wise intersections AB and CH, AC and BH, BC and AH.*
- Midpoints of sides AB, BC and CA.*
- Midpoints of intervals AH, BH and CH.*

There are many further interesting properties, e.g. nine-point circle is externally tangent to that triangle three excircles and internally tangent to its incircle as it seen from Fig. I.13.4(a).

To adopt the statement for cycles geometry we need to find a FLT-invariant meaning of the midpoint A_m of an interval BC, because the equality of distances BA_m and A_mC is not FLT-invariant. The definition in cycles geometry can be done by either of the following equivalent relations:

- The midpoint A_m of an interval BC is defined by the cross-ratio $\frac{BA_m}{CA_m} : \frac{BI}{CI} = 1$, where I is the point at infinity.
- We construct the midpoint A_m of an interval BC as the intersection of the interval and the line orthogonal to BC and to the cycle, which uses BC as its diameter. The latter condition means that the cycle passes both points B and C and is orthogonal to the line BC.

Both procedures are meaningful if we replace the point at infinity I by an arbitrary fixed point N of the plane. In the second case all lines will be replaced by cycles passing through N, for example the line through B and C shall be replaced by a cycle through B, C and N. If we similarly replace “lines” by “cycles passing through N” in Thm. I.13.7 it turns into a valid FLT-invariant version, cf. Fig. I.13.4(b). Some additional properties,

e.g. the tangency of the nine-points circle to the ex-/in-circles, are preserved in the new version as well. Furthermore, we can illustrate the connection between two versions of the theorem by an animation, where the infinity is transformed to a finite point N by a continuous one-parameter group of FLT. Fig. I.13.5 in the electronic version of this paper shows such an animation; the printed version of this figure presents two intermediate steps in the transition from Fig. I.13.4(a) to I.13.4(b). Further examples of animations can be found at [207].

It is natural to test the nine-point theorem in the hyperbolic and the parabolic spaces. Fortunately, it is very easy under the given implementation: we only need to change the defining metric of the point space, cf. [6], this can be done for an already defined figure. The corresponding figures Fig. I.13.4(c) and (d) suggest that the hyperbolic version of the theorem is still true in the plain and even FLT-invariant forms. We shall clarify that the hyperbolic version of the Thm. I.13.7 specialises the nine-point conic of a complete quadrilateral [61, 76]: in addition to the existence of this conic, our theorem specifies its type for this particular arrangement as equilateral hyperbola with the vertical axis of symmetry.

The computational power of the package is sufficient not only to hint that the new theorem is true but also to make a complete proof. To this end we define an ensemble of cycles with exactly same interrelations, but populate the generation-0 with points A , B and C with symbolic coordinates, that is, objects of the GiNaC class `realsymbol`. Thus, the entire figure defined from them will be completely general. Then, we may define the hyperbola passing through three bases of altitudes and check by the symbolic computations that this hyperbola passes another six “midpoints” as well.

In the parabolic space the nine-point Thm. I.13.7 is not preserved in this manner. It is already observed [19, 190, 191, 196, 198, 203, 209, 261], that the degeneracy of parabolic metric in the point space requires certain revision of traditional definitions. The parabolic variation of nine-point theorem may prompt some further considerations as well. An expanded discussion of various aspects of the nine-point construction shall be the subject of a separate paper.

I.13.5. To Do List

The library is still under active development. Along with continuous bug fixing there is an intention to extend both functionality and usability. Here are several nearest tasks planned so far:

- Expand class `subfigure` in a way suitable for encoding loxodromes and other objects of an extended Möbius–Lie geometry [209, 218].
- Add non-point transformations, extending the package to Lie sphere geometry.
- Provide an effective parametrisation of solutions of a single quadratics condition.
- Expand drawing facilities in three dimensions to hyperboloids and paraboloids.
- Maintain and improve the Graphical User Interface which makes the library accessible to users without programming skills.

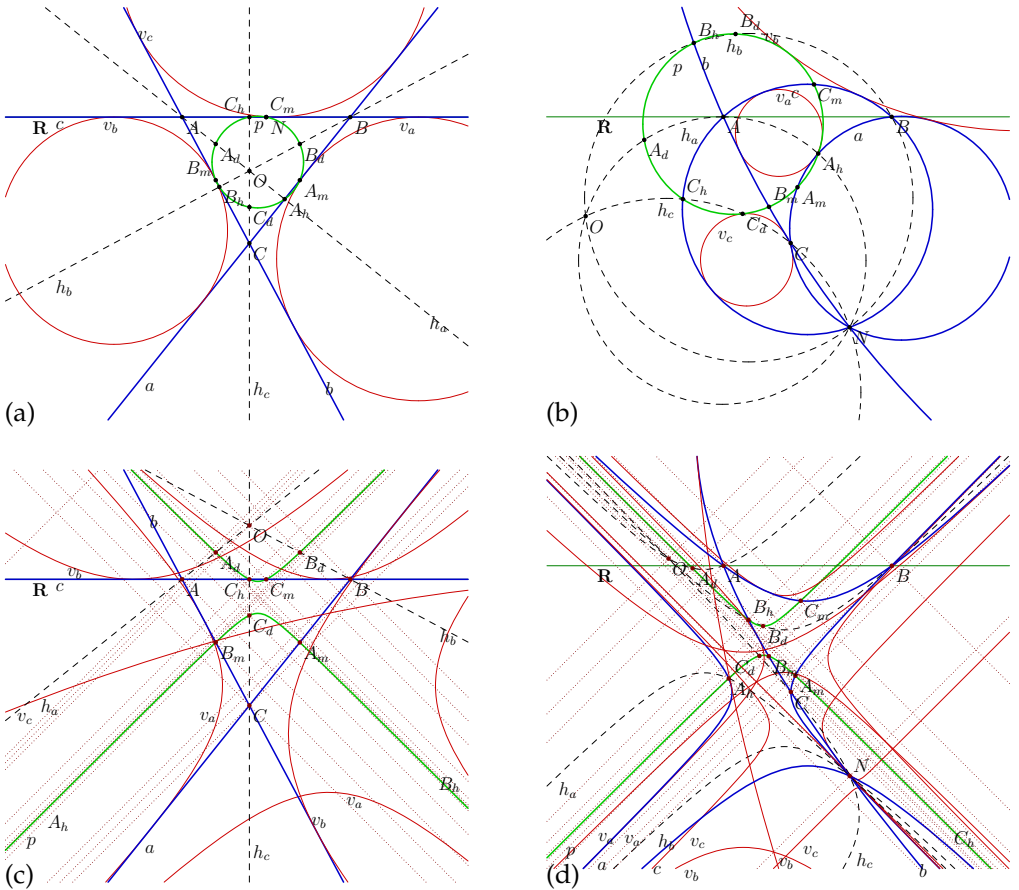


FIGURE I.13.4. The illustration of the conformal nine-points theorem. The left column is the statement for a triangle with straight sides (the point N is at infinity), the right column is its conformal version (the point N is at the finite part). The first row show the elliptic point space, the second row—the hyperbolic point space. Thus, the top-left picture shows the traditional theorem, three other pictures—its different modifications.

- Investigate cloud computing options which can free a user from the burden of software installation.

Being an open-source project the library is open for contributions and suggestions of other developers and users.

FIGURE I.13.5. Animated transition between the classical and conformal versions of the nine-point theorem. Use control buttons to activate it. You may need Adobe Acrobat Reader for this feature.

Poincaré Extension of Möbius Transformations

Given sphere preserving (Möbius) transformations in n -dimensional Euclidean space one can use the Poincaré extension to obtain sphere preserving transformations in a half-space of $n + 1$ dimensions. The Poincaré extension is usually provided either by an explicit formula or by some geometric construction. We investigate its algebraic background and describe all available options. The solution is given in terms of one-parameter subgroups of Möbius transformations acting on triples of quadratic forms. To focus on the concepts, this paper deals with the Möbius transformations of the real line only.

It is not surprising that we will arrive to the three possible situation—elliptic, parabolic, hyperbolic—considered above. The interesting feature of this chapter is what we completely avoid usage of complex, dual and double numbers which were are permanent companions so far.

I.14.1. Introduction

It is known, that Möbius transformations on \mathbb{R}^n can be expanded to the “upper” half-space in \mathbb{R}^{n+1} using the Poincaré extension [24, § 3.3; 273, § 5.2]. An explicit formula is usually presented without a discussion of its origin. In particular, one may get an impression that the solution is unique. This paper considers various aspects of such extension and describes different possible realisations. Our consideration is restricted to the case of extension from the real line to the upper half-plane. However, we made an effort to present it in a way, which allows numerous further generalisations.

I.14.2. Geometric construction

We start from the geometric procedure in the standard situation. The group $SL_2(\mathbb{R})$ consists of real 2×2 matrices with the unit determinant. $SL_2(\mathbb{R})$ acts on the real line by linear-fractional maps:

$$(I.14.1) \quad \begin{pmatrix} a & b \\ c & d \end{pmatrix} : x \mapsto \frac{ax + b}{cx + d}, \quad \text{where } x \in \mathbb{R} \text{ and } \begin{pmatrix} a & b \\ c & d \end{pmatrix} \in SL_2(\mathbb{R}).$$

A pair of (possibly equal) real numbers x and y uniquely determines a semicircle C_{xy} in the upper half-plane with the diameter $[x, y]$. For a linear-fractional transformation M (I.14.1), the images $M(x)$ and $M(y)$ define the semicircle with the diameter $[M(x), M(y)]$, thus, we can define the action of M on semicircles: $M(C_{xy}) = C_{M(x)M(y)}$. Geometrically, the *Poincaré extension* is based on the following lemma, see Fig. I.14.1(a) and more general Lem. I.14.18 below:

LEMMA I.14.1. *If a pencil of semicircles in the upper half-plane has a common point, then the images of these semicircles under a transformation (I.14.1) have a common point as well.*

Elementary geometry of right triangles tells that a pair of intersecting intervals $[x, y], [x', y']$, where $x < x' < y < y'$, defines the point

$$(I.14.2) \quad \left(\frac{xy - x'y'}{x + y - x' - y'}, \frac{\sqrt{(x - y')(x - x')(x' - y)(y - y')}}{x + y - x' - y'} \right) \in \mathbb{R}_+^2.$$

An alternative demonstration uses three observations:

- i. the scaling $x \mapsto ax, a > 0$ on the real line produces the scaling $(u, v) \mapsto (au, av)$ on pairs (I.14.2);
- ii. the horizontal shift $x \mapsto x + b$ on the real line produces the horizontal shift $(u, v) \mapsto (u + b, v)$ on pairs (I.14.2);
- iii. for the special case $y = -x^{-1}$ and $y' = -x'^{-1}$ the pair (I.14.2) is $(0, 1)$.

Finally, expression (I.14.2), as well as (I.14.3)–(I.14.4) below, can be calculated by the specialised CAS for Möbius invariant geometries [186, 211].

This standard approach can be widened as follows. The above semicircle can be equivalently described through the unique circle passing x and y and orthogonal to the real axis. Similarly, an interval $[x, y]$ uniquely defines a right-angle hyperbola in \mathbb{R}^2 orthogonal to the real line and passing (actually, having her vertices at) $(x, 0)$ and $(y, 0)$. An intersection with the second such hyperbola having vertices $(x', 0)$ and $(y', 0)$ defines a point with coordinates, see Fig. I.14.1(f):

$$(I.14.3) \quad \left(\frac{xy - x'y'}{x + y - x' - y'}, \frac{\sqrt{(x - y')(x - x')(x' - y)(y' - y)}}{x + y - x' - y'} \right),$$

where $x < y < x' < y'$. Note, the opposite sign of the product under the square roots in (I.14.2) and (I.14.3).

If we wish to consider the third type of conic sections—parabolas—we cannot use the unaltered procedure: there is no a non-degenerate parabola orthogonal to the real line and intersecting the real line in two points. We may recall, that a circle (or hyperbola) is orthogonal to the real line if its centre belongs to the real line. Analogously, a parabola is *focally orthogonal* (see [198, § 6.6] for a general consideration) to the real line if its focus belongs to the real line. Then, an interval $[x, y]$ uniquely defines a downward-opened parabola with the real roots x and y and focally orthogonal to the real line. Two such parabolas defined by intervals $[x, y]$ and $[x', y']$ have a common point, see Fig. I.14.1(c):

$$(I.14.4) \quad \left(\frac{xy' - yx' + D}{x - y - x' + y'}, \frac{(x' - x)(y' - y)(y - x + y' - x') + (x + y - x' - y')D}{(x - y - x' + y')^2} \right),$$

where $D = \pm\sqrt{(x - x')(y - y')(y - x)(y' - x')}$. For pencils of such hyperbolas and parabolas respective variants of Lem. I.14.1 hold.

Focally orthogonal parabolas make the angle 45° with the real line. This suggests to replace orthogonal circles and hyperbolas by conic sections with a fixed angle to the real line, see Fig. I.14.1(b)–(e). Of course, to be consistent this procedure requires a suitable modification of Lem. I.14.1, we will obtain it as a byproduct of our study, see

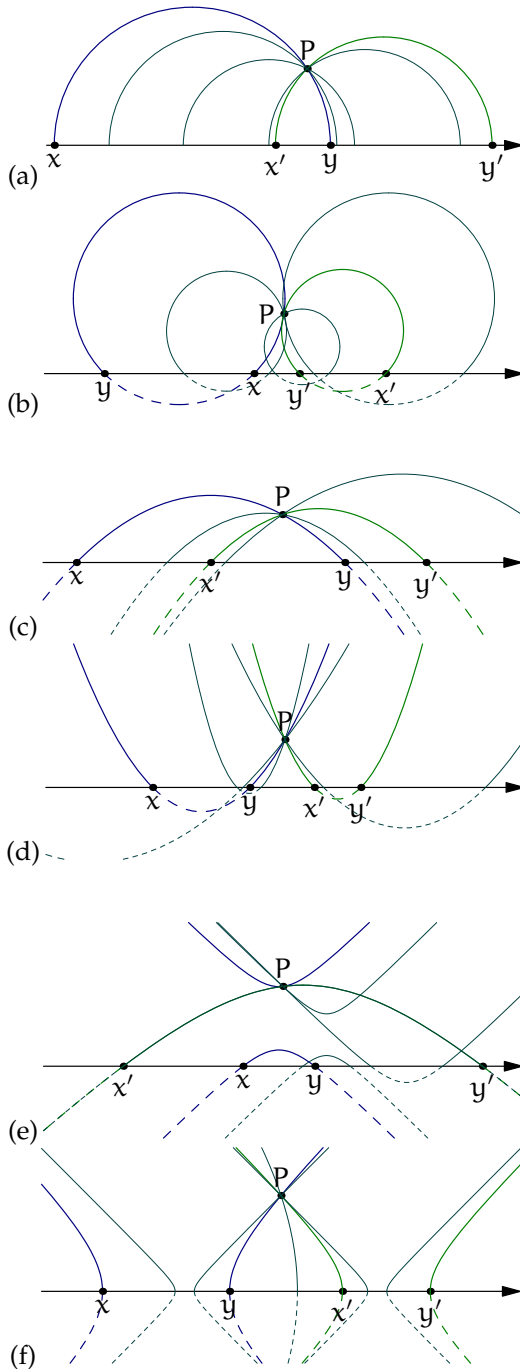


FIGURE I.14.1. Poincaré extensions: first column presents points defined by the intersecting intervals $[x, y]$ and $[x', y']$, the second column—by disjoint intervals. Each row uses the same type of conic sections—circles, parabolas and hyperbolas respectively. Pictures are

Lem. I.14.18. However, the respective alterations of the above formulae (I.14.2)–(I.14.4) become more complicated in the general case.

The considered geometric construction is elementary and visually appealing. Now we turn to respective algebraic consideration.

I.14.3. Möbius transformations and Cycles

The group $SL_2(\mathbb{R})$ acts on \mathbb{R}^2 by matrix multiplication on column vectors:
(I.14.5)

$$\mathcal{L}_g : \begin{pmatrix} x_1 \\ x_2 \end{pmatrix} \mapsto \begin{pmatrix} ax_1 + bx_2 \\ cx_1 + dx_2 \end{pmatrix} = \begin{pmatrix} a & b \\ c & d \end{pmatrix} \begin{pmatrix} x_1 \\ x_2 \end{pmatrix}, \quad \text{where } g = \begin{pmatrix} a & b \\ c & d \end{pmatrix} \in SL_2(\mathbb{R}).$$

A linear action respects the equivalence relation $\begin{pmatrix} x_1 \\ x_2 \end{pmatrix} \sim \begin{pmatrix} \lambda x_1 \\ \lambda x_2 \end{pmatrix}$, $\lambda \neq 0$ on \mathbb{R}^2 . The collection of all cosets for non-zero vectors in \mathbb{R}^2 is the *projective line* $\mathbb{P}\mathbb{R}^1$. Explicitly, a non-zero vector $\begin{pmatrix} x_1 \\ x_2 \end{pmatrix} \in \mathbb{R}^2$ corresponds to the point with homogeneous coordinates $[x_1 : x_2] \in \mathbb{P}\mathbb{R}^1$. If $x_2 \neq 0$ then this point is represented by $[\frac{x_1}{x_2} : 1]$ as well. The embedding $\mathbb{R} \rightarrow \mathbb{P}\mathbb{R}^1$ defined by $x \mapsto [x : 1]$, $x \in \mathbb{R}$ covers the all but one of points in $\mathbb{P}\mathbb{R}^1$. The exceptional point $[1 : 0]$ is naturally identified with the infinity.

The linear action (I.14.5) induces a morphism of the projective line $\mathbb{P}\mathbb{R}^1$, which is called a Möbius transformation. Considered on the real line within $\mathbb{P}\mathbb{R}^1$, Möbius transformations takes fraction-linear form:

$$g : [x : 1] \mapsto \left[\frac{ax + b}{cx + d} : 1 \right], \quad \text{where } g = \begin{pmatrix} a & b \\ c & d \end{pmatrix} \in SL_2(\mathbb{R}) \text{ and } cx + d \neq 0.$$

This $SL_2(\mathbb{R})$ -action on $\mathbb{P}\mathbb{R}^1$ is denoted as $g : x \mapsto g \cdot x$. We note that the correspondence of column vectors and row vectors $i : \begin{pmatrix} x_1 \\ x_2 \end{pmatrix} \mapsto (x_2, -x_1)$ intertwines the left multiplication \mathcal{L}_g (I.14.5) and the right multiplication $\mathcal{R}_{g^{-1}}$ by the inverse matrix:

$$(I.14.6) \quad \mathcal{R}_{g^{-1}} : (x_2, -x_1) \mapsto (cx_1 + dx_2, -ax_1 - bx_2) = (x_2, -x_1) \begin{pmatrix} d & -b \\ -c & a \end{pmatrix}.$$

We extended the map i to 2×2 -matrices by the rule:

$$(I.14.7) \quad i : \begin{pmatrix} x_1 & y_1 \\ x_2 & y_2 \end{pmatrix} \mapsto \begin{pmatrix} y_2 & -y_1 \\ x_2 & -x_1 \end{pmatrix}.$$

Two columns $\begin{pmatrix} x \\ 1 \end{pmatrix}$ and $\begin{pmatrix} y \\ 1 \end{pmatrix}$ form the 2×2 matrix $M_{xy} = \begin{pmatrix} x & y \\ 1 & 1 \end{pmatrix}$. For geometrical reasons appearing in Cor. I.14.3, we call a *cycle* the 2×2 -matrix C_{xy} defined by

$$(I.14.8) \quad C_{xy} = \frac{1}{2} M_{xy} \cdot i(M_{xy}) = \frac{1}{2} M_{yx} \cdot i(M_{yx}) = \begin{pmatrix} \frac{x+y}{2} & -xy \\ 1 & -\frac{x+y}{2} \end{pmatrix}.$$

We note that $\det C_{xy} = -(x-y)^2/4$, thus $\det C_{xy} = 0$ if and only if $x = y$. Also, we can consider the Möbius transformation produced by the 2×2 -matrix C_{xy} and calculate:

$$(I.14.9) \quad C_{xy} \begin{pmatrix} x \\ 1 \end{pmatrix} = \lambda \begin{pmatrix} x \\ 1 \end{pmatrix} \quad \text{and} \quad C_{xy} \begin{pmatrix} y \\ 1 \end{pmatrix} = -\lambda \begin{pmatrix} y \\ 1 \end{pmatrix} \quad \text{where } \lambda = \frac{x-y}{2}.$$

Thus, points $[x : 1], [y : 1] \in \mathbb{P}\mathbb{R}^1$ are fixed by C_{xy} . Also, C_{xy} swaps the interval $[x, y]$ and its complement.

Due to their structure, matrices C_{xy} can be parametrised by points of \mathbb{R}^3 . Furthermore, the map from $\mathbb{R}^2 \rightarrow \mathbb{R}^3$ given by $(x, y) \mapsto C_{xy}$ naturally induces the projective map $(\mathbb{P}\mathbb{R}^1)^2 \rightarrow \mathbb{P}\mathbb{R}^2$ due to the identity:

$$\frac{1}{2} \begin{pmatrix} \lambda x & \mu y \\ \lambda & \mu \end{pmatrix} \begin{pmatrix} \mu & -\mu y \\ \lambda & -\lambda x \end{pmatrix} = \lambda \mu \begin{pmatrix} \frac{x+y}{2} & -xy \\ 1 & -\frac{x+y}{2} \end{pmatrix} = \lambda \mu C_{xy}.$$

Conversely, a zero-trace matrix $\begin{pmatrix} a & b \\ c & -a \end{pmatrix}$ with a non-positive determinant is projectively equivalent to a product C_{xy} (I.14.8) with $x, y = \frac{a \pm \sqrt{a^2 + bc}}{c}$. In particular, we can embed a point $[x : 1] \in \mathbb{P}\mathbb{R}^1$ to 2×2 -matrix C_{xx} with zero determinant.

The combination of (I.14.5)–(I.14.8) implies that the correspondence $(x, y) \mapsto C_{xy}$ is $\text{SL}_2(\mathbb{R})$ -covariant in the following sense:

$$(I.14.10) \quad g C_{xy} g^{-1} = C_{x'y'}, \quad \text{where } x' = g \cdot x \text{ and } y' = g \cdot y.$$

To achieve a geometric interpretation of all matrices, we consider the bilinear form $Q : \mathbb{R}^2 \times \mathbb{R}^2 \rightarrow \mathbb{R}$ generated by a 2×2 -matrix $\begin{pmatrix} a & b \\ c & d \end{pmatrix}$:

$$(I.14.11) \quad Q(x, y) = \begin{pmatrix} x_1 & x_2 \end{pmatrix} \begin{pmatrix} a & b \\ c & d \end{pmatrix} \begin{pmatrix} y_1 \\ y_2 \end{pmatrix}, \quad \text{where } x = (x_1, x_2), y = (y_1, y_2).$$

Due to linearity of Q , the null set

$$(I.14.12) \quad \{(x, y) \in \mathbb{R}^2 \times \mathbb{R}^2 \mid Q(x, y) = 0\}$$

factors to a subset of $\mathbb{P}\mathbb{R}^1 \times \mathbb{P}\mathbb{R}^1$. Furthermore, for the matrices C_{xy} (I.14.8), a direct calculation shows that:

LEMMA I.14.2. *The following identity holds:*

$$(I.14.13) \quad C_{xy}(i(x'), y') = \text{tr}(C_{xy} C_{x'y'}) = \frac{1}{2}(x+y)(x'+y') - (xy + x'y').$$

In particular, the above expression is a symmetric function of the pairs (x, y) and (x', y') .

The map i appearance in (I.14.13) is justified once more by the following result.

COROLLARY I.14.3. *The null set of the quadratic form $C_{xy}(x') = C_{xy}(i(x'), x')$ consists of two points x and y .*

Alternatively, the identities $C_{xy}(x) = C_{xy}(y) = 0$ follows from (I.14.9) and the fact that $i(z)$ is orthogonal to z for all $z \in \mathbb{R}^2$. Also, we note that:

$$i \left(\begin{pmatrix} x_1 \\ x_2 \end{pmatrix} \right) \begin{pmatrix} a & b \\ c & d \end{pmatrix} \begin{pmatrix} y_1 \\ y_2 \end{pmatrix} = \begin{pmatrix} x_1 & x_2 \end{pmatrix} \begin{pmatrix} -c & -d \\ a & b \end{pmatrix} \begin{pmatrix} y_1 \\ y_2 \end{pmatrix}.$$

Motivated by Lem. I.14.2, we call $\langle C_{xy}, C_{x'y'} \rangle := -\text{tr}(C_{xy} C_{x'y'})$ the *pairing* of two cycles. It shall be noted that the pairing is *not* positively defined, this follows from the explicit expression (I.14.13). The sign is chosen in such way, that

$$\langle C_{xy}, C_{xy} \rangle = -2 \det(C_{xy}) = \frac{1}{2}(x - y)^2 \geq 0.$$

Also, an immediate consequence of Lem. I.14.2 or identity (I.14.11) is

COROLLARY I.14.4. *The pairing of cycles is invariant under the action (I.14.10) of $SL_2(\mathbb{R})$:*

$$\langle g \cdot C_{xy} \cdot g^{-1}, g \cdot C_{x'y'} \cdot g^{-1} \rangle = \langle C_{xy}, C_{x'y'} \rangle.$$

From (I.14.13), the null set (I.14.12) of the form $Q = C_{xy}$ can be associated to the family of cycles $\{C_{x'y'} \mid \langle C_{xy}, C_{x'y'} \rangle = 0, (x', y') \in \mathbb{R}^2 \times \mathbb{R}^2\}$ which we will call *orthogonal* to C_{xy} .

I.14.4. Extending cycles

Since bilinear forms with matrices C_{xy} have numerous geometric connections with $\mathbb{P}\mathbb{R}^1$, we are looking for a similar interpretation of the generic matrices. The previous discussion identified the key ingredient of the recipe: $SL_2(\mathbb{R})$ -invariant pairing (I.14.13) of two forms. Keeping in mind the structure of C_{xy} , we will parameterise¹

a generic 2×2 matrix as $\begin{pmatrix} l+n & -m \\ k & -l+n \end{pmatrix}$ and consider the corresponding four dimensional vector (n, l, k, m) . Then, the similarity with $\begin{pmatrix} a & b \\ c & d \end{pmatrix} \in SL_2(\mathbb{R})$:

$$(I.14.14) \quad \begin{pmatrix} l'+n' & -m' \\ k' & -l'+n' \end{pmatrix} = \begin{pmatrix} a & b \\ c & d \end{pmatrix} \begin{pmatrix} l+n & -m \\ k & -l+n \end{pmatrix} \begin{pmatrix} a & b \\ c & d \end{pmatrix}^{-1},$$

corresponds to the linear transformation of \mathbb{R}^4 , cf. [198, Ex. 4.15]:

$$(I.14.15) \quad \begin{pmatrix} n' \\ l' \\ k' \\ m' \end{pmatrix} = \begin{pmatrix} 1 & 0 & 0 & 0 \\ 0 & cb+ad & bd & ca \\ 0 & 2cd & d^2 & c^2 \\ 0 & 2ab & b^2 & a^2 \end{pmatrix} \begin{pmatrix} n \\ l \\ k \\ m \end{pmatrix}.$$

In particular, this action commutes with the scaling of the first component:

$$(I.14.16) \quad \lambda : (n, l, k, m) \mapsto (\lambda n, l, k, m).$$

This expression is helpful in proving the following statement.

LEMMA I.14.5. *Any $SL_2(\mathbb{R})$ -invariant (in the sense of the action (I.14.15)) pairing in \mathbb{R}^4 is isomorphic to*

$$2\check{n}\check{n} - 2\check{l}\check{l} + \check{k}\check{m} + \check{m}\check{k} = \begin{pmatrix} \check{n} & \check{l} & \check{k} & \check{m} \end{pmatrix} \begin{pmatrix} 2\check{\sigma} & 0 & 0 & 0 \\ 0 & -2 & 0 & 0 \\ 0 & 0 & 0 & 1 \\ 0 & 0 & 1 & 0 \end{pmatrix} \begin{pmatrix} n \\ l \\ k \\ m \end{pmatrix},$$

¹Further justification of this parametrisation will be obtained from the equation of a quadratic curve (I.14.18).

where $\check{\sigma} = -1, 0$ or 1 and $(n, l, k, m), (\tilde{n}, \tilde{l}, \tilde{k}, \tilde{m}) \in \mathbb{R}^4$.

PROOF. Let T be 4×4 a matrix from (I.14.15), if a $SL_2(\mathbb{R})$ -invariant pairing is defined by a 4×4 matrix $J = (j_{fg})$, then $T'JT = J$, where T' is transpose of T . The equivalent identity $T'J = JT^{-1}$ produces a system of homogeneous linear equations which has the generic solution:

$$\begin{aligned} j_{12} &= j_{13} = j_{14} = j_{21} = j_{31} = j_{41} = 0, \\ j_{22} &= \frac{(d-a)j_{42} - 2bj_{44}}{c} - 2j_{43}, & j_{23} &= -\frac{b}{c}j_{42}, & j_{24} &= -\frac{cj_{42} + 2(a-d)j_{44}}{c}, \\ j_{34} &= \frac{c(a-d)j_{42} + (a-d)^2j_{44}}{c^2} + j_{43}, & j_{33} &= \frac{b^2}{c^2}j_{44}, & j_{32} &= \frac{bcj_{42} + 2(a-d)j_{44}}{c}, \end{aligned}$$

with four free variables j_{11}, j_{42}, j_{43} and j_{44} . Since a solution shall not depend on a, b, c, d , we have to put $j_{42} = j_{44} = 0$. Then by the homogeneity of the identity $T'J = JT^{-1}$, we can scale j_{43} to 1. Thereafter, an independent (sign-preserving) scaling (I.14.16) of n leaves only three non-isomorphic values $-1, 0, 1$ of j_{11} . \square

The appearance of the three essential different cases $\check{\sigma} = -1, 0$ or 1 in Lem. I.14.5 is a manifestation of the common division of mathematical objects into elliptic, parabolic and hyperbolic cases [185; 198, Ch. 1]. Thus, we will use letters “e”, “p”, “h” to encode the corresponding three values of $\check{\sigma}$.

Now we may describe all $SL_2(\mathbb{R})$ -invariant pairings of bilinear forms.

COROLLARY I.14.6. Any $SL_2(\mathbb{R})$ -invariant (in the sense of the similarity (I.14.14)) pairing between two bilinear forms $Q = \begin{pmatrix} l+n & -m \\ k & -l+n \end{pmatrix}$ and $\tilde{Q} = \begin{pmatrix} \tilde{l}+\tilde{n} & -\tilde{m} \\ \tilde{k} & -\tilde{l}+\tilde{n} \end{pmatrix}$ is isomorphic to:

$$\begin{aligned} \text{(I.14.17)} \quad \langle Q, \tilde{Q} \rangle_\tau &= -\text{tr}(Q_\tau \tilde{Q}) \\ &= 2\tau\tilde{n}n - 2\tilde{l}l + \tilde{k}m + \tilde{m}k, \quad \text{where } Q_\tau = \begin{pmatrix} l-\tau n & -m \\ k & -l-\tau n \end{pmatrix} \end{aligned}$$

and $\tau = -1, 0$ or 1 .

Note that we can explicitly write Q_τ for $Q = \begin{pmatrix} a & b \\ c & d \end{pmatrix}$ as follows:

$$Q_e = \begin{pmatrix} a & b \\ c & d \end{pmatrix}, \quad Q_p = \begin{pmatrix} \frac{1}{2}(a-d) & b \\ c & -\frac{1}{2}(a-d) \end{pmatrix}, \quad Q_h = \begin{pmatrix} -d & b \\ c & -a \end{pmatrix}.$$

In particular, $Q_h = -Q^{-1}$ and $Q_p = \frac{1}{2}(Q_e + Q_h)$. Furthermore, Q_p has the same structure as C_{xy} . Now, we are ready to extend the projective line $\mathbb{P}R^1$ to two dimensions using the analogy with properties of cycles C_{xy} .

- DEFINITION I.14.7.
- i. Two bilinear forms Q and \tilde{Q} are τ -orthogonal if $\langle Q, \tilde{Q} \rangle_\tau = 0$.
 - ii. A form is τ -isotropic if it is τ -orthogonal to itself.

If a form $Q = \begin{pmatrix} l+n & -m \\ k & -l+n \end{pmatrix}$ has $k \neq 0$ then we can scale it to obtain $k = 1$, this form of Q is called *normalised*. A normalised τ -isotropic form is completely determined by its diagonal values: $\begin{pmatrix} u+v & -u^2 + \tau v^2 \\ 1 & -u+v \end{pmatrix}$. Thus, the set of such forms is in a one-to-one correspondence with points of \mathbb{R}^2 . Finally, a form $Q = \begin{pmatrix} l+n & -m \\ k & -l+n \end{pmatrix}$ is e-orthogonal to the τ -isotropic form $\begin{pmatrix} u+v & -u^2 + \tau v^2 \\ 1 & -u+v \end{pmatrix}$ if:

$$(I.14.18) \quad k(u^2 - \tau v^2) - 2lu - 2nv + m = 0,$$

that is the point $(u, v) \in \mathbb{R}^2$ belongs to the quadratic curve with coefficients (k, l, n, m) .

I.14.5. Homogeneous spaces of cycles

Obviously, the group $SL_2(\mathbb{R})$ acts on $\mathbb{P}\mathbb{R}^1$ transitively, in fact it is even 3-transitive in the following sense. We say that a triple $\{x_1, x_2, x_3\} \subset \mathbb{P}\mathbb{R}^1$ of distinct points is *positively oriented* if

$$\text{either } x_1 < x_2 < x_3, \quad \text{or } x_3 < x_1 < x_2,$$

where we agree that the ideal point $\infty \in \mathbb{P}\mathbb{R}^1$ is greater than any $x \in \mathbb{R}$. Equivalently, a triple $\{x_1, x_2, x_3\}$ of reals is positively oriented if:

$$(x_1 - x_2)(x_2 - x_3)(x_3 - x_1) > 0.$$

Also, a triple of distinct points, which is not positively oriented, is *negatively oriented*. A simple calculation based on the resolvent-type identity:

$$\frac{ax + b}{cx + d} - \frac{ay + b}{cy + d} = \frac{(x - y)(ad - bc)}{(cx + b)(cy + d)}$$

shows that both the positive and negative orientations of triples are $SL_2(\mathbb{R})$ -invariant. On the other hand, the reflection $x \mapsto -x$ swaps orientations of triples. Note, that the reflection is a Moebius transformation associated to the cycle

$$(I.14.19) \quad C_{0\infty} = \begin{pmatrix} 1 & 0 \\ 0 & -1 \end{pmatrix}, \quad \text{with } \det C_{0\infty} = -1.$$

A significant amount of information about Möbius transformations follows from the fact, that any continuous one-parametric subgroup of $SL_2(\mathbb{R})$ is conjugated to one of the three following subgroups²:

$$(I.14.20) \quad A = \left\{ \begin{pmatrix} e^{-t} & 0 \\ 0 & e^t \end{pmatrix} \right\}, \quad N = \left\{ \begin{pmatrix} 1 & t \\ 0 & 1 \end{pmatrix} \right\}, \quad K = \left\{ \begin{pmatrix} \cos t & -\sin t \\ \sin t & \cos t \end{pmatrix} \right\},$$

²A reader may know that A, N and K are factors in the Iwasawa decomposition $SL_2(\mathbb{R}) = ANK$ (cf. Cor. I.14.10, however this important result does not play any rôle in our consideration.

where $t \in \mathbb{R}$. Also, it is useful to introduce subgroups A' and N' conjugated to A and N respectively:

$$(I.14.21) \quad A' = \left\{ \begin{pmatrix} \cosh t & \sinh t \\ \sinh t & \cosh t \end{pmatrix} \mid t \in \mathbb{R} \right\}, \quad N' = \left\{ \begin{pmatrix} 1 & 0 \\ t & 1 \end{pmatrix} \mid t \in \mathbb{R} \right\}.$$

Thereafter, all three one-parameter subgroups A' , N' and K consist of all matrices with the universal structure

$$(I.14.22) \quad \begin{pmatrix} a & \tau b \\ b & a \end{pmatrix} \quad \text{where } \tau = 1, 0, -1 \text{ for } A', N' \text{ and } K \text{ respectively.}$$

We use the notation H_τ for these subgroups. Again, any continuous one-dimensional subgroup of $SL_2(\mathbb{R})$ is conjugated to H_τ for an appropriate τ .

We note, that matrices from A , N and K with $t \neq 0$ have two, one and none different real eigenvalues respectively. Eigenvectors in \mathbb{R}^2 correspond to fixed points of Möbius transformations on $\mathbb{P}\mathbb{R}^1$. Clearly, the number of eigenvectors (and thus fixed points) is limited by the dimensionality of the space, that is two. For this reason, if g_1 and g_2 take equal values on three different points of $\mathbb{P}\mathbb{R}^1$, then $g_1 = g_2$.

Also, eigenvectors provide an effective classification tool: $g \in SL_2(\mathbb{R})$ belongs to a one-dimensional continuous subgroup conjugated to A , N or K if and only if the characteristic polynomial $\det(g - \lambda I)$ has two, one and none different real root(s) respectively. We will illustrate an application of fixed points techniques through the following well-known result, which will be used later.

LEMMA I.14.8. *Let $\{x_1, x_2, x_3\}$ and $\{y_1, y_2, y_3\}$ be positively oriented triples of points in \mathbb{R} . Then, there is a unique (computable!) Möbius map $\phi \in SL_2(\mathbb{R})$ with $\phi(x_j) = y_j$ for $j = 1, 2, 3$.*

PROOF. Often, the statement is quickly demonstrated through an explicit expression for ϕ , cf. [26, Thm. 13.2.1]. We will use properties of the subgroups A , N and K to describe an algorithm to find such a map. First, we notice that it is sufficient to show the Lemma for the particular case $y_1 = 0, y_2 = 1, y_3 = \infty$. The general case can be obtained from composition of two such maps. Another useful observation is that the fixed point for N , that is ∞ , is also a fixed point of A .

Now, we will use subgroups K , N and A in order of increasing number of their fixed points. First, for any x_3 the matrix $g' = \begin{pmatrix} \cos t & \sin t \\ -\sin t & \cos t \end{pmatrix} \in K$ such that $\cot t = x_3$ maps x_3 to $y_3 = \infty$. Let $x'_1 = g'x_1$ and $x'_2 = g'x_2$. Then the matrix $g'' = \begin{pmatrix} 1 & -x'_1 \\ 0 & 1 \end{pmatrix} \in N$, fixes $\infty = g'x_3$ and sends x'_1 to $y_1 = 0$. Let $x''_2 = g''x'_2$, from positive orientation of triples we have $0 < x''_2 < \infty$. Next, the matrix $g''' = \begin{pmatrix} a^{-1} & 0 \\ 0 & a \end{pmatrix} \in A$ with $a = \sqrt{x''_2}$ sends x''_2 to 1 and fixes both $\infty = g''g'x_3$ and $0 = g''g'x_1$. Thus, $g = g'''g''g'$ makes the required transformation $(x_1, x_2, x_3) \mapsto (0, 1, \infty)$. \square

COROLLARY I.14.9. *Let $\{x_1, x_2, x_3\}$ and $\{y_1, y_2, y_3\}$ be two triples with the opposite orientations. Then, there is a unique Möbius map $\phi \in SL_2(\mathbb{R})$ with $\phi \circ C_{0\infty}(x_j) = y_j$ for $j = 1, 2, 3$.*

We will denote by ϕ_{XY} the unique map from Lem. I.14.8 defined by triples $X = \{x_1, x_2, x_3\}$ and $Y = \{y_1, y_2, y_3\}$.

Although we are not going to use it in this paper, we note that the following important result [240, § III.1] is an immediate consequence of our proof of Lem. I.14.8.

COROLLARY I.14.10 (Iwasawa decomposition). *Any element of $g \in \text{SL}_2(\mathbb{R})$ is a product $g = g_A g_N g_K$, where g_A, g_N and g_K belong to subgroups A, N, K respectively and those factors are uniquely defined.*

In particular, we note that it is not a coincidence that the subgroups appear in the Iwasawa decomposition $\text{SL}_2(\mathbb{R}) = \text{ANK}$ in order of decreasing number of their fixed points.

I.14.6. Triples of intervals

We change our point of view and instead of two ordered triples of points consider three ordered pairs, that is—three intervals. For them we will need the following definition.

DEFINITION I.14.11. We say that a triple of intervals $\{[x_1, y_1], [x_2, y_2], [x_3, y_3]\}$ is *aligned* if the triples $X = \{x_1, x_2, x_3\}$ and $Y = \{y_1, y_2, y_3\}$ of their endpoints have the same orientation.

Aligned triples determine certain one-parameter subgroups of Möbius transformations as follows:

PROPOSITION I.14.12. *Let $\{[x_1, y_1], [x_2, y_2], [x_3, y_3]\}$ be an aligned triple of intervals.*

i. *If ϕ_{XY} has at most one fixed point, then there is a unique (up to a parametrisation) one-parameter semigroup of Möbius map $\psi(t) \subset \text{SL}_2(\mathbb{R})$, which maps $[x_1, y_1]$ to $[x_2, y_2]$ and $[x_3, y_3]$:*

$$\psi(t_j)(x_1) = x_j, \quad \psi(t_j)(y_1) = y_j, \quad \text{for some } t_j \in \mathbb{R} \text{ and } j = 2, 3.$$

ii. *Let ϕ_{XY} have two fixed points $x < y$ and C_{xy} be the orientation inverting Möbius transformation with the matrix (I.14.8). For $j = 1, 2, 3$, we define:*

$$\begin{aligned} x'_j &= x_j, & y'_j &= y_j, & x''_j &= C_{xy}x_j, & y''_j &= C_{xy}y_j & \text{if } x < x_j < y; \\ x'_j &= C_{xy}x_j, & y'_j &= C_{xy}y_j, & x''_j &= x_j, & y''_j &= y_j, & \text{otherwise.} \end{aligned}$$

Then, there is a one-parameter semigroup of Möbius map $\psi(t) \subset \text{SL}_2(\mathbb{R})$, and $t_2, t_3 \in \mathbb{R}$ such that:

$$\psi(t_j)(x'_1) = x'_j, \quad \psi(t_j)(x''_1) = x''_j, \quad \psi(t_j)(y'_1) = y'_j, \quad \psi(t_j)(y''_1) = y''_j,$$

where $j = 2, 3$.

PROOF. Consider the one-parameter subgroup of $\psi(t) \subset \text{SL}_2(\mathbb{R})$ such that $\phi_{XY} = \psi(1)$. Note, that $\psi(t)$ and ϕ_{XY} have the same fixed points (if any) and no point x_j is fixed since $x_j \neq y_j$. If the number of fixed points is less than 2, then $\psi(t)x_1, t \in \mathbb{R}$ produces the entire real line except a possible single fixed point. Therefore, there are

t_2 and t_3 such that $\psi(t_2)x_1 = x_2$ and $\psi(t_3)x_1 = x_3$. Since $\psi(t)$ and ϕ_{XY} commute for all t we also have:

$$\psi(t_j)y_1 = \psi(t_j)\phi_{XY}x_1 = \phi_{XY}\psi(t_j)x_1 = \phi_{XY}x_j = y_j, \quad \text{for } j = 2, 3.$$

If there are two fixed points $x < y$, then the open interval (x, y) is an orbit for the subgroup $\psi(t)$. Since all x'_1, x'_2 and x'_3 belong to this orbit and C_{xy} commutes with ϕ_{XY} we may repeat the above reasoning for the dashed intervals $[x'_j, y'_j]$. Finally, $x''_j = C_{xy}x'_j$ and $y''_j = C_{xy}y'_j$, where C_{xy} commutes with ϕ and $\psi(t_j)$, $j = 2, 3$. Uniqueness of the subgroup follows from Lemma I.14.13. \square

The group $SL_2(\mathbb{R})$ acts transitively on collection of all cycles C_{xy} , thus this is a $SL_2(\mathbb{R})$ -homogeneous space. It is easy to see that the fix-group of the cycle $C_{-1,1}$ is A' (I.14.21). Thus the homogeneous space of cycles is isomorphic to $SL_2(\mathbb{R})/A'$.

LEMMA I.14.13. *Let H be a one-parameter continuous subgroup of $SL_2(\mathbb{R})$ and $X = SL_2(\mathbb{R})/H$ be the corresponding homogeneous space. If two orbits of one-parameter continuous subgroups on X have at least three common points then these orbits coincide.*

PROOF. Since H is conjugated either to A' , N' or K , the homogeneous space $X = SL_2(\mathbb{R})/H$ is isomorphic to the upper half-plane in double, dual or complex numbers [198, § 3.3.4]. Orbits of one-parameter continuous subgroups in X are conic sections, which are circles, parabolas (with vertical axis) or equilateral hyperbolas (with vertical axis) for the respective type of geometry. Any two different orbits of the same type intersect at most at two points, since an analytic solution reduces to a quadratic equation. \square

Alternatively, we can reformulate Prop. I.14.12 as follows: three different cycles $C_{x_1y_1}, C_{x_2y_2}, C_{x_3y_3}$ define a one-parameter subgroup, which generate either one orbit or two related orbits passing the three cycles.

We have seen that the number of fixed points is the key characteristics for the map ϕ_{XY} . The next result gives an explicit expression for it.

PROPOSITION I.14.14. *The map ϕ_{XY} has zero, one or two fixed points if the expression*

$$(I.14.23) \quad \det \begin{pmatrix} 1 & x_1y_1 & y_1 - x_1 \\ 1 & x_2y_2 & y_2 - x_2 \\ 1 & x_3y_3 & y_3 - x_3 \end{pmatrix}^2 - 4 \det \begin{pmatrix} x_1 & 1 & y_1 \\ x_2 & 1 & y_2 \\ x_3 & 1 & y_3 \end{pmatrix} \cdot \det \begin{pmatrix} x_1 & -x_1y_1 & y_1 \\ x_2 & -x_2y_2 & y_2 \\ x_3 & -x_3y_3 & y_3 \end{pmatrix}$$

is negative, zero or positive respectively.

PROOF. If a Möbius transformation $\begin{pmatrix} a & b \\ c & d \end{pmatrix}$ maps $x_1 \mapsto y_1, x_2 \mapsto y_2, x_3 \mapsto y_3$ and $s \mapsto s$, then we have a homogeneous linear system, cf. [26, Ex. 13.2.4]:

$$(I.14.24) \quad \begin{pmatrix} x_1 & 1 & -x_1y_1 & -y_1 \\ x_2 & 1 & -x_2y_2 & -y_2 \\ x_3 & 1 & -x_3y_3 & -y_3 \\ s & 1 & -s^2 & -s \end{pmatrix} \begin{pmatrix} a \\ b \\ c \\ d \end{pmatrix} = \begin{pmatrix} 0 \\ 0 \\ 0 \\ 0 \end{pmatrix}.$$

A non-zero solution exists if the determinant of the 4×4 matrix is zero. Expanding it over the last row and rearranging terms we obtain the quadratic equation for the fixed point s :

$$s^2 \det \begin{pmatrix} x_1 & 1 & y_1 \\ x_2 & 1 & y_2 \\ x_3 & 1 & y_3 \end{pmatrix} + s \det \begin{pmatrix} 1 & x_1 y_1 & y_1 - x_1 \\ 1 & x_2 y_2 & y_2 - x_2 \\ 1 & x_3 y_3 & y_3 - x_3 \end{pmatrix} + \det \begin{pmatrix} x_1 & -x_1 y_1 & y_1 \\ x_2 & -x_2 y_2 & y_2 \\ x_3 & -x_3 y_3 & y_3 \end{pmatrix} = 0.$$

The value (I.14.23) is the discriminant of this equation. \square

REMARK I.14.15. It is interesting to note, that the relation $ax + b - cxy - dy = 0$ used in (I.14.24) can be stated as e-orthogonality of the cycle $\begin{pmatrix} a & b \\ c & d \end{pmatrix}$ and the isotropic bilinear form $\begin{pmatrix} x & -xy \\ 1 & -y \end{pmatrix}$.

If $y = g_0 \cdot x$ for some $g_0 \in H_\tau$, then for any $g \in H_\tau$ we also have $y_g = g_0 \cdot x_g$, where $x_g = g \cdot x$ and $y_g = g \cdot y$. Thus, we demonstrated the first part of the following result.

LEMMA I.14.16. *Let $\tau = 1, 0$ or -1 and a real constant $t \neq 0$ be such that $1 - \tau t^2 > 0$.*

i. *The collections of intervals:*

$$(I.14.25) \quad I_{\tau,t} = \left\{ \left[x, \frac{x+\tau t}{tx+1} \right] \mid x \in \mathbb{R} \right\}$$

is preserved by the actions of subgroup H_τ . Any three different intervals from $I_{\tau,t}$ define the subgroup H_τ in the sense of Prop. I.14.12.

ii. *All H_τ -invariant bilinear forms compose the family $P_{\tau,t} = \left\{ \begin{pmatrix} a & \tau b \\ b & a \end{pmatrix} \right\}$.*

The family $P_{\tau,t}$ consists of the eigenvectors of the 4×4 matrix from (I.14.15) with suitably substituted entries. There is (up to a factor) exactly one τ -isotropic form in $P_{\tau,t}$, namely $\begin{pmatrix} 1 & \tau \\ 1 & 1 \end{pmatrix}$. We denote this form by ι . It corresponds to the point $(0, 1) \in \mathbb{R}^2$ as discussed after Defn. I.14.7. We may say that the subgroup H_τ fixes the point ι , this will play an important rôle below.

I.14.7. Geometrisation of cycles

We return to the geometric version of the Poincaré extension considered in Sec. I.14.2 in terms of cycles. Cycles of the form $\begin{pmatrix} x & -x^2 \\ 1 & -x \end{pmatrix}$ are τ -isotropic for any τ and are parametrised by the point x of the real line. For a fixed τ , the collection of all τ -isotropic cycles is a larger set containing the image of the real line from the previous sentence. Geometrisation of this embedding is described in the following result.

LEMMA I.14.17. i. *The transformation $x \mapsto \frac{x+\tau t}{tx+1}$ from the subgroup H_τ , which maps $x \mapsto y$, corresponds to the value $t = \frac{x-y}{xy-\tau}$.*

ii. *The unique (up to a factor) bilinear form Q orthogonal to C_{xx} , C_{yy} and ι is*

$$Q = \begin{pmatrix} \frac{1}{2}(x+y+xy-\tau) & -xy \\ 1 & \frac{1}{2}(-x-y+xy-\tau) \end{pmatrix}.$$

iii. The defined above t and Q are connected by the cycles cross ratio (I.12.15) identity:

$$(I.14.26) \quad \langle Q, \mathbb{R}; \mathbb{R}, Q \rangle = \frac{\langle Q, \mathbb{R} \rangle_\tau}{\langle Q, Q \rangle_\tau} : \frac{\langle \mathbb{R}, \mathbb{R} \rangle_\tau}{\langle \mathbb{R}, Q \rangle_\tau} = \frac{\tau^2}{t^2 - \tau}.$$

Here, the real line is represented by the bilinear form $\mathbb{R} = \begin{pmatrix} 1 & 0 \\ 0 & 1 \end{pmatrix}$ defined by the identity matrix.

iv. For a cycle $Q = \begin{pmatrix} l+n & -m \\ k & -l+n \end{pmatrix}$, the value of the cycles cross ratio

$$\langle Q, \mathbb{R}; \mathbb{R}, Q \rangle = \frac{\langle Q, \mathbb{R} \rangle_e}{\langle Q, Q \rangle_e} : \frac{\langle \mathbb{R}, \mathbb{R} \rangle_e}{\langle \mathbb{R}, Q \rangle_e} = \frac{n^2}{l^2 + n^2 - km}$$

is equal to the square of cosine of the angle between the curve $k(u^2 + \tau v^2) - 2lu - 2nv + m = 0$ (I.14.18) and the real line, cf. Ex. I.5.23.i and Ex I.12.8.

PROOF. The first statement is verified by a short calculation. A form $Q = \begin{pmatrix} l+n & -m \\ k & -l+n \end{pmatrix}$ in the second statement may be calculated from the homogeneous system:

$$\begin{pmatrix} 0 & -2x & x^2 & 1 \\ 0 & -2y & y^2 & 1 \\ -2 & 0 & -\tau & 1 \end{pmatrix} \begin{pmatrix} n \\ l \\ k \\ m \end{pmatrix} = \begin{pmatrix} 0 \\ 0 \\ 0 \end{pmatrix},$$

which has the rank 3 if $x \neq y$. The third statement can be checked by a calculation as well. Finally, the last item is a particular case of the more general statement as indicated. Yet, we can derive it here from the implicit derivative $\frac{dv}{du} = \frac{ku-1}{n}$ of the function $k(u^2 + \tau v^2) - 2lu - 2nv + m = 0$ (I.14.18) at the point $(u, 0)$. Note that this value is independent from τ . Since this is the tangent of the intersection angle with the real line, the square of the cosine of this angle is:

$$\frac{1}{1 + \left(\frac{dv}{du}\right)^2} = \frac{n^2}{l^2 + k^2u^2 + n^2 - 2kul} = \frac{n^2}{l^2 + n^2 - km} = \frac{\langle Q, \mathbb{R} \rangle^2}{\langle Q, Q \rangle_e \langle \mathbb{R}, \mathbb{R} \rangle},$$

if $ku^2 - 2ul + m = 0$. □

Also, we note that, the independence of the left-hand side of (I.14.26) from x can be shown from basic principles. Indeed, for a fixed t the subgroup H_τ acts transitively on the family of triples $\{x, \frac{x+\tau t}{1+x}, l\}$, thus H_τ acts transitively on all bilinear forms orthogonal to such triples. However, the left-hand side of (I.14.26) is $SL_2(\mathbb{R})$ -invariant, thus may not depend on x . This simple reasoning cannot provide the exact expression in the right-hand side of (I.14.26), which is essential for the geometric interpretation of the Poincaré extension.

To restore a cycle from its intersection points with the real line we need also to know its cycle product with the real line. If this product is non-zero then the sign of the parameter n is additionally required. At the cycles' language, a common point of

cycles C and \tilde{C} is encoded by a cycle \hat{C} such that:

$$(I.14.27) \quad \langle \hat{C}, C \rangle_e = \langle \hat{C}, \tilde{C} \rangle_e = \langle \hat{C}, \hat{C} \rangle_\tau = 0.$$

For a given value of τ , this produces two linear and one quadratic equation for parameters of \hat{C} . Thus, a pair of cycles may not have a common point or have up to two such points. Furthermore, Möbius-invariance of the above conditions (I.14.26) and (I.14.27) supports the geometrical construction of Poincaré extension, cf. Lem. I.14.1:

LEMMA I.14.18. *Let a family consist of cycles, which are e -orthogonal to a given τ -isotropic cycle \hat{C} and have the fixed value of the fraction in the left-hand side of (I.14.26). Then, for a given Möbius transformation g and any cycle C from the family, gC is e -orthogonal to the τ -isotropic cycle $g\hat{C}$ and has the same fixed value of the fraction in the left-hand side of (I.14.26) as C .*

Summarising the geometrical construction, the Poincaré extension based on two intervals and the additional data produces two situations:

- i. If the cycles C and \tilde{C} are orthogonal to the real line, then a pair of overlapping cycles produces a point of the elliptic upper half-plane, a pair of disjoint cycles defines a point of the hyperbolic. However, there is no orthogonal cycles uniquely defining a parabolic extension.
- ii. If we admit cycles, which are not orthogonal to the real line, then the same pair of cycles may define any of the three different types (EPH) of extension.

These peculiarities make the extension based on three intervals, described above, a bit more preferable.

I.14.8. Concluding remarks

Based on the consideration in Sections I.14.3–I.14.7 we describe the following steps to carry out the generalised extension procedure:

- i. Points of the extended space are equivalence classes of aligned triples of cycles in $\mathbb{P}\mathbb{R}^1$, see Defn. I.14.11. The equivalence relation between triples will emerge at step I.14.18.iii.
- ii. A triple T of different cycles defines the unique one-parameter continuous subgroup $S(t)$ of Möbius transformations as defined in Prop. I.14.12.
- iii. Two triples of cycles are equivalent if and only if the subgroups defined in step I.14.18.ii coincide (up to a parametrisation).
- iv. The geometry of the extended space, defined by the equivalence class of a triple T , is elliptic, parabolic or hyperbolic depending on the subgroup $S(t)$ being similar $S(t) = gH_\tau(t)g^{-1}$, $g \in \text{SL}_2(\mathbb{R})$ (up to parametrisation) to H_τ (I.14.22) with $\tau = -1, 0$ or 1 respectively. The value of τ may be identified from the triple using Prop. I.14.14.
- v. For the above τ and $g \in \text{SL}_2(\mathbb{R})$, the point of the extended space, defined by the the equivalence class of a triple T , is represented by τ -isotropic (see Defn. I.14.7(I.14.7.ii)) bilinear form $g^{-1} \begin{pmatrix} 1 & \tau \\ 1 & 1 \end{pmatrix} g$, which is S -invariant, see the end of Section I.14.6.

Obviously, the above procedure is more complicated than the geometric construction from Section I.14.2. There are reasons for this, as discussed in Section I.14.7: our procedure is uniform and we are avoiding consideration of numerous subcases created by an incompatible selection of parameters. Furthermore, our presentation is aimed for generalisations to Möbius transformations of moduli over other rings. This can be considered as an analog of Cayley–Klein geometries [284; 339, Apps. A–B].

It shall be rather straightforward to adopt the extension for \mathbb{R}^n . Möbius transformations in \mathbb{R}^n are naturally expressed as linear-fractional transformations in Clifford algebras [65] with a similar classification of subgroups based on fixed points [2, 343]. The Möbius invariant matrix presentation of cycles in \mathbb{R}^n is already known [65, (4.12); 100; 208, § 5]. Of course, it is necessary to enlarge the number of defining cycles from 3 to, say, $n + 2$. This shall have a connection with Cauchy–Kovalevskaya extension considered in Clifford analysis [295, 310]. Naturally, a consideration of other moduli and rings may require some more serious adjustments in our scheme.

Our construction is based on the matrix presentations of cycles. This technique is effective in many different cases [198, 208]. Thus, it is not surprising that such ideas (with some technical variation) appeared independently on many occasions [65, (4.12); 100; 163, § 4.2; 300, § 1.1]. The interesting feature of the present work is the complete absence of any (hyper)complex numbers. It is deemed to be unavoidable [198, § 3.3.4] to employ complex, dual and double numbers to represent three different types of Möbius transformations extended from the real line to a plane. Also (hyper)complex numbers were essential in [185, 198] to define three possible types of cycle product (I.14.17), and now we managed without them.

Apart from having real entries, our matrices for cycles share the structure of matrices from [65, (4.12); 100; 185; 198]. To obtain another variant, one replaces the map i (I.14.7) by

$$t : \begin{pmatrix} x_1 & y_1 \\ x_2 & y_2 \end{pmatrix} \mapsto \begin{pmatrix} y_1 & y_2 \\ x_1 & x_2 \end{pmatrix}.$$

Then, we may define symmetric matrices in a manner similar to (I.14.8):

$$C_{xy}^t = \frac{1}{2} M_{xy} \cdot t(M_{xy}) = \begin{pmatrix} xy & \frac{x+y}{2} \\ \frac{x+y}{2} & 1 \end{pmatrix}.$$

This is the form of matrices for cycles similar to [163, § 4.2; 300, § 1.1]. The property (I.14.10) with matrix similarity shall be replaced by the respective one with matrix congruence: $g \cdot C_{xy}^t \cdot g^t = C_{x'y'}^t$. The rest of our construction may be adjusted for these matrices accordingly.

Conformal Parametrisation of Loxodromes by Triples of Circles

We provide a parametrisation of a loxodrome by three specially arranged cycles. The parametrisation is covariant under fractional linear transformations of the complex plane and naturally encodes conformal properties of loxodromes. Selected geometric examples illustrate the use of parametrisation. Our work extends the set of objects in Lie sphere geometry—circle, lines and points—to the natural maximal conformally-invariant family, which also includes loxodromes.

I.15.1. Introduction

It is easy to come across shapes of logarithmic spirals, as in Fig. I.15.1(a), one can find them on a sunflower, a snail shell or a remote galaxy. This is not surprising since the fundamental differential equation $\dot{y} = \lambda y$, $\lambda \in \mathbb{C}$ serves as a first approximation to many natural processes. The main symmetries of complex analysis are built on the

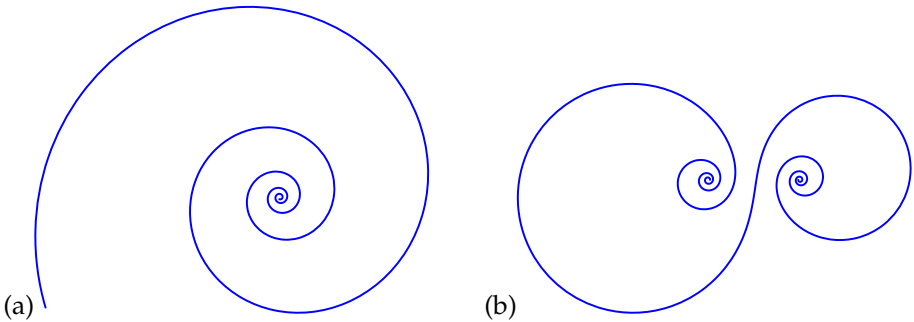


FIGURE I.15.1. A logarithmic spiral (a) and its image under a fractional linear transformation—loxodrome (b).

fractional linear transformation (FLT):

$$(I.15.1) \quad \begin{pmatrix} \alpha & \beta \\ \gamma & \delta \end{pmatrix} : z \mapsto \frac{\alpha z + \beta}{\gamma z + \delta}, \quad \text{where } \alpha, \beta, \gamma, \delta \in \mathbb{C} \text{ and } \det \begin{pmatrix} \alpha & \beta \\ \gamma & \delta \end{pmatrix} \neq 0.$$

Thus, images of logarithmic spirals under FLT, called loxodromes, as in Fig. I.15.1(b) are not rare. Indeed, they appear in many instances from the stereographic projection

of a rhumb line in navigation to a preferred model of a Carleson arc in the theory of singular integral operators [40, 46]. Furthermore, loxodromes are orbits of one-parameter continuous groups of FLT of loxodromic type [24, § 4.3; 306, § 9.2; 330, § 9.2].

This setup motivates a search for effective tools to deal with FLT-invariant properties of loxodromes. They were studied from a differential-geometric point of view in many papers [43, 290–293, 317], see also [270, § 2.7.6]. In this work we develop a “global” description that matches the Lie sphere geometry framework, see Rem. I.15.3.

The outline of the paper is as follows. After preliminaries on FLTs and invariant geometry of cycles (Section II.6.2) we review the basics of logarithmic spirals and loxodromes (Section I.15.3). A new parametrisation of loxodromes is introduced in Section I.15.4 and several examples illustrate its use in Section I.15.5. Section I.15.6 frames our work within a wider approach [209, 211, 212], which extends Lie sphere geometry. A brief list of open questions concludes the paper.

I.15.2. Preliminaries: Fractional Linear Transformations and Cycles

In this section we provide some necessary background in Lie geometry of circles, fractional-linear transformations and the Fillmore–Springer–Cnops construction (FSCc). Regrettably, the latter remains largely unknown in the context of complex analysis despite its numerous advantages. We will have some further discussion of this in Rem. I.15.3 below.

The right way [306, § 9.2] to think about FLT (I.15.1) is through the *projective complex line* $\mathbb{P}\mathbb{C}$. This is the family of cosets in $\mathbb{C}^2 \setminus \{(0, 0)\}$ with respect to the equivalence relation $\begin{pmatrix} w_1 \\ w_2 \end{pmatrix} \sim \begin{pmatrix} \alpha w_1 \\ \alpha w_2 \end{pmatrix}$ for all nonzero $\alpha \in \mathbb{C}$. Conveniently \mathbb{C} is identified with a part of $\mathbb{P}\mathbb{C}$ by assigning the coset of $\begin{pmatrix} z \\ 1 \end{pmatrix}$ to $z \in \mathbb{C}$. Loosely speaking $\mathbb{P}\mathbb{C} = \mathbb{C} \cup \{\infty\}$, where ∞ is the coset of $\begin{pmatrix} 1 \\ 0 \end{pmatrix}$. The pair $[w_1 : w_2]$ with $w_2 \neq 0$ gives *homogeneous coordinates* for $z = w_1/w_2 \in \mathbb{C}$. Then, the linear map $\mathbb{C}^2 \rightarrow \mathbb{C}^2$

$$(I.15.2) \quad M : \begin{pmatrix} w_1 \\ w_2 \end{pmatrix} \mapsto \begin{pmatrix} w'_1 \\ w'_2 \end{pmatrix} = \begin{pmatrix} \alpha w_1 + \beta w_2 \\ \gamma w_1 + \delta w_2 \end{pmatrix}, \text{ where } M = \begin{pmatrix} \alpha & \beta \\ \gamma & \delta \end{pmatrix} \in \text{GL}_2(\mathbb{C})$$

factors from \mathbb{C}^2 to $\mathbb{P}\mathbb{C}$ and coincides with (I.15.1) on $\mathbb{C} \subset \mathbb{P}\mathbb{C}$.

Generic equations of cycles in real and complex coordinates $z = x + iy$ are:

$$(I.15.3) \quad k(x^2 + y^2) - 2lx - 2ny + m = 0 \quad \text{or} \quad kz\bar{z} - \bar{L}z - L\bar{z} + m = 0,$$

where $(k, l, n, m) \in \mathbb{R}^4$ and $L = l + in$. This includes lines (if $k = 0$), points as zero-radius circles (if $l^2 + n^2 - mk = 0$) and proper circles otherwise. Homogeneity of (I.15.3) suggests that (k, l, m, n) can be considered as homogeneous coordinates $[k : l : m : n]$ of a point in three-dimensional projective space $\mathbb{P}\mathbb{R}^3$.

The homogeneous form of the cycle equation (I.15.3) for $z = [w_1 : w_2]$ can be written¹ using matrices as follows:

$$(I.15.4) \quad kw_1\bar{w}_1 - \bar{L}w_1\bar{w}_2 - L\bar{w}_1w_2 + mw_2\bar{w}_2 = (-\bar{w}_2 \quad \bar{w}_1) \begin{pmatrix} \bar{L} & -m \\ k & -L \end{pmatrix} \begin{pmatrix} w_1 \\ w_2 \end{pmatrix} = 0.$$

From now on we identify a cycle C given by (I.15.3) with its 2×2 matrix $\begin{pmatrix} \bar{L} & -m \\ k & -L \end{pmatrix}$, this is called the *Fillmore–Springer–Cnops construction* (FSCc). Again, C shall be treated up to the equivalence relation $C \sim tC$ for all real $t \neq 0$. Then, the linear action (I.15.2) corresponds to the action on 2×2 cycle matrices by the intertwining identity:

$$(I.15.5) \quad (-\bar{w}'_2 \quad \bar{w}'_1) \begin{pmatrix} \bar{L}' & -m' \\ k' & -L' \end{pmatrix} \begin{pmatrix} w'_1 \\ w'_2 \end{pmatrix} = (-\bar{w}_2 \quad \bar{w}_1) \begin{pmatrix} \bar{L} & -m \\ k & -L \end{pmatrix} \begin{pmatrix} w_1 \\ w_2 \end{pmatrix}.$$

Explicitly, for $M \in GL_2(\mathbb{C})$ those actions are:

$$(I.15.6) \quad \begin{pmatrix} w'_1 \\ w'_2 \end{pmatrix} = M \begin{pmatrix} w_1 \\ w_2 \end{pmatrix}, \quad \text{and} \quad \begin{pmatrix} \bar{L}' & -m' \\ k' & -L' \end{pmatrix} = \bar{M} \begin{pmatrix} \bar{L} & -m \\ k & -L \end{pmatrix} M^{-1},$$

where \bar{M} is the component-wise complex conjugation of M . Note, that the FLT with matrix M (I.15.1) corresponds to a linear transformation $C \mapsto M(C) := \bar{M}CM^{-1}$ of cycle matrices in (I.15.6). A quick calculation shows that $M(C)$ indeed has real off-diagonal elements as required for a FSCc matrix.

This paper essentially depends on the following result.

PROPOSITION I.15.1. *Define a cycle product of two cycles C and C' by:*

$$(I.15.7) \quad \langle C, C' \rangle := \text{tr}(C\bar{C}') = L\bar{L}' + \bar{L}L' - mk' - km'.$$

Then, the cycle product is FLT-invariant:

$$(I.15.8) \quad \langle M(C), M(C') \rangle = \langle C, C' \rangle \quad \text{for any } M \in SL_2(\mathbb{C}).$$

PROOF. Indeed, we have:

$$\begin{aligned} \langle M(C), M(C') \rangle &= \text{tr}(M(C)\overline{M(C')}) \\ &= \text{tr}(\bar{M}CM^{-1}\bar{M}\bar{C}'\bar{M}^{-1}) \\ &= \text{tr}(\bar{M}\bar{C}\bar{C}'\bar{M}^{-1}) \\ &= \text{tr}(C\bar{C}') \\ &= \langle C, C' \rangle, \end{aligned}$$

using the invariance of trace. □

Note that the cycle product (I.15.7) is *not* positive definite, it produces a Lorentz-type metric in \mathbb{R}^4 . Here are some relevant examples of geometric properties expressed through the cycle product:

¹Of course, this is not the only possible presentation. However, this form is particularly suitable to demonstrate FLT-invariance (I.15.8) of the cycle product below.

- EXAMPLE I.15.2.
- i. If $k = 1$ (and C is a proper circle), then $\langle C, C \rangle / 2$ is equal to the square of the radius of C . In particular $\langle C, C \rangle = 0$ indicates a zero-radius circle representing a point.
 - ii. If $\langle C_1, C_2 \rangle = 0$ for nonzero radius cycles C_1 and C_2 , then they intersect at a right angle.
 - iii. If $\langle C_1, C_2 \rangle = 0$ and C_2 is a zero-radius circle, then C_1 passes the point represented by C_2 .

In general, a combination of (I.15.6) and (I.15.8) yields that consideration of FLTs in \mathbb{C} can be replaced by linear algebra in the space of cycles \mathbb{R}^4 (or rather $\mathbb{P}\mathbb{R}^3$) with an indefinite metric, see [113] for the latter.

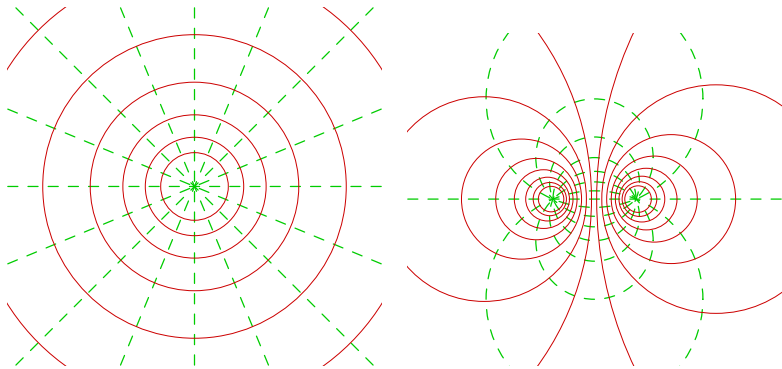


FIGURE I.15.2. Orthogonal elliptic (green-dashed) and hyperbolic (red-solid) pencils of cycles. The left drawing shows the standard case and the right the generic one, which is the image of the standard pencils under an FLT.

A spectacular illustration of this approach that we will need later is orthogonal pencils of cycles. Consider a collection of all cycles passing through two different points in \mathbb{C} , it is called an *elliptic pencil*. A beautiful and non-elementary fact of Euclidean geometry is that cycles orthogonal to every cycle in the elliptic pencil fill the entire plane and are disjoint, such a family is called a *hyperbolic pencil*. This statement is obvious in the standard arrangement when the elliptic pencil is formed by straight lines—cycles passing the origin and infinity. Then, the hyperbolic pencil consists of concentric circles, see Fig. I.15.2. For the sake of completeness, a *parabolic pencil* (not used in this paper) formed by all circles touching a given line at a given point, [198, Ex. 6.10] provides further extensions and illustrations. See [330, § 11.8] for an example of cycle pencils’ appearance in operator theory.

This picture becomes a bit trivial in the language of cycles. A pencil of cycles (of any type!) is a linear span $tC_1 + (1 - t)C_2$ of two arbitrary different cycles C_1 and C_2 from the pencil. Again, this is easier to check for standard pencils. A pencil is elliptic, parabolic or hyperbolic depending on which inequality holds [198, Ex. 5.28.ii]:

$$(I.15.9) \quad \langle C_1, C_2 \rangle^2 \stackrel{\leq}{\geq} \langle C_1, C_1 \rangle \langle C_2, C_2 \rangle.$$

Then, the orthogonality of cycles in the plane is exactly their orthogonality as vectors with respect to the indefinite cycle product (I.15.7). For cycles in the standard pencils this is immediately seen from the explicit expression of the product $\langle C, C' \rangle = \bar{L}\bar{L}' + \bar{L}\bar{L}' - m\bar{k}' - k\bar{m}'$ in cycle components. Finally, linearization (I.15.6) of FLT in the cycle space shows that a pencil (i.e., a linear span) is transformed to a pencil and FLT-invariance (I.15.8) of the cycle product guarantees that the orthogonality of two pencils is preserved.

REMARK I.15.3. A sketchy historical overview (we apologise for any important omission!) starts from the concept of Lie sphere geometry, see [32, Ch. 3] for a detailed presentation. It unifies circles, lines and points, which are all called cycles in this context (analytically this is already embodied by equation (I.15.3)). The main invariant property of Lie sphere geometry is *tangential contact*. The first radical advance came from the observation that cycles (through their parameters in (I.15.3)) naturally form a linear or projective space, see [276; 300, Ch. 1]. The second crucial step is the recognition that the cycle space carries out the FLT-invariant indefinite metric [32, Ch. 3; 163, § F.4]. At the same time some presentations of cycles by 2×2 matrices were used [163, § F.4; 300, Ch. 1; 306, § 9.2]. Their main feature is that the FLT in \mathbb{C} corresponds to a some sort of linear transform by matrix conjugation in the cycle space. However, the metric in the cycle space was not expressed in terms of those matrices.

All three ingredients—matrix presentation with linear structure and the invariant product—came happily together as the Fillmore–Springer–Cnops construction (FSCc) in the context of Clifford algebras [65, Ch. 4; 100]. Regrettably, the FSCc has not yet propagated back to the most fundamental case of complex numbers, cf. [306, § 9.2] or the somewhat cumbersome techniques used in [32, Ch. 3]. Interestingly, even the founding fathers were not always strict followers of their own techniques, see [101].

A combination of all three components of Lie cycle geometry within FSCc facilitates further development. It was discovered that for the smaller group $SL_2(\mathbb{R})$ there exist more types—elliptic, parabolic and hyperbolic—of invariant metrics in the cycle space [185; 191; 198, Ch. 5]. Based on the earlier work [163], the key concept of Lie sphere geometry—*tangency of two cycles* C_1 and C_2 —can be expressed through the cycle product (I.15.7) as [198, Ex. 5.26.ii]:

$$\langle C_1 + C_2, C_1 + C_2 \rangle = 0$$

for C_1, C_2 normalised such that $\langle C_1, C_1 \rangle = \langle C_2, C_2 \rangle = 1$. Furthermore, $C_1 + C_2$ is the zero-radius cycle representing the point of contact.

The FSCc is useful in the consideration of the Poincaré extension of Möbius maps [209] and continued fractions [208]. In theoretical physics, FSCc nicely describes conformal compactifications of various space-time models [128; 130; 187; 198, § 8.1]. Last but not least, FSCc is behind the Computer Algebra System (CAS) operating in Lie sphere geometry [186, 211]. FSCc equally well applies to not only the field of complex numbers but rings of dual and double numbers as well [198]. New use of the FSCc will be given in the following sections in applications to loxodromes.

I.15.3. Fractional Linear Transformations and Loxodromes

In aiming for a covariant description of loxodromes we start from the following definition.

DEFINITION I.15.4. A *standard logarithmic spiral* (SLS) with parameter $\lambda \in \mathbb{C}$ is the orbit of the point 1 under the (disconnected) one-parameter subgroup of the FLT of diagonal matrices

$$(I.15.10) \quad D_\lambda(t) = \begin{pmatrix} \pm e^{\lambda t/2} & 0 \\ 0 & e^{-\lambda t/2} \end{pmatrix}, \quad t \in \mathbb{R}.$$

REMARK I.15.5. Our SLS is a *union* of two branches, each of them is a logarithmic spiral in the usual sense. The three-cycle parametrisation of loxodromes presented below becomes less elegant if those two branches need to be separated. Yet, we draw just one “positive” branch on Fig. I.15.3 to make the situation more transparent.

The SLS is the solution of the differential equation $z' = \lambda z$ with the initial value $z(0) = \pm 1$ and has the parametric equation $z(t) = \pm e^{\lambda t}$. Furthermore, we obtain the same orbit for λ_1 and $\lambda_2 \in \mathbb{C}$ if $\lambda_1 = \alpha \lambda_2$ for real $\alpha \neq 0$ through a re-parametrisation of the time $t \mapsto \alpha t$. Thus, an SLS is identified by the point $[\Re(\lambda) : \Im(\lambda)]$ of the real projective line $\mathbb{P}\mathbb{R}$. Thereafter the following classification is useful:

DEFINITION I.15.6. The SLS is

- *positive*, if $\Re(\lambda) \cdot \Im(\lambda) > 0$;
- *degenerate*, if $\Re(\lambda) \cdot \Im(\lambda) = 0$;
- *negative*, if $\Re(\lambda) \cdot \Im(\lambda) < 0$.

Informally: a positive SLS unwinds counterclockwise, a negative SLS clockwise. A degenerate SLS is the unit circle if $\Im(\lambda) \neq 0$ and the punctured real axis $\mathbb{R} \setminus \{0\}$ if $\Re(\lambda) \neq 0$. If $\Re(\lambda) = \Im(\lambda) = 0$ then the SLS is the single point 1.

DEFINITION I.15.7. A *logarithmic spiral* is the image of an SLS under a complex affine transformation $z \mapsto \alpha z + \beta$, with $\alpha, \beta \in \mathbb{C}$. A *loxodrome* is any image of an SLS under a generic FLT (I.15.1).

Obviously, a complex affine transformation is an FLT with the upper triangular matrix $\begin{pmatrix} \alpha & \beta \\ 0 & 1 \end{pmatrix}$. Thus, logarithmic spirals form an affine-invariant (but not FLT-invariant) subset of loxodromes. Thereafter, loxodromes (and their degenerate forms—circles, straight lines and points) extend the notion of cycles from the Lie sphere geometry, cf. Rem. I.15.3.

By the nature of Defn. I.15.7, the parameter λ and the corresponding classification from Defn. I.15.6 remain meaningful for logarithmic spirals and loxodromes. FLTs eliminate distinctions between circles and straight lines, but for degenerate loxodromes ($\Re(\lambda) \cdot \Im(\lambda) = 0$) we still can note the difference between the two cases of $\Re(\lambda) \neq 0$ and $\Im(\lambda) \neq 0$: orbits of former are whole circles (or straight lines) while latter orbits are only arcs of circles (or segments of lines).

The immediate consequence of Defn. I.15.7 is

PROPOSITION I.15.8. *The collection of all loxodromes is an FLT-invariant family. Degenerate loxodromes—(arcs of) circles and (segments) of straight lines—form an FLT-invariant subset of loxodromes.*

As mentioned above, an SLS is completely characterised by the point $[\Re(\lambda) : \Im(\lambda)]$ of the real projective line $\mathbb{P}\mathbb{R}$ extended by the additional point $[0 : 0]^2$. In the standard way, $[\Re(\lambda) : \Im(\lambda)]$ is associated with the real value $\tilde{\lambda} := 2\pi\Re(\lambda)/\Im(\lambda)$ extended by ∞ for $\Im(\lambda) = 0$ and with symbol $\frac{0}{0}$ for the $\Re(\lambda) = \Im(\lambda) = 0$ cases. Geometrically, $\alpha = \exp(\tilde{\lambda}) \in \mathbb{R}_+$ represents the next point after 1, where the given SLS branch meets the real positive half-axis after one full counterclockwise turn. Obviously, $\alpha > 1$ and $\alpha < 1$ for positive and negative SLS, respectively. For a degenerate SLS:

- i. with $\Im(\lambda) \neq 0$ we obtain $\tilde{\lambda} = 0$ and $\alpha = 1$;
- ii. with $\Re(\lambda) \neq 0$ we consistently define $\alpha = \infty$.

In essence, a loxodrome Λ is defined by the pair $(\tilde{\lambda}, M)$, where M is the FLT mapping Λ to the SLS with parameter $\tilde{\lambda}$. While $\tilde{\lambda}$ is completely determined by Λ , the map M is not.

PROPOSITION I.15.9. i. *The subgroup of FLT that maps SLS with the parameter $\tilde{\lambda}$ to itself consists of products $D_{\tilde{\lambda}}(t)\mathbb{R}^\varepsilon$, $\varepsilon = 0, 1$ of transformations $D_{\tilde{\lambda}}(t) = D_\lambda(t)$, $\lambda = \tilde{\lambda} + 2\pi i$ (I.15.10) and branch-swapping reflections:*

$$(I.15.11) \quad R = \begin{pmatrix} 0 & -1 \\ 1 & 0 \end{pmatrix} : z \mapsto -z^{-1}.$$

- ii. *Pairs $(\tilde{\lambda}, M)$ and $(\tilde{\lambda}', M')$ define the same loxodrome if and only if*
 - (a) $\tilde{\lambda} = \tilde{\lambda}'$;
 - (b) $M = D_{\tilde{\lambda}}(t)\mathbb{R}^\varepsilon M'$ for $\varepsilon = 0, 1$ and $t \in \mathbb{R}$.

REMARK I.15.10. Often loxodromes appear as orbits of one-parameter continuous subgroups of loxodromic FLT, which are characterised by non-real traces [24, § 4.3; 306, § 9.2; 330, § 9.2]. In the above notations such a subgroup is $MD_{\tilde{\lambda}}(t)M^{-1}$, thus the common presentation is not much different from the above $(\tilde{\lambda}, M)$ -parametrisation. Furthermore, we need to pick any point on a loxodrome to present it as an orbit.

I.15.4. Three-cycle Parametrisation of Loxodromes

Although pairs $(\tilde{\lambda}, M)$ provide a parametrisation of loxodromes, the following alternative is more operational. It is inspired by the orthogonal pairs of elliptic and hyperbolic pencils described in Section II.6.2.

DEFINITION I.15.11. *A three-cycle parametrisation $\{C_1, C_2, C_3\}$ of a non-degenerate SLS $\tilde{\lambda}$ satisfies the following conditions:*

- i. C_1 is any straight line passing through the origin;
- ii. C_2 and C_3 are two circles with their centres at the origin;
- iii. Λ passes the intersection points $C_1 \cap C_2$ and $C_1 \cap C_3$; and

²Pedantic consideration of the trivial case $\Re(\lambda) = \Im(\lambda) = 0$ will be often omitted in the following discussion.

- iv. A branch of Λ makes one full counterclockwise turn between intersection points $C_1 \cap C_2$ and $C_1 \cap C_3$ belonging to a ray in C_1 from the origin.

We say that a three-cycle parametrisation is *standard* if C_1 is the real axis and C_2 is the unit circle, then $C_3 = \{z : |z| = \exp(\tilde{\lambda})\}$. A three-cycle parametrisation can be consistently extended to a degenerate SLS Λ as follows:

- $\tilde{\lambda} = 0$: any straight line C_1 passing the origin and the unit circle $C_2 = C_3 = \Lambda$;
 $\tilde{\lambda} = \infty$: the real axis as $C_1 = \Lambda$, the unit circle as C_2 and $C_3 = (0, 0, 0, 1)$ being the zero-radius circle at infinity.

Since cycles are elements of the projective space, the following *normalised cycle product*:

$$(I.15.12) \quad [C_1, C_2] := \frac{\langle C_1, C_2 \rangle}{\sqrt{\langle C_1, C_1 \rangle \langle C_2, C_2 \rangle}}$$

is more meaningful than the cycle product (I.15.7) itself. Note that, $[C_1, C_2]$ is defined only if neither C_1 nor C_2 is a zero-radius cycle (i.e., a point). Also, the normalised cycle product is $GL_2(\mathbb{C})$ -invariant in comparison to the $SL_2(\mathbb{C})$ -invariance in (I.15.8).

A reader will instantly recognise the familiar pattern of the cosine of angle between two vectors appeared in (I.15.12). Simple calculations show that this geometric interpretation is very explicit in two special cases of interest.

LEMMA I.15.12. i. Let C_1 and C_2 be two straight lines passing the origin with slopes $\tan \phi_1$ and $\tan \phi_2$ respectively. Then $C_2 = D_{x+iy}(1)C_1$ for transformation (I.15.10) with any $x \in \mathbb{R}$ and $y = \phi_2 - \phi_1$ satisfying the relations:

$$(I.15.13) \quad [C_1, C_2] = \cos y.$$

ii. Let C_1 and C_2 be two circles centred at the origin with radii r_1 and r_2 respectively. Then $C_2 = D_{x+iy}(1)C_1$ for transformation (I.15.10) with any $y \in \mathbb{R}$ and $x = \log(r_2) - \log(r_1)$ satisfies the relation:

$$(I.15.14) \quad [C_1, C_2] = \cosh x.$$

Note the explicit elliptic-hyperbolic analogy between (I.15.13) and (I.15.14). By the way, both expressions produce real x and y due to inequality (I.15.9) for the respective types of pencils. Now we can deduce the following properties of a three-cycle parametrisation.

PROPOSITION I.15.13. For a given SLS Λ with a parameter λ :

- i. Any transformation (I.15.10) maps a three-cycle parametrisation of Λ to another three-cycle parametrisation of Λ .
- ii. For any two three-cycle parametrisations $\{C_1, C_2, C_3\}$ and $\{C'_1, C'_2, C'_3\}$, there exists $t_0 \in \mathbb{R}$ such that $C'_j = D_\lambda(t_0)C_j$ for $D_\lambda(t_0)$ (I.15.10) and $j = 1, 2, 3$.
- iii. The parameter $\tilde{\lambda} = 2\pi\Re(\lambda)/\Im(\lambda)$ of SLS can be recovered from its three-cycle parametrisation by the relation:

$$(I.15.15) \quad \tilde{\lambda} = \operatorname{arccosh} [C_2, C_3] \quad \text{and} \quad \lambda \sim \tilde{\lambda} + 2\pi i.$$

PROOF. The first statement is obvious. For the second we take $D_\lambda(t_0) : \Lambda \rightarrow \Lambda$ which maps $C_1 \cap C_2$ to $C'_1 \cap C'_2$, this transformation maps $C_j \mapsto C'_j$ for $j = 1, 2, 3$. Finally, the last statement follows from (I.15.14). \square

Note that expression (I.15.15) is FLT-invariant. Since any loxodrome is an image of SLS under FLT we obtain a three-cycle parametrisation of loxodromes as follows.

PROPOSITION I.15.14. i. Any three-cycle parametrisation $\{C_1, C_2, C_3\}$ of SLS has the following FLT-invariant properties:

- (a) C_1 is orthogonal to C_2 and C_3 ;
 - (b) C_2 and C_3 either disjoint or coincide.³
- ii. For any FLT M and three-cycle parametrisation $\{C'_1, C'_2, C'_3\}$ of an SLS, the three cycles $C_j = M(C'_j)$, $j = 1, 2, 3$ satisfy the above conditions (I.15.14.i(a)) and (I.15.14.i(b)).
- iii. For any triple of cycles $\{C_1, C_2, C_3\}$ satisfying the above conditions (I.15.14.i(a)) and (I.15.14.i(b)) there exists an FLT M such that cycles $\{M(C_1), M(C_2), M(C_3)\}$ provide a three-cycle parametrisation of the SLS with the parameter $\tilde{\lambda}$ (I.15.15). The FLT M is uniquely defined by the additional condition that $\{M(C_1), M(C_2), M(C_3)\}$ is a standard parametrisation of the SLS.

PROOF. The first statement is obvious, the second follows because properties (I.15.14.i(a)) and (I.15.14.i(b)) are FLT-invariant.

For (I.15.14.iii) in the degenerate case $C_2 = C_3$: any M that sends $C_2 = C_3$ to the unit circle will do the job. If $C_2 \neq C_3$ we explicitly describe below the procedure, which produces FLT M mapping the loxodrome to the SLS. \square

PROCEDURE I.15.15. Two disjoint cycles C_2 and C_3 span a hyperbolic pencil H as described in Section II.6.2. Then C_1 belongs to the elliptic E pencil orthogonal to H . Let C_0 and C_∞ be the two zero-radius cycles (points) from the hyperbolic pencil H . Every cycle in E , including C_1 , passes through C_0 and C_∞ . We label these points in such a way that

- for a positive $\tilde{\lambda}$, cycle C_3 is between C_2 and C_∞ ; and
- for a negative $\tilde{\lambda}$, cycle C_3 is between C_2 and C_0 .

Here “between” for cycles means “between” for their intersection points with C_1 . Finally, let C_u be any of two intersection points $C_1 \cap C_2$. Then, there exists a unique FLT M such that $M : C_0 \mapsto 0$, $M : C_u \mapsto 1$ and $M : C_\infty \mapsto \infty$. We will call M the *standard FLT associated* to the three-cycle parametrisation $\{C_1, C_2, C_3\}$ of the loxodrome.

REMARK I.15.16. To complement the construction of the standard FLT M associated to the three-cycle parametrisation $\{C_1, C_2, C_3\}$ from Procedure I.15.15, we can describe the inverse operation. For the loxodrome, which is the image of SLS with the parameter λ under an FLT M , we define the *standard three-cycle parametrisation* $\{M(\mathbb{R}), M(C_u), M(C_\lambda)\}$ as the image of the standard parametrisation of the SLS under M . Here \mathbb{R} is the real axis, $C_u = \{z : |z| = 1\}$ is the unit circle and $C_\lambda = \{z : |z| = \exp(\tilde{\lambda})\}$.

In essence, the previous proposition says that a three-cycle and (λ, M) parametrisations are equivalent and delivers an explicit procedure producing one from another.

³Recall that if $C_2 = C_3$, then SLS is degenerate and coincides with $C_2 = C_3$.

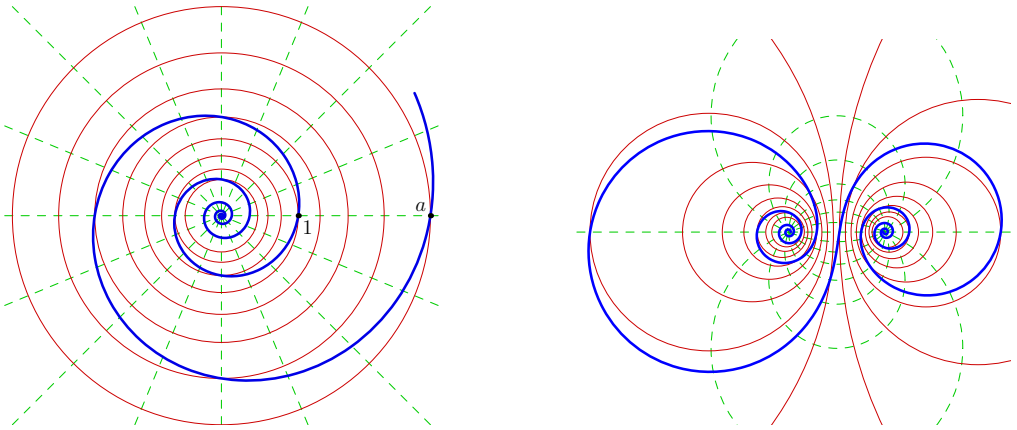


FIGURE I.15.3. Logarithmic spirals (left) and loxodrome (right) with associated pencils of cycles. This is a combination of Figs. I.15.1 and I.15.2.

However, three-cycle parametrisation is more geometric, since it links a loxodrome to a pair of orthogonal pencils, see Fig. I.15.3. Furthermore, cycles C_1, C_2, C_3 (unlike parameters λ and M) can be directly drawn in the plane to represent a loxodrome, which may be even omitted.

I.15.5. Applications of Three-Cycle Parametrisation

Now we present some examples of the use of three-cycle parametrisation of loxodromes. Any parametrisation mentioned in this paper has some arbitrariness. For pairs $(\tilde{\lambda}, M)$ this is described in Proposition I.15.9. Characterisation as orbits from Rem. I.15.10 seems to be most ambiguous: besides the previous freedom in the choice of one-parameter subgroup, we can pick any point of the loxodrome as well. Now we want to resolve non-uniqueness in the three-cycle parametrisation. Recall, that a triple $\{C_1, C_2, C_3\}$ is non-degenerate if $C_2 \neq C_3$ and C_3 is not zero-radius.

PROPOSITION I.15.17. *Two non-degenerate triples $\{C_1, C_2, C_3\}$ and $\{C'_1, C'_2, C'_3\}$ parameterise the same loxodrome if and only if all the following conditions are satisfied:*

- i. Pairs $\{C_2, C_3\}$ and $\{C'_2, C'_3\}$ span the same hyperbolic pencil. That is, cycles C'_2 and C'_3 are linear combinations of C_2 and C_3 and vice versa.
- ii. Pairs $\{C_2, C_3\}$ and $\{C'_2, C'_3\}$ define the same parameter $\tilde{\lambda}$:

$$(I.15.16) \quad [C_2, C_3] = [C'_2, C'_3].$$

- iii. The elliptic-hyperbolic identity holds:

$$(I.15.17) \quad \frac{\operatorname{arccosh} [C_j, C'_j]}{\operatorname{arccosh} [C_2, C_3]} \equiv \frac{1}{2\pi} \arccos [C_1, C'_1] \pmod{1},$$

where j is either 2 or 3.

PROOF. Necessity of (I.15.17.i) is obvious, since hyperbolic pencils spanned by $\{C_2, C_3\}$ and $\{C'_2, C'_3\}$ are both the image of concentric circles centred at origin under the FLT M defining the loxodrome. Necessity of (I.15.17.ii) is also obvious since $\tilde{\lambda}$ is uniquely defined by the loxodrome. Necessity of (I.15.17.iii) follows from the analysis of the following demonstration of sufficiency.

For sufficiency, let M be FLT constructed through Procedure I.15.15 from $\{C_1, C_2, C_3\}$. Then (I.15.17.i) implies that $M(C'_2)$ and $M(C'_3)$ are also circles centred at the origin. Then Lem. I.15.12 implies that the transformation $D_{x+iy}(1)$, where $x = \operatorname{arccosh}[C_2, C'_2]$ and $y = \arccos[C_1, C'_1]$, maps C'_1 and C'_2 to C_1 and C_2 , respectively. Furthermore, from identity (I.15.16) it follows that the same $D_{x+iy}(1)$ maps C'_3 to C_3 . Finally, condition (I.15.17) means that $x+i(y+2\pi n) = a(\tilde{\lambda}+2\pi i)$ for $a = x/\tilde{\lambda}$ and some $n \in \mathbb{Z}$. In other words $D_{x+iy}(1) = D_{\tilde{\lambda}}(a)$, thus $D_{x+iy}(1)$ maps the SLS with parameter $\tilde{\lambda}$ to itself. Since $\{M(C_1), M(C_2), M(C_3)\}$ and $\{M(C'_1), M(C'_2), M(C'_3)\}$ are two three-cycle parametrisations of the same SLS, $\{C_1, C_2, C_3\}$ and $\{C'_1, C'_2, C'_3\}$ are two three-cycle parametrisations of the same loxodrome. \square

See Fig. I.13.1 for an animated family of equivalent three-cycle parametrisations of the same loxodrome (also posted at [207]). Relation (I.15.17), which correlates elliptic and hyperbolic rotations for the loxodrome, regularly appears in this context. The next topic provides another illustration of this.

PROCEDURE I.15.18. To verify whether a loxodrome parametrised by three cycles $\{C_1, C_2, C_3\}$ passes a point parametrised by a zero-radius cycle, C_0 we perform the following steps:

- i. Define the cycle

$$(I.15.18) \quad C_h = tC_2 + (1-t)C_3, \quad \text{where } t = -\frac{\langle C_0, C_3 \rangle}{\langle C_0, C_2 - C_3 \rangle},$$

which belongs to the hyperbolic pencil spanned by $\{C_2, C_3\}$ and is orthogonal to C_0 , that is, passes the respective point.

- ii. Find the cycle C_e from the elliptic pencil orthogonal to $\{C_2, C_3\}$ that passes through C_0 . C_e is the solution of the system of three linear (equation with respect to parameters of C_e) equations, cf. Ex I.15.2:

$$\begin{aligned} \langle C_e, C_0 \rangle &= 0, \\ \langle C_e, C_2 \rangle &= 0, \\ \langle C_e, C_3 \rangle &= 0. \end{aligned}$$

- iii. Verify the elliptic-hyperbolic relation:

$$(I.15.19) \quad \frac{\operatorname{arccosh}[C_h, C_2]}{\operatorname{arccosh}[C_2, C_3]} \equiv \frac{1}{2\pi} \arccos[C_e, C_1] \pmod{1}.$$

PROOF. Let M be the standard FLT associated with $\{C_1, C_2, C_3\}$ from Procedure I.15.15. The point C_0 belongs to the loxodrome if the transformation $D_{\tilde{\lambda}}(t)$ for some t maps $M(C_0)$ to the intersection $M(C_1) \cap M(C_2)$. But $D_{x+iy}(1)$ with $x = \operatorname{arccosh}[C_h, C_2]$ and $y = \arccos[C_e, C_1]$ maps $M(C_h) \rightarrow M(C_2)$ and $M(C_e) \rightarrow M(C_1)$, thus it also

maps $M(C_0) \subset M(C_h) \cap M(C_e)$ to $M(C_1) \cap M(C_2)$. Condition (I.15.19) guaranties that $D_{x+iy}(1) = D_{\tilde{\lambda}}(x/\tilde{\lambda})$, as in the previous Prop. \square

Our final example considers two loxodromes that may have completely different associated pencils.

PROCEDURE I.15.19. Let two loxodromes be parametrised by $\{C_1, C_2, C_3\}$ and $\{C'_1, C'_2, C'_3\}$. Assume they intersect at some point parametrised by a zero-radius cycle C_0 (this can be checked by Procedure I.15.18, if needed). To find the angle of intersection we perform the following steps:

- i. Use (I.15.18) to find cycles C_h and C'_h belonging to hyperbolic pencils, spanned by $\{C_2, C_3\}$ and $\{C'_2, C'_3\}$, respectively, and both passing C_0 .
- ii. The intersection angle is

$$(I.15.20) \quad \arccos [C_h, C'_h] = \arctan \left(\frac{\tilde{\lambda}}{2\pi} \right) + \arctan \left(\frac{\tilde{\lambda}'}{2\pi} \right),$$

where $\tilde{\lambda}$ and $\tilde{\lambda}'$ are determined by (I.15.15).

PROOF. A non-degenerate loxodrome intersects any cycle from its hyperbolic pencil with the fixed angle $\arctan(\tilde{\lambda}/(2\pi))$. This is used to amend the intersection angle $\arccos [C_h, C'_h]$ of cycles from the respective hyperbolic pencils. \square

COROLLARY I.15.20. *Let a loxodrome parametrised by $\{C_1, C_2, C_3\}$ pass through a point parametrised by a zero-radius cycle C_0 as in Procedure I.15.18. Then, a non-zero radius cycle C is tangent to the loxodrome at C_0 if and only if the following two conditions hold:*

$$(I.15.21) \quad \begin{aligned} \langle C, C_0 \rangle &= 0, \\ \arccos [C, C_h] &= \arctan \left(\frac{\tilde{\lambda}}{2\pi} \right), \end{aligned}$$

where C_h is given by (I.15.18) and $\tilde{\lambda}$ is determined by (I.15.15).

PROOF. The first condition simply verifies that C passes C_0 , cf. Ex I.15.2. Cycle C , as a degenerate loxodrome, is parametrised by $\{C_e, C, C\}$, where C_e is any cycle orthogonal to C and C_e is not relevant in the following. The hyperbolic pencil spanned by two copies of C consists of C only. Thus we put $C'_h = C$, $\tilde{\lambda}' = 0$ in (I.15.20) and set that expression equal it to 0 to obtain the second equation in (I.15.21). \square

I.15.6. Discussion and Open Questions

It was mentioned at the end of Section I.15.4 that a three-cycle parametrisation of loxodromes is more geometric than their presentation by a pair (λ, M) . Furthermore, three-cycle parametrisation reveals the natural analogy between elliptic and hyperbolic features of loxodromes, see (I.15.17) as an illustration. Examples in Section I.15.5 show that various geometric questions are explicitly answered in term of three-cycle parametrisation. Thus, our work extends the set of objects in Lie sphere geometry—circles, lines and points—to the natural maximal conformally-invariant family, which also includes loxodromes. In practical terms, three-cycle parametrisation allows one

to extend the library figure for Möbuis invariant geometry [211, 212] to operate with loxodromes as well.

It is even more important that the presented technique is another implementation of a general framework [208, 209, 211, 212], which provides a significant advance in Lie sphere geometry. The Poincaré extension of FLT from the real line to the upper half-plane was performed by a pair of orthogonal cycles in [209]. A similar extension of FLT from the complex plane to the upper half-space can be done by a *triple of pairwise orthogonal cycles*. Thus, triples satisfying FLT-invariant properties (I.15.14.i(a)) and (I.15.14.i(b)) of Prop. I.15.14 present another non-equivalent class of cycle ensembles in the sense of [209]. In general, Lie sphere geometry *can be enriched by consideration of cycle ensembles* interrelated by a list of FLT-invariant properties [209]. Such ensembles become new objects in the extended Lie spheres geometry and can be represented by points in a *cycle ensemble space*.

There are several natural directions to extend this work further, here are just few of them:

- i. Link our “global” parametrisation of loxodromes with the differential geometric approach from [43, 290, 293]. Our last Cor. I.15.20 can be a first step in this direction.
- ii. Consider all FLT-invariant non-equivalent classes of three-cycle ensembles on \mathbb{C} : pairwise orthogonal triples (representing points in the upper half-space [209]), triples satisfying properties (I.15.14.i(a)) and (I.15.14.i(b)) of Prop. I.15.14 (representing loxodromes), etc.
- iii. Extend this consideration to quaternions or Clifford algebras [122, 258]. The previous works [291, 292] and availability of FSCc in this setup [65, Ch. 4; 100] make it rather promising.
- iv. Consider Möbius transformations in rings of dual and double numbers [19, 190, 191, 196, 198, 203, 209, 261]. There are enough indications that the story will not be quite the same as for complex numbers.
- v. Explore further connections of loxodromes with
 - Carleson curves and microlocal properties of singular integral operators [18, 40, 46]; or
 - applications to operator theory [306, 330].

Some combinations of those topics may be fruitful as well.

Continued Fractions, Möbius Transformations and Cycles

We review interrelations between continued fractions, Möbius transformations and representations of cycles by 2×2 matrices. This leads us to several descriptions of continued fractions through chains of orthogonal or touching horocycles. One of these descriptions was proposed in paper by A. Beardon and I. Short [28]. The approach is extended to several dimensions in a way which is compatible to the early propositions of A. Beardon based on Clifford algebras [22].

I.16.1. Introduction

Continued fractions remain an important and attractive topic of current research [45; 149; 158; 163, § E.3]. A fruitful and geometrically appealing method considers a continued fraction as an (infinite) product of linear-fractional transformations from the Möbius group. see Sec. I.16.2 of this paper for an overview, papers [23; 274; 285; 299; 300, Ex. 10.2] and in particular [25] contain further references and historical notes. Partial products of linear-fractional maps form a sequence in the Moebius group, the corresponding sequence of transformations can be viewed as a discrete dynamical system [25, 249]. Many important questions on continued fractions, e.g. their convergence, can be stated in terms of asymptotic behaviour of the associated dynamical system. Geometrical generalisations of continued fractions to many dimensions were introduced recently as well [22, 149].

Any consideration of the Möbius group introduces cycles—the Möbius invariant set of all circles and straight lines. Furthermore, an efficient treatment cycles and Möbius transformations is realised through certain 2×2 matrices, which we will review in Sec. I.16.3, see also [65, § 4.1; 100; 163, § 4.2; 185; 198; 300]. Linking the above relations we may propose the main thesis of the present note:

COROLLARY I.16.1 (Continued fractions and cycles). *Properties of continued fractions may be illustrated and demonstrated using related cycles, in particular, in the form of respective 2×2 matrices.*

One may expect that such an observation has been made a while ago, e.g. in the book [300], where both topics were studied. However, this seems did not happened for some reasons. It is only the recent paper [28], which pioneered a connection between continued fractions and cycles. We hope that the explicit statement of the claim will stimulate its further fruitful implementations. In particular, Sec. I.16.4 reveals all three possible cycle arrangements similar to one used in [28]. Secs. I.16.5–I.16.6 shows that

relations between continued fractions and cycles can be used in the multidimensional case as well.

As an illustration, we draw on Fig. I.16.1 chains of tangent horocycles (circles tangent to the real line, see [28] and Sec. I.16.4) for two classical simple continued fractions:

$$e = 2 + \frac{1}{1 + \frac{1}{2 + \frac{1}{1 + \frac{1}{1 + \dots}}}}, \quad \pi = 3 + \frac{1}{7 + \frac{1}{15 + \frac{1}{1 + \frac{1}{292 + \dots}}}}.$$

One can immediately see, that the convergence for π is much faster: already the third

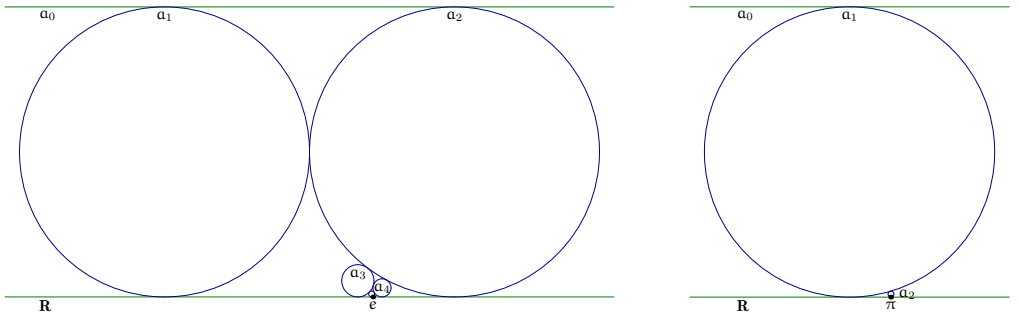


FIGURE I.16.1. Continued fractions for e and π visualised. The convergence rate for π is pictorially faster.

horocycle is too small to be visible even if it is drawn. This is related to larger coefficients in the continued fraction for π .

Paper [28] also presents examples of proofs based on chains of horocycles. This intriguing construction was introduced in [28] *ad hoc*. Guided by the above claim we reveal sources of this and other similar arrangements of horocycles. Also, we can produce multi-dimensional variant of the framework.

I.16.2. Continued Fractions

We use the following compact notation for a continued fraction:

$$(I.16.1) \quad K(a_n|b_n) = \frac{a_1}{b_1 + \frac{a_2}{b_2 + \frac{a_3}{b_3 + \dots}}} = \frac{a_1}{b_1} + \frac{a_2}{b_2} + \frac{a_3}{b_3} + \dots$$

Without loss of generality we can assume $a_j \neq 0$ for all j . The important particular case of *simple* continued fractions, with $a_n = 1$ for all n , is denoted by $K(b_n) = K(1|b_n)$. Any continued fraction can be transformed to an equivalent simple one.

It is easy to see, that continued fractions are related to the following linear-fractional (Möbius) transformation, cf. [23, 274, 285, 299]:

$$(I.16.2) \quad S_n = s_1 \circ s_2 \circ \dots \circ s_n, \quad \text{where } s_j(z) = \frac{a_j}{b_j + z}.$$

These Möbius transformation are considered as bijective maps of the Riemann sphere $\hat{\mathbb{C}} = \mathbb{C} \cup \{\infty\}$ onto itself. If we associate the matrix $\begin{pmatrix} a & b \\ c & d \end{pmatrix}$ to a liner-fractional transformation $z \mapsto \frac{az+b}{cz+d}$, then the composition of two such transformations corresponds to multiplication of the respective matrices. Thus, relation (I.16.2) has the matrix form:

$$(I.16.3) \quad \begin{pmatrix} P_{n-1} & P_n \\ Q_{n-1} & Q_n \end{pmatrix} = \begin{pmatrix} 0 & a_1 \\ 1 & b_1 \end{pmatrix} \begin{pmatrix} 0 & a_2 \\ 1 & b_2 \end{pmatrix} \dots \begin{pmatrix} 0 & a_n \\ 1 & b_n \end{pmatrix}.$$

The last identity can be fold into the recursive formula:

$$(I.16.4) \quad \begin{pmatrix} P_{n-1} & P_n \\ Q_{n-1} & Q_n \end{pmatrix} = \begin{pmatrix} P_{n-2} & P_{n-1} \\ Q_{n-2} & Q_{n-1} \end{pmatrix} \begin{pmatrix} 0 & a_n \\ 1 & b_n \end{pmatrix}.$$

This is equivalent to the main recurrence relation:

$$(I.16.5) \quad \begin{aligned} P_n &= b_n P_{n-1} + a_n P_{n-2}, & n &= 1, 2, 3, \dots, & \text{with } P_1 &= a_1, & P_0 &= 0, \\ Q_n &= b_n Q_{n-1} + a_n Q_{n-2}, & & & Q_1 &= b_1, & Q_0 &= 1. \end{aligned}$$

The meaning of entries P_n and Q_n from the matrix (I.16.3) is revealed as follows. Möbius transformation (I.16.2)–(I.16.3) maps 0 and ∞ to

$$(I.16.6) \quad \frac{P_n}{Q_n} = S_n(0), \quad \frac{P_{n-1}}{Q_{n-1}} = S_n(\infty).$$

It is easy to see that $S_n(0)$ is the *partial quotient* of (I.16.1):

$$(I.16.7) \quad \frac{P_n}{Q_n} = \frac{a_1}{b_1 + \frac{a_2}{b_2 + \dots + \frac{a_n}{b_n}}}.$$

Properties of the sequence of partial quotients $\left\{ \frac{P_n}{Q_n} \right\}$ in terms of sequences $\{a_n\}$ and $\{b_n\}$ are the core of the continued fraction theory. Equation (I.16.6) links partial quotients with the Möbius map (I.16.2). Circles form an invariant family under Möbius transformations, thus their appearance for continued fractions is natural. Surprisingly, this happened only recently in [28].

I.16.3. Möbius Transformations and Cycles

If $M = \begin{pmatrix} a & b \\ c & d \end{pmatrix}$ is a matrix with real entries then for the purpose of the associated Möbius transformations $M : z \mapsto \frac{az+b}{cz+d}$ we may assume that $\det M = \pm 1$. The collection of all such matrices form a group. Möbius maps commute with the complex conjugation $z \mapsto \bar{z}$. If $\det M > 0$ then both the upper and the lower half-planes are preserved; if $\det M < 0$ then the two half-planes are swapped. Thus, we can treat M as the map of equivalence classes $z \sim \bar{z}$, which are labelled by respective points of the closed upper half-plane. Under this identification we consider any map produced by M with $\det M = \pm 1$ as the map of the closed upper-half plane to itself.

The characteristic property of Möbius maps is that circles and lines are transformed to circles and lines. We use the word *cycles* for elements of this Möbius-invariant family [185, 198, 339]. We abbreviate a cycle given by the equation

$$(I.16.8) \quad k(u^2 + v^2) - 2lv - 2nu + m = 0$$

to the point (k, l, n, m) of the three dimensional projective space $\mathbb{P}\mathbb{R}^3$. The equivalence relation $z \sim \bar{z}$ is lifted to the equivalence relation

$$(I.16.9) \quad (k, l, n, m) \sim (k, l, -n, m)$$

in the space of cycles, which again is compatible with the Möbius transformations acting on cycles.

The most efficient connection between cycles and Möbius transformations is realised through the construction, which may be traced back to [300] and was subsequently rediscovered by various authors [65, § 4.1; 100; 163, § 4.2], see also [185, 198]. The construction associates a cycle (k, l, n, m) with the 2×2 matrix $C = \begin{pmatrix} l + in & -m \\ k & -l + in \end{pmatrix}$, see discussion in [198, § 4.4] for a justification. This identification is Möbius covariant: the Möbius transformation defined by $M = \begin{pmatrix} a & b \\ c & d \end{pmatrix}$ maps a cycle with matrix C to the cycle with matrix MCM^{-1} . Therefore, any Möbius-invariant relation between cycles can be expressed in terms of corresponding matrices. The central role is played by the Möbius-invariant inner product [198, § 5.3]:

$$(I.16.10) \quad \langle C, \tilde{C} \rangle = \Re \operatorname{tr}(C\tilde{C}),$$

which is a cousin of the product used in GNS construction of C^* -algebras. Notably, the relation:

$$(I.16.11) \quad \langle C, \tilde{C} \rangle = 0 \quad \text{or} \quad k\tilde{m} + m\tilde{k} - 2n\tilde{n} - 2\tilde{l}l = 0,$$

describes two cycles $C = (k, l, m, n)$ and $\tilde{C} = (\tilde{k}, \tilde{l}, \tilde{m}, \tilde{n})$ orthogonal in Euclidean geometry. Also, the inner product (I.16.10) expresses the Descartes–Kirillov condition [163, Lem. 4.1(c); 198, Ex. 5.26] of C and \tilde{C} to be externally tangent:

$$(I.16.12) \quad \langle C + \tilde{C}, C + \tilde{C} \rangle = 0 \quad \text{or} \quad (l + \tilde{l})^2 + (n + \tilde{n})^2 - (m + \tilde{m})(k + \tilde{k}) = 0,$$

where the representing vectors $C = (k, l, n, m)$ and $\tilde{C} = (\tilde{k}, \tilde{l}, \tilde{m}, \tilde{n})$ from $\mathbb{P}\mathbb{R}^3$ need to be normalised by the conditions $\langle C, C \rangle = 1$ and $\langle \tilde{C}, \tilde{C} \rangle = 1$.

I.16.4. Continued Fractions and Cycles

Let $M = \begin{pmatrix} a & b \\ c & d \end{pmatrix}$ be a matrix with real entries and the determinant $\det M$ equal to ± 1 , we denote this by $\delta = \det M$. As mentioned in the previous section, to calculate the image of a cycle C under Möbius transformations M we can use matrix similarity

MCM^{-1} . If $M = \begin{pmatrix} P_{n-1} & P_n \\ Q_{n-1} & Q_n \end{pmatrix}$ is the matrix (I.16.3) associated to a continued fraction and we are interested in the partial fractions $\frac{P_n}{Q_n}$, it is natural to ask:

Which cycles C have transformations MCM^{-1} depending on the first (or on the second) columns of M only?

It is a straightforward calculation with matrices¹ to check the following statements:

LEMMA I.16.2. *The cycles $(0, 0, 1, m)$ (the horizontal lines $v = m$) are the only cycles, such that their images under the Möbius transformation $\begin{pmatrix} a & b \\ c & d \end{pmatrix}$ are independent from the column $\begin{pmatrix} b \\ d \end{pmatrix}$. The image associated to the column $\begin{pmatrix} a \\ c \end{pmatrix}$ is the horocycle $(c^2m, acm, \delta, a^2m)$, which touches the real line at $\frac{a}{c}$ and has the radius $\frac{1}{mc^2}$.*

In particular, for the matrix (I.16.4) the horocycle is touching the real line at the point $\frac{P_{n-1}}{Q_{n-1}} = S_n(\infty)$ (I.16.6).

LEMMA I.16.3. *The cycles $(k, 0, 1, 0)$ (with the equation $k(u^2 + v^2) - 2v = 0$) are the only cycles, such that their images under the Möbius transformation $\begin{pmatrix} a & b \\ c & d \end{pmatrix}$ are independent from the column $\begin{pmatrix} a \\ c \end{pmatrix}$. The image associated to the column $\begin{pmatrix} b \\ d \end{pmatrix}$ is the horocycle $(d^2k, bdk, \delta, b^2k)$, which touches the real line at $\frac{b}{d}$ and has the radius $\frac{1}{kd^2}$.*

In particular, for the matrix (I.16.4) the horocycle is touching the real line at the point $\frac{P_n}{Q_n} = S_n(0)$ (I.16.6). In view of these partial quotients the following cycles joining them are of interest.

LEMMA I.16.4. *A cycle $(0, 1, n, 0)$ (any non-horizontal line passing 0) is transformed by (I.16.2)–(I.16.3) to the cycle $(2Q_nQ_{n-1}, P_nQ_{n-1} + Q_nP_{n-1}, \delta n, 2P_nP_{n-1})$, which passes points $\frac{P_n}{Q_n} = S_n(0)$ and $\frac{P_{n-1}}{Q_{n-1}} = S(\infty)$ on the real line.*

The above three families contain cycles with specific relations to partial quotients through Möbius transformations. There is one degree of freedom in each family: m , k and n , respectively. We can use the parameters to create an ensemble of three cycles (one from each family) with some Möbius-invariant interconnections. Three most natural arrangements are illustrated by Fig. I.16.2. The first row presents the initial selection of cycles, the second row—their images after a Möbius transformation (colours are preserved). The arrangements are as follows:

- i. The left column shows the arrangement used in the paper [28]: two horocycles are tangent, the third cycle, which we call *connecting*, passes three points of pair-wise contact between horocycles and the real line. The connecting cycle is also orthogonal to horocycles and the real line. The arrangement corresponds to the following values $m = 2$, $k = 2$, $n = 0$. These parameters

¹This calculation can be done with the help of the tailored Computer Algebra System (CAS) as described in [186; 198, App. B].

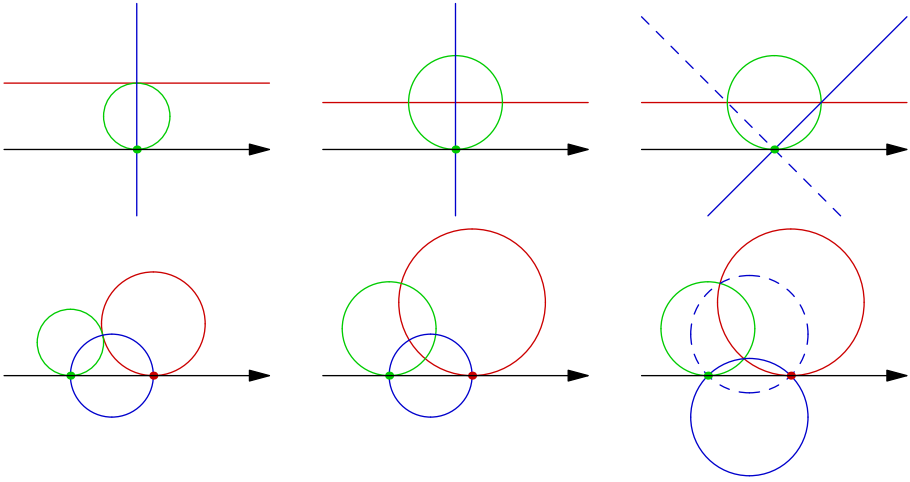


FIGURE I.16.2. Various arrangements for three cycles. The first row shows the initial position, the second row—after a Möbius transformation (colours are preserved).

The left column shows the arrangement used in the paper [28]: two horocycles touching, the connecting cycle is passing their common point and is orthogonal to the real line.

The central column presents two orthogonal horocycles and the connecting cycle orthogonal to them.

The horocycles in the right column are again orthogonal but the connecting cycle passes one of their intersection points and makes 45° with the real axis.

are uniquely defined by the above tangent and orthogonality conditions together with the requirement that the horocycles' radii agreeably depend from the consecutive partial quotients' denominators: $\frac{1}{2Q_{n-1}^2}$ and $\frac{1}{2Q_n^2}$ respectively. This follows from the explicit formulae of image cycles calculated in Lemmas I.16.2 and I.16.3.

- ii. The central column of Fig. I.16.2 presents two orthogonal horocycles and the connecting cycle orthogonal to them. The initial cycles have parameters $m = \sqrt{2}$, $k = \sqrt{2}$, $n = 0$. Again, these values follow from the geometric conditions and the alike dependence of radii from the partial quotients' denominators: $\frac{\sqrt{2}}{2Q_{n-1}^2}$ and $\frac{\sqrt{2}}{2Q_n^2}$.
- iii. Finally, the right column have the same two orthogonal horocycles, but the connecting cycle passes one of two horocycles' intersection points. Its mirror reflection in the real axis satisfying (I.16.9) (drawn in the dashed style) passes the second intersection point. This corresponds to the values $m = \sqrt{2}$, $k = \sqrt{2}$, $n = \pm 1$. The connecting cycle makes the angle 45° at the points

of intersection with the real axis. It also has the radius $\frac{\sqrt{2}}{2} \left| \frac{p_n}{Q_n} - \frac{p_{n-1}}{Q_{n-1}} \right| = \frac{\sqrt{2}}{2} \frac{1}{|Q_n Q_{n-1}|}$ —the geometric mean of radii of two other cycles. This again repeats the relation between cycles' radii in the first case.

Three configurations have fixed ratio $\sqrt{2}$ between respective horocycles' radii. Thus, they are equally suitable for the proofs based on the size of horocycles, e.g. [28, Thm. 4.1].

On the other hand, there is a tiny computational advantage in the case of orthogonal horocycles. Let we have the sequence p_j of partial fractions $p_j = \frac{p_j}{Q_j}$ and want to rebuild the corresponding chain of horocycles. A horocycle with the point of contact p_j has components $(1, p_j, n_j, p_j^2)$, thus only the value of n_j need to be calculated at every step. If we use the condition “to be tangent to the previous horocycle”, then the quadratic relation (I.16.12) shall be solved. Meanwhile, the orthogonality relation (I.16.11) is linear in n_j .

I.16.5. Multi-dimensional Möbius maps and cycles

It is natural to look for multidimensional generalisations of continued fractions. A geometric approach based on Möbius transformation and Clifford algebras was proposed in [22]. The Clifford algebra $\mathcal{C}(\mathfrak{n})$ is the associative unital algebra over \mathbb{R} generated by the elements e_1, \dots, e_n satisfying the following relation:

$$e_i e_j + e_j e_i = -2\delta_{ij},$$

where δ_{ij} is the Kronecker delta. An element of $\mathcal{C}(\mathfrak{n})$ having the form $x = x_1 e_1 + \dots + x_n e_n$ can be associated with the vector $(x_1, \dots, x_n) \in \mathbb{R}^n$. The *reversion* $a \mapsto a^*$ in $\mathcal{C}(\mathfrak{n})$ [65, (1.19(ii))] is defined on vectors by $x^* = x$ and extended to other elements by the relation $(\overline{ab})^* = b^* a^*$. Similarly the *conjugation* is defined on vectors by $\bar{x} = -x$ and the relation $\overline{a\bar{b}} = \bar{b}a$. We also use the notation $|a|^2 = a\bar{a} \geq 0$ for any product a of vectors. An important observation is that any non-zero vectors x has a multiplicative inverse: $x^{-1} = \frac{\bar{x}}{|x|^2}$.

By Ahlfors [3] (see also [22, § 5; 65, Thm. 4.10]) a matrix $M = \begin{pmatrix} a & b \\ c & d \end{pmatrix}$ with Clifford entries defines a linear-fractional transformation of \mathbb{R}^n if the following conditions are satisfied:

- i. a, b, c and d are products of vectors in \mathbb{R}^n ;
- ii. ab^*, cd^*, c^*a and d^*b are vectors in \mathbb{R}^n ;
- iii. the pseudodeterminant $\delta := ad^* - bc^*$ is a non-zero real number.

Clearly we can scale the matrix to have the pseudodeterminant $\delta = \pm 1$ without an effect on the related linear-fractional transformation. Define, cf. [65, (4.7)]

$$(I.16.13) \quad \bar{M} = \begin{pmatrix} d^* & -b^* \\ -c^* & a^* \end{pmatrix} \quad \text{and} \quad M^* = \begin{pmatrix} \bar{d} & \bar{b} \\ \bar{c} & \bar{a} \end{pmatrix}.$$

Then $M\bar{M} = \delta I$ and $\bar{M} = \kappa M^*$, where $\kappa = 1$ or -1 depending either d is a product of even or odd number of vectors.

To adopt the discussion from Section I.16.3 to several dimensions we use vector rather than paravector formalism, see [65, (1.42)] for a discussion. Namely, we consider

vectors $x \in \mathbb{R}^{n+1}$ as elements $x = x_1 e_1 + \dots + x_n e_n + x_{n+1} e_{n+1}$ in $\mathcal{O}(n+1)$. Therefore we can extend the Möbius transformation defined by $M = \begin{pmatrix} a & b \\ c & d \end{pmatrix}$ with $a, b, c, d \in \mathcal{O}(n)$ to act on \mathbb{R}^{n+1} . Again, such transformations commute with the reflection R in the hyperplane $x_{n+1} = 0$:

$$R: \quad x_1 e_1 + \dots + x_n e_n + x_{n+1} e_{n+1} \quad \mapsto \quad x_1 e_1 + \dots + x_n e_n - x_{n+1} e_{n+1}.$$

Thus we can consider the Möbius maps acting on the equivalence classes $x \sim R(x)$.

Spheres and hyperplanes in \mathbb{R}^{n+1} —which we continue to call cycles—can be associated to 2×2 matrices [65, (4.12); 100]:

$$(I.16.14) \quad k\bar{x}x - l\bar{x} - x\bar{l} + m = 0 \quad \leftrightarrow \quad C = \begin{pmatrix} l & m \\ k & \bar{l} \end{pmatrix},$$

where $k, m \in \mathbb{R}$ and $l \in \mathbb{R}^{n+1}$. For brevity we also encode a cycle by its coefficients (k, l, m) . A justification of (I.16.14) is provided by the identity:

$$(1 \quad \bar{x}) \begin{pmatrix} l & m \\ k & \bar{l} \end{pmatrix} \begin{pmatrix} x \\ 1 \end{pmatrix} = kx\bar{x} - l\bar{x} - x\bar{l} + m, \quad \text{since } \bar{\bar{x}} = -x \text{ for } x \in \mathbb{R}^n.$$

The identification is also Möbius-covariant in the sense that the transformation associated with the Ahlfors matrix M sends a cycle C to the cycle MCM^* [65, (4.16)]. The equivalence $x \sim R(x)$ is extended to spheres:

$$\begin{pmatrix} l & m \\ k & \bar{l} \end{pmatrix} \sim \begin{pmatrix} R(l) & m \\ k & R(\bar{l}) \end{pmatrix}$$

since it is preserved by the Möbius transformations with coefficients from $\mathcal{O}(n)$.

Similarly to (I.16.10) we define the Möbius-invariant inner product of cycles by the identity $\langle C, \tilde{C} \rangle = \Re \operatorname{tr}(C\tilde{C})$, where \Re denotes the scalar part of a Clifford number. The orthogonality condition $\langle C, \tilde{C} \rangle = 0$ means that the respective cycle are geometrically orthogonal in \mathbb{R}^{n+1} .

I.16.6. Continued fractions from Clifford algebras and horocycles

There is an association between the triangular matrices and the elementary Möbius maps of \mathbb{R}^n , cf. (I.16.2):

$$(I.16.15) \quad \begin{pmatrix} 0 & 1 \\ 1 & b \end{pmatrix} : x \mapsto (x+b)^{-1}, \quad \text{where } x = x_1 e_1 + \dots + x_n e_n, b = b_1 e_1 + \dots + b_n e_n,$$

Similar to the real line case in Section I.16.2, Beardon proposed [22] to consider the composition of a series of such transformations as multidimensional continued fraction, cf. (I.16.2). It can be again represented as the the product (I.16.3) of the respective 2×2 matrices. Another construction of multidimensional continued fractions based on horocycles was hinted in [28]. We wish to clarify the connection between them. The bridge is provided by the respective modifications of Lem. I.16.2–I.16.4.

LEMMA I.16.5. *The cycles $(0, e_{n+1}, m)$ (the “horizontal” hyperplane $x_{n+1} = m$) are the only cycles, such that their images under the Möbius transformation $\begin{pmatrix} a & b \\ c & d \end{pmatrix}$ are independent from the column $\begin{pmatrix} b \\ d \end{pmatrix}$. The image associated to the column $\begin{pmatrix} a \\ c \end{pmatrix}$ is the horocycle $(-m|c|^2, -ma\bar{c} + \delta e_{n+1}, m|a|^2)$, which touches the hyperplane $x_{n+1} = 0$ at $\frac{a\bar{c}}{|c|^2}$ and has the radius $\frac{1}{m|c|^2}$.*

LEMMA I.16.6. *The cycles $(k, e_{n+1}, 0)$ (with the equation $k(u^2 + v^2) - 2v = 0$) are the only cycles, such that their images under the Möbius transformation $\begin{pmatrix} a & b \\ c & d \end{pmatrix}$ are independent from the column $\begin{pmatrix} a \\ c \end{pmatrix}$. The image associated to the column $\begin{pmatrix} b \\ d \end{pmatrix}$ is the horocycle $(k|d|^2, kb\bar{d} + \delta e_{n+1}, -kb\bar{b})$, which touches the hyperplane $x_{n+1} = 0$ at $\frac{b\bar{d}}{|d|^2}$ and has the radius $\frac{1}{k|d|^2}$.*

The proof of the above lemmas are reduced to multiplications of respective matrices with Clifford entries.

LEMMA I.16.7. *A cycle $C = (0, l, 0)$, where $l = x + re_{n+1}$ and $0 \neq x \in \mathbb{R}^n$, $r \in \mathbb{R}$, that is any non-horizontal hyperplane passing the origin, is transformed into $MCM^* = (cx\bar{d} + d\bar{x}\bar{c}, \alpha x\bar{d} + b\bar{x}\bar{c} + \delta re_{n+1}, \alpha x\bar{b} + b\bar{x}\bar{a})$. This cycle passes points $\frac{a\bar{c}}{|c|^2}$ and $\frac{b\bar{d}}{|d|^2}$.*

If $x = \bar{c}d$, then the centre of

$$MCM^* = (2|c|^2|d|^2, a\bar{c}|d|^2 + b\bar{d}|c|^2, (a\bar{c})(d\bar{b}) + (b\bar{d})(c\bar{a}))$$

is $\frac{1}{2}(\frac{a\bar{c}}{|c|^2} + \frac{b\bar{d}}{|d|^2}) + \frac{\delta r}{2|c|^2|d|^2}e_{n+1}$, that is, the centre belongs to the two-dimensional plane passing the points $\frac{a\bar{c}}{|c|^2}$ and $\frac{b\bar{d}}{|d|^2}$ and orthogonal to the hyperplane $x_{n+1} = 0$.

PROOF. We note that $e_{n+1}x = -xe_{n+1}$ for all $x \in \mathbb{R}^n$. Thus, for a product of vectors $d \in \mathcal{C}(n)$ we have $e_{n+1}\bar{d} = d^*e_{n+1}$. Then

$$ce_{n+1}\bar{d} + d\bar{e}_{n+1}\bar{c} = (cd^* - dc^*)e_{n+1} = (cd^* - (cd^*)^*)e_{n+1} = 0,$$

due to the Ahlfors condition I.16.4.ii. Similarly, $ae_{n+1}\bar{b} + b\bar{e}_{n+1}\bar{a} = 0$ and $ae_{n+1}\bar{d} + b\bar{e}_{n+1}\bar{c} = (ad^* - bc^*)e_{n+1} = \delta e_{n+1}$.

The image MCM^* of the cycle $C = (0, l, 0)$ is $(c\bar{l}\bar{d} + d\bar{l}\bar{c}, a\bar{l}\bar{d} + b\bar{l}\bar{c}, a\bar{l}\bar{b} + b\bar{l}\bar{a})$. From the above calculations for $l = x + re_{n+1}$ it becomes $(cx\bar{d} + d\bar{x}\bar{c}, \alpha x\bar{d} + b\bar{x}\bar{c} + \delta re_{n+1}, \alpha x\bar{b} + b\bar{x}\bar{a})$. The rest of statement is verified by the substitution. \square

Thus, we have exactly the same freedom to choose representing horocycles as in Section I.16.4: make two consecutive horocycles either tangent or orthogonal. To visualise this, we may use the two-dimensional plane V passing the points of contacts of two consecutive horocycles and orthogonal to $x_{n+1} = 0$. It is natural to choose the connecting cycle (drawn in blue on Fig. I.16.2) with the centre belonging to V , this eliminates excessive degrees of freedom. The corresponding parameters are described in the second part of Lem. I.16.7. Then, the intersection of horocycles with V are the same as on Fig. I.16.2.

Thus, the continued fraction with the partial quotients $\frac{P_n \bar{Q}_n}{|Q_n|^2} \in \mathbb{R}^n$ can be represented by the chain of tangent/orthogonal horocycles. The observation made at the end of Section I.16.4 on computational advantage of orthogonal horocycles remains valid in multidimensional situation as well.

As a further alternative we may shift the focus from horocycles to the connecting cycle (drawn in blue on Fig. I.16.2). The part of the space \mathbb{R}^n enclosed inside the connecting cycle is the image under the corresponding Möbius transformation of the half-space of \mathbb{R}^n cut by the hyperplane $(0, l, 0)$ from Lem. I.16.7. Assume a sequence of connecting cycles C_j satisfies the following two conditions, e.g. in Seidel–Stern-type theorem [28, Thm 4.1]:

- i. for any j , the cycle C_j is enclosed within the cycle C_{j-1} ;
- ii. the sequence of radii of C_j tends to zero.

Under the above assumption the sequence of partial fractions converges. Furthermore, if we use the connecting cycles in the third arrangement, that is generated by the cycle $(0, x + e_{n+1}, 0)$, where $\|x\| = 1, x \in \mathbb{R}^n$, then the above second condition can be replaced by following

- (2') the sequence of $x_{n+1}^{(j)}$ of $(n+1)$ -th coordinates of the centres of the connecting cycles C_j tends to zero.

Thus, the sequence of connecting cycles is a useful tool to describe a continued fraction even without a relation to horocycles.

Summing up, we started from multidimensional continued fractions defined through the composition of Möbius transformations in Clifford algebras and associated to it the respective chain of horocycles. This establishes the equivalence of two approaches proposed in [22] and [28] respectively.

Part II

Harmonic Analysis

Elements of the Representation Theory

II.1.1. Representations of Groups

Objects unveil their nature in actions. Groups act on other sets by means of *representations*. A representation of a group G is a group homomorphism of G in a transformation group of a set. It is a fundamental observation that *linear* objects are easier to study. Therefore we begin from linear representations of groups.

DEFINITION II.1.1. A linear continuous *representation of a group* G is a continuous function $T(g)$ on G with values in the group of non-degenerate linear continuous transformation in a linear space H (either finite or infinite dimensional) such that $T(g)$ satisfies to the functional identity:

$$(II.1.1) \quad T(g_1 g_2) = T(g_1) T(g_2).$$

REMARK II.1.2. If we have a representation of a group G by its action on a set X we can use the following *linearization procedure*. Let us consider a linear space $L(X)$ of functions $X \rightarrow \mathbb{C}$ which may be restricted by some additional requirements (e.g. integrability, boundedness, continuity, etc.). There is a natural representation of G on $L(X)$ which produced by its action on X :

$$(II.1.2) \quad g : f(x) \mapsto \rho_g f(x) = f(g^{-1} \cdot x), \quad \text{where } g \in G, x \in X.$$

Clearly this representation is already linear. However in many practical cases the formula for linearization (II.1.2) has some additional terms which are required to make it, for example, unitary.

EXERCISE II.1.3. Show that $T(g^{-1}) = T^{-1}(g)$ and $T(e) = I$, where I is the identity operator on H .

EXERCISE II.1.4. Show that these are linear continuous representations of corresponding groups:

- i. Operators $T(x)$ such that $[T(x) f](t) = f(t + x)$ form a representation of \mathbb{R} in $L_2(\mathbb{R})$.
- ii. Operators $T(n)$ such that $T(n)a_k = a_{k+n}$ form a representation of \mathbb{Z} in ℓ_2 .
- iii. Operators $T(a, b)$ defined by

$$(II.1.3) \quad [T(a, b) f](x) = \sqrt{a} f(ax + b), \quad a \in \mathbb{R}_+, b \in \mathbb{R}$$

form a representation of **$ax + b$ group** in $L_2(\mathbb{R})$.

iv. Operators $T(s, x, y)$ defined by

$$(II.1.4) \quad [T(s, x, y) f](t) = e^{i(2s - \sqrt{2}yt + xy)} f(t - \sqrt{2}x)$$

form *Schrödinger representation* of the **Heisenberg group** \mathbb{H}^1 in $L_2(\mathbb{R})$.

v. Operators $T(g)$ defined by

$$(II.1.5) \quad [T(g)f](t) = \frac{1}{ct+d} f\left(\frac{at+b}{ct+d}\right), \quad \text{where } g^{-1} = \begin{pmatrix} a & b \\ c & d \end{pmatrix},$$

form a representation of **$SL_2(\mathbb{R})$** in $L_2(\mathbb{R})$.

In the sequel a representation *always means* linear continuous representation. $T(g)$ is an *exact representation* (or *faithful representation* if $T(g) = I$ only for $g = e$). The opposite case when $T(g) = I$ for all $g \in G$ is a *trivial representation*. The space H is *representation space* and in most cases will be a *Hilber space* [164, § III.5]. If dimensionality of H is finite then T is a *finite dimensional representation*, in the opposite case it is *infinite dimensional representation*.

We denote the *scalar product* on H by $\langle \cdot, \cdot \rangle$. Let $\{e_j\}$ be an (finite or infinite) *orthonormal basis* in H , i.e.

$$\langle e_j, e_j \rangle = \delta_{jk},$$

where δ_{jk} is the *Kroneker delta*, and linear span of $\{e_j\}$ is dense in H .

DEFINITION II.1.5. The *matrix elements* $t_{jk}(g)$ of a representation T of a group G (with respect to a basis $\{e_j\}$ in H) are complex valued functions on G defined by

$$(II.1.6) \quad t_{jk}(g) = \langle T(g)e_j, e_k \rangle.$$

EXERCISE II.1.6. Show that [333, § 1.1.3]

- i. $T(g) e_k = \sum_j t_{jk}(g) e_j$.
- ii. $t_{jk}(g_1 g_2) = \sum_n t_{jn}(g_1) t_{nk}(g_2)$.

It is typical mathematical questions to determine identical objects which may have a different appearance. For representations it is solved in the following definition.

DEFINITION II.1.7. Two representations T_1 and T_2 of the same group G in spaces H_1 and H_2 correspondingly are *equivalent representations* if there exist a linear operator $A : H_1 \rightarrow H_2$ with the continuous inverse operator A^{-1} such that:

$$T_2(g) = A T_1(g) A^{-1}, \quad \forall g \in G.$$

EXERCISE II.1.8. Show that representation $T(a, b)$ of **$ax + b$ group** in $L_2(\mathbb{R})$ from Exercise II.1.4.iii is equivalent to the representation

$$(II.1.7) \quad [T_1(a, b) f](x) = \frac{e^{i\frac{b}{a}}}{\sqrt{a}} f\left(\frac{x}{a}\right).$$

HINT. Use the Fourier transform. □

The *relation of equivalence* is reflexive, symmetric, and transitive. Thus it splits the set of all representations of a group G into *classes of equivalent representations*. In the sequel we study *group representations up to their equivalence classes only*.

EXERCISE II.1.9. Show that equivalent representations have the same **matrix elements** in appropriate basis.

DEFINITION II.1.10. Let T be a representation of a group G in a Hilbert space H . The *adjoint representation* $T'(g)$ of G in H is defined by

$$T'(g) = (T(g^{-1}))^*,$$

where $*$ denotes the adjoint operator in H .

EXERCISE II.1.11. Show that

- i. T' is indeed a representation.
- ii. $t'_{jk}(g) = \bar{t}_{kj}(g^{-1})$.

Recall [164, § III.5.2] that a bijection $U : H \rightarrow H$ is a *unitary operator* if

$$\langle Ux, Uy \rangle = \langle x, y \rangle, \quad \forall x, y \in H.$$

EXERCISE II.1.12. Show that $UU^* = I$.

DEFINITION II.1.13. T is a *unitary representation* of a group G in a space H if $T(g)$ is a unitary operator for all $g \in G$. T_1 and T_2 are *unitary equivalent representations* if $T_1 = UT_2U^{-1}$ for a unitary operator U .

- EXERCISE II.1.14.
- i. Show that all representations from Exercises II.1.4 are unitary.
 - ii. Show that representations from Exercises II.1.4.iii and II.1.8 are unitary equivalent.

HINT. Take that the Fourier transform is unitary for granted. □

EXERCISE II.1.15. Show that if a Lie group G is represented by unitary operators in H then its Lie algebra \mathfrak{g} is represented by selfadjoint (possibly unbounded) operators in H .

The following definition have a sense for *finite* dimensional representations.

DEFINITION II.1.16. A *character of representation* T is equal $\chi(g) = \text{tr}(T(g))$, where tr is the *trace* [164, § III.5.2 (Probl.)] of operator.

EXERCISE II.1.17. Show that

- i. Characters of a representation T are constant on the **adjoint elements** $g^{-1}hg$, for all $g \in G$.
- ii. Character is an algebra homomorphism from an algebra of representations with Kronecker's (tensor) multiplication [333, § 1.9] to complex numbers.

HINT. Use that $\text{tr}(AB) = \text{tr}(BA)$, $\text{tr}(A+B) = \text{tr} A + \text{tr} B$, and $\text{tr}(A \otimes B) = \text{tr} A \text{tr} B$. □

For *infinite* dimensional representation characters can be defined either as distributions [159, § 11.2] or in infinitesimal terms of Lie algebras [159, § 11.3].

The characters of a representation should not be confused with the following notion.

DEFINITION II.1.18. A *character* of a group G is a one-dimensional representation of G .

- EXERCISE II.1.19.
- i. Let χ be a **character of a group** G . Show that a **character of representation** χ coincides with it and thus is a character of G .
 - ii. A **matrix element** of a group character χ coincides with χ .
 - iii. Let χ_1 and χ_2 be **characters of a group** G . Show that $\chi_1 \otimes \chi_2 = \chi_1 \chi_2$ and $\chi'(g) = \chi_1(g^{-1})$ are again characters of G . In other words *characters of a group form a group themselves*.

II.1.2. Decomposition of Representations

The important part of any mathematical theory is classification theorems on structural properties of objects. Very well known examples are:

- i. The main theorem of arithmetic on unique representation an integer as a product of powers of prime numbers.
- ii. *Jordan's normal form of a matrix*.

The similar structural results in the representation theory are very difficult. The easiest (but still rather difficult) questions are on classification of **unitary representations** up to **unitary equivalence**.

DEFINITION II.1.20. Let T be a representation of G in H . A linear subspace $L \subset H$ is *invariant subspace* for T if for any $x \in L$ and any $g \in G$ the vector $T(g)x$ again belong to L .

There are always two trivial invariant subspaces: the null space and entire H . All other are *non-trivial invariant subspaces*.

DEFINITION II.1.21. If there are only two trivial invariant subspaces then T is *irreducible representation*. Otherwise we have *reducible representation*.

For any non-trivial invariant subspace we can define the *restriction of representation* of T on it. In this way we obtain a *subrepresentation* of T .

EXAMPLE II.1.22. Let $T(a)$, $a \in \mathbb{R}_+$ be defined as follows: $[T(a)]f(x) = f(ax)$. Then spaces of **even and odd functions** are invariant.

DEFINITION II.1.23. If the closure of linear span of all vectors $T(g)v$ is dense in H then v is called *cyclic vector* for T .

EXERCISE II.1.24. Show that for an irreducible representation any non-zero vector is cyclic.

The following important result of representation theory of compact groups is a consequence of the Exercise I.2.33 and we state here it without a proof.

THEOREM II.1.25. [159, § 9.2]

- i. *Every topologically irreducible representation of a compact group G is finite-dimensional and unitarizable.*
- ii. *If T_1 and T_2 are two inequivalent irreducible representations, then every **matrix element** of T_1 is orthogonal in $L_2(G)$ to every matrix element of T_2 .*

iii. For a compact group G its dual space \hat{G} is discrete.

The important property of unitary representation is complete reducibility.

EXERCISE II.1.26. Let a unitary representation T has an invariant subspace $L \subset H$, then its orthogonal completion L^\perp is also invariant.

DEFINITION II.1.27. A representation on H is called decomposable if there are two non-trivial invariant subspaces H_1 and H_2 of H such that $H = H_1 \oplus H_2$.

If a representation is not decomposable then its primary.

THEOREM II.1.28. [159, § 8.4] Any unitary representation T of a locally compact group G can be decomposed in a (continuous) direct sum irreducible representations: $T = \int_X T_x \, d\mu(x)$.

The necessity of continuous sums appeared in very simple examples:

EXERCISE II.1.29. Let T be a representation of \mathbb{R} in $L_2(\mathbb{R})$ as follows: $[T(a)f](x) = e^{iax}f(x)$. Show that

- i. Any measurable set $E \subset \mathbb{R}$ define an invariant subspace of functions vanishing outside E .
- ii. T does not have invariant irreducible subrepresentations.

DEFINITION II.1.30. The set of equivalence classes of unitary irreducible representations of a group G is denoted by \hat{G} and called *dual object* (or *dual space*) of the group G .

DEFINITION II.1.31. A *left regular representation* $\Lambda(g)$ of a group G is the representation by **left shifts** in the space $L_2(G)$ of square-integrable function on G with the **left Haar measure**

$$(II.1.8) \quad \Lambda g : f(h) \mapsto f(g^{-1}h).$$

The *main problem of representation theory* is to decompose a left regular representation $\Lambda(g)$ into irreducible components.

II.1.3. Invariant Operators and Schur's Lemma

It is a pleasant feature of an abstract theory that we obtain important general statements from simple observations. **Finiteness of invariant measure** on a compact group is one such example. Another example is **Schur's Lemma** presented here.

To find different classes of representations we need to compare them each other. This is done by *intertwining operators*.

DEFINITION II.1.32. Let T_1 and T_2 are representations of a group G in a spaces H_1 and H_2 correspondingly. An operator $A : H_1 \rightarrow H_2$ is called an *intertwining operator* if

$$A T_1(g) = T_2(g) A, \quad \forall g \in G.$$

If $T_1 = T_2 = T$ then A is *interntwinig operator* or *commuting operator* for T .

EXERCISE II.1.33. Let $G, H, T(g)$, and A be as above. Show the following: [333, § 1.3.1]

- i. Let $\mathbf{x} \in H$ be an eigenvector for A with eigenvalue λ . Then $T(g)\mathbf{x}$ for all $g \in G$ are eigenvectors of A with the same eigenvalue λ .
- ii. All eigenvectors of A with a fixed eigenvalue λ for a linear subspace invariant under all $T(g)$, $g \in G$.
- iii. If an operator A is commuting with **irreducible representation** T then $A = \lambda I$.

HINT. Use the spectral decomposition of selfadjoint operators [164, § V.2.2]. \square

The next result have very important applications.

LEMMA II.1.34 (Schur). [159, § 8.2] *If two representations T_1 and T_2 of a group G are irreducible, then every **intertwining operator** between them is either zero or invertible.*

HINT. Consider subspaces $\ker A \subset H_1$ and $\text{im} A \subset H_2$. \square

EXERCISE II.1.35. Show that

- i. Two irreducible representations are either equivalent or disjunctive.
- ii. All operators commuting with an irreducible representation form a field.
- iii. Irreducible representation of commutative group are one-dimensional.
- iv. If T is unitary irreducible representation in H and $B(\cdot, \cdot)$ is a bounded semi linear form in H invariant under T : $B(T(g)\mathbf{x}, T(g)\mathbf{y}) = B(\mathbf{x}, \mathbf{y})$ then $B(\cdot, \cdot) = \lambda \langle \cdot, \cdot \rangle$.

HINT. Use that $B(\cdot, \cdot) = \langle A\cdot, \cdot \rangle$ for some A [164, § III.5.1]. \square

II.1.4. Induced Representations

The general scheme of induced representations is as follows, see [105, Ch. 6; 159, § 13.2; 170, § 3.1; 321, Ch. 5] and subsection I.2.2.2. Let G be a group and let H be its subgroup. Let $X = G/H$ be the corresponding left homogeneous space and $s : X \rightarrow G$ be a continuous function (section) [159, § 13.2] which is a right inverse to the natural projection $p : G \rightarrow G/H$.

Then any $g \in G$ has a unique decomposition of the form $g = s(x)h^{-1}$ where $x = p(g) \in X$ and $h \in H$. We define the map $r : G \rightarrow H$:

$$(II.1.9) \quad r(g) = s(x)^{-1}g, \quad \text{where } x = p(g).$$

Note that X is a left homogeneous space with the G -action defined in terms of p and s as follows, see Ex. I.2.22:

$$(II.1.10) \quad g : x \mapsto g \cdot x = p(g * s(x)),$$

where $*$ is the multiplication on G . A useful consequences of the above formulae is:

$$(II.1.11) \quad s(x) = g * s(y) * (r(g * s(y)))^{-1},$$

$$(II.1.12) \quad r(g^{-1} * s(x)) = r(g * s(y)), \quad \text{where } y = g^{-1} \cdot x \text{ for } x, y \in X \text{ and } g \in G.$$

Let $\chi : H \rightarrow B(V)$ be a linear representation of H in a vector space V , e.g. by unitary rotations in the algebra of either complex, dual or double numbers. Then χ induces a linear representation of G , which is known as *induced representation* in the sense of

Mackey [159, § 13.2]. This representation has the canonical realisation ρ in a space of V -valued functions on X . It is given by the formula (cf. [159, § 13.2.(7)–(9)]):

$$(II.1.13) \quad [\rho_\chi(g)f](x) = \chi(r(g^{-1} * s(x))) f(g^{-1} \cdot x),$$

where $g \in G$, $x \in X$, $h \in H$ and $r : G \rightarrow H$, $s : X \rightarrow G$ are maps defined above; $*$ denotes multiplication on G and \cdot denotes the action (II.1.10) of G on X from the left.

In the case of complex numbers this representation automatically becomes unitary in the space $L_2(X)$ of the functions square integrable with respect to a measure $d\mu$ if instead of the representation χ one uses the following substitute:

$$(II.1.14) \quad \chi_0(h) = \chi(h) \left(\frac{d\mu(h \cdot x)}{d\mu(x)} \right)^{\frac{1}{2}}.$$

However in our study the unitarity of representations or its proper replacements is a more subtle issue and we will consider it separately.

An alternative construction of induced representations is realised on the space of functions on G which have the following property:

$$(II.1.15) \quad F(gh) = \chi(h)F(g), \quad \text{for all } h \in H.$$

This space is invariant under the left shifts. The restriction of the left regular representation to this subspace is equivalent to the induced representation described above.

- EXERCISE II.1.36. i. Write the intertwining operator for this equivalence.
 ii. Define the corresponding inner product on the space of functions II.1.15 in such a way that the above intertwining operator becomes unitary.

HINT. Use the map $s : X \rightarrow G$.

□

Wavelets on Groups and Square Integrable Representations

A matured mathematical theory looks like a tree. There is a solid trunk which supports all branches and leaves but could not be alive without them. In the case of group approach to wavelets the trunk of the theory is a construction of wavelets from a *square integrable representation* [38], [5, Chap. 8]. We begin from this trunk which is a model for many different generalisations and will continue with some smaller “generalising” branches later.

II.2.1. Wavelet Transform on Groups

Let G be a group with a left Haar measure $d\mu$ and let ρ be a unitary irreducible representation of a group G by operators $\rho_g, g \in G$ in a Hilbert space H .

DEFINITION II.2.1. Let us fix a vector $w_0 \in H$. We call $w_0 \in H$ a *vacuum vector* or a *mother wavelet* (other less-used names are *ground state*, *fiducial vector*, etc.). We will say that set of vectors $w_g = \rho(g)w_0, g \in G$ form a family of *coherent states (wavelets)*.

EXERCISE II.2.2. If ρ is irreducible then $w_g, g \in G$ is a *total set* in H , i.e. the linear span of these vectors is dense in H .

The *wavelet transform* can be defined as a mapping from H to a space of functions over G via its *representational coefficients* (also known as *matrix coefficients*):

$$(II.2.1) \quad \mathcal{W} : v \mapsto \hat{v}(g) = \langle \rho(g^{-1})v, w_0 \rangle = \langle v, \rho(g)w_0 \rangle = \langle v, w_g \rangle.$$

EXERCISE II.2.3. Show that the wavelet transform \mathcal{W} is a continuous linear mapping and the image of a vector is a bounded continuous function on G . The linear space of all such images is denoted by $W(G)$.

EXERCISE II.2.4. Let a Hilbert space H has a basis $e_j, j \in \mathbb{Z}$ and a unitary representation ρ of $G = \mathbb{Z}$ defined by $\rho(k)e_j = e_{j+k}$. Write a formula for wavelet transform with $w_0 = e_0$ and characterise $W(\mathbb{Z})$.

ANSWER. $\hat{v}(n) = \langle v, e_n \rangle$. □

EXERCISE II.2.5. Let G be $ax + b$ group and ρ is given by (cf. (II.1.3)):

$$(II.2.2) \quad [\Gamma(a, b) f](x) = \frac{1}{\sqrt{a}} f\left(\frac{x-b}{a}\right),$$

in $L_2(\mathbb{R})$. Show that

- i. The representation is reducible and describe its irreducible components.
- ii. for $w_0(x) = \frac{1}{2\pi i(x+i)}$ coherent states are $v_{(a,b)}(x) = \frac{\sqrt{a}}{2\pi i(x-(b-ia))}$.
- iii. Wavelet transform is given by

$$\hat{v}(a, b) = \frac{\sqrt{a}}{2\pi i} \int_{\mathbb{R}} \frac{v(x)}{x - (b + ia)} dx,$$

which resembles the *Cauchy integral formula*.

- iv. Give a characteristic of $W(G)$.
- v. Write the wavelet transform for the same representation of the group $ax + b$ and the *Gaussian* (or *Gauss function*) $e^{-x^2/2}$ (see Fig. II.2.1) as a mother wavelets.

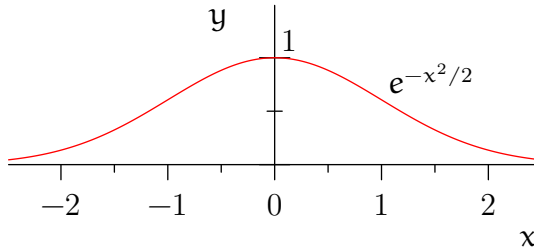


FIGURE II.2.1. The Gaussian function $e^{-x^2/2}$.

PROPOSITION II.2.6. *The wavelet transform \mathcal{W} intertwines ρ and the left regular representation Λ (II.1.8) of G :*

$$\mathcal{W}\rho(g) = \Lambda(g)\mathcal{W}.$$

PROOF. We have:

$$\begin{aligned} [\mathcal{W}(\rho(g)v)](h) &= \langle \rho(h^{-1})\rho(g)v, w_0 \rangle \\ &= \langle \rho((g^{-1}h)^{-1})v, w_0 \rangle \\ &= [\mathcal{W}v](g^{-1}h) \\ &= [\Lambda(g)\mathcal{W}v](h). \end{aligned}$$

□

COROLLARY II.2.7. *The function space $W(G)$ is invariant under the representation Λ of G .*

Wavelet transform maps vectors of H to functions on G . We can consider a map in the opposite direction sends a function on G to a vector in H .

DEFINITION II.2.8. The *inverse wavelet transform* $\mathcal{M}_{w'_0}$ associated with a vector $w'_0 \in H$ maps $L_1(G)$ to H and is given by the formula:

$$(II.2.3) \quad \begin{aligned} \mathcal{M}_{w'_0} : L_1(G) \rightarrow H : \hat{v}(g) \mapsto \mathcal{M}[\hat{v}(g)] &= \int_G \hat{v}(g) w'_g \, d\mu(g) \\ &= \int_G \hat{v}(g) \rho(g) \, d\mu(g) w'_0, \end{aligned}$$

where in the last formula the integral express an operator acting on vector w'_0 .

EXERCISE II.2.9. Write inverse wavelet transforms for Exercises II.2.4 and II.2.5.

ANSWER. i. For Exercises II.2.4: $v = \sum_{-\infty}^{\infty} \hat{v}(n) e_n$.

ii. For Exercises II.2.5:

$$v(x) = \frac{1}{2\pi i} \int_{\mathbb{R}_+^2} \frac{\hat{v}(a, b)}{x - (b - ia)} \frac{da \, db}{a^{\frac{3}{2}}}.$$

□

LEMMA II.2.10. If the wavelet transform \mathcal{W} and inverse wavelet transform \mathcal{M} are defined by the same vector w_0 then they are adjoint operators: $\mathcal{W}^* = \mathcal{M}$.

PROOF. We have:

$$\begin{aligned} \langle \mathcal{M}\hat{v}, w_g \rangle &= \left\langle \int_G \hat{v}(g') w_{g'} \, d\mu(g'), w_g \right\rangle \\ &= \int_G \hat{v}(g') \langle w_{g'}, w_g \rangle \, d\mu(g') \\ &= \int_G \hat{v}(g') \overline{\langle w_g, w_{g'} \rangle} \, d\mu(g') \\ &= \langle \hat{v}, \mathcal{W}w_g \rangle, \end{aligned}$$

where the scalar product in the first line is on H and in the last line is on $L_2(G)$. Now the result follows from the totality of coherent states w_g in H . □

PROPOSITION II.2.11. The inverse wavelet transform \mathcal{M} intertwines the representation Λ (II.1.8) on $L_2(G)$ and ρ on H :

$$\mathcal{M}\Lambda(g) = \rho(g)\mathcal{M}.$$

PROOF. We have:

$$\begin{aligned} \mathcal{M}[\Lambda(g)\hat{v}(h)] &= \mathcal{M}[\hat{v}(g^{-1}h)] \\ &= \int_G \hat{v}(g^{-1}h) w_h \, d\mu(h) \\ &= \int_G \hat{v}(h') w'_{g'h'} \, d\mu(h') \\ &= \rho(g) \int_G \hat{v}(h') w'_h \, d\mu(h') \\ &= \rho(g) \mathcal{M}[\hat{v}(h')], \end{aligned}$$

where $h' = g^{-1}h$. □

COROLLARY II.2.12. *The image $\mathcal{M}(L_1(G)) \subset H$ of subspace under the inverse wavelet transform \mathcal{M} is invariant under the representation ρ .*

An important particular case of such an invariant subspace is Gårding space.

DEFINITION II.2.13. Let $C_\infty^0(G)$ be the space of infinitely differentiable functions with compact supports. Then for the given representation ρ in H the Gårding space $\mathcal{G}(\rho) \subset H$ is the image of $C_\infty^0(G)$ under the inverse wavelet transform with all possible reconstruction vectors:

$$\mathcal{G}(\rho) = \{\mathcal{M}_w \phi \mid w \in H, \phi \in C_\infty^0(G)\}.$$

COROLLARY II.2.14. *The Gårding space is invariant under the derived representation $d\rho$.*

The following proposition explain the usage of the name “inverse” (not “adjoint” as it could be expected from Lemma II.2.10) for \mathcal{M} .

THEOREM II.2.15. *The operator*

$$(II.2.4) \quad \mathcal{P} = \mathcal{M}\mathcal{W} : H \rightarrow H$$

maps H into its linear subspace for which w'_0 is cyclic. Particularly if ρ is an irreducible representation then \mathcal{P} is cI for some constant c depending from w_0 and w'_0 .

PROOF. It follows from Propositions II.6.27 and II.2.11 that operator $\mathcal{M}\mathcal{W} : H \rightarrow H$ intertwines ρ with itself. Then Corollaries II.6.28 and II.6.31 imply that the image $\mathcal{M}\mathcal{W}$ is a ρ -invariant subspace of H containing w_0 . From irreducibility of ρ by Schur's Lemma [159, § 8.2] one concludes that $\mathcal{M}\mathcal{W} = cI$ on C for a constant $c \in \mathbb{C}$. \square

REMARK II.2.16. From Exercises II.2.4 and II.2.9 it follows that irreducibility of ρ is not necessary for $\mathcal{M}\mathcal{W} = cI$, it is sufficient that w_0 and w'_0 are cyclic only.

We have similarly

THEOREM II.2.17. *Operator $\mathcal{W}\mathcal{M}$ is up to a complex multiplier a projection of $L_1(G)$ to $W(G)$.*

II.2.2. Square Integrable Representations

So far our consideration of wavelets was mainly algebraic. Usually in analysis we wish that the wavelet transform can preserve an analytic structure, e.g. values of scalar product in Hilbert spaces. This accomplished if a representation ρ possesses the following property.

DEFINITION II.2.18. [159, § 9.3] Let a group G with a left Haar measure $d\mu$ have a unitary representation $\rho : G \rightarrow \mathcal{L}(H)$. A vector $w \in H$ is called *admissible vector* if the function $\hat{w}(g) = \langle \rho(g)w, w \rangle$ is non-void and square integrable on G with respect to $d\mu$:

$$(II.2.5) \quad 0 < c^2 = \int_G \langle \rho(g)w, w \rangle \langle w, \rho(g)w \rangle d\mu(g) < \infty.$$

If an admissible vector exists then ρ is a *square integrable representation*.

Square integrable representations of groups have many interesting properties (see [85, § 14] for unimodular groups and [87], [5, Chap. 8] for not unimodular generalisation) which are crucial in the construction of wavelets. For example, for a square integrable representation all functions $\langle \rho(g)v_1, v_2 \rangle$ with an admissible vector v_1 and any $v_2 \in H$ are square integrable on G ; such representation belong to *discrete series*; etc.

EXERCISE II.2.19. Show that

- i. Admissible vectors form a linear space.
- ii. For an irreducible ρ the set of admissible vectors is dense in H or empty.

HINT. The set of all admissible vectors is an ρ -invariant subspace of H . □

EXERCISE II.2.20. i. Find a condition for a vector to be admissible for the representation (II.2.2) (and therefore the representation is square integrable).

ii. Show that $w_0(x) = \frac{1}{2\pi i(x+i)}$ is admissible for $ax + b$ group.

iii. Show that the Gaussian e^{-x^2} is *not* admissible for $ax + b$ group.

For an admissible vector w we take its normalisation $w_0 = \frac{\|w\|}{c} w$ to obtain:

$$(II.2.6) \quad \int_G |\langle \rho(g)w_0, w_0 \rangle|^2 d\mu(g) = \|w_0\|^2.$$

Such a w_0 as a vacuum state produces many useful properties.

PROPOSITION II.2.21. *If both wavelet transform \mathcal{W} and inverse wavelet transform \mathcal{M} for an irreducible square integrable representation ρ are defined by the same admissible vector w_0 then the following three statements are equivalent:*

- i. w_0 satisfy (II.2.6);
- ii. $\mathcal{M}\mathcal{W} = I$;
- iii. for any vectors $v_1, v_2 \in H$:

$$(II.2.7) \quad \langle v_1, v_2 \rangle = \int_G \hat{v}_1(g) \overline{\hat{v}_2(g)} d\mu(g).$$

PROOF. We **already knew** that $\mathcal{M}\mathcal{W} = cI$ for a constant $c \in \mathbb{C}$. Then (II.2.6) exactly says that $c = 1$. Because \mathcal{W} and \mathcal{M} **are adjoint operators** it follows from $\mathcal{M}\mathcal{W} = I$ on H that:

$$\langle v_1, v_2 \rangle = \langle \mathcal{M}\mathcal{W}v_1, v_2 \rangle = \langle \mathcal{W}v_1, \mathcal{M}^*v_2 \rangle = \langle \mathcal{W}v_1, \mathcal{W}v_2 \rangle,$$

which is exactly the isometry of \mathcal{W} (II.2.7). Finally condition (II.2.6) is a particular case of general isometry of \mathcal{W} for vector w_0 . □

EXERCISE II.2.22. Write the isometry conditions (II.2.7) for wavelet transforms for \mathbb{Z} and $ax + b$ groups (Exercises II.2.4 and II.2.5).

Wavelets from square integrable representation closely related to the following notion:

DEFINITION II.2.23. A *reproducing kernel* on a set X with a measure is a function $K(x, y)$ such that:

$$(II.2.8) \quad K(x, x) > 0, \quad \forall x \in X,$$

$$(II.2.9) \quad K(x, y) = \overline{K(y, x)},$$

$$(II.2.10) \quad K(x, z) = \int_X K(x, y)K(y, z) \, dy.$$

PROPOSITION II.2.24. The image $W(G)$ of the wavelet transform \mathcal{W} has a reproducing kernel $K(g, g') = \langle w_g, w_{g'} \rangle$. The reproducing formula is in fact a convolution:

$$(II.2.11) \quad \begin{aligned} \hat{v}(g') &= \int_G K(g', g)\hat{v}(g) \, d\mu(g) \\ &= \int_G \hat{w}_0(g^{-1}g')\hat{v}(g) \, d\mu(g) \end{aligned}$$

with a wavelet transform of the vacuum vector $\hat{w}_0(g) = \langle w_0, \rho(g)w_0 \rangle$.

PROOF. Again we have a simple application of the previous formulas:

$$(II.2.12) \quad \begin{aligned} \hat{v}(g') &= \langle \rho(g'^{-1})v, w_0 \rangle \\ &= \int_G \langle \rho(h^{-1})\rho(g'^{-1})v, w_0 \rangle \overline{\langle \rho(h^{-1})w_0, w_0 \rangle} \, d\mu(h) \\ &= \int_G \langle \rho((g'h)^{-1})v, w_0 \rangle \langle \rho(h)w_0, w_0 \rangle \, d\mu(h) \\ &= \int_G \hat{v}(g'h) \hat{w}_0(h^{-1}) \, d\mu(h) \\ &= \int_G \hat{v}(g) \hat{w}_0(g^{-1}g') \, d\mu(g), \end{aligned}$$

where transformation (II.2.12) is due to (II.2.7). \square

EXERCISE II.2.25. Write reproducing kernels for wavelet transforms for \mathbb{Z} and $ax+b$ groups (Exercises II.2.4 and II.2.5).

EXERCISE* II.2.26. Operator (II.2.11) of convolution with \hat{w}_0 is an orthogonal projection of $L_2(G)$ onto $W(G)$.

HINT. Use that an left invariant subspace of $L_2(G)$ is in fact an right ideal in convolution algebra, see Lemma I.2.36. \square

REMARK II.2.27. To possess a reproducing kernel—is a well-known property of spaces of analytic functions. The space $W(G)$ shares also another important property of analytic functions: it belongs to a kernel of a certain first order differential operator with Clifford coefficients (the Dirac operator) and a second order operator with scalar coefficients (the Laplace operator) [15, 170, 172, 223], which we will consider that later too.

We consider only fundamentals of the wavelet construction here. There are much results which can be stated in an abstract level. To avoid repetition we will formulate it later on together with an interesting examples of applications.

The construction of wavelets from square integrable representations is general and straightforward. However we can not use it everywhere we may wish:

- i. Some important representations are not square integrable.
- ii. Some groups, e.g. \mathbb{H}^n , do not have square representations at all.
- iii. Even if representation is square integrable, some important vacuum vectors are not admissible, e.g. the Gaussian e^{-x^2} in **II.2.20.iii**.
- iv. Sometimes we are interested in Banach spaces, while unitary square integrable representations are acting only on Hilbert spaces.

To be vivid the trunk of the wavelets theory should split into several branches adopted to particular cases and we describe some of them in the next lectures.

II.2.3. Fundamentals of Wavelets on Homogeneous Spaces

Let G be a group and H be its closed normal subgroup. Let $X = G/H$ be the corresponding **homogeneous space** with a left invariant measure $d\mu$. Let $s : X \rightarrow G$ be a Borel section in the principal bundle of the natural projection $p : G \rightarrow G/H$. Let ρ be a continuous representation of a group G by invertible unitary operators $\rho(g)$, $g \in G$ in a Hilbert space H .

For any $g \in G$ there is a unique decomposition of the form $g = s(x)h$, $h \in H$, $x = p(g) \in X$. We will define $r : G \rightarrow H : r(g) = h = (s(p(g)))^{-1}g$ from the previous equality. Then there is a geometric action of G on $X \rightarrow X$ defined as follows

$$g : x \mapsto g^{-1} \cdot x = p(g^{-1}s(x)).$$

EXAMPLE II.2.28. As a subgroup H we select now the center of \mathbb{H}^n consisting of elements $(t, 0)$. Of course $X = G/H$ isomorphic to \mathbb{C}^n and mapping $s : \mathbb{C}^n \rightarrow G$ simply is defined as $s(z) = (0, z)$. The Haar measure on \mathbb{H}^n coincides with the standard Lebesgue measure on \mathbb{R}^{2n+1} [321, § 1.1] thus the invariant measure on X also coincides with the Lebesgue measure on \mathbb{C}^n . Note also that composition law $p(g \cdot s(z))$ reduces to Euclidean shifts on \mathbb{C}^n . We also find $p((s(z_1))^{-1} \cdot s(z_2)) = z_2 - z_1$ and $r((s(z_1))^{-1} \cdot s(z_2)) = \frac{1}{2} \mathcal{J} \bar{z}_1 z_2$.

Let $\rho : G \rightarrow \mathcal{L}(V)$ be a unitary representation of the group G by operators in a Hilbert space V .

DEFINITION II.2.29. Let $G, H, X = G/H, s : X \rightarrow G, \rho : G \rightarrow \mathcal{L}(V)$ be as above. We say that $w_0 \in H$ is a *vacuum vector* if it satisfies to the following two conditions:

$$(II.2.13) \quad \rho(h)w_0 = \chi(h)w_0, \quad \chi(h) \in \mathbb{C}, \quad \text{for all } h \in H;$$

$$(II.2.14) \quad \int_X |\langle w_0, \rho(s(x))w_0 \rangle|^2 dx = \|w_0\|^2.$$

We will say that set of vectors $w_x = \rho(x)w_0$, $x \in X$ form a family of *coherent states*.

Note that mapping $h \rightarrow \chi(h)$ from (II.2.13) defines a character of the subgroup H . The condition (II.2.14) can be easily achieved by a renormalisation w_0 as soon as we sure that the integral in the left hand side is finite and non-zero.

CONVENTION II.2.30. In that follow we will usually write $x \in X$ and $x^{-1} \in X$ instead of $s(x) \in G$ and $s(x)^{-1} \in G$ correspondingly. The right meaning of “ x ” can be easily found from the context (whether an element of X or G is expected there).

EXAMPLE II.2.31. As a “vacuum vector” we will select the original *vacuum vector of quantum mechanics*—the *Gauss function* $w_0(q) = e^{-q^2/2}$ (see Figure II.2.1), which belongs to all $L_2(\mathbb{R}^n)$. Its transformations are defined as follow:

$$\begin{aligned} w_g(q) = [\rho_{(s,z)}w_0](q) &= e^{i(2s-\sqrt{2}xq+xy)} e^{-(q-\sqrt{2}y)^2/2} \\ &= e^{2is-(x^2+y^2)/2} e^{((x+iy)^2-q^2)/2-\sqrt{2}i(x+iy)q} \\ &= e^{2is-z\bar{z}/2} e^{(z^2-q^2)/2-\sqrt{2}izq}. \end{aligned}$$

Particularly $[\rho_{(t,0)}w_0](q) = e^{-2it}w_0(q)$, i.e., it really is a vacuum vector in the sense of our definition with respect to H .

EXERCISE II.2.32. Check the square integrability condition (II.2.14) for $w_0(q) = e^{-q^2/2}$.

The wavelet transform (similarly to **the group case**) can be defined as a mapping from V to a space of bounded continuous functions over G via representational coefficients

$$v \mapsto \hat{v}(g) = \langle \rho(g^{-1})v, w_0 \rangle = \langle v, \rho(g)w_0 \rangle.$$

Due to (II.2.13) such functions have simple transformation properties along H -orbits:

$$\begin{aligned} \hat{v}(gh) &= \langle v, \rho(gh)w_0 \rangle \\ &= \langle v, \rho(g)\rho(h)w_0 \rangle \\ &= \langle v, \rho(g)\chi(h)w_0 \rangle \\ &= \bar{\chi}(h) \langle v, \rho(g)w_0 \rangle \\ &= \bar{\chi}(h)\hat{v}(g), \quad \text{where } g \in G, h \in H. \end{aligned}$$

Thus the wavelet transform is completely defined by its values indexed by points of $X = G/H$. Therefore we prefer to consider so called induced wavelet transform.

REMARK II.2.33. In the earlier papers [170], [173] we use name *reduced* wavelet transform since it produces functions on a homogeneous space rather than the entire group. From now on we prefer the name *induced wavelet transform* due to its explicit connection with induced representations.

DEFINITION II.2.34. The *induced wavelet transform* \mathcal{W} from a Hilbert space H to a space of function $W(X)$ on a homogeneous space $X = G/H$ defined by a representation ρ of G on H , a vacuum vector w_0 is given by the formula

$$(II.2.15) \quad \mathcal{W} : H \rightarrow W(X) : v \mapsto \hat{v}(x) = [\mathcal{W}v](x) = \langle \rho(x^{-1})v, w_0 \rangle = \langle v, \rho(x)w_0 \rangle.$$

EXAMPLE II.2.35. The transformation (II.2.15) with the kernel $[\rho_{(0,z)}w_0](q)$ is an embedding $L_2(\mathbb{R}^n) \rightarrow L_2(\mathbb{C}^n)$ and is given by the formula

$$\begin{aligned}
 \hat{f}(z) &= \langle f, \rho_{s(z)}f_0 \rangle \\
 &= \pi^{-n/4} \int_{\mathbb{R}^n} f(q) e^{-z\bar{z}/2} e^{-(z^2+q^2)/2+\sqrt{2}zq} dq \\
 \text{(II.2.16)} \quad &= e^{-z\bar{z}/2} \pi^{-n/4} \int_{\mathbb{R}^n} f(q) e^{-(z^2+q^2)/2+\sqrt{2}zq} dq.
 \end{aligned}$$

Then $\hat{f}(g)$ belongs to $L_2(\mathbb{C}^n, dg)$ or its preferably to say that function $\check{f}(z) = e^{z\bar{z}/2}\hat{f}(t_0, z)$ belongs to space $L_2(\mathbb{C}^n, e^{-|z|^2} dg)$ because $\check{f}(z)$ is analytic in z . Such functions form the Segal-Bargmann space $F_2(\mathbb{C}^n, e^{-|z|^2} dg)$ of functions [17, 301], which are analytic by z and square-integrable with respect to the Gaussian measure Gauss measure $e^{-|z|^2} dz$. We use notation \check{W} for the mapping $v \mapsto \check{v}(z) = e^{z\bar{z}/2}\mathcal{W}v$. Analyticity of $\check{f}(z)$ is equivalent to the condition $(\frac{\partial}{\partial \bar{z}_j} + \frac{1}{2}z_j I)\check{f}(z) = 0$. The integral in (II.2.16) is the well-known Segal-Bargmann transform [17, 301].

EXERCISE II.2.36. Check that $\check{w}_0(z) = 1$ for the vacuum vector $w_0(q) = e^{-q^2/2}$.

There is a natural representation of G in $W(X)$. It can be obtained if we first lift functions from X to G , apply the left regular representation Λ and then pul them back to X . The result defines a representation $\lambda(g) : W(X) \rightarrow W(X)$ as follow

$$\text{(II.2.17)} \quad [\lambda(g)f](x) = \bar{\chi}(r(g^{-1} \cdot x))f(g^{-1} \cdot x).$$

We recall that $\chi(h)$ is a character of H defined in (II.2.13) by the vacuum vector w_0 . Of course, for the case of trivial $H = \{e\}$ (II.2.17) becomes the left regular representation $\Lambda(g)$ of G .

PROPOSITION II.2.37. The induced wavelet transform \mathcal{W} intertwines ρ and the representation λ (II.2.17) on $W(X)$:

$$\mathcal{W}\rho(g) = \lambda(g)\mathcal{W}.$$

PROOF. We have with obvious adjustments in comparison with Proposition II.6.27:

$$\begin{aligned}
 [\mathcal{W}(\rho(g)v)](x) &= \langle \rho(g)v, \rho(x)w_0 \rangle \\
 &= \langle v, \rho(g^{-1}s(x))w_0 \rangle \\
 &= \langle v, \rho(s(g^{-1} \cdot x))\rho(r(g^{-1} \cdot x))w_0 \rangle \\
 &= \langle v, \rho(s(g^{-1} \cdot x))\chi(r(g^{-1} \cdot x))w_0 \rangle \\
 &= \bar{\chi}(r(g^{-1} \cdot x)) \langle v, \rho(s(g^{-1} \cdot x))w_0 \rangle \\
 &= \bar{\chi}(r(g^{-1} \cdot x))[\mathcal{W}v](g^{-1}x) \\
 &= \lambda(g)[\mathcal{W}v](x).
 \end{aligned}$$

□

COROLLARY II.2.38. The function space $W(X)$ is invariant under the representation λ of G .

EXAMPLE II.2.39. Integral transformation (II.2.16) intertwines the Schrödinger representation (II.1.4) with the following realisation of representation (II.2.17):

$$(II.2.18) \quad \begin{aligned} \lambda(s, z)\hat{f}(\mathbf{u}) &= \hat{f}_0(z^{-1} \cdot \mathbf{u})\bar{\chi}(s + r(z^{-1} \cdot \mathbf{u})) \\ &= \hat{f}_0(\mathbf{u} - z)\mathbf{e}^{is + i\mathcal{J}(\bar{z}\mathbf{u})} \end{aligned}$$

EXERCISE II.2.40. i. Using relation $\check{\mathcal{W}} = e^{-|z|^2/2}\mathcal{W}$ derive from above that $\check{\mathcal{W}}$ intertwines the Schrödinger representation with the following:

$$\check{\lambda}(s, z)\check{f}(\mathbf{u}) = \check{f}_0(\mathbf{u} - z)\mathbf{e}^{2is - \bar{z}\mathbf{u} - |z|^2/2}.$$

ii. Show that infinitesimal generators of representation $\check{\lambda}$ are:

$$\partial\check{\lambda}(s, 0, 0) = i\mathbf{I}, \quad \partial\check{\lambda}(0, x, 0) = -\partial_{\mathbf{u}} - \mathbf{u}\mathbf{I}, \quad \partial\check{\lambda}(0, 0, y) = i(-\partial_z + z\mathbf{I})$$

We again introduce a transform adjoint to \mathcal{W} .

DEFINITION II.2.41. The *inverse wavelet transform* \mathcal{M} from $W(X)$ to H is given by the formula:

$$(II.2.19) \quad \begin{aligned} \mathcal{M} : W(X) \rightarrow H : \hat{v}(x) \mapsto \mathcal{M}[\hat{v}(x)] &= \int_X \hat{v}(x)w_x \, d\mu(x) \\ &= \int_X \hat{v}(x)\rho(x) \, d\mu(x)w_0. \end{aligned}$$

PROPOSITION II.2.42. The *inverse wavelet transform* \mathcal{M} intertwines the representation λ on $W(X)$ and ρ on H :

$$\mathcal{M}\lambda(g) = \rho(g)\mathcal{M}.$$

PROOF. We have:

$$\begin{aligned} \mathcal{M}[\lambda(g)\hat{v}(x)] &= \mathcal{M}[\chi(r(g^{-1} \cdot x))\hat{v}(g^{-1} \cdot x)] \\ &= \int_X \chi(r(g^{-1} \cdot x))\hat{v}(g^{-1} \cdot x)w_x \, d\mu(x) \\ &= \chi(r(g^{-1} \cdot x)) \int_X \hat{v}(x')w_{g \cdot x'} \, d\mu(x') \\ &= \rho_g \int_X \hat{v}(x')w_{x'} \, d\mu(x') \\ &= \rho_g \mathcal{M}[\hat{v}(x')], \end{aligned}$$

where $x' = g^{-1} \cdot x$. □

COROLLARY II.2.43. The *image* $\mathcal{M}(W(X)) \subset H$ of subspace $W(X)$ under the *inverse wavelet transform* \mathcal{M} is *invariant* under the representation ρ .

EXAMPLE II.2.44. Inverse transformation to (II.2.16) is given by a realisation of (II.2.19):

$$\begin{aligned}
 (II.2.20) \quad f(q) &= \int_{\mathbb{C}^n} \hat{f}(z) f_{s(z)}(q) \, dz \\
 &= \int_{\mathbb{C}^n} \hat{f}(x, y) e^{iy(x-\sqrt{2}y)} e^{-(q-\sqrt{2}y)^2/2} \, dx \, dy \\
 &= \int_{\mathbb{C}^n} \check{f}(z) e^{-(z^2+q^2)/2+\sqrt{2}zq} e^{-|z|^2} \, dz.
 \end{aligned}$$

The transformation (II.2.20) intertwines the representations (II.2.18) and the Schrödinger representation (II.1.4) of the Heisenberg group.

The following proposition explain the usage of the name for \mathcal{M} .

THEOREM II.2.45. *The operator*

$$(II.2.21) \quad \mathcal{P} = \mathcal{M}\mathcal{W} : H \rightarrow H$$

is a projection of H to its linear subspace for which w_0 is cyclic. Particularly if ρ is an irreducible representation then the inverse wavelet transform \mathcal{M} is a left inverse operator on H for the wavelet transform \mathcal{W} :

$$\mathcal{M}\mathcal{W} = I.$$

PROOF. It follows from Propositions II.2.37 and II.2.42 that operator $\mathcal{M}\mathcal{W} : H \rightarrow H$ intertwines ρ with itself. Then Corollaries II.2.38 and II.2.43 imply that the image $\mathcal{M}\mathcal{W}$ is a ρ -invariant subspace of H containing w_0 . Because of $\mathcal{M}\mathcal{W}w_0 = w_0$ we conclude that $\mathcal{M}\mathcal{W}$ is a projection.

From irreducibility of ρ by Schur’s Lemma [159, § 8.2] one concludes that $\mathcal{M}\mathcal{W} = cI$ on H for a constant $c \in \mathbb{C}$. Particularly

$$\mathcal{M}\mathcal{W}w_0 = \int_X \langle \rho(x^{-1})w_0, w_0 \rangle \rho(x)w_0 \, d\mu(x) = cw_0.$$

From the condition (II.2.14) it follows that $\langle cw_0, w_0 \rangle = \langle \mathcal{M}\mathcal{W}w_0, w_0 \rangle = \langle w_0, w_0 \rangle$ and therefore $c = 1$. □

We have similar

THEOREM II.2.46. *Operator $\mathcal{W}\mathcal{M}$ is a projection of $L_1(X)$ to $W(X)$.*

COROLLARY II.2.47. *In the space $W(X)$ the strong convergence implies point-wise convergence.*

PROOF. From the definition of the wavelet transform:

$$\left| \hat{f}(x) \right| = |\langle f, \rho(x)w_0 \rangle| \leq \|f\| \|w_0\|.$$

Since the wavelet transform is an isometry we conclude that $\left| \hat{f}(x) \right| \leq c \|f\|$ for $c = \|w_0\|$, which implies the assertion about two types of convergence. □

EXAMPLE II.2.48. The corresponding operator for the Segal-Bargmann space \mathcal{P} (II.2.21) is an identity operator $L_2(\mathbb{R}^n) \rightarrow L_2(\mathbb{R}^n)$ and (II.2.21) gives an integral presentation of the Dirac delta.

While the orthoprojection $L_2(\mathbb{C}^n, e^{-|z|^2} dg) \rightarrow F_2(\mathbb{C}^n, e^{-|z|^2} dg)$ is of a separate interest and is a principal ingredient in Berezin quantization [35, 67]. We can easily find its kernel from (II.2.24). Indeed, $\hat{f}_0(z) = e^{-|z|^2}$, then the kernel is

$$\begin{aligned} K(z, w) &= \hat{f}_0(z^{-1} \cdot w) \bar{\chi}(r(z^{-1} \cdot w)) \\ &= \hat{f}_0(w - z) e^{i\Im(\bar{z}w)} \\ &= \exp\left(\frac{1}{2}(-|w - z|^2 + w\bar{z} - z\bar{w})\right) \\ &= \exp\left(\frac{1}{2}(-|z|^2 - |w|^2) + w\bar{z}\right). \end{aligned}$$

To receive the reproducing kernel for functions $\check{f}(z) = e^{|z|^2} \hat{f}(z)$ in the Segal-Bargmann space we should multiply $K(z, w)$ by $e^{(-|z|^2 + |w|^2)/2}$ which gives the standard reproducing kernel $= \exp(-|z|^2 + w\bar{z})$ [17, (1.10)].

We denote by $W^* : W^*(X) \rightarrow H$ and $\mathcal{M}^* : H \rightarrow W^*(X)$ the adjoint (in the standard sense) operators to W and \mathcal{M} respectively.

COROLLARY II.2.49. *We have the following identity:*

$$(II.2.22) \quad \langle Wv, \mathcal{M}^*l \rangle_{W(X)} = \langle v, l \rangle_H, \quad \forall v, l \in H,$$

or equivalently

$$(II.2.23) \quad \int_X \langle \rho(x^{-1})v, w_0 \rangle \langle \rho(x)w_0, l \rangle d\mu(x) = \langle v, l \rangle.$$

PROOF. We show the equality in the first form (II.2.23) (but we will apply it often in the second one):

$$\langle Wv, \mathcal{M}^*l \rangle_{W(X)} = \langle \mathcal{M}Wv, l \rangle_H = \langle v, l \rangle_H.$$

□

COROLLARY II.2.50. *The space $W(X)$ has the reproducing formula*

$$(II.2.24) \quad \hat{v}(y) = \int_X \hat{v}(x) \hat{b}_0(x^{-1} \cdot y) d\mu(x),$$

where $\hat{b}_0(y) = [Ww_0](y)$ is the wavelet transform of the vacuum vector w_0 .

PROOF. Again we have a simple application of the previous formulas:

$$\begin{aligned}
 \hat{v}(y) &= \langle \rho(y^{-1})v, w_0 \rangle \\
 \text{(II.2.25)} \quad &= \int_X \langle \rho(x^{-1})\rho(y^{-1})v, w_0 \rangle \langle \rho(x)w_0, w_0 \rangle \, d\mu(x) \\
 &= \int_X \langle \rho(s(y \cdot x)^{-1})v, w_0 \rangle \langle \rho(x)w_0, w_0 \rangle \, d\mu(x) \\
 &= \int_X \hat{v}(y \cdot x) \hat{b}_0(x^{-1}) \, d\mu(x) \\
 &= \int_X \hat{v}(x) \hat{b}_0(x^{-1}y) \, d\mu(x),
 \end{aligned}$$

where transformation (II.2.25) is due to (II.2.23). □

Hypercomplex Linear Representations

A consideration of the symmetries in analysis is natural to start from *linear representations*. The previous geometrical actions (I.1.1) can be naturally extended to such representations by **induction** [159, § 13.2; 170, § 3.1] from a representation of a subgroup H . If H is one-dimensional then its irreducible representation is a character, which is always supposed to be a complex valued. However, hypercomplex numbers naturally appeared in the $SL_2(\mathbb{R})$ action (I.1.1), see Subsection I.3.3.4 and [194], why shall we admit only $i^2 = -1$ to deliver a character then?

II.3.1. Hypercomplex Characters

As we already mentioned the typical discussion of induced representations of $SL_2(\mathbb{R})$ is centred around the case $H = K$ and a complex valued character of K . A linear transformation defined by a matrix (I.3.8) in K is a rotation of \mathbb{R}^2 by the angle t . After identification $\mathbb{R}^2 = \mathbb{C}$ this action is given by the multiplication e^{it} , with $i^2 = -1$. The rotation preserve the (elliptic) metric given by:

$$(II.3.1) \quad x^2 + y^2 = (x + iy)(x - iy).$$

Therefore the orbits of rotations are circles, any line passing the origin (a “spoke”) is rotated by the angle t , see Fig. II.3.1.

Dual and double numbers produces the most straightforward adaptation of this result.

PROPOSITION II.3.1. *The following table show correspondences between three types of algebraic characters:*

<i>Elliptic</i>	<i>Parabolic</i>	<i>Hyperbolic</i>
$i^2 = -1$	$\varepsilon^2 = 0$	$j^2 = 1$
$w = x + iy$	$w = x + \varepsilon y$	$w = x + jy$
$\bar{w} = x - iy$	$\bar{w} = x - \varepsilon y$	$\bar{w} = x - jy$
$e^{it} = \cos t + i \sin t$	$e^{\varepsilon t} = 1 + \varepsilon t$	$e^{jt} = \cosh t + j \sinh t$
$ w _e^2 = w\bar{w} = x^2 + y^2$	$ w _p^2 = w\bar{w} = x^2$	$ w _h^2 = w\bar{w} = x^2 - y^2$
$\arg w = \tan^{-1} \frac{y}{x}$	$\arg w = \frac{y}{x}$	$\arg w = \tanh^{-1} \frac{y}{x}$
<i>unit circle</i> $ w _e^2 = 1$	<i>“unit” strip</i> $x = \pm 1$	<i>unit hyperbola</i> $ w _h^2 = 1$

Geometrical action of multiplication by e^{it} is drawn in Fig. II.3.1 for all three cases.

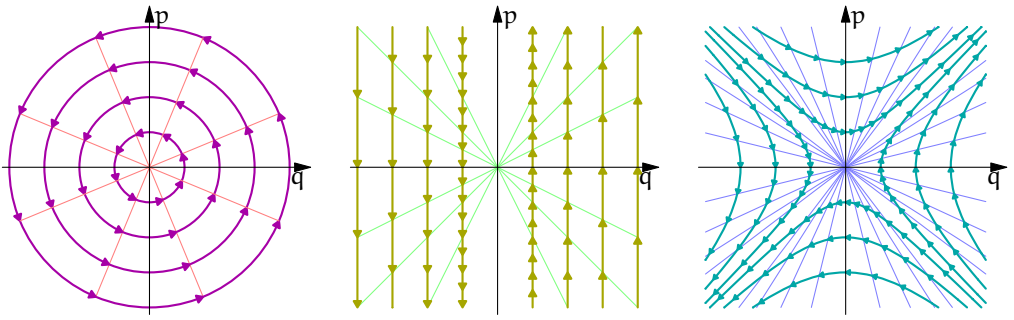


FIGURE II.3.1. Rotations of algebraic wheels, i.e. the multiplication by $e^{t\epsilon}$: elliptic (E), trivial parabolic (P_0) and hyperbolic (H). All blue orbits are defined by the identity $x^2 - t^2y^2 = r^2$. Thin “spokes” (straight lines from the origin to a point on the orbit) are “rotated” from the real axis. This is symplectic linear transformations of the classical phase space as well.

Explicitly parabolic rotations associated with $e^{\epsilon t}$ acts on dual numbers as follows:

$$(II.3.2) \quad e^{\epsilon x} : a + \epsilon b \mapsto a + \epsilon(ax + b).$$

This links the parabolic case with the Galilean group [339] of symmetries of the classic mechanics, with the absolute time disconnected from space.

The obvious algebraic similarity and the connection to classical kinematic is a wide spread justification for the following viewpoint on the parabolic case, cf. [129, 339]:

- the parabolic trigonometric functions are trivial:

$$(II.3.3) \quad \text{cosp } t = \pm 1, \quad \text{sinp } t = t;$$

- the parabolic distance is independent from y if $x \neq 0$:

$$(II.3.4) \quad x^2 = (x + \epsilon y)(x - \epsilon y);$$

- the polar decomposition of a dual number is defined by [339, App. C(30')]:

$$(II.3.5) \quad u + \epsilon v = u(1 + \epsilon \frac{v}{u}), \quad \text{thus} \quad |u + \epsilon v| = u, \quad \arg(u + \epsilon v) = \frac{v}{u};$$

- the parabolic wheel looks rectangular, see Fig. II.3.1.

Those algebraic analogies are quite explicit and widely accepted as an ultimate source for parabolic trigonometry [129, 241, 339]. Moreover, those three rotations are all non-isomorphic symplectic linear transformations of the phase space, which makes them useful in the context of classical and quantum mechanics [196, 199], see Chap. IV.1. There exist also alternative characters [188] based on Möbius transformations with geometric motivation and connections to equations of mathematical physics.

II.3.2. Induced Representations

Let G be a group, H be its closed subgroup with the corresponding homogeneous space $X = G/H$ with an invariant measure. We are using notations and definitions of

maps $p : G \rightarrow X$, $s : X \rightarrow G$ and $r : G \rightarrow H$ from Subsection ???. Let χ be an irreducible representation of H in a vector space V , then it induces a representation of G in the sense of Mackey [159, § 13.2]. This representation has the realisation ρ_χ in the space $L_2(X)$ of V -valued functions by the formula [159, § 13.2.(7)–(9)]:

$$(II.3.6) \quad [\rho_\chi(g)f](x) = \chi(r(g^{-1} * s(x)))f(g^{-1} \cdot x),$$

where $g \in G$, $x \in X$, $h \in H$ and $r : G \rightarrow H$, $s : X \rightarrow G$ are maps defined above; $*$ denotes multiplication on G and \cdot denotes the action (II.1.10) of G on X .

Consider this scheme for representations of $SL_2(\mathbb{R})$ induced from characters of its one-dimensional subgroups. We can notice that only the subgroup K requires a complex valued character due to the fact of its compactness. For subgroups N' and A' we can consider characters of all three types—elliptic, parabolic and hyperbolic. Therefore we have seven essentially different induced representations. We will write explicitly only three of them here.

EXAMPLE II.3.2. Consider the subgroup $H = K$, due to its compactness we are limited to complex valued characters of K only. All of them are of the form χ_k :

$$(II.3.7) \quad \chi_k \begin{pmatrix} \cos t & \sin t \\ -\sin t & \cos t \end{pmatrix} = e^{-ikt}, \quad \text{where } k \in \mathbb{Z}.$$

Using the explicit form (??) of the map s we find the map r given in (??) as follows:

$$r \begin{pmatrix} a & b \\ c & d \end{pmatrix} = \frac{1}{\sqrt{c^2 + d^2}} \begin{pmatrix} d & -c \\ c & d \end{pmatrix} \in K.$$

Therefore:

$$r(g^{-1} * s(u, v)) = \frac{1}{\sqrt{(cu + d)^2 + (cv)^2}} \begin{pmatrix} cu + d & -cv \\ cv & cu + d \end{pmatrix}, \quad \text{where } g^{-1} = \begin{pmatrix} a & b \\ c & d \end{pmatrix}.$$

Substituting this into (II.3.7) and combining with the Möbius transformation of the domain (I.1.1) we get the explicit realisation ρ_k of the induced representation (II.3.6):

$$(II.3.8) \quad \rho_k(g)f(w) = \frac{|cw + d|^k}{(cw + d)^k} f\left(\frac{aw + b}{cw + d}\right), \quad \text{where } g^{-1} = \begin{pmatrix} a & b \\ c & d \end{pmatrix}, \quad w = u + iv.$$

This representation acts on complex valued functions in the upper half-plane $\mathbb{R}_+^2 = SL_2(\mathbb{R})/K$ and belongs to the discrete series [240, § IX.2]. It is common to get rid of the factor $|cw + d|^k$ from that expression in order to keep analyticity:

$$(II.3.9) \quad \rho_k(g)f(w) = \frac{1}{(cw + d)^k} f\left(\frac{aw + b}{cw + d}\right), \quad \text{where } g^{-1} = \begin{pmatrix} a & b \\ c & d \end{pmatrix}, \quad w = u + iv.$$

We will often follow this practise for a convenience as well.

EXAMPLE II.3.3. In the case of the subgroup N there is a wider choice of possible characters.

- i. Traditionally only complex valued characters of the subgroup N are considered, they are:

$$(II.3.10) \quad \chi_\tau^c \begin{pmatrix} 1 & 0 \\ t & 1 \end{pmatrix} = e^{i\tau t}, \quad \text{where } \tau \in \mathbb{R}.$$

A direct calculation shows that:

$$r \begin{pmatrix} a & b \\ c & d \end{pmatrix} = \begin{pmatrix} 1 & 0 \\ \frac{c}{d} & 1 \end{pmatrix} \in N'.$$

Thus:

$$(II.3.11) \quad r(g^{-1} * s(u, v)) = \begin{pmatrix} 1 & 0 \\ \frac{cv}{d+cu} & 1 \end{pmatrix}, \quad \text{where } g^{-1} = \begin{pmatrix} a & b \\ c & d \end{pmatrix}.$$

A substitution of this value into the character (II.3.10) together with the Möbius transformation (I.1.1) we obtain the next realisation of (II.3.6):

$$\rho_{\tau}^{\mathbb{C}}(g)f(w) = \exp\left(i \frac{\tau cv}{cu + d}\right) f\left(\frac{aw + b}{cw + d}\right), \quad \text{where } w = u + \varepsilon v, \quad g^{-1} = \begin{pmatrix} a & b \\ c & d \end{pmatrix}.$$

The representation acts on the space of *complex* valued functions on the upper half-plane \mathbb{R}_+^2 , which is a subset of *dual* numbers as a homogeneous space $SL_2(\mathbb{R})/N'$. The mixture of complex and dual numbers in the same expression is confusing.

- ii. The parabolic character χ_{τ} with the algebraic flavour is provided by multiplication (II.3.2) with the dual number:

$$\chi_{\tau} \begin{pmatrix} 1 & 0 \\ t & 1 \end{pmatrix} = e^{\varepsilon \tau t} = 1 + \varepsilon \tau t, \quad \text{where } \tau \in \mathbb{R}.$$

If we substitute the value (II.3.11) into this character, then we receive the representation:

$$\rho_{\tau}(g)f(w) = \left(1 + \varepsilon \frac{\tau cv}{cu + d}\right) f\left(\frac{aw + b}{cw + d}\right),$$

where w , τ and g are as above. The representation is defined on the space of dual numbers valued functions on the upper half-plane of dual numbers. Thus expression contains only dual numbers with their usual algebraic operations. Thus it is linear with respect to them.

All characters in the previous Example are unitary. Then the general scheme of induced representations [159, § 13.2] implies their unitarity in proper senses.

THEOREM II.3.4 ([194]). *Both representations of $SL_2(\mathbb{R})$ from Example II.3.3 are unitary on the space of function on the upper half-plane \mathbb{R}_+^2 of dual numbers with the inner product:*

$$(II.3.12) \quad \langle f_1, f_2 \rangle = \int_{\mathbb{R}_+^2} f_1(w) \bar{f}_2(w) \frac{du dv}{v^2}, \quad \text{where } w = u + \varepsilon v,$$

and we use the conjugation and multiplication of functions' values in algebras of complex and dual numbers for representations $\rho_{\tau}^{\mathbb{C}}$ and ρ_{τ} respectively.

The inner product (II.3.12) is positive defined for the representation $\rho_{\tau}^{\mathbb{C}}$ but is not for the other. The respective spaces are parabolic cousins of the *Krein spaces* [12], which are hyperbolic in our sense.

II.3.3. Similarity and Correspondence: Ladder Operators

From the above observation we can deduce the following empirical principle, which has a heuristic value.

- PRINCIPLE II.3.5 (Similarity and correspondence). i. Subgroups K , N' and A' play a similar rôle in the structure of the group $SL_2(\mathbb{R})$ and its representations.
- ii. The subgroups shall be swapped simultaneously with the respective replacement of hypercomplex unit ι .

The first part of the Principle (similarity) does not look sound alone. It is enough to mention that the subgroup K is compact (and thus its spectrum is discrete) while two other subgroups are not. However in a conjunction with the second part (correspondence) the Principle have received the following confirmations so far, see [194] for details:

- The action of $SL_2(\mathbb{R})$ on the homogeneous space $SL_2(\mathbb{R})/H$ for $H = K, N'$ or A' is given by linear-fractional transformations of complex, dual or double numbers respectively.
- Subgroups K, N' or A' are isomorphic to the groups of unitary rotations of respective unit cycles in complex, dual or double numbers.
- Representations induced from subgroups K, N' or A' are unitary if the inner product spaces of functions with values in complex, dual or double numbers.

REMARK II.3.6. The principle of similarity and correspondence resembles supersymmetry between bosons and fermions in particle physics, but we have similarity between three different types of entities in our case.

Let us give another illustration to the Principle. Consider the Lie algebra \mathfrak{sl}_2 of the group $SL_2(\mathbb{R})$. Pick up the following basis in \mathfrak{sl}_2 [321, § 8.1]:

$$(II.3.13) \quad A = \frac{1}{2} \begin{pmatrix} -1 & 0 \\ 0 & 1 \end{pmatrix}, \quad B = \frac{1}{2} \begin{pmatrix} 0 & 1 \\ 1 & 0 \end{pmatrix}, \quad Z = \begin{pmatrix} 0 & 1 \\ -1 & 0 \end{pmatrix}.$$

The commutation relations between the elements are:

$$(II.3.14) \quad [Z, A] = 2B, \quad [Z, B] = -2A, \quad [A, B] = -\frac{1}{2}Z.$$

Let ρ be a representation of the group $SL_2(\mathbb{R})$ in a space V . Consider the derived representation $d\rho$ of the Lie algebra \mathfrak{sl}_2 [240, § VI.1] and denote $\tilde{X} = d\rho(X)$ for $X \in \mathfrak{sl}_2$. To see the structure of the representation ρ we can decompose the space V into eigenspaces of the operator \tilde{X} for some $X \in \mathfrak{sl}_2$, cf. the Taylor series in Section II.5.4.

EXAMPLE II.3.7. It would not be surprising that we are going to consider three cases:

- i. Let $X = Z$ be a generator of the subgroup K (I.3.8). Since this is a compact subgroup the corresponding eigenspaces $\tilde{Z}v_k = ikv_k$ are parametrised by an integer $k \in \mathbb{Z}$. The raising/lowering or ladder operators L^\pm [240, § VI.2; 321, § 8.2] are defined by the following commutation relations:

$$(II.3.15) \quad [\tilde{Z}, L^\pm] = \lambda_\pm L^\pm.$$

In other words L^\pm are eigenvectors for operators $\text{ad } Z$ of adjoint representation of \mathfrak{sl}_2 [240, § VI.2].

REMARK II.3.8. The existence of such ladder operators follows from the general properties of Lie algebras if the element $X \in \mathfrak{sl}_2$ belongs to a *Cartan subalgebra*. This is the case for vectors Z and B , which are the only two non-isomorphic types of Cartan subalgebras in \mathfrak{sl}_2 . However the third case considered in this paper, the parabolic vector $B + Z/2$, does not belong to a Cartan subalgebra, yet a sort of ladder operators is still possible with dual number coefficients. Moreover, for the hyperbolic vector B , besides the standard ladder operators an additional pair with double number coefficients will also be described.

From the commutators (II.3.15) we deduce that L^+v_k are eigenvectors of \tilde{Z} as well:

$$\begin{aligned} \tilde{Z}(L^+v_k) &= (L^+\tilde{Z} + \lambda_+L^+)v_k = L^+(\tilde{Z}v_k) + \lambda_+L^+v_k = ikL^+v_k + \lambda_+L^+v_k \\ &= (ik + \lambda_+)L^+v_k. \end{aligned}$$

Thus action of ladder operators on respective eigenspaces can be visualised by the diagram:

$$(II.3.16) \quad \dots \begin{array}{c} \xleftarrow{L^+} \\ \xrightarrow{L^-} \end{array} V_{ik-\lambda} \begin{array}{c} \xleftarrow{L^+} \\ \xrightarrow{L^-} \end{array} V_{ik} \begin{array}{c} \xleftarrow{L^+} \\ \xrightarrow{L^-} \end{array} V_{ik+\lambda} \begin{array}{c} \xleftarrow{L^+} \\ \xrightarrow{L^-} \end{array} \dots$$

Assuming $L^+ = a\tilde{A} + b\tilde{B} + c\tilde{Z}$ from the relations (II.3.14) and defining condition (II.3.15) we obtain linear equations with unknown a , b and c :

$$c = 0, \quad 2a = \lambda_+b, \quad -2b = \lambda_+a.$$

The equations have a solution if and only if $\lambda_+^2 + 4 = 0$, and the raising/lowering operators are

$$(II.3.17) \quad L^\pm = \pm i\tilde{A} + \tilde{B}.$$

- ii. Consider the case $X = 2B$ of a generator of the subgroup A' (I.3.10). The subgroup is not compact and eigenvalues of the operator \tilde{B} can be arbitrary, however raising/lowering operators are still important [140, § II.1; 251, § 1.1]. We again seek a solution in the form $L_h^+ = a\tilde{A} + b\tilde{B} + c\tilde{Z}$ for the commutator $[2\tilde{B}, L_h^+] = \lambda L_h^+$. We will get the system:

$$4c = \lambda a, \quad b = 0, \quad a = \lambda c.$$

A solution exists if and only if $\lambda^2 = 4$. There are obvious values $\lambda = \pm 2$ with the ladder operators $L_h^\pm = \pm 2\tilde{A} + \tilde{Z}$, see [140, § II.1; 251, § 1.1]. Each indecomposable \mathfrak{sl}_2 -module is formed by a one-dimensional chain of eigenvalues with a transitive action of ladder operators.

Admitting double numbers we have an extra possibility to satisfy $\lambda^2 = 4$ with values $\lambda = \pm 2j$. Then there is an additional pair of hyperbolic ladder operators $L_j^\pm = \pm 2j\tilde{A} + \tilde{Z}$, which shift eigenvectors in the ‘‘orthogonal’’ direction to the standard operators L_h^\pm . Therefore an indecomposable \mathfrak{sl}_2 -module can

be parametrised by a two-dimensional lattice of eigenvalues on the double number plane, see Fig. II.3.2

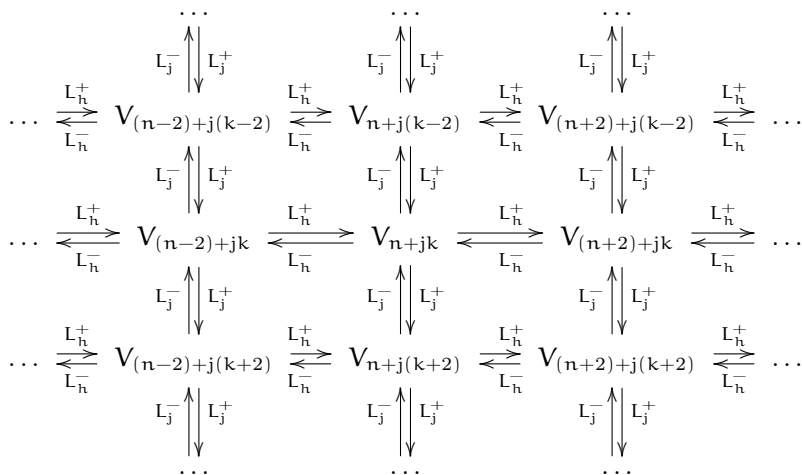


FIGURE II.3.2. The action of hyperbolic ladder operators on a 2D lattice of eigenspaces. Operators L_h^\pm move the eigenvalues by 2, making shifts in the horizontal direction. Operators L_j^\pm change the eigenvalues by $2j$, shown as vertical shifts.

iii. Finally consider the case of a generator $X = -B+Z/2$ of the subgroup N' (I.3.11). According to the above procedure we get the equations:

$$b + 2c = \lambda a, \quad -a = \lambda b, \quad \frac{a}{2} = \lambda c,$$

which can be resolved if and only if $\lambda^2 = 0$. If we restrict ourselves with the only real (complex) root $\lambda = 0$, then the corresponding operators $L_p^\pm = -\tilde{B} + \tilde{Z}/2$ will not affect eigenvalues and thus are useless in the above context. However the dual number roots $\lambda = \pm \epsilon t$, $t \in \mathbb{R}$ lead to the operators $L_\epsilon^\pm = \pm \epsilon t \tilde{A} - \tilde{B} + \tilde{Z}/2$. These operators are suitable to build an \mathfrak{sl}_2 -modules with a one-dimensional chain of eigenvalues.

REMARK II.3.9. It is noteworthy that:

- the introduction of complex numbers is a necessity for the *existence* of ladder operators in the elliptic case;
- in the parabolic case we need dual numbers to make ladder operators *useful*;
- in the hyperbolic case double numbers are not required neither for the existence or for the usability of ladder operators, but they do provide an enhancement.

We summarise the above consideration with a focus on the Principle of similarity and correspondence:

PROPOSITION II.3.10. *Let a vector $X \in \mathfrak{sl}_2$ generates the subgroup K , N' or A' , that is $X = Z$, $B - Z/2$, or B respectively. Let ι be the respective hypercomplex unit.*

Then raising/lowering operators L^\pm satisfying to the commutation relation:

$$[X, L^\pm] = \pm \iota L^\pm, \quad [L^-, L^+] = 2\iota X.$$

are:

$$L^\pm = \pm \iota \tilde{A} + \tilde{Y}.$$

Here $Y \in \mathfrak{sl}_2$ is a linear combination of B and Z with the properties:

- $Y = [A, X]$.
- $X = [A, Y]$.
- *Killings form $K(X, Y)$ [159, § 6.2] vanishes.*

Any of the above properties defines the vector $Y \in \text{span}\{B, Z\}$ up to a real constant factor.

The usability of the Principle of similarity and correspondence will be illustrated by more examples below.

Covariant Transform

A general group-theoretical construction [5, 63, 95, 106, 173, 220, 279] of *wavelets* (or *coherent state*) starts from an irreducible square integrable representation—in the proper sense or modulo a subgroup. Then a mother wavelet is chosen to be *admissible*. This leads to a wavelet transform which is an isometry to L_2 space with respect to the Haar measure on the group or (quasi)invariant measure on a homogeneous space.

The importance of the above situation shall not be diminished, however an exclusive restriction to such a setup is not necessary, in fact. Here is a classical example from complex analysis: the Hardy space $H_2(\mathbb{T})$ on the unit circle and Bergman spaces $B_2^n(\mathbb{D})$, $n \geq 2$ in the unit disk produce wavelets associated with representations ρ_1 and ρ_n of the group $SL_2(\mathbb{R})$ respectively [170]. While representations ρ_n , $n \geq 2$ are from square integrable discrete series, the mock discrete series representation ρ_1 is not square integrable [240, § VI.5; 321, § 8.4]. However it would be natural to treat the Hardy space in the same framework as Bergman ones. Some more examples will be presented below.

II.4.1. Extending Wavelet Transform

To make a sharp but still natural generalisation of wavelets we give the following definition.

DEFINITION II.4.1. [192] Let ρ be a representation of a group G in a space V and F be an operator from V to a space U . We define a *covariant transform* \mathcal{W} from V to the space $L(G, U)$ of U -valued functions on G by the formula:

$$(II.4.1) \quad \mathcal{W} : v \mapsto \hat{v}(g) = F(\rho(g^{-1})v), \quad v \in V, g \in G.$$

Operator F will be called *fiducial operator* in this context.

We borrow the name for operator F from fiducial vectors of Klauder and Skagerstam [220].

REMARK II.4.2. We do not require that fiducial operator F shall be linear. Sometimes the positive homogeneity, i.e. $F(tv) = tF(v)$ for $t > 0$, alone can be already sufficient, see Example II.6.14.

REMARK II.4.3. Usefulness of the covariant transform is in the reverse proportion to the dimensionality of the space U . The covariant transform encodes properties of v in a function $\mathcal{W}v$ on G . For a low dimensional U this function can be ultimately investigated by means of harmonic analysis. Thus $\dim U = 1$ (scalar-valued functions)

is the ideal case, however, it is unattainable sometimes, see Example II.4.12 below. We may have to use a higher dimensions of U if the given group G is not rich enough.

Moreover, the relation between the dimensionality of U and usefulness of the covariant transform shall not be taking dogmatically. Paper [201] gives an important example of covariant transform which provides a simplification even in the case of $\dim U = \dim V$.

As we will see below covariant transform is a close relative of wavelet transform. The name is chosen due to the following common property of both transformations.

THEOREM II.4.4. *The covariant transform (II.6.17) intertwines ρ and the left regular representation Λ on $L(G, U)$:*

$$\mathcal{W}\rho(g) = \Lambda(g)\mathcal{W}.$$

Here Λ is defined as usual by:

$$(II.4.2) \quad \Lambda(g) : f(h) \mapsto f(g^{-1}h).$$

PROOF. We have a calculation similar to wavelet transform [173, Prop. 2.6]. Take $u = \rho(g)v$ and calculate its covariant transform:

$$\begin{aligned} [\mathcal{W}(\rho(g)v)](h) &= [\mathcal{W}(\rho(g)v)](h) = F(\rho(h^{-1})\rho(g)v) \\ &= F(\rho((g^{-1}h)^{-1})v) \\ &= [\mathcal{W}v](g^{-1}h) \\ &= \Lambda(g)[\mathcal{W}v](h). \end{aligned}$$

□

The next result follows immediately:

COROLLARY II.4.5. *The image space $\mathcal{W}(V)$ is invariant under the left shifts on G .*

REMARK II.4.6. A further generalisation of the covariant transform can be obtained if we relax the group structure. Consider, for example, a cancellative semigroup \mathbb{Z}_+ of non-negative integers. It has a linear presentation on the space of polynomials in a variable t defined by the action $m : t^n \mapsto t^{m+n}$ on the monomials. Application of a linear functional l , e.g. defined by an integration over a measure on the real line, produces umbral calculus $l(t^n) = c_n$, which has a magic efficiency in many areas, notably in combinatorics [174, 238]. In this direction we also find fruitful to expand the notion of an intertwining operator to a token [178].

II.4.2. Examples of Covariant Transform

In this Subsection we will provide several examples of covariant transforms. Some of them will be expanded in subsequent sections, however a detailed study of all aspects will not fit into the present work. We start from the classical example of the group-theoretical wavelet transform:

EXAMPLE II.4.7. [5, 95, 95, 173, 220, 279] Let V be a Hilbert space with an inner product $\langle \cdot, \cdot \rangle$ and ρ be a unitary representation of a group G in the space V . Let $F : V \rightarrow \mathbb{C}$ be the functional $v \mapsto \langle v, v_0 \rangle$ defined by a vector $v_0 \in V$. The vector v_0 is often called

the *mother wavelet* in areas related to signal processing, the *vacuum state* in the quantum framework, etc.

In this set-up, the transformation (II.6.17) is the well-known expression for a *wavelet transform* [5, (7.48)] (or *representation coefficients*):

$$(II.4.3) \quad \mathcal{W} : v \mapsto \hat{v}(g) = \langle \rho(g^{-1})v, v_0 \rangle = \langle v, \rho(g)v_0 \rangle, \quad v \in V, g \in G.$$

The family of vectors $v_g = \rho(g)v_0$ is called *wavelets* or *coherent states*. In this case we obtain scalar valued functions on G , cf. Rem. II.6.10.

This scheme is typically carried out for a square integrable representation ρ with v_0 being an admissible vector [5, 63, 87, 95, 106, 279]. In this case the wavelet (covariant) transform is a map into the square integrable functions [87] with respect to the left Haar measure on G . The map becomes an isometry if v_0 is properly scaled. Moreover, we are able to recover the input v from its wavelet transform through the reconstruction formula, which requires an admissible vector as well, see Example II.6.20 below. The most popularised case of the above scheme is as follows.

EXAMPLE II.4.8. An isometric representation of the $ax + b$ group on $V = L_p(\mathbb{R})$ is given by the formula:

$$(II.4.4) \quad [\rho_p(a, b) f](x) = a^{-\frac{1}{p}} f\left(\frac{x-b}{a}\right).$$

The representation (II.4.4) is square integrable for $p = 2$. Any function v_0 , such that its Fourier transform $\hat{v}_0(\xi)$ satisfy to

$$(II.4.5) \quad \int_0^\infty \frac{|\hat{v}_0(\xi)|^2}{\xi} d\xi < \infty,$$

is admissible [5, § 12.2]. The continuous wavelet transform is generated by the representation (II.4.4) acting on an admissible vector v_0 in the expression (II.6.18). The image of a function from $L_2(\mathbb{R})$ is a function on the upper half-plane square integrable with respect to the measure $a^{-2} da db$. For sufficiently regular \hat{v}_0 the admissibility (II.6.20) of v_0 follows from a weaker condition

$$(II.4.6) \quad \int_{\mathbb{R}} v_0(x) dx = 0.$$

However, square integrable representations and admissible vectors do not cover all interesting cases.

EXAMPLE II.4.9. For the above $G = \text{Aff}$ and the representation (II.4.4), we consider the operators $F_\pm : L_p(\mathbb{R}) \rightarrow \mathbb{C}$ defined by:

$$(II.4.7) \quad F_\pm(f) = \frac{1}{2\pi i} \int_{\mathbb{R}} \frac{f(t) dt}{x \mp i}.$$

Then the covariant transform (II.6.17) is the Cauchy integral from $L_p(\mathbb{R})$ to the space of functions $\hat{f}(a, b)$ such that $a^{-\frac{1}{p}} \hat{f}(a, b)$ is in the Hardy space in the upper/lower half-plane $H_p(\mathbb{R}_\pm^2)$. Although the representation (II.4.4) is square integrable for $p =$

2, the function $\frac{1}{x \pm i}$ used in (II.6.22) is not an admissible vacuum vector. Thus the complex analysis become decoupled from the traditional wavelet theory. As a result the application of wavelet theory shall rely on an extraneous mother wavelets [146].

Many important objects in complex analysis are generated by inadmissible mother wavelets like (II.6.22). For example, if $F : L_2(\mathbb{R}) \rightarrow \mathbb{C}$ is defined by $F : f \mapsto F_+ f - F_- f$ then the covariant transform (II.6.17) reduces to the *Poisson integral*. If $F : L_2(\mathbb{R}) \rightarrow \mathbb{C}^2$ is defined by $F : f \mapsto (F_+ f, F_- f)$ then the covariant transform (II.6.17) represents a function f on the real line as a jump:

$$(II.4.8) \quad f(z) = f_+(z) - f_-(z), \quad f_{\pm}(z) \in H_p(\mathbb{R}_{\pm}^2)$$

between functions analytic in the upper and the lower half-planes. This makes a decomposition of $L_2(\mathbb{R})$ into irreducible components of the representation (II.4.4). Another interesting but non-admissible vector is the *Gaussian* e^{-x^2} .

EXAMPLE II.4.10. For the group $G = SL_2(\mathbb{R})$ [240] let us consider the unitary representation ρ (II.3.9) on the space of square integrable function $L_2(\mathbb{R}_{\pm}^2)$ on the upper half-plane through the Möbius transformations (I.1.1):

$$(II.4.9) \quad \rho(g) : f(z) \mapsto \frac{1}{(cz + d)^2} f\left(\frac{az + b}{cz + d}\right), \quad g^{-1} = \begin{pmatrix} a & b \\ c & d \end{pmatrix}.$$

This is a representation from the discrete series and $L_2(\mathbb{D})$ and irreducible invariant subspaces are parametrised by integers. Let F_k be the functional $L_2(\mathbb{R}_{\pm}^2) \rightarrow \mathbb{C}$ of pairing with the lowest/highest k -weight vector in the corresponding irreducible component (Bergman space) $B_k(\mathbb{R}_{\pm}^2)$, $k \geq 2$ of the discrete series [240, Ch. VI]. Then we can build an operator F from various F_k similarly to the previous Example. In particular, the jump representation (II.4.8) on the real line generalises to the representation of a square integrable function f on the upper half-plane as a sum

$$f(z) = \sum_k a_k f_k(z), \quad f_k \in B_n(\mathbb{R}_{\pm}^2)$$

for prescribed coefficients a_k and analytic functions f_k in question from different irreducible subspaces.

Covariant transform is also meaningful for principal and complementary series of representations of the group $SL_2(\mathbb{R})$, which are not square integrable [170].

EXAMPLE II.4.11. Let $G = SU(2) \times \text{Aff}$ be the Cartesian product of the groups $SU(2)$ of unitary rotations of \mathbb{C}^2 and the $ax + b$ group Aff . This group has a unitary linear representation on the space $L_2(\mathbb{R}, \mathbb{C}^2)$ of square-integrable (vector) \mathbb{C}^2 -valued functions by the formula:

$$\rho(g) \begin{pmatrix} f_1(t) \\ f_2(t) \end{pmatrix} = \begin{pmatrix} \alpha f_1(at + b) + \beta f_2(at + b) \\ \gamma f_1(at + b) + \delta f_2(at + b) \end{pmatrix},$$

where $g = \begin{pmatrix} \alpha & \beta \\ \gamma & \delta \end{pmatrix} \times (a, b) \in SU(2) \times \text{Aff}$. It is obvious that the vector Hardy space, that is functions with both components being analytic, is invariant under such action of G .

As a fiducial operator $F : L_2(\mathbb{R}, \mathbb{C}^2) \rightarrow \mathbb{C}$ we can take, cf. (II.6.22):

$$(II.4.10) \quad F \begin{pmatrix} f_1(t) \\ f_2(t) \end{pmatrix} = \frac{1}{2\pi i} \int_{\mathbb{R}} \frac{f_1(t) dt}{x - i}.$$

Thus the image of the associated covariant transform is a subspace of scalar valued bounded functions on G . In this way we can transform (without a loss of information) vector-valued problems, e.g. matrix *Wiener–Hopf factorisation* [47], to scalar question of harmonic analysis on the group G .

EXAMPLE II.4.12. A straightforward generalisation of Ex. II.6.11 is obtained if V is a Banach space and $F : V \rightarrow \mathbb{C}$ is an element of V^* . Then the covariant transform coincides with the construction of wavelets in Banach spaces [173].

EXAMPLE II.4.13. The next stage of generalisation is achieved if V is a Banach space and $F : V \rightarrow \mathbb{C}^n$ is a linear operator. Then the corresponding covariant transform is a map $\mathcal{W} : V \rightarrow L(G, \mathbb{C}^n)$. This is closely related to M.G. Krein’s works on *directing functionals* [236], see also *multiresolution wavelet analysis* [51], Clifford-valued Fock–Segal–Bargmann spaces [66] and [5, Thm. 7.3.1].

EXAMPLE II.4.14. Let F be a projector $L_p(\mathbb{R}) \rightarrow L_p(\mathbb{R})$ defined by the relation $(Ff)\hat{\ }(\lambda) = \chi(\lambda)\hat{f}(\lambda)$, where the hat denotes the Fourier transform and $\chi(\lambda)$ is the characteristic function of the set $[-2, -1] \cup [1, 2]$. Then the covariant transform $L_p(\mathbb{R}) \rightarrow C(\text{Aff}, L_p(\mathbb{R}))$ generated by the representation (II.4.4) of the affine group from F contains all information provided by the *Littlewood–Paley operator* [114, § 5.1.1].

EXAMPLE II.4.15. A step in a different direction is a consideration of non-linear operators. Take again the “ $ax + b$ ” group and its representation (II.4.4). We define F to be a homogeneous but non-linear functional $V \rightarrow \mathbb{R}_+$:

$$(II.4.11) \quad F_m(f) = \frac{1}{2} \int_{-1}^1 |f(x)| dx.$$

The covariant transform (II.6.17) becomes:

$$(II.4.12) \quad [\mathcal{W}_p f](a, b) = F(\rho_p(a, b)f) = \frac{1}{2} \int_{-1}^1 \left| a^{\frac{1}{p}} f(ax + b) \right| dx = a^{\frac{1}{p}} \frac{1}{2a} \int_{b-a}^{b+a} |f(x)| dx.$$

We will see its connections with the Hardy–Littlewood maximal functions in Example II.6.43

Since linearity has clear advantages, we may prefer to reformulate the last example through linear covariant transforms. The idea is similar to the representation of a convex function as an envelope of linear ones, cf. [108, Ch. I, Lem. 6.1]. To this end, we take a collection \mathcal{F} of linear fiducial functionals and, for a given function f , consider the set of all covariant transforms $\mathcal{W}_F f, F \in \mathcal{F}$.

EXAMPLE II.4.16. Let us return to the setup of the previous Example for $G = \text{Aff}$ and its representation (II.4.4). Consider the unit ball B in $L_\infty[-1, 1]$. Then, any $\omega \in B$

defines a bounded linear functional F_ω on $L_1(\mathbb{R})$:

$$F_\omega(f) = \frac{1}{2} \int_{-1}^1 f(x) \omega(x) dx = \frac{1}{2} \int_{\mathbb{R}} f(x) \omega(x) dx.$$

Of course, $\sup_{\omega \in B} F_\omega(f) = F_m(f)$ with F_m from (II.6.25) and for all $f \in L_1(\mathbb{R})$. Then, for the non-linear covariant transform (II.6.26) we have the following expression in terms of the linear covariant transforms generated by F_ω :

$$(II.4.13) \quad [W_1^m f](a, b) = \sup_{\omega \in B} [W_1^\omega f](a, b).$$

The presence of supremum is the price to pay for such a “linearisation”.

REMARK II.4.17. The above construction is not much different to the *grand maximal function* [314, § III.1.2]. Although, it may look like a generalisation of covariant transform, grand maximal function can be realised as a particular case of Defn. II.6.8. Indeed, let $M(V)$ be a subgroup of the group of all invertible isometries of a metric space V . If ρ represents a group G by isometries of V then we can consider the group \tilde{G} generated by all finite products of $M(V)$ and $\rho(g)$, $g \in G$ with the straightforward action $\tilde{\rho}$ on V . The grand maximal functions is produced by the covariant transform for the representation $\tilde{\rho}$ of \tilde{G} .

EXAMPLE II.4.18. Let $V = L_c(\mathbb{R}^2)$ be the space of compactly supported bounded functions on the plane. We take F be the linear operator $V \rightarrow \mathbb{C}$ of integration over the real line:

$$F : f(x, y) \mapsto F(f) = \int_{\mathbb{R}} f(x, 0) dx.$$

Let G be the group of Euclidean motions of the plane represented by ρ on V by a change of variables. Then the wavelet transform $F(\rho(g)f)$ is the *Radon transform* [127].

II.4.3. Symbolic Calculi

There is a very important class of the covariant transforms which maps operators to functions. Among numerous sources we wish to single out works of Berezin [34, 35]. We start from the Berezin *covariant symbol*.

EXAMPLE II.4.19. Let a representation ρ of a group G act on a space X . Then there is an associated representation ρ_B of G on a space $V = B(X, Y)$ of linear operators $X \rightarrow Y$ defined by the identity [35, 173]:

$$(II.4.14) \quad (\rho_B(g)A)x = A(\rho(g^{-1})x), \quad x \in X, g \in G, A \in B(X, Y).$$

Following the Remark II.6.10 we take F to be a functional $V \rightarrow \mathbb{C}$, for example F can be defined from a pair $x \in X, l \in Y^*$ by the expression $F : A \mapsto \langle Ax, l \rangle$. Then the covariant transform is:

$$W : A \mapsto \hat{A}(g) = F(\rho_B(g)A).$$

This is an example of *covariant calculus* [34, 173].

There are several variants of the last Example which are of a separate interest.

EXAMPLE II.4.20. A modification of the previous construction is obtained if we have two groups G_1 and G_2 represented by ρ_1 and ρ_2 on X and Y^* respectively. Then we have a covariant transform $B(X, Y) \rightarrow L(G_1 \times G_2, \mathbb{C})$ defined by the formula:

$$\mathcal{W} : A \mapsto \hat{A}(g_1, g_2) = \langle A\rho_1(g_1)x, \rho_2(g_2)l \rangle.$$

This generalises the above *Berezin covariant calculi* [173].

EXAMPLE II.4.21. Let us restrict the previous example to the case when $X = Y$ is a Hilbert space, $\rho_1 = \rho_2 = \rho$ and $x = l$ with $\|x\| = 1$. Then the range of the covariant transform:

$$\mathcal{W} : A \mapsto \hat{A}(g) = \langle A\rho(g)x, \rho(g)x \rangle$$

is a subset of the *numerical range* of the operator A . As a function on a group $\hat{A}(g)$ provides a better description of A than the set of its values—numerical range.

EXAMPLE II.4.22. The group $SU(1, 1) \simeq SL_2(\mathbb{R})$ consists of 2×2 matrices of the form $\begin{pmatrix} \alpha & \beta \\ \bar{\beta} & \bar{\alpha} \end{pmatrix}$ with the unit determinant [240, § IX.1]. Let T be an operator with the spectral radius less than 1. Then the associated Möbius transformation

$$(II.4.15) \quad g : T \mapsto g \cdot T = \frac{\alpha T + \beta I}{\bar{\beta} T + \bar{\alpha} I}, \quad \text{where } g = \begin{pmatrix} \alpha & \beta \\ \bar{\beta} & \bar{\alpha} \end{pmatrix} \in SL_2(\mathbb{R}),$$

produces a well-defined operator with the spectral radius less than 1 as well. Thus we have a representation of $SU(1, 1)$.

Let us introduce the *defect operators* $D_T = (I - T^*T)^{1/2}$ and $D_{T^*} = (I - TT^*)^{1/2}$. For the fiducial operator $F = D_{T^*}$ the covariant transform is, cf. [318, § VI.1, (1.2)]:

$$[\mathcal{W}T](g) = F(g \cdot T) = -e^{i\phi} \Theta_T(z) D_T, \quad \text{for } g = \begin{pmatrix} e^{i\phi/2} & 0 \\ 0 & e^{-i\phi/2} \end{pmatrix} \begin{pmatrix} 1 & -z \\ -\bar{z} & 1 \end{pmatrix},$$

where the *characteristic function* $\Theta_T(z)$ [318, § VI.1, (1.1)] is:

$$\Theta_T(z) = -T + D_{T^*} (I - zT^*)^{-1} z D_T.$$

Thus we approached the *functional model* of operators from the covariant transform. In accordance with Remark II.6.10 the model is most fruitful for the case of operator $F = D_{T^*}$ being one-dimensional.

The intertwining property in the previous examples was obtained as a consequence of the general Prop. II.6.27 about the covariant transform. However it may be worth to select it as a separate definition:

DEFINITION II.4.23. A *covariant calculus*, also known as *symbolic calculus*, is a map from operators to functions, which intertwines two representations of the same group in the respective spaces.

There is a dual class of covariant transforms acting in the opposite direction: from functions to operators. The prominent examples are the *Berezin contravariant symbol* [34, 173] and symbols of a *pseudodifferential operators* (PDO) [139, 173].

EXAMPLE II.4.24. The classical *Riesz–Dunford functional calculus* [88, § VII.3; 266, § IV.2] maps analytical functions on the unit disk to the linear operators, it is defined through the Cauchy-type formula with the resolvent. The calculus is an intertwining operator [182] between the Möbius transformations of the unit disk, cf. (II.5.23), and the actions (II.4.15) on operators from the Example II.4.22. This topic will be developed in Subsection III.1.2.

In line with the Defn. II.4.23 we can directly define the corresponding calculus through the intertwining property [168, 182]:

DEFINITION II.4.25. A *contravariant calculus*, also know as *functional calculus*, is a map from functions to operators, which intertwines two representations of the same group in the respective spaces.

The duality between co- and contravariant calculi is the particular case of the duality between covariant transform and the contravariant transform defined in the next Subsection. In many cases a proper choice of spaces makes covariant and/or contravariant calculus a bijection between functions and operators. Subsequently only one form of calculus, either co- or contravariant, is defined explicitly, although both of them are there in fact.

II.4.4. Contravariant Transform

An object invariant under the left action Λ (II.6.29) is called *left invariant*. For example, let L and L' be two left invariant spaces of functions on G . We say that a pairing $\langle \cdot, \cdot \rangle : L \times L' \rightarrow \mathbb{C}$ is *left invariant* if

$$(II.4.16) \quad \langle \Lambda(g)f, \Lambda(g)f' \rangle = \langle f, f' \rangle, \quad \text{for all } f \in L, f' \in L'.$$

- REMARK II.4.26.
- i. We do not require the pairing to be linear in general.
 - ii. If the pairing is invariant on space $L \times L'$ it is not necessarily invariant (or even defined) on the whole $C(G) \times C(G)$.
 - iii. In a more general setting we shall study an invariant pairing on a homogeneous spaces instead of the group. However due to length constraints we cannot consider it here beyond the Example II.4.29.
 - iv. An invariant pairing on G can be obtained from an *invariant functional* \mathfrak{l} by the formula $\langle f_1, f_2 \rangle = \mathfrak{l}(f_1 \bar{f}_2)$.

For a representation ρ of G in V and $w_0 \in V$, we construct a function $w(g) = \rho(g)w_0$. We assume that the pairing can be extended in its second component to this V -valued functions. For example, such an extension can be defined in the weak sense.

DEFINITION II.4.27. Let $\langle \cdot, \cdot \rangle$ be a left invariant pairing on $L \times L'$ as above, let ρ be a representation of G in a space V , we define the function $w(g) = \rho(g)v_0$ for $v_0 \in V$. The *contravariant transform* \mathcal{M} is a map $L \rightarrow V$ defined by the pairing:

$$(II.4.17) \quad \mathcal{M}_{w_0}^\rho : f \mapsto \langle f, w \rangle, \quad \text{where } f \in L.$$

We can drop out sup/subscripts in $\mathcal{M}_{w_0}^\rho$ as we are doing for \mathcal{W}_F^ρ .

EXAMPLE II.4.28 (Haar pairing). The most well-known example of an invariant pairing on $L_2(G, d\mu) \times L_2(G, d\mu)$ is integration over the Haar measure:

$$(II.4.18) \quad \langle f_1, f_2 \rangle = \int_G f_1(g) f_2(g) dg.$$

If ρ is a unitary square integrable representation of G and w_0 is an admissible vector, see Example II.6.11, then this pairing can be extended to $w(g) = \rho(g)w_0$. The contravariant transform is known in this setup as the *reconstruction formula*, cf. [5, (8.19)]:

$$(II.4.19) \quad \mathcal{M}_{w_0} f = \int_G f(g) w(g) dg, \quad \text{where } w(g) = \rho(g)w_0.$$

It is possible to use different admissible vectors v_0 and w_0 for the wavelet transform (II.6.18) and the reconstruction formula (II.6.33), respectively, cf. Example II.6.41.

EXAMPLE II.4.29. Let ρ be a square integrable representation of G modulo a subgroup $H \subset G$ and let $X = G/H$ be the corresponding homogeneous space with a quasi-invariant measure dx . Then integration over dx with an appropriate weight produces an invariant pairing. The contravariant transform is a more general version [5, (7.52)] of the *reconstruction formula* mentioned in the previous example.

If the invariant pairing is defined by integration over the Haar measure, cf. Example II.6.20, then we can show an intertwining property for the contravariant transform as well.

PROPOSITION II.4.30 ([173, Prop. 2.9]). *The inverse wavelet transform \mathcal{M}_{w_0} (II.6.33) intertwines the left regular representation Λ (II.6.29) on $L_2(G)$ and ρ :*

$$(II.4.20) \quad \mathcal{M}_{w_0} \Lambda(g) = \rho(g) \mathcal{M}_{w_0}.$$

COROLLARY II.4.31. *The image $\mathcal{M}_{w_0}(L(G)) \subset V$ of a left invariant space $L(G)$ under the inverse wavelet transform \mathcal{M}_{w_0} is invariant under the representation ρ .*

REMARK II.4.32. It is an important observation, that the above intertwining property is also true for some contravariant transforms which are not based on pairing (II.6.32). For example, in the case of the affine group all pairings (II.6.34), (II.6.39) and (non-linear!) (II.6.35) satisfy to (IV.5.22) for the respective representation ρ_p (II.4.4).

Let

- ρ be not a square integrable representation (even modulo a subgroup); or
- w_0 be an inadmissible vector of a square integrable representation ρ .

A suitable invariant pairing in this case is not associated with integration over the Haar measure on G . In this case we speak about a *Hardy pairing*. The following example explains the name.

EXAMPLE II.4.33 (Hardy pairing). Let G be the “ $ax + b$ ” group and its representation ρ (II.4.4) from Ex. II.6.12. An invariant pairing on G , which is not generated by the Haar measure $a^{-2} da db$, is:

$$(II.4.21) \quad \langle f_1, f_2 \rangle_H = \lim_{\alpha \rightarrow 0} \int_{-\infty}^{\infty} f_1(a, b) f_2(a, b) \frac{db}{a}.$$

For this pairing we can consider functions $\frac{1}{2\pi i(x+i)}$ or e^{-x^2} , which are not admissible vectors in the sense of square integrable representations. Then the contravariant transform provides an *integral resolutions* of the identity. For example, for $v_0 = \frac{1}{2\pi i(x+i)}$ we obtain:

$$[\mathcal{M}f](x) = \lim_{a \rightarrow 0} \int_{-\infty}^{\infty} f(a, b) \frac{a^{-\frac{1}{p}}}{2\pi i(x + ia - b)} db = - \lim_{a \rightarrow 0} \frac{a^{-\frac{1}{p}}}{2\pi i} \int_{-\infty}^{\infty} \frac{f(a, b) db}{b - (x + ia)}.$$

In other words, it expresses the boundary values at $a = 0$ of the Cauchy integral $-[\mathcal{C}f](a, x + ai)$.

Similar pairings can be defined for other semi-direct products of two groups. We can also extend a Hardy pairing to a group, which has a subgroup with such a pairing.

EXAMPLE II.4.34. Let G be the group $SL_2(\mathbb{R})$ from the Ex. II.4.10. Then the “ $ax + b$ ” group is a subgroup of $SL_2(\mathbb{R})$, moreover we can parametrise $SL_2(\mathbb{R})$ by triples (a, b, θ) , $\theta \in (-\pi, \pi]$ with the respective Haar measure [240, III.1(3)]. Then the Hardy pairing

$$(II.4.22) \quad \langle f_1, f_2 \rangle = \lim_{a \rightarrow 0} \int_{-\infty}^{\infty} f_1(a, b, \theta) \bar{f}_2(a, b, \theta) db d\theta.$$

is invariant on $SL_2(\mathbb{R})$ as well. The corresponding contravariant transform provides even a finer resolution of the identity which is invariant under conformal mappings of the Lobachevsky half-plane.

Here is an important example of non-linear pairing.

EXAMPLE II.4.35. Let $G = \text{Aff}$, an invariant homogeneous functional on G is given by the L_∞ version of the Haar functional (II.6.32):

$$(II.4.23) \quad \langle f_1, f_2 \rangle_\infty = \sup_{g \in G} |f_1(g)f_2(g)|.$$

Define the following two functions on \mathbb{R} :

$$(II.4.24) \quad v_0^+(t) = \begin{cases} 1, & \text{if } t = 0; \\ 0, & \text{if } t \neq 0, \end{cases} \quad \text{and} \quad v_0^*(t) = \begin{cases} 1, & \text{if } |t| \leq 1; \\ 0, & \text{if } |t| > 1. \end{cases}$$

The respective contravariant transforms are generated by the representation ρ_∞ (II.4.4) are:

$$(II.4.25) \quad [\mathcal{M}_{v_0^+} f](t) = f^+(t) = \langle f(a, b), \rho_\infty(a, b)v_0^+(t) \rangle_\infty = \sup_a |f(a, t)|,$$

$$(II.4.26) \quad [\mathcal{M}_{v_0^*} f](t) = f^*(t) = \langle f(a, b), \rho_\infty(a, b)v_0^*(t) \rangle_\infty = \sup_{a > |b-t|} |f(a, b)|.$$

The transforms (II.6.37) and (II.6.38) are the *vertical* and *non-tangential maximal functions* [231, § VIII.C.2], respectively.

EXAMPLE II.4.36. Consider again $G = \text{Aff}$ equipped now with an invariant linear functional, which is a Hardy-type modification (cf. (II.6.34)) of L_∞ -functional (II.6.35):

$$(II.4.27) \quad \langle f_1, f_2 \rangle_\infty^H = \overline{\lim}_{a \rightarrow 0} \sup_{b \in \mathbb{R}} (f_1(a, b) f_2(a, b)),$$

where $\overline{\lim}$ is the limit superior. Then, the covariant transform \mathcal{M}^H for this pairing from functions v^+ and v^* (II.6.36) becomes:

$$(II.4.28) \quad [\mathcal{M}_{v_0^+}^H f](t) = \langle f(a, b), \rho_\infty(a, b) v_0^+(t) \rangle_\infty^H = \overline{\lim}_{a \rightarrow 0} f(a, t),$$

$$(II.4.29) \quad [\mathcal{M}_{v_0^*}^H f](t) = \langle f(a, b), \rho_\infty(a, b) v_0^*(t) \rangle_\infty^H = \overline{\lim}_{\substack{a \rightarrow 0 \\ |b-t| < a}} f(a, b).$$

They are the *normal* and *non-tangential* limits superior from the upper-half plane to the real line, respectively.

There is the obvious inequality $\langle f_1, f_2 \rangle_\infty \geq \langle f_1, f_2 \rangle_\infty^H$ between pairings (II.6.35) and (II.6.39), which produces the corresponding relation between respective contravariant transforms.

There is an explicit duality between the covariant transform and the contravariant transform. Discussion of the grand maximal function in the Rem. II.6.16 shows usefulness of the covariant transform over the a family of fiducial functional. Thus, we shall not be surprised by the contravariant transform over a family of reconstructing vectors as well.

DEFINITION II.4.37. Let $w : \text{Aff} \rightarrow L_1(\mathbb{R})$ be a function. We define a new function $\rho_1 w$ on Aff with values in $L_1(\mathbb{R})$ through the point-wise action $[\rho_1 w](g) = \rho_1(g) w(g)$ of ρ_∞ (II.4.4). If $\sup_g \|w(g)\|_1 < \infty$, then, for $f \in L_1(\text{Aff})$, we define the *extended contravariant transform* by:

$$(II.4.30) \quad [\mathcal{M}_w f](x) = \int_{\text{Aff}} f(g) [\rho_1 w](g) dg.$$

Note, that (II.6.42) reduces to the contravariant transform (II.6.33) if we start from the constant function $w(g) = w_0$.

DEFINITION II.4.38. We call a function r on \mathbb{R} a *nucleus* if:

- i. r is supported in $[-1, 1]$,
- ii. $|r| < \frac{1}{2}$ almost everywhere, and
- iii. $\int_{\mathbb{R}} r(x) dx = 0$, cf. (II.6.21).

Clearly, for a nucleus r , the function $s = \rho_1(a, b)r$ has properties:

- i. s is supported in a ball centred at b and radius a ,
- ii. $|s| < \frac{1}{2a}$ almost everywhere, and
- iii. $\int_{\mathbb{R}} s(x) dx = 0$.

In other words, $s = \rho_1(a, b)r$ is an *atom*, cf. [314, § III.2.2] and any atom may be obtained in this way from some nucleus and certain $(a, b) \in \text{Aff}$.

EXAMPLE II.4.39. Let $f(g) = \sum_j \lambda_j \delta_{g_j}(g)$ with $\sum_j |\lambda_j| < \infty$ be a countable sum of point masses on Aff. If all values of $w(g_j)$ are nucleuses, then (II.6.42) becomes:

$$(II.4.31) \quad [\mathcal{M}_w f](x) = \int_{\text{Aff}} f(g) [\rho_1 w](g) dg = \sum_j \lambda_j s_j,$$

where $s_j = \rho_1(g_j)w(g_j)$ are atoms. The right-hand side of (II.6.43) is known as an *atomic decomposition* of a function $h(x) = [\mathcal{M}_w f](x)$, see [314, § III.2.2].

II.4.5. Composing the Co- and Contravariant Transforms

In the case of classical wavelets, the relation between the wavelet transform (II.6.18) and the inverse wavelet transform (II.6.33) is suggested by their names.

EXAMPLE II.4.40. For a square integrable representation and admissible vectors v_0 and w_0 , there is the relation [5, (8.52)]:

$$\mathcal{M}_{w_0} \mathcal{W}_{v_0} = kI,$$

where the constant k depends on v_0 , w_0 and the Duflo–Moore operator [5, § 8.2; 87].

It is of interest, that two different vectors can be used as analysing vector in (II.6.18) and for the reconstructing formula (II.6.33). Even a greater variety can be achieved if we use additional fiducial operators and invariant pairings.

EXAMPLE II.4.41. The composition of the contravariant transform $\mathcal{M}_{v_0^*}$ (II.6.38) with the covariant transform \mathcal{W}_∞ (II.6.26) is:

$$(II.4.32) \quad \begin{aligned} [\mathcal{M}_{v_0^*} \mathcal{W}_\infty f](t) &= \sup_{a > |b-t|} \left\{ \frac{1}{2a} \int_{b-a}^{b+a} |f(x)| dx \right\} \\ &= \sup_{b_1 < t < b_2} \left\{ \frac{1}{b_2 - b_1} \int_{b_1}^{b_2} |f(x)| dx \right\}. \end{aligned}$$

Thus, $\mathcal{M}_{v_0^*} \mathcal{W}_\infty f$ coincides with the *Hardy–Littlewood maximal function* f^M [231, § VIII.B.1], which contains important information on the original function f . Combining Props. II.6.27 and II.6.30 (through Rem. II.6.32), we deduce that the operator $M : f \mapsto f^M$ intertwines ρ_p with itself: $\rho_p M = M \rho_p$ (yet, M is non-linear).

EXAMPLE II.4.42. Let the mother wavelet $v_0(x) = \delta(x)$ be the Dirac delta function, then the wavelet transform \mathcal{W}_δ generated by ρ_∞ (II.4.4) on $C(\mathbb{R})$ is $[\mathcal{W}_\delta f](a, b) = f(b)$. Take the reconstruction vector $w_0(x) = (1 - \chi_{[-1,1]}(x))/x$ and consider the respective inverse wavelet transform \mathcal{M}_{w_0} produced by the Hardy pairing (II.6.34). Then, the

composition of both maps is:

$$\begin{aligned}
 [\mathcal{M}_{w_0} \circ \mathcal{W}_\delta f](t) &= \lim_{a \rightarrow 0} \int_{-\infty}^{\infty} f(b) \rho_\infty(a, b) w_0(t) \frac{db}{a} \\
 &= \lim_{a \rightarrow 0} \int_{-\infty}^{\infty} f(b) \frac{1 - \chi_{[-a, a]}(t - b)}{t - b} db \\
 &= \lim_{a \rightarrow 0} \int_{|b| > a} \frac{f(b)}{t - b} db.
 \end{aligned}$$

The last expression is a *singular integral operator* (SIO) [257, § 2.6; 314, § I.5] defined through the principal value (in the sense of Cauchy).

EXAMPLE II.4.43. Let \mathcal{W} be a covariant transform generated either by the functional F_\pm (II.6.22) (i.e. the Cauchy integral) or $(F_+ - F_-)$ (i.e. the Poisson integral) from the Example II.6.13. Then, for the contravariant transform $\mathcal{M}_{v_0^+}^H$ (II.6.37) the composition $\mathcal{M}_{v_0^+}^H \mathcal{W}$ becomes the normal boundary value of the Cauchy/Poisson integral, respectively. The similar composition $\mathcal{M}_{v_0^*}^H \mathcal{W}$ for the reconstructing vector v_0^* (II.6.36) turns to be the non-tangential limit of the Cauchy/Poisson integrals.

It is the classical question of harmonic analysis to identify a class of functions on the real line such that $\mathcal{M}_{v_0^+}^H \mathcal{W}$ becomes the identity operator on it. Combining intertwining properties of the covariant and contravariant transforms (Props. II.6.27, II.6.30 and Rem. II.6.32) we conclude that $\mathcal{M}_{v_0^+}^H \mathcal{W}$ will intertwine the representation ρ with itself. If we restrict our attention to ρ -irreducible subspace, then a sort of Schur's lemma suggests that such an operator is a (possible zero) multiple of the identity operator. This motivates the following template definition, cf. [203, § 1].

DEFINITION II.4.44. For a representation ρ of a group G in a space V , a *generalised Hardy space* H is an ρ -irreducible subspace of V .

EXAMPLE II.4.45. Let $G = \text{Aff}$ and the representation ρ_p is defined in $V = L_p(\mathbb{R})$ by (II.4.4). Then the classical Hardy spaces $H_p(\mathbb{R})$ are ρ_p -irreducible, thus are provided by the above definition.

We illustrate the group-theoretical technique by the following statement.

PROPOSITION II.4.46. *Let B be the spaces of bounded uniformly continuous functions on the real line. Let $F : B \rightarrow \mathbb{R}$ be a fiducial functional such that:*

$$(II.4.33) \quad \lim_{a \rightarrow 0} F(\rho_\infty(1/a, 0)f) = 0, \quad \text{for all } f \in B \text{ such that } f(0) = 0$$

and $F(\rho_\infty(1, b)f)$ is a continuous function of $b \in \mathbb{R}$ for a given $f \in B$.

Then, $\mathcal{M}_{v_0^*}^H \circ \mathcal{W}_F$ is a constant times the identity operator on B .

PROOF. First of all we note that $\mathcal{M}_{v_0^+}^H \mathcal{W}_F$ is a bounded operator on B . Let $v_{(a,b)}^* = \rho_\infty(a, b)v^*$. Obviously, $v_{(a,b)}^*(0) = v^*(-\frac{b}{a})$ is an eigenfunction for operators $\Lambda(a', 0)$,

$\mathfrak{a}' \in \mathbb{R}_+$ of the left regular representation of Aff:

$$(II.4.34) \quad \Lambda(\mathfrak{a}', 0)v_{(\mathfrak{a}, \mathfrak{b})}^*(0) = v_{(\mathfrak{a}, \mathfrak{b})}^*(0).$$

This and the left invariance of the pairing (II.6.30) imply $\mathcal{M}_{v_0^*}^H \circ \Lambda(1/\mathfrak{a}, 0) = \mathcal{M}_{v_0^*}^H$ for any $(\mathfrak{a}, 0) \in \text{Aff}$. Then, applying the intertwining properties (II.6.44) we obtain:

$$\begin{aligned} [\mathcal{M}_{v_0^*}^H \circ \mathcal{W}_F f](0) &= [\mathcal{M}_{v_0^*}^H \circ \Lambda(1/\mathfrak{a}, 0) \circ \mathcal{W}_F f](0) \\ &= [\mathcal{M}_{v_0^*}^H \circ \mathcal{W}_F \circ \rho_\infty(1/\mathfrak{a}, 0) f](0) \end{aligned}$$

Using the limit $\mathfrak{a} \rightarrow 0$ (II.6.53) and the continuity of $F \circ \rho_\infty(1, \mathfrak{b})$ we conclude that the linear functional $\mathfrak{l} : f \mapsto [\mathcal{M}_{v_0^*}^H \circ \mathcal{W}_F f](0)$ vanishes for any $f \in \mathbb{B}$ such that $f(0) = 0$. Take a function $f_1 \in \mathbb{B}$ such that $f_1(0) = 1$ and define $\mathfrak{c} = \mathfrak{l}(f_1)$. From linearity of \mathfrak{l} , for any $f \in \mathbb{B}$ we have:

$$\mathfrak{l}(f) = \mathfrak{l}(f - f(0)f_1 + f(0)f_1) = \mathfrak{l}(f - f(0)f_1) + f(0)\mathfrak{l}(f_1) = \mathfrak{c}f(0).$$

Furthermore, using the intertwining properties (II.6.44) and (IV.5.22):

$$\begin{aligned} [\mathcal{M}_{v_0^*}^H \circ \mathcal{W}_F f](t) &= [\rho_\infty(1, -t) \circ \mathcal{M}_{v_0^*}^H \circ \mathcal{W}_F f](0) \\ &= [\mathcal{M}_{v_0^*}^H \circ \mathcal{W}_F \circ \rho_\infty(1, -t) f](0) \\ &= \mathfrak{l}(\rho_\infty(1, -t)f) \\ &= \mathfrak{c}[\rho_\infty(1, -t)f](0) \\ &= \mathfrak{c}f(t). \end{aligned}$$

This finishes the proof. □

To get the classical statement we need the following lemma.

LEMMA II.4.47. For $w(t) \in L_1(\mathbb{R})$, define the fiducial functional on \mathbb{B} :

$$(II.4.35) \quad F(f) = \int_{\mathbb{R}} f(t) w(t) dt.$$

Then F satisfies to the condition (and thus conclusions) of Prop. II.6.48.

PROOF. Let f be a continuous bounded function such that $f(0) = 0$. For $\varepsilon > 0$ chose

- $\delta > 0$ such that $|f(t)| < \varepsilon$ for all $|t| < \delta$;
- $M > 0$ such that $\int_{|t| > M} |w(t)| dt < \varepsilon$.

Then, for $\mathfrak{a} < \delta/M$, we have the estimation:

$$\begin{aligned} |F(\rho_\infty(1/\mathfrak{a}, 0)f)| &= \left| \int_{\mathbb{R}} f(\mathfrak{a}t) w(t) dt \right| \\ &\leq \left| \int_{|t| < M} f(\mathfrak{a}t) w(t) dt \right| + \left| \int_{|t| > M} f(\mathfrak{a}t) w(t) dt \right| \\ &\leq \varepsilon(\|w\|_1 + \|f\|_\infty). \end{aligned}$$

Finally, for a uniformly continuous function g : for $\varepsilon > 0$ there is $\delta > 0$ such that $|g(t+b) - g(t)| < \varepsilon$ for all $b < \delta$ and $t \in \mathbb{R}$. Then:

$$|F(\rho_\infty(1, b)g) - F(g)| = \left| \int_{\mathbb{R}} (g(t+b) - g(t)) w(t) dt \right| \leq \varepsilon \|w\|_1.$$

That demonstrates the continuity of $F(\rho_\infty(1, b)g)$ at $b = 0$ and, by the group property, at any other point as well. \square

REMARK II.4.48. A direct evaluation shows, that the constant $c = \iota(f_1)$ from the proof of Prop. II.6.48 for the fiducial functional (II.6.55) is equal to $c = \int_{\mathbb{R}} w(t) dt$. Of course, for non-trivial boundary values we need $c \neq 0$. On the other hand, the admissibility condition (II.6.21) requires $c = 0$. In this sense, the classical harmonic analysis and the traditional wavelet construction are two orthogonal parts of the same covariant transform theory.

The table integral $\int_{\mathbb{R}} \frac{dx}{x^2+1} = \pi$ tells that the “wavelet” $p(t) = \frac{1}{\pi} \frac{1}{1+t^2}$ is in $L_1(\mathbb{R})$ with $c = 1$, the corresponding wavelet transform is the Poisson integral. Its boundary behaviour from Prop. II.6.48 is the classical result, cf. [108, Ch. I, Cor. 3.2].

The comparison between our demonstrations and the traditional proofs, e.g. in [108], does not reveal any significant distinctions. We simply made an explicit usage of the relevant group structure, which is implicitly employed in traditional texts anyway.

II.4.5.1. Real and Complex Technique in Harmonic Analysis. There are two main approaches in harmonic analysis on the real line. The real variables technique uses various maximal functions, dyadic cubes and, occasionally, the Poisson integral [314]. The complex variable technique is based on the Cauchy integral and fine properties of analytic functions [264, 265].

Both methods seem to have clear advantages. The real variable technique:

- i. does not require an introduction of the imaginary unit for a study of real-valued harmonic functions of a real variable (Occam’s Razor);
- ii. allows a straightforward generalisation to several dimensions.

By contrast, access to the beauty and power of analytic functions (e.g., Möbius transformations, factorisation of zeroes, etc. [231]) is the main reason to use the complex variable technique. A posteriori, a multidimensional analytic version was also discovered [252], it is based on the monogenic Clifford-valued functions [49].

Therefore, propensity for either techniques becomes a personal choice of a researcher. Some of them prefer the real variable method, explicitly cleaning out any reference to analytic or harmonic functions [314, Ch. III, p. 88]. Others, e.g. [233], happily combine the both techniques. However, the reasons for switching between two methods at particular places may look mysterious.

We demonstrated above that both—real and complex—techniques in harmonic analysis have the same group-theoretical origin. Moreover, they are complemented by the wavelet construction. Therefore, there is no any confrontation between these approaches. In other words, the binary opposition of the real and complex methods resolves into Kant’s triad thesis-antithesis-synthesis: complex-real-covariant.

Analytic Functions

We saw in the first section that an inspiring geometry of cycles can be recovered from the properties of $SL_2(\mathbb{R})$. In this section we consider a realisation of the function theory within Erlangen approach [170, 172, 175, 176]. The covariant transform will be our principal tool in this construction.

II.5.1. Induced Covariant Transform

The choice of a mother wavelet or fiducial operator F from Section II.4.1 can significantly influence the behaviour of the covariant transform. Let G be a group and H be its closed subgroup with the corresponding homogeneous space $X = G/H$. Let ρ be a representation of G by operators on a space V , we denote by ρ_H the restriction of ρ to the subgroup H .

DEFINITION II.5.1. Let χ be a representation of the subgroup H in a space U and $F : V \rightarrow U$ be an intertwining operator between χ and the representation ρ_H :

$$(II.5.1) \quad F(\rho(h)v) = F(v)\chi(h), \quad \text{for all } h \in H, v \in V.$$

Then the covariant transform (II.6.17) generated by F is called the *induced covariant transform*.

The following is the main motivating example.

EXAMPLE II.5.2. Consider the traditional wavelet transform as outlined in Ex. II.6.11. Chose a vacuum vector v_0 to be a joint eigenvector for all operators $\rho(h)$, $h \in H$, that is $\rho(h)v_0 = \chi(h)v_0$, where $\chi(h)$ is a complex number depending of h . Then χ is obviously a character of H .

The image of wavelet transform (II.6.18) with such a mother wavelet will have a property:

$$\hat{v}(gh) = \langle v, \rho(gh)v_0 \rangle = \langle v, \rho(g)\chi(h)v_0 \rangle = \chi(h)\hat{v}(g).$$

Thus the wavelet transform is uniquely defined by cosets on the homogeneous space G/H . In this case we previously spoke about the *reduced wavelet transform* [172]. A representation ρ_0 is called *square integrable mod H* if the induced wavelet transform $[\mathcal{W}f_0](w)$ of the vacuum vector $f_0(x)$ is square integrable on X .

The image of induced covariant transform have the similar property:

$$(II.5.2) \quad \hat{v}(gh) = F(\rho((gh)^{-1})v) = F(\rho(h^{-1})\rho(g^{-1})v) = F(\rho(g^{-1})v)\chi(h^{-1}).$$

Thus it is enough to know the value of the covariant transform only at a single element in every coset G/H in order to reconstruct it for the entire group G by the representation χ . Since coherent states (wavelets) are now parametrised by points homogeneous space G/H they are referred sometimes as coherent states which are not connected to a group [219], however this is true only in a very narrow sense as explained above.

EXAMPLE II.5.3. To make it more specific we can consider the representation of $SL_2(\mathbb{R})$ defined on $L_2(\mathbb{R})$ by the formula, cf. (II.3.8):

$$\rho(g) : f(z) \mapsto \frac{1}{(cx + d)} f\left(\frac{ax + b}{cx + d}\right), \quad g^{-1} = \begin{pmatrix} a & b \\ c & d \end{pmatrix}.$$

Let $K \subset SL_2(\mathbb{R})$ be the compact subgroup of matrices $h_t = \begin{pmatrix} \cos t & \sin t \\ -\sin t & \cos t \end{pmatrix}$. Then for the fiducial operator F_{\pm} (II.6.22) we have $F_{\pm} \circ \rho(h_t) = e^{\mp it} F_{\pm}$. Thus we can consider the covariant transform only for points in the homogeneous space $SL_2(\mathbb{R})/K$, moreover this set can be naturally identified with the $ax + b$ group. Thus we do not obtain any advantage of extending the group in Ex. II.6.12 from $ax + b$ to $SL_2(\mathbb{R})$ if we will be still using the fiducial operator F_{\pm} (II.6.22).

Functions on the group G , which have the property $\hat{v}(gh) = \hat{v}(g)\chi(h)$ (II.5.2), provide a space for the representation of G induced by the representation χ of the subgroup H . This explains the choice of the name for induced covariant transform.

REMARK II.5.4. Induced covariant transform uses the fiducial operator F which passes through the action of the subgroup H . This reduces information which we obtained from this transform in some cases.

There is also a simple connection between a covariant transform and right shifts:

PROPOSITION II.5.5. *Let G be a Lie group and ρ be a representation of G in a space V . Let $[Wf](g) = F(\rho(g^{-1})f)$ be a covariant transform defined by the fiducial operator $F : V \rightarrow \mathcal{U}$. Then the right shift $[Wf](gg')$ by g' is the covariant transform $[W'f](g) = F'(\rho(g^{-1})f)$ defined by the fiducial operator $F' = F \circ \rho(g^{-1})$.*

In other words the covariant transform intertwines right shifts on the group G with the associated action ρ_B (II.4.14) on fiducial operators.

Although the above result is obvious, its infinitesimal version has interesting consequences.

COROLLARY II.5.6 ([193]). *Let G be a Lie group with a Lie algebra \mathfrak{g} and ρ be a smooth representation of G . We denote by $d\rho_B$ the derived representation of the associated representation ρ_B (II.4.14) on fiducial operators.*

Let a fiducial operator F be a null-solution, i.e. $AF = 0$, for the operator $A = \sum_j a_j d\rho_B^{X_j}$, where $X_j \in \mathfrak{g}$ and a_j are constants. Then the covariant transform $[Wf](g) = F(\rho(g^{-1})f)$ for any f satisfies:

$$DF(g) = 0, \quad \text{where } D = \sum_j \bar{a}_j \mathcal{L}^{X_j}.$$

Here \mathcal{L}^{X_j} are the left invariant fields (Lie derivatives) on G corresponding to X_j .

EXAMPLE II.5.7. Consider the representation ρ (II.4.4) of the $ax + b$ group with the $p = 1$. Let A and N be the basis of \mathfrak{g} generating one-parameter subgroups $(e^t, 0)$ and $(0, t)$, respectively. Then, the derived representations are:

$$[d\rho^A f](x) = -f(x) - xf'(x), \quad [d\rho^N f](x) = -f'(x).$$

The corresponding left invariant vector fields on $ax + b$ group are:

$$\mathfrak{L}^A = a\partial_a, \quad \mathfrak{L}^N = a\partial_b.$$

The mother wavelet $\frac{1}{x+i}$ in (II.6.22) is a null solution of the operator

$$-d\rho^A - id\rho^N = I + (x + i)\frac{d}{dx}.$$

Therefore, the image of the covariant transform with the fiducial operator F_+ (II.6.22) consists of the null solutions to the operator $-\mathfrak{L}^A + i\mathfrak{L}^N = ia(\partial_b + i\partial_a)$, that is in the essence the Cauchy–Riemann operator in the upper half-plane.

EXAMPLE II.5.8. In the above setting, the function $p(x) = \frac{1}{\pi} \frac{1}{x^2+1}$ is a null solution of the operator:

$$(d\rho^A)^2 - d\rho^A + (d\rho^N)^2 = 2I + 4x\frac{d}{dx} + (1 + x^2)\frac{d^2}{dx^2}.$$

The covariant transform with the mother wavelet $p(x)$ is the Poisson integral, its values are null solutions to the operator $(\mathfrak{L}^A)^2 - \mathfrak{L}^A + (\mathfrak{L}^N)^2 = a^2(\partial_b^2 + \partial_a^2)$ —the Laplace operator.

EXAMPLE II.5.9. Using the setup of the previous Examples, we observe that the Gaussian $e^{-x^2/2}$ is the null solution of the operator $d\rho^A + (d\rho^N)^2 = I + x\frac{d}{dx} + \frac{d^2}{dx^2}$. Therefore, the covariant transform with the Gaussian as a mother wavelet consists of the null solutions to the operator $\mathfrak{L}^A + (\mathfrak{L}^N)^2 = a(\partial_a + a\partial_b^2)$, that is a parabolic equation related to the heat equation (I.11.12). The second null-solution to the operator $d\rho^A + (d\rho^N)^2$ is $\text{erf}(ix)e^{-x^2/2}$, where the error function erf satisfies to the identity $\text{erf}'(x) = e^{-x^2/2}$. For the normalised mother wavelet, the corresponding wavelet transform is:

$$\begin{aligned} [\mathcal{W}\phi](a, b) &= \frac{1}{\sqrt{2\pi}} \int_{\mathbb{R}} \phi(ax + b) e^{-x^2/2} dx \\ \text{(II.5.3)} \quad &= \frac{1}{\sqrt{2\pi}a} \int_{\mathbb{R}} \phi(y) \exp\left(-\frac{(y - b)^2}{2a^2}\right) dy. \end{aligned}$$

It consists of null-solutions $[\mathcal{W}\phi](a, b)$ to the operator $\partial_a + a\partial_b^2$ as mentioned above. To obtain solutions $f(x, t)$ of the heat equation $\partial_t - k\partial_x^2$ (I.11.12) we can use the change of variables: $f(x, t) = [\mathcal{W}\phi](2\sqrt{kt}, x)$. Then the wavelet transform (II.5.3) mutates to the integral formula (I.11.13).

EXAMPLE II.5.10. The fiducial functional F_m (II.6.25) is a null solution of the following functional equation:

$$F_m - F_m \circ \rho_\infty\left(\frac{1}{2}, \frac{1}{2}\right) - F_m \circ \rho_\infty\left(\frac{1}{2}, -\frac{1}{2}\right) = 0.$$

Consequently, the image of wavelet transform \mathcal{W}_p^m (II.6.26) consists of functions which solve the equation:

$$(I - R(\frac{1}{2}, \frac{1}{2}) - R(\frac{1}{2}, -\frac{1}{2}))f = 0 \quad \text{or} \quad f(a, b) = f(\frac{1}{2}a, b + \frac{1}{2}a) + f(\frac{1}{2}a, b - \frac{1}{2}a).$$

The last relation is the key to the dyadic cubes technique, see for example [108, Ch. VII, Thm. 1.1] or the picture on the front cover of this book.

The moral of the above Examples II.6.35–II.6.37 is: there is a significant freedom in choice of the covariant transforms. However, some fiducial functionals has special properties, which suggest the suitable technique (e.g., analytic, harmonic, dyadic, etc.) following from this selection.

There is a statement which extends Corollary II.6.34 from differential operators to integro-differential ones. We will formulate it for the wavelets setting.

COROLLARY II.5.11. *Let G be a group and ρ be a unitary representation of G, which can be extended to a vector space V of functions or distributions on G. Let a mother wavelet $w \in V'$ satisfy the equation*

$$\int_G \alpha(g) \rho(g)w \, dg = 0,$$

for a fixed distribution $\alpha(g)$ and a (not necessarily invariant) measure dg . Then any wavelet transform $F(g) = \mathcal{W}f(g) = \langle f, \rho(g)w \rangle$ obeys the condition:

$$DF = 0, \quad \text{where} \quad D = \int_G \bar{\alpha}(g) R(g) \, dg,$$

with R being the right regular representation of G.

Clearly, the Corollary II.6.34 is a particular case of the Corollary IV.5.3 with a distribution α , which is a combination of derivatives of Dirac's delta functions. The last Corollary will be illustrated at the end of Section III.1.2.

REMARK II.5.12. We note that Corollaries II.6.34 and IV.5.3 are true whenever we have an intertwining property between ρ with the right regular representation of G.

II.5.2. Induced Wavelet Transform and Cauchy Integral

We again use the general scheme from Subsection II.3.2. The $ax + b$ group is isomorphic to a subgroups of $SL_2(\mathbb{R})$ consisting of the lower-triangular matrices:

$$F = \left\{ \frac{1}{\sqrt{a}} \begin{pmatrix} a & 0 \\ b & 1 \end{pmatrix}, a > 0 \right\}.$$

The corresponding homogeneous space $X = SL_2(\mathbb{R})/F$ is one-dimensional and can be parametrised by a real number. The natural projection $p : SL_2(\mathbb{R}) \rightarrow \mathbb{R}$ and its left inverse $s : \mathbb{R} \rightarrow SL_2(\mathbb{R})$ can be defined as follows:

$$(II.5.4) \quad p : \begin{pmatrix} a & b \\ c & d \end{pmatrix} \mapsto \frac{b}{d}, \quad s : u \mapsto \begin{pmatrix} 1 & u \\ 0 & 1 \end{pmatrix}.$$

Thus we calculate the corresponding map $r : SL_2(\mathbb{R}) \rightarrow F$, see Subsection ??:

$$(II.5.5) \quad r : \begin{pmatrix} a & b \\ c & d \end{pmatrix} \mapsto \begin{pmatrix} d^{-1} & 0 \\ c & d \end{pmatrix}.$$

Therefore the action of $SL_2(\mathbb{R})$ on the real line is exactly the Möbius map (I.1.1):

$$g : u \mapsto p(g^{-1} * s(u)) = \frac{au + b}{cu + d}, \quad \text{where } g^{-1} = \begin{pmatrix} a & b \\ c & d \end{pmatrix}.$$

We also calculate that

$$r(g^{-1} * s(u)) = \begin{pmatrix} (cu + d)^{-1} & 0 \\ c & cu + d \end{pmatrix}.$$

To build an induced representation we need a character of the affine group. A generic character of F is a power of its diagonal element:

$$\rho_\kappa \begin{pmatrix} a & 0 \\ c & a^{-1} \end{pmatrix} = a^\kappa.$$

Thus the corresponding realisation of induced representation (II.3.6) is:

$$(II.5.6) \quad \rho_\kappa(g) : f(u) \mapsto \frac{1}{(cu + d)^\kappa} f\left(\frac{au + b}{cu + d}\right) \quad \text{where } g^{-1} = \begin{pmatrix} a & b \\ c & d \end{pmatrix}.$$

The only freedom remaining by the scheme is in a choice of a value of *number* κ and the corresponding functional space where our representation acts. At this point we have a wider choice of κ than it is usually assumed: it can belong to different hypercomplex systems.

One of the important properties which would be nice to have is the unitarity of the representation (II.5.6) with respect to the standard inner product:

$$\langle f_1, f_2 \rangle = \int_{\mathbb{R}^2} f_1(u) \bar{f}_2(u) \, du.$$

A change of variables $x = \frac{au+b}{cu+d}$ in the integral suggests the following property is necessary and sufficient for that:

$$(II.5.7) \quad \kappa + \bar{\kappa} = 2.$$

A mother wavelet for an induced wavelet transform shall be an eigenvector for the action of a subgroup \tilde{H} of $SL_2(\mathbb{R})$, see (II.5.1). Let us consider the most common case of $\tilde{H} = K$ and take the infinitesimal condition with the derived representation: $d\rho_n^Z w_0 = \lambda w_0$, since Z (II.3.13) is the generator of the subgroup K . In other word the restriction of w_0 to a K -orbit should be given by $e^{\lambda t}$ in the exponential coordinate t along the K -orbit. However we usually need its expression in other “more natural” coordinates. For example [195], an eigenvector of the derived representation of $d\rho_n^Z$ should satisfy the differential equation in the ordinary parameter $x \in \mathbb{R}$:

$$(II.5.8) \quad -\kappa x f(x) - f'(x)(1 + x^2) = \lambda f(x).$$

The equation does not have singular points, the general solution is globally defined (up to a constant factor) by:

$$(II.5.9) \quad w_{\lambda, \kappa}(x) = \frac{1}{(1 + x^2)^{\kappa/2}} \begin{pmatrix} x - i \\ x + i \end{pmatrix}^{i\lambda/2} = \frac{(x - i)^{(i\lambda - \kappa)/2}}{(x + i)^{(i\lambda + \kappa)/2}}.$$

To avoid multivalent functions we need 2π -periodicity along the exponential coordinate on K . This implies that the parameter $m = -i\lambda$ is an integer. Therefore the solution becomes:

$$(II.5.10) \quad w_{m,\kappa}(x) = \frac{(x+i)^{(m-\kappa)/2}}{(x-i)^{(m+\kappa)/2}}.$$

The corresponding wavelets resemble the Cauchy kernel normalised to the invariant metric in the Lobachevsky half-plane:

$$w_{m,\kappa}(u, v; x) = \rho_{\kappa}^F(s(u, v))w_{m,\kappa}(x) = v^{\kappa/2} \frac{(x-u+iv)^{(m-\kappa)/2}}{(x-u-iv)^{(m+\kappa)/2}}$$

Therefore the wavelet transform (II.6.18) from function on the real line to functions on the upper half-plane is:

$$\hat{f}(u, v) = \langle f, \rho_{\kappa}^F(u, v)w_{m,\kappa} \rangle = v^{\kappa/2} \int_{\mathbb{R}} f(x) \frac{(x-(u+iv))^{(m-\kappa)/2}}{(x-(u-iv))^{(m+\kappa)/2}} dx.$$

Introduction of a complex variable $z = u + iv$ allows to write it as:

$$(II.5.11) \quad \hat{f}(z) = (\Im z)^{\kappa/2} \int_{\mathbb{R}} f(x) \frac{(x-z)^{(m-\kappa)/2}}{(x-\bar{z})^{(m+\kappa)/2}} dx.$$

According to the general theory this wavelet transform intertwines representations ρ_{κ}^F (II.5.6) on the real line (induced by the character α^{κ} of the subgroup F) and ρ_m^K (II.3.8) on the upper half-plane (induced by the character e^{imt} of the subgroup K).

II.5.3. The Cauchy-Riemann (Dirac) and Laplace Operators

Ladder operators $L^{\pm} = \pm iA + B$ act by raising/lowering indexes of the K -eigenfunctions $w_{m,\kappa}$ (II.5.9), see Subsection II.3.3. More explicitly [195]:

$$(II.5.12) \quad d\rho_{\kappa}^{L^{\pm}} : w_{m,\kappa} \mapsto -\frac{i}{2}(m \pm \kappa)w_{m \pm 2, \kappa}.$$

There are two possibilities here: $m \pm \kappa$ is zero for some m or not. In the first case the chain (II.5.12) of eigenfunction $w_{m,\kappa}$ terminates on one side under the transitive action (II.3.16) of the ladder operators; otherwise the chain is infinite in both directions. That is, the values $m = \mp \kappa$ and only those correspond to the maximal (minimal) weight function $w_{\mp \kappa, \kappa}(x) = \frac{1}{(x \pm i)^{\kappa}} \in L_2(\mathbb{R})$, which are annihilated by L^{\pm} :

$$(II.5.13) \quad d\rho_{\kappa}^{L^{\pm}} w_{\mp \kappa, \kappa} = (\pm i d\rho_{\kappa}^A + d\rho_{\kappa}^B) w_{\mp \kappa, \kappa} = 0.$$

By the Cor. II.6.34 for the mother wavelets $w_{\mp \kappa, \kappa}$, which are annihilated by (II.5.13), the images of the respective wavelet transforms are null solutions to the left-invariant differential operator $D_{\pm} = \overline{\mathcal{L}^{\pm}}$:

$$(II.5.14) \quad D_{\pm} = \mp i \mathcal{L}^A + \mathcal{L}^B = -\frac{i\kappa}{2} + v(\partial_u \pm i\partial_v).$$

This is a conformal version of the Cauchy-Riemann equation. The second order conformal Laplace-type operators $\Delta_+ = \overline{\mathcal{L}^L \mathcal{L}^L}$ and $\Delta_- = \mathcal{L}^L \overline{\mathcal{L}^L}$ are:

$$(II.5.15) \quad \Delta_{\pm} = (v\partial_u - \frac{i\kappa}{2})^2 + v^2\partial_v^2 \pm \frac{\kappa}{2}.$$

For the mother wavelets $w_{m,\kappa}$ in (II.5.13) such that $m = \mp\kappa$ the unitarity condition $\kappa + \bar{\kappa} = 2$, see (II.5.7), together with $m \in \mathbb{Z}$ implies $\kappa = \mp m = 1$. In such a case the wavelet transforms (II.5.11) are:

$$(II.5.16) \quad \hat{f}^+(z) = (\mathcal{J}z)^{\frac{1}{2}} \int_{\mathbb{R}} \frac{f(x) dx}{x - z} \quad \text{and} \quad \hat{f}^-(z) = (\mathcal{J}z)^{\frac{1}{2}} \int_{\mathbb{R}} \frac{f(x) dx}{x - \bar{z}},$$

for $w_{-1,1}$ and $w_{1,1}$ respectively. The first one is the Cauchy integral formula up to the factor $2\pi i \sqrt{\mathcal{J}z}$. Clearly, one integral is the complex conjugation of another. Moreover, the minimal/maximal weight cases can be intertwined by the following automorphism of the Lie algebra \mathfrak{sl}_2 :

$$A \rightarrow B, \quad B \rightarrow A, \quad Z \rightarrow -Z.$$

As explained before $\hat{f}^{\pm}(w)$ are null solutions to the operators D_{\pm} (II.5.14) and Δ_{\pm} (II.5.15). These transformations intertwine unitary equivalent representations on the real line and on the upper half-plane, thus they can be made unitary for proper spaces. This is the source of two faces of the Hardy spaces: they can be defined either as square-integrable on the real line with an analytic extension to the half-plane, or analytic on the half-plane with square-integrability on an infinitesimal displacement of the real line.

For the third possibility, $m \pm \kappa \neq 0$, there is no an operator spanned by the derived representation of the Lie algebra \mathfrak{sl}_2 which kills the mother wavelet $w_{m,\kappa}$. However the remarkable *Casimir operator* $C = Z^2 - 2(L^-L^+ + L^+L^-)$, which spans the centre of the universal enveloping algebra of \mathfrak{sl}_2 [240, § X.1; 321, § 8.1], produces a second order operator which does the job. Indeed from the identities (II.5.12) we get:

$$(II.5.17) \quad d\rho_{\kappa}^C w_{m,\kappa} = (2\kappa - \kappa^2)w_{m,\kappa}.$$

Thus we get $d\rho_{\kappa}^C w_{m,\kappa} = 0$ for $\kappa = 2$ or 0 . The mother wavelet $w_{0,2}$ turns to be the *Poisson kernel* [114, Ex. 1.2.17]. The associated wavelet transform

$$(II.5.18) \quad \hat{f}(z) = \mathcal{J}z \int_{\mathbb{R}} \frac{f(x) dx}{|x - z|^2}$$

consists of null solutions of the left-invariant second-order Laplacian, image of the Casimir operator, cf. (II.5.15):

$$\Delta(=:\mathcal{L}^C) = v^2 \partial_u^2 + v^2 \partial_v^2.$$

Another integral formula producing solutions to this equation delivered by the mother wavelet $w_{m,0}$ with the value $\kappa = 0$ in (II.5.17):

$$(II.5.19) \quad \hat{f}(z) = \int_{\mathbb{R}} f(x) \left(\frac{x - z}{x - \bar{z}} \right)^{m/2} dx.$$

Furthermore, we can introduce higher order differential operators. The functions $w_{\mp 2m+1,1}$ are annihilated by n -th power of operator $d\rho_{\kappa}^{L^{\pm}}$ with $1 \leq m \leq n$. By the Cor. II.6.34 the the image of wavelet transform (II.5.11) from a mother wavelet $\sum_1^n a_m w_{\mp 2m,1}$ will consist of null-solutions of the n -th power D_{\pm}^n of the conformal Cauchy-Riemann operator (II.5.14). They are a conformal flavour of *polyanalytic* functions [16].

We can similarly look for mother wavelets which are eigenvectors for other types of one dimensional subgroups. Our consideration of subgroup K is simplified by several facts:

- The parameter κ takes only complex values.
- The derived representation does not have singular points on the real line.

For both subgroups A' and N' this will not be true. The further consideration will be given in [195].

II.5.4. The Taylor Expansion

Consider an induced wavelet transform generated by a Lie group G , its representation ρ and a mother wavelet w which is an eigenvector of a one-dimensional subgroup $\tilde{H} \subset G$. Then by Prop. II.6.33 the wavelet transform intertwines ρ with a representation $\rho^{\tilde{H}}$ induced by a character of \tilde{H} .

If the mother wavelet is itself in the domain of the induced wavelet transform then the chain (II.3.16) of \tilde{H} -eigenvectors w_m will be mapped to the similar chain of their images \hat{w}_m . The corresponding derived induced representation $d\rho^{\tilde{H}}$ produces ladder operators with the transitive action of the ladder operators on the chain of \hat{w}_m . Then the vector space of “formal power series”:

$$(II.5.20) \quad \hat{f}(z) = \sum_{m \in \mathbb{Z}} a_m \hat{w}_m(z)$$

is a module for the Lie algebra of the group G .

Coming back to the case of the group $G = \text{SL}_2(\mathbb{R})$ and subgroup $\tilde{H} = K$. Images $\hat{w}_{m,1}$ of the eigenfunctions (II.5.10) under the Cauchy integral transform (II.5.16) are:

$$\hat{w}_{m,1}(z) = (\mathcal{J}z)^{1/2} \frac{(z+i)^{(m-1)/2}}{(z-i)^{(m+1)/2}}.$$

They are eigenfunctions of the derived representation on the upper half-plane and the action of ladder operators is given by the same expressions (II.5.12). In particular, the \mathfrak{sl}_2 -module generated by $\hat{w}_{1,1}$ will be one-sided since this vector is annihilated by the lowering operator. Since the Cauchy integral produces an unitary intertwining operator between two representations we get the following variant of Taylor series:

$$\hat{f}(z) = \sum_{m=0}^{\infty} c_m \hat{w}_{m,1}(z), \quad \text{where } c_m = \langle f, w_{m,1} \rangle.$$

For two other types of subgroups, representations and mother wavelets this scheme shall be suitably adapted and detailed study will be presented elsewhere [195].

II.5.5. Wavelet Transform in the Unit Disk and Other Domains

We can similarly construct an analytic function theories in unit disks, including parabolic and hyperbolic ones [191]. This can be done simply by an application of the *Cayley transform* to the function theories in the upper half-plane. Alternatively we can apply the full procedure for properly chosen groups and subgroups. We will briefly outline such a possibility here, see also [170].

Elements of $SL_2(\mathbb{R})$ can be also represented by 2×2 -matrices with complex entries such that, cf. Example II.4.24:

$$g = \begin{pmatrix} \alpha & \bar{\beta} \\ \beta & \bar{\alpha} \end{pmatrix}, \quad g^{-1} = \begin{pmatrix} \bar{\alpha} & -\bar{\beta} \\ -\beta & \alpha \end{pmatrix}, \quad |\alpha|^2 - |\beta|^2 = 1.$$

This realisations of $SL_2(\mathbb{R})$ (or rather $SU(2, \mathbb{C})$) is more suitable for function theory in the unit disk. It is obtained from the form, which we used before for the upper half-plane, by means of the Cayley transform [191, § 8.1].

We may identify the *unit disk* \mathbb{D} with the homogeneous space $SL_2(\mathbb{R})/\mathbb{T}$ for the *unit circle* \mathbb{T} through the important decomposition $SL_2(\mathbb{R}) \sim \mathbb{D} \times \mathbb{T}$ with $K = \mathbb{T}$ —the compact subgroup of $SL_2(\mathbb{R})$:

$$(II.5.21) \quad \begin{pmatrix} \alpha & \bar{\beta} \\ \beta & \bar{\alpha} \end{pmatrix} = |\alpha| \begin{pmatrix} 1 & \bar{\beta}\bar{\alpha}^{-1} \\ \beta\alpha^{-1} & 1 \end{pmatrix} \begin{pmatrix} \frac{\alpha}{|\alpha|} & 0 \\ 0 & \frac{\bar{\alpha}}{|\alpha|} \end{pmatrix} \\ = \frac{1}{\sqrt{1-|u|^2}} \begin{pmatrix} 1 & u \\ \bar{u} & 1 \end{pmatrix} \begin{pmatrix} e^{ix} & 0 \\ 0 & e^{-ix} \end{pmatrix},$$

where

$$x = \arg \alpha, \quad u = \bar{\beta}\bar{\alpha}^{-1}, \quad |u| < 1.$$

Each element $g \in SL_2(\mathbb{R})$ acts by the linear-fractional transformation (the Möbius map) on \mathbb{D} and \mathbb{T} $H_2(\mathbb{T})$ as follows:

$$(II.5.22) \quad g : z \mapsto \frac{\alpha z + \beta}{\bar{\beta}z + \bar{\alpha}}, \quad \text{where } g = \begin{pmatrix} \alpha & \beta \\ \bar{\beta} & \bar{\alpha} \end{pmatrix}.$$

In the decomposition (II.5.21) the first matrix on the right hand side acts by transformation (II.5.22) as an orthogonal rotation of \mathbb{T} or \mathbb{D} ; and the second one—by transitive family of maps of the unit disk onto itself.

The representation induced by a complex-valued character $\chi_k(z) = z^{-k}$ of \mathbb{T} according to the Section II.3.2 is:

$$(II.5.23) \quad \rho_k(g) : f(z) \mapsto \frac{1}{(\alpha - \beta z)^k} f\left(\frac{\bar{\alpha}z - \bar{\beta}}{\alpha - \beta z}\right) \quad \text{where } g = \begin{pmatrix} \alpha & \beta \\ \bar{\beta} & \bar{\alpha} \end{pmatrix}.$$

The representation ρ_1 is unitary on square-integrable functions and irreducible on the *Hardy space* on the unit circle.

We choose [173, 175] K -invariant function $v_0(z) \equiv 1$ to be a *vacuum vector*. Thus the associated *coherent states*

$$v(g, z) = \rho_1(g)v_0(z) = (u - z)^{-1}$$

are completely determined by the point on the unit disk $u = \bar{\beta}\bar{\alpha}^{-1}$. The family of coherent states considered as a function of both u and z is obviously the *Cauchy kernel* [170]. The *wavelet transform* [170, 173] $\mathcal{W} : L_2(\mathbb{T}) \rightarrow H_2(\mathbb{D}) : f(z) \mapsto \mathcal{W}f(g) = \langle f, v_g \rangle$ is the *Cauchy integral*:

$$(II.5.24) \quad \mathcal{W}f(u) = \frac{1}{2\pi i} \int_{\mathbb{T}} f(z) \frac{1}{u - z} dz.$$

This approach can be extended to arbitrary connected simply-connected domain. Indeed, it is known that Möbius maps is the whole group of biholomorphic automorphisms of the unit disk or upper half-plane. Thus we can state the following corollary from the *Riemann mapping theorem*:

COROLLARY II.5.13. *The group of biholomorphic automorphisms of a connected simply connected domain with at least two points on its boundary is isomorphic to $SL_2(\mathbb{R})$.*

If a domain is non-simply connected, then the group of its biholomorphic mapping can be trivial [27, 257]. However we may look for a rich group acting on function spaces rather than on geometric sets. Let a connected non-simply connected domain D be bounded by a finite collection of non-intersecting contours Γ_i , $i = 1, \dots, n$. For each Γ_i consider the isomorphic image G_i of the $SL_2(\mathbb{R})$ group which is defined by the Corollary II.5.13. Then define the group $G = G_1 \times G_2 \times \dots \times G_n$ and its action on $L_2(\partial D) = L_2(\Gamma_1) \oplus L_2(\Gamma_2) \oplus \dots \oplus L_2(\Gamma_n)$ through the Moebius action of G_i on $L_2(\Gamma_i)$.

EXAMPLE II.5.14. Consider an *annulus* defined by $r < |z| < R$. It is bounded by two circles: $\Gamma_1 = \{z : |z| = r\}$ and $\Gamma_2 = \{z : |z| = R\}$. For Γ_1 the Möbius action of $SL_2(\mathbb{R})$ is

$$\begin{pmatrix} \alpha & \bar{\beta} \\ \beta & \bar{\alpha} \end{pmatrix} : z \mapsto \frac{\alpha z + \bar{\beta}/r}{\beta z/r + \bar{\alpha}}, \quad \text{where } |\alpha|^2 - |\beta|^2 = 1,$$

with the respective action on Γ_2 . Those action can be linearised in the spaces $L_2(\Gamma_1)$ and $L_2(\Gamma_2)$. If we consider a subrepresentation reduced to analytic function on the annulus, then one copy of $SL_2(\mathbb{R})$ will act on the part of functions analytic outside of Γ_1 and another copy—on the part of functions analytic inside of Γ_2 .

Thus all classical objects of complex analysis (the Cauchy-Riemann equation, the Taylor series, the Bergman space, etc.) for a rather generic domain D can be also obtained from suitable representations similarly to the case of the upper half-plane [170, 175].

Affine Group: the Real and Complex Techniques in Harmonic Analysis

In this chapter we reviews complex and real techniques in harmonic analysis. We demonstrated that both, real and complex, techniques in harmonic analysis have the same group-theoretical origin: the covariant transform generated by the affine group. Moreover, they are complemented by the wavelet construction. Therefore, there is no any confrontation between these approaches and they can be lined up as in Table II.6.1. In other words, the binary opposition of the real and complex methods resolves via Kant's triad thesis-antithesis-synthesis: complex-real-covariant.

II.6.1. Introduction

There are two main approaches in harmonic analysis on the real line. The real variables technique uses various maximal functions, dyadic cubes and, occasionally, the Poisson integral [314]. The complex variable technique is based on the Cauchy integral and fine properties of analytic functions [264, 265].

Both methods seem to have clear advantages. The real variable technique:

- i. does not require an introduction of the imaginary unit for a study of real-valued harmonic functions of a real variable (Occam's Razor: among competing hypotheses, the one with the fewest assumptions should be selected);
- ii. allows a straightforward generalization to several real variables.

By contrast, access to the beauty and power of analytic functions (e.g., Möbius transformations, factorisation of zeroes, etc. [231]) is the main reason to use the complex variable technique. A posteriori, a multidimensional analytic version was also discovered [252], it is based on the monogenic Clifford-valued functions [49].

Therefore, propensity for either techniques becomes a personal choice of a researcher. Some of them prefer the real variable method, explicitly cleaning out any reference to analytic or harmonic functions [314, Ch. III, p. 88]. Others, e.g. [68, 233], happily combine the both techniques. However, the reasons for switching between two methods at particular places may look mysterious.

The purpose of the present paper is to revise the origins of the real and complex variable techniques. Thereafter, we describe the common group-theoretical root of both. Such a unification deepens our understanding of both methods and illuminates their interaction.

REMARK II.6.1. In this paper, we consider only examples which are supported by the affine group Aff of the real line. In the essence, Aff is the semidirect product of

the group of dilations acting on the group of translations. Thus, our consideration can be generalized to the semidirect product of dilations and homogeneous (nilpotent) Lie groups, cf. [103, 201]. Other important extensions are the group $SL_2(\mathbb{R})$ and associated hypercomplex algebras, see Rems. II.6.6, II.6.17 and [191, 197, 198]. However, we do not aim here to a high level of generality, it can be developed in subsequent works once the fundamental issues are sufficiently clarified.

II.6.2. Two approaches to harmonic analysis

As a starting point of our discussion, we provide a schematic outline of complex and real variables techniques in the one-dimensional harmonic analysis. The application of complex analysis may be summarised in the following sequence of principal steps:

Integral transforms.: For a function $f \in L_p(\mathbb{R})$, we apply the Cauchy or Poisson integral transforms:

$$(II.6.1) \quad [Cf](x + iy) = \frac{1}{2\pi i} \int_{\mathbb{R}} \frac{f(t)}{t - (x + iy)} dt,$$

$$(II.6.2) \quad [Pf](x, y) = \frac{1}{\pi} \int_{\mathbb{R}} \frac{y}{(t - x)^2 + y^2} f(t) dt.$$

An equivalent transformation on the unit circle replaces the Fourier series $\sum_k c_k e^{ikt}$ by the Taylor series $\sum_{k=0}^{\infty} c_k z^k$ in the complex variable $z = re^{it}$, $0 \leq r < 1$. It is used for the Abel summation of trigonometric series [344, § III.6]. Some other summations methods are in use as well [245].

Domains.: Above integrals (II.6.1)–(II.6.2) map the domain of functions from the real line to the upper half-plane, which can be conveniently identified with the set of complex numbers having a positive imaginary part. The larger domain allows us to inspect functions in greater details.

Differential operators.: The image of integrals (II.6.1) and (II.6.2) consists of functions, belonging to the kernel of the Cauchy–Riemann operator $\partial_{\bar{z}}$ and Laplace operator Δ respectively, i.e.:

$$(II.6.3) \quad \partial_{\bar{z}} = \frac{\partial}{\partial x} + i \frac{\partial}{\partial y}, \quad \Delta = \frac{\partial^2}{\partial x^2} + \frac{\partial^2}{\partial y^2}.$$

Such functions have numerous nice properties in the upper half-plane, e.g. they are infinitely differentiable, which make their study interesting and fruitful.

Boundary values and SIO.: To describe properties of the initial function f on the real line we consider the boundary values of $[Cf](x + iy)$ or $[Pf](x, y)$, i.e. their limits as $y \rightarrow 0$ in some sense. The Sokhotsky–Plemelj formula provides the boundary value of the Cauchy integral [257, (2.6.6)]:

$$(II.6.4) \quad [Cf](x, 0) = \frac{1}{2} f(x) + \frac{1}{2\pi i} \int_{\mathbb{R}} \frac{f(t)}{t - x} dt.$$

The last term is a singular integral operator defined through the principal value in the Cauchy sense:

$$(II.6.5) \quad \frac{1}{2\pi i} \int_{\mathbb{R}} \frac{f(t)}{t-x} dt = \lim_{\varepsilon \rightarrow 0} \frac{1}{2\pi i} \int_{-\infty}^{x-\varepsilon} + \int_{x+\varepsilon}^{\infty} \frac{f(t)}{t-x} dt.$$

For the Abel summation the boundary values are replaced by the limit as $r \rightarrow 1^-$ in the series $\sum_{k=0}^{\infty} c_k (re^{it})^k$.

Hardy space.: Sokhotsky–Plemelj formula (II.6.4) shows, that the boundary value $[\mathcal{C}f](x, 0)$ may be different from $f(x)$. The vector space of functions $f(x)$ such that $[\mathcal{C}f](x, 0) = f(x)$ is called the Hardy space on the real line [264, A.6.3].

Summing up this scheme: we replace a function (distribution) on the real line by a nicer (analytic or harmonic) function on a larger domain—the upper half-plane. Then, we trace down properties of the extensions to its boundary values and, eventually, to the initial function.

The real variable approach does not have a clearly designated path in the above sense. Rather, it looks like a collection of interrelated tools, which are efficient for various purposes. To highlight similarity and differences between real and complex analysis, we line up the elements of the real variable technique in the following way:

Hardy–Littlewood maximal function: is, probably, the most important component [54; 108, § I.4; 231, § VIII.B.1; 314, Ch. 2] of this technique. The maximal function f^M is defined on the real line by the identity:

$$(II.6.6) \quad f^M(t) = \sup_{a>0} \left\{ \frac{1}{2a} \int_{t-a}^{t+a} |f(x)| dx \right\}.$$

Domain: is not apparently changed, the maximal function f^M is again defined on the real line. However, an efficient treatment of the maximal functions requires consideration of tents [314, § II.2], which are parametrised by their vertices, i.e. points (a, b) , $a > 0$, of the upper half-plane. In other words, we repeatedly need values of all integrals $\frac{1}{2a} \int_{t-a}^{t+a} |f(x)| dx$, rather than the single value of the supremum over a .

Littlewood–Paley theory: [68, § 3] and associated dyadic squares technique [108, Ch. VII, Thm. 1.1; 314, § IV.3] as well as stopping time argument [108, Ch. VI, Lem. 2.2] are based on bisection of a function’s domain into two equal parts.

SIO: is a natural class of bounded linear operators in $L_p(\mathbb{R})$. Moreover, maximal operator $M : f \rightarrow f^M$ (II.6.6) and singular integrals are intimately related [314, Ch. I].

Hardy space: can be defined in several equivalent ways from previous notions.

For example, it is the class of such functions that their image under maximal operator (II.6.6) or singular integral (II.6.5) belongs to $L_p(\mathbb{R})$ [314, Ch. III].

The following discussion will line up real variable objects along the same axis as complex variables. We will summarize this in Table II.6.1.

II.6.3. Affine group and its representations

It is hard to present harmonic analysis and wavelets without touching the affine group one way or another, e.g. through the *doubling condition* on the measure, cf. [340]. Unfortunately, many sources only mention the group and do not use it explicitly. On the other hand, it is equally difficult to speak about the affine group without a reference to results in harmonic analysis: two theories are intimately intertwined. In this section we collect fundamentals of the affine group and its representations, which are not yet a standard background of an analyst.

Let $G = \text{Aff}$ be the $ax + b$ (or the *affine*) group [5, § 8.2], which is represented (as a topological set) by the upper half-plane $\{(a, b) \mid a \in \mathbb{R}_+, b \in \mathbb{R}\}$. The group law is:

$$(II.6.7) \quad (a, b) \cdot (a', b') = (aa', ab' + b).$$

As any other group, Aff has the *left regular representation* by shifts on functions $\text{Aff} \rightarrow \mathbb{C}$:

$$(II.6.8) \quad \Lambda(a, b) : f(a', b') \mapsto f_{(a,b)}(a', b') = f\left(\frac{a'}{a}, \frac{b' - b}{a}\right).$$

A left invariant measure on Aff is $dg = a^{-2} da db$, $g = (a, b)$. By the definition, the left regular representation (II.6.8) acts by unitary operators on $L_2(\text{Aff}, dg)$. The group is not unimodular and a right invariant measure is $a^{-1} da db$.

There are two important subgroups of the $ax + b$ group:

$$(II.6.9) \quad A = \{(a, 0) \in \text{Aff} \mid a \in \mathbb{R}_+\} \quad \text{and} \quad N = \{(1, b) \in \text{Aff} \mid b \in \mathbb{R}\}.$$

An isometric representation of Aff on $L_p(\mathbb{R})$ is given by the formula:

$$(II.6.10) \quad [\rho_p(a, b) f](x) = a^{-\frac{1}{p}} f\left(\frac{x - b}{a}\right).$$

Here, we identify the real line with the subgroup N or, even more accurately, with the homogeneous space Aff/N [92, § 2]. This representation is known as *quasi-regular* for its similarity with (II.6.8). The action of the subgroup N in (II.6.10) reduces to shifts, the subgroup A acts by dilations.

REMARK II.6.2. The $ax + b$ group definitely escapes Occam's Razor in harmonic analysis, cf. the arguments against the imaginary unit in the Introduction. Indeed, shifts are required to define convolutions on \mathbb{R}^n , and an *approximation of the identity* [314, § I.6.1] is a convolution with the dilated kernel. The same scaled convolutions define the fundamental *maximal functions*, see [314, § III.1.2] cf. Example II.6.43 below. Thus, we can avoid usage of the upper half-plane \mathbb{C}_+ , but the same set will anyway re-invent itself in the form of the $ax + b$ group.

The representation (II.6.10) in $L_2(\mathbb{R})$ is reducible and the space can be split into irreducible subspaces. Following the philosophy presented in the Introduction to the paper [203, § 1] we give the following

DEFINITION II.6.3. For a representation ρ of a group G in a space V , a *generalized Hardy space* H is an ρ -irreducible (or ρ -primary, as discussed in Section II.6.7) subspace of V .

EXAMPLE II.6.4. Let $G = \text{Aff}$ and the representation ρ_p be defined in $V = L_p(\mathbb{R})$ by (II.6.10). Then the classical Hardy spaces $H_p(\mathbb{R})$ are ρ_p -irreducible, thus are covered by the above definition.

Some ambiguity in picking the Hardy space out of all (well, two, as we will see below) irreducible components is resolved by the traditional preference.

REMARK II.6.5. We have defined the Hardy space completely in terms of representation theory of $ax + b$ group. The traditional descriptions, via the Fourier transform or analytic extensions, will be corollaries in our approach, see Prop. II.6.7 and Example II.6.35.

REMARK II.6.6. It is an interesting and important observation, that the Hardy space in $L_p(\mathbb{R})$ is invariant under the action of a larger group $SL_2(\mathbb{R})$, the group of 2×2 matrices with real entries and determinant equal to 1, the group operation coincides with the multiplication of matrices. The $ax + b$ group is isomorphic to the subgroup of the upper-triangular matrices in $SL_2(\mathbb{R})$. The group $SL_2(\mathbb{R})$ has an isometric representation in $L_p(\mathbb{R})$:

$$(II.6.11) \quad \begin{pmatrix} a & b \\ c & d \end{pmatrix} : f(x) \mapsto \frac{1}{|a - cx|^{\frac{2}{p}}} f\left(\frac{dx - b}{a - cx}\right),$$

which produces quasi-regular representation (II.6.10) by the restriction to upper-triangular matrices. The Hardy space $H_p(\mathbb{R})$ is invariant under the above action as well. Thus, $SL_2(\mathbb{R})$ produces a refined version in comparison with the harmonic analysis of the $ax + b$ group considered in this paper. Moreover, as representations of the $ax + b$ group are connected with complex numbers, the structure of $SL_2(\mathbb{R})$ links all three types of hypercomplex numbers [191; 197, § 3; 198, § 3.3.4], see also Rem. II.6.17.

To clarify a decomposition of $L_p(\mathbb{R})$ into irreducible subspaces of representation (II.6.10) we need another realization of this representation. It is called *co-adjoint* and is related to the *orbit method* of Kirillov [105, § 6.7.1; 162, § 4.1.4]. Again, this isometric representation can be defined on $L_p(\mathbb{R})$ by the formula:

$$(II.6.12) \quad [(a, b) f](\lambda) = a^{\frac{1}{p}} e^{-2\pi i b \lambda} f(a\lambda).$$

Since $a > 0$, there is an obvious decomposition into invariant subspaces of :

$$(II.6.13) \quad L_p(\mathbb{R}) = L_p(-\infty, 0) \oplus L_p(0, \infty).$$

It is possible to demonstrate, that these components are irreducible. This decomposition has a spatial nature, i.e., the subspaces have disjoint supports. Each half-line can be identified with the subgroup A or with the homogeneous space Aff/N .

The restrictions and of the co-adjoint representation to invariant subspaces (II.6.13) for $p = 2$ are not unitary equivalent. Any irreducible unitary representation of Aff is unitary equivalent either to or . Although there is no intertwining operator between and , the map:

$$(II.6.14) \quad J : L_p(\mathbb{R}) \rightarrow L_p(\mathbb{R}) : f(\lambda) \mapsto f(-\lambda),$$

has the property

$$(II.6.15) \quad (a, -b) \circ J = J \circ (a, b)$$

which corresponds to the outer automorphism $(a, b) \mapsto (a, -b)$ of Aff.

As was already mentioned, for the Hilbert space $L_2(\mathbb{R})$, representations (II.6.10) and (II.6.12) are unitary equivalent, i.e., there is a unitary intertwining operator between them. We may guess its nature as follows. The eigenfunctions of the operators $\rho_2(1, b)$ are $e^{2\pi i \omega x}$ and the eigenfunctions of $(1, b)$ are $\delta(\lambda - \omega)$. Both sets form “continuous bases” of $L_2(\mathbb{R})$ and the unitary operator which maps one to another is the Fourier transform:

$$(II.6.16) \quad \mathcal{F} : f(x) \mapsto \hat{f}(\lambda) = \int_{\mathbb{R}} e^{-2\pi i \lambda x} f(x) dx.$$

Although, the above arguments were informal, the intertwining property $\mathcal{F}\rho_2(a, b) = (1, b)\mathcal{F}$ can be directly verified by the appropriate change of variables in the Fourier transform. Thus, cf. [264, Lem. A.6.2.2]:

PROPOSITION II.6.7. *The Fourier transform maps irreducible invariant subspaces H_2 and H_2^\perp of (II.6.10) to irreducible invariant subspaces $L_2(0, \infty) = \mathcal{F}(H_2)$ and $L_2(-\infty, 0) = \mathcal{F}(H_2^\perp)$ of co-adjoint representation (II.6.12). In particular, $L_2(\mathbb{R}) = H_2 \oplus H_2^\perp$.*

Reflection J (II.6.14) anticommutes with the Fourier transform: $\mathcal{F}J = -J\mathcal{F}$. Thus, J also interchange the irreducible components ρ_p^+ and ρ_p^- of quasi-regular representation (II.6.10) according to (II.6.15).

Summing up, the unique rôle of the Fourier transform in harmonic analysis is based on the following facts from the representation theory. The Fourier transform

- intertwines shifts in quasi-regular representation (II.6.10) to operators of multiplication in co-adjoint representation (II.6.12);
- intertwines dilations in (II.6.10) to dilations in (II.6.12);
- maps the decomposition $L_2(\mathbb{R}) = H_2 \oplus H_2^\perp$ into spatially separated spaces with disjoint supports;
- anticommutes with J , which interchanges ρ_2^+ and ρ_2^- .

Armed with this knowledge we are ready to proceed to harmonic analysis.

II.6.4. Covariant transform

We make an extension of the wavelet construction defined in terms of group representations. See [159] for a background in the representation theory, however, the only treated case in this paper is the $ax + b$ group.

DEFINITION II.6.8. [192, 197] Let ρ be a representation of a group G in a space V and F be an operator acting from V to a space U . We define a *covariant transform* \mathcal{W}_F^ρ acting from V to the space $L(G, U)$ of U -valued functions on G by the formula:

$$(II.6.17) \quad \mathcal{W}_F^\rho : v \mapsto \hat{v}(g) = F(\rho(g^{-1})v), \quad v \in V, g \in G.$$

The operator F will be called a *fiducial operator* in this context (cf. the fiducial vector in [220]).

We may drop the sup/subscripts from \mathcal{W}_F^ρ if the functional F and/or the representation ρ are clear from the context.

REMARK II.6.9. We do not require that the fiducial operator F be linear. Sometimes the positive homogeneity, i.e. $F(tv) = tF(v)$ for $t > 0$, alone can be already sufficient, see Example II.6.14.

REMARK II.6.10. It looks like the usefulness of the covariant transform is in the reverse proportion to the dimension of the space U . The covariant transform encodes properties of v in a function $\mathcal{W}_F^\rho v$ on G , which is a scalar-valued function if $\dim U = 1$. However, such a simplicity is not always possible. Moreover, the paper [201] gives an important example of a covariant transform which provides a simplification even in the case $\dim U = \dim V$.

We start the list of examples with the classical case of the group-theoretical wavelet transform.

EXAMPLE II.6.11. [5, 95, 95, 173, 220, 279] Let V be a Hilbert space with an inner product $\langle \cdot, \cdot \rangle$ and ρ be a unitary representation of a group G in the space V . Let $F : V \rightarrow \mathbb{C}$ be the functional $v \mapsto \langle v, v_0 \rangle$ defined by a vector $v_0 \in V$. The vector v_0 is often called the *mother wavelet* in areas related to signal processing, the *vacuum state* in the quantum framework, etc.

In this set-up, transformation (II.6.17) is the well-known expression for a *wavelet transform* [5, (7.48)] (or *representation coefficients*):

$$(II.6.18) \quad \mathcal{W} : v \mapsto \tilde{v}(g) = \langle \rho(g^{-1})v, v_0 \rangle = \langle v, \rho(g)v_0 \rangle, \quad v \in V, g \in G.$$

The family of the vectors $v_g = \rho(g)v_0$ is called *wavelets* or *coherent states*. The image of (II.6.18) consists of scalar valued functions on G .

This scheme is typically carried out for a square integrable representation ρ with v_0 being an admissible vector [5, 63, 87, 95, 106, 279], i.e. satisfying the condition:

$$(II.6.19) \quad 0 < \|\tilde{v}_0\|^2 = \int_G |\langle v_0, \rho_2(g)v_0 \rangle|^2 dg < \infty.$$

In this case the wavelet (covariant) transform is a map into the square integrable functions [87] with respect to the left Haar measure on G . The map becomes an isometry if v_0 is properly scaled. Moreover, we are able to recover the input v from its wavelet transform through the reconstruction formula, which requires an admissible vector as well, see Example II.6.20 below. The most popularized case of the above scheme is provided by the affine group.

EXAMPLE II.6.12. For the $ax + b$ group, representation (II.6.10) is square integrable for $p = 2$. Any function v_0 , such that its Fourier transform $\hat{v}_0(\lambda)$ satisfies

$$(II.6.20) \quad \int_0^\infty \frac{|\hat{v}_0(\lambda)|^2}{\lambda} d\lambda < \infty,$$

is admissible in the sense of (II.6.19) [5, § 12.2]. The *continuous wavelet transform* is generated by representation (II.6.10) acting on an admissible vector v_0 in expression (II.6.18).

The image of a function from $L_2(\mathbb{R})$ is a function on the upper half-plane square integrable with respect to the measure $a^{-2} da db$. There are many examples [5, § 12.2] of useful admissible vectors, say, the *Mexican hat* wavelet: $(1 - x^2)e^{-x^2/2}$. For sufficiently regular \hat{v}_0 admissibility (II.6.20) of v_0 follows by a weaker condition

$$(II.6.21) \quad \int_{\mathbb{R}} v_0(x) dx = 0.$$

We dedicate Section II.6.8 to isometric properties of this transform.

However, square integrable representations and admissible vectors do not cover all interesting cases.

EXAMPLE II.6.13. For the above $G = \text{Aff}$ and representation (II.6.10), we consider the operators $F_{\pm} : L_p(\mathbb{R}) \rightarrow \mathbb{C}$ defined by:

$$(II.6.22) \quad F_{\pm}(f) = \frac{1}{\pi i} \int_{\mathbb{R}} \frac{f(x) dx}{i \mp x}.$$

In $L_2(\mathbb{R})$ we note that $F_+(f) = \langle f, c \rangle$, where $c(x) = \frac{1}{\pi i} \frac{1}{i+x}$. Computing the Fourier transform $\hat{c}(\lambda) = \chi_{(0,+\infty)}(\lambda) e^{-\lambda}$, we see that $\bar{c} \in H_2(\mathbb{R})$. Moreover, \hat{c} does not satisfy admissibility condition (II.6.20) for representation (II.6.10).

Then, covariant transform (II.6.17) is Cauchy integral (II.6.1) from $L_p(\mathbb{R})$ to the space of functions $\tilde{f}(a, b)$ such that $a^{-\frac{1}{p}} \tilde{f}(a, b)$ is in the Hardy space on the upper-/lower half-plane $H_p(\mathbb{R}_{\pm}^2)$ [264, § A.6.3]. Due to inadmissibility of $c(x)$, the complex analysis become decoupled from the traditional wavelet theory.

Many important objects in harmonic analysis are generated by inadmissible mother wavelets like (II.6.22). For example, the functionals $P = \frac{1}{2}(F_+ + F_-)$ and $Q = \frac{1}{2i}(F_+ - F_-)$ are defined by kernels:

$$(II.6.23) \quad p(x) = \frac{1}{2\pi i} \left(\frac{1}{i-x} + \frac{1}{i+x} \right) = \frac{1}{\pi} \frac{1}{1+x^2},$$

$$(II.6.24) \quad q(x) = -\frac{1}{2\pi} \left(\frac{1}{i-x} - \frac{1}{i+x} \right) = -\frac{1}{\pi} \frac{x}{1+x^2}$$

which are *Poisson kernel* (II.6.2) and the *conjugate Poisson kernel* [108, § III.1; 114, § 4.1; 231, Ch. 5; 264, § A.5.3], respectively. Another interesting non-admissible vector is the *Gaussian* e^{-x^2} .

EXAMPLE II.6.14. A step in a different direction is a consideration of non-linear operators. Take again the $ax + b$ group and its representation (II.6.10). We define F to be a homogeneous (but non-linear) functional $V \rightarrow \mathbb{R}_+$:

$$(II.6.25) \quad F_m(f) = \frac{1}{2} \int_{-1}^1 |f(x)| dx.$$

Covariant transform (II.6.17) becomes:

$$(II.6.26) \quad [\mathcal{W}_p^m f](a, b) = F(\rho_p(\frac{1}{a}, -\frac{1}{b})f) = \frac{1}{2} \int_{-1}^1 \left| a^{\frac{1}{p}} f(ax + b) \right| dx = \frac{a^{\frac{1}{q}}}{2} \int_{b-a}^{b+a} |f(x)| dx,$$

where $\frac{1}{p} + \frac{1}{q} = 1$, as usual. We will see its connections with the Hardy–Littlewood maximal functions in Example II.6.43.

Since linearity has clear advantages, we may prefer to reformulate the last example using linear covariant transforms. The idea is similar to the representation of a convex function as an envelope of linear ones, cf. [108, Ch. I, Lem. 6.1]. To this end, we take a collection \mathbf{F} of linear fiducial functionals and, for a given function f , consider the set of all covariant transforms $\mathcal{W}_F f$, $F \in \mathbf{F}$.

EXAMPLE II.6.15. Let us return to the setup of the previous Example for $G = \text{Aff}$ and its representation (II.6.10). Consider the unit ball B in $L_\infty[-1, 1]$. Then, any $\omega \in B$ defines a bounded linear functional F_ω on $L_1(\mathbb{R})$:

$$(II.6.27) \quad F_\omega(f) = \frac{1}{2} \int_{-1}^1 f(x) \omega(x) dx = \frac{1}{2} \int_{\mathbb{R}} f(x) \omega(x) dx.$$

Of course, $\sup_{\omega \in B} F_\omega(f) = F_m(f)$ with F_m from (II.6.25) and for all $f \in L_1(\mathbb{R})$. Then, for the non-linear covariant transform (II.6.26) we have the following expression in terms of the linear covariant transforms generated by F_ω :

$$(II.6.28) \quad [\mathcal{W}_1^m f](a, b) = \sup_{\omega \in B} [\mathcal{W}_1^\omega f](a, b).$$

The presence of supremum is the price to pay for such a “linearization”.

REMARK II.6.16. The above construction is not much different to the *grand maximal function* [314, § III.1.2]. Although, it may look like a generalisation of covariant transform, grand maximal function can be realised as a particular case of Defn. II.6.8. Indeed, let $M(V)$ be a subgroup of the group of all invertible isometries of a metric space V . If ρ represents a group G by isometries of V then we can consider the group \tilde{G} generated by all finite products of $M(V)$ and $\rho(g)$, $g \in G$ with the straightforward action $\tilde{\rho}$ on V . The grand maximal functions is produced by the covariant transform for the representation $\tilde{\rho}$ of \tilde{G} .

REMARK II.6.17. It is instructive to compare action (II.6.11) of the large $SL_2(\mathbb{R})$ group on the mother wavelet $\frac{1}{x+i}$ for the Cauchy integral and the principal case $\omega(x) = \chi_{[-1,1]}(x)$ (the characteristic function of $[-1, 1]$) for functional (II.6.27). The wavelet $\frac{1}{x+i}$ is an eigenvector for all matrices $\begin{pmatrix} \cos t & \sin t \\ -\sin t & \cos t \end{pmatrix}$, which form the one-parameter compact subgroup $K \subset SL_2(\mathbb{R})$. The respective covariant transform (i.e., the Cauchy integral) maps functions to the homogeneous space $SL_2(\mathbb{R})/K$, which is the upper half-plane with the Möbius (linear-fractional) transformations of complex numbers [191; 197, § 3; 198, § 3.3.4]. By contrast, the mother wavelet $\chi_{[-1,1]}$ is an eigenvector for all

matrices $\begin{pmatrix} \cosh t & \sinh t \\ \sinh t & \cosh t \end{pmatrix}$, which form the one-parameter subgroup $A \in \text{SL}_2(\mathbb{R})$. The covariant transform (i.e., the averaging) maps functions to the homogeneous space $\text{SL}_2(\mathbb{R})/A$, which can be identified with a set of double numbers with corresponding Möbius transformations [191; 197, § 3; 198, § 3.3.4]. Conformal geometry of double numbers is suitable for real variables technique, in particular, tents [314, § II.2] make a Möbius-invariant family.

II.6.5. The contravariant transform

Define the left action Λ of a group G on a space of functions over G by:

$$(II.6.29) \quad \Lambda(g) : f(h) \mapsto f(g^{-1}h).$$

For example, in the case of the affine group it is (II.6.8). An object invariant under the left action Λ is called *left invariant*. In particular, let L and L' be two left invariant spaces of functions on G . We say that a pairing $\langle \cdot, \cdot \rangle : L \times L' \rightarrow \mathbb{C}$ is *left invariant* if

$$(II.6.30) \quad \langle \Lambda(g)f, \Lambda(g)f' \rangle = \langle f, f' \rangle, \quad \text{for all } f \in L, f' \in L', g \in G.$$

- REMARK II.6.18.
- i. We do not require the pairing to be linear in general, in some cases it is sufficient to have only homogeneity, see Example II.6.22.
 - ii. If the pairing is invariant on space $L \times L'$ it is not necessarily invariant (or even defined) on large spaces of functions.
 - iii. In some cases, an invariant pairing on G can be obtained from an *invariant functional* \mathfrak{l} by the formula $\langle f_1, f_2 \rangle = \mathfrak{l}(f_1 f_2)$.

For a representation ρ of G in V and $w_0 \in V$, we construct a function $w(g) = \rho(g)w_0$ on G . We assume that the pairing can be extended in its second component to this V -valued functions. For example, such an extension can be defined in the weak sense.

DEFINITION II.6.19. [192,197] Let $\langle \cdot, \cdot \rangle$ be a left invariant pairing on $L \times L'$ as above, let ρ be a representation of G in a space V , we define the function $w(g) = \rho(g)w_0$ for $w_0 \in V$ such that $w(g) \in L'$ in a suitable sense. The *contravariant transform* $\mathcal{M}_{w_0}^\rho$ is a map $L \rightarrow V$ defined by the pairing:

$$(II.6.31) \quad \mathcal{M}_{w_0}^\rho : f \mapsto \langle f, w \rangle, \quad \text{where } f \in L.$$

We can drop out sup/subscripts in $\mathcal{M}_{w_0}^\rho$ as we did for \mathcal{W}_F^ρ .

EXAMPLE II.6.20 (Haar paring). The most used example of an invariant pairing on $L_2(G, d\mu) \times L_2(G, d\mu)$ is the integration with respect to the Haar measure:

$$(II.6.32) \quad \langle f_1, f_2 \rangle = \int_G f_1(g)f_2(g) dg.$$

If ρ is a square integrable representation of G and w_0 is an admissible vector, see Example II.6.11, then this pairing can be extended to $w(g) = \rho(g)w_0$. The contravariant transform is known in this setup as the *reconstruction formula*, cf. [5, (8.19)]:

$$(II.6.33) \quad \mathcal{M}_{w_0} f = \int_G f(g) w(g) dg, \quad \text{where } w(g) = \rho(g)w_0.$$

It is possible to use different admissible vectors v_0 and w_0 for wavelet transform (II.6.18) and reconstruction formula (II.6.33), respectively, cf. Example II.6.41.

Let either

- ρ be not a square integrable representation (even modulo a subgroup); or
- w_0 be an inadmissible vector of a square integrable representation ρ .

A suitable invariant pairing in this case is not associated with integration over the Haar measure on G . In this case we speak about a *Hardy pairing*. The following example explains the name.

EXAMPLE II.6.21 (Hardy pairing). Let G be the $ax + b$ group and its representation ρ (II.6.10) in Example II.6.12. An invariant pairing on G , which is not generated by the Haar measure $a^{-2}da db$, is:

$$(II.6.34) \quad \langle f_1, f_2 \rangle_H = \lim_{a \rightarrow 0} \int_{-\infty}^{\infty} f_1(a, b) f_2(a, b) \frac{db}{a}.$$

For this pairing, we can consider functions $\frac{1}{\pi i} \frac{1}{x+i}$ or e^{-x^2} , which are not admissible vectors in the sense of square integrable representations. For example, for $v_0 = \frac{1}{\pi i} \frac{1}{x+i}$ we obtain:

$$[\mathcal{M}f](x) = \lim_{a \rightarrow 0} \int_{-\infty}^{\infty} f(a, b) \frac{a^{-\frac{1}{p}}}{\pi i(x + ia - b)} db = - \lim_{a \rightarrow 0} \frac{a^{-\frac{1}{p}}}{\pi i} \int_{-\infty}^{\infty} \frac{f(a, b) db}{b - (x + ia)}.$$

In other words, it expresses the boundary values at $a = 0$ of the Cauchy integral $[-\mathcal{C}f](x + ia)$.

Here is an important example of non-linear pairing.

EXAMPLE II.6.22. Let $G = \text{Aff}$ and an invariant homogeneous functional on G be given by the L_∞ -version of Haar functional (II.6.32):

$$(II.6.35) \quad \langle f_1, f_2 \rangle_\infty = \sup_{g \in G} |f_1(g)f_2(g)|.$$

Define the following two functions on \mathbb{R} :

$$(II.6.36) \quad v_0^+(t) = \begin{cases} 1, & \text{if } t = 0; \\ 0, & \text{if } t \neq 0, \end{cases} \quad \text{and} \quad v_0^*(t) = \begin{cases} 1, & \text{if } |t| \leq 1; \\ 0, & \text{if } |t| > 1. \end{cases}$$

The respective contravariant transforms are generated by representation ρ_∞ (II.6.10) are:

$$(II.6.37) \quad [\mathcal{M}_{v_0^+} f](t) = f^+(t) = \langle f(a, b), \rho_\infty(a, b)v_0^+(t) \rangle_\infty = \sup_a |f(a, t)|,$$

$$(II.6.38) \quad [\mathcal{M}_{v_0^*} f](t) = f^*(t) = \langle f(a, b), \rho_\infty(a, b)v_0^*(t) \rangle_\infty = \sup_{a > |b-t|} |f(a, b)|.$$

Transforms (II.6.37) and (II.6.38) are the *vertical* and *non-tangential maximal functions* [231, § VIII.C.2], respectively.

EXAMPLE II.6.23. Consider again $G = \text{Aff}$ equipped now with an invariant linear functional, which is a Hardy-type modification (cf. (II.6.34)) of L_∞ -functional (II.6.35):

$$(II.6.39) \quad \langle f_1, f_2 \rangle_\infty^H = \overline{\lim}_{a \rightarrow 0} \sup_{b \in \mathbb{R}} (f_1(a, b) f_2(a, b)),$$

where $\overline{\lim}$ is the upper limit. Then, the covariant transform \mathcal{M}^H for this pairing for functions v^+ and v^* (II.6.36) becomes:

$$(II.6.40) \quad [\mathcal{M}_{v_0^+}^H f](t) = \langle f(a, b), \rho_\infty(a, b) v_0^+(t) \rangle_\infty^H = \overline{\lim}_{a \rightarrow 0} f(a, t),$$

$$(II.6.41) \quad [\mathcal{M}_{v_0^*}^H f](t) = \langle f(a, b), \rho_\infty(a, b) v_0^*(t) \rangle_\infty^H = \overline{\lim}_{\substack{a \rightarrow 0 \\ |b-t| < a}} f(a, b).$$

They are the *normal* and *non-tangential* upper limits from the upper-half plane to the real line, respectively.

Note the obvious inequality $\langle f_1, f_2 \rangle_\infty \geq \langle f_1, f_2 \rangle_\infty^H$ between pairings (II.6.35) and (II.6.39), which produces the corresponding relation between respective contravariant transforms.

There is an explicit duality between the covariant transform and the contravariant transform. Discussion of the grand maximal function in the Rem. II.6.16 shows usefulness of the covariant transform over a family of fiducial functionals. Thus, we shall not be surprised by the contravariant transform over a family of reconstructing vectors as well.

DEFINITION II.6.24. Let $w : \text{Aff} \rightarrow L_1(\mathbb{R})$ be a function. We define a new function $\rho_1 w$ on Aff with values in $L_1(\mathbb{R})$ via the point-wise action $[\rho_1 w](g) = \rho_1(g)w(g)$ of ρ_∞ (II.6.10). If $\sup_g \|w(g)\|_1 < \infty$, then, for $f \in L_1(\text{Aff})$, we define the *extended contravariant transform* by:

$$(II.6.42) \quad [\mathcal{M}_w f](x) = \int_{\text{Aff}} f(g) [\rho_1 w](g) dg.$$

Note, that (II.6.42) reduces to the contravariant transform (II.6.33) if we start from the constant function $w(g) = w_0$.

DEFINITION II.6.25. We call a function r on \mathbb{R} a *nucleus* if:

- i. r is supported in $[-1, 1]$,
- ii. $|r| < \frac{1}{2}$ almost everywhere, and
- iii. $\int_{\mathbb{R}} r(x) dx = 0$, cf. (II.6.21).

Clearly, for a nucleus r , the function $s = \rho_1(a, b)r$ has the following properties:

- i. s is supported in a ball centred at b and radius a ,
- ii. $|s| < \frac{1}{2a}$ almost everywhere, and
- iii. $\int_{\mathbb{R}} s(x) dx = 0$.

In other words, $s = \rho_1(a, b)r$ is an *atom*, cf. [314, § III.2.2] and any atom may be obtained in this way from some nucleus and certain $(a, b) \in \text{Aff}$.

EXAMPLE II.6.26. Let $f(g) = \sum_j \lambda_j \delta_{g_j}(g)$ with $\sum_j |\lambda_j| < \infty$ be a countable sum of point masses on Aff. If all values of $w(g_j)$ are nucleuses, then (II.6.42) becomes:

$$(II.6.43) \quad [\mathcal{M}_w f](x) = \int_{\text{Aff}} f(g) [\rho_1 w](g) dg = \sum_j \lambda_j s_j,$$

where $s_j = \rho_1(g_j)w(g_j)$ are atoms. The right-hand side of (II.6.43) is known as an *atomic decomposition* of a function $h(x) = [\mathcal{M}_w f](x)$, see [314, § III.2.2].

II.6.6. Intertwining properties of covariant transforms

The covariant transform has obtained its name because of the following property.

THEOREM II.6.27. [192, 197] *Covariant transform (II.6.17) intertwines ρ and the left regular representation Λ (II.6.29) on $L(G, \mathcal{U})$:*

$$(II.6.44) \quad \mathcal{W}\rho(g) = \Lambda(g)\mathcal{W}.$$

COROLLARY II.6.28. *The image space $\mathcal{W}(V)$ is invariant under the left shifts on G .*

The covariant transform is also a natural source of *relative convolutions* [171, 204], which are operators $A_k = \int_G k(g)\rho(g) dg$ obtained by integration a representation ρ of a group G with a suitable kernel k on G . In particular, inverse wavelet transform $\mathcal{M}_{w_0} f$ (II.6.33) can be defined from the relative convolution A_f as well: $\mathcal{M}_{w_0} f = A_f w_0$.

COROLLARY II.6.29. *Covariant transform (II.6.17) intertwines the operator of convolution K (with kernel k) and the operator of relative convolution A_k , i.e. $K\mathcal{W} = \mathcal{W}A_k$.*

If the invariant pairing is defined by integration with respect to the Haar measure, cf. Example II.6.20, then we can show an intertwining property for the contravariant transform as well.

PROPOSITION II.6.30. [173, Prop. 2.9] *Inverse wavelet transform \mathcal{M}_{w_0} (II.6.33) intertwines left regular representation Λ (II.6.29) on $L_2(G)$ and ρ :*

$$(II.6.45) \quad \mathcal{M}_{w_0} \Lambda(g) = \rho(g) \mathcal{M}_{w_0}.$$

COROLLARY II.6.31. *The image $\mathcal{M}_{w_0}(L(G)) \subset V$ of a left invariant space $L(G)$ under the inverse wavelet transform \mathcal{M}_{w_0} is invariant under the representation ρ .*

REMARK II.6.32. It is an important observation, that the above intertwining property is also true for some contravariant transforms which are not based on pairing (II.6.32). For example, in the case of the affine group all pairings (II.6.34), (II.6.39) and (non-linear!) (II.6.35) satisfy to (IV.5.22) for the respective representation ρ_p (II.6.10).

There is also a simple connection between a covariant transform and right shifts.

PROPOSITION II.6.33. [193, 197] *Let G be a Lie group and ρ be a representation of G in a space V . Let $[\mathcal{W}f](g) = F(\rho(g^{-1})f)$ be a covariant transform defined by a fiducial operator $F : V \rightarrow \mathcal{U}$. Then the right shift $[\mathcal{W}f](gg')$ by g' is the covariant transform $[\mathcal{W}'f](g) = F'(\rho(g^{-1})f)$ defined by the fiducial operator $F' = F \circ \rho(g^{-1})$.*

In other words the covariant transform intertwines right shifts $R(g) : f(h) \mapsto f(hg)$ on the group G with the associated action

$$(II.6.46) \quad \rho_B(g) : F \mapsto F \circ \rho(g^{-1})$$

on fiducial operators:

$$(II.6.47) \quad R(g) \circ \mathcal{W}_F = \mathcal{W}_{\rho_B(g)F}, \quad g \in G.$$

Although the above result is obvious, its infinitesimal version has interesting consequences. Let G be a Lie group with a Lie algebra \mathfrak{g} and ρ be a smooth representation of G . We denote by $d\rho_B$ the derived representation of the associated representation ρ_B (II.6.46) on fiducial operators.

COROLLARY II.6.34. [193, 197] *Let a fiducial operator F be a null-solution, i.e. $AF = 0$, for the operator $A = \sum_j a_j d\rho_B^{X_j}$, where $X_j \in \mathfrak{g}$ and a_j are constants. Then the covariant transform $[\mathcal{W}_F f](g) = F(\rho(g^{-1})f)$ for any f satisfies*

$$D(\mathcal{W}_F f) = 0, \quad \text{where } D = \sum_j \bar{a}_j \mathfrak{L}^{X_j}.$$

Here, \mathfrak{L}^{X_j} are the left invariant fields (Lie derivatives) on G corresponding to X_j .

EXAMPLE II.6.35. Consider representation ρ (II.6.10) of the $ax + b$ group with the $p = 1$. Let A and N be the basis of \mathfrak{g} generating one-parameter subgroups A and N (II.6.9), respectively. Then, the derived representations are:

$$[d\rho^A f](x) = -f(x) - xf'(x), \quad [d\rho^N f](x) = -f'(x).$$

The corresponding left invariant vector fields on $ax + b$ group are:

$$\mathfrak{L}^A = a\partial_a, \quad \mathfrak{L}^N = a\partial_b.$$

The mother wavelet $\frac{1}{x+i}$ in (II.6.22) is a null solution of the operator

$$(II.6.48) \quad -d\rho^A - id\rho^N = I + (x+i)\frac{d}{dx}.$$

Therefore, the image of the covariant transform with fiducial operator F_+ (II.6.22) consists of the null solutions to the operator $-\mathfrak{L}^A + i\mathfrak{L}^N = ia(\partial_b + i\partial_a)$, that is in the essence Cauchy–Riemann operator $\partial_{\bar{z}}$ (II.6.3) in the upper half-plane.

EXAMPLE II.6.36. In the above setting, the function $p(x) = \frac{1}{\pi} \frac{1}{x^2+1}$ (II.6.23) is a null solution of the operator:

$$(d\rho^A)^2 - d\rho^A + (d\rho^N)^2 = 2I + 4x\frac{d}{dx} + (1+x^2)\frac{d^2}{dx^2}.$$

The covariant transform with the mother wavelet $p(x)$ is the Poisson integral, its values are null solutions to the operator $(\mathfrak{L}^A)^2 - \mathfrak{L}^A + (\mathfrak{L}^N)^2 = a^2(\partial_b^2 + \partial_a^2)$, which is Laplace operator Δ (II.6.3).

EXAMPLE II.6.37. Fiducial functional F_m (II.6.25) is a null solution of the following functional equation:

$$F_m - F_m \circ \rho_\infty(\frac{1}{2}, \frac{1}{2}) - F_m \circ \rho_\infty(\frac{1}{2}, -\frac{1}{2}) = 0.$$

Consequently, the image of wavelet transform \mathcal{W}_p^m (II.6.26) consists of functions which solve the equation:

$$(I - R(\frac{1}{2}, \frac{1}{2}) - R(\frac{1}{2}, -\frac{1}{2}))f = 0 \quad \text{or} \quad f(a, b) = f(\frac{1}{2}a, b + \frac{1}{2}a) + f(\frac{1}{2}a, b - \frac{1}{2}a).$$

The last relation is the key to the stopping time argument [108, Ch. VI, Lem. 2.2] and the dyadic squares technique, see for example [314, § IV.3], [108, Ch. VII, Thm. 1.1] or the picture on the front cover of the latter book.

The moral of the above Examples II.6.35–II.6.37 is: there is a significant freedom in choice of covariant transforms. However, some fiducial functionals have special properties, which suggest the suitable technique (e.g., analytic, harmonic, dyadic, etc.) following from this choice.

II.6.7. Composing the covariant and the contravariant transforms

From Props. II.6.27, II.6.30 and Rem. II.6.32 we deduce the following

COROLLARY II.6.38. *The composition $\mathcal{M}_w \circ \mathcal{W}_F$ of a covariant \mathcal{M}_w and contravariant \mathcal{W}_F transforms is a map $V \rightarrow V$, which commutes with ρ , i.e., intertwines ρ with itself.*

In particular for the affine group and representation (II.6.10), $\mathcal{M}_w \circ \mathcal{W}_F$ commutes with shifts and dilations of the real line.

Since the image space of $\mathcal{M}_w \circ \mathcal{W}_F$ is an Aff-invariant space, we shall be interested in the smallest building blocks with the same property. For the Hilbert spaces, any group invariant subspace V can be decomposed into a direct integral $V = \oplus \int V_\mu \, d\mu$ of irreducible subspaces V_μ , i.e. V_μ does not have any non-trivial invariant subspace [159, § 8.4]. For representations in Banach spaces complete reducibility may not occur and we shall look for *primary* subspace, i.e. space which is not a direct sum of two invariant subspaces [159, § 8.3]. We already identified such subspaces as generalized Hardy spaces in Defn. II.6.3. They are also related to covariant functional calculus [182; 197, § 6].

For irreducible Hardy spaces, we can use the following general principle, which has several different formulations, cf. [159, Thm. 8.2.1]:

LEMMA II.6.39 (Schur). [5, Lem. 4.3.1] *Let ρ be a continuous unitary irreducible representation of G on the Hilbert space H . If a bounded operator $T : H \rightarrow T$ commutes with $\rho(g)$, for all $g \in G$, then $T = \kappa I$, for some $\lambda \in \mathbb{C}$.*

REMARK II.6.40. A revision of proofs of the Schur’s Lemma, even in different formulations, show that the result is related to the existence of joint invariant subspaces for all operators $\rho(g)$, $g \in G$.

In the case of classical wavelets, the relation between wavelet transform (II.6.18) and inverse wavelet transform (II.6.33) is suggested by their names.

EXAMPLE II.6.41. For an irreducible square integrable representation and admissible vectors v_0 and w_0 , there is the relation [5, (8.52)]:

$$(II.6.49) \quad \mathcal{M}_{w_0} \mathcal{W}_{v_0} = kI,$$

as an immediate consequence from the Schur’s lemma. Furthermore, square integrability condition (II.6.19) ensures that $k \neq 0$. The exact value of the constant k depends on v_0, w_0 and the Duflo–Moore operator [5, § 8.2; 87].

It is of interest here, that two different vectors can be used as analysing vector in (II.6.18) and for the reconstructing formula (II.6.33). Even a greater variety can be achieved if we use additional fiducial operators and invariant pairings.

For the affine group, recall the decomposition from Prop. II.6.7 into invariant subspaces $L_2(\mathbb{R}) = H_2 \oplus H_2^\perp$ and the fact, that the restrictions ρ_2^+ and ρ_2^- of ρ_2 (II.6.10) on H_2 and H_2^\perp are not unitary equivalent. Then, Schur’s lemma implies:

COROLLARY II.6.42. Any bounded linear operator $T : L_2(\mathbb{R}) \rightarrow L_2(\mathbb{R})$ commuting with ρ_2 has the form $k_1 I_{H_2} \oplus k_2 I_{H_2^\perp}$ for some constants $k_1, k_2 \in \mathbb{C}$. Consequently, the Fourier transform maps T to the operator of multiplication by $k_1 \chi_{(0,+\infty)} + k_2 \chi_{(-\infty,0)}$.

Of course, Corollary II.6.42 is applicable to the composition of covariant and contravariant transforms. In particular, the constants k_1 and k_2 may have zero values: for example, the zero value occurs for \mathcal{W} (II.6.18) with an admissible vector v_0 and non-tangential limit $\mathcal{M}_{v_0^*}^H$ (II.6.41)—because a square integrable function $f(a, b)$ on Aff vanishes for $a \rightarrow 0$.

EXAMPLE II.6.43. The composition of contravariant transform $\mathcal{M}_{v_0^*}$ (II.6.38) with covariant transform \mathcal{W}_∞ (II.6.26) is:

$$(II.6.50) \quad \begin{aligned} [\mathcal{M}_{v_0^*} \mathcal{W}_\infty f](t) &= \sup_{a > |b-t|} \left\{ \frac{1}{2a} \int_{b-a}^{b+a} |f(x)| dx \right\} \\ &= \sup_{b_1 < t < b_2} \left\{ \frac{1}{b_2 - b_1} \int_{b_1}^{b_2} |f(x)| dx \right\}. \end{aligned}$$

Thus, $\mathcal{M}_{v_0^*} \mathcal{W}_\infty f$ coincides with *Hardy–Littlewood maximal function* f^M (II.6.6), which contains important information on the original function f [231, § VIII.B.1]. Combining Props. II.6.27 and II.6.30 (through Rem. II.6.32), we deduce that the operator $M : f \mapsto f^M$ commutes with ρ_p : $\rho_p M = M \rho_p$. Yet, M is non-linear and Cor. II.6.42 is not applicable in this case.

EXAMPLE II.6.44. Let the mother wavelet $v_0(x) = \delta(x)$ be the Dirac delta function, then the wavelet transform \mathcal{W}_δ generated by ρ_∞ (II.6.10) on $C(\mathbb{R})$ is $[\mathcal{W}_\delta f](a, b) = f(b)$. Take the reconstruction vector $w_0(t) = (1 - \chi_{[-1,1]}(t))/t/\pi$ and consider the respective inverse wavelet transform \mathcal{M}_{w_0} produced by Hardy pairing (II.6.34). Then,

the composition of both maps is:

$$\begin{aligned}
 (\mathcal{M}_{w_0} \circ \mathcal{W}_\delta f)(t) &= \lim_{a \rightarrow 0} \frac{1}{\pi} \int_{-\infty}^{\infty} f(b) \rho_\infty(a, b) w_0(t) \frac{db}{a} \\
 &= \lim_{a \rightarrow 0} \frac{1}{\pi} \int_{-\infty}^{\infty} f(b) \frac{1 - \chi_{[-a, a]}(t - b)}{t - b} db \\
 (II.6.51) \qquad &= \lim_{a \rightarrow 0} \frac{1}{\pi} \int_{|b| > a} \frac{f(b)}{t - b} db.
 \end{aligned}$$

The last expression is the *Hilbert transform* $\mathcal{H} = \mathcal{M}_{w_0} \circ \mathcal{W}_\delta$, which is an example of a *singular integral operator* (SIO) [257, § 2.6; 314, § I.5] defined through the principal value (II.6.5) (in the sense of Cauchy). By Cor. II.6.42 we know that $\mathcal{H} = k_1 I_{H_2} \oplus k_2 I_{H_2^+}$ for some constants $k_1, k_2 \in \mathbb{C}$. Furthermore, we can directly check that $\mathcal{H}J = -J\mathcal{H}$, for the reflection J from (II.6.14), thus $k_1 = -k_2$. An evaluation of \mathcal{H} on a simple function from H_2 (say, the Cauchy kernel $\frac{1}{x+i}$) gives the value of the constant $k_1 = -i$. Thus, $\mathcal{H} = (-iI_{H_2}) \oplus (iI_{H_2^+})$.

In fact, the previous reasons imply the following

PROPOSITION II.6.45. [313, § III.1.1] *Any bounded linear operator on $L_2(\mathbb{R})$ commuting with quasi-regular representation ρ_2 (II.6.10) and anticommuting with reflection J (II.6.14) is a constant multiple of Hilbert transform (II.6.51).*

EXAMPLE II.6.46. Consider the covariant transform \mathcal{W}_q defined by the inadmissible wavelet $q(t)$ (II.6.24), the conjugated Poisson kernel. Its composition with the contravariant transform $\mathcal{M}_{v_0^+}^H$ (II.6.40) is

$$(II.6.52) \qquad \mathcal{M}_{v_0^+}^H \circ \mathcal{W}_q f(t) = \overline{\lim}_{a \rightarrow 0} \frac{1}{\pi} \int_{\mathbb{R}} \frac{f(x) (t - x)}{(t - x)^2 + a^2} dx$$

We can see that this composition satisfies to Prop. II.6.45, the constant factor can again be evaluated from the Cauchy kernel $f(x) = \frac{1}{x+i}$ and is equal to 1. Of course, this is a classical result [114, Thm. 4.1.5] in harmonic analysis that (II.6.52) provides an alternative expression for Hilbert transform (II.6.51).

EXAMPLE II.6.47. Let \mathcal{W} be a covariant transform generated either by the functional F_\pm (II.6.22) (i.e. the Cauchy integral) or $\frac{1}{2}(F_+ - F_-)$ (i.e. the Poisson integral) from the Example II.6.13. Then, for contravariant transform $\mathcal{M}_{v_0^+}^H$ (II.6.37) the composition $\mathcal{M}_{v_0^+}^H \mathcal{W}$ becomes the normal boundary value of the Cauchy/Poisson integral, respectively. The similar composition $\mathcal{M}_{v_0^*}^H \mathcal{W}$ for reconstructing vector v_0^* (II.6.36) turns to be the non-tangential limit of the Cauchy/Poisson integrals.

The maximal function and SIO are often treated as elementary building blocks of harmonic analysis. In particular, it is common to define the Hardy space as a closed subspace of $L_p(\mathbb{R})$ which is mapped to $L_p(\mathbb{R})$ by either the maximal operator (II.6.50)

or by the SIO (II.6.51) [89; 314, § III.1.2 and § III.4.3]. From this perspective, the coincidence of both characterizations seems to be non-trivial. On the contrast, we presented both the maximal operator and SIO as compositions of certain co- and contravariant transforms. Thus, these operators act between certain Aff-invariant subspaces, which we associated with generalized Hardy spaces in Defn. II.6.3. For the right choice of fiducial functionals, the coincidence of the respective invariant subspaces is quite natural.

The potential of the group-theoretical approach is not limited to the Hilbert space $L_2(\mathbb{R})$. One of possibilities is to look for a suitable modification of Schur's Lemma II.6.39, say, to Banach spaces. However, we can proceed with the affine group without such a generalisation. Here is an illustration to a classical question of harmonic analysis: to identify the class of functions on the real line such that $\mathcal{M}_{v_0^*}^H \mathcal{W}$ becomes the identity operator on it.

PROPOSITION II.6.48. *Let B be the space of bounded uniformly continuous functions on the real line. Let $F : B \rightarrow \mathbb{R}$ be a fiducial functional such that:*

$$(II.6.53) \quad \lim_{\alpha \rightarrow 0} F(\rho_\infty(1/\alpha, 0)f) = 0, \quad \text{for all } f \in B \text{ such that } f(0) = 0$$

and $F(\rho_\infty(1, b)f)$ is a continuous function of $b \in \mathbb{R}$ for a given $f \in B$.

Then, $\mathcal{M}_{v_0^*}^H \circ \mathcal{W}_F$ is a constant multiple of the identity operator on B .

PROOF. First of all we note that $\mathcal{M}_{v_0^*}^H \mathcal{W}_F$ is a bounded operator on B . Let $v_{(a,b)}^* = \rho_\infty(a, b)v^*$. Obviously, $v_{(a,b)}^*(0) = v^*(-\frac{b}{a})$ is an eigenfunction for operators $\Lambda(a', 0)$, $a' \in \mathbb{R}_+$ of the left regular representation of Aff:

$$(II.6.54) \quad \Lambda(a', 0)v_{(a,b)}^*(0) = v_{(a,b)}^*(0).$$

This and the left invariance of pairing (II.6.30) imply that $\mathcal{M}_{v_0^*}^H \circ \Lambda(1/\alpha, 0) = \mathcal{M}_{v_0^*}^H$ for any $(\alpha, 0) \in \text{Aff}$. Then, applying intertwining properties (II.6.44) we obtain that

$$\begin{aligned} [\mathcal{M}_{v_0^*}^H \circ \mathcal{W}_F f](0) &= [\mathcal{M}_{v_0^*}^H \circ \Lambda(1/\alpha, 0) \circ \mathcal{W}_F f](0) \\ &= [\mathcal{M}_{v_0^*}^H \circ \mathcal{W}_F \circ \rho_\infty(1/\alpha, 0)f](0). \end{aligned}$$

Using the limit $\alpha \rightarrow 0$ (II.6.53) and the continuity of $F \circ \rho_\infty(1, b)$ we conclude that the linear functional $l : f \mapsto [\mathcal{M}_{v_0^*}^H \circ \mathcal{W}_F f](0)$ vanishes for any $f \in \mathbb{B}$ such that $f(0) = 0$. Take a function $f_1 \in B$ such that $f_1(0) = 1$ and define $c = l(f_1)$. From linearity of l , for any $f \in B$ we have:

$$l(f) = l(f - f(0)f_1 + f(0)f_1) = l(f - f(0)f_1) + f(0)l(f_1) = cf(0).$$

Furthermore, using intertwining properties (II.6.44) and (IV.5.22):

$$\begin{aligned} [\mathcal{M}_{v_0^*}^H \circ \mathcal{W}_F f](t) &= [\rho_\infty(1, -t) \circ \mathcal{M}_{v_0^*}^H \circ \mathcal{W}_F f](0) \\ &= [\mathcal{M}_{v_0^*}^H \circ \mathcal{W}_F \circ \rho_\infty(1, -t)f](0) \\ &= l(\rho_\infty(1, -t)f) \\ &= c[\rho_\infty(1, -t)f](0) \\ &= cf(t). \end{aligned}$$

This completes the proof. □

To get the classical statement we need the following lemma.

LEMMA II.6.49. *For a non-zero $w(t) \in L_1(\mathbb{R})$, define the fiducial functional on B :*

$$(II.6.55) \quad F(f) = \int_{\mathbb{R}} f(t) w(t) dt.$$

Then F satisfies the conditions (and thus the conclusions) of Prop. II.6.48.

PROOF. Let f be a continuous bounded function such that $f(0) = 0$. For $\varepsilon > 0$ chose

- $\delta > 0$ such that $|f(t)| < \varepsilon$ for all $|t| < \delta$;
- $M > 0$ such that $\int_{|t|>M} |w(t)| dt < \varepsilon$.

Then, for $\alpha < \delta/M$, we have the estimation:

$$\begin{aligned} |F(\rho_{\infty}(1/\alpha, 0)f)| &= \left| \int_{\mathbb{R}} f(\alpha t) w(t) dt \right| \\ &\leq \left| \int_{|t|<M} f(\alpha t) w(t) dt \right| + \left| \int_{|t|>M} f(\alpha t) w(t) dt \right| \\ &\leq \varepsilon(\|w\|_1 + \|f\|_{\infty}). \end{aligned}$$

Finally, for a uniformly continuous function g for $\varepsilon > 0$ there is $\delta > 0$ such that $|g(t+b) - g(t)| < \varepsilon$ for all $b < \delta$ and $t \in \mathbb{R}$. Then

$$|F(\rho_{\infty}(1, b)g) - F(g)| = \left| \int_{\mathbb{R}} (g(t+b) - g(t)) w(t) dt \right| \leq \varepsilon \|w\|_1.$$

This proves the continuity of $F(\rho_{\infty}(1, b)g)$ at $b = 0$ and, by the group property, at any other point as well. □

REMARK II.6.50. A direct evaluation shows, that the constant $c = l(f_1)$ from the proof of Prop. II.6.48 for fiducial functional (II.6.55) is equal to $c = \int_{\mathbb{R}} w(t) dt$. Of course, for non-trivial boundary values we need $c \neq 0$. On the other hand, admissibility condition (II.6.21) requires $c = 0$. Moreover, the classical harmonic analysis and the traditional wavelet construction are two “orthogonal” parts of the same covariant transform theory in the following sense. We can present a rather general bounded function $w = w_{\alpha} + w_p$ as a sum of an admissible mother wavelet w_{α} and a suitable multiple w_p of the Poisson kernel. An extension of this technique to unbounded functions leads to *Calderón–Zygmund decomposition* [314, § I.4].

The table integral $\int_{\mathbb{R}} \frac{dx}{x^2+1} = \pi$ tells that the “wavelet” $p(t) = \frac{1}{\pi} \frac{1}{1+t^2}$ (II.6.23) is in $L_1(\mathbb{R})$ with $c = 1$, the corresponding wavelet transform is the Poisson integral. Its boundary behaviour from Prop. II.6.48 is the classical result, cf. [108, Ch. I, Cor. 3.2]. The comparison of our arguments with the traditional proofs, e.g. in [108], does not reveal any significant distinctions. We simply made an explicit usage of the relevant group structure, which is implicitly employed in traditional texts anyway, cf. [54]. Further demonstrations of this type can be found in [4, 92].

II.6.8. Transported norms

If the functional F and the representation ρ in (II.6.17) are both linear, then the resulting covariant transform is a linear map. If \mathcal{W}_F is injective, e.g. due to irreducibility of ρ , then \mathcal{W}_F transports a norm $\|\cdot\|$ defined on V to a norm $\|\cdot\|_F$ defined on the image space $\mathcal{W}_F V$ by the simple rule:

$$(II.6.56) \quad \|\mathbf{u}\|_F := \|\mathbf{v}\|, \quad \text{where the unique } \mathbf{v} \in V \text{ is defined by } \mathbf{u} = \mathcal{W}_F \mathbf{v}.$$

By the very definition, we have the following

- PROPOSITION II.6.51. i. \mathcal{W}_F is an isometry $(V, \|\cdot\|) \rightarrow (\mathcal{W}_F V, \|\cdot\|_F)$.
 ii. If the representation ρ acts on $(V, \|\cdot\|)$ by isometries then $\|\cdot\|_F$ is left invariant.

A touch of non-triviality occurs if the transported norm can be naturally expressed in the original terms of G .

EXAMPLE II.6.52. It is common to consider a unitary square integrable representation ρ and an admissible mother wavelet $f \in V$. In this case, wavelet transform (II.6.18) becomes an isometry to square integrable functions on G with respect to a Haar measure [5, Thm. 8.1.3]. In particular, for the affine group and setup of Example II.6.12, the wavelet transform with an admissible vector is a multiple of an isometry map from $L_2(\mathbb{R})$ to the functions on the upper half-plane, i.e., the $ax + b$ group, which are square integrable with respect to the Haar measure $a^{-2} da db$.

A reader expects that there are other interesting examples of the transported norms, which are not connected to the Haar integration.

EXAMPLE II.6.53. In the setup of Example II.6.13, consider the space $L_p(\mathbb{R})$ with representation (II.6.10) of Aff and Poisson kernel $p(t)$ (II.6.23) as an inadmissible mother wavelet. The norm transported by \mathcal{W}_p to the image space on Aff is [264, § A.6.3]:

$$(II.6.57) \quad \|\mathbf{u}\|_p = \sup_{a>0} \left(\int_{-\infty}^{\infty} |\mathbf{u}(a, b)|^p \frac{db}{a} \right)^{\frac{1}{p}}.$$

In the theory of Hardy spaces, the L_p -norm on the real line and transported norm (II.6.57) are naturally intertwined, cf. [264, Thm. A.3.4.1(iii)], and are used interchangeably.

The second possibility to transport a norm from V to a function space on G uses an contravariant transform \mathcal{M}_v :

$$(II.6.58) \quad \|\mathbf{u}\|_v := \|\mathcal{M}_v \mathbf{u}\|.$$

- PROPOSITION II.6.54. i. The contravariant transform \mathcal{M}_v is an isometry $(L, \|\cdot\|_v) \rightarrow (V, \|\cdot\|)$.
 ii. If the composition $\mathcal{M}_v \circ \mathcal{W}_F = cI$ is a multiple of the identity on V then transported norms $\|\cdot\|_v$ (II.6.58) and $\|\cdot\|_F$ (II.6.56) differ only by a constant multiplier.

The above result is well-known for traditional wavelets.

EXAMPLE II.6.55. In the setup of Example II.6.41, for a square integrable representation and two admissible mother wavelets v_0 and w_0 we know that $\mathcal{M}_{w_0} \mathcal{W}_{v_0} = kI$ (II.6.49), thus transported norms (II.6.56) and (II.6.58) differ by a constant multiplier. Thus, norm (II.6.58) is also provided by the integration with respect to the Haar measure on G .

In the theory of Hardy spaces the result is also classical.

EXAMPLE II.6.56. For the fiducial functional F with property (II.6.53) and the contravariant transform $\mathcal{M}_{v_0}^H$ (II.6.41), Prop. II.6.48 implies $\mathcal{M}_{v_0}^H \circ \mathcal{W}_F = cI$. Thus, the norm transported to Aff by $\mathcal{M}_{v_0}^H$ from $L_p(\mathbb{R})$ up to factor coincides with (II.6.57). In other words, the transition to the boundary limit on the Hardy space is an isometric operator. This is again a classical result of the harmonic analysis, cf. [264, Thm. A.3.4.1(ii)].

The co- and contravariant transforms can be used to transport norms in the opposite direction: from a classical space of functions on G to a representation space V .

EXAMPLE II.6.57. Let V be the space of σ -finite signed measures of a bounded variation on the upper half-plane. Let the $ax + b$ group acts on V by the representation adjoint to $[\rho_1(a, b)f](x, y) = a^{-1}f(\frac{x-b}{a}, \frac{y}{a})$ on $L_2(\mathbb{R}_+^2)$, cf. (II.6.8). If the mother wavelet v_0 is the indicator function of the square $\{0 < x < 1, 0 < y < 1\}$, then the covariant transform of a measure μ is $\tilde{\mu}(a, b) = a^{-1}\mu(Q_{a,b})$, where $Q_{a,b}$ is the square $\{b < x < b + a, 0 < y < a\}$. If we request that $\tilde{\mu}(a, b)$ is a bounded function on the affine group, then μ is a Carleson measure [108, § I.5]. A norm transported from $L_\infty(\text{Aff})$ to the appropriate subset of V becomes the Carleson norm of measures. Indicator function of a tent taken as a mother wavelet will lead to an equivalent definition.

It was already mentioned in Rem. II.6.16 and Example II.6.26 that we may be interested to mix several different covariant and contravariant transforms. This motivate the following statement.

PROPOSITION II.6.58. *Let $(V, \|\cdot\|)$ be a normed space and ρ be a continuous representation of a topological locally compact group G on V . Let two fiducial operators F_1 and F_2 define the respective covariant transforms \mathcal{W}_1 and \mathcal{W}_2 to the same image space $W = \mathcal{W}_1V = \mathcal{W}_2V$. Assume, there exists an contravariant transform $\mathcal{M} : W \rightarrow V$ such that $\mathcal{M} \circ \mathcal{W}_1 = c_1I$ and $\mathcal{M} \circ \mathcal{W}_2 = c_2I$. Define by $\|\cdot\|_{\mathcal{M}}$ the norm on U transported from V by \mathcal{M} . Then*

$$(II.6.59) \quad \|\mathcal{W}_1v_1 + \mathcal{W}_2v_2\|_{\mathcal{M}} = \|c_1v_1 + c_2v_2\|, \quad \text{for any } v_1, v_2 \in V.$$

PROOF. Indeed:

$$\begin{aligned} \|\mathcal{W}_1v_1 + \mathcal{W}_2v_2\|_{\mathcal{M}} &= \|\mathcal{M} \circ \mathcal{W}_1v_1 + \mathcal{M} \circ \mathcal{W}_2v_2\| \\ &= \|c_1v_1 + c_2v_2\|, \end{aligned}$$

by the definition of transported norm (II.6.58) and the assumptions $\mathcal{M} \circ \mathcal{W}_i = c_iI$. \square

Although the above result is simple, it does have important consequences.

COROLLARY II.6.59 (Orthogonality Relation). *Let ρ be a square integrable representation of a group G in a Hilbert space V . Then, for any two admissible mother wavelets f and f'*

there exists a constant c such that:

$$(II.6.60) \quad \int_G \langle v, \rho(g)f \rangle \overline{\langle v', \rho(g)f' \rangle} dg = c \langle v, v' \rangle \quad \text{for any } v_1, v_2 \in V.$$

Moreover, the constant $c = c(f', f)$ is a sesquilinear form of vectors f' and f .

PROOF. We can derive (II.6.60) from (II.6.59) as follows. Let \mathcal{M}_f be the inverse wavelet transform (II.6.33) defined by the admissible vector f , then $\mathcal{M}_f \circ \mathcal{W}_f = I$ on V providing the right scaling of f . Furthermore, $\mathcal{M}_f \circ \mathcal{W}_{f'} = \bar{c}I$ by (II.6.49) for some complex constant c . Thus, by (II.6.59):

$$\|\mathcal{W}_f v + \mathcal{W}_{f'} v'\|_{\mathcal{M}} = \|v + \bar{c}v'\|.$$

Now, through the polarisation identity [164, Problem 476] we get the equality (II.6.60) of inner products. □

The above result is known as the *orthogonality relation* in the theory of wavelets, for some further properties of the constant c see [5, Thm. 8.2.1].

Here is an application of Prop. II.6.58 to harmonic analysis, cf. [114, Thm. 4.1.7]:

COROLLARY II.6.60. *The covariant transform \mathcal{W}_q with conjugate Poisson kernel q (II.6.24) is a bounded map from $(L_2(\mathbb{R}), \|\cdot\|)$ to $(L(\text{Aff}), \|\cdot\|_2)$ with norm $\|\cdot\|_2$ (II.6.57). Moreover:*

$$\|\mathcal{W}_q f\|_2 = \|f\|, \quad \text{for all } f \in L_2(\mathbb{R}).$$

PROOF. As we establish in Example II.6.46 for contravariant transform $\mathcal{M}_{v_0^+}^H$ (II.6.40), $\mathcal{M}_{v_0^+}^H \circ \mathcal{W}_q = -iI$ and iI on H_2 and H_2^\perp , respectively. Take the unique presentation $f = u + u^\perp$, for $u \in H_2$ and $u^\perp \in H_2^\perp$. Then, by (II.6.59)

$$\|\mathcal{W}_q f\|_2 = \|-iu + iu^\perp\| = \|u + u^\perp\| = \|f\|.$$

This completes the proof. □

Covariant scheme	Complex variable	Real variable
<p>Covariant transform is $\mathcal{W}_F^{\rho} : v \mapsto \hat{v}(g) = F(\rho(g^{-1})v)$. In particular, the wavelet transform for the mother wavelet v_0 is $\tilde{v}(g) = \langle v, \rho(g)v_0 \rangle$.</p>	<p>The Cauchy integral is generated by the mother wavelet $\frac{1}{2\pi i} \frac{1}{x+i}$. The Poisson integral is generated by the mother wavelet $\frac{1}{\pi} \frac{1}{x^2+1}$</p>	<p>The averaging operator $\tilde{f}(b) = \frac{1}{2a} \int_{b-a}^{b+a} f(t) dt$ is defined by the mother wavelet $\chi_{[-1,1]}(t)$, to average the modulus of $f(t)$ we use all elements of the unit ball in $L_{\infty}[-1, 1]$.</p>
<p>The covariant transform maps vectors to functions on G or, in the induced case, to functions on the homogeneous space G/H.</p>	<p>Functions are mapped from the real line to the upper half-plane parametrised by either the $ax + b$-group or the homogeneous space $SL_2(\mathbb{R})/K$.</p>	<p>Functions are mapped from the real line to the upper half-plane parametrised by either the $ax + b$-group or the homogeneous space $SL_2(\mathbb{R})/A$.</p>
<p>Annihilating action on the mother wavelet produces functional relation on the image of the covariant transform</p>	<p>The operator $-\delta\rho^A - i\delta\rho^N = I + (x+i)\frac{d}{dx}$ annihilates the mother wavelet $\frac{1}{2\pi i} \frac{1}{x+i}$, thus the image of wavelet transform is in the kernel of the Cauchy-Riemann operator $-\mathcal{L}^A + i\mathcal{L}^N = i\alpha(\partial_b + i\partial_a)$. Similarly, for the Laplace operator.</p>	<p>The mother wavelet $v_0 = \chi_{[-1,1]}$ satisfies the equality $\chi_{[-1,1]} = \chi_{[-1,0]} + \chi_{[0,1]}$, where both terms are again scaled and shifted v_0. The image of the wavelet transform is suitable for the stopping time argument and the dyadic squares technique.</p>
<p>An invariant pairing $\langle \cdot, \cdot \rangle$ generates the contravariant transform $[\mathcal{M}_{v_0}^{\rho} f](f(g), \rho(g)v_0)$ for</p>	<p>The contravariant transform with the invariant Hardy pairing on the $ax + b$ group produces boundary values of functions on the real line.</p>	<p>The covariant transform with the invariant sup pairing produces the vertical and non-tangential maximal functions.</p>
<p>The composition $\mathcal{M}_{\circ} \mathcal{W}_F$ of the covariant and contravariant transforms is a multiple of the identity on irreducible components.</p>	<p>SIO is a composition of the Cauchy integral and its boundary value.</p>	<p>The Hardy-Littlewood maximal function is the composition of the averaging operator and the contravariant transform from the invariant sup pairing.</p>
<p>The Hardy space is an invariant subspace of the group representation.</p>	<p>The Hardy space consists of the limiting values of the Cauchy integral. SIO is bounded on this space.</p>	<p>The Hardy-Littlewood maximal operator is bounded on the Hardy space H_p.</p>

FIGURE II.6.1. The correspondence between different elements of harmonic analysis.

Part III

Functional Calculi and Spectra

Covariant and Contravariant Calculi

United in the trinity functional calculus, spectrum, and spectral mapping theorem play the exceptional rôle in functional analysis and could not be substituted by anything else.

III.1.1. Functional Calculus as an Algebraic Homomorphism

Many traditional definitions of functional calculus are covered by the following rigid template based on the *algebra homomorphism* property:

DEFINITION III.1.1. An *functional calculus* for an element $a \in \mathfrak{A}$ is a continuous linear mapping $\Phi : \mathcal{A} \rightarrow \mathfrak{A}$ such that

i. Φ is a unital *algebra homomorphism*

$$\Phi(f \cdot g) = \Phi(f) \cdot \Phi(g).$$

ii. There is an initialisation condition: $\Phi[v_0] = a$ for a fixed function v_0 , e.g. $v_0(z) = z$.

The most typical definition of the spectrum is seemingly independent and uses the important notion of resolvent:

DEFINITION III.1.2. A *resolvent* of element $a \in \mathfrak{A}$ is the function $R(\lambda) = (a - \lambda e)^{-1}$, which is the image under Φ of the Cauchy kernel $(z - \lambda)^{-1}$.

A *spectrum* of $a \in \mathfrak{A}$ is the set $\text{sp } a$ of singular points of its resolvent $R(\lambda)$.

Then the following important theorem links spectrum and functional calculus together.

THEOREM III.1.3 (Spectral Mapping). *For a function f suitable for the functional calculus:*

$$(III.1.1) \quad f(\text{sp } a) = \text{sp } f(a).$$

However the power of the classic spectral theory rapidly decreases if we move beyond the study of one normal operator (e.g. for quasinilpotent ones) and is virtually nil if we consider several non-commuting ones. Sometimes these severe limitations are seen to be irresistible and alternative constructions, i.e. model theory cf. Example II.4.22 and [266], were developed.

Yet the spectral theory can be revived from a fresh start. While three components—functional calculus, spectrum, and spectral mapping theorem—are highly interdependent in various ways we will nevertheless arrange them as follows:

- i. Functional calculus is an *original* notion defined in some independent terms;
- ii. Spectrum (or more specifically *contravariant spectrum*) (or spectral decomposition) is derived from previously defined functional calculus as its *support* (in some appropriate sense);
- iii. Spectral mapping theorem then should drop out naturally in the form (III.1.1) or some its variation.

Thus the entire scheme depends from the notion of the functional calculus and our ability to escape limitations of Definition III.1.1. The first known to the present author definition of functional calculus not linked to algebra homomorphism property was the Weyl functional calculus defined by an integral formula [8]. Then its intertwining property with affine transformations of Euclidean space was proved as a theorem. However it seems to be the only “non-homomorphism” calculus for decades.

The different approach to whole range of calculi was given in [168] and developed in [173,180,182,193] in terms of *intertwining operators* for group representations. It was initially targeted for several non-commuting operators because no non-trivial algebra homomorphism is possible with a commutative algebra of function in this case. However it emerged later that the new definition is a useful replacement for classical one across all range of problems.

In the following Subsections we will support the last claim by consideration of the simple known problem: characterisation a $n \times n$ matrix up to similarity. Even that “freshman” question can be only sorted out by the classical spectral theory for a small set of diagonalisable matrices. Our solution in terms of new spectrum will be full and thus unavoidably coincides with one given by the Jordan normal form of matrices. Other more difficult questions are the subject of ongoing research.

III.1.2. Intertwining Group Actions on Functions and Operators

Any functional calculus uses properties of *functions* to model properties of *operators*. Thus changing our viewpoint on functions, as was done in Section II.5, we can get another approach to operators. The two main possibilities are encoded in Definitions II.4.23 and II.4.25: we can assign a certain function to the given operator or *vice versa*. Here we consider the second possibility and treat the first in the Subsection III.1.5.

The representation ρ_1 (II.5.23) is unitary irreducible when acts on the Hardy space H_2 . Consequently we have one more reason to abolish the template definition III.1.1: H_2 is *not* an algebra. Instead we replace the *homomorphism property* by a *symmetric covariance*:

DEFINITION III.1.4 ([168]). An *contravariant analytic calculus* for an element $a \in \mathfrak{A}$ and an \mathfrak{A} -module M is a *continuous linear mapping* $\Phi : A(\mathbb{D}) \rightarrow A(\mathbb{D}, M)$ such that

- i. Φ is an *intertwining operator*

$$\Phi \rho_1 = \rho_a \Phi$$

between two representations of the $SL_2(\mathbb{R})$ group ρ_1 (II.5.23) and ρ_a defined below in (III.1.5).

- ii. There is an initialisation condition: $\Phi[v_0] = m$ for $v_0(z) \equiv 1$ and $m \in M$, where M is a left \mathfrak{A} -module.

Note that our functional calculus released from the homomorphism condition can take value in any left \mathfrak{A} -module M , which however could be \mathfrak{A} itself if suitable. This add much flexibility to our construction.

The earliest functional calculus, which is *not* an algebraic homomorphism, was the Weyl functional calculus and was defined just by an integral formula as an operator valued distribution [8]. In that paper (joint) spectrum was defined as support of the Weyl calculus, i.e. as the set of point where this operator valued distribution does not vanish. We also define the spectrum as a support of functional calculus, but due to our Definition III.1.4 it will means the set of non-vanishing intertwining operators with primary subrepresentations.

DEFINITION III.1.5. A corresponding *spectrum* of $a \in \mathfrak{A}$ is the *support* of the functional calculus Φ , i.e. the collection of intertwining operators of ρ_a with *primary representations* [159, § 8.3].

More variations of contravariant functional calculi are obtained from other groups and their representations [168, 173, 180, 182, 193].

A simple but important observation is that the Möbius transformations (I.1.1) can be easily extended to any Banach algebra. Let \mathfrak{A} be a Banach algebra with the unit e , an element $a \in \mathfrak{A}$ with $\|a\| < 1$ be fixed, then for for transformations

$$(III.1.2) \quad g : a \mapsto g \cdot a = (\alpha a + \bar{\beta} e)(\beta a + \bar{\alpha} e)^{-1}, \quad g = \begin{pmatrix} \alpha & \bar{\beta} \\ \beta & \bar{\alpha} \end{pmatrix} \in \mathrm{SL}_2(\mathbb{R})$$

we introduce $\mathrm{SL}_2(\mathbb{R})$ -orbit

$$\mathbb{A} = \{g \cdot a \mid g \in \mathrm{SL}_2(\mathbb{R})\} \subset \mathfrak{A}.$$

Clearly, \mathbb{A} is a left (right) $\mathrm{SL}_2(\mathbb{R})$ -homogeneous space with the natural left (right) action:

$$g_1 : b = g \cdot a \mapsto g_1^{-1} \cdot b := (g_1^{-1} g) \cdot a \quad (g_1 : g \cdot a \mapsto (g g_1) \cdot a),$$

where $g_1, g \in \mathrm{SL}_2(\mathbb{R})$ and $b = g \cdot a \in \mathbb{A}$. That is, for a fixed $a \in \mathfrak{A}$ the set \mathbb{A} and the $\mathrm{SL}_2(\mathbb{R})$ -action on it are completely parametrised by correspondence $b = g \cdot a \leftrightarrow g$.

Let us define the *resolvent* function $R(g, b) : \mathrm{SL}_2(\mathbb{R}) \times \mathbb{A} \rightarrow \mathfrak{A}$ by:

$$(III.1.3) \quad R(g_1, b) := (\alpha_1 e - \beta_1 b)^{-1} = (\beta a + \bar{\alpha})(\alpha' e - \beta' a)^{-1},$$

where

$$g_1 = \begin{pmatrix} \alpha_1 & \bar{\beta}_1 \\ \beta_1 & \bar{\alpha}_1 \end{pmatrix}, \quad g = \begin{pmatrix} \alpha & \bar{\beta} \\ \beta & \bar{\alpha} \end{pmatrix} \in \mathrm{SL}_2(\mathbb{R}), \quad b = g \cdot a \in \mathbb{A}$$

and

$$\begin{pmatrix} \alpha' & \bar{\beta}' \\ \beta' & \bar{\alpha}' \end{pmatrix} = g^{-1} g_1 = \begin{pmatrix} \bar{\alpha} & -\bar{\beta} \\ -\beta & \alpha \end{pmatrix} \cdot \begin{pmatrix} \alpha_1 & \bar{\beta}_1 \\ \beta_1 & \bar{\alpha}_1 \end{pmatrix}$$

Then, we can directly check that:

$$(III.1.4) \quad R(g_1, b) R(g_2, g_1^{-1} \cdot b) = R(g_1 g_2, b),$$

for all $g_1, g_2 \in \mathrm{SL}_2(\mathbb{R})$ and $b \in \mathbb{A}$.

The last identity is well known in representation theory [159, § 13.2(10)] and is a key ingredient of *induced representations*. Thus we can again linearise (III.1.2), cf. (II.5.23), in the space of continuous functions $C(\mathbb{A}, M)$ with values in a left \mathfrak{A} -module M :

$$(III.1.5) \quad \begin{aligned} \rho_a(g) : f(b) &\mapsto R(g, b)f(g^{-1} \cdot b) \\ &= (\alpha e - \beta b)^{-1} f\left(\frac{\bar{\alpha}b - \bar{\beta}e}{\alpha e - \beta b}\right), \end{aligned}$$

where $g \in SL_2(\mathbb{R})$ and $b \in \mathbb{A}$.

For any $m \in M$ we can define a K -invariant *vacuum vector* as $v_m(g^{-1} \cdot a) = m \otimes v_0(g^{-1} \cdot a) \in C(\mathbb{A}, M)$. It generates the associated with v_m family of *coherent states* $v_m(u, a) = (ue - a)^{-1}m$, where $u \in \mathbb{D}$.

The *wavelet transform* defined by the same common formula based on coherent states (cf. (II.5.24)):

$$(III.1.6) \quad \mathcal{W}_m f(g) = \langle f, \rho_a(g)v_m \rangle,$$

is a version of Cauchy integral, which maps $L_2(\mathbb{A})$ to $C(SL_2(\mathbb{R}), M)$. It is closely related (but not identical!) to the Riesz-Dunford functional calculus: the traditional functional calculus is given by the case:

$$\Phi : f \mapsto \mathcal{W}_m f(0) \quad \text{for } M = \mathfrak{A} \text{ and } m = e.$$

The both conditions—the intertwining property and initial value—required by Definition III.1.4 easily follows from our construction. Finally, we wish to provide an example of application of the Corollary IV.5.3.

EXAMPLE III.1.6. Let a be an operator and ϕ be a function which annihilates it, i.e. $\phi(a) = 0$. For example, if a is a matrix ϕ can be its minimal polynomial. From the integral representation of the contravariant calculus on $G = SL_2(\mathbb{R})$ we can rewrite the annihilation property like this:

$$\int_G \phi(g)R(g, a) dg = 0.$$

Then the vector-valued function $[\mathcal{W}_m f](g)$ defined by (III.1.6) shall satisfy to the following condition:

$$\int_G \phi(g') [\mathcal{W}_m f](gg') dg' = 0$$

due to the Corollary IV.5.3.

III.1.3. Jet Bundles and Prolongations of ρ_1

Spectrum was defined in III.1.5 as the *support* of our functional calculus. To elaborate its meaning we need the notion of a *prolongation* of representations introduced by S. Lie, see [267, 268] for a detailed exposition.

DEFINITION III.1.7. [268, Chap. 4] Two holomorphic functions have *n*th order *contact* in a point if their value and their first n derivatives agree at that point, in other words their Taylor expansions are the same in first $n + 1$ terms.

A point $(z, u^{(n)}) = (z, u, u_1, \dots, u_n)$ of the *jet space* $\mathbb{J}^n \sim \mathbb{D} \times \mathbb{C}^n$ is the equivalence class of holomorphic functions having n th contact at the point z with the polynomial:

$$(III.1.7) \quad p_n(w) = u_n \frac{(w-z)^n}{n!} + \dots + u_1 \frac{(w-z)}{1!} + u.$$

For a fixed n each holomorphic function $f : \mathbb{D} \rightarrow \mathbb{C}$ has n th *prolongation* (or *n-jet*) $j_n f : \mathbb{D} \rightarrow \mathbb{C}^{n+1}$:

$$(III.1.8) \quad j_n f(z) = (f(z), f'(z), \dots, f^{(n)}(z)).$$

The graph $\text{amma}_f^{(n)}$ of $j_n f$ is a submanifold of \mathbb{J}^n which is section of the *jet bundle* over \mathbb{D} with a fibre \mathbb{C}^{n+1} . We also introduce a notation J_n for the map $J_n : f \mapsto \text{amma}_f^{(n)}$ of a holomorphic f to the graph $\text{amma}_f^{(n)}$ of its n -jet $j_n f(z)$ (III.1.8).

One can prolong any map of functions $\psi : f(z) \mapsto [\psi f](z)$ to a map $\psi^{(n)}$ of n -jets by the formula

$$(III.1.9) \quad \psi^{(n)}(J_n f) = J_n(\psi f).$$

For example such a prolongation $\rho_1^{(n)}$ of the representation ρ_1 of the group $SL_2(\mathbb{R})$ in $H_2(\mathbb{D})$ (as any other representation of a Lie group [268]) will be again a representation of $SL_2(\mathbb{R})$. Equivalently we can say that J_n *intertwines* ρ_1 and $\rho_1^{(n)}$:

$$J_n \rho_1(g) = \rho_1^{(n)}(g) J_n \quad \text{for all } g \in SL_2(\mathbb{R}).$$

Of course, the representation $\rho_1^{(n)}$ is not irreducible: any jet subspace $\mathbb{J}^k, 0 \leq k \leq n$ is $\rho_1^{(n)}$ -invariant subspace of \mathbb{J}^n . However the representations $\rho_1^{(n)}$ are *primary* [159, § 8.3] in the sense that they are not sums of two subrepresentations.

The following statement explains why jet spaces appeared in our study of functional calculus.

PROPOSITION III.1.8. *Let matrix a be a Jordan block of a length k with the eigenvalue $\lambda = 0$, and m be its root vector of order k , i.e. $a^{k-1}m \neq a^k m = 0$. Then the restriction of ρ_a on the subspace generated by v_m is equivalent to the representation ρ_1^k .*

III.1.4. Spectrum and Spectral Mapping Theorem

Now we are prepared to describe a spectrum of a matrix. Since the functional calculus is an intertwining operator its support is a decomposition into intertwining operators with primary representations (we can not expect generally that these primary subrepresentations are irreducible).

Recall the transitive on \mathbb{D} group of inner automorphisms of $SL_2(\mathbb{R})$, which can send any $\lambda \in \mathbb{D}$ to 0 and are actually parametrised by such a λ . This group extends Proposition III.1.8 to the complete characterisation of ρ_a for matrices.

PROPOSITION III.1.9. *Representation ρ_a is equivalent to a direct sum of the prolongations $\rho_1^{(k)}$ of ρ_1 in the k th jet space \mathbb{J}^k intertwined with inner automorphisms. Consequently the spectrum of a (defined via the functional calculus $\Phi = \mathcal{W}_m$) labelled exactly by n pairs of numbers $(\lambda_i, k_i), \lambda_i \in \mathbb{D}, k_i \in \mathbb{Z}_+, 1 \leq i \leq n$ some of whom could coincide.*

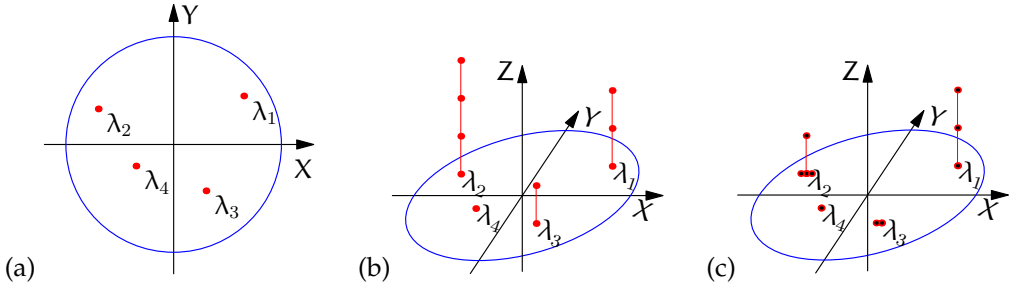


FIGURE III.1.1. Classical spectrum of the matrix from the Ex. III.1.10 is shown at (a). Contravariant spectrum of the same matrix in the jet space is drawn at (b). The image of the contravariant spectrum under the map from Ex. III.1.12 is presented at (c).

Obviously this spectral theory is a fancy restatement of the *Jordan normal form* of matrices.

EXAMPLE III.1.10. Let $J_k(\lambda)$ denote the Jordan block of the length k for the eigenvalue λ . In Fig. III.1.1 there are two pictures of the spectrum for the matrix

$$a = J_3(\lambda_1) \oplus J_4(\lambda_2) \oplus J_1(\lambda_3) \oplus J_2(\lambda_4),$$

where

$$\lambda_1 = \frac{3}{4}e^{i\pi/4}, \quad \lambda_2 = \frac{2}{3}e^{i5\pi/6}, \quad \lambda_3 = \frac{2}{5}e^{-i3\pi/4}, \quad \lambda_4 = \frac{3}{5}e^{-i\pi/3}.$$

Part (a) represents the conventional two-dimensional image of the spectrum, i.e. eigenvalues of a , and (b) describes spectrum $sp\ a$ arising from the wavelet construction. The first image did not allow to distinguish a from many other essentially different matrices, e.g. the diagonal matrix

$$\text{diag}(\lambda_1, \lambda_2, \lambda_3, \lambda_4),$$

which even have a different dimensionality. At the same time Fig. III.1.1(b) completely characterise a up to a similarity. Note that each point of $sp\ a$ in Fig. III.1.1(b) corresponds to a particular root vector, which spans a primary subrepresentation.

As was mentioned in the beginning of this section a reasonable spectrum should be linked to the corresponding functional calculus by an appropriate spectral mapping theorem. The new version of spectrum is based on prolongation of ρ_1 into jet spaces (see Section III.1.3). Naturally a correct version of spectral mapping theorem should also operate in jet spaces.

Let $\phi : \mathbb{D} \rightarrow \mathbb{D}$ be a holomorphic map, let us define its action on functions $[\phi_*f](z) = f(\phi(z))$. According to the general formula (III.1.9) we can define the prolongation $\phi_*^{(n)}$ onto the jet space \mathbb{J}^n . Its associated action $\rho_1^k \phi_*^{(n)} = \phi_*^{(n)} \rho_1^n$ on the pairs (λ, k) is given by the formula:

$$(III.1.10) \quad \phi_*^{(n)}(\lambda, k) = \left(\phi(\lambda), \left[\frac{k}{\text{deg}_\lambda \phi} \right] \right),$$

where $\text{deg}_\lambda \phi$ denotes the degree of zero of the function $\phi(z) - \phi(\lambda)$ at the point $z = \lambda$ and $[x]$ denotes the integer part of x .

THEOREM III.1.11 (Spectral mapping). *Let ϕ be a holomorphic mapping $\phi : \mathbb{D} \rightarrow \mathbb{D}$ and its prolonged action $\phi_*^{(n)}$ defined by (III.1.10), then*

$$\text{sp } \phi(\alpha) = \phi_*^{(n)} \text{sp } \alpha.$$

The explicit expression of (III.1.10) for $\phi_*^{(n)}$, which involves derivatives of ϕ upto n th order, is known, see for example [137, Thm. 6.2.25], but was not recognised before as form of spectral mapping.

EXAMPLE III.1.12. Let us continue with Example III.1.10. Let ϕ map all four eigenvalues $\lambda_1, \dots, \lambda_4$ of the matrix α into themselves. Then Fig. III.1.1(a) will represent the classical spectrum of $\phi(\alpha)$ as well as α .

However Fig. III.1.1(c) shows mapping of the new spectrum for the case ϕ has orders of zeros at these points as follows: the order 1 at λ_1 , exactly the order 3 at λ_2 , an order at least 2 at λ_3 , and finally any order at λ_4 .

III.1.5. Functional Model and Spectral Distance

Let α be a matrix and $\mu(z)$ be its *minimal polynomial*:

$$\mu_\alpha(z) = (z - \lambda_1)^{m_1} \cdot \dots \cdot (z - \lambda_n)^{m_n}.$$

If all eigenvalues λ_i of α (i.e. all roots of $\mu(z)$) belong to the unit disk we can consider the respective *Blaschke product*

$$B_\alpha(z) = \prod_{i=1}^n \left(\frac{z - \lambda_i}{1 - \overline{\lambda_i}z} \right)^{m_i},$$

such that its numerator coincides with the minimal polynomial $\mu(z)$. Moreover, for an unimodular z we have $B_\alpha(z) = \mu_\alpha(z) \overline{\mu_\alpha^{-1}(z)} z^{-m}$, where $m = m_1 + \dots + m_n$. We also have the following covariance property:

PROPOSITION III.1.13. *The above correspondence $\alpha \mapsto B_\alpha$ intertwines the $\text{SL}_2(\mathbb{R})$ action (III.1.2) on the matrices with the action (II.5.23) with $k = 0$ on functions.*

The result follows from the observation that every elementary product $\frac{z - \lambda_i}{1 - \overline{\lambda_i}z}$ is the Moebius transformation of z with the matrix $\begin{pmatrix} 1 & -\lambda_i \\ -\overline{\lambda_i} & 1 \end{pmatrix}$. Thus the correspondence $\alpha \mapsto B_\alpha(z)$ is a covariant (symbolic) calculus in the sense of the Defn. II.4.23. See also the Example II.4.22.

The Jordan normal form of a matrix provides a description, which is equivalent to its contravariant spectrum. From various viewpoints, e.g. numerical approximations, it is worth to consider its stability under a perturbation. It is easy to see, that an arbitrarily small disturbance breaks the Jordan structure of a matrix. However, the result of random small perturbation will not be random, its nature is described by the following remarkable theorem:

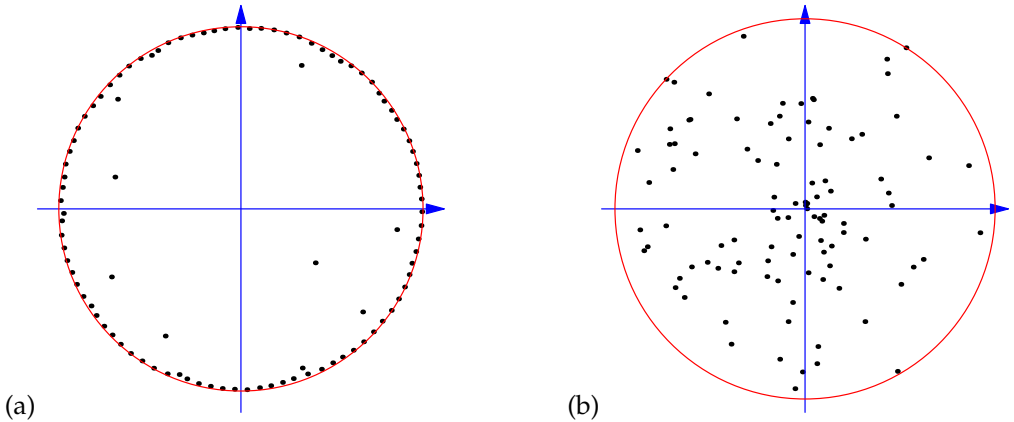


FIGURE III.1.2. Perturbation of the Jordan block's spectrum: (a) The spectrum of the perturbation $J_{100} + \epsilon^{100}K$ of the Jordan block J_{100} by a random matrix K . (b) The spectrum of the random matrix K .

THEOREM III.1.14 (Lidskii [244], see also [259]). *Let J_n be a Jordan block of a length $n > 1$ with zero eigenvalues and K be an arbitrary matrix. Then eigenvalues of the perturbed matrix $J_n + \epsilon^n K$ admit the expansion*

$$\lambda_j = \epsilon \xi_j^{1/n} + o(\epsilon), \quad j = 1, \dots, n,$$

where $\xi_j^{1/n}$ represents all n -th complex roots of certain $\xi \in \mathbb{C}$.

The left picture in Fig. III.1.2 presents a perturbation of a Jordan block J_{100} by a random matrix. Perturbed eigenvalues are close to vertices of a right polygon with 100 vertices. Those regular arrangements occur despite of the fact that eigenvalues of the matrix K are dispersed through the unit disk (the right picture in Fig. III.1.2). In a sense it is rather the Jordan block regularises eigenvalues of K than K perturbs the eigenvalue of the Jordan block.

Although the Jordan structure itself is extremely fragile, it still can be easily guessed from a perturbed eigenvalues. Thus there exists a certain characterisation of matrices which is stable under small perturbations. We will describe a sense, in which the covariant spectrum of the matrix $J_n + \epsilon^n K$ is stable for small ϵ . For this we introduce the covariant version of spectral distances motivated by the functional model. Our definition is different from other types known in the literature [324, Ch. 5].

DEFINITION III.1.15. Let a and b be two matrices with all their eigenvalues sitting inside of the unit disk and $B_a(z)$ and $B_b(z)$ be respective Blaschke products as defined above. The (covariant) spectral distance $d(a, b)$ between a and b is equal to the distance $\|B_a - B_b\|_2$ between $B_a(z)$ and $B_b(z)$ in the Hardy space on the unit circle.

Since the spectral distance is defined through the distance in H_2 all standard axioms of a distance are automatically satisfied. For a Blaschke products we have $|B_a(z)| =$

1 if $|z| = 1$, thus $\|B_a\|_p = 1$ in any L_p on the unit circle. Therefore an alternative expression for the spectral distance is:

$$d(a, b) = 2(1 - \langle B_a, B_b \rangle).$$

In particular, we always have $0 \leq d(a, b) \leq 2$. We get an obvious consequence of Prop. III.1.13, which justifies the name of the covariant spectral distance:

COROLLARY III.1.16. *For any $g \in SL_2(\mathbb{R})$ we have $d(a, b) = d(g \cdot a, g \cdot b)$, where \cdot denotes the Möbius action (III.1.2).*

An important property of the covariant spectral distance is its stability under small perturbations.

THEOREM III.1.17. *For $n = 2$ let $\lambda_1(\varepsilon)$ and $\lambda_2(\varepsilon)$ be eigenvalues of the matrix $J_2 + \varepsilon^2 \cdot K$ for some matrix K . Then*

$$(III.1.11) \quad |\lambda_1(\varepsilon)| + |\lambda_2(\varepsilon)| = O(\varepsilon), \quad \text{however} \quad |\lambda_1(\varepsilon) + \lambda_2(\varepsilon)| = O(\varepsilon^2).$$

The spectral distance from the 1-jet at 0 to two 0-jets at points λ_1 and λ_2 bounded only by the first condition in (III.1.11) is $O(\varepsilon^2)$. However the spectral distance between J_2 and $J_2 + \varepsilon^2 \cdot K$ is $O(\varepsilon^4)$.

In other words, a matrix with eigenvalues satisfying to the Lisdkii condition from the Thm. III.1.14 is much closer to the Jordan block J_2 than a generic one with eigenvalues of the same order. Thus the covariant spectral distance is more stable under perturbation that magnitude of eigenvalues. For $n = 2$ a proof can be forced through a direct calculation. We also conjecture that the similar statement is true for any $n \geq 2$.

III.1.6. Covariant Pencils of Operators

Let H be a real Hilbert space, possibly of finite dimensionality. For bounded linear operators A and B consider the *generalised eigenvalue problem*, that is finding a scalar λ and a vector $x \in H$ such that:

$$(III.1.12) \quad Ax = \lambda Bx \quad \text{or equivalently} \quad (A - \lambda B)x = 0.$$

The standard eigenvalue problem corresponds to the case $B = I$, moreover for an invertible B the generalised problem can be reduced to the standard one for the operator $B^{-1}A$. Thus it is sensible to introduce the equivalence relation on the pairs of operators:

$$(III.1.13) \quad (A, B) \sim (DA, DB) \quad \text{for any invertible operator } D.$$

We may treat the pair (A, B) as a column vector $\begin{pmatrix} A \\ B \end{pmatrix}$. Then there is an action of the $SL_2(\mathbb{R})$ group on the pairs:

$$(III.1.14) \quad g \cdot \begin{pmatrix} A \\ B \end{pmatrix} = \begin{pmatrix} aA + bB \\ cA + dB \end{pmatrix}, \quad \text{where } g = \begin{pmatrix} a & b \\ c & d \end{pmatrix} \in SL_2(\mathbb{R}).$$

If we consider this $SL_2(\mathbb{R})$ -action subject to the equivalence relation (III.1.13) then we will arrive to a version of the linear-fractional transformation of the operator defined in (III.1.2). There is a connection of the $SL_2(\mathbb{R})$ -action (III.1.14) to the problem (III.1.12) through the following intertwining relation:

PROPOSITION III.1.18. Let λ and $\chi \in H$ solve the generalised eigenvalue problem (III.1.12) for the pair (A, B) . Then the pair $(C, D) = g \cdot (A, B)$, $g \in SL_2(\mathbb{R})$ has a solution μ and χ , where

$$\mu = g \cdot \lambda = \frac{a\lambda + b}{c\lambda + d}, \quad \text{for } g = \begin{pmatrix} a & b \\ c & d \end{pmatrix} \in SL_2(\mathbb{R}),$$

is defined by the Möbius transformation (I.1.1).

In other words the correspondence

$$(A, B) \mapsto \text{all generalised eigenvalues}$$

is another realisation of a covariant calculus in the sense of Defn. II.4.23. The collection of all pairs $g \cdot (A, B)$, $g \in SL_2(\mathbb{R})$ is an example of *covariant pencil* of operators. This set is a $SL_2(\mathbb{R})$ -homogeneous spaces, thus it shall be within the classification of such homogeneous spaces provided in the Subsection ??.

EXAMPLE III.1.19. It is easy to demonstrate that all existing homogeneous spaces can be realised by matrix pairs.

- i. Take the pair (O, I) where O and I are the zero and identity $n \times n$ matrices respectively. Then any transformation of this pair by a lower-triangular matrix from $SL_2(\mathbb{R})$ is equivalent to (O, I) . The respective homogeneous space is isomorphic to the real line with the Möbius transformations (I.1.1).
- ii. Consider $H = \mathbb{R}^2$. Using the notations ι from Subsection I.3.4 we define three realisations (elliptic, parabolic and hyperbolic) of an operator A_ι :

$$(III.1.15) \quad A_i = \begin{pmatrix} 0 & 1 \\ -1 & 0 \end{pmatrix}, \quad A_\epsilon = \begin{pmatrix} 0 & 1 \\ 0 & 0 \end{pmatrix}, \quad A_j = \begin{pmatrix} 0 & 1 \\ 1 & 0 \end{pmatrix}.$$

Then for an arbitrary element h of the subgroup K , N or A the respective (in the sense of the Principle II.3.5) pair $h \cdot (A_\iota, I)$ is equivalent to (A_ι, I) itself. Thus those three homogeneous spaces are isomorphic to the elliptic, parabolic and hyperbolic half-planes under respective actions of $SL_2(\mathbb{R})$. Note, that $A_\iota^2 = \iota^2 I$, that is A_ι is a model for hypercomplex units.

- iii. Let A be a direct sum of any two different matrices out of the three A_ι from (III.1.15) then the fix group of the equivalence class of the pair (A, I) is the identity of $SL_2(\mathbb{R})$. Thus the corresponding homogeneous space coincides with the group itself.

Hawing homogeneous spaces generated by pairs of operators we can define respective functions on those spaces. The special attention is due the following paraphrase of the resolvent:

$$R_{(A,B)}(g) = (cA + dB)^{-1} \quad \text{where } g^{-1} = \begin{pmatrix} a & b \\ c & d \end{pmatrix} \in SL_2(\mathbb{R}).$$

Obviously $R_{(A,B)}(g)$ contains the essential information about the pair (A, B) . Probably, the function $R_{(A,B)}(g)$ contains too much simultaneous information, we may restrict it to get a more detailed view. For vectors $u, v \in H$ we also consider vector and scalar-valued functions related to the generalised resolvent:

$$R_{(A,B)}^u(g) = (cA + dB)^{-1}u, \quad \text{and} \quad R_{(A,B)}^{(u,v)}(g) = \langle (cA + dB)^{-1}u, v \rangle,$$

where $(cA + dB)^{-1}u$ is understood as a solution w of the equation $u = (cA + dB)w$ if it exists and is unique, this does not require the full invertibility of $cA + dB$.

It is easy to see that the map $(A, B) \mapsto R_{(A,B)}^{(u,v)}(g)$ is a covariant calculus as well. It worth to notice that function $R_{(A,B)}$ can again fall into three EPH cases.

EXAMPLE III.1.20. For the three matrices A_t considered in the previous Example we denote by $R_t(g)$ the resolvent-type function of the pair (A_t, I) . Then:

$$R_i(g) = \frac{1}{c^2 + d^2} \begin{pmatrix} d & -c \\ c & d \end{pmatrix}, \quad R_\varepsilon(g) = \frac{1}{d^2} \begin{pmatrix} d & -c \\ 0 & d \end{pmatrix}, \quad R_j(g) = \frac{1}{d^2 - c^2} \begin{pmatrix} d & -c \\ -c & d \end{pmatrix}.$$

Put $u = (1, 0) \in H$, then $R_t(g)u$ is a two-dimensional real vector valued functions with components equal to real and imaginary part of hypercomplex Cauchy kernel considered in [195].

Consider the space $L(G)$ of functions spanned by all left translations of $R_{(A,B)}(g)$. As usual, a closure in a suitable metric, say L_p , can be taken. The left action $g : f(h) \mapsto f(g^{-1}h)$ of $SL_2(\mathbb{R})$ on this space is a linear representation of this group. Afterwards the representation can be decomposed into a sum of primary subrepresentations.

EXAMPLE III.1.21. For the matrices A_t the irreducible components are isomorphic to analytic spaces of hypercomplex functions under the fraction-linear transformations build in Subsection II.3.2.

An important observation is that a decomposition into irreducible or primary components can reveal an EPH structure even in the cases hiding it on the homogeneous space level.

EXAMPLE III.1.22. Take the operator $A = A_i \oplus A_j$ from the Example III.1.19(III.1.19.iii). The corresponding homogeneous space coincides with the entire $SL_2(\mathbb{R})$. However if we take two vectors $u_i = (1, 0) \oplus (0, 0)$ and $u_j = (0, 0) \oplus (1, 0)$ then the respective linear spaces generated by functions $R_A(g)u_i$ and $R_A(g)u_j$ will be of elliptic and hyperbolic types respectively.

Let us briefly consider a *quadratic eigenvalue* problem: for given operators (matrices) A_0, A_1 and A_2 from $B(H)$ find a scalar λ and a vector $x \in H$ such that

$$(III.1.16) \quad Q(\lambda)x = 0, \quad \text{where} \quad Q(\lambda) = \lambda^2 A_2 + \lambda A_1 + A_0.$$

There is a connection with our study of conic sections from Subsection ?? which we will only hint for now. Comparing (III.1.16) with the equation of the cycle (I.4.3) we can associate the respective Fillmore–Springer–Cnops–type matrix to $Q(\lambda)$, cf. (??):

$$(III.1.17) \quad Q(\lambda) = \lambda^2 A_2 + \lambda A_1 + A_0 \quad \longleftrightarrow \quad C_Q = \begin{pmatrix} A_1 & A_0 \\ A_2 & -A_1 \end{pmatrix}.$$

Then we can state the following analogue of Thm. ?? for the quadratic eigenvalues:

PROPOSITION III.1.23. *Let two quadratic matrix polynomials Q and \tilde{Q} are such that their FSCc matrices (III.1.17) are conjugated $C_{\tilde{Q}} = gC_Q g^{-1}$ by an element $g \in SL_2(\mathbb{R})$. Then λ is a solution of the quadratic eigenvalue problem for Q and $x \in H$ if and only if $\mu = g \cdot \lambda$ is a solution of the quadratic eigenvalue problem for \tilde{Q} and x . Here $\mu = g \cdot \lambda$ is the Möbius transformation (I.1.1) associated to $g \in SL_2(\mathbb{R})$.*

So quadratic matrix polynomials are non-commuting analogues of the cycles and it would be exciting to extend the geometry from Section ?? to this non-commutative setting as much as possible.

REMARK III.1.24. It is beneficial to extend a notion of a scalar in an (generalised) eigenvalue problem to an abstract field or ring. For example, we can consider pencils of operators/matrices with polynomial coefficients. In many circumstances we may factorise the polynomial ring by an ideal generated by a collection of algebraic equations. Our work with hypercomplex units is the most elementary realisation of this setup. Indeed, the algebra of hypercomplex numbers with the hypercomplex unit ι is a realisation of the polynomial ring in a variable t factored by the single quadratic relation $t^2 + \sigma = 0$, where $\sigma = \iota^2$.

Part IV

The Heisenberg Group and Physics

Preview: Quantum and Classical Mechanics

... it was on a Sunday that the idea first occurred to me that a $b - b a$ might correspond to a Poisson bracket.

P.A.M. Dirac,

The following lectures describe some links between the group $SL_2(\mathbb{R})$, the Heisenberg group and hypercomplex numbers. The described relations appear in a natural way without any enforcement from our side. The discussion is illustrated by mathematical models of various physical systems.

In this chapter we will demonstrate that a Poisson bracket do not only corresponds to a commutator, in fact a Poisson bracket is the image of the commutator under a transformation which uses dual numbers.

IV.1.1. Axioms of Mechanics

There is a recent revival of interest in foundations of quantum mechanics, which is essentially motivated by engineering challenges at the nano-scale. There are strong indications that we need to revise the development of the quantum theory from its early days.

In 1926, Dirac discussed the idea that quantum mechanics can be obtained from classical description through a change in the only rule, cf. [81]:

... there is one basic assumption of the classical theory which is false, and that if this assumption were removed and replaced by something more general, the whole of atomic theory would follow quite naturally. Until quite recently, however, one has had no idea of what this assumption could be.

In Dirac's view, such a condition is provided by the Heisenberg commutation relation of coordinate and momentum variables [81, (1)]:

$$(IV.1.1) \quad q_r p_r - p_r q_r = i\hbar.$$

Algebraically, this identity declares noncommutativity of q_r and p_r . Thus, Dirac stated [81] that classical mechanics is formulated through commutative quantities ("c-numbers" in his terms) while quantum mechanics requires noncommutative quantities ("q-numbers"). The rest of theory may be unchanged if it does not contradict to the above algebraic rules. This was explicitly re-affirmed at the first sentence of the subsequent paper [80]:

The new mechanics of the atom introduced by Heisenberg may be based on the assumption that the variables that describe a dynamical system do not obey the commutative law of multiplication, but satisfy instead certain quantum conditions.

The same point of view is expressed in his later works [82, p. 26; 83, p. 6].

Dirac's approach was largely approved, especially by researchers on the mathematical side of the board. Moreover, the vague version – “quantum is something noncommutative” – of the original statement was lightly reverted to “everything noncommutative is quantum”. For example, there is a fashion to label any noncommutative algebra as a “quantum space” [72].

Let us carefully review Dirac's idea about noncommutativity as the principal source of quantum theory.

IV.1.2. “Algebra” of Observables

Dropping the commutativity hypothesis on observables, Dirac made [81] the following (apparently flexible) assumption:

All one knows about q-numbers is that if z_1 and z_2 are two q-numbers, or one q-number and one c-number, there exist the numbers $z_1 + z_2$, $z_1 z_2$, $z_2 z_1$, which will in general be q-numbers but may be c-numbers.

Mathematically, this (together with some natural identities) means that observables form an algebraic structure known as a *ring*. Furthermore, the linear *superposition principle* imposes a linear structure upon observables, thus their set becomes an *algebra*. Some mathematically-oriented texts, e.g. [94, § 1.2], directly speak about an “algebra of observables” which is not far from the above quote [81]. It is also deducible from two connected statements in Dirac's canonical textbook:

- i. “the linear operators corresponds to the dynamical variables at that time” [82, § 7, p. 26].
- ii. “Linear operators can be added together” [82, § 7, p. 23].

However, the assumption that any two observables may be added cannot fit into a physical theory. To admit addition, observables need to have the same dimensionality. In the simplest example of the observables of coordinate q and momentum p , which units shall be assigned to the expression $q + p$? Meters or $\frac{\text{kilos} \times \text{meters}}{\text{seconds}}$? If we get the value 5 for $p + q$ in the metric units, what is then the result in the imperial ones? Since these questions cannot be answered, the above Dirac's assumption is not a part of any physical theory.

Another common definition suffering from the same problem is used in many excellent books written by distinguished mathematicians, see for example [104, § 1.1; 248, § 2-2]. It declares that quantum observables are projection-valued Borel measures on the *dimensionless* real line. Such a definition permit an instant construction (through the functional calculus) of new observables, including algebraically formed [248, § 2-2, p. 63]:

Because of Axiom III, expressions such as A^2 , $A^3 + A$, $1 - A$, and e^A all make sense whenever A is an observable.

However, if A has a physical dimension (is not a scalar) then the expression $A^3 + A$ cannot be assigned a dimension in a consistent manner.¹

Of course, physical defects of the above (otherwise perfect) mathematical constructions do not prevent physicists from making correct calculations, which are in a good agreement with experiments. We are not going to analyse methods which allow researchers to escape the indicated dangers. Instead, it will be more beneficial to outline alternative mathematical foundations of quantum theory, which do not have those shortcomings.

IV.1.3. Non-Essential Noncommutativity

While we can add two observables if they have the same dimension only, physics allows us to multiply any observables freely. Of course, the dimensionality of a product is the product of dimensionalities, thus the commutator $[A, B] = AB - BA$ is well defined for any two observables A and B . In particular, the commutator (IV.1.1) is also well-defined, but is it indeed so important?

In fact, it is easy to argue that noncommutativity of observables is not an essential prerequisite for quantum mechanics: there are constructions of quantum theory which do not rely on it at all. The most prominent example is the Feynman path integral. To focus on the really cardinal moments, we firstly take the popular lectures [97], which present the main elements in a very enlightening way. Feynman managed to tell the fundamental features of quantum electrodynamics without any reference to (non-)commutativity: the entire text does not mention it anywhere.

Is this an artefact of the popular nature of these lecture? Take the academic presentation of path integral technique given in [98]. It mentioned (non-)commutativity only on pages 115–6 and 176. In addition, page 355 contains a remark on noncommutativity of quaternions, which is irrelevant to our topic. Moreover, page 176 highlights that noncommutativity of quantum observables is a consequence of the path integral formalism rather than an indispensable axiom.

But what is the mathematical source of quantum theory if noncommutativity is not? The vivid presentation in [97] uses stopwatch with a single hand to explain the calculation of path integrals. The angle of stopwatch's hand presents the *phase* for a path $x(t)$ between two points in the configuration space. The mathematical expression for the path's phase is [98, (2-15)]:

$$(IV.1.2) \quad \phi[x(t)] = \text{const} \cdot e^{(i/\hbar)S[x(t)]},$$

where $S[x(t)]$ is the *classic action* along the path $x(t)$. Summing up contributions (IV.1.2) along all paths between two points a and b we obtain the amplitude $K(a, b)$. This

¹These arguments are rooted in history. Vieta, the founding father of the symbolic algebra, always wrote $x^2 + x \cdot 1$ instead of $x^2 + x$: the former avoids “meaningless addition of an area to a length” expressed by the later. However, very soon Descartes said that Vieta's notations used unnecessary geometric justifications.

amplitude presents very accurate description of many quantum phenomena. Therefore, expression (IV.1.2) is also a strong contestant for the rôle of the cornerstone of quantum theory.

Is there anything common between two “principal” identities (IV.1.1) and (IV.1.2)? Seemingly, not. A more attentive reader may say that there are only two common elements there (in order of believed significance):

- i. The non-zero Planck constant \hbar .
- ii. The imaginary unit i .

The Planck constant was the first manifestation of quantum (discrete) behaviour and it is at the heart of the whole theory. In contrast, classical mechanics is oftenly obtained as a semiclassical limit $\hbar \rightarrow 0$. Thus, the non-zero Planck constant looks like a clear marker of quantum world in its opposition to the classical one. Regrettably, there is a common practice to “chose our units such that $\hbar = 1$ ”. Thus, the Planck constant becomes oftenly invisible in many formulae even being implicitly present there. Note also, that 1 in the identity $\hbar = 1$ is not a scalar but a physical quantity with the dimensionality of the action. Thus, the simple omission of the Planck constant invalidates dimensionalities of physical equations.

The complex imaginary unit is also a mandatory element of quantum mechanics in all its possible formulations. It is enough to point out that the popular lectures [97] managed to avoid any mention of noncommutativity but did uses complex numbers both explicitly (see the Index there) and implicitly (as rotations of the hand of a stop-watch). However, it is a common perception that complex numbers are a useful but manly technical tool in quantum theory.

IV.1.4. Quantum Mechanics from the Heisenberg Group

Looking for a source of quantum theory we again return to the Heisenberg commutation relations (IV.1.1): they are an important part of quantum mechanics (either as a prerequisite or as a consequence). It was observed for a long time that these relations are a representation of the structural identities of the Lie algebra of the Heisenberg group [104, 138, 139]. In the simplest case of one dimension, the Heisenberg group $\mathbb{H} = \mathbb{H}^1$ can be realised by the Euclidean space \mathbb{R}^3 with the group law:

$$(IV.1.3) \quad (s, x, y) * (s', x', y') = (s + s' + \frac{1}{2}\omega(x, y; x', y'), x + x', y + y'),$$

where ω is the *symplectic form* on \mathbb{R}^2 [11, § 37], which is behind the entire classical Hamiltonian formalism:

$$(IV.1.4) \quad \omega(x, y; x', y') = xy' - x'y.$$

Here, like for the path integral, we see another example of a quantum notion being defined through a classical object.

The Heisenberg group is noncommutative since $\omega(x, y; x', y') = -\omega(x', y'; x, y)$. The collection of points $(s, 0, 0)$ forms the centre of \mathbb{H} , that is $(s, 0, 0)$ commutes with any other element of the group. We are interested in the unitary irreducible representations (UIRs) ρ of \mathbb{H} in an infinite-dimensional Hilbert space H , that is a group homomorphism ($\rho(g_1)\rho(g_2) = \rho(g_1 * g_2)$) from \mathbb{H} to unitary operators on H . By Schur’s

lemma, for such a representation ρ , the action of the centre shall be multiplication by an unimodular complex number, i.e. $\rho(s, 0, 0) = e^{2\pi i \hbar s} \mathbb{1}$ for some real $\hbar \neq 0$.

Furthermore, the celebrated Stone–von Neumann theorem [104, § 1.5] tells that all UIRs of \mathbb{H} in complex Hilbert spaces with the same value of \hbar are unitary equivalent. In particular, this implies that any realisation of quantum mechanics, e.g. the Schrödinger wave mechanics, which provides the commutation relations (IV.1.1) shall be unitary equivalent to the Heisenberg matrix mechanics based on these relations.

In particular, any UIR of \mathbb{H} is equivalent to a subrepresentation of the following representation on $L_2(\mathbb{R}^2)$:

$$(IV.1.5) \quad \rho_{\hbar}(s, x, y) : f(q, p) \mapsto e^{-2\pi i(\hbar s + qx + py)} f\left(q - \frac{\hbar}{2}y, p + \frac{\hbar}{2}x\right).$$

Here \mathbb{R}^2 has the physical meaning of the classical *phase space* with q representing the coordinate in the configurational space and p —the respective momentum. The function $f(q, p)$ in (IV.1.5) presents a state of the physical system as an amplitude over the phase space. Thus, the action (IV.1.5) is more intuitive and has many technical advantages [104, 139, 341] in comparison with the well-known Schrödinger representation (cf. (IV.4.16)), to which it is unitary equivalent, of course.

Infinitesimal generators of the one-parameter subgroups $\rho_{\hbar}(0, x, 0)$ and $\rho_{\hbar}(0, 0, y)$ from (IV.1.5) are the operators $\frac{1}{2}\hbar\partial_p - 2\pi iq$ and $-\frac{1}{2}\hbar\partial_q - 2\pi ip$. For these, we can directly verify the commutator identity:

$$\left[-\frac{1}{2}\hbar\partial_q - 2\pi ip, \frac{1}{2}\hbar\partial_p - 2\pi iq\right] = i\hbar, \quad \text{where } \hbar = 2\pi\hbar.$$

Since we have a representation of (IV.1.1), these operators can be used as a model of the quantum coordinate and momentum.

For a Hamiltonian $H(q, p)$ we can integrate the representation ρ_{\hbar} with the Fourier transform $\hat{H}(x, y)$ of $H(q, p)$:

$$(IV.1.6) \quad \tilde{H} = \int_{\mathbb{R}^2} \hat{H}(x, y) \rho_{\hbar}(0, x, y) dx dy$$

and obtain (possibly unbounded) operator \tilde{H} on $L_2(\mathbb{R}^2)$. This assignment of the operator \tilde{H} (quantum observable) to a function $H(q, p)$ (classical observable) is known as the Weyl quantization or a Weyl calculus [104, § 2.1]. The Hamiltonian \tilde{H} defines the dynamics of a quantum observable \tilde{k} by the *Heisenberg equation*:

$$(IV.1.7) \quad i\hbar \frac{d\tilde{k}}{dt} = \tilde{H}\tilde{k} - \tilde{k}\tilde{H}.$$

This is sketch of the well-known construction of quantum mechanics from infinite-dimensional UIRs of the Heisenberg group, which can be found in numerous sources [104, 139, 181].

IV.1.5. Classical Noncommutativity

Now we are going to show that the priority of importance in quantum theory shall be shifted from the Planck constant towards the imaginary unit. Namely, we describe a model of *classical* mechanics with a *non-zero* Planck constant but with a different hypercomplex unit. Instead of the imaginary unit with the property $i^2 = -1$ we will

use the nilpotent unit ε such that $\varepsilon^2 = 0$. The *dual numbers* generated by nilpotent unit were already known for there connections with Galilean relativity [115, 339] – the fundamental symmetry of classical mechanics – thus its appearance in our discussion shall not be very surprising after all. Rather, we may wonder why the following construction was unnoticed for such a long time.

Another important feature of our scheme is that the classical mechanics is presented by a noncommutative model. Therefore, it will be a refutation of Dirac’s claim about the exclusive rôle of noncommutativity for quantum theory. Moreover, the model is developed from the same Heisenberg group, which were used above to describe the quantum mechanics.

Consider a four-dimensional algebra \mathfrak{C} spanned by 1, i , ε and $i\varepsilon$. We can define the following representation $\rho_{\varepsilon\hbar}$ of the Heisenberg group in a space of \mathfrak{C} -valued smooth functions [197, 199]:

$$(IV.1.8) \rho_{\varepsilon\hbar}(s, x, y) : f(q, p) \mapsto e^{-2\pi i(xq + yp)} \left(f(q, p) + \varepsilon\hbar \left(2\pi i s f(q, p) - \frac{iy}{2} f'_q(q, p) + \frac{ix}{2} f'_p(q, p) \right) \right).$$

A simple calculation shows the representation property

$$\rho_{\varepsilon\hbar}(s, x, y) \rho_{\varepsilon\hbar}(s', x', y') = \rho_{\varepsilon\hbar}((s, x, y) * (s', x', y'))$$

for the multiplication (IV.1.3) on \mathbb{H} . Since this is not a unitary representation in a complex-valued Hilbert space its existence does not contradict the Stone–von Neumann theorem. Both representations (IV.1.5) and (IV.1.8) are *noncommutative* and act on functions over the phase space. The important distinction is:

- The representation (IV.1.5) is induced (in the sense of Mackey [159, § 13.4]) by the *complex-valued* unitary character $\rho_{\hbar}(s, 0, 0) = e^{2\pi i\hbar s}$ of the centre of \mathbb{H} .
- The representation (IV.1.8) is similarly induced by the *dual number-valued* character $\rho_{\varepsilon\hbar}(s, 0, 0) = e^{\varepsilon\hbar s} = 1 + \varepsilon\hbar s$ of the centre of \mathbb{H} , cf. [194]. Here dual numbers are the associative and commutative two-dimensional algebra spanned by 1 and ε .

Similarity between (IV.1.5) and (IV.1.8) is even more striking if (IV.1.8) is written² as:

$$(IV.1.9) \quad \rho_{\hbar}(s, x, y) : f(q, p) \mapsto e^{-2\pi(\varepsilon\hbar s + i(qx + py))} f\left(q - \frac{i\hbar}{2}\varepsilon y, p + \frac{i\hbar}{2}\varepsilon x\right).$$

Here, for a differentiable function k of a real variable t , the expression $k(t + \varepsilon a)$ is understood as $k(t) + \varepsilon a k'(t)$, where $a \in \mathbb{C}$ is a constant. For a real-analytic function k this can be justified through its Taylor’s expansion, see [58; 78; 79; 115; 342, § I.2(10)]. The same expression appears within the non-standard analysis based on the idempotent unit ε [30].

The infinitesimal generators of one-parameter subgroups $\rho_{\varepsilon\hbar}(0, x, 0)$ and $\rho_{\varepsilon\hbar}(0, 0, y)$ in (IV.1.8) are

$$d\rho_{\varepsilon\hbar}^X = -2\pi i q - \frac{\varepsilon\hbar}{4\pi i} \partial_p \quad \text{and} \quad d\rho_{\varepsilon\hbar}^Y = -2\pi i p + \frac{\varepsilon\hbar}{4\pi i} \partial_q,$$

²I am grateful to Prof. N.A.Gromov, who suggested this expression.

respectively. We calculate their commutator:

$$(IV.1.10) \quad d\rho_{\varepsilon\hbar}^X \cdot d\rho_{\varepsilon\hbar}^Y - d\rho_{\varepsilon\hbar}^Y \cdot d\rho_{\varepsilon\hbar}^X = \varepsilon\hbar.$$

It is similar to the Heisenberg relation (IV.1.1): the commutator is non-zero and is proportional to the Planck constant. The only difference is the replacement of the imaginary unit by the nilpotent one. The radical nature of this change becomes clear if we integrate this representation with the Fourier transform $\hat{H}(x, y)$ of a Hamiltonian function $H(q, p)$:

$$(IV.1.11) \quad \mathring{H} = \int_{\mathbb{R}^{2n}} \hat{H}(x, y) \rho_{\varepsilon\hbar}(0, x, y) dx dy = H + \frac{\varepsilon\hbar}{2} \left(\frac{\partial H}{\partial p} \frac{\partial}{\partial q} - \frac{\partial H}{\partial q} \frac{\partial}{\partial p} \right).$$

This is a first order differential operator on the phase space. It generates a dynamics of a classical observable k – a smooth real-valued function on the phase space – through the equation isomorphic to the Heisenberg equation (IV.1.7):

$$\varepsilon\hbar \frac{d\mathring{k}}{dt} = \mathring{H}k - k\mathring{H}.$$

Making a substitution from (IV.1.11) and using the identity $\varepsilon^2 = 0$ we obtain:

$$(IV.1.12) \quad \frac{dk}{dt} = \frac{\partial H}{\partial p} \frac{\partial k}{\partial q} - \frac{\partial H}{\partial q} \frac{\partial k}{\partial p}.$$

This is, of course, the *Hamilton equation* of classical mechanics based on the *Poisson bracket*. Dirac suggested, see the paper's epigraph, that the commutator *corresponds* to the Poisson bracket. However, the commutator in the representation (IV.1.8) is *exactly* the Poisson bracket.

Note also, that both the Planck constant and the nilpotent unit disappeared from (IV.1.12) however we did use the fact $\hbar \neq 0$ to make this cancellation. Also, the shy disappearance of the nilpotent unit ε at the very last minute can explain why its rôle remain unnoticed for a long time.

IV.1.6. Summary

We revised mathematical foundations of quantum and classical mechanics and the rôle of hypercomplex units $i^2 = -1$ and $\varepsilon^2 = 0$ there. To make the consideration complete, one may wish to consider the third logical possibility of the hyperbolic unit j with the property $j^2 = 1$ [142, 156, 194, 198, 199, 281, 327], see Section IV.4.4.

The above discussion provides the following observations [200]:

- i. Noncommutativity is not a crucial prerequisite for quantum theory, it can be obtained as a consequence of other fundamental assumptions.
- ii. Noncommutativity is not a distinguished feature of quantum theory, there are noncommutative formulations of classical mechanics as well.
- iii. The non-zero Planck constant is compatible with classical mechanics. Thus, there is no a necessity to consider the semiclassical limit $\hbar \rightarrow 0$, where the *constant* has to tend to zero.

- iv. There is no a necessity to request that physical observables form an algebra, which is a physical non-sense since we cannot add two observables of different dimensionalities. Quantization can be performed by the Weyl recipe, which requires only a structure of a linear space in the collection of all observables with the same physical dimensionality.
- v. It is the imaginary unit in (IV.1.1), which is ultimately responsible for most of quantum effects. Classical mechanics can be obtained from the similar commutator relation (IV.1.10) using the nilpotent unit $\varepsilon^2 = 0$.

In Dirac's opinion, quantum noncommutativity was so important because it guarantees a non-trivial commutator, which is required to substitute the Poisson bracket. In our model, multiplication of classical observables is also non-commutative and the Poisson bracket exactly is the commutator. Thus, these elements do not separate quantum and classical models anymore.

Our consideration illustrates the following statement on the exceptional rôle of the complex numbers in quantum theory:

...for the first time, the complex field \mathbb{C} was brought into physics at a fundamental and universal level, not just as a useful or elegant device, as had often been the case earlier for many applications of complex numbers to physics, but at the very basis of physical law. [277]

In the 1960s it was said (in a certain connection) that the most important discovery of recent years in physics was the complex numbers. [250, p. 90]

Thus, Dirac may be right that we need to change a single assumption to get a transition between classical mechanics and quantum. But, it shall not be a move from commutative to noncommutative. Instead, we need to replace a representation of the Heisenberg group induced from a dual number-valued character by the representation induced by a complex-valued character. Our conclusion can be stated like a proportionality:

Classical/Quantum=Dual numbers/Complex numbers.

The Heisenberg Group

The relations, which define the Heisenberg group or its Lie algebra, are of a fundamental nature and appeared in very different areas. For example, the basic operators of differentiation and multiplication by an independent variable in analysis satisfy to the same commutation relations as observables of momentum and coordinate in quantum mechanics.

It is very easy to oversee those common structures. Roger Howe said in [138]:

An investigator might be able to get what he wanted out of a situation while overlooking the extra structure imposed by the Heisenberg group, structure which might enable him to get much more.

We shall start from the general properties the Heisenberg group and its representations. Many important applications will follow.

REMARK IV.2.1. It is worth to mention that the Heisenberg group is also known as the *Weyl* (or Heisenberg–Weyl) group in physical literature. It is another illustration of its perception as an extraneous object: physicists call it by the name of a mathematician, and mathematicians by the name of a physicists.

To add more confusion the Lie algebra of the Heisenberg group is called Weyl algebra. However, the commutator relations $[Q, P] = I$ in the Weyl algebra are called Heisenberg commutator relations, however the commutation relation $sm = qms$ in the representation the Heisenberg group are known as the Weyl commutation relation. The most obvious simplification would be to call every above object the Heisenberg–Weyl. However we will use the most common names in this work.

IV.2.1. The Symplectic Form and the Heisenberg group

Let $n \geq 1$ be an integer. For two real n -vectors $x, y \in \mathbb{R}^n$, we write xy for their inner product:

(IV.2.1)

$$xy = x_1y_1 + x_2y_2 + \cdots + x_ny_n, \quad \text{where } x = (x_1, x_2, \dots, x_n), \quad y = (y_1, y_2, \dots, y_n).$$

Similarly for complex vectors $z, w \in \mathbb{C}^n$, we define:

(IV.2.2)

$$z\bar{w} = z_1\bar{w}_1 + z_2\bar{w}_2 + \cdots + z_n\bar{w}_n, \quad \text{where } z = (z_1, z_2, \dots, z_n), \quad w = (w_1, w_2, \dots, w_n).$$

The following notion is the central for Hamiltonian formulation of classical mechanics [11, § 37].

DEFINITION IV.2.2. The *symplectic form* ω on \mathbb{R}^{2n} is a function of two vectors such that:

$$(IV.2.3) \quad \omega(x, y; x', y') = xy' - x'y, \quad \text{where } (x, y), (x', y') \in \mathbb{R}^{2n}.$$

EXERCISE IV.2.3. Check the following properties:

- i. ω is anti-symmetric $\omega(x, y; x', y') = -\omega(x', y'; x, y)$.
- ii. ω is bilinear:

$$\begin{aligned} \omega(x, y; \alpha x', \alpha y') &= \alpha \omega(x, y; x', y'), \\ \omega(x, y; x' + x'', y' + y'') &= \alpha \omega(x, y; x', y') + \omega(x, y; x'', y''). \end{aligned}$$

- iii. Let $z = x + iy$ and $w = x' + iy'$ then ω can be expressed through the complex inner product (IV.2.2) as $\omega(x, y; x', y') = -\Im(z\bar{w})$.
- iv. The symplectic form on \mathbb{R}^2 is equal to $\det \begin{pmatrix} x & x' \\ y & y' \end{pmatrix}$. Consequently it vanishes if and only if (x, y) and (x', y') are collinear.
- v. Let $A \in \text{SL}_2(\mathbb{R})$ be a real 2×2 matrix with the unit determinant. Define:

$$(IV.2.4) \quad \begin{pmatrix} \tilde{x} \\ \tilde{y} \end{pmatrix} = A \begin{pmatrix} x \\ y \end{pmatrix} \quad \text{and} \quad \begin{pmatrix} \tilde{x}' \\ \tilde{y}' \end{pmatrix} = A \begin{pmatrix} x' \\ y' \end{pmatrix}.$$

Then, $\omega(\tilde{x}, \tilde{y}; \tilde{x}', \tilde{y}') = \omega(x, y; x', y')$. Moreover, the *symplectic group* $\text{Sp}(2)$ —the set of all linear transformations of \mathbb{R}^2 preserving ω —coincides with $\text{SL}_2(\mathbb{R})$.

Now we define the main object of our consideration.

DEFINITION IV.2.4. An element of the n -dimensional *Heisenberg group* \mathbb{H}^n [104, 139] is $(s, x, y) \in \mathbb{R}^{2n+1}$, where $s \in \mathbb{R}$ and $x, y \in \mathbb{R}^n$. The group law on \mathbb{H}^n is given as follows:

$$(IV.2.5) \quad (s, x, y) \cdot (s', x', y') = (s + s' + \frac{1}{2}\omega(x, y; x', y'), x + x', y + y'),$$

where ω the symplectic form.

For the sake of simplicity, we will work with the one-dimensional Heisenberg group \mathbb{H}^1 on several occasions. This shall be mainly in the cases involving the symplectic group, since we want to stay the basic case $\text{Sp}(2) \sim \text{SL}_2(\mathbb{R})$. However, consideration of the general case of \mathbb{H}^n is similar in most respects.

EXERCISE IV.2.5. For the Heisenberg group \mathbb{H}^n , check that:

- i. The unit is $(0, 0, 0)$ and the inverse $(s, x, y)^{-1} = (-s, -x, -y)$.
- ii. It is a non-commutative Lie group. HINT: Use the properties of the symplectic form from the Exercise IV.2.3. For example, the associativity follows from the linearity of ω . \diamond
- iii. It has the *centre*

$$(IV.2.6) \quad Z = \{(s, 0, 0) \in \mathbb{H}^n, s \in \mathbb{R}\}.$$

The group law on \mathbb{H}^n can be expressed in several equivalent forms.

EXERCISE IV.2.6. i. Introduce complexified coordinates (s, z) on \mathbb{H}^1 with $z = x + iy$. Then the group law can be written as:

$$(s, z) \cdot (s', z') = (s + s' + \frac{1}{2}\mathcal{J}(z'\bar{z}), z + z').$$

ii. Show that the set \mathbb{R}^3 with the group law

$$(IV.2.7) \quad (s, x, y) \cdot (s', x', y') = (s + s' + xy', x + x', y + y')$$

is isomorphic to the Heisenberg group \mathbb{H}^1 . It is called *polarised Heisenberg group* [104, § 1.2]. HINT: Use the explicit form of the homomorphism $(s, x, y) \mapsto (s + \frac{1}{2}xy, x, y)$. \diamond

iii. Define the map $\phi : \mathbb{H}^1 \rightarrow M_3(\mathbb{R})$ by

$$(IV.2.8) \quad \phi(s, x, y) = \begin{pmatrix} 1 & x & s + \frac{1}{2}xy \\ 0 & 1 & y \\ 0 & 0 & 1 \end{pmatrix}.$$

This is a group homomorphism from \mathbb{H}^1 to the group of 3×3 matrices with the unit determinant and the matrix multiplication as the group operation. Write also a group homomorphism from the polarised Heisenberg group to $M_3(\mathbb{R})$.

iv. Expand the above items from this Exercise to \mathbb{H}^n .

IV.2.2. Lie algebra of the Heisenberg group

The Lie algebra of the Heisenberg group \mathfrak{h}_1 is also called *Weyl algebra*. From the general theory we know, that \mathfrak{h}_1 is a three-dimensional real vector space, thus, it can be identified as a set with the group $\mathbb{H}^1 \sim \mathbb{R}^3$ itself.

There are several standard possibilities to realise \mathfrak{h}_1 , cf. Sect. I.2.3. Firstly, we link \mathfrak{h}_1 with one-parameter subgroups as in Sect. I.2.3.1.

EXERCISE IV.2.7. i. Show that 3×3 matrices from (IV.2.8) are created by the following exponential map:

$$(IV.2.9) \quad \exp \begin{pmatrix} 0 & x & s \\ 0 & 0 & y \\ 0 & 0 & 0 \end{pmatrix} = \begin{pmatrix} 1 & x & s + \frac{1}{2}xy \\ 0 & 1 & y \\ 0 & 0 & 1 \end{pmatrix}.$$

Thus \mathfrak{h}_1 isomorphic to the vector space of matrices in the left-hand side. We can define the explicit identification $\exp : \mathfrak{h}_1 \rightarrow \mathbb{H}^1$ by (IV.2.9), which is also known as the exponential coordinates on \mathbb{H}^1 .

ii. Define the basis of \mathfrak{h}_1 :

$$(IV.2.10) \quad S = \begin{pmatrix} 0 & 0 & 1 \\ 0 & 0 & 0 \\ 0 & 0 & 0 \end{pmatrix}, \quad X = \begin{pmatrix} 0 & 1 & 0 \\ 0 & 0 & 0 \\ 0 & 0 & 0 \end{pmatrix}, \quad Y = \begin{pmatrix} 0 & 0 & 0 \\ 0 & 0 & 1 \\ 0 & 0 & 0 \end{pmatrix}.$$

Write the one-parameter subgroups of \mathbb{H}^1 generated by S, X and Y .

Another possibility is a description of \mathfrak{h}_1 as the collection of invariant vector fields, see Sect. I.2.3.2.

EXERCISE IV.2.8. i. Check that the following vector fields on \mathbb{H}^1 are left (right) invariant:

$$(IV.2.11) \quad S^{l(r)} = \pm \partial_s, \quad X^{l(r)} = \pm \partial_x - \frac{1}{2}y\partial_s, \quad Y^{l(r)} = \pm \partial_y + \frac{1}{2}x\partial_s.$$

Show also that they are linearly independent and, thus, are bases the Lie algebra \mathfrak{h}_1 in two different realisations.

ii. Calculate one-parameter groups of right (left) shifts on \mathbb{H}^1 generated by these vector fields.

The principal operation on a Lie algebra, besides the linear structure, is the commutator $[A, B] = AB - BA$, see Sect. I.2.3.3. In the above exercises we can define the commutator for matrices and vector fields through the corresponding algebraic operations in these algebras.

EXERCISE IV.2.9. i. Check that bases from (IV.2.10) and (IV.2.11) satisfy the Heisenberg commutator relation

$$(IV.2.12) \quad [X^{l(r)}, Y^{l(r)}] = S^{l(r)}$$

and all other commutators vanishing. More generally:

$$(IV.2.13) \quad [A, A'] = \omega(x, y; x', y')S, \quad \text{where } A^{(r)} = s^{(r)}S + x^{(r)}X + y^{(r)}Y,$$

and ω is the symplectic form.

ii. Show that any second (and, thus, any higher) commutator $[[A, B], C]$ on \mathfrak{h}_1 vanishes. This property can be stated as “the Heisenberg group is a step 2 nilpotent Lie group”.

iii. Check the formula

$$(IV.2.14) \quad \exp(A)\exp(B) = \exp\left(A + B + \frac{1}{2}[A, B]\right), \quad \text{where } A, B \in \mathfrak{h}_1.$$

The formula is also true for any step 2 nilpotent Lie group and is a particular case of the Baker–Campbell–Hausdorff formula. HINT: In the case of \mathbb{H}^1 you can use the explicit form of the exponential map (IV.2.9).◊

iv. Define the vector space decomposition

$$(IV.2.15) \quad \mathfrak{h}_1 = V_0 \oplus V_1, \quad \text{such that } V_0 = [V_1, V_1].$$

Consequently, we can start from definition of the Lie algebra \mathfrak{h}_n through the commutation relations (IV.2.12). Thereafter, \mathbb{H}^n and the group law (IV.2.5) can be derived from the exponentiation of \mathfrak{h}_n .

We note that any element $A \in \mathfrak{h}_1$ defines an adjoint map $\text{ad}(A) : B \mapsto [A, B]$ on \mathfrak{h}_1 .

EXERCISE IV.2.10. Write matrices corresponding to transformations $\text{ad}(S)$, $\text{ad}(X)$, $\text{ad}(Y)$ of \mathfrak{h}_1 in the basis S, X, Y .

IV.2.3. Automorphisms of the Heisenberg group

Erlangen programme suggest investigate invariants under group action. This recipe can be applied recursively to groups themselves. Transformations of a group which preserve its structure are called *group automorphisms*.

EXERCISE IV.2.11. Check that the following are automorphisms of \mathbb{H}^1 :

i. *Inner automorphisms or conjugation* with $(s, x, y) \in \mathbb{H}^1$:

$$(IV.2.16) \quad \begin{aligned} (s', x', y') \mapsto (s, x, y) \cdot (s', x', y') \cdot (s, x, y)^{-1} &= (s' + \omega(x, y; x', y'), x', y') \\ &= (s' + xy' - x'y, x', y'). \end{aligned}$$

ii. *Symplectic maps* $(s, x, y) = (s, \tilde{x}, \tilde{y})$, where $\begin{pmatrix} \tilde{x} \\ \tilde{y} \end{pmatrix} = A \begin{pmatrix} x \\ y \end{pmatrix}$ with A from the symplectic group $\text{Sp}(2) \sim \text{SL}_2(\mathbb{R})$, see Exercise IV.2.3.v.

iii. *Dilations*: $(s, x, y) \mapsto (r^2s, rx, ry)$ for a positive real r .

iv. *Inversion*: $(s, x, y) \mapsto (-s, y, x)$.

The last three types of transformations are *outer automorphisms*.

In fact we listed all ingredients of the automorphism group.

EXERCISE IV.2.12. Show that

- i. Automorphism groups of \mathbb{H}^1 and \mathfrak{h}_1 coincide as groups of maps of \mathbb{R}^3 onto itself. HINT: Use the exponent map and the relation (IV.2.14). The crucial step is a demonstration that any automorphism of \mathbb{H}^1 is a linear map of \mathbb{R}^3 . See details in [104, Ch. 1, (1.21)]. \diamond
- ii. All transforms from Exercise IV.2.11 viewed as automorphisms of \mathfrak{h}_1 preserve the decomposition (IV.2.15).
- iii. Every automorphism of \mathbb{H}^1 can be written uniquely as composition of a symplectic map, an inner automorphism, a dilation and a power (mod 2) of the inversion from Exercise IV.2.11. HINT: Any automorphism is a linear map (by the previous item) of \mathbb{R}^3 which maps the centre Z to itself. Thus it shall have the form $(s, x, y) \mapsto (cs + ax + by, T(x, y))$, where a, b and c are real and T is a linear map of \mathbb{R}^2 , see [104, Ch. 1, (1.22)]. \diamond

The symplectic automorphisms from Exercise IV.2.11.ii can be characterised as the group of outer automorphisms of \mathbb{H}^1 , which trivially acts on the centre of \mathbb{H}^1 . It is the group of symmetries of the symplectic form ω in (IV.2.5) [104, Thm. 1.22; 138, p. 830]. The symplectic group is isomorphic to $\text{SL}_2(\mathbb{R})$ considered in the first half of this work, see Exercise IV.2.3.v. For future use we will need $\widetilde{\text{Sp}}(2)$ which is the double cover of $\text{Sp}(2)$.

We can build the semidirect product $G = \mathbb{H}^1 \rtimes \widetilde{\text{Sp}}(2)$ with the standard group law for semidirect products:

$$(IV.2.17) \quad (h, g) * (h', g') = (h * g(h'), g * g'), \quad \text{where } h, h' \in \mathbb{H}^1, \quad g, g' \in \widetilde{\text{Sp}}(2),$$

and the stars denote the respective group operations while the action $g(h')$ is defined as the composition of the projection map $\widetilde{\text{Sp}}(2) \rightarrow \text{Sp}(2)$ and the action (IV.2.4). This group is sometimes called the *Schrödinger group* and it is known as the maximal kinematical invariance group of both the free Schrödinger equation and the quantum harmonic oscillator [263]. This group is of interest not only in quantum mechanics but also in optics [322, 323].

Consider the Lie algebra \mathfrak{sp}_2 of the group $\text{Sp}(2)$. We again use the basis A, B, Z (II.3.13) with commutators (II.3.14). Vectors $Z, B - Z/2$ and B are generators of the one-parameter subgroups K, N' and A' (I.3.8–I.3.10) respectively. Furthermore we

can consider the basis $\{S, X, Y, A, B, Z\}$ of the Lie algebra \mathfrak{g} of the Schrödinger group $G = \mathbb{H}^1 \times \widetilde{\text{Sp}}(2)$. All non-zero commutators besides those already listed in (IV.2.12) and (II.3.14) are:

$$(IV.2.18) \quad [A, X] = \frac{1}{2}X, \quad [B, X] = -\frac{1}{2}Y, \quad [Z, X] = Y;$$

$$(IV.2.19) \quad [A, Y] = -\frac{1}{2}Y, \quad [B, Y] = -\frac{1}{2}X, \quad [Z, Y] = -X.$$

IV.2.4. Subgroups of \mathbb{H}^n and Homogeneous Spaces

We want to classify up to certain equivalences all possible \mathbb{H}^1 -homogeneous spaces. According to Sect. I.2.2.2 we will look for *continuous* subgroups of \mathbb{H}^1 .

One-dimensional continuous subgroups of \mathbb{H}^1 can be classified up to group automorphism. Two one-dimensional subgroups of \mathbb{H}^1 are the centre Z (IV.2.6) and

$$(IV.2.20) \quad H_x = \{(0, t, 0) \in \mathbb{H}^n, t \in \mathbb{R}\}.$$

EXERCISE IV.2.13. Show that

- i. There is no an automorphism of \mathbb{H}^1 which maps Z to H_x .
- ii. For any one-parameter continuous subgroup H of \mathbb{H}^1 there is an automorphism of \mathbb{H}^1 which maps H either to Z or H_x .

Next, for a subgroup H we wish to describe the respective homogeneous space $X = \mathbb{H}^1/H$ and actions of \mathbb{H}^1 on X . See, Section I.2.2.2 for the background general theory and definitions of maps $p : \mathbb{H}^1 \rightarrow X$ and $s : X \rightarrow \mathbb{H}^1$.

EXERCISE IV.2.14. Check that:

- i. Both homogeneous spaces \mathbb{H}^1/Z and \mathbb{H}^1/H_x are parametrised by \mathbb{R}^2 ;
- ii. The \mathbb{H}^1 -action on \mathbb{H}^1/Z is:

$$(IV.2.21) \quad (s, x, y) : (x', y') \mapsto (x + x', y + y').$$

HINT: Use the following maps: $p : (s', x', y') \mapsto (x', y')$, $s : (x', y') \mapsto (0, x', y')$. \diamond

- iii. The \mathbb{H}^1 -action on \mathbb{H}^1/H_x is:

$$(IV.2.22) \quad (s, x, y) : (s', y') \mapsto (s + s' + \frac{1}{2}xy', y + y').$$

HINT: Use the following maps: $p : (s', x', y') \mapsto x'$, $s : x' \mapsto (0, x', 0)$. \diamond

The classification of two-dimensional subgroups is as follows:

EXERCISE IV.2.15. Show that

- i. For any two-dimensional continuous subgroup of \mathbb{H}^1 there is an automorphism of \mathbb{H}^1 which maps the subgroup to

$$(IV.2.23) \quad H'_x = \{(s, 0, y) \in \mathbb{H}^1, s, y \in \mathbb{R}\}.$$

- ii. The homogeneous space \mathbb{H}^1/H'_x is parametrised by \mathbb{R} .
- iii. \mathbb{H}^1 -action on \mathbb{H}^1/H'_x is

$$(IV.2.24) \quad (s, x, y) : x' \mapsto x + x'$$

HINT: Use the maps $p : (s', x', y') \mapsto x'$ and $s : x' \mapsto (0, x', 0)$. \diamond

Actions (IV.2.21) and (IV.2.24) are Euclidean shifts and much more simple than the Möbius action of the group $SL_2(\mathbb{R})$ (I.1.1). Nevertheless, the associated representations of the Heisenberg group will be far from trivial.

Representations of the Heisenberg Group

The Heisenberg group, as many other things, is worth to be seen in action. We are going to describe various form of its actions on linear spaces, that is, representations of \mathbb{H}^n .

IV.3.1. Left Regular Representations and Its Subrepresentations

As usual, we can extend geometrical action of \mathbb{H}^1 on itself by left shift to a linear representation

$$(IV.3.1) \quad \Lambda(g) : f(g') \mapsto f(g^{-1}g'), \quad g, g' \in \mathbb{H}^1$$

on a certain linear space of functions.

EXERCISE IV.3.1. Check that the Lebesgue measure $dg = ds dx dy$ on $\mathbb{H}^1 \sim \mathbb{R}^3$ is invariant under the left shift (IV.3.1).

Thus the (left invariant) *Haar measure* on \mathbb{H}^1 coincides with the Lebesgue measure. The same measure is also invariant under the right shifts, thus \mathbb{H}^1 is *unimodular*. Consequently, the action (IV.3.1) on $L_2(\mathbb{H}, dg)$ is unitary, it is called the *left regular representation*. Moreover, the action (IV.3.1) on the Banach space $L_p(\mathbb{H}, dg)$ for any $1 \leq p < \infty$ is also an isometry.

The left regular representation (IV.3.1) is reducible on $L_2(\mathbb{H}, dg)$. To find its (possibly irreducible) subrepresentations, we can construct linear representations of \mathbb{H}^1 by induction from a character χ of the centre Z , see Section II.3 and [159, § 13]. There are several equivalent forms for the construction, here we prefer the following one, cf. § II.3.2 and [159, § 13; 321, Ch. 5].

Let χ be a character of Z , that is, a group homomorphism of Z to the group of unimodular complex numbers. Let $F_2^X(\mathbb{H}^1)$ be the space of functions on \mathbb{H}^1 having the properties:

$$(IV.3.2) \quad f(gh) = \chi(h)f(g), \quad \text{for all } g \in \mathbb{H}^n, h \in Z$$

and

$$(IV.3.3) \quad \int_{\mathbb{R}^2} |f(0, x, y)|^2 dx dy < \infty.$$

Then $F_2^X(\mathbb{H}^1)$ is invariant under the left shifts (IV.3.1) and those shifts restricted to $F_2^X(\mathbb{H}^1)$ make a representation ρ_χ of \mathbb{H}^1 induced by χ .

EXERCISE IV.3.2. Check that the induced representation is unitary if $F_2^X(\mathbb{H}^1)$ is considered as a Hilbert space with the norm defined by the integral in (IV.3.3).

However, the representation ρ_χ is not necessarily irreducible. Indeed, left shifts are commuting with the right action of the group. Thus, any subspace of null-solutions of a linear combination $aS + \sum_{j=1}^n (b_j X_j + c_j Y_j)$ of left-invariant vector fields is left-invariant and we can restrict ρ_χ to this subspace. The left-invariant differential operators define analytic condition for functions, cf. Cor. II.6.34.

EXAMPLE IV.3.3. The function $f_0(s, x, y) = e^{i\hbar s - \hbar(x^2 + y^2)/4}$, where $\hbar = 2\pi\hbar$ is a real number, belongs to $F_2^X(\mathbb{H}^n)$ for the character $\chi(s) = e^{i\hbar s}$. It is also a null solution for all the operators $X_j - iY_j$. The closed linear span of functions $f_g = \Lambda(g)f_0$ is invariant under left shifts and provide a model for the representation Heisenberg group, cf. below (IV.3.7).

IV.3.2. Induced Representations on Homogeneous Spaces

We can also build representations on the homogeneous spaces using the formula (II.3.6). We briefly remind this alternative construction of induced representations here [159, § 13.2]. Consider a subgroup H of a group G . Let a smooth section $s : G/H \rightarrow G$ be a right inverse of the natural projection $p : G \rightarrow G/H$. Thus any element $g \in G$ can be uniquely decomposed as $g = s(p(g)) * r(g)$ where the map $r : G \rightarrow H$ is defined by the previous identity. For a character χ of H we can define a *lifting* $\mathcal{L}_\chi : L_2(G/H) \rightarrow L_2^X(G)$ as follows:

$$(IV.3.4) \quad [\mathcal{L}_\chi f](g) = \chi(r(g))f(p(g)) \quad \text{where } f(x) \in L_2(G/H).$$

The image space of the lifting \mathcal{L}_χ satisfies to (IV.3.2) and is invariant under left shifts. We also define the *pulling* $\mathcal{P} : L_2^X(G) \rightarrow L_2(G/H)$, which is a left inverse of the lifting and explicitly can be given, for example, by $[\mathcal{P}F](x) = F(s(x))$. Then the induced representation on $L_2(G/H)$ is generated by the formula

$$(IV.3.5) \quad \rho_\chi(g) = \mathcal{P} \circ \Lambda(g) \circ \mathcal{L}$$

It implies the formula (II.3.6) for induced representations on the homogeneous spaces:

$$(IV.3.6) \quad [\rho_\chi(g)f](x) = \chi(r(g^{-1} * s(x)))f(g^{-1} \cdot x).$$

The corresponding forms of the induced representations are:

- i. For $H = Z$ the map $r : \mathbb{H}^1 \rightarrow Z$ is $r(s, x, y) = (s, 0, 0)$. For the character $\chi_\hbar(s, 0, 0) = e^{2\pi i \hbar s}$, the representation of \mathbb{H}^1 on $L_2(\mathbb{R}^2)$ is, cf. (IV.2.21):

$$(IV.3.7) \quad [\rho_\hbar(s, x, y)f](x', y') = e^{2\pi i \hbar (-s - \frac{1}{2} \omega(x, y; x' y'))} f(x' - x, y' - y).$$

The Fourier transform maps this representation to the *Fock–Segal–Bargmann (FSB) representation* (IV.3.20), see Exercise IV.3.5.

- ii. For $H = H_\chi$ the map $r(s, x, y) = (0, x, 0)$. For the character $\chi(0, x, 0) = e^{2\pi i \hbar x}$, the representation \mathbb{H}^1 on $L_2(\mathbb{R}^2)$ is, cf. (IV.2.22):

$$(IV.3.8) \quad [\rho_\hbar(s, x, y)f](s', y') = e^{-2\pi i \hbar x} f(s' - s - xy' + \frac{1}{2}xy, y' - y).$$

iii. For $H = H'_x = \{(s, 0, y) \in \mathbb{H}^1\}$ the map $r : \mathbb{H}^1 \rightarrow H'_x$ is $r(s, x, y) = (s - \frac{1}{2}xy, 0, y)$. For the character $\chi_h(s, 0, y) = e^{2\pi i(\hbar s + qy)}$, the representation of \mathbb{H}^1 on $L_2(\mathbb{R}^1)$ is, cf. (IV.2.24):

$$(IV.3.9) \quad [\rho_h(s, x, y)f](x') = \exp(2\pi i(\hbar(-s + yx' - \frac{1}{2}xy) - qy)) f(x' - x).$$

For $q = 0$, this is a key to the *Schrödinger representation* of the Heisenberg group, which is obtained by the Fourier transform.

We will see below that all these (and many others) representations with the same value \hbar are unitary equivalent.

IV.3.3. Co-adjoint Representation and Method of Orbits

Let \mathfrak{h}_1^* be the dual space to \mathfrak{h}_1 , that is the space of all linear functional on $\mathfrak{h}_1 \sim \mathbb{R}^3$. For physical reasons, we use letter (h, q, p) to denote bi-orthonormal coordinates to the exponential ones (s, x, y) on \mathfrak{h}^n .

The inner automorphism from the Exercise IV.2.11.i map the unit $(0, 0, 0)$ of \mathbb{H}^1 to itself. Thus inner automorphisms generate a transformation of the tangent space at $(0, 0, 0)$ to itself, which is a linear map given by the same formula (IV.2.16).

EXERCISE IV.3.4. Check that the adjoint of the linear transformation (IV.2.16) is:

$$(IV.3.10) \quad \text{ad}^*(s, x, y) : (h, q, p) \mapsto (h, q + hy, p - hx),$$

where $(s, x, y) \in \mathbb{H}^n$.

The above map is called the *co-adjoint representation* [159, § 15.1] $\text{Ad}^* : \mathfrak{h}_n^* \rightarrow \mathfrak{h}_n^*$ of \mathbb{H}^n . There are two types of orbits in (IV.3.10) for Ad^* , i.e. Euclidean spaces \mathbb{R}^{2n} and single points:

$$(IV.3.11) \quad \mathcal{O}_h = \{(h, q, p) : \text{for a fixed } h \neq 0, (q, p) \in \mathbb{R}^{2n}\},$$

$$(IV.3.12) \quad \mathcal{O}_{(q,p)} = \{(0, q, p) : \text{for a fixed } (q, p) \in \mathbb{R}^{2n}\}.$$

All complex representations are *induced* [159, § 13] by a character $\chi_h(s, 0, 0) = e^{ihs}$ of the centre of \mathbb{H}^n generated by $(h, 0, 0) \in \mathfrak{h}_n^*$ and shifts (IV.3.10) from the *left* on orbits (IV.3.11). The explicit formula respecting *physical units* [181] is:

$$(IV.3.13) \quad \rho_\chi(s, x, y) : f_h(q, p) \mapsto e^{-i(\hbar s + qx + py)} f_h(q - \frac{\hbar}{2}y, p + \frac{\hbar}{2}x).$$

This is the Fock–Segal–Bargmann (FSB) type representation

EXERCISE IV.3.5. Check that the Fourier transform

$$\hat{f}(q, p) = \int_{\mathbb{R}^2} f(x', y') e^{-\hbar(x'p + y'q)} dx' dy'$$

intertwines representations (IV.3.7) and (IV.3.20).

The Stone–von Neumann Theorem IV.3.6 describes all unitary irreducible representations of \mathbb{H}^n parametrised up to equivalence by two classes of orbits (IV.3.11) and (IV.3.12):

- The infinite dimensional representations by transformation ρ_χ (IV.3.20) for $h \neq 0$ in Fock [104, 139] space $F_2(\mathcal{O}_h) \subset L_2(\mathcal{O}_h)$ of null solutions of Cauchy–Riemann type operators [181].

- The one-dimensional representations as multiplication by a constant on $\mathbb{C} = L_2(\mathcal{O}_{(q,p)})$ which drops out from (IV.3.20) for $\hbar = 0$:

$$(IV.3.14) \quad \rho_{(q,p)}(s, x, y) : c \mapsto e^{-i(qx+py)}c.$$

IV.3.4. Stone–von Neumann Theorem

The following result [159, § 18.4], [104, Chap. 1, § 5] reduces

THEOREM IV.3.6 (The Stone–von Neumann). *Let ρ be a unitary representation of \mathbb{H}^n on a Hilbert space H , such that $\rho(s, 0, 0) = e^{2i\hbar s}I$ for a non-zero real \hbar . Then $H = \bigoplus H_\alpha$ where the H_α 's are mutually orthogonal subspaces of H , each invariant under ρ , such that the restriction $\rho|_{H_\alpha}$ is unitary equivalent to ρ_\hbar for each α . In particular, if ρ is irreducible then ρ is equivalent to ρ_\hbar .*

PROOF. □

IV.3.5. Shale–Weil Representation

The Shale–Weil theorem [104, § 4.2; 138, p. 830] states that any representation ρ_\hbar of the Heisenberg groups generates a unitary oscillator (or metaplectic) representation ρ_\hbar^{SW} of the $\widetilde{Sp}(2)$, the two-fold cover of the symplectic group [104, Thm. 4.58]. The Shale–Weil theorem allows us also to expand any representation ρ_\hbar of the Heisenberg group to the representation $\rho_\hbar^2 = \rho_\hbar \oplus \rho_\hbar^{SW}$ of the group Schrödinger group G .

Of course, there is the derived form of the Shale–Weil representation for \mathfrak{g} . It can often be explicitly written in contrast to the Shale–Weil representation.

EXAMPLE IV.3.7. Let ρ_\hbar be the Schrödinger representation [104, § 1.3] of \mathbb{H}^1 in $L_2(\mathbb{R})$, that is [199, (3.5)]:

$$[\rho_\chi(s, x, y)f](q) = e^{2\pi i\hbar(s-x y/2)+2\pi i x q} f(q - \hbar y).$$

Thus the action of the derived representation on the Lie algebra \mathfrak{h}_1 is:

$$(IV.3.15) \quad \rho_\hbar(X) = 2\pi i q, \quad \rho_\hbar(Y) = -\hbar \frac{d}{dq}, \quad \rho_\hbar(S) = 2\pi i \hbar I.$$

Then the associated Shale–Weil representation of $Sp(2)$ in $L_2(\mathbb{R})$ has the derived action, cf. [104, § 4.3; 322, (2.2)]:

(IV.3.16)

$$\rho_\hbar^{SW}(A) = -\frac{q}{2} \frac{d}{dq} - \frac{1}{4}, \quad \rho_\hbar^{SW}(B) = -\frac{\hbar i}{8\pi} \frac{d^2}{dq^2} - \frac{\pi i q^2}{2\hbar}, \quad \rho_\hbar^{SW}(Z) = \frac{\hbar i}{4\pi} \frac{d^2}{dq^2} - \frac{\pi i q^2}{\hbar}.$$

We can verify commutators (IV.2.12) and (II.3.14), (IV.2.19) for operators (IV.3.15–IV.3.16). It is also obvious that in this representation the following algebraic relations hold:

$$(IV.3.17) \quad \begin{aligned} \rho_{\hbar}^{\text{SW}}(A) &= \frac{i}{4\pi\hbar} (\rho_{\hbar}(X)\rho_{\hbar}(Y) - \frac{1}{2}\rho_{\hbar}(S)) \\ &= \frac{i}{8\pi\hbar} (\rho_{\hbar}(X)\rho_{\hbar}(Y) + \rho_{\hbar}(Y)\rho_{\hbar}(X)), \end{aligned}$$

$$(IV.3.18) \quad \rho_{\hbar}^{\text{SW}}(B) = \frac{i}{8\pi\hbar} (\rho_{\hbar}(X)^2 - \rho_{\hbar}(Y)^2),$$

$$(IV.3.19) \quad \rho_{\hbar}^{\text{SW}}(Z) = \frac{i}{4\pi\hbar} (\rho_{\hbar}(X)^2 + \rho_{\hbar}(Y)^2).$$

Thus it is common in quantum optics to name \mathfrak{g} as a Lie algebra with quadratic generators, see [109, § 2.2.4].

Note that $\rho_{\hbar}^{\text{SW}}(Z)$ is the Hamiltonian of the harmonic oscillator (up to a factor). Then we can consider $\rho_{\hbar}^{\text{SW}}(B)$ as the Hamiltonian of a repulsive (hyperbolic) oscillator. The operator $\rho_{\hbar}^{\text{SW}}(B - Z/2) = \frac{\hbar i}{4\pi} \frac{d^2}{dq^2}$ is the parabolic analog. A graphical representation of all three transformations defined by those Hamiltonian is given in Fig. II.3.1 and a further discussion of these Hamiltonians can be found in [338, § 3.8].

An important observation, which is often missed, is that the three linear symplectic transformations are unitary rotations in the corresponding hypercomplex algebra, cf. [194, § 3]. This means, that the symplectomorphisms generated by operators $Z, B - Z/2, B$ within time t coincide with the multiplication of hypercomplex number $q + ip$ by e^{it} , see Section II.3.1 and Fig. II.3.1, which is just another illustration of the Similarity and Correspondence Principle II.3.5.

EXAMPLE IV.3.8. There are many advantages of considering representations of the Heisenberg group on the phase space [74; 104, § 1.6; 139, § 1.7]. A convenient expression for Fock–Segal–Bargmann (FSB) representation on the phase space is, cf. § IV.4.2.1 and [74, (1); 181, (2.9)]:

$$(IV.3.20) \quad [\rho_{\mathbb{F}}(s, x, y)f](q, p) = e^{-2\pi i(\hbar s + qx + py)} f\left(q - \frac{\hbar}{2}y, p + \frac{\hbar}{2}x\right).$$

Then the derived representation of \mathfrak{h}_1 is:

$$(IV.3.21) \quad \rho_{\mathbb{F}}(X) = -2\pi i q + \frac{\hbar}{2} \partial_p, \quad \rho_{\mathbb{F}}(Y) = -2\pi i p - \frac{\hbar}{2} \partial_q, \quad \rho_{\mathbb{F}}(S) = -2\pi i \hbar I.$$

This produces the derived form of the Shale–Weil representation:

$$(IV.3.22) \quad \rho_{\mathbb{F}}^{\text{SW}}(A) = \frac{1}{2} (q \partial_q - p \partial_p), \quad \rho_{\mathbb{F}}^{\text{SW}}(B) = -\frac{1}{2} (p \partial_q + q \partial_p), \quad \rho_{\mathbb{F}}^{\text{SW}}(Z) = p \partial_q - q \partial_p.$$

Note that this representation does not contain the parameter \hbar unlike the equivalent representation (IV.3.16). Thus the FSB model explicitly shows the equivalence of $\rho_{\hbar_1}^{\text{SW}}$ and $\rho_{\hbar_2}^{\text{SW}}$ if $\hbar_1 \hbar_2 > 0$ [104, Thm. 4.57].

As we will also see below the FSB-type representations in hypercomplex numbers produce almost the same Shale–Weil representations.

Harmonic Oscillator and Ladder Operators

Complex valued representations of the Heisenberg group (also known as Weyl or Heisenberg-Weyl group) provide a natural framework for quantum mechanics [104, 139]. This is the most fundamental example of the Kirillov orbit method, induced representations and geometrical quantisation technique [160, 161]. Following the presentation in Section II.3 we will consider representations of the Heisenberg group which are induced by hypercomplex characters of its centre: complex (which correspond to the elliptic case), dual (parabolic) and double (hyperbolic).

To describe dynamics of a physical system we use a universal equation based on inner derivations (commutator) of the convolution algebra [177, 181]. The complex valued representations produce the standard framework for quantum mechanics with the Heisenberg dynamical equation [336].

The double number valued representations, with the hyperbolic unit $j^2 = 1$, is a natural source of hyperbolic quantum mechanics developed for a while [142, 143, 151, 154, 155]. The universal dynamical equation employs hyperbolic commutator in this case. This can be seen as a *Moyal bracket* based on the hyperbolic sine function. The hyperbolic observables act as operators on a Krein space with an indefinite inner product. Such spaces are employed in study of \mathcal{PT} -symmetric Hamiltonians and hyperbolic unit $j^2 = 1$ naturally appear in this setup [121].

The representations with values in dual numbers provide a convenient description of the classical mechanics. For this we do not take any sort of semiclassical limit, rather the nilpotency of the parabolic unit ($\varepsilon^2 = 0$) do the task. This removes the vicious necessity to consider the Planck *constant* tending to zero. The dynamical equation takes the Hamiltonian form. We also describe classical non-commutative representations of the Heisenberg group which acts in the first jet space.

REMARK IV.4.1. It is worth to note that our technique is different from contraction technique in the theory of Lie groups [119, 242]. Indeed a contraction of the Heisenberg group \mathbb{H}^n is the commutative Euclidean group \mathbb{R}^{2n} which does not recreate neither quantum nor classical mechanics.

The approach provides not only three different types of dynamics, it also generates the respective rules for addition of probabilities as well. For example, the quantum interference is the consequence of the same complex-valued structure, which directs the Heisenberg equation. The absence of an interference (a particle behaviour) in the classical mechanics is again the consequence the nilpotency of the parabolic unit. Double

numbers creates the hyperbolic law of additions of probabilities, which was extensively investigated [151, 154]. There are still unresolved issues with positivity of the probabilistic interpretation in the hyperbolic case [142, 143].

REMARK IV.4.2. It is commonly accepted since the Dirac's paper [81] that the striking (or even *the only*) difference between quantum and classical mechanics is non-commutativity of observables in the first case. In particular the Heisenberg commutation relations (IV.2.12) imply the uncertainty principle, the Heisenberg equation of motion and other quantum features. However, the entire book of Feynman on QED [97] does not contain any reference to non-commutativity. Moreover, our work shows that there is a non-commutative formulation of classical mechanics. Non-commutative representations of the Heisenberg group in dual numbers implies the Poisson dynamical equation and local addition of probabilities in Section IV.4.5, which are completely classical.

This entirely dispels any illusive correlation between classical/quantum and commutative/commutative. Instead we show that quantum mechanics is fully determined by the properties of complex numbers. In Feynman's exposition [97] complex numbers are presented by a clock, rotations of its arm encode multiplications by unimodular complex numbers. Moreover, there is no presentation of quantum mechanics, which does not employ complex phases (numbers) in one or another form. Analogous parabolic and hyperbolic phases (or characters produced by associated hypercomplex numbers, see Section II.3.1) lead to classical and hypercomplex mechanics respectively.

This section clarifies foundations of quantum and classical mechanics. We recovered the existence of three non-isomorphic models of mechanics from the representation theory. They were already derived in [142, 143] from translation invariant formulation, that is from the group theory as well. It also hinted that hyperbolic counterpart is (at least theoretically) as natural as classical and quantum mechanics are. The approach provides a framework for a description of aggregate system which have say both quantum and classical components. This can be used to model quantum computers with classical terminals [189].

Remarkably, simultaneously with the work [142] group-invariant axiomatics of geometry led R.I. Pimenov [284] to description of 3^n Cayley–Klein constructions. The connection between group-invariant geometry and respective mechanics were explored in many works of N.A. Gromov, see for example [115, 116, 119]. They already highlighted the rôle of three types of hypercomplex units for the realisation of elliptic, parabolic and hyperbolic geometry and kinematic.

There is a further connection between representations of the Heisenberg group and hypercomplex numbers. The symplectomorphism of phase space are also automorphism of the Heisenberg group [104, § 1.2]. We recall that the symplectic group $\text{Sp}(2)$ [104, § 1.2] is isomorphic to the group $\text{SL}_2(\mathbb{R})$ [140, 240, 251] and provides linear symplectomorphisms of the two-dimensional phase space. It has three types of non-isomorphic one-dimensional continuous subgroups (I.3.8–I.3.10) with symplectic action on the phase space illustrated by Fig. II.3.1. Hamiltonians, which produce those

symplectomorphism, are of interest [322; 323; 338, § 3.8]. An analysis of those Hamiltonians from Section II.3.3 by means of ladder operators recreates hypercomplex coefficients as well [196].

Harmonic oscillators, which we shall use as the main illustration here, are treated in most textbooks on quantum mechanics. This is efficiently done through creation/annihilation (ladder) operators, cf. § II.3.3 and [48, 109]. The underlying structure is the representation theory of the Heisenberg and symplectic groups [104; 139; 240, § VI.2; 321, § 8.2]. As we will see, they are naturally connected with respective hypercomplex numbers. As a result we obtain further illustrations to the Similarity and Correspondence Principle II.3.5.

We work with the simplest case of a particle with only one degree of freedom. Higher dimensions and the respective group of symplectomorphisms $\text{Sp}(2n)$ may require consideration of Clifford algebras [66, 69, 121, 166, 289].

IV.4.1. p-Mechanic Formalism

Here we briefly outline a formalism [53, 169, 177, 181, 294], which allows to unify quantum and classical mechanics.

IV.4.1.1. Convolutions (Observables) on \mathbb{H}^n and Commutator. Using an invariant measure $dg = ds dx dy$ on \mathbb{H}^n we can define the convolution of two functions:

$$(IV.4.1) \quad (k_1 * k_2)(g) = \int_{\mathbb{H}^n} k_1(g_1) k_2(g_1^{-1}g) dg_1.$$

This is a non-commutative operation, which is meaningful for functions from various spaces including $L_1(\mathbb{H}^n, dg)$, the Schwartz space S and many classes of distributions, which form algebras under convolutions. Convolutions on \mathbb{H}^n are used as *observables* in p-mechanic [169, 181].

A unitary representation ρ of \mathbb{H}^n extends to $L_1(\mathbb{H}^n, dg)$ by the formula:

$$(IV.4.2) \quad \rho(k) = \int_{\mathbb{H}^n} k(g)\rho(g) dg.$$

This is also an algebra homomorphism of convolutions to linear operators.

For a dynamics of observables we need inner *derivations* D_k of the convolution algebra $L_1(\mathbb{H}^n)$, which are given by the *commutator*:

$$(IV.4.3) \quad \begin{aligned} D_k : f \mapsto [k, f] &= k * f - f * k \\ &= \int_{\mathbb{H}^n} k(g_1) (f(g_1^{-1}g) - f(gg_1^{-1})) dg_1, \quad f, k \in L_1(\mathbb{H}^n). \end{aligned}$$

To describe dynamics of a time-dependent observable $f(t, g)$ we use the universal equation, cf. [167, 169]:

$$(IV.4.4) \quad S\dot{f} = [H, f],$$

where S is the left-invariant vector field (IV.2.11) generated by the centre of \mathbb{H}^n . The presence of operator S fixes the dimensionality of both sides of the equation (IV.4.4) if the observable H (Hamiltonian) has the dimensionality of energy [181, Rem 4.1]. If

we apply a right inverse \mathcal{A} of S to both sides of the equation (IV.4.4) we obtain the equivalent equation

$$(IV.4.5) \quad \dot{f} = \llbracket H, f \rrbracket,$$

based on the universal bracket $\llbracket k_1, k_2 \rrbracket = k_1 * \mathcal{A}k_2 - k_2 * \mathcal{A}k_1$ [181].

EXAMPLE IV.4.3 (Harmonic oscillator). Let $H = \frac{1}{2}(mk^2q^2 + \frac{1}{m}p^2)$ be the Hamiltonian of a one-dimensional harmonic oscillator, where k is a constant frequency and m is a constant mass. Its p -mechanisation will be the second order differential operator on \mathbb{H}^n [53, § 5.1]:

$$H = \frac{1}{2}(mk^2X^2 + \frac{1}{m}Y^2),$$

where we dropped sub-indexes of vector fields (IV.2.11) in one dimensional setting. We can express the commutator as a difference between the left and the right action of the vector fields:

$$\llbracket H, f \rrbracket = \frac{1}{2}(mk^2((X^r)^2 - (X^l)^2) + \frac{1}{m}((Y^r)^2 - (Y^l)^2))f.$$

Thus the equation (IV.4.4) becomes [53, (5.2)]:

$$(IV.4.6) \quad \frac{\partial}{\partial s} \dot{f} = \frac{\partial}{\partial s} \left(mk^2y \frac{\partial}{\partial x} - \frac{1}{m}x \frac{\partial}{\partial y} \right) f.$$

Of course, the derivative $\frac{\partial}{\partial s}$ can be dropped from both sides of the equation and the general solution is found to be:

$$(IV.4.7) \quad f(t; s, x, y) = f_0 \left(s, x \cos(kt) + mky \sin(kt), -\frac{x}{mk} \sin(kt) + y \cos(kt) \right),$$

where $f_0(s, x, y)$ is the initial value of an observable on \mathbb{H}^n .

EXAMPLE IV.4.4 (Unharmonic oscillator). We consider unharmonic oscillator with cubic potential, see [55] and references therein:

$$(IV.4.8) \quad H = \frac{mk^2}{2}q^2 + \frac{\lambda}{6}q^3 + \frac{1}{2m}p^2.$$

Due to the absence of non-commutative products p -mechanisation is straightforward:

$$H = \frac{mk^2}{2}X^2 + \frac{\lambda}{6}X^3 + \frac{1}{m}Y^2.$$

Similarly to the harmonic case the dynamic equation, after cancellation of $\frac{\partial}{\partial s}$ on both sides, becomes:

$$(IV.4.9) \quad \dot{f} = \left(mk^2y \frac{\partial}{\partial x} + \frac{\lambda}{6} \left(3y \frac{\partial^2}{\partial x^2} + \frac{1}{4}y^3 \frac{\partial^2}{\partial s^2} \right) - \frac{1}{m}x \frac{\partial}{\partial y} \right) f.$$

Unfortunately, it cannot be solved analytically as easy as in the harmonic case.

IV.4.1.2. States and Probability. Let an observable $\rho(k)$ (IV.4.2) is defined by a kernel $k(g)$ on the Heisenberg group and its representation ρ at a Hilbert space \mathcal{H} . A state on the convolution algebra is given by a vector $v \in \mathcal{H}$. A simple calculation:

$$\begin{aligned} \langle \rho(k)v, v \rangle_{\mathcal{H}} &= \left\langle \int_{\mathbb{H}^n} k(g)\rho(g)v \, dg, v \right\rangle_{\mathcal{H}} \\ &= \int_{\mathbb{H}^n} k(g) \langle \rho(g)v, v \rangle_{\mathcal{H}} \, dg \\ &= \int_{\mathbb{H}^n} k(g) \overline{\langle v, \rho(g)v \rangle_{\mathcal{H}}} \, dg \end{aligned}$$

can be restated as:

$$\langle \rho(k)v, v \rangle_{\mathcal{H}} = \langle k, l \rangle, \quad \text{where } l(g) = \langle v, \rho(g)v \rangle_{\mathcal{H}}.$$

Here the left-hand side contains the inner product on \mathcal{H} , while the right-hand side uses a skew-linear pairing between functions on \mathbb{H}^n based on the Haar measure integration. In other words we obtain, cf. [53, Thm. 3.11]:

PROPOSITION IV.4.5. *A state defined by a vector $v \in \mathcal{H}$ coincides with the linear functional given by the wavelet transform*

$$(IV.4.10) \quad l(g) = \langle v, \rho(g)v \rangle_{\mathcal{H}}$$

of v used as the mother wavelet as well.

The addition of vectors in \mathcal{H} implies the following operation on states:

$$(IV.4.11) \quad \begin{aligned} \langle v_1 + v_2, \rho(g)(v_1 + v_2) \rangle_{\mathcal{H}} &= \langle v_1, \rho(g)v_1 \rangle_{\mathcal{H}} + \langle v_2, \rho(g)v_2 \rangle_{\mathcal{H}} \\ &\quad + \langle v_1, \rho(g)v_2 \rangle_{\mathcal{H}} + \overline{\langle v_1, \rho(g^{-1})v_2 \rangle_{\mathcal{H}}} \end{aligned}$$

The last expression can be conveniently rewritten for kernels of the functional as

$$(IV.4.12) \quad l_{12} = l_1 + l_2 + 2A\sqrt{l_1 l_2}$$

for some real number A . This formula is behind the contextual law of addition of conditional probabilities [153] and will be illustrated below. Its physical interpretation is an interference, say, from two slits. Despite of a common belief, the mechanism of such interference can be both causal and local, see [152, 179].

IV.4.2. Elliptic characters and Quantum Dynamics

In this section we consider the representation ρ_h of \mathbb{H}^n induced by the elliptic character $\chi_h(s) = e^{ihs}$ in complex numbers parametrised by $h \in \mathbb{R}$. We also use the convenient agreement $h = 2\pi\hbar$ borrowed from physical literature.

IV.4.2.1. Fock–Segal–Bargmann and Schrödinger Representations. The realisation of ρ_h by the left shifts (IV.3.1) on $L_2^h(\mathbb{H}^n)$ is rarely used in quantum mechanics. Instead two unitary equivalent forms are more common: the Schrödinger and Fock–Segal–Bargmann (FSB) representations.

The FSB representation can be obtained from the FSB orbit method of Kirillov [160]. It allows spatially separate irreducible components of the left regular representation,

each of them become located on the orbit of the co-adjoint representation, see [160; 181, § 2.1] for details, we only present a brief summary here.

We identify \mathbb{H}^n and its Lie algebra \mathfrak{h}_n through the exponential map [159, § 6.4]. The dual \mathfrak{h}_n^* of \mathfrak{h}_n is presented by the Euclidean space \mathbb{R}^{2n+1} with coordinates (\hbar, q, p) . The pairing \mathfrak{h}_n^* and \mathfrak{h}_n given by

$$\langle (s, x, y), (\hbar, q, p) \rangle = \hbar s + q \cdot x + p \cdot y.$$

This pairing defines the Fourier transform $\hat{\cdot} : L_2(\mathbb{H}^n) \rightarrow L_2(\mathfrak{h}_n^*)$ given by [161, § 2.3]:

$$(IV.4.13) \quad \hat{\phi}(F) = \int_{\mathfrak{h}_n} \phi(\exp X) e^{-2\pi i \langle X, F \rangle} dX \quad \text{where } X \in \mathfrak{h}^n, F \in \mathfrak{h}_n^*.$$

For a fixed \hbar the left regular representation (IV.3.1) is mapped by the Fourier transform to the FSB type representation (IV.3.20). The collection of points $(\hbar, q, p) \in \mathfrak{h}_n^*$ for a fixed \hbar is naturally identified with the *phase space* of the system.

REMARK IV.4.6. It is possible to identify the case of $\hbar = 0$ with classical mechanics [181]. Indeed, a substitution of the zero value of \hbar into (IV.3.20) produces the commutative representation:

$$(IV.4.14) \quad \rho_0(s, x, y) : f(q, p) \mapsto e^{-2\pi i (qx + py)} f(q, p).$$

It can be decomposed into the direct integral of one-dimensional representations parametrised by the points (q, p) of the phase space. The classical mechanics, including the Hamilton equation, can be recovered from those representations [181]. However the condition $\hbar = 0$ (as well as the *semiclassical limit* $\hbar \rightarrow 0$) is not completely physical. Commutativity (and subsequent relative triviality) of those representation is the main reason why they are often neglected. The commutativity can be outweighed by special arrangements, e.g. an antiderivative [181, (4.1)], but the procedure is not straightforward, see discussion in [1, 184, 188]. A direct approach using dual numbers will be shown below, cf. Rem. IV.4.18.

To recover the Schrödinger representation we use notations and technique of induced representations from § II.3.2, see also [173, Ex. 4.1]. The subgroup $H = \{(s, 0, y) \mid s \in \mathbb{R}, y \in \mathbb{R}^n\} \subset \mathbb{H}^n$ defines the homogeneous space $X = G/H$, which coincides with \mathbb{R}^n as a manifold. The natural projection $\mathbf{p} : G \rightarrow X$ is $\mathbf{p}(s, x, y) = x$ and its left inverse $\mathbf{s} : X \rightarrow G$ can be as simple as $\mathbf{s}(x) = (0, x, 0)$. For the map $\mathbf{r} : G \rightarrow H$, $\mathbf{r}(s, x, y) = (s - xy/2, 0, y)$ we have the decomposition

$$(s, x, y) = \mathbf{s}(\mathbf{p}(s, x, y)) * \mathbf{r}(s, x, y) = (0, x, 0) * (s - \frac{1}{2}xy, 0, y).$$

For a character $\chi_h(s, 0, y) = e^{ihs}$ of H the lifting $\mathcal{L}_\chi : L_2(G/H) \rightarrow L_2^X(G)$ is as follows:

$$[\mathcal{L}_\chi f](s, x, y) = \chi_h(\mathbf{r}(s, x, y)) f(\mathbf{p}(s, x, y)) = e^{ih(s - xy/2)} f(x).$$

Thus the representation $\rho_\chi(g) = \mathcal{P} \circ \Lambda(g) \circ \mathcal{L}$ becomes:

$$(IV.4.15) \quad [\rho_\chi(s', x', y') f](x) = e^{-2\pi i \hbar (s' + x y' - x' y' / 2)} f(x - x').$$

After the Fourier transform $x \mapsto q$ we get the Schrödinger representation on the *configuration space*:

$$(IV.4.16) \quad [\rho_\chi(s', x', y') \hat{f}](q) = e^{-2\pi i \hbar (s' + x' y' / 2) - 2\pi i x' q} \hat{f}(q + \hbar y').$$

Note that this again turns into a commutative representation (multiplication by an unimodular function) if $\hbar = 0$. To get the full set of commutative representations in this way we need to use the character $\chi_{(\hbar, p)}(s, 0, y) = e^{2\pi i(\hbar + py)}$ in the above consideration.

IV.4.2.2. Commutator and the Heisenberg Equation. The property (IV.3.2) of $F_2^X(\mathbb{H}^n)$ implies that the restrictions of two operators $\rho_\chi(k_1)$ and $\rho_\chi(k_2)$ to this space are equal if

$$\int_{\mathbb{R}} k_1(s, x, y) \chi(s) ds = \int_{\mathbb{R}} k_2(s, x, y) \chi(s) ds.$$

In other words, for a character $\chi(s) = e^{2\pi i \hbar s}$ the operator $\rho_\chi(k)$ depends only on

$$\hat{k}_s(\hbar, x, y) = \int_{\mathbb{R}} k(s, x, y) e^{-2\pi i \hbar s} ds,$$

which is the partial Fourier transform $s \mapsto \hbar$ of $k(s, x, y)$. The restriction to $F_2^X(\mathbb{H}^n)$ of the composition formula for convolutions is [181, (3.5)]:

$$(IV.4.17) \quad (k' * k)_s^\wedge = \int_{\mathbb{R}^{2n}} e^{i\hbar(xy' - yx')/2} \hat{k}'_s(\hbar, x', y') \hat{k}_s(\hbar, x - x', y - y') dx' dy'.$$

Under the Schrödinger representation (IV.4.16) the convolution (IV.4.17) defines a rule for composition of two pseudo-differential operators (PDO) in the Weyl calculus [104, § 2.3; 139].

Consequently the representation (IV.4.2) of commutator (IV.4.3) depends only on its partial Fourier transform [181, (3.6)]:

$$(IV.4.18) \quad [k', k]_s^\wedge = 2i \int_{\mathbb{R}^{2n}} \sin\left(\frac{\hbar}{2}(xy' - yx')\right) \times \hat{k}'_s(\hbar, x', y') \hat{k}_s(\hbar, x - x', y - y') dx' dy'.$$

Under the Fourier transform (IV.4.13) this commutator is exactly the *Moyal bracket* [341] for \hat{k}' and \hat{k} on the phase space.

For observables in the space $F_2^X(\mathbb{H}^n)$ the action of S is reduced to multiplication, e.g. for $\chi(s) = e^{i\hbar s}$ the action of S is multiplication by $i\hbar$. Thus the equation (IV.4.4) reduced to the space $F_2^X(\mathbb{H}^n)$ becomes the Heisenberg type equation [181, (4.4)]:

$$(IV.4.19) \quad \dot{f} = \frac{1}{i\hbar} [H, f]_s^\wedge,$$

based on the above bracket (IV.4.18). The Schrödinger representation (IV.4.16) transforms this equation to the original Heisenberg equation.

EXAMPLE IV.4.7. i. Under the Fourier transform $(x, y) \mapsto (q, p)$ the p -dynamic equation (IV.4.6) of the harmonic oscillator becomes:

$$(IV.4.20) \quad \dot{f} = \left(mk^2 q \frac{\partial}{\partial p} - \frac{1}{m} p \frac{\partial}{\partial q} \right) f.$$

The same transform creates its solution out of (IV.4.7).

ii. Since $\frac{\partial}{\partial s}$ acts on $F_2^X(\mathbb{H}^n)$ as multiplication by $i\hbar$, the quantum representation of unharmonic dynamics equation (IV.4.9) is:

$$(IV.4.21) \quad \dot{f} = \left(mk^2 q \frac{\partial}{\partial p} + \frac{\lambda}{6} \left(3q^2 \frac{\partial}{\partial p} - \frac{\hbar^2}{4} \frac{\partial^3}{\partial p^3} \right) - \frac{1}{m} p \frac{\partial}{\partial q} \right) f.$$

This is exactly the equation for the Wigner function obtained in [55, (30)].

IV.4.2.3. Quantum Probabilities. For the elliptic character $\chi_h(s) = e^{ihs}$ we can use the Cauchy–Schwarz inequality to demonstrate that the real number A in the identity (IV.4.12) is between -1 and 1 . Thus we can put $A = \cos \alpha$ for some angle (phase) α to get the formula for counting quantum probabilities, cf. [154, (2)]:

$$(IV.4.22) \quad l_{12} = l_1 + l_2 + 2 \cos \alpha \sqrt{l_1 l_2}$$

REMARK IV.4.8. It is interesting to note that the both trigonometric functions are employed in quantum mechanics: sine is in the heart of the Moyal bracket (IV.4.18) and cosine is responsible for the addition of probabilities (IV.4.22). In the essence the commutator and probabilities took respectively the odd and even parts of the elliptic character e^{ihs} .

EXAMPLE IV.4.9. Take a vector $v_{(a,b)} \in L_2^h(\mathbb{H}^n)$ defined by a Gaussian with mean value (a, b) in the phase space for a harmonic oscillator of the mass m and the frequency k :

$$(IV.4.23) \quad v_{(a,b)}(q, p) = \exp \left(-\frac{2\pi km}{\hbar} (q - a)^2 - \frac{2\pi}{\hbar km} (p - b)^2 \right).$$

A direct calculation shows:

$$\begin{aligned} \langle v_{(a,b)}, \rho_{\hbar}(s, x, y) v_{(a',b')} \rangle &= \frac{4}{\hbar} \exp \left(\pi i (2s\hbar + x(a + a') + y(b + b')) \right. \\ &\quad \left. - \frac{\pi}{2\hbar km} ((\hbar x + b - b')^2 + (b - b')^2) - \frac{\pi km}{2\hbar} ((\hbar y + a' - a)^2 + (a' - a)^2) \right) \\ &= \frac{4}{\hbar} \exp \left(\pi i (2s\hbar + x(a + a') + y(b + b')) \right. \\ &\quad \left. - \frac{\pi}{\hbar km} \left((b - b' + \frac{\hbar x}{2})^2 + (\frac{\hbar x}{2})^2 \right) - \frac{\pi km}{\hbar} \left((a - a' - \frac{\hbar y}{2})^2 + (\frac{\hbar y}{2})^2 \right) \right) \end{aligned}$$

Thus the kernel $l_{(a,b)} = \langle v_{(a,b)}, \rho_{\hbar}(s, x, y) v_{(a,b)} \rangle$ (IV.4.10) for a state $v_{(a,b)}$ is:

$$(IV.4.24) \quad l_{(a,b)} = \frac{4}{\hbar} \exp \left(2\pi i (s\hbar + xa + yb) - \frac{\pi\hbar}{2km} x^2 - \frac{\pi km\hbar}{2\hbar} y^2 \right)$$

An observable registering a particle at a point $q = c$ of the configuration space is $\delta(q - c)$. On the Heisenberg group this observable is given by the kernel:

$$(IV.4.25) \quad X_c(s, x, y) = e^{2\pi i (s\hbar + xc)} \delta(y).$$

The measurement of X_c on the state (IV.4.23) (through the kernel (IV.4.24)) predictably is:

$$\langle X_c, l_{(a,b)} \rangle = \sqrt{\frac{2km}{\hbar}} \exp \left(-\frac{2\pi km}{\hbar} (c - a)^2 \right).$$

EXAMPLE IV.4.10. Now take two states $v_{(0,b)}$ and $v_{(0,-b)}$, where for the simplicity we assume the mean values of coordinates vanish in the both cases. Then the corresponding kernel (IV.4.11) has the interference terms:

$$\begin{aligned} l_i &= \langle v_{(0,b)}, \rho_{\hbar}(s, x, y) v_{(0,-b)} \rangle \\ &= \frac{4}{\hbar} \exp \left(2\pi i s \hbar - \frac{\pi}{2\hbar k m} ((\hbar x + 2b)^2 + 4b^2) - \frac{\pi \hbar k m}{2} y^2 \right). \end{aligned}$$

The measurement of X_c (IV.4.25) on this term contains the oscillating part:

$$\langle X_c, l_i \rangle = \sqrt{\frac{2km}{\hbar}} \exp \left(-\frac{2\pi km}{\hbar} c^2 - \frac{2\pi}{km\hbar} b^2 + \frac{4\pi i}{\hbar} cb \right)$$

Therefore on the kernel l corresponding to the state $v_{(0,b)} + v_{(0,-b)}$ the measurement is

$$\langle X_c, l \rangle = 2\sqrt{\frac{2km}{\hbar}} \exp \left(-\frac{2\pi km}{\hbar} c^2 \right) \left(1 + \exp \left(-\frac{2\pi}{km\hbar} b^2 \right) \cos \left(\frac{4\pi}{\hbar} cb \right) \right).$$

The presence of the cosine term in the last expression can generate an interference

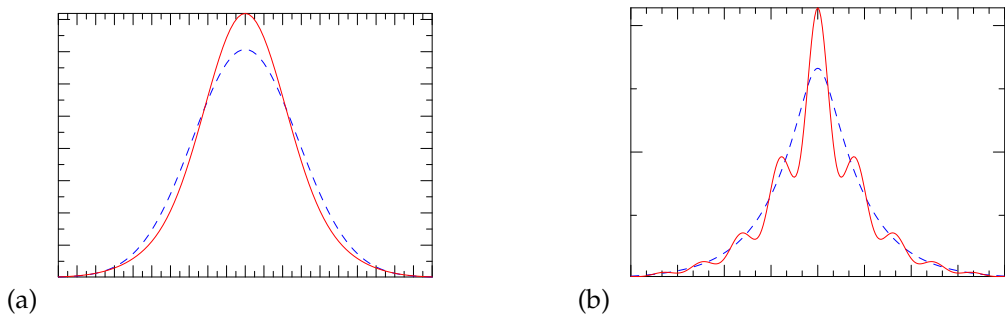


FIGURE IV.4.1. Quantum probabilities: the blue (dashed) graph shows the addition of probabilities without interaction, the red (solid) graph present the quantum interference. Left picture shows the Gaussian state (IV.4.23), the right—the rational state (IV.4.26)

picture. In practise it does not happen for the minimal uncertainty state (IV.4.23) which we are using here: it rapidly vanishes outside of the neighbourhood of zero, where oscillations of the cosine occurs, see Fig. IV.4.1(a).

EXAMPLE IV.4.11. To see a traditional interference pattern one can use a state which is far from the minimal uncertainty. For example, we can consider the state:

$$(IV.4.26) \quad u_{(a,b)}(q, p) = \frac{\hbar^2}{((q - a)^2 + \hbar/km)((p - b)^2 + \hbar km)}.$$

To evaluate the observable X_c (IV.4.25) on the state $l(g) = \langle u_1, \rho_{\hbar}(g) u_2 \rangle$ (IV.4.10) we use the following formula:

$$\langle X_c, l \rangle = \frac{2}{\hbar} \int_{\mathbb{R}^n} \hat{u}_1(q, 2(q - c)/\hbar) \overline{\hat{u}_2(q, 2(q - c)/\hbar)} dq,$$

where $\hat{u}_i(q, x)$ denotes the partial Fourier transform $p \mapsto x$ of $u_i(q, p)$. The formula is obtained by swapping order of integrations. The numerical evaluation of the state obtained by the addition $u_{(0,b)} + u_{(0,-b)}$ is plotted on Fig. IV.4.1(b), the red curve shows the canonical interference pattern.

IV.4.3. Ladder Operators and Harmonic Oscillator

Let ρ be a representation of the Schrödinger group $G = \mathbb{H}^1 \times \widetilde{\text{Sp}}(2)$ (IV.2.17) in a space V . Consider the derived representation of the Lie algebra \mathfrak{g} [240, § VI.1] and denote $\tilde{X} = \rho(X)$ for $X \in \mathfrak{g}$. To see the structure of the representation ρ we can decompose the space V into eigenspaces of the operator \tilde{X} for some $X \in \mathfrak{g}$. The canonical example is the Taylor series in complex analysis.

We are going to consider three cases corresponding to three non-isomorphic subgroups (I.3.8–I.3.10) of $\text{Sp}(2)$ starting from the compact case. Let $H = Z$ be a generator of the compact subgroup K . Corresponding symplectomorphisms (IV.2.4) of the phase space are given by orthogonal rotations with matrices $\begin{pmatrix} \cos t & \sin t \\ -\sin t & \cos t \end{pmatrix}$. The Shale–Weil representation (IV.3.16) coincides with the Hamiltonian of the harmonic oscillator in Schrödinger representation.

Since $\widetilde{\text{Sp}}(2)$ is a two-fold cover the corresponding eigenspaces of a compact group $\tilde{Z}v_k = ikv_k$ are parametrised by a half-integer $k \in \mathbb{Z}/2$. Explicitly for a half-integer k eigenvectors are:

$$(IV.4.27) \quad v_k(q) = H_{k+\frac{1}{2}} \left(\sqrt{\frac{2\pi}{\hbar}} q \right) e^{-\frac{\pi}{\hbar} q^2},$$

where H_k is the *Hermite polynomial* [93, 8.2(9); 104, § 1.7].

From the point of view of quantum mechanics as well as the representation theory it is beneficial to introduce the ladder operators L^\pm (II.3.15), known also as *creation/annihilation* in quantum mechanics [48; 104, p. 49]. There are two ways to search for ladder operators: in (complexified) Lie algebras \mathfrak{h}_1 and \mathfrak{sp}_2 . The later coincides with our consideration in Section II.3.3 in the essence.

IV.4.3.1. Ladder Operators from the Heisenberg Group. Assuming $L^+ = a\tilde{X} + b\tilde{Y}$ we obtain from the relations (IV.2.18–IV.2.19) and (II.3.15) the linear equations with unknown a and b :

$$a = \lambda_+ b, \quad -b = \lambda_+ a.$$

The equations have a solution if and only if $\lambda_+^2 + 1 = 0$, and the raising/lowering operators are $L^\pm = \tilde{X} \mp i\tilde{Y}$.

REMARK IV.4.12. Here we have an interesting asymmetric response: due to the structure of the semidirect product $\mathbb{H}^1 \times \widetilde{\text{Sp}}(2)$ it is the symplectic group which acts on \mathbb{H}^1 , not *vice versa*. However the Heisenberg group has a weak action in the opposite direction: it shifts eigenfunctions of $\text{Sp}(2)$.

In the Schrödinger representation (IV.3.15) the ladder operators are

$$(IV.4.28) \quad \rho_{\hbar}(L^{\pm}) = 2\pi i q \pm i\hbar \frac{d}{dq}.$$

The standard treatment of the harmonic oscillator in quantum mechanics, which can be found in many textbooks, e.g. [104, § 1.7; 109, § 2.2.3], is as follows. The vector $v_{-1/2}(q) = e^{-\pi q^2/\hbar}$ is an eigenvector of \tilde{Z} with the eigenvalue $-\frac{i}{2}$. In addition $v_{-1/2}$ is annihilated by L^+ . Thus the chain (II.3.16) terminates to the right and the complete set of eigenvectors of the harmonic oscillator Hamiltonian is presented by $(L^-)^k v_{-1/2}$ with $k = 0, 1, 2, \dots$

We can make a wavelet transform generated by the Heisenberg group with the mother wavelet $v_{-1/2}$, and the image will be the Fock–Segal–Bargmann (FSB) space [104, § 1.6; 139]. Since $v_{-1/2}$ is the null solution of $L^+ = \tilde{X} - i\tilde{Y}$, then by Cor. II.6.34 the image of the wavelet transform will be null-solutions of the corresponding linear combination of the Lie derivatives (IV.2.11):

$$(IV.4.29) \quad D = \overline{X^r} - i\overline{Y^r} = (\partial_x + i\partial_y) - \pi\hbar(x - iy),$$

which turns out to be the Cauchy–Riemann equation on a weighted FSB-type space, see Section IV.5.4 below.

IV.4.3.2. Symplectic Ladder Operators. We can also look for ladder operators within the Lie algebra \mathfrak{sp}_2 , see Subsection IV.4.3.1 and [194, § 8]. Assuming $L_2^+ = a\tilde{A} + b\tilde{B} + c\tilde{Z}$ from the relations (II.3.14) and defining condition (II.3.15) we obtain the linear equations with unknown a , b and c :

$$c = 0, \quad 2a = \lambda_+ b, \quad -2b = \lambda_+ a.$$

The equations have a solution if and only if $\lambda_+^2 + 4 = 0$, and the raising/lowering operators are $L_2^{\pm} = \pm i\tilde{A} + \tilde{B}$. In the Shale–Weil representation (IV.3.16) they turn out to be:

$$(IV.4.30) \quad L_2^{\pm} = \pm i \left(\frac{q}{2} \frac{d}{dq} + \frac{1}{4} \right) - \frac{\hbar i}{8\pi} \frac{d^2}{dq^2} - \frac{\pi i q^2}{2\hbar} = -\frac{i}{8\pi\hbar} \left(\mp 2\pi q + \hbar \frac{d}{dq} \right)^2.$$

Since this time $\lambda_+ = 2i$ the ladder operators L_2^{\pm} produce a shift on the diagram (II.3.16) twice bigger than the operators L^{\pm} from the Heisenberg group. After all, this is not surprising since from the explicit representations (IV.4.28) and (IV.4.30) we get:

$$L_2^{\pm} = -\frac{i}{8\pi\hbar} (L^{\pm})^2.$$

IV.4.4. Hyperbolic Quantum Mechanics

Now we turn to double numbers also known as hyperbolic, split-complex, etc. numbers [157; 325; 339, App. C]. They form a two dimensional algebra \mathbb{O} spanned by 1 and j with the property $j^2 = 1$. There are zero divisors:

$$j_{\pm} = \frac{1}{\sqrt{2}}(1 \pm j), \quad \text{such that} \quad j_+ j_- = 0 \quad \text{and} \quad j_{\pm}^2 = j_{\pm}.$$

Thus double numbers algebraically isomorphic to two copies of \mathbb{R} spanned by j_{\pm} . Being algebraically dull double numbers are nevertheless interesting as a homogeneous space [191, 194] and they are relevant in physics [151, 325, 326]. The combination of p-mechanical approach with hyperbolic quantum mechanics was already discussed in [53, § 6].

For the hyperbolic character $\chi_{jh}(s) = e^{jhs} = \cosh hs + j \sinh hs$ of \mathbb{R} one can define the hyperbolic Fourier-type transform:

$$\hat{k}(q) = \int_{\mathbb{R}} k(x) e^{-jqx} dx.$$

It can be understood in the sense of distributions on the space dual to the set of analytic functions [155, § 3]. Hyperbolic Fourier transform intertwines the derivative $\frac{d}{dx}$ and multiplication by jq [155, Prop. 1].

EXAMPLE IV.4.13. For the Gaussian the hyperbolic Fourier transform is the ordinary function (note the sign difference!):

$$\int_{\mathbb{R}} e^{-x^2/2} e^{-jqx} dx = \sqrt{2\pi} e^{q^2/2}.$$

However the opposite identity:

$$\int_{\mathbb{R}} e^{x^2/2} e^{-jqx} dx = \sqrt{2\pi} e^{-q^2/2}$$

is true only in a suitable distributional sense. To this end we may note that $e^{x^2/2}$ and $e^{-q^2/2}$ are null solutions to the differential operators $\frac{d}{dx} - x$ and $\frac{d}{dq} + q$ respectively, which are intertwined (up to the factor j) by the hyperbolic Fourier transform. The above differential operators $\frac{d}{dx} - x$ and $\frac{d}{dq} + q$ are images of the ladder operators (IV.4.28) in the Lie algebra of the Heisenberg group. They are intertwining by the Fourier transform, since this is an automorphism of the Heisenberg group [138].

An elegant theory of hyperbolic Fourier transform may be achieved by a suitable adaptation of [138], which uses representation theory of the Heisenberg group.

IV.4.4.1. Hyperbolic Representations of the Heisenberg Group. Consider the space $F_h^j(\mathbb{H}^n)$ of \mathbb{O} -valued functions on \mathbb{H}^n with the property:

$$(IV.4.31) \quad f(s + s', h, y) = e^{jhs'} f(s, x, y), \quad \text{for all } (s, x, y) \in \mathbb{H}^n, s' \in \mathbb{R},$$

and the square integrability condition (IV.3.3). Then the hyperbolic representation is obtained by the restriction of the left shifts to $F_h^j(\mathbb{H}^n)$. To obtain an equivalent representation on the phase space we take \mathbb{O} -valued functional of the Lie algebra \mathfrak{h}_n :

$$(IV.4.32) \quad \chi_{(h,q,p)}^j(s, x, y) = e^{j(hs + qx + py)} = \cosh(hs + qx + py) + j \sinh(hs + qx + py).$$

The hyperbolic Fock–Segal–Bargmann type representation is intertwined with the left group action by means of the Fourier transform (IV.4.13) with the hyperbolic functional (IV.4.32). Explicitly this representation is:

$$(IV.4.33) \quad \rho_h(s, x, y) : f(q, p) \mapsto e^{-j(hs + qx + py)} f\left(q - \frac{h}{2}y, p + \frac{h}{2}x\right).$$

For a hyperbolic Schrödinger type representation we again use the scheme described in § II.3.2. Similarly to the elliptic case one obtains the formula, resembling (IV.4.15):

$$(IV.4.34) \quad [\rho_{\chi}^j(s', x', y')f](x) = e^{-jh(s'+xy'-x'y'/2)}f(x-x').$$

Application of the hyperbolic Fourier transform produces a Schrödinger type representation on the configuration space, cf. (IV.4.16):

$$[\rho_{\chi}^j(s', x', y')\hat{f}](q) = e^{-jh(s'+x'y'/2)-jx'q}\hat{f}(q+hy').$$

The extension of this representation to kernels according to (IV.4.2) generates hyperbolic pseudodifferential operators introduced in [155, (3.4)].

IV.4.4.2. Hyperbolic Dynamics. Similarly to the elliptic (quantum) case we consider a convolution of two kernels on \mathbb{H}^n restricted to $F_h^j(\mathbb{H}^n)$. The composition law becomes, cf. (IV.4.17):

$$(IV.4.35) \quad (k' * k)_s^{\wedge} = \int_{\mathbb{R}^{2n}} e^{jh(xy'-yx')} \hat{k}'_s(h, x', y') \hat{k}_s(h, x-x', y-y') dx' dy'.$$

This is close to the calculus of hyperbolic PDO obtained in [155, Thm. 2]. Respectively for the commutator of two convolutions we get, cf. (IV.4.18):

$$(IV.4.36) \quad [k', k]_s^{\wedge} = \int_{\mathbb{R}^{2n}} \sinh(h(xy'-yx')) \hat{k}'_s(h, x', y') \hat{k}_s(h, x-x', y-y') dx' dy'.$$

This the hyperbolic version of the Moyal bracket, cf. [155, p. 849], which generates the corresponding image of the dynamic equation (IV.4.4).

- EXAMPLE IV.4.14. i. For a quadratic Hamiltonian, e.g. harmonic oscillator from Example IV.4.3, the hyperbolic equation and respective dynamics is identical to quantum considered before.
- ii. Since $\frac{\partial}{\partial s}$ acts on $F_2^j(\mathbb{H}^n)$ as multiplication by jh and $j^2 = 1$, the hyperbolic image of the unharmonic equation (IV.4.9) becomes:

$$\dot{f} = \left(mk^2q \frac{\partial}{\partial p} + \frac{\lambda}{6} \left(3q^2 \frac{\partial}{\partial p} + \frac{\hbar^2}{4} \frac{\partial^3}{\partial p^3} \right) - \frac{1}{m} p \frac{\partial}{\partial q} \right) f.$$

The difference with quantum mechanical equation (IV.4.21) is in the sign of the cubic derivative.

IV.4.4.3. Hyperbolic Probabilities. To calculate probability distribution generated by a hyperbolic state we are using the general procedure from Section IV.4.1.2. The main differences with the quantum case are as follows:

- i. The real number A in the expression (IV.4.12) for the addition of probabilities is bigger than 1 in absolute value. Thus it can be associated with the hyperbolic cosine $\cosh \alpha$, cf. Rem. IV.4.8, for certain phase $\alpha \in \mathbb{R}$ [155].
- ii. The nature of hyperbolic interference on two slits is affected by the fact that e^{jhs} is not periodic and the hyperbolic exponent e^{jt} and cosine $\cosh t$ do not oscillate. It is worth to notice that for Gaussian states the hyperbolic interference is exactly the same as quantum one, cf. Figs. IV.4.1(a) and IV.4.2(a). This

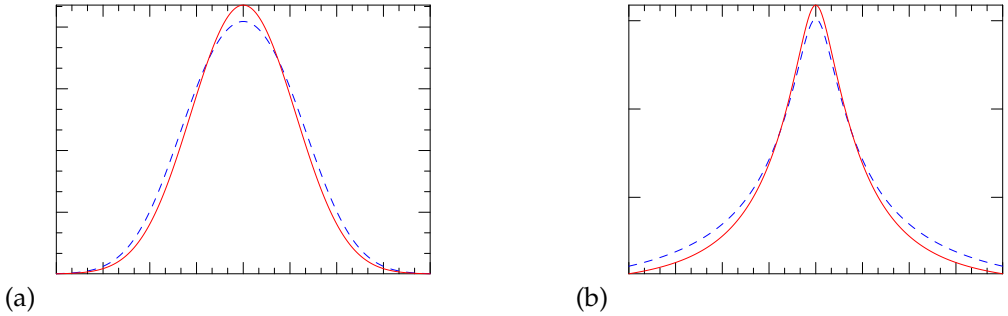


FIGURE IV.4.2. Hyperbolic probabilities: the blue (dashed) graph shows the addition of probabilities without interaction, the red (solid) graph present the quantum interference. Left picture shows the Gaussian state (IV.4.23), with the same distribution as in quantum mechanics, cf. Fig. IV.4.1(a). The right picture shows the rational state (IV.4.26), note the absence of interference oscillations in comparison with the quantum state on Fig. IV.4.1(b).

is similar to coincidence of quantum and hyperbolic dynamics of harmonic oscillator.

The contrast between two types of interference is prominent for the rational state (IV.4.26), which is far from the minimal uncertainty, see the different patterns on Figs. IV.4.1(b) and IV.4.2(b).

IV.4.4.4. Ladder Operators for the Hyperbolic Subgroup. Consider the case of the Hamiltonian $H = 2B$, which is a repulsive (hyperbolic) harmonic oscillator [338, § 3.8]. The corresponding one-dimensional subgroup of symplectomorphisms produces hyperbolic rotations of the phase space, see Fig. II.3.1. The eigenvectors v_μ of the operator

$$\rho_{\hbar}^{\text{SW}}(2B)v_\nu = -i \left(\frac{\hbar}{4\pi} \frac{d^2}{dq^2} + \frac{\pi q^2}{\hbar} \right) v_\nu = i\nu v_\nu,$$

are *Weber–Hermite* (or *parabolic cylinder*) functions $v_\nu = D_{\nu-\frac{1}{2}}(\pm 2e^{i\frac{\pi}{4}}\sqrt{\frac{\pi}{\hbar}}q)$, see [93, § 8.2; 312] for fundamentals of Weber–Hermite functions and [322] for further illustrations and applications in optics.

The corresponding one-parameter group is not compact and the eigenvalues of the operator $2\tilde{B}$ are not restricted by any integrality condition, but the raising/lowering operators are still important [140, § II.1; 251, § 1.1]. We again seek solutions in two subalgebras \mathfrak{h}_1 and \mathfrak{sp}_2 separately. However the additional options will be provided by a choice of the number system: either complex or double.

EXAMPLE IV.4.15 (Complex Ladder Operators). Assuming $L_{\hbar}^+ = a\tilde{X} + b\tilde{Y}$ from the commutators (IV.2.18–IV.2.19) we obtain the linear equations:

$$(IV.4.37) \quad -a = \lambda_+ b, \quad -b = \lambda_+ a.$$

The equations have a solution if and only if $\lambda_+^2 - 1 = 0$. Taking the real roots $\lambda = \pm 1$ we obtain that the raising/lowering operators are $L_{\hbar}^{\pm} = \tilde{X} \mp \tilde{Y}$. In the Schrödinger representation (IV.3.15) the ladder operators are

$$(IV.4.38) \quad L_{\hbar}^{\pm} = 2\pi i q \pm \hbar \frac{d}{dq}.$$

The null solutions $v_{\pm \frac{1}{2}}(q) = e^{\pm \frac{\pi i}{\hbar} q^2}$ to operators $\rho_{\hbar}(L^{\pm})$ are also eigenvectors of the Hamiltonian $\rho_{\hbar}^{SW}(2B)$ with the eigenvalue $\pm \frac{1}{2}$. However the important distinction from the elliptic case is, that they are not square-integrable on the real line anymore.

We can also look for ladder operators within the \mathfrak{sp}_2 , that is in the form $L_{2\hbar}^{\pm} = a\tilde{A} + b\tilde{B} + c\tilde{Z}$ for the commutator $[2\tilde{B}, L_{\hbar}^{\pm}] = \lambda L_{\hbar}^{\pm}$, see § ?? . Within complex numbers we get only the values $\lambda = \pm 2$ with the ladder operators $L_{2\hbar}^{\pm} = \pm 2\tilde{A} + \tilde{Z}/2$, see [140, § II.1; 251, § 1.1]. Each indecomposable \mathfrak{h}_1 - or \mathfrak{sp}_2 -module is formed by a one-dimensional chain of eigenvalues with a transitive action of ladder operators L_{\hbar}^{\pm} or $L_{2\hbar}^{\pm}$ respectively. And we again have a quadratic relation between the ladder operators:

$$L_{2\hbar}^{\pm} = \frac{i}{4\pi\hbar} (L_{\hbar}^{\pm})^2.$$

IV.4.4.5. Double Ladder Operators. There are extra possibilities in in the context of hyperbolic quantum mechanics [151, 154, 155]. Here we use the representation of \mathbb{H}^1 induced by a hyperbolic character $e^{jht} = \cosh(ht) + j \sinh(ht)$, see [199, (4.5)], and obtain the hyperbolic representation of \mathbb{H}^1 , cf. (IV.4.16):

$$(IV.4.39) \quad [\rho_{\hbar}^j(s', x', y')\hat{f}](q) = e^{jh(s' - x'y'/2) + jx'y'q} \hat{f}(q - hy').$$

The corresponding derived representation is

$$(IV.4.40) \quad \rho_{\hbar}^j(X) = jq, \quad \rho_{\hbar}^j(Y) = -\hbar \frac{d}{dq}, \quad \rho_{\hbar}^j(S) = j\hbar I.$$

Then the associated Shale–Weil derived representation of \mathfrak{sp}_2 in the Schwartz space $S(\mathbb{R})$ is, cf. (IV.3.16):

$$(IV.4.41) \quad \rho_{\hbar}^{SW}(A) = -\frac{q}{2} \frac{d}{dq} - \frac{1}{4}, \quad \rho_{\hbar}^{SW}(B) = \frac{j\hbar}{4} \frac{d^2}{dq^2} - \frac{jq^2}{4\hbar}, \quad \rho_{\hbar}^{SW}(Z) = -\frac{j\hbar}{2} \frac{d^2}{dq^2} - \frac{jq^2}{2\hbar}.$$

Note that $\rho_{\hbar}^{SW}(B)$ now generates a usual harmonic oscillator, not the repulsive one like $\rho_{\hbar}^{SW}(B)$ in (IV.3.16). However the expressions in the quadratic algebra are still the same (up to a factor), cf. (IV.3.17–IV.3.19):

$$(IV.4.42) \quad \begin{aligned} \rho_{\hbar}^{SW}(A) &= -\frac{j}{2\hbar} (\rho_{\hbar}^j(X)\rho_{\hbar}^j(Y) - \frac{1}{2}\rho_{\hbar}^j(S)) \\ &= -\frac{j}{4\hbar} (\rho_{\hbar}^j(X)\rho_{\hbar}^j(Y) + \rho_{\hbar}^j(Y)\rho_{\hbar}^j(X)), \end{aligned}$$

$$(IV.4.43) \quad \rho_{\hbar}^{SW}(B) = \frac{j}{4\hbar} (\rho_{\hbar}^j(X)^2 - \rho_{\hbar}^j(Y)^2),$$

$$(IV.4.44) \quad \rho_{\hbar}^{SW}(Z) = -\frac{j}{2\hbar} (\rho_{\hbar}^j(X)^2 + \rho_{\hbar}^j(Y)^2).$$

This is due to the Principle II.3.5 of similarity and correspondence: we can swap operators Z and B with simultaneous replacement of hypercomplex units i and j .

The eigenspace of the operator $2\rho_h^{SW}(B)$ with an eigenvalue $j\nu$ are spanned by the Weber–Hermite functions $D_{-\nu-\frac{1}{2}}\left(\pm\sqrt{\frac{2}{h}}x\right)$, see [93, § 8.2]. Functions D_ν are generalisations of the Hermit functions (IV.4.27).

The compatibility condition for a ladder operator within the Lie algebra \mathfrak{h}_1 will be (IV.4.37) as before, since it depends only on the commutators (IV.2.18–IV.2.19). Thus we still have the set of ladder operators corresponding to values $\lambda = \pm 1$:

$$L_h^\pm = \tilde{X} \mp \tilde{Y} = jq \pm h \frac{d}{dq}.$$

Admitting double numbers we have an extra way to satisfy $\lambda^2 = 1$ in (IV.4.37) with values $\lambda = \pm j$. Then there is an additional pair of hyperbolic ladder operators, which are identical (up to factors) to (IV.4.28):

$$L_j^\pm = \tilde{X} \mp j\tilde{Y} = jq \pm jh \frac{d}{dq}.$$

Pairs L_h^\pm and L_j^\pm shift eigenvectors in the “orthogonal” directions changing their eigenvalues by ± 1 and $\pm j$. Therefore an indecomposable \mathfrak{sp}_2 -module can be parametrised by a two-dimensional lattice of eigenvalues in double numbers, see Fig. II.3.2.

The following functions

$$\begin{aligned} v_{\frac{1}{2}}^{\pm h}(q) &= e^{\mp jq^2/(2h)} = \cosh \frac{q^2}{2h} \mp j \sinh \frac{q^2}{2h}, \\ v_{\frac{1}{2}}^{\pm j}(q) &= e^{\mp q^2/(2h)} \end{aligned}$$

are null solutions to the operators L_h^\pm and L_j^\pm respectively. They are also eigenvectors of $2\rho_h^{SW}(B)$ with eigenvalues $\mp \frac{j}{2}$ and $\mp \frac{1}{2}$ respectively. If these functions are used as mother wavelets for the wavelet transforms generated by the Heisenberg group, then the image space will consist of the null-solutions of the following differential operators, see Cor. II.6.34:

$$D_h = \overline{X^r - Y^r} = (\partial_x - \partial_y) + \frac{h}{2}(x + y), \quad D_j = \overline{X^r - jY^r} = (\partial_x + j\partial_y) - \frac{h}{2}(x - jy),$$

for $v_{\frac{1}{2}}^{\pm h}$ and $v_{\frac{1}{2}}^{\pm j}$ respectively. This is again in line with the classical result (IV.4.29). However annihilation of the eigenvector by a ladder operator does not mean that the part of the 2D-lattice becomes void since it can be reached via alternative routes on this lattice. Instead of multiplication by a zero, as it happens in the elliptic case, a half-plane of eigenvalues will be multiplied by the divisors of zero $1 \pm j$.

We can also search ladder operators within the algebra \mathfrak{sp}_2 and admitting double numbers we will again find two sets of them, cf. § ??:

$$\begin{aligned} L_{2h}^\pm &= \pm \tilde{A} + \tilde{Z}/2 = \mp \frac{q}{2} \frac{d}{dq} \mp \frac{1}{4} - \frac{jh}{4} \frac{d^2}{dq^2} - \frac{jq^2}{4h} = -\frac{j}{4h} (L_h^\pm)^2, \\ L_{2j}^\pm &= \pm j\tilde{A} + \tilde{Z}/2 = \mp \frac{jq}{2} \frac{d}{dq} \mp \frac{j}{4} - \frac{jh}{4} \frac{d^2}{dq^2} - \frac{jq^2}{4h} = -\frac{j}{4h} (L_j^\pm)^2. \end{aligned}$$

Again the operators $L_{2\hbar}^{\pm}$ and $L_{-2\hbar}^{\pm}$ produce double shifts in the orthogonal directions on the same two-dimensional lattice in Fig. II.3.2.

IV.4.5. Parabolic (Classical) Representations on the Phase Space

After the previous two cases it is natural to link classical mechanics with dual numbers generated by the parabolic unit $\varepsilon^2 = 0$. Connection of the parabolic unit ε with the Galilean group of symmetries of classical mechanics is around for a while [339, App. C].

However the nilpotency of the parabolic unit ε make it difficult if we will work with dual number valued functions only. To overcome this issue we consider a commutative real algebra \mathfrak{C} spanned by $1, i, \varepsilon$ and $i\varepsilon$ with identities $i^2 = -1$ and $\varepsilon^2 = 0$. A seminorm on \mathfrak{C} is defined as follows:

$$|a + bi + c\varepsilon + di\varepsilon|^2 = a^2 + b^2.$$

IV.4.5.1. Classical Non-Commutative Representations. We wish to build a representation of the Heisenberg group which will be a classical analog of the Fock–Segal–Bargmann representation (IV.3.20). To this end we introduce the space $F_{\hbar}^{\varepsilon}(\mathbb{H}^n)$ of \mathfrak{C} -valued functions on \mathbb{H}^n with the property:

$$(IV.4.45) \quad f(s + s', \hbar, y) = e^{\varepsilon \hbar s'} f(s, x, y), \quad \text{for all } (s, x, y) \in \mathbb{H}^n, s' \in \mathbb{R},$$

and the square integrability condition (IV.3.3). It is invariant under the left shifts and we restrict the left group action to $F_{\hbar}^{\varepsilon}(\mathbb{H}^n)$.

An equivalent form of the induced representation acts on $F_{\hbar}^{\varepsilon}(\mathbb{R}^{2n})$, where \mathbb{R}^{2n} is the homogeneous space of \mathbb{H}^n over its centre. The Fourier transform $(x, y) \mapsto (q, p)$ intertwines the last representation with the following action on \mathfrak{C} -valued functions on the phase space:

$$(IV.4.46) \quad \rho_{\hbar}^{\varepsilon}(s, x, y) : f(q, p) \mapsto e^{-2\pi i(xq + yp)} (f(q, p) + \varepsilon \hbar (sf(q, p) + \frac{y}{2\pi i} f'_q(q, p) - \frac{x}{2\pi i} f'_p(q, p))).$$

REMARK IV.4.16. Comparing the traditional infinite-dimensional (IV.3.20) and one-dimensional (IV.4.14) representations of \mathbb{H}^n we can note that the properties of the representation (IV.4.46) are a non-trivial mixture of the former:

- i. The action (IV.4.46) is non-commutative, similarly to the quantum representation (IV.3.20) and unlike the classical one (IV.4.14). This non-commutativity will produce the Hamilton equations below in a way very similar to Heisenberg equation, see Rem. IV.4.18.
- ii. The representation (IV.4.46) does not change the support of a function f on the phase space, similarly to the classical representation (IV.4.14) and unlike the quantum one (IV.3.20). Such a localised action will be responsible later for an absence of an interference in classical probabilities.
- iii. The parabolic representation (IV.4.46) can not be derived from either the elliptic (IV.3.20) or hyperbolic (IV.4.33) by the plain substitution $\hbar = 0$.

We may also write a classical Schrödinger type representation. According to § II.3.2 we get a representation formally very similar to the elliptic (IV.4.15) and hyperbolic

versions (IV.4.34):

$$\begin{aligned}
 \text{(IV.4.47)} \quad [\rho_x^\varepsilon(s', x', y')f](x) &= e^{-\varepsilon h(s' + xy' - x'y'/2)}f(x - x') \\
 &= (1 - \varepsilon h(s' + xy' - \frac{1}{2}x'y'))f(x - x').
 \end{aligned}$$

However due to nilpotency of ε the (complex) Fourier transform $x \mapsto q$ produces a different formula for parabolic Schrödinger type representation in the configuration space, cf. (IV.4.16) and (IV.4.39):

$$[\rho_x^\varepsilon(s', x', y')\hat{f}](q) = e^{2\pi i x' q} \left((1 - \varepsilon h(s' - \frac{1}{2}x'y'))\hat{f}(q) + \frac{\varepsilon h y'}{2\pi i}\hat{f}'(q) \right).$$

This representation shares all properties mentioned in Rem. IV.4.16 as well.

IV.4.5.2. Hamilton Equation. The identity $e^{\varepsilon t} - e^{-\varepsilon t} = 2\varepsilon t$ can be interpreted as a parabolic version of the sine function, while the parabolic cosine is identically equal to one, cf. § II.3.1 and [129, 190]. From this we obtain the parabolic version of the commutator (IV.4.18):

$$\begin{aligned}
 [k', k]_s^\wedge(\varepsilon h, x, y) &= \varepsilon h \int_{\mathbb{R}^{2n}} (xy' - yx') \\
 &\quad \times \hat{k}'_s(\varepsilon h, x', y') \hat{k}_s(\varepsilon h, x - x', y - y') \, dx' dy',
 \end{aligned}$$

for the partial parabolic Fourier-type transform \hat{k}'_s of the kernels. Thus the parabolic representation of the dynamical equation (IV.4.4) becomes:

(IV.4.48)

$$\varepsilon h \frac{d\hat{f}_s}{dt}(\varepsilon h, x, y; t) = \varepsilon h \int_{\mathbb{R}^{2n}} (xy' - yx') \hat{H}_s(\varepsilon h, x', y') \hat{f}_s(\varepsilon h, x - x', y - y'; t) \, dx' dy',$$

Although there is no possibility to divide by ε (since it is a zero divisor) we can obviously eliminate εh from the both sides if the rest of the expressions are real. Moreover this can be done “in advance” through a kind of the antiderivative operator considered in [181, (4.1)]. This will prevent “imaginary parts” of the remaining expressions (which contain the factor ε) from vanishing.

REMARK IV.4.17. It is noteworthy that the Planck constant completely disappeared from the dynamical equation. Thus the only prediction about it following from our construction is $h \neq 0$, which was confirmed by experiments, of course.

Using the duality between the Lie algebra of \mathbb{H}^n and the phase space we can find an adjoint equation for observables on the phase space. To this end we apply the usual Fourier transform $(x, y) \mapsto (q, p)$. It turn to be the Hamilton equation [181, (4.7)]. However the transition to the phase space is more a custom rather than a necessity and in many cases we can efficiently work on the Heisenberg group itself.

REMARK IV.4.18. It is noteworthy, that the non-commutative representation (IV.4.46) allows to obtain the Hamilton equation directly from the commutator $[\rho_h^\varepsilon(k_1), \rho_h^\varepsilon(k_2)]$. Indeed its straightforward evaluation will produce exactly the above expression. By contrast, such a commutator for the commutative representation (IV.4.14) is zero and to obtain the Hamilton equation we have to work with an additional tools, e.g. an anti-derivative [181, (4.1)].

- EXAMPLE IV.4.19. i. For the harmonic oscillator in Example IV.4.3 the equation (IV.4.48) again reduces to the form (IV.4.6) with the solution given by (IV.4.7). The adjoint equation of the harmonic oscillator on the phase space is not different from the quantum written in Example IV.4.7(IV.4.7.i). This is true for any Hamiltonian of at most quadratic order.
- ii. For non-quadratic Hamiltonians classical and quantum dynamics are different, of course. For example, the cubic term of ∂_s in the equation (IV.4.9) will generate the factor $\varepsilon^3 = 0$ and thus vanish. Thus the equation (IV.4.48) of the unharmonic oscillator on \mathbb{H}^n becomes:

$$\dot{f} = \left(mk^2 y \frac{\partial}{\partial x} + \frac{\lambda y}{2} \frac{\partial^2}{\partial x^2} - \frac{1}{m} x \frac{\partial}{\partial y} \right) f.$$

The adjoint equation on the phase space is:

$$\dot{f} = \left(\left(mk^2 q + \frac{\lambda}{2} q^2 \right) \frac{\partial}{\partial p} - \frac{1}{m} p \frac{\partial}{\partial q} \right) f.$$

The last equation is the classical Hamilton equation generated by the cubic potential (IV.4.8). Qualitative analysis of its dynamics can be found in many textbooks [11, § 4.C, Pic. 12; 278, § 4.4].

REMARK IV.4.20. We have obtained the *Poisson bracket* from the commutator of convolutions on \mathbb{H}^n without any quasiclassical limit $\hbar \rightarrow 0$. This has a common source with the deduction of main calculus theorems in [58] based on dual numbers. As explained in [191, Rem. 6.9] this is due to the similarity between the parabolic unit ε and the infinitesimal number used in non-standard analysis [73]. In other words, we never need to take care about terms of order $O(\hbar^2)$ because they will be wiped out by $\varepsilon^2 = 0$.

An alternative derivation of classical dynamics from the Heisenberg group is given in the recent paper [247].

IV.4.5.3. Classical probabilities. It is worth to notice that dual numbers are not only helpful in reproducing classical Hamiltonian dynamics, they also provide the classic rule for addition of probabilities. We use the same formula (IV.4.10) to calculate kernels of the states. The important difference now that the representation (IV.4.46) does not change the support of functions. Thus if we calculate the correlation term $\langle v_1, \rho(g)v_2 \rangle$ in (IV.4.11), then it will be zero for every two vectors v_1 and v_2 which have disjoint supports in the phase space. Thus no interference similar to quantum or hyperbolic cases (Section IV.4.2.3) is possible.

IV.4.5.4. Ladder Operator for the Nilpotent Subgroup. Finally we look for ladder operators for the Hamiltonian $\tilde{B} + \tilde{Z}/2$ or, equivalently, $-\tilde{B} + \tilde{Z}/2$. It can be identified with a free particle [338, § 3.8].

We can look for ladder operators in the representation (IV.3.15–IV.3.16) within the Lie algebra \mathfrak{h}_1 in the form $L_\varepsilon^\pm = a\tilde{X} + b\tilde{Y}$. This is possible if and only if

$$(IV.4.49) \quad -b = \lambda a, \quad 0 = \lambda b.$$

The compatibility condition $\lambda^2 = 0$ implies $\lambda = 0$ within complex numbers. However such a “ladder” operator produces only the zero shift on the eigenvectors, cf. (??).

Another possibility appears if we consider the representation of the Heisenberg group induced by dual-valued characters. On the configuration space such a representation is [199, (4.11)]:

$$(IV.4.50) \quad [\rho_\chi^\varepsilon(s, x, y)f](q) = e^{2\pi i x q} \left((1 - \varepsilon h(s - \frac{1}{2}xy)) f(q) + \frac{\varepsilon h y}{2\pi i} f'(q) \right).$$

The corresponding derived representation of \mathfrak{h}_1 is

$$(IV.4.51) \quad \rho_h^p(X) = 2\pi i q, \quad \rho_h^p(Y) = \frac{\varepsilon h}{2\pi i} \frac{d}{dq}, \quad \rho_h^p(S) = -\varepsilon h I.$$

However the Shale–Weil extension generated by this representation is inconvenient. It is better to consider the FSB–type parabolic representation (IV.4.46) on the phase space induced by the same dual-valued character. Then the derived representation of \mathfrak{h}_1 is:

$$(IV.4.52) \quad \rho_h^p(X) = -2\pi i q - \frac{\varepsilon h}{4\pi i} \partial_p, \quad \rho_h^p(Y) = -2\pi i p + \frac{\varepsilon h}{4\pi i} \partial_q, \quad \rho_h^p(S) = \varepsilon h I.$$

An advantage of the FSB representation is that the derived form of the parabolic Shale–Weil representation coincides with the elliptic one (IV.3.22).

Eigenfunctions with the eigenvalue μ of the parabolic Hamiltonian $\tilde{B} + \tilde{Z}/2 = q\partial_p$ have the form

$$(IV.4.53) \quad v_\mu(q, p) = e^{\mu p/q} f(q), \text{ with an arbitrary function } f(q).$$

The linear equations defining the corresponding ladder operator $L_\varepsilon^\pm = a\tilde{X} + b\tilde{Y}$ in the algebra \mathfrak{h}_1 are (IV.4.49). The compatibility condition $\lambda^2 = 0$ implies $\lambda = 0$ within complex numbers again. Admitting dual numbers we have additional values $\lambda = \pm \varepsilon \lambda_1$ with $\lambda_1 \in \mathbb{C}$ with the corresponding ladder operators

$$L_\varepsilon^\pm = \tilde{X} \mp \varepsilon \lambda_1 \tilde{Y} = -2\pi i q - \frac{\varepsilon h}{4\pi i} \partial_p \pm 2\pi \varepsilon \lambda_1 i p = -2\pi i q + \varepsilon i (\pm 2\pi \lambda_1 p + \frac{h}{4\pi} \partial_p).$$

For the eigenvalue $\mu = \mu_0 + \varepsilon \mu_1$ with $\mu_0, \mu_1 \in \mathbb{C}$ the eigenfunction (IV.4.53) can be rewritten as:

$$(IV.4.54) \quad v_\mu(q, p) = e^{\mu p/q} f(q) = e^{\mu_0 p/q} \left(1 + \varepsilon \mu_1 \frac{p}{q} \right) f(q)$$

due to the nilpotency of ε . Then the ladder action of L_ε^\pm is $\mu_0 + \varepsilon \mu_1 \mapsto \mu_0 + \varepsilon (\mu_1 \pm \lambda_1)$. Therefore these operators are suitable for building \mathfrak{sp}_2 -modules with a one-dimensional chain of eigenvalues.

Finally, consider the ladder operator for the same element $B + Z/2$ within the Lie algebra \mathfrak{sp}_2 , cf. § ?? . There is the only operator $L_\varepsilon^\pm = \tilde{B} + \tilde{Z}/2$ corresponding to complex coefficients, which does not affect the eigenvalues. However the dual numbers lead to the operators

$$L_\varepsilon^\pm = \pm \varepsilon \lambda_2 \tilde{A} + \tilde{B} + \tilde{Z}/2 = \pm \frac{\varepsilon \lambda_2}{2} (q\partial_q - p\partial_p) + q\partial_p, \quad \lambda_2 \in \mathbb{C}.$$

These operator act on eigenvalues in a non-trivial way.

IV.4.5.5. Similarity and Correspondence. We wish to summarise our findings. Firstly, the appearance of hypercomplex numbers in ladder operators for \mathfrak{h}_1 follows exactly the same pattern as was already noted for \mathfrak{sp}_2 , see Rem. II.3.9:

- the introduction of complex numbers is a necessity for the *existence* of ladder operators in the elliptic case;
- in the parabolic case we need dual numbers to make ladder operators *useful*;
- in the hyperbolic case double numbers are not required neither for the existence or for the usability of ladder operators, but they do provide an enhancement.

In the spirit of the Similarity and Correspondence Principle II.3.5 we have the following extension of Prop. II.3.10:

PROPOSITION IV.4.21. *Let a vector $H \in \mathfrak{sp}_2$ generates the subgroup K, N' or A' , that is $H = Z, B + Z/2$, or $2B$ respectively. Let ι be the respective hypercomplex unit. Then the ladder operators L^\pm satisfying to the commutation relation:*

$$[H, L_2^\pm] = \pm \iota L^\pm$$

are given by:

- i. Within the Lie algebra \mathfrak{h}_1 : $L^\pm = \tilde{X} \mp \iota \tilde{Y}$.
- ii. Within the Lie algebra \mathfrak{sp}_2 : $L_2^\pm = \pm \iota \tilde{A} + \tilde{E}$. Here $E \in \mathfrak{sp}_2$ is a linear combination of B and Z with the properties:
 - $E = [A, H]$.
 - $H = [A, E]$.
 - Killings form $K(H, E)$ [159, § 6.2] vanishes.

Any of the above properties defines the vector $E \in \text{span}\{B, Z\}$ up to a real constant factor.

It is worth continuing this investigation and describing in details hyperbolic and parabolic versions of FSB spaces.

Wavelet Transform, Uncertainty Relation and Analyticity

There are two and a half main examples of reproducing kernel spaces of analytic function. One is the Fock–Segal–Bargmann (FSB) space and others (one and a half) – the Bergman and Hardy spaces on the upper half-plane. The first space is generated by the Heisenberg group [104, § 1.6; 197, § 7.3], two others – by the group $SL_2(\mathbb{R})$ [197, § 4.2] (this explains our way of counting).

Those spaces have the following properties, which make their study particularly pleasant and fruitful:

- i. There is a group, which acts transitively on functions' domain.
- ii. There is a reproducing kernel.
- iii. The space consists of holomorphic functions.

Furthermore, for FSB space there is the following property:

- iv. The reproducing kernel is generated by a function, which minimises the uncertainty for coordinate and momentum observables.

It is known, that a transformation group is responsible for the appearance of the reproducing kernel [5, Thm. 8.1.3]. This paper shows that the last two properties are equivalent and connected to the group as well.

IV.5.1. Induced Wavelet (Covariant) Transform

The following object is common in quantum mechanics [181], signal processing, harmonic analysis [205], operator theory [201, 204] and many other areas [197]. Therefore, it has various names [5]: coherent states, wavelets, matrix coefficients, etc. In the most fundamental situation [5, Ch. 8], we start from an irreducible unitary representation ρ of a Lie group G in a Hilbert space H . For a vector $f \in H$ (called mother wavelet, vacuum state, etc.), we define the map \mathcal{W}_f from H to a space of functions on G by:

$$(IV.5.1) \quad [\mathcal{W}_f v](g) = \tilde{v}(g) := \langle v, \rho(g)f \rangle.$$

Under the above assumptions, $\tilde{v}(g)$ is a bounded continuous function on G . The map \mathcal{W}_f intertwines $\rho(g)$ with the left shifts on G :

$$(IV.5.2) \quad \mathcal{W}_f \circ \rho(g) = \Lambda(g) \circ \mathcal{W}_f, \quad \text{where } \Lambda(g) : \tilde{v}(g') \mapsto \tilde{v}(g^{-1}g').$$

Thus, the image $\mathcal{W}_f H$ is invariant under the left shifts on G . If ρ is square integrable and f is admissible [5, § 8.1], then $\tilde{v}(g)$ is square-integrable with respect to the Haar measure on G . Moreover, it is a reproducing kernel Hilbert space and the kernel is $k(g) = [\mathcal{W}_f f](g)$. At this point, none of admissible vectors has an advantage over others.

It is common [197, § 5.1], that there exists a closed subgroup $H \subset G$ and a respective $f \in H$ such that $\rho(h)f = \chi(h)f$ for some character χ of H . In this case, it is enough to know values of $\tilde{v}(s(x))$, for any continuous section s from the homogeneous space $X = G/H$ to G . The map $v \mapsto \tilde{v}(x) = \tilde{v}(s(x))$ intertwines ρ with the representation ρ_χ in a certain function space on X induced by the character χ of H [159, § 13.2]. We call the map

$$(IV.5.3) \quad \mathcal{W}_f : v \mapsto \tilde{v}(x) = \langle v, \rho(s(x))f \rangle, \quad \text{where } x \in G/H$$

the *induced wavelet transform* [197, § 5.1].

For example, if $G = \mathbb{H}$, $H = \{(s, 0, 0) \in \mathbb{H} : s \in \mathbb{R}\}$ and its character $\chi_h(s, 0, 0) = e^{2\pi i h s}$, then any vector $f \in L_2(\mathbb{R})$ satisfies $\rho_h(s, 0, 0)f = \chi_h(s)f$ for the representation (IV.4.16). Thus, we still do not have a reason to prefer any admissible vector to others.

IV.5.2. The Uncertainty Relation

In quantum mechanics [104, § 1.1], an observable (that is, a self-adjoint operator on a Hilbert space H) A produces the expectation value \bar{A} on a pure state (that is, a unit vector) $\phi \in H$ by $\bar{A} = \langle A\phi, \phi \rangle$. Then, the dispersion is evaluated as follow:

$$(IV.5.4) \quad \Delta_\phi^2(A) = \langle (A - \bar{A})^2 \phi, \phi \rangle = \langle (A - \bar{A})\phi, (A - \bar{A})\phi \rangle = \|(A - \bar{A})\phi\|^2.$$

The next theorem links obstructions of exact simultaneous measurements with non-commutativity of observables.

THEOREM IV.5.1 (The Uncertainty relation). *If A and B are self-adjoint operators on a Hilbert space H , then*

$$(IV.5.5) \quad \|(A - a)u\| \|(B - b)u\| \geq \frac{1}{2} |\langle (AB - BA)u, u \rangle|,$$

for any $u \in H$ from the domains of AB and BA and $a, b \in \mathbb{R}$. Equality holds precisely when u is a solution of $((A - a) + ir(B - b))u = 0$ for some real r .

PROOF. The proof is well-known [104, § 1.3], but it is short, instructive and relevant for the following discussion, thus we include it in full. We start from simple algebraic transformations:

$$(IV.5.6) \quad \begin{aligned} \langle (AB - BA)u, u \rangle &= \langle ((A - a)(B - b) - (B - b)(A - a))u, u \rangle \\ &= \langle (B - b)u, (A - a)u \rangle - \langle (A - a)u, (B - b)u \rangle \\ &= 2i\Im \langle (B - b)u, (A - a)u \rangle \end{aligned}$$

Then by the Cauchy–Schwartz inequality:

$$\frac{1}{2} \langle (AB - BA)u, u \rangle \leq |\langle (B - b)u, (A - a)u \rangle| \leq \|(B - b)u\| \|(A - a)u\|.$$

The equality holds if and only if $(B - b)u$ and $(A - a)u$ are proportional by a *purely imaginary* scalar. \square

The famous application of the above theorem is the following fundamental relation in quantum mechanics. We use [199, (3.5)] the Schrödinger representation (IV.4.16) of the Heisenberg group (IV.4.16):

$$(IV.5.7) \quad [\rho_h(s', x', y')\hat{f}](q) = e^{-2\pi i h (s' + x'y'/2) - 2\pi i x'q} \hat{f}(q + \hbar y').$$

Elements of the Lie algebra \mathfrak{h} , corresponding to the infinitesimal generators X and Y of one-parameter subgroups $(0, t/(2\pi), 0)$ and $(0, 0, t)$ in \mathbb{H} , are represented in (IV.5.7) by the (unbounded) operators \tilde{M} and \tilde{D} on $L_2(\mathbb{R})$:

$$(IV.5.8) \quad \tilde{M} = -iq, \quad \tilde{D} = \hbar \frac{d}{dq}, \quad \text{with the commutator} \quad [\tilde{M}, \tilde{D}] = i\hbar I.$$

In the Schrödinger model of quantum mechanics, $f(q) \in L_2(\mathbb{R})$ is interpreted as a wave function (a state) of a particle, with $M = i\tilde{M}$ and $\frac{1}{\hbar}\tilde{D}$ are the observables of its coordinate and momentum.

COROLLARY IV.5.2 (Heisenberg–Kennard uncertainty relation). *For the coordinate M and momentum D observables we have the Heisenberg–Kennard uncertainty relation:*

$$(IV.5.9) \quad \Delta_\phi(M) \cdot \Delta_\phi(D) \geq \frac{\hbar}{2}.$$

The equality holds if and only if $\phi(q) = e^{-cq^2}$, $c \in \mathbb{R}_+$ is the Gaussian—the vacuum state in the Schrödinger model.

PROOF. The relation follows from the commutator $[M, D] = i\hbar I$, which, in turn, is the representation of the Lie algebra \mathfrak{h} of the Heisenberg group. By Thm. IV.5.1, the minimal uncertainty state in the Schrödinger representation is a solution of the differential equation: $(M - irD)\phi = 0$ for some $r \in \mathbb{R}$, or, explicitly:

$$(IV.5.10) \quad (M - irD)\phi = -i \left(q + r\hbar \frac{d}{dq} \right) \phi(q) = 0.$$

The solution is the Gaussian $\phi(q) = e^{-cq^2}$, $c = \frac{1}{2r\hbar}$. For $c > 0$, this function is in the state space $L_2(\mathbb{R})$. \square

IV.5.3. The Gaussian

The Gaussian is the crucial element in the theory of the Heisenberg group and will repeatedly use its remarkable properties. For this reasons we devote a separate section to their description.

Cor. IV.5.2 identifies the Gaussian $\phi(q) = e^{-cq^2}$ as the vector with minimal uncertainty. It is also common to say that the Gaussian $\phi(q) = e^{-cq^2}$ represents the ground state, which minimises the uncertainty of coordinate and momentum.

IV.5.4. Right Shifts and Analyticity

To discover some preferable mother wavelets, we use the following general result from [197, § 5]. Let G be a locally compact group and ρ be its representation in a Hilbert space H . Let $[\mathcal{W}_f v](g) = \langle v, \rho(g)f \rangle$ be the wavelet transform defined by a vacuum state $f \in H$. Then, the right shift $R(g) : [\mathcal{W}_f v](g') \mapsto [\mathcal{W}_f v](g'g)$ for $g \in G$ coincides with the wavelet transform $[\mathcal{W}_{f_g} v](g') = \langle v, \rho(g')f_g \rangle$ defined by the vacuum state $f_g = \rho(g)f$. In other words, the covariant transform intertwines right shifts on the group G with the associated action ρ on vacuum states, cf. (IV.5.2):

$$(IV.5.11) \quad R(g) \circ \mathcal{W}_f = \mathcal{W}_{\rho(g)f}.$$

Although, the above observation is almost trivial, applications of the following corollary are not.

COROLLARY IV.5.3 (Analyticity of the wavelet transform, [197, § 5]). *Let G be a group and dg be a measure on G . Let ρ be a unitary representation of G , which can be extended by integration to a vector space V of functions or distributions on G . Let a mother wavelet $f \in H$ satisfy the equation*

$$\int_G a(g) \rho(g) f dg = 0,$$

for a fixed distribution $a(g) \in V$. Then any wavelet transform $\tilde{v}(g) = \langle v, \rho(g) f \rangle$ obeys the condition:

$$(IV.5.12) \quad D\tilde{v} = 0, \quad \text{where } D = \int_G \bar{a}(g) R(g) dg,$$

with R being the right regular representation of G .

Some applications (including discrete one) produced by the $ax + b$ group can be found in [205, § 6]. We turn to the Heisenberg group now.

EXAMPLE IV.5.4 (Gaussian and FSB transform). The Gaussian $\phi(q) = e^{-cq^2/2}$ is a null-solution of the operator $\hbar cM - iD$. For the centre $Z = \{(s, 0, 0) : s \in \mathbb{R}\} \subset \mathbb{H}$, we define the section $s : \mathbb{H}/Z \rightarrow \mathbb{H}$ by $s(x, y) = (0, x, y)$. Then, the corresponding induced wavelet transform (IV.5.3) is:

$$(IV.5.13) \quad \tilde{v}(x, y) = \langle v, \rho(s(x, y)) \phi \rangle = \int_{\mathbb{R}} v(q) e^{\pi i \hbar x y - 2\pi i x q} e^{-c(q + \hbar y)^2/2} dq.$$

The transformation intertwines the Schrödinger and Fock–Segal–Bargmann representations. Furthermore,

The infinitesimal generators X and Y of one-parameters subgroups $(0, t/(2\pi), 0)$ and $(0, 0, t)$ are represented through the right shift in (IV.2.5) by

$$R_*(X) = -\frac{1}{4\pi} y \partial_s + \frac{1}{2\pi} \partial_x, \quad R_*(Y) = \frac{1}{2} x \partial_s + \partial_y.$$

For the representation induced by the character $\chi_{\hbar}(s, 0, 0) = e^{2\pi i \hbar s}$ we have $\partial_s = 2\pi i \hbar I$. Cor. IV.5.3 ensures that the operator

$$(IV.5.14) \quad \hbar c \cdot R_*(X) + i \cdot R_*(Y) = -\frac{\hbar}{2} (2\pi x + i \hbar c y) + \frac{\hbar c}{2\pi} \partial_x + i \partial_y$$

annihilate any $\tilde{v}(x, y)$ from (IV.5.13). The integral (IV.5.13) is known as Fock–Segal–Bargmann (FSB) transform and in the most common case the values $\hbar = 1$ and $c = 2\pi$ are used. For these, operator (IV.5.14) becomes $-\pi(x + iy) + (\partial_x + i \partial_y) = -\pi z + 2\partial_{\bar{z}}$ with $z = x + iy$. Then the function $V(z) = e^{\pi z \bar{z}/2} \tilde{v}(z) = e^{\pi(x^2 + y^2)/2} \tilde{v}(x, y)$ satisfies the Cauchy–Riemann equation $\partial_{\bar{z}} V(z) = 0$.

This example shows, that the Gaussian is a preferred vacuum state (as producing analytic functions through FSB transform) exactly for the same reason as being the minimal uncertainty state: the both are derived from the identity $(\hbar cM + iD)e^{-cq^2/2} = 0$.

IV.5.5. Uncertainty and Analyticity

The main result of this paper is a generalisation of the previous observation, which bridges together Cor. IV.5.3 and Thm. IV.5.1. Let G, H, ρ and H be as before. Assume, that the homogeneous space $X = G/H$ has a (quasi-)invariant measure $d\mu(x)$ [159, § 13.2]. Then, for a function (or a suitable distribution) k on X we can define the integrated representation:

$$(IV.5.15) \quad \rho(k) = \int_X k(x)\rho(s(x)) d\mu(x),$$

which is (possibly, unbounded) operators on (possibly, dense subspace of) H . It is a homomorphism of the convolution algebra $L_1(G, dg)$ to an algebra of bounded operators on H . In particular, $R(k)$ denotes the integrated right shifts, for $H = \{e\}$.

THEOREM IV.5.5 ([206]). *Let k_1 and k_2 be two distributions on X with the respective integrated representations $\rho(k_1)$ and $\rho(k_2)$. The following are equivalent:*

i. *A vector $f \in H$ satisfies the identity*

$$\Delta_f(\rho(k_1)) \cdot \Delta_f(\rho(k_2)) = |\langle [\rho(k_1), \rho(k_2)]f, f \rangle|.$$

ii. *The image of the wavelet transform $\mathcal{W}_f : v \mapsto \tilde{v}(g) = \langle v, \rho(g)f \rangle$ consists of functions satisfying the equation $R(k_1 + irk_2)\tilde{v} = 0$ for some $r \in \mathbb{R}$, where R is the integrated form (IV.5.15) of the right regular representation on G .*

PROOF. This is an immediate consequence of a combination of Thm. IV.5.1 and Cor. IV.5.3. □

Example IV.5.4 is a particular case of this theorem with $k_1(x, y) = \delta'_x(x, y)$ and $k_2(x, y) = \delta'_y(x, y)$ (partial derivatives of the delta function), which represent vectors X and Y from the Lie algebra \mathfrak{h} . The next example will be of this type as well.

IV.5.6. Hardy Space on the Real Line

We consider the induced representation ρ_1 (II.3.8) for $k = 1$ of the group $SL_2(\mathbb{R})$. A $SL_2(\mathbb{R})$ -quasi-invariant measure on the real line is $|cx + d|^{-2} dx$. Thus, the following form of the representation (II.3.8)

$$(IV.5.16) \quad \rho_1(g)f(w) = \frac{1}{cx + d} f\left(\frac{ax + b}{cx + d}\right), \quad \text{where } g^{-1} = \begin{pmatrix} a & b \\ c & d \end{pmatrix},$$

is unitary in $L_2(\mathbb{R})$ with the Lebesgue measure dx .

We can calculate the derived representations for the basis of \mathfrak{sl}_2 (II.3.13):

$$\begin{aligned} d\rho_1^A &= \frac{1}{2} \cdot I + x\partial_x, \\ d\rho_1^B &= \frac{1}{2}x \cdot I + \frac{1}{2}(x^2 - 1)\partial_x, \\ d\rho_1^Z &= -x \cdot I - (x^2 + 1)\partial_x. \end{aligned}$$

The linear combination of the above vector fields producing ladder operators $L^\pm = \pm iA + B$ are, cf. (II.3.17):

$$(IV.5.17) \quad d\rho_1^{L^\pm} = \frac{1}{2}((x \pm i) \cdot I + (x \pm i)^2 \cdot \partial_x).$$

Obviously, the function $f_+(x) = (x + i)^{-1}$ satisfies $d\rho_1^{L^+} f_+ = 0$. Recalling the commutator $[A, B] = -\frac{1}{2}Z$ we note that $d\rho_1^Z f_+ = -if_+$. Therefore, there is the following identity for dispersions on this state:

$$\Delta_{f_+}(\rho_1^A) \cdot \Delta_{f_+}(\rho_1^B) = \frac{1}{2},$$

with the minimal value of uncertainty among all eigenvectors of the operator $d\rho_1^Z$.

Furthermore, the vacuum state f_+ generates the induced wavelet transform for the subgroup $K = \{e^{tZ} \mid t \in \mathbb{R}\}$. We identify $SL_2(\mathbb{R})/K$ with the upper half-plane $\mathbb{C}_+ = \{z \in \mathbb{C} \mid \Im z > 0\}$ [197, § 5.5; 204]. The map $s : SL_2(\mathbb{R})/K \rightarrow SL_2(\mathbb{R})$ is defined as $s(x + iy) = \frac{1}{\sqrt{y}} \begin{pmatrix} y & x \\ 0 & 1 \end{pmatrix}$ (I.3.13). Then, the induced wavelet transform (IV.5.3) is:

$$\begin{aligned} \tilde{v}(x + iy) &= \langle v, \rho_1(s(x + iy))f_+ \rangle = \frac{1}{2\pi\sqrt{y}} \int_{\mathbb{R}} \frac{v(t) dt}{\frac{t-x}{y} - i} \\ &= \frac{\sqrt{y}}{2\pi} \int_{\mathbb{R}} \frac{v(t) dt}{t - (x + iy)}. \end{aligned}$$

Clearly, this is the Cauchy integral up to the factor \sqrt{y} , which is related to the conformal metric on the upper half-plane. Similarly, we can consider the operator $\rho_1^{B-iA} = \frac{1}{2}((x \pm i) \cdot I + (x \pm i)^2 \cdot \partial_x)$ and the function $f_-(z) = \frac{1}{x-i}$ simultaneously solving the equations $\rho_1^{B-iA} f_- = 0$ and $d\rho_1^Z f_- = if_-$. It produces the integral with the conjugated Cauchy kernel.

Finally, we can calculate the operator (IV.5.12) annihilating the image of the wavelet transform. In the coordinates $(x + iy, t) \in (SL_2(\mathbb{R})/K) \times K$, the restriction to the induced subrepresentation is, cf. [240, § IX.5]:

$$(IV.5.18) \quad \mathfrak{L}^A = \frac{i}{2} \sin 2t \cdot I - y \sin 2t \cdot \partial_x - y \cos 2t \cdot \partial_y,$$

$$(IV.5.19) \quad \mathfrak{L}^B = -\frac{i}{2} \cos 2t \cdot I + y \cos 2t \cdot \partial_x - y \sin 2t \cdot \partial_y.$$

Then, the left-invariant vector field corresponding to the ladder operator contains the Cauchy–Riemann operator as the main ingredient:

$$(IV.5.20) \quad \mathfrak{L}^{L^-} = e^{2it}(-\frac{i}{2}I + y(\partial_x + i\partial_y)), \quad \text{where } L^- = \overline{L^+} = -iA + B.$$

Furthermore, if $\mathfrak{L}^{-iA+B} \tilde{v}(x + iy) = 0$, then $(\partial_x + i\partial_y)(\tilde{v}(x + iy)/\sqrt{y}) = 0$. That is, $V(x + iy) = \tilde{v}(x + iy)/\sqrt{y}$ is a holomorphic function on the upper half-plane.

Similarly, we can treat representations of $SL_2(\mathbb{R})$ in the space of square integrable functions on the upper half-plane. The irreducible components of this representation are isometrically isomorphic [197, § 4–5] to the weighted Bergman spaces of (purely poly-)analytic functions on the unit disk, cf. [329]. Further connections between analytic function theory and group representations can be found in [170, 197].

IV.5.7. Contravariant Transform and Relative Convolutions

For a square integrable unitary irreducible representation ρ and a fixed admissible vector $\psi \in V$, the integrated representation (IV.5.15) produces the *contravariant transform* $\mathcal{M}_\psi : L_1(G) \rightarrow V$, cf. [173, 204]:

$$(IV.5.21) \quad \mathcal{M}_\psi^\rho(k) = \rho(k)\psi, \quad \text{where } k \in L_1(G).$$

The contravariant transform \mathcal{M}_ψ^ρ intertwines the left regular representation Λ on $L_2(G)$ and ρ :

$$(IV.5.22) \quad \mathcal{M}_\psi^\rho \Lambda(g) = \rho(g) \mathcal{M}_\psi^\rho.$$

Combining with (IV.5.2), we see that the composition $\mathcal{M}_\psi^\rho \circ \mathcal{W}_\phi^\rho$ of the covariant and contravariant transform intertwines ρ with itself. For an irreducible square integrable ρ and suitably normalised admissible ϕ and ψ , we use the Schur’s lemma [5, Lem. 4.3.1], [159, Thm. 8.2.1] to conclude that:

$$(IV.5.23) \quad \mathcal{M}_\psi^\rho \circ \mathcal{W}_\phi^\rho = \langle \psi, \phi \rangle I.$$

Similarly to induced wavelet transform (IV.5.3), we may define integrated representation and contravariant transform for a homogeneous space. Let H be a subgroup of G and $X = G/H$ be the respective homogeneous space with a (quasi-)invariant measure dx [159, § 9.1]. For the natural projection $p : G \rightarrow X$ we fix a continuous section $s : X \rightarrow G$ [159, § 13.2], which is a right inverse to p . Then, we define an operator of *relative convolution* on V [171, 204], cf. (IV.5.15):

$$(IV.5.24) \quad \rho(k) = \int_X k(x) \rho(s(x)) dx,$$

with a kernel k defined on $X = G/H$. There are many important classes of operators described by (IV.5.24), notably pseudodifferential operators (PDO) and Toeplitz operators [139, 171, 173, 204]. Thus, it is important to have various norm estimations of $\rho(k)$. We already mentioned a straightforward inequality $\|\rho(k)\| \leq C \|k\|_1$ for $k \in L_1(G, dg)$, however, other classes are of interest as well.

IV.5.8. Norm Estimations of Relative Convolution

If G is the Heisenberg group and ρ is its Schrödinger representation, then $\rho(\hat{a})$ (IV.5.24) is a PDO $\alpha(X, D)$ with the symbol α [104, 139, 204], which is the Weyl quantization (IV.1.6) of a classical observable a defined on phase space \mathbb{R}^2 . Here, \hat{a} is the Fourier transform of a , as usual. The Calderón–Vaillancourt theorem [320, Ch. XIII] estimates $\|\alpha(X, D)\|$ by L_∞ -norm of a finite number of partial derivatives of a .

In this section we revise the method used in [139, § 3.1] to prove the Calderón–Vaillancourt estimations. It was described as “rather magical” in [104, § 2.5]. We hope, that a usage of the covariant transform dispel the mystery without undermining the power of the method.

We start from the following lemma, which has a transparent proof in terms of covariant transform, cf. [139, § 3.1] and [104, (2.75)]. For the rest of the section we assume that ρ is an irreducible square integrable representation of an exponential Lie group G in V and mother wavelet $\phi, \psi \in V$ are admissible.

LEMMA IV.5.6. *Let $\phi \in V$ be such that, for $\Phi = \mathcal{W}_\phi \phi$, the reciprocal Φ^{-1} is bounded on G or $X = G/H$. Then, for the integrated representation (IV.5.15) or relative convolution (IV.5.24), we have the inequality:*

$$(IV.5.25) \quad \|\rho(f)\| \leq \| \Lambda \otimes R(f\Phi^{-1}) \|,$$

where $(\Lambda \otimes R)(g) : k(g') \mapsto k(g^{-1}g'g)$ acts on the image of \mathcal{W}_ϕ .

PROOF. We know from (IV.5.23) that $\mathcal{M}_\phi \circ \mathcal{W}_{\rho(g)\phi} = \langle \phi, \rho(g)\phi \rangle I$ on V , thus:

$$\mathcal{M}_\phi \circ \mathcal{W}_{\rho(g)\phi} \circ \rho(g) = \langle \phi, \rho(g)\phi \rangle \rho(g) = \Phi(g)\rho(g).$$

On the other hand, the intertwining properties (IV.5.2) and (IV.5.11) of the wavelet transform imply:

$$\mathcal{M}_\phi \circ \mathcal{W}_{\rho(g)\phi} \circ \rho(g) = \mathcal{M}_\phi \circ (\Lambda \otimes R)(g) \circ \mathcal{W}_\phi.$$

Integrating the identity $\Phi(g)\rho(g) = \mathcal{M}_\phi \circ (\Lambda \otimes R)(g) \circ \mathcal{W}_\phi$ with the function $f\Phi^{-1}$ and use the partial isometries \mathcal{W}_ϕ and \mathcal{M}_ϕ we get the inequality. \square

The Lemma is most efficient if $\Lambda \otimes R$ acts in a simple way. Thus, we give the following

DEFINITION IV.5.7. We say that the subgroup H has the *complemented commutator property*, if there exists a continuous section $s : X \rightarrow G$ such that:

$$(IV.5.26) \quad \rho(s(x)^{-1}gs(x)) = \rho(g), \quad \text{for all } x \in X = G/H, g \in G.$$

For a Lie group G with the Lie algebra \mathfrak{g} define the Lie algebra $\mathfrak{h} = [\mathfrak{g}, \mathfrak{g}]$. The subgroup $H = \exp(\mathfrak{h})$ (as well as any larger subgroup) has the complemented commutator property (IV.5.26). Of course, $X = G/H$ is non-trivial if $H \neq G$ and this happens, for example, for a nilpotent G . In particular, for the Heisenberg group, its centre has the complemented commutator property.

Note, that the complemented commutator property (IV.5.26) implies:

$$(IV.5.27) \quad \Lambda \otimes R(s(x)) : g \mapsto gh, \quad \text{for the unique } h = g^{-1}s(x)^{-1}gs(x) \in H.$$

For a character χ of the subgroup H , we introduce an integral transformation $\hat{\cdot} : L_1(X) \rightarrow C(G)$:

$$(IV.5.28) \quad \hat{k}(g) = \int_X k(x)\chi(g^{-1}s(x)^{-1}gs(x)) dx,$$

where $h(x, g) = g^{-1}s(x)^{-1}gs(x)$ is in H due to the relations (IV.5.26). This transformation generalises the isotropic symbol defined for the Heisenberg group in [139, § 2.1].

PROPOSITION IV.5.8 ([202]). *Let a subgroup H of G have the complemented commutator property (IV.5.26) and ρ_χ be an irreducible representation of G induced from a character χ of H , then*

$$(IV.5.29) \quad \|\rho_\chi(f)\| \leq \|f\widehat{\Phi^{-1}}\|_\infty,$$

with the sup-norm of the function $f\widehat{\Phi^{-1}}$ on the right.

PROOF. For an induced representation ρ_χ [159, § 13.2], the covariant transform \mathcal{W}_ϕ maps V to a space $L_2^X(G)$ of functions having the property $F(gh) = \chi(h)F(g)$ [204, § 3.1]. From (IV.5.27), the restriction of $\Lambda \otimes R$ to the space $L_2^X(G)$ is:

$$\Lambda \otimes R(s(x)) : \psi(g) \mapsto \psi(gh) = \chi(h(x, g))\psi(g).$$

In other words, $\Lambda \otimes R$ acts by multiplication on $L_2^X(G)$. Then, integrating the representation $\Lambda \otimes R$ over X with a function k we get an operator $(\Lambda \otimes R)(k)$, which reduces on the irreducible component to multiplication by the function $\hat{k}(g)$. Put $k = f\Phi^{-1}$

for $\Phi = \mathcal{W}_\phi \phi$. Then, from the inequality (IV.5.25), the norm of operator $\rho_\chi(f)$ can be estimated by $\|\Lambda \otimes \mathcal{R}(f\Phi^{-1})\| = \|\widehat{f\Phi^{-1}}\|_\infty$. \square

For a nilpotent step 2 Lie group, the transformation (IV.5.28) is almost the Fourier transform, cf. the case of the Heisenberg group in [139, § 2.1]. This allows to estimate $\|\widehat{f\Phi^{-1}}\|_\infty$ through $\|\widehat{f}\|_\infty$, where \widehat{f} is in the essence the symbol of the respective PDO. For other groups, the expression $g^{-1}s(x)^{-1}gs(x)$ in (IV.5.28) contains non-linear terms and its analysis is more difficult. In some circumstance the integral Fourier operators [320, Ch. VIII] may be useful for this purpose.

Open Problems

A reader may already note numerous objects and results, which deserve a further consideration. It may also worth to state some open problems explicitly. In this section we indicate several directions for further work, which go through four main areas described in the paper.

A.1. Geometry

Geometry is most elaborated area so far, yet many directions are waiting for further exploration.

- i. Möbius transformations (I.1.1) with three types of hypercomplex units appear from the action of the group $SL_2(\mathbb{R})$ on the homogeneous space $SL_2(\mathbb{R})/H$ [194], where H is any subgroup A, N, K from the Iwasawa decomposition (I.3.12). Which other actions and hypercomplex numbers can be obtained from other Lie groups and their subgroups?
- ii. Lobachevsky geometry of the upper half-plane is extremely beautiful and well-developed subject [26, 71]. However the traditional study is limited to one subtype out of nine possible: with the complex numbers for Möbius transformation and the complex imaginary unit used in FSCc (??). The remaining eight cases shall be explored in various directions, notably in the context of discrete subgroups [24].
- iii. The Fillmore-Springer-Cnops construction, see subsection ??, is closely related to the *orbit method* [161] applied to $SL_2(\mathbb{R})$. An extension of the orbit method from the Lie algebra dual to matrices representing cycles may be fruitful for semisimple Lie groups.
- iv.
- v. A development of a discrete version of the geometrical notions can be derived from suitable discrete groups. A natural first example is the group $SL_2(\mathbb{F})$, where \mathbb{F} is a finite field, e.g. \mathbb{Z}_p the field of integers modulo a prime p .

A.2. Analytic Functions

It is known that in several dimensions there are different notions of analyticity, e.g. several complex variables and Clifford analysis. However, analytic functions of a complex variable are usually thought to be the only options in a plane domain. The following seems to be promising:

- i. Development of the basic components of analytic function theory (the Cauchy integral, the Taylor expansion, the Cauchy-Riemann and Laplace equations, etc.) from the same construction and principles in the elliptic, parabolic and hyperbolic cases and respective subcases.
- ii. Identification of Hilbert spaces of analytic functions of Hardy and Bergman types, investigation of their properties. Consideration of the corresponding Toeplitz operators and algebras generated by them.
- iii. Application of analytic methods to elliptic, parabolic and hyperbolic equations and corresponding boundary and initial values problems.
- iv. Generalisation of the results obtained to higher dimensional spaces. Detailed investigation of physically significant cases of three and four dimensions.
- v. There is a current interest in construction of analytic function theory on discrete sets. Our approach is ready for application to an analytic functions in discrete geometric set-up outlined in item [A.1.0.v](#) above.

A.3. Functional Calculus

The functional calculus of a finite dimensional operator considered in Section [III.1](#) is elementary but provides a coherent and comprehensive treatment. It shall be extended to further cases where other approaches seems to be rather limited.

- i. Nilpotent and quasinilpotent operators have the most trivial spectrum possible (the single point $\{0\}$) while their structure can be highly non-trivial. Thus the standard spectrum is insufficient for this class of operators. In contract, the covariant calculus and the spectrum give complete description of nilpotent operators—the basic prototypes of quasinilpotent ones. For quasinilpotent operators the construction will be more complicated and shall use analytic functions mentioned in [A.2.0.i](#).
- ii. The version of covariant calculus described above is based on the *discrete series* representations of $SL_2(\mathbb{R})$ group and is particularly suitable for the description of the *discrete spectrum* (note the remarkable coincidence in the names).

It is interesting to develop similar covariant calculi based on the two other representation series of $SL_2(\mathbb{R})$: *principal* and *complementary* [\[240\]](#). The corresponding versions of analytic function theories for principal [\[170\]](#) and complementary series [\[191\]](#) were initiated within a unifying framework. The classification of analytic function theories into elliptic, parabolic, hyperbolic [\[185, 191\]](#) hints the following associative chains:

Representations	—	Function Theory	—	Type of Spectrum
discrete series	—	elliptic	—	discrete spectrum
principal series	—	hyperbolic	—	continuous spectrum
complementary series	—	parabolic	—	residual spectrum

- iii. Let a be an operator with $\text{sp } a \in \mathbb{D}$ and $\|a^k\| < Ck^p$. It is typical to consider instead of a the *power bounded* operator ra , where $0 < r < 1$, and consequently develop its H_∞ calculus. However such a regularisation is very rough and

hides the nature of extreme points of $\text{sp } a$. To restore full information a subsequent limit transition $r \rightarrow 1$ of the regularisation parameter r is required. This makes the entire technique rather cumbersome and many results have an indirect nature.

The regularisation $a^k \rightarrow a^k/k^p$ is more natural and accurate for polynomially bounded operators. However it cannot be achieved within the homomorphic calculus Defn. III.1.1 because it is not compatible with any algebra homomorphism. Albeit this may be achieved within the covariant calculus Defn. III.1.4 and Bergman type space from A.2.0.ii.

- iv. Several non-commuting operators are especially difficult to treat with functional calculus Defn. III.1.1 or a joint spectrum. For example, deep insights on joint spectrum of commuting tuples [319] refused to be generalised to non-commuting case so far. The covariant calculus was initiated [168] as a new approach to this hard problem and was later found useful elsewhere as well. Multidimensional covariant calculus [180] shall use analytic functions described in A.2.0.iv.
- v. As we noted above there is a duality between the co- and contravariant calculi from Defns. II.4.23 and II.4.25. We also seen in Section III.1 that functional calculus is an example of contravariant calculus and the functional model is a case of a covariant one. It is interesting to explore the duality between them further.

A.4. Quantum Mechanics

Due to the space restrictions we only touched quantum mechanics, further details can be found in [169, 181, 183, 184, 188, 199]. In general, Erlangen approach is much more popular among physicists rather than mathematicians. Nevertheless its potential is not exhausted even there.

- i. There is a possibility to build representation of the Heisenberg group using characters of its centre with values in dual and double numbers rather than in complex ones. This will naturally unifies classical mechanics, traditional QM and hyperbolic QM [155]. In particular, a full construction of the corresponding Fock–Segal–Bargmann spaces would be of interest.
- ii. Representations of nilpotent Lie groups with multidimensional centres in Clifford algebras as a framework for consistent quantum field theories based on De Donder–Weyl formalism [183].

REMARK A.1. This work is performed within the “Erlangen programme at large” framework [185, 191], thus it would be suitable to explain the numbering of various papers. Since the logical order may be different from chronological one the following numbering scheme is used:

Prefix	Branch description
"0" or no prefix	Mainly geometrical works, within the classical field of Erlangen programme by F. Klein, see [191, 194]
"1"	Papers on analytical functions theories and wavelets, e.g. [170]
"2"	Papers on operator theory, functional calculi and spectra, e.g. [182]
"3"	Papers on mathematical physics, e.g. [199]

For example, [199] is the first paper in the mathematical physics area. The present paper [197] outlines the whole framework and thus does not carry a subdivision number. The on-line version of this paper may be updated in due course to reflect the achieved progress.

Supplementary Material

B.1. Dual and Double Numbers

Complex numbers form a two-dimensional commutative associative algebra with an identity. Up to a suitable choice of a basis there are exactly three different types of such algebras—see [241]. They are spanned by a basis consisting of 1 and a hypercomplex unit ι . The square of ι is -1 for complex numbers, 0 for dual numbers and 1 for double numbers. In these cases, we write the hypercomplex unit ι as i , ε and j , respectively.

The arithmetic of hypercomplex numbers is defined by associative, commutative and distributive laws. For example, the product is

$$(u + \iota v)(u' + \iota v') = (uu' + \iota^2 vv') + \iota(uv' + u'v), \quad \text{where } \iota^2 = -1, 0, \text{ or } 1.$$

Further comparison of hypercomplex numbers is presented in Fig. B.2.

Despite significant similarities, only complex numbers belong to mainstream mathematics. Among their obvious advantages is the following:

- i. A product of complex numbers is equal to zero if and only if at least one factor is zero. This property is called the absence of *zero divisors*. Dual and double numbers both have large set of zero divisors.
- ii. Complex numbers are *algebraically closed*, that is, any polynomial with one variable with complex coefficients has a complex root. It is easy to see that dual and double numbers are not algebraically closed for the same reason as real numbers.

The first property is not very crucial, since zero divisors can be treated through appropriate techniques, e.g. projective coordinates, cf. Section I.8.1. The property of being algebraically-closed was not used in the present work. Thus, the absence of these properties is not an insuperable obstacle in the study of hypercomplex numbers. On the other hand, hypercomplex numbers naturally appeared in Section I.3.3 from $SL_2(\mathbb{R})$ action on the three different types of homogeneous spaces.

B.2. Classical Properties of Conic Sections

We call cycles three types of curves: circles, parabolas and equilateral hyperbolas. They belong to a large class of conic sections, i.e. they are the intersection of a cone with a plane, see Fig. I.1.3. Algebraically, cycles are defined by a quadratic equation (I.15.3) and are a subset of *quadrics*.

The beauty of conic sections has attracted mathematicians for several thousand years. There is an extensive literature—see [123, § 6] for an entry-level introduction and [36, Ch. 17] for a comprehensive coverage. We list below the basic definitions only in order to clarify the distinction between the classical foci, the centres of conic sections and our usage.

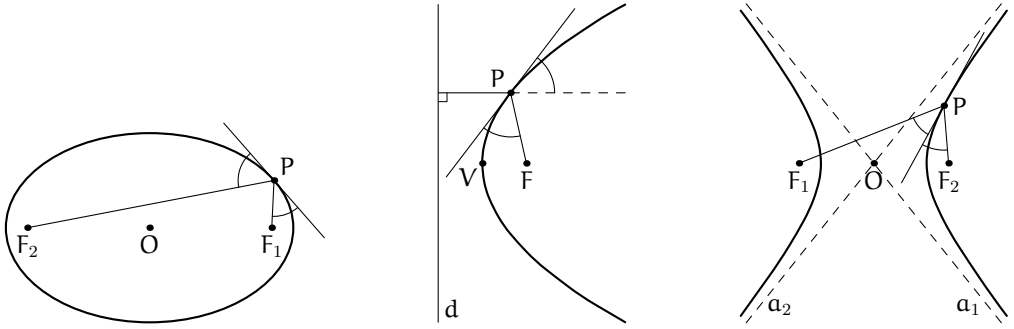


FIGURE B.1. Classical definitions of conic sections through the distances from foci. Equality of some angles can be derived and results in corresponding ray reflection.

We use the notation $|P_1P_2|$ and $|P l|$ for the Euclidean distance between points P_1 , P_2 and between a point P and a line l .

Ellipse: — a set of points P such that $|PF_1| + |PF_2| = \text{const}$ for two fixed points F_1 and F_2 , called the *foci* of the ellipse—see Fig. B.1. The midpoint O of the interval F_1F_2 is the ellipse’s *centre*. A *circle* is a particular case of an ellipse with $F_1 = F_2 = O$.

Parabola: — a set of points P such that $|PF| = |P d|$ for a fixed point F and a line d . They are called the *focus* and *directrix*, respectively. The point of the parabola nearest to the directrix is its *vertex*. The centre of a parabola is not usually defined.

Hyperbola: — a set of points P such that $|PF_1| - |PF_2| = \pm \text{const}$ for two fixed points F_1 and F_2 called the *foci* of the hyperbola. A hyperbola has two disjoint branches which tend to their *asymptotes*—see lines a_1 and a_2 in Fig. B.1. The midpoint O of the interval F_1F_2 , which is also the intersection of the asymptotes, is the hyperbola’s *centre*.

The above definition in terms of distances allows us to deduce the equality of the respective angles in each case—see Fig. B.1 and [123, § 6]. This implies reflection of the respective rays. For example, any ray perpendicular to the directrix is reflected by the parabola to pass its focus—the “burning point”. There are many applications of this, from the legendary burning of the Roman fleet by Archimedes to practical (parabolic) satellite dishes.

B.3. Comparison with Yaglom's Book

The profound book by Yaglom [339] is already a golden classic appreciated by several generations of mathematicians and physicists. To avoid confusion, we provide a comparison of our notions and results with Yaglom's.

Firstly, there is a methodological difference. Yaglom started from notions of length and angles and then derived objects (notably parabolas) which carry them out in an invariant way. We worked in the opposite direction by taking invariant objects (FSCC matrices) and deriving the respective notions and properties, which were also invariant. This leads to significant distinctions in our results which are collected in Fig. B.3.

In short, we tried to avoid an overlap with Yaglom's book [339]—our results are either new or obtained in a different manner.

We may also note some later attempts to axiomatize the theory, see for example [315]. As it often happens with axiomatisation, the result may be compared with sun-dried fruits: it is suitable for long-term preservation but does not keep all its test, aroma and vitamins. Also, the fruit needs to be grown up within the synthetic approach beforehand.

B.4. Other Approaches and Results

The development of parabolic and hyperbolic analogues of complex analysis has a long but sporadic history. In the absence of continuity, there are many examples when a researcher started from a scratch without any knowledge of previous works. There may be even more forgotten papers on the subject. To improve the situation, we list here some papers without trying to be comprehensive or even representative.

The survey and history of Cayley–Klein geometries is presented in Yaglom's book [339] and this will be completed by the work [284] which provides the full axiomatic classification of EPH cases. See also [270, 304, 311] for modern discussion of the Erlangen programme. A search for hyperbolic function theory was attempted several times starting from the 1930s—see, for example, [241, 253, 260, 286, 332]. Despite some important advances, the obtained hyperbolic theory is not yet as natural and complete as complex analysis is. Parabolic geometry was considered in [339] with rather trivial “parabolic calculus” described in [58]. There is also interest in this topic from different areas: differential geometry [19, 29, 44, 57, 58, 79, 102, 229, 230, 308, 342], kinematics [78, 232, 331, 339], quantum mechanics [9, 118, 120, 133, 142, 143, 151, 154, 155, 157, 325, 327], group representations [115, 116], space-time geometry [42, 130, 131, 141, 256], hypercomplex analysis [60; 90; 91; 170; 234; 235, Part IV; 243] and non-linear dynamics [281–283], integrability of discrete equations [41, 226–228, 297].

B.5. FSCc with Clifford Algebras

Our CAS uses FSCc, which is expressed through Clifford algebras [191, 211]. Clifford algebras also admit straightforward generalisation to higher dimensions. There are two slightly different forms: so called vector (all versions of CAS) and paravector (since v.3.0 only) formalisms. In paravector formalism a point with coordinates (u, v) is represented by the paravector $u\mathbf{1} + v\mathbf{e}_0$ from the Clifford algebra with the single generator \mathbf{e}_0 and unit $\mathbf{1}$. Such Clifford algebra is commutative and effectively isomorphic to

complex, dual or double numbers depending on the value e_0^2 . Therefore, all FSCc matrix formulae for the paravector formalism coincide with ones presented in this book.

In vector formalism a point with coordinates (u, v) is represented by the vector $ue_0 + ve_1$ from the Clifford algebra with two generators e_0 and e_1 which anticommute: $e_0e_1 = -e_1e_0$. Although, in this case, we need to take care on the non-commutativity of Clifford numbers, many matrix expressions have a simpler form. We briefly outline differences in FSCc for vector formalism below.

Let $\mathcal{C}(\sigma)$ be the four-dimensional Clifford algebra with unit 1 , two generators e_0 and e_1 , and the fourth element of the basis, their product e_0e_1 . The multiplication table is $e_0^2 = -1$, $e_1^2 = \sigma$ and $e_0e_1 = -e_1e_0$. Here, $\sigma = -1, 0$ and 1 in the respective EPH cases. The point space \mathbb{A} consists of vectors $ue_0 + ve_1$. An isomorphic realisation of $SL_2(\mathbb{R})$ is obtained if we replace a matrix $\begin{pmatrix} a & b \\ c & d \end{pmatrix}$ by $\begin{pmatrix} a & be_0 \\ -ce_0 & d \end{pmatrix}$ for any σ . The Möbius transformation of $\mathbb{A} \rightarrow \mathbb{A}$ for all three algebras $\mathcal{C}(\sigma)$ by the same expression, cf. (I.3.24), is

$$(B.1) \quad \begin{pmatrix} a & be_0 \\ -ce_0 & d \end{pmatrix} : ue_0 + ve_1 \mapsto \frac{a(ue_0 + ve_1) + be_0}{-ce_0(ue_0 + ve_1) + d},$$

where the expression $\frac{a}{b}$ in a non-commutative algebra is understood as ab^{-1} .

In Clifford algebras, the FSCc matrix of a cycle (k, l, n, m) is, cf. (I.4.5),

$$(B.2) \quad C_{\check{\sigma}}^s = \begin{pmatrix} l\check{e}_0 + sn\check{e}_1 & m \\ k & -l\check{e}_0 - sn\check{e}_1 \end{pmatrix}, \quad \text{with } \check{e}_0^2 = -1, \check{e}_1^2 = \check{\sigma},$$

where the EPH type of $\mathcal{C}(\check{\sigma})$ may be different from the type of $\mathcal{C}(\sigma)$. In terms of matrices (B.1) and (B.2) the $SL_2(\mathbb{R})$ -similarity (I.4.7) has exactly the same form $\tilde{C}_{\check{\sigma}}^s = gC_{\check{\sigma}}^s g^{-1}$. However, the cycle similarity (I.6.10) becomes simpler, e.g. there is no need in conjugation:

$$(B.3) \quad C_{\check{\sigma}}^s : \tilde{C}_{\check{\sigma}}^s \mapsto C_{\check{\sigma}}^s \tilde{C}_{\check{\sigma}}^s C_{\check{\sigma}}^s.$$

The cycle product is $\Re \operatorname{tr}(C_{\check{\sigma}}^s \tilde{C}_{\check{\sigma}}^s)$ [191]. Its “imaginary” part (vanishing for hypercomplex numbers) is equal to the symplectic form of cycles’ centres.

Unit	
Number	w
Conjugation	w
Euler formula	$e^{it} =$
Modulus	$ w _e^2 =$
Argument	\arg
Zero divisors	
Inverse	
Unit cycle	cir

FIGURE B.2. The correspondence between complex, dual and double numbers.

Notion	Yaglom's usage	This work
Circle	Defined as a locus of equidistant points in metric $d(u, v; u', v') = u - u' $. Effectively is a pair of vertical lines.	A limiting case of p-cycles with $n = 0$. Forms a Möbius-invariant subfamily of selfadjoint p-cycles (Definition 1.6.12). In this case, all three centres coincide. We use term "circle" only to describe a drawing of a cycle in the elliptic point space \mathbb{C} .
Cycle	Defined as locus of points having fixed angle view to a segment. Effectively is a non-degenerate parabola with a vertical axis.	We use this word for a point of the projective cycle space \mathbb{P}^3 . Its drawing in various point spaces can be a circle, parabola, hyperbola, single or pair of lines, single point or an empty set.
Centre	Absent, Yaglom's cycles are "centreless".	A cycle has three EPH centres.
Diameter	A quarter of the parabola's focal length.	The distance between real roots.
Special lines	Vertical lines, special role reflects absolute time in Galilean mechanics.	The intersection of invariant sets of selfadjoint and zero radius p-cycles, i.e. having the form $(1, 1, 0, 1^2)$.
Orthogonal, perpendicular	The relation between two lines, if one of them is special. Delivers the shortest distance.	We have a variety of different orthogonality and perpendicularity relations, which are not necessary local and symmetric.
Inversion in circles.	Defined through the degenerated p-metric	Conjugation with a degenerate parabola ($n = 0$).
Reflection in cycles	Defined as a reflection in the parabola along the special lines.	Composition of conjugation with three parabolas—see Exercise 1.6.33.

FIGURE B.3. Comparison with the Yaglom book

How to Use the Software

This is information about Open Source Software project [Moebinv \[211\]](#), see its Webpage¹ for updates.

It is easier to use the MoebInv package than ever. The simplest options are:

- i. Download [precompiled GUI](#) for your OS. The GUI has self-contained help system, please use it for further advise.
- ii. Work with Jupyter notebooks at your Web-browser. You can access these at either:
 - on [Google Colab \[214\]](#); or
 - on [CodeOcean capsule \[213\]](#).

Once you started a Jupyter notebook you can skip to Section [C.3](#) for introduction.

The third possibility is live DVD (ISO image), its installation is explained in Section [C.2](#). You can skip to Section [C.3](#) if you are not using this route. The live DVD/ISO images are derived from several open-source projects, notably Debian GNU–Linux [\[309\]](#), GiNaC library of symbolic calculations [\[21\]](#), Asymptote [\[126\]](#) and many others. Thus, our work is distributed under the *GNU General Public License (GPL) 3.0* [\[112\]](#).

You can download an ISO image of a Live GNU–Linux DVD with our CAS from several locations. The initial (now outdated) version was posted through the Data Conservancy Project [arXiv.org](#) associated to paper [\[186\]](#). A newer version of ISO is now included as an auxiliary file to the same paper, see the subdirectory:

<http://arxiv.org/src/cs/0512073v11/anc>

Also, an updated versions (v3.5.8) of the ISO image for **amd64** architecture is uploaded to clouds:

<https://tinyurl.com/rvhyyv2>

<https://drive.google.com/file/d/1I3XT91pfXY2BbZbxSOXJLfVvthSb4hkb/view?usp=sharing>

In this Appendix, we only briefly outline how to start using the enclosed DVD or ISO image. As soon as the DVD is running or the ISO image is mounted as a virtual file system, further help may be obtained on the computer screen. We also describe how to run most of the software on the disk on computers without a DVD drive at the end of Sections [C.1](#), [C.2.1](#) and [C.2.2](#).

¹<http://moebinv.sourceforge.net/>

C.1. Viewing Colour Graphics

The easiest part is to view colour illustrations on your computer. There are not many hardware and software demands for this task—your computer should have a DVD drive and be able to render HTML pages. The last task can be done by any web browser. If these requirements are satisfied, perform the following steps:

1. Insert the DVD disk into the drive of your computer.
2. Mount the disk, if required by your OS.
3. Open the contents of the DVD in a file browser.
4. Open the file `index.html` from the top-level folder of the DVD in a web browser, which may be done simply by clicking on its icon.
5. Click in the browser on the link [View book illustrations](#).

If your computer does not have a DVD drive (e.g. is a netbook), but you can gain brief access to a computer with a drive, then you can copy the top-level folder `doc` from the enclosed DVD to a portable medium, say a memory stick. Illustrations (and other documentation) can be accessed by opening the `index.html` file from this folder.

In a similar way, the reader can access ISO images of bootable disks, software sources and other supplementary information described below.

C.2. Installation of CAS

There are three major possibilities of using the enclosed CAS:

- A. To boot your computer from the DVD itself.
- B. To run it in a Linux emulator.
- C. *Advanced*: recompile it from the enclosed sources for your platform.

Method A is straightforward and can bring some performance enhancement. However, it requires hardware compatibility; in particular, you must have the so-called `amd64` (or `i386` for previous versions up to `v3.0`) architecture. Method B will run on a much wider set of hardware and you can use CAS from the comfort of your standard desktop. However, this may require an additional third-party programme to be installed.

C.2.1. Booting from the DVD Disk. WARNING: it is a general principle, that running a software within an emulator is more secure than to boot your computer in another OS. Thus we recommend using the method described in Section [C.2.2](#).

It is difficult to give an exact list of hardware requirements for DVD booting, but your computer must be based on the `amd64` architecture. If you are ready to have a try, follow these steps:

1. Insert the DVD disk into the drive of your computer.
2. Switch off or reboot the computer.
3. Depending on your configuration, the computer may itself attempt to boot from the DVD instead of its hard drive. In this case you can proceed to step 5.
4. If booting from the DVD does not happen, then you need to reboot again and bring up the “boot menu”, which allows you to chose the boot device manually. This menu is usually prompted by a “magic key” pressed just after

the computer is powered on—see your computer documentation. In the boot menu, chose the CD/DVD drive.

5. You will be presented with the screen shown on the left in Fig. C.1. Simply press Enter to chose the “Live (486)” or “Live (686-pae)” (for more advanced processors) to boot. To run 686-pae kernel in an emulator, e.g. VirtualBox, you may need to allow “PAE option” in settings.
6. If the DVD booted well on your computer you will be presented with the GUI screen shown on the right in Fig. C.1. Congratulations, you can proceed to Section C.3.

If the DVD boots but the graphic X server did not start for any reason and you have the text command prompt only, you can still use most of the CAS. This is described in the last paragraph of Section C.3.

If your computer does not have a DVD drive you may still boot the CAS on your computer from a spare USB stick of at least 1Gb capacity. For this, use UNetbootin [13] or a similar tool to put an ISO image of a boot disk on the memory stick. The ISO image(s) is located at the top-level folder `iso-images` of the DVD and the file `README` in this folder describes them. You can access this folder as described in Section C.1.

C.2.2. Running a Linux Emulator. You can also use the enclosed CAS on a wide range of hardware running various operating systems, e.g. Linux, Windows, Mac OS, etc. To this end you need to install a so-called *virtual machine*, which can emulate amd64 architecture. I would recommend VirtualBox [271]—a free, open-source program which works well on many existing platforms. There are many alternatives (including open-source), for example: Qemu [31], Open Virtual Machine [272] and some others.

Here, we outline the procedure for VirtualBox—for other emulators you may need to make some adjustments. To use VirtualBox, follow these steps:

1. Insert the DVD disk in your computer.
2. Open the `index.html` file from the top directory of the DVD disk and follow the link “Installing VirtualBox”. This is a detailed guide with all screenshots. Below we list only the principal steps from this guide.
3. Go to the web site of VirtualBox [271] and proceed to the download page for your platform.
4. Install VirtualBox on your computer and launch it.
5. Create a new virtual machine. Use either the entire DVD or the enclosed ISO images for the virtual DVD drive. If you are using the ISO images, you may wish to copy them first to your hard drive for better performance and silence. See the file `README` in the top-level folder `iso-images` for a description of the image(s).
6. Since a computer emulation is rather resource-demanding, it is better to close all other applications on slower computers (e.g. with a RAM less than 1Gb).
7. Start the newly-created machine. You will need to proceed through steps 5–6 from the previous subsections, as if the DVD is booting on your real computer. As soon as the machine presents the GUI, shown on the right in Fig. C.1, you are ready to use the software.

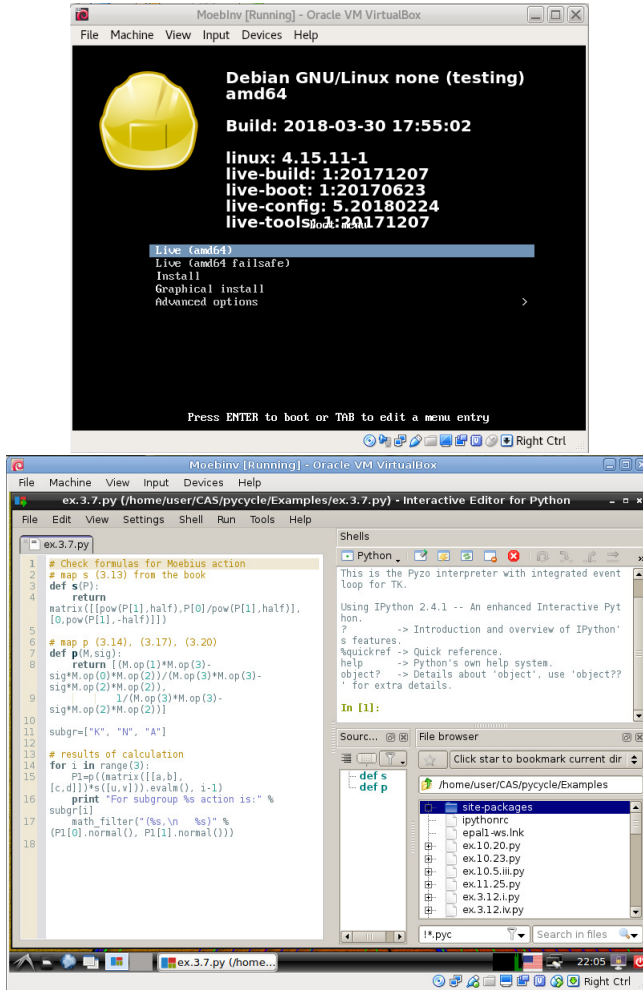


FIGURE C.1. Initial screens of software start up. First, DVD boot menu; second, IDE screen after the booting.

If you succeeded in this you may proceed to Section C.3. Some tips to improve your experience with emulations are described in the detailed electronic manual.

C.2.3. Recompiling the CAS on Your OS. The core of our software is a C++ library which is based on GiNaC [21]—see its web page for up-to-date information. The latter can be compiled and installed on both Linux and Windows. Subsequently, our library can also be compiled on these computers from the provided sources. Then, the library can be used in your C++ programmes. See the top-level folder `src` on the DVD and the documentation therein. Also, the library source code (files `cycle.h` and `cycle.cpp`) is

produced in the current directory if you pass the \TeX file of the paper [186] through \LaTeX .

Our interactive tool is based on pyGiNaC [50]—a Python binding for GiNaC. This may work on many flavours of Linux as well. Please note that, in order to use pyGiNaC with the recent GiNaC, you need to apply my patches to the official version. The DVD contains the whole pyGiNaC source tree which is already patched and is ready to use.

There is also a possibility to use our library interactively with swiGiNaC [307], which is another Python binding for GiNaC and is included in many Linux distributions. The complete sources for binding our library to swiGiNaC are in the corresponding folder of the enclosed DVD. However, swiGiNaC does not implement full functionality of our library.

C.3. Using the CAS and Computer Exercises

Once you have booted to the GUI with the open CAS window as described in Subsections C.2.1 or C.2.2, a window with Pyzo (an integrated development environment—IDE) shall start. The left frame is an editor for your code, some exercises from the book will appear there. Top right frame is a IPython shell, where your code will be executed. Bottom left frame presents the files tree.

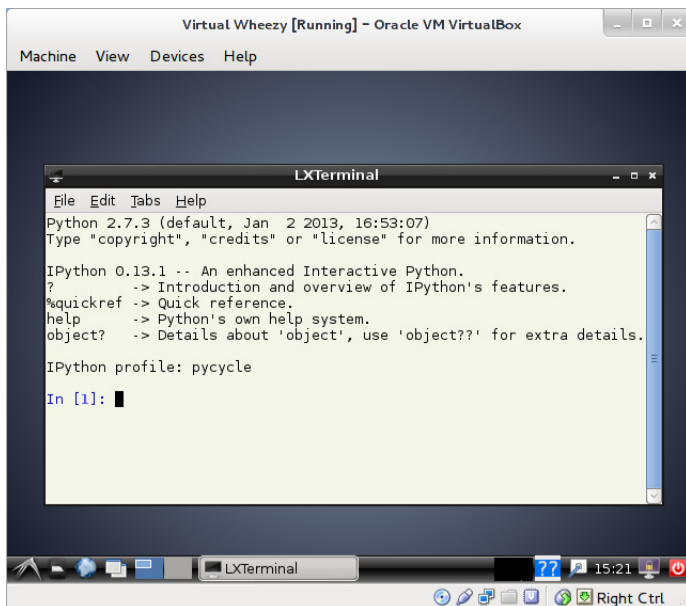


FIGURE C.2. IPython shell.

Pyzo has a modern graphical user interface (GUI) and a detailed help system, thus we do not need to describe its work here. On the other hand, if a user wish to work with IPython shell alone (see Fig. C.2), he may start the shall from

Main Me

The presentation below will be given in terms of IPython shell, an interactions with Pyzo is even more intuitive.

Initially, you may need to configure your keyboard (if it is not a US layout). To install, for example, a Portuguese keyboard, you may type the following command at the IPython prompt (e.g. the top right frame of Pyzo):

```
In [2]: !change-xkb pt
```

The keyboard will be switched and the corresponding national flag displayed at the bottom-left corner of the window. For another keyboard you need to use the international two-letter country code instead of `pt` in the above command. The first exclamation mark tells that the interpreter needs to pass this command to the shell.

C.3.1. Warming Up. The first few lines at the top of the CAS windows suggest several commands to receive a quick introduction or some help on the IPython interpreter [280]. Our CAS was loaded with many predefined objects—see Section C.5. Let us see what `C` is, for example:

```
In [3]: print C
-----> print(C)
[cycle2D object]
```

```
In [4]: print C.string()
-----> print(C.string())
(k, [L,n],m)
```

Thus, `C` is a two-dimensional cycle defined with the quadruple (k, l, n, m) . Its determinant is:

```
In [5]: print C.hdet()
-----> print(C.hdet())
k*m-L**2+si*n**2
```

Here, `si` stands for σ —the signature of the point space metric. Thus, the answer reads $km - l^2 + \sigma n^2$ —the determinant of the FSCc matrix of `C`. Note, that terms of the expression can appear in a different order: GiNaC does not have a predefined sorting preference in output.

As an exercise, the reader may now follow the proof of Theorem I.4.13, remembering that the point `P` and cycle `C` are already defined. In fact, all statements and exercises marked by the symbol ∇ on the margins are already present on the DVD. For example, to access the proof of Theorem I.4.13, type the following at the prompt:

```
In [6]: %ed ex.4.13.py
```

Here, the *special* `%ed` instructs the external editor `jed` to visit the file `ex.I.4.13.py`. This file is a Python script containing the same lines as the proof of Theorem I.4.13 in the book. The editor `jed` may be manipulated from its menu and has command keystrokes compatible with GNU Emacs. For example, to exit the editor, press `Ctrl-X Ctrl-C`. After that, the interactive shell executes the visited file and outputs:

```
In [6]: %ed ex.4.13.py
Editing... done. Executing edited code...
Conjugated cycle passes the Moebius image of P: True
```

Thus, our statement is proven.

For any other CAS-assisted statement or exercise you can also visit the corresponding solution using its number next to the symbol ∇ in the margin. For example, for Exercise I.6.22, open file `ex.I.6.22.py`. However, the next mouse sign marks the item I.6.24.i, thus you need to visit file `ex.I.6.24.i.py` in this case. These files are located on a read-only file system, so to modify them you need to save them first with a new name (Ctrl-X Ctrl-W), exit the editor, and then use %ed special to edit the freshly-saved file.

C.3.2. Drawing Cycles. You can visualise cycles instantly. First, we open an Asymptote instance and define a picture size:

```
In [7]: A=asy()
```

Asymptote session is open. Available methods are:

```
help(), size(int), draw(str), fill(str), clip(str), ...
```

```
In [8]: A.size(100)
```

Then, we define a cycle with centre $(0, 1)$ and σ -radius 2:

```
In [9]: Cn=cycle2D([0,1],e,2)
```

```
In [10]: print Cn.string()
```

```
-----> print(Cn.string())
```

```
(1, [0,1],-2-si)
```

This cycle depends on a variable `sign` and it must be substituted with a numeric value before a visualisation becomes possible:

```
In [11]: A.send(cycle2D(Cn.subs(sign==1)).asy_string())
```

```
In [12]: A.send(cycle2D(Cn.subs(sign==0)).asy_string())
```

```
In [13]: A.send(cycle2D(Cn.subs(sign==1)).asy_string())
```

```
In [14]: A.shipout("cycles")
```

```
In [15]: del(A)
```

By now, a separate window will have opened with cycle `Cn` drawn triply as a circle, parabola and hyperbola. The image is also saved in the Encapsulated Postscript (EPS) file `cycles.eps` in the current directory.

Note that you do not need to retype inputs 12 and 13 from scratch. Up/down arrows scroll the input history, so you can simply edit the value of `sign` in the input line 11. Also, since you are in Linux, the Tab key will do a completion for you whenever possible.

The interactive shell evaluates and remember all expressions, so it may sometime be useful to restart it. It can be closed by Ctrl-D and started from the Main Menu (the bottom-left corner of the screen) using Accessories \rightarrow CAS pycyle. In the same menu

folder, there are two items which open documentation about the library in PDF and HTML formats.

C.3.3. Library figure. There is a high-level library figure, which allows to describe ensembles of cycles through various relations between elements. Let us start from the example. First, we create an empty figure F with the elliptic geometry, given by the diagonal matrix $\begin{pmatrix} -1 & 0 \\ 0 & -1 \end{pmatrix}$:

```
$ from figure import *
$ F=figure([-1,-1])
```

Every (even “empty”) figure comes with two predefined cycles: the real line and infinity. Since they will be used later, we get an access to them:

```
$ RL=F.get_real_line()
$ inf=F.get_infinity()
```

We can add new cycles to the figure explicitly specifying their parameters. For example, for $k = 1, l = 3, n = 2, m = 12$:

```
$ A=F.add_cycle(cycle2D(1, [3,2], 12), "A")
```

A point (zero-radius cycle) can be specified by its coordinates (coordinates of its centre):

```
$ B=F.add_point([0,1], "B")
```

Now we use the main feature of this library and add a new cycles c through its relations to existing members of the figure F :

```
$ c=F.add_cycle_rel([is_orthogonal(A), is_orthogonal(B), \
$ is_orthogonal(RL)], "c")
```

Cycle c will be orthogonal to cycle A , passes through point B (that is orthogonal to the zero-radius cycle representin B), and orthogonal to the real line. The last condition characterises a line in the Lobachevsky half-plane. We can add a straight line requesting its orthogonality to the infinity. For example:

```
$ d=F.add_cycle_rel([is_orthogonal(A), is_orthogonal(B), \
$ is_orthogonal(inf)], "d")
```

We may want to find parameters of automatically calculated cycles c and d :

```
$ print F.string()
```

This produces an output, showing parameters of all cycles together with their mutual relations:

```
infy: {(0, [[0,0]]~infy, 1), -2} --> (d); <-- ()
R: {(0, [[0,1]]~R, 0), -1} --> (c); <-- ()
A: {(1, [[3,2]]~A, 12), 0} --> (c,d); <-- ()
B: {(1, [[0,1]]~B, 1), 0} --> (c,d); <-- (B/o,infy|d,B-(0)|o,B-(1)|o)
c: {(6/11, [[1,0]]~c, -6/11), 1} --> (); <-- (A|o,B|o,R|o)
d: {(0, [[-1/6,1/2]]~d, 1), 1} --> (); <-- (A|o,B|o,infy|o)
B-(0): {(0, [[1,0]]~B-(0), 0), -3} --> (B); <-- ()
B-(1): {(0, [[0,1]]~B-(1), 2), -3} --> (B); <-- ()
```

Note, two cycles $B-(0)$ and $B-(1)$ were automatically created as “invisible” parents of cycle (point) B .

Finally, we may want to see the drawing:


```
$ F.asy_write(300,-1.5,5,-5,5,"figure-example")
```

This creates an encapsulated PostScript file `figure-example.eps`, which is shown on Fig. C.3. See [211] for further documentation of `figure` library. Examples include symbolic calculations and *automatic theorem proving*.

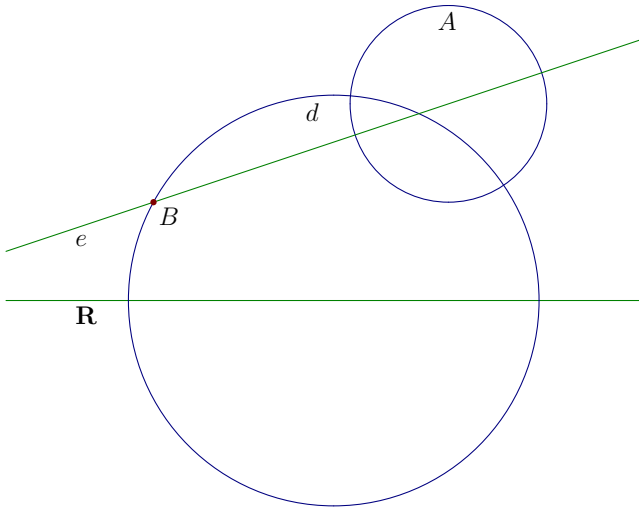


FIGURE C.3. Example of `figure` library usage.

C.3.4. Further Usage. There are several batch checks which can be performed with CAS. Open a terminal window from Main Menu → Accessories → LXTerminal. Type at the command prompt:

```
$ cd ~/CAS/pycycle/
$ ./run-pyGiNaC.sh test_pycycle.py
```

A comprehensive test of the library will be performed and the end of the output will look like this:

```
True: sl2_clifford_list: (0)
True: sl2_clifford_matrix: (0)
True: jump_fnct (-1)
```

Finished. The total number of errors is 0

Under normal circumstances, the reported total number of errors will, of course, be zero. You can also run all exercises from this book in a batch. From a new terminal window, type:

```
$ cd ~/CAS/pycycle/Examples/
$ ./check_all_exercises.sh
```

Exercises will be performed one by one with their numbers reported. Numerous graphical windows will be opened to show pencils of cycles. These windows can be closed by pressing the `q` key for each of them. This batch file suppresses all output from the exercises, except those containing the `False` string. Under normal circumstances, these are only Exercises I.7.14.i and I.7.14.ii.

You may also access the CAS from a command line. This may be required if the graphic X server failed to start for any reason. From the command prompt, type the following:

```
$ cd ~/CAS/pycycle/Examples/
$ ./run-pyGiNaC.sh
```

The full capacity of the CAS is also accessible from the command prompt, except for the preview of drawn cycles in a graphical window. However, EPS files can still be created with `Asymptote`—see `shipout()` method.

C.4. Library for Cycles

Our C++ library defines the class `cycle` to manipulate cycles of arbitrary dimension in a symbolic manner. The derived class `cycle2D` is tailored to manipulate two-dimensional cycles. For the purpose of the book, we briefly list here some methods for `cycle2D` in the `pyGiNaC` binding form only.

constructors: There are two main forms of `cycle2D` constructors:

```
C=cycle2D(k,[l,n],m,e) # Cycle defined by a quadruple
Cr=(u,v),e,r) # Cycle with center at [u,v] and radius r2
```

In both cases, we use a metric defined by a Clifford unit `e`.

operations: Cycles can be added (+), subtracted (-) or multiplied by a scalar (method `exmul()`). A simplification is done by `normal()` and substitution by `subs()`. Coefficients of cycles can be normalised by the methods `normalize()` (k-normalisation), `normalize_det()` and `normalize_norm()`.

evaluations: For a given cycle, we can make the following evaluations: `hdet()`—determinant of its (hypercomplex) FSCc matrix, `radius_sq()`—square of the radius, `val()`—value of a cycle at a point, which is the power of the point to the cycle.

similarities: There are the following methods for building cycle similarities: `s12_similarity()`, `matrix_similarity()` and `cycle_similarity()` with an element of $SL_2(\mathbb{R})$, a matrix or another cycle, respectively.

checks: There are several checks for cycles, which return `GiNaC` relations. The latter may be converted to Boolean values if no variables are presented within them. The checks for a single cycle are: `is_linear()`, `is_normalized()` and `passing()`, the latter requires a parameter (point). For two cycles, they are `is_orthogonal()` and `is_f_orthogonal()`.

specialisation: Having a cycle defined through several variables, we may try to specialise it to satisfy some further conditions. If these conditions are *linear* with respect to the cycle's variables, this can be achieved through the very useful method `subject_to()`. For example, for the above defined cycle `C`, we can find

```
C2=C.subject_to([C.passing([u,v]), C.is_orthogonal(C1)])
```

where `C2` will be a generic cycle passing the point `[u,v]` and orthogonal to `C1`. See the proof of Theorem I.4.13 for an application.

specific: There are the following methods specific to two dimensions: `focus()`, `focal_length()`—evaluation of a cycle's focus and focal length and `roots()`—finding intersection points with a vertical or horizontal line. For a generic line, use method `line_intersect()` instead.

drawing: For visualisation through `Asymptote`, you can use various methods: `asy_draw()`, `asy_path()` and `asy_string()`. They allow you to define the bounding box, colour and style of the cycle's drawing. See the examples or full documentation for details of usage.

Further information can be obtained from [electronic documentation](#) on the enclosed DVD, an inspection of the test file `CAS/pycycle/test_pycycle.py` and solutions of the exercises.

C.5. Predefined Objects at Initialisation

For convenience, we predefine many GiNaC objects which may be helpful. Here is a brief indication of the most-used:

```

realsymbol.: a, b, c, d: elements of  $SL_2(\mathbb{R})$  matrix.
u, v, u1, v1, u2, v2: coordinates of points.
r, r1, r2: radii.
k, l, n, m, k1, l1, n1, m1: components of cycles.
sign, sign1, sign2, sign3, sign4: signatures of various metrics.
s, s1, s2, s3: s parameters of FSCc matrices.
x, y, t: spare to use.
varidx.: mu, nu, rho, tau: two-dimensional (in vector formalism) or one-dimensional
indexes for Clifford units.
matrix.: M, M1, M2, M3: diagonal  $2 \times 2$  matrices with entries  $-1$  and  $i$ -th sign on their
diagonal.
sign_mat, sign_mat1, sign_mat2: similar matrices with  $i$ -th  $s$  instead of sign.
clifford_unit.: e, es, er, et: Clifford units with metrics derived from matrices M,
M1, M2, M3, respectively.
cycle2D.: The following cycles are predefined:
C=cycle2D(k,[l,n],m,e) # A generic cycle
C1=cycle2D(k1,[l1,n1],m1,e)# Another generic cycle
Cr=( [u,v],e,r2) # Cycle with centre at [u,v] and radius r2
Cu=cycle2D(1,[0,0],1,e) # Unit cycle
real_line=cycle2D(0,[0,1],0,e)
Z=cycle2D([u,v], e) # Zero radius cycles at [u,v]
Z1=cycle2D([u1,v1], e) # Zero radius cycles at [u1,v1]
Zinf=cycle2D(0,[0,0],1,e) # Zero radius cycles at infinity

```

The solutions of the exercises make heavy use of these objects. Their exact definition can be found in the file `CAS/pycycle/init_cycle.py` from the home directory.

Bibliography

- [1] F. Agostini, S. Caprara, and G. Ciccotti. Do we have a consistent non-adiabatic quantum-classical mechanics?. *Europhys. Lett. EPL*, **78** (3):Art. 30001, 6, 2007. doi: [10.1209/0295-5075/78/30001](https://doi.org/10.1209/0295-5075/78/30001). ↑[342](#)
- [2] L. V. Ahlfors. On the fixed points of Möbius transformations in \mathbf{R}^n . *Ann. Acad. Sci. Fenn. Ser. A I Math.*, **10**:15–27, 1985. ↑[191](#)
- [3] L. V. Ahlfors. Möbius transformations in \mathbb{R}^n expressed through 2×2 matrices of Clifford numbers. *Complex Variables Theory Appl.*, **5** (2):215–224, 1986. ↑[213](#)
- [4] A. Albargi. Some estimations for covariant transforms, 2013. (In preparation). ↑[293](#)
- [5] S. T. Ali, J.-P. Antoine, and J.-P. Gazeau. *Coherent states, wavelets and their generalizations*. Graduate Texts in Contemporary Physics. Springer-Verlag, New York, 2000. ↑[227](#), [231](#), [249](#), [250](#), [251](#), [253](#), [257](#), [260](#), [278](#), [281](#), [282](#), [284](#), [289](#), [290](#), [294](#), [296](#), [359](#), [365](#)
- [6] E. F. Allen. On a triangle inscribed in a rectangular hyperbola. *Amer. Math. Monthly*, **48**:675–681, 1941. ↑[173](#)
- [7] F. Almalki and V. V. Kisil. Geometric dynamics of a harmonic oscillator, arbitrary minimal uncertainty states and the smallest step 3 nilpotent Lie group. *J. Phys. A: Math. Theor*, **52**:025301, 2019. E-print: [arXiv:1805.01399](https://arxiv.org/abs/1805.01399). ↑[164](#)
- [8] R. F. V. Anderson. The Weyl functional calculus. *J. Functional Analysis*, **4**:240–267, 1969. ↑[302](#), [303](#)
- [9] F. Antonuccio. Hyperbolic numbers and the Dirac spinor. In V. V. Dvoeglazov (ed.) *The photon and Poincare group*, Nova Science Publisher, Inc., Commack, 1999. E-print: [arXiv:hep-th/9812036](https://arxiv.org/abs/hep-th/9812036). ↑[375](#)
- [10] D. N. Arnold and J. Rogness. Möbius transformations revealed. *Notices Amer. Math. Soc.*, **55** (10):1226–1231, 2008. ↑[3](#)
- [11] V. I. Arnol’d. *Mathematical methods of classical mechanics*. Graduate Texts in Mathematics, vol. 60. Springer-Verlag, New York, 1991. Translated from the 1974 Russian original by K. Vogtmann and A. Weinstein, corrected reprint of the second (1989) edition. ↑[53](#), [108](#), [113](#), [318](#), [323](#), [355](#)
- [12] D. Z. Arov and H. Dym. *J-contractive matrix valued functions and related topics*. Encyclopedia of Mathematics and its Applications, vol. 116. Cambridge University Press, Cambridge, 2008. ↑[244](#)
- [13] Arpad and G. Kovacs. *UNetbootin—create bootable Live USB drives for Linux*, 2011. URL: <http://unetbootin.sourceforge.net/>. ↑[381](#)
- [14] W. Arveson. *An invitation to C^* -algebras*. Springer-Verlag, 1976. ↑[150](#)
- [15] M. Atiyah and W. Schmid. A geometric construction of the discrete series for semisimple Lie group. In J. A. Wolf, M. Cahen, and M. D. Wilde (eds.) *Harmonic analysis and representations of semisimple Lie group*, pages 317–383, D. Reidel Publishing Company, Dordrecht, Holland, 1980. ↑[232](#)
- [16] M. B. Balk. Polyanalytic functions and their generalizations [MR1155418 (93f:30050)]. *Complex analysis, I*, pages 195–253, Springer, Berlin, 1997. ↑[271](#)
- [17] V. Bargmann. On a Hilbert space of analytic functions and an associated integral transform. Part I. *Comm. Pure Appl. Math.*, **3**:215–228, 1961. ↑[235](#), [238](#)
- [18] D. E. Barrett and M. Bolt. Cauchy integrals and Möbius geometry of curves. *Asian J. Math.*, **11** (1):47–53, 2007. ↑[205](#)
- [19] D. E. Barrett and M. Bolt. Laguerre arc length from distance functions. *Asian J. Math.*, **14** (2):213–233, 2010. ↑[173](#), [205](#), [375](#)
- [20] H. Bateman. *The mathematical analysis of electrical and optical wave-motion on the basis of Maxwell’s equations*. Dover Publications, Inc., New York, 1955. ↑[166](#)

- [21] C. Bauer, A. Frink, and R. Kreckel. Introduction to the GiNaC framework for symbolic computation within the C++ programming language. *J. Symbolic Computation*, **33** (1):1–12, 2002. Web: <http://www.ginac.de/>. E-print: [arXiv:cs/0004015](https://arxiv.org/abs/cs/0004015). ↑[160](#), [379](#), [382](#)
- [22] A. F. Beardon. Continued fractions, Möbius transformations and Clifford algebras. *Bull. London Math. Soc.*, **35** (3):302–308, 2003. ↑[207](#), [213](#), [214](#), [216](#)
- [23] A. F. Beardon and L. Lorentzen. Continued fractions and restrained sequences of Möbius maps. *Rocky Mountain J. Math.*, **34** (2):441–466, 2004. ↑[207](#), [209](#)
- [24] A. F. Beardon. *The geometry of discrete groups*. Graduate Texts in Mathematics, vol. 91. Springer-Verlag, New York, 1995. Corrected reprint of the 1983 original. ↑[64](#), [115](#), [125](#), [147](#), [151](#), [155](#), [156](#), [166](#), [177](#), [194](#), [199](#), [369](#)
- [25] A. F. Beardon. Continued fractions, discrete groups and complex dynamics. *Comput. Methods Funct. Theory*, **1** (2):535–594, 2001. ↑[207](#)
- [26] A. F. Beardon. *Algebra and geometry*. Cambridge University Press, Cambridge, 2005. ↑[3](#), [34](#), [53](#), [115](#), [122](#), [155](#), [185](#), [187](#), [369](#)
- [27] A. F. Beardon and I. Short. Conformal symmetries of regions. *Irish Math. Soc. Bull.*, **59**:49–60, 2007. ↑[64](#), [274](#)
- [28] A. F. Beardon and I. Short. A geometric representation of continued fractions. *Amer. Math. Monthly*, **121** (5):391–402, 2014. ↑[160](#), [166](#), [207](#), [208](#), [209](#), [211](#), [212](#), [213](#), [214](#), [216](#)
- [29] E. Bekkara, C. Frances, and A. Zeghib. On lightlike geometry: Isometric actions, and rigidity aspects. *C. R. Math. Acad. Sci. Paris*, **343** (5):317–321, 2006. ↑[375](#)
- [30] J. L. Bell. *A primer of infinitesimal analysis*. Cambridge University Press, Cambridge, Second, 2008. ↑[320](#)
- [31] F. Bellard. *QEMU—a generic and open source machine emulator and virtualizer*, 2011. URL: <http://qemu.org/>. ↑[381](#)
- [32] W. Benz. *Classical geometries in modern contexts. Geometry of real inner product spaces*. Birkhäuser Verlag, Basel, Second edition, 2007. ↑[118](#), [147](#), [159](#), [160](#), [162](#), [197](#)
- [33] W. Benz. A fundamental theorem for dimension-free Möbius sphere geometries. *Aequationes Math.*, **76** (1–2):191–196, 2008. ↑[45](#), [161](#)
- [34] F. A. Berezin. Covariant and contravariant symbols of operators. *Izv. Akad. Nauk SSSR Ser. Mat.*, **36**:1134–1167, 1972. Reprinted in [[35](#)], pp. 228–261]. ↑[254](#), [255](#)
- [35] F. A. Berezin. *Metod vtorichnogo kvantovaniya*. “Nauka”, Moscow, Second ed., 1986. Edited and with a preface by M. K. Polivanov. ↑[238](#), [254](#), [392](#)
- [36] M. Berger. *Geometry. II*. Universitext. Springer-Verlag, Berlin, 1987. Translated from the French by M. Cole and S. Levy. ↑[102](#), [147](#), [374](#)
- [37] M. Berger. *Geometry. I*. Universitext. Springer-Verlag, Berlin, 1994. Translated from the 1977 French original by M. Cole and S. Levy, Corrected reprint of the 1987 translation. ↑[58](#), [73](#)
- [38] D. Bernier and K. F. Taylor. Wavelets from square-integrable representations. *SIAM J. Math. Anal.*, **27** (2):594–608, 1996. MR97h:22004. ↑[227](#)
- [39] G. Birkhoff. Orthogonality in linear metric spaces. *Duke Math. J.*, **1** (2):169–172, 1935. ↑[94](#)
- [40] C. J. Bishop, A. Böttcher, Yu. I. Karlovich, and I. Spitkovsky. Local spectra and index of singular integral operators with piecewise continuous coefficients on composed curves. *Math. Nachr.*, **206**:5–83, 1999. ↑[194](#), [205](#)
- [41] A. I. Bobenko and W. K. Schief. Circle complexes and the discrete CKP equation. *Int. Math. Res. Not. IMRN*, **5**:1504–1561, 2017. ↑[166](#), [375](#)
- [42] D. Boccaletti, F. Catoni, R. Cannata, V. Catoni, E. Nichelatti, and P. Zampetti. *The mathematics of Minkowski space-time and an introduction to commutative hypercomplex numbers*. Birkhäuser Verlag, Basel, 2008. ↑[109](#), [111](#), [116](#), [375](#)
- [43] M. Bolt. Extremal properties of logarithmic spirals. *Beiträge Algebra Geom.*, **48** (2):493–520, 2007. ↑[194](#), [205](#)
- [44] M. Bolt, T. Ferdinands, and L. Kavlie. The most general planar transformations that map parabolas into parabolas. *Involve*, **2** (1):79–88, 2009. ↑[156](#), [375](#)
- [45] J. Borwein, A. van der Poorten, J. Shallit, and W. Zudilin. *Neverending fractions. An introduction to continued fractions*. Australian Mathematical Society Lecture Series, vol. 23. Cambridge University Press, Cambridge, 2014. ↑[207](#)

- [46] A. Böttcher and Yu. I. Karlovich. Cauchy's singular integral operator and its beautiful spectrum. *Systems, approximation, singular integral operators, and related topics (Bordeaux, 2000)*, pages 109–142, Birkhäuser, Basel, 2001. ↑[194](#), [205](#)
- [47] A. Böttcher, Y. I. Karlovich, and I. M. Spitkovsky. *Convolution operators and factorization of almost periodic matrix functions*. Operator Theory: Advances and Applications, vol. 131. Birkhäuser Verlag, Basel, 2002. ↑[253](#)
- [48] C. P. Boyer and W. Miller Jr. A classification of second-order raising operators for Hamiltonians in two variables. *J. Mathematical Phys.*, **15**:1484–1489, 1974. ↑[339](#), [346](#)
- [49] F. Brackx, R. Delanghe, and F. Sommen. *Clifford analysis*. Research Notes in Mathematics, vol. 76. Pitman (Advanced Publishing Program), Boston, MA, 1982. ↑[263](#), [275](#)
- [50] J. Brandmeyer and V. V. Kisil. *PyGiNaC—a Python interface to the C++ symbolic math library GiNaC*, 2004. The project currently URL: <http://moebinv.sourceforge.net/pyGiNaC.html>. ↑[383](#)
- [51] O. Bratteli and P. E. T. Jorgensen. Isometries, shifts, Cuntz algebras and multiresolution wavelet analysis of scale N . *Integral Equations Operator Theory*, **28** (4):382–443, 1997. E-print: [arXiv:funct-an/9612003](http://arxiv.org/abs/funct-an/9612003). ↑[253](#)
- [52] S. Brewer. Projective cross-ratio on hypercomplex numbers. *Adv. Appl. Clifford Algebras*, **23** (1):1–14, 2013March. doi: [10.1007/s00006-012-0335-7](https://doi.org/10.1007/s00006-012-0335-7). E-print: [arXiv:1203.2554](http://arxiv.org/abs/1203.2554). ↑[53](#), [54](#), [123](#), [156](#), [157](#)
- [53] A. Brodlie and V. V. Kisil. Observables and states in p -mechanics. *Advances in mathematics research*. vol. 5, pages 101–136, Nova Sci. Publ., Hauppauge, NY, 2003. E-print: [arXiv:quant-ph/0304023](http://arxiv.org/abs/quant-ph/0304023). ↑[339](#), [340](#), [341](#), [348](#)
- [54] V. I. Burenkov. Recent progress in studying the boundedness of classical operators of real analysis in general Morrey-type spaces. I. *Eurasian Math. J.*, **3** (3):11–32, 2012. ↑[277](#), [293](#)
- [55] E. Calzetta and E. Verdager. Real-time approach to tunnelling in open quantum systems: Decoherence and anomalous diffusion. *J. Phys. A*, **39** (30):9503–9532, 2006. ↑[340](#), [344](#)
- [56] T. K. Carne. *Geometry and groups*, 2006. URL: <http://www.dpms.cam.ac.uk/~tkc/GeometryandGroups>. ↑[114](#)
- [57] F. Catoni, R. Cannata, V. Catoni, and P. Zampetti. N -dimensional geometries generated by hypercomplex numbers. *Adv. Appl. Clifford Algebras*, **15** (1), 2005. ↑[375](#)
- [58] F. Catoni, R. Cannata, and E. Nichelatti. The parabolic analytic functions and the derivative of real functions. *Adv. Appl. Clifford Algebras*, **14** (2):185–190, 2004. ↑[100](#), [320](#), [355](#), [375](#)
- [59] T. E. Cecil. *Lie sphere geometry: With applications to submanifolds*. Universitext. Springer, New York, Second, 2008. ↑[45](#), [147](#), [159](#), [161](#)
- [60] P. Cerejeiras, U. Kähler, and F. Sommen. Parabolic Dirac operators and the Navier-Stokes equations over time-varying domains. *Math. Methods Appl. Sci.*, **28** (14):1715–1724, 2005. ↑[375](#)
- [61] Z. Cerin and G. M. Gianella. On improvements of the butterfly theorem. *Far East J. Math. Sci. (FJMS)*, **20** (1):69–85, 2006. ↑[173](#)
- [62] S.-S. Chern. Finsler geometry is just Riemannian geometry without the quadratic restriction. *Notices Amer. Math. Soc.*, **43** (9):959–963, 1996. ↑[85](#)
- [63] J. G. Christensen and G. Ólafsson. Examples of coorbit spaces for dual pairs. *Acta Appl. Math.*, **107** (1–3):25–48, 2009. ↑[249](#), [251](#), [281](#)
- [64] J. Cnops. *Hurwitz pairs and applications of Möbius transformations*. Habilitation Dissertation, Universiteit Gent, 1994. See also [\[65\]](#). ↑[51](#), [148](#), [150](#), [156](#)
- [65] J. Cnops. *An introduction to Dirac operators on manifolds*. Progress in Mathematical Physics, vol. 24. Birkhäuser Boston Inc., Boston, MA, 2002. ↑[7](#), [45](#), [48](#), [50](#), [51](#), [52](#), [55](#), [72](#), [84](#), [94](#), [148](#), [150](#), [156](#), [160](#), [161](#), [162](#), [163](#), [191](#), [197](#), [205](#), [207](#), [210](#), [213](#), [214](#), [393](#)
- [66] J. Cnops and V. V. Kisil. Monogenic functions and representations of nilpotent Lie groups in quantum mechanics. *Math. Methods Appl. Sci.*, **22** (4):353–373, 1999. E-print: [arXiv:math/9806150](http://arxiv.org/abs/math/9806150). Zbl[1005.22003](#). ↑[253](#), [339](#)
- [67] L. A. Coburn. Berezin-Toeplitz quantization. *Algebraic methods in operator theory*, pages 101–108, Birkhäuser Verlag, New York, 1994. ↑[238](#)
- [68] R. R. Coifman, P. W. Jones, and S. Semmes. Two elementary proofs of the L^2 boundedness of Cauchy integrals on Lipschitz curves. *J. Amer. Math. Soc.*, **2** (3):553–564, 1989. ↑[275](#), [277](#)
- [69] D. Constaes, N. Faustino, and R. S. Kraußhar. Fock spaces, Landau operators and the time-harmonic Maxwell equations. *J. Phys. A*, **44** (13):135303, 2011. ↑[339](#)

- [70] H. S. M. Coxeter. *Introduction to geometry*. Wiley Classics Library. John Wiley & Sons, Inc., New York, 1989. Reprint of the 1969 edition. ↑[63](#)
- [71] H. S. M. Coxeter and S. L. Greitzer. *Geometry revisited*. Random House, New York, 1967. Zbl[0166.16402](#). ↑[xiii](#), [40](#), [46](#), [58](#), [64](#), [73](#), [84](#), [91](#), [148](#), [150](#), [172](#), [369](#)
- [72] J. Cuntz. Quantum spaces and their noncommutative topology. *Notices Amer. Math. Soc.*, **48** (8):793–799, 2001. ↑[316](#)
- [73] M. Davis. *Applied nonstandard analysis*. Wiley-Interscience [John Wiley & Sons], New York, 1977. ↑[96](#), [355](#)
- [74] M. A. de Gosson. Spectral properties of a class of generalized Landau operators. *Comm. Partial Differential Equations*, **33** (10–12):2096–2104, 2008. ↑[335](#)
- [75] R. Delanghe, F. Sommen, and V. Souček. *Clifford algebra and spinor-valued functions. A function theory for the Dirac operator*. Mathematics and its Applications, vol. 53. Kluwer Academic Publishers Group, Dordrecht, 1992. Related REDUCE software by F. Brackx and D. Constaes, With 1 IBM-PC floppy disk (3.5 inch). ↑[162](#)
- [76] M. DeVilliers. The nine-point conic: a rediscovery and proof by computer. *International Journal of Mathematical Education in Science and Technology*, **37** (1):7–14, 2006. ↑[173](#)
- [77] D. Devriese et al. *Kig*, <https://edu.kde.org/kig/>, since 2006. Free and Open-Source Interactive Geometry Software. ↑[168](#)
- [78] F. M. Dimentberg. The method of screws and calculus of screws applied to the theory of three-dimensional mechanisms. *Adv. in Mech.*, **1** (3–4):91–106, 1978. ↑[320](#), [375](#)
- [79] F. M. Dimentberg. *Теория винтов и ее приложения [Theory of screws and its applications]*. “Nauka”, Moscow, 1978. ↑[320](#), [375](#)
- [80] P. A. M. Dirac. On the theory of quantum mechanics. *Proceedings of the Royal Society of London. Series A*, **112** (762):661–677, 1926. ↑[315](#)
- [81] P. A. M. Dirac. Quantum mechanics and a preliminary investigation of the hydrogen atom. *Proceedings of the Royal Society of London. Series A, Containing Papers of a Mathematical and Physical Character*, **110** (755):561–579, 1926. ↑[315](#), [316](#), [338](#)
- [82] P. A. M. Dirac. *The principles of quantum mechanics*. Oxford University Press, London, 4th ed., 1958. ↑[316](#)
- [83] P. A. M. Dirac. *Directions in physics*. Wiley-Interscience [John Wiley & Sons], New York, 1978. Five lectures delivered during a visit to Australia and New Zealand, August–September, 1975, With a foreword by Mark Oliphant, Edited by H. Hora and J. R. Shepanski. ↑[316](#)
- [84] J. Dixmier. *Les C*-algèbres et leurs représentations*. Gauthier-Villars, Paris, 1964. ↑[26](#)
- [85] J. Dixmier. *C*-algebras*. North-Holland Publishing Co., Amsterdam, 1977. Translated from the French by Francis Jellet, North-Holland Mathematical Library, Vol. 15. ↑[231](#)
- [86] L. Dorst, C. Doran, and J. Lasenby (eds.) *Applications of geometric algebra in computer science and engineering*. Birkhäuser Boston, Inc., Boston, MA, 2002. Papers from the conference (AGACSE 2001) held at Cambridge University, Cambridge, July 9–13, 2001. ↑[160](#)
- [87] M. Duflou and C. C. Moore. On the regular representation of a nonunimodular locally compact group. *J. Functional Analysis*, **21** (2):209–243, 1976. ↑[231](#), [251](#), [260](#), [281](#), [290](#)
- [88] N. Dunford and J. T. Schwartz. *Linears operators. part i: General theory*. Pure and Applied Mathematics, vol. VII. John Wiley & Sons, Inc., New York, 1957. ↑[256](#)
- [89] J. Dziubański and M. Preisner. Riesz transform characterization of Hardy spaces associated with Schrödinger operators with compactly supported potentials. *Ark. Mat.*, **48** (2):301–310, 2010. ↑[292](#)
- [90] D. Eelbode and F. Sommen. Taylor series on the hyperbolic unit ball. *Bull. Belg. Math. Soc. Simon Stevin*, **11** (5):719–737, 2004. ↑[375](#)
- [91] D. Eelbode and F. Sommen. The fundamental solution of the hyperbolic Dirac operator on $\mathbb{R}^{1,m}$: a new approach. *Bull. Belg. Math. Soc. Simon Stevin*, **12** (1):23–37, 2005. ↑[375](#)
- [92] A. S. Elmabrok and O. Hutník. Induced representations of the affine group and intertwining operators: I. Analytical approach. *J. Phys. A*, **45** (24):244017, 15, 2012. ↑[278](#), [293](#)
- [93] A. Erdélyi, W. Magnus, F. Oberhettinger, and F. G. Tricomi. *Higher transcendental functions. Vol. II*. Robert E. Krieger Publishing Co. Inc., Melbourne, Fla., 1981. Based on notes left by Harry Bateman, Reprint of the 1953 original. ↑[346](#), [350](#), [352](#)

- [94] L. D. Faddeev and O. A. Yakubovskii. *Lectures on quantum mechanics for mathematics students*. Student Mathematical Library, vol. 47. American Mathematical Society (AMS), Providence, RI, 2009. Translated by Harold McFaden. xii, 234 p. ↑316
- [95] H. G. Feichtinger and K. H. Gröchenig. Banach spaces related to integrable group representations and their atomic decompositions. I. *J. Funct. Anal.*, **86** (2):307–340, 1989. ↑249, 250, 251, 281
- [96] H. Fernandes et al. *GNU Dr. Geo*, <http://www.drgeo.eu/>, since 1996. Interactive Geometry Software. ↑168
- [97] R. P. Feynman. *QED: the strange theory of light and matter*. Penguin Press Science Series. Penguin, 1990. ↑317, 318, 338
- [98] R. P. Feynman and A. R. Hibbs. *Quantum mechanics and path integral*. McGraw-Hill Book Company, New York, 1965. ↑317
- [99] J. P. Fillmore and M. Paluszny. The Apollonius contact problem and representational geometry. *Seminarberichte, FernUniversität in Hagen*, **Band 62** (Teil 1):45–72, 1997. ISSN 0944–0838, <http://www.math.ucsd.edu/~fillmore/papers/FPHR.pdf>. ↑47
- [100] J. P. Fillmore and A. Springer. Möbius groups over general fields using Clifford algebras associated with spheres. *Internat. J. Theoret. Phys.*, **29** (3):225–246, 1990. ↑7, 45, 48, 51, 80, 84, 148, 150, 156, 160, 161, 163, 164, 191, 197, 205, 207, 210, 214
- [101] J. P. Fillmore and A. Springer. Determining circles and spheres satisfying conditions which generalize tangency, 2000. preprint, <http://www.math.ucsd.edu/~fillmore/papers/2000LGalgorithm.pdf>. ↑47, 55, 67, 148, 150, 162, 164, 165, 197
- [102] P. Fjelstad and S. G. Gal. Two-dimensional geometries, topologies, trigonometries and physics generated by complex-type numbers. *Adv. Appl. Clifford Algebras*, **11** (1):81–107 (2002), 2001. ↑375
- [103] G. B. Folland and E. M. Stein. *Hardy spaces on homogeneous group*. Princeton University Press, Princeton, New Jersey, 1982. ↑276
- [104] G. B. Folland. *Harmonic analysis in phase space*. Annals of Mathematics Studies, vol. 122. Princeton University Press, Princeton, NJ, 1989. ↑316, 318, 319, 324, 325, 327, 333, 334, 335, 337, 338, 339, 343, 346, 347, 359, 360, 365
- [105] G. B. Folland. *A course in abstract harmonic analysis*. Studies in Advanced Mathematics. Boca Raton, FL: CRC Press. viii, 276 p. \$ 61.95, 1995. ↑224, 279
- [106] H. Führ. *Abstract harmonic analysis of continuous wavelet transforms*. Lecture Notes in Mathematics, vol. 1863. Springer-Verlag, Berlin, 2005. ↑249, 251, 281
- [107] G. I. Garas'ko. *Начала финслеровой геометрии для физиков*. [Elements of Finsler geometry for physicists]. TETRU, Moscow, 2009. 268 pp. URL: <http://hypercomplex.xpsweb.com/articles/487/ru/pdf/00-gbook.pdf>. ↑85
- [108] J. B. Garnett. *Bounded analytic functions*. Graduate Texts in Mathematics, vol. 236. Springer, New York, first, 2007. ↑253, 263, 268, 277, 282, 283, 289, 293, 295
- [109] J.-P. Gazeau. *Coherent States in Quantum Physics*. Wiley-VCH Verlag, 2009. ↑335, 339, 347
- [110] A. Gerrard and J. M. Burch. *Introduction to matrix methods in optics*. Dover Publications Inc., New York, 1994. Corrected reprint of the 1975 original. ↑107, 108
- [111] I. M. Glazman and Ju. I. Ljubič. *Finite-dimensional linear analysis*. Dover Publications Inc., Mineola, NY, 2006. Translated from the Russian and edited by G. P. Barker and G. Kuerti, Reprint of the 1974 edition. ↑xiv
- [112] GNU. *General Public License (GPL)*. Free Software Foundation, Inc., Boston, USA, version 3, 2007. URL: <http://www.gnu.org/licenses/gpl.html>. ↑160, 379
- [113] I. Gohberg, P. Lancaster, and L. Rodman. *Indefinite linear algebra and applications*. Birkhäuser Verlag, Basel, 2005. ↑60, 73, 75, 150, 196
- [114] L. Grafakos. *Classical Fourier analysis*. Graduate Texts in Mathematics, vol. 249. Springer, New York, Second, 2008. ↑253, 271, 282, 291, 296
- [115] N. A. Gromov. *Контракции и аналитические продолжения классических групп. Единый подход*. (Russian) [Contractions and analytic extensions of classical groups. Unified approach]. Akad. Nauk SSSR Ural. Otdel. Komi Nauchn. Tsentr, Syktyvkar, 1990. ↑157, 320, 338, 375
- [116] N. A. Gromov. Transitions: Contractions and analytical continuations of the Cayley–Klein groups. *Int. J. Theor. Phys.*, **29**:607–620, 1990. ↑94, 338, 375

- [117] N. A. Gromov. Possible quantum kinematics. II. Nonminimal case. *J. Math. Phys.*, **51** (8):083515, 12, 2010. ↑[156](#), [162](#)
- [118] N. A. Gromov. *Контракции Классических и Квантовых Групп. [Contractions of classic and quantum groups]*. Moskva: Fizmatlit, 2012. ↑[156](#), [162](#), [375](#)
- [119] N. A. Gromov and V. V. Kuratov. All possible Cayley-Klein contractions of quantum orthogonal groups. *Yadernaya Fiz.*, **68** (10):1752–1762, 2005. ↑[337](#), [338](#)
- [120] N. A. Gromov and V. V. Kuratov. Possible quantum kinematics. *J. Math. Phys.*, **47** (1):013502, 9, 2006. ↑[162](#), [375](#)
- [121] U. Günther and S. Kuzhel. \mathcal{PT} -symmetry, Cartan decompositions, Lie triple systems and Krein space-related Clifford algebras. *J. Phys. A*, **43** (39):392002, 2010. ↑[337](#), [339](#)
- [122] K. Gürlebeck, K. Habetha, and W. Sprößig. *Holomorphic functions in the plane and n-dimensional space*. Birkhäuser Verlag, Basel, 2008. Translated from the 2006 German original, With 1 CD-ROM (Windows and UNIX). ↑[205](#)
- [123] V. Gutenmacher and N. B. Vasilyev. *Lines and curves. A practical geometry handbook*. Birkhäuser Verlag, Basel, 2004. Based on an English translation of the original Russian edition by A. Kundu. Foreword by Mark Saul. ↑[374](#)
- [124] E. Hakenholz et al. *CaRMetal*, <http://carmetal.org/>, since 2006. Free Software on Dynamical Geometry. ↑[168](#)
- [125] B. Hall. *Lie groups, Lie algebras, and representations*. Graduate Texts in Mathematics, vol. 222. Springer, Cham, Second, 2015. An Elementary Introduction. ↑[32](#)
- [126] A. Hammerlindl, J. Bowman, and T. Prince. *Asymptote—powerful descriptive vector graphics language for technical drawing, inspired by MetaPost*, 2004. URL: <http://asymptote.sourceforge.net/>. ↑[163](#), [379](#)
- [127] S. Helgason. *Integral geometry and Radon transforms*. Springer, New York, 2011. ↑[254](#)
- [128] F. J. Herranz, J. de Lucas, and M. Tobolski. Lie-Hamilton systems on curved spaces: a geometrical approach. *J. Phys. A*, **50** (49):495201, 23, 2017. ↑[197](#)
- [129] F. J. Herranz, R. Ortega, and M. Santander. Trigonometry of spacetimes: a new self-dual approach to a curvature/signature (in)dependent trigonometry. *J. Phys. A*, **33** (24):4525–4551, 2000. E-print: [arXiv:math-ph/9910041](https://arxiv.org/abs/math-ph/9910041). ↑[119](#), [136](#), [138](#), [242](#), [354](#)
- [130] F. J. Herranz and M. Santander. Conformal compactification of spacetimes. *J. Phys. A*, **35** (31):6619–6629, 2002. E-print: [arXiv:math-ph/0110019](https://arxiv.org/abs/math-ph/0110019). ↑[94](#), [102](#), [103](#), [104](#), [162](#), [197](#), [375](#)
- [131] F. J. Herranz and M. Santander. Conformal symmetries of spacetimes. *J. Phys. A*, **35** (31):6601–6618, 2002. E-print: [arXiv:math-ph/0110019](https://arxiv.org/abs/math-ph/0110019). ↑[94](#), [375](#)
- [132] D. Hestenes. *Space-time algebra*. Birkhäuser/Springer, Cham, Second, 2015. With a foreword by Anthony Lasenby. ↑[160](#), [162](#)
- [133] D. Hestenes and G. Sobczyk. *Clifford algebra to geometric calculus. A unified language for mathematics and physics*. Fundamental Theories of Physics. D. Reidel Publishing Co., Dordrecht, 1984. ↑[160](#), [162](#), [375](#)
- [134] D. Hildenbrand. *Foundations of geometric algebra computing*. Geometry and Computing, vol. 8. Springer, Heidelberg, 2013. With a foreword by Alyn Rockwood. ↑[160](#)
- [135] M. Hohenwarter et al. *GeoGebra*, <https://www.geogebra.org/>, since 2001. An Interactive Geometry, Algebra, Statistics and Calculus Application. ↑[168](#)
- [136] L. Hörmander. *The analysis of linear partial differential operators III: Pseudodifferential operators*. Springer-Verlag, Berlin, 1985. ↑[24](#)
- [137] R. A. Horn and C. R. Johnson. *Topics in matrix analysis*. Cambridge University Press, Cambridge, 1994. Corrected reprint of the 1991 original. ↑[60](#), [307](#)
- [138] R. Howe. On the role of the Heisenberg group in harmonic analysis. *Bull. Amer. Math. Soc. (N.S.)*, **3** (2):821–843, 1980. ↑[3](#), [19](#), [318](#), [323](#), [327](#), [334](#), [348](#)
- [139] R. Howe. Quantum mechanics and partial differential equations. *J. Funct. Anal.*, **38** (2):188–254, 1980. ↑[255](#), [318](#), [319](#), [324](#), [333](#), [335](#), [337](#), [339](#), [343](#), [347](#), [365](#), [366](#), [367](#)
- [140] R. Howe and E.-C. Tan. *Nonabelian harmonic analysis. Applications of SL(2, R)*. Springer-Verlag, New York, 1992. ↑[19](#), [246](#), [338](#), [350](#), [351](#)
- [141] J. Hucks. Hyperbolic complex structures in physics. *J. Math. Phys.*, **34** (12):5986–6008, 1993. ↑[375](#)
- [142] R. Hudson. *Generalised translation-invariant mechanics*. D. Phil. thesis, Bodleian Library, Oxford, 1966. ↑[321](#), [337](#), [338](#), [375](#)

- [143] R. Hudson. Translation invariant phase space mechanics. In A. Khrennikov (ed.) *Quantum theory: reconsideration of foundations—2*, pages 301–314, Växjö Univ. Press, Växjö, 2004. ↑[337](#), [338](#), [375](#)
- [144] N. Hungerbühler and K. Kusejko. Steiner’s porism in finite Miquelian Möbius planes. *Adv. Geom.*, **18** (1):55–68, 2018. ↑[152](#), [156](#)
- [145] N. Hungerbühler and G. Villiger. Exotic Steiner chains in Miquelian Möbius planes of odd order. *Adv. Geom.*, **21** (2):207–220, 2021. ↑[152](#), [156](#)
- [146] O. Hutník. On Toeplitz-type operators related to wavelets. *Integral Equations Operator Theory*, **63** (1):29–46, 2009. ↑[252](#)
- [147] A. Jadczyk. Compactified Minkowski space: Myths and facts. *ArXiv e-prints*, May 2011. ↑[103](#)
- [148] M. L. Juhász. A universal linear algebraic model for conformal geometries. *J. Geom.*, **109** (3):Art. 48, 18, 2018. E-print: [arXiv:1603.06863](#). ↑[147](#), [159](#)
- [149] O. Karpenkov. *Geometry of continued fractions*. Algorithms and Computation in Mathematics, vol. 26. Springer, Heidelberg, 2013. ↑[207](#)
- [150] H. A. Kastrup. On the advancements of conformal transformations and their associated symmetries in geometry and theoretical physics. *Annalen der Physik*, **17** (9–10):631–690, 2008. E-print: [arXiv:0808.2730](#). ↑[147](#), [156](#), [166](#)
- [151] A. Yu. Khrennikov. Hyperbolic quantum mechanics. *Dokl. Akad. Nauk*, **402** (2):170–172, 2005. ↑[337](#), [338](#), [348](#), [351](#), [375](#)
- [152] A. Yu. Khrennikov and Ya. I. Volovich. Numerical experiment on interference for macroscopic particles, 2001. E-print: [arXiv:quant-ph/0111159](#). ↑[341](#)
- [153] A. Khrennikov. Linear representations of probabilistic transformations induced by context transitions. *J. Phys. A*, **34** (47):9965–9981, 2001. E-print: [arXiv:quant-ph/0106073](#). ↑[341](#)
- [154] A. Khrennikov. Hyperbolic Quantum Mechanics. *Adv. Appl. Clifford Algebras*, **13** (1):1–9, 2003. E-print: [arXiv:quant-ph/0101002](#). ↑[337](#), [338](#), [344](#), [351](#), [375](#)
- [155] A. Khrennikov. Hyperbolic quantization. *Adv. Appl. Clifford Algebr.*, **18** (3–4):843–852, 2008. ↑[337](#), [348](#), [349](#), [351](#), [371](#), [375](#)
- [156] A. Khrennikov. *Contextual approach to quantum formalism*. Fundamental Theories of Physics, vol. 160. Springer, New York, 2009. ↑[321](#)
- [157] A. Khrennikov and G. Segre. Hyperbolic quantization. In L. Accardi, W. Freudenberg, and M. Schürman (eds.) *Quantum probability and infinite dimensional analysis*, pages 282–287, World Scientific Publishing, Hackensack, NJ, 2007. ↑[347](#), [375](#)
- [158] S. Khrushchev. *Orthogonal polynomials and continued fractions: from Euler’s point of view*. Encyclopedia of Mathematics and its Applications, vol. 122. Cambridge University Press, Cambridge, 2008. ↑[207](#)
- [159] A. A. Kirillov. *Elements of the theory of representations*. Springer-Verlag, Berlin, 1976. Translated from the Russian by Edwin Hewitt, Grundlehren der Mathematischen Wissenschaften, Band 220. ↑[17](#), [18](#), [19](#), [21](#), [22](#), [53](#), [109](#), [221](#), [222](#), [223](#), [224](#), [225](#), [230](#), [237](#), [241](#), [243](#), [244](#), [248](#), [280](#), [289](#), [303](#), [304](#), [305](#), [320](#), [331](#), [332](#), [333](#), [334](#), [342](#), [357](#), [360](#), [363](#), [365](#), [366](#)
- [160] A. A. Kirillov. Introduction to the theory of representations and noncommutative harmonic analysis [MR90a:22005]. *Representation theory and noncommutative harmonic analysis, i*, pages 1–156, 227–234, Springer, Berlin, 1994. MR1311488. ↑[337](#), [341](#), [342](#)
- [161] A. A. Kirillov. Merits and demerits of the orbit method. *Bull. Amer. Math. Soc. (N.S.)*, **36** (4):433–488, 1999. ↑[53](#), [337](#), [342](#), [369](#)
- [162] A. A. Kirillov. *Lectures on the orbit method*. Graduate Studies in Mathematics, vol. 64. American Mathematical Society, Providence, RI, 2004. ↑[279](#)
- [163] A. A. Kirillov. *A tale of two fractals*. Springer, New York, 2013. Draft: <http://www.math.upenn.edu/~kirillov/MATH480-F07/xf.pdf>. ↑[9](#), [45](#), [48](#), [51](#), [52](#), [55](#), [58](#), [61](#), [66](#), [150](#), [151](#), [160](#), [161](#), [191](#), [197](#), [207](#), [210](#)
- [164] A. A. Kirillov and A. D. Gvishiani. *Theorems and problems in functional analysis*. Problem Books in Mathematics. Springer-Verlag, New York, 1982. ↑[xiv](#), [17](#), [65](#), [89](#), [113](#), [220](#), [221](#), [224](#), [296](#)
- [165] A. V. Kisil. Isometric action of $SL_2(\mathbb{R})$ on homogeneous spaces. *Adv. App. Clifford Algebras*, **20** (2):299–312, 2010. E-print: [arXiv:0810.0368](#). MR2012b:32019. ↑[113](#), [131](#), [157](#)
- [166] V. Y. Kisil. Clifford valued convolution operator algebras on the Heisenberg group. A quantum field theory model. In F. Brackx, R. Delanghe, and H. Serras (eds.) *Clifford algebras and their applications in mathematical physics, proceedings of the Third international conference held in Deinze*, pages 287–294, Kluwer Academic Publishers Group, Dordrecht, 1993. MR1266878. ↑[339](#)

- [167] V. V. Kisil. Quantum probabilities and non-commutative Fourier transform on the Heisenberg group. In N. Kalton, E. Saab, and Montgomery-Smith (eds.) *Interaction between functional analysis, harmonic analysis and probability* (Columbia, MO, 1994), pages 255–266, Dekker, New York, 1995. MR97b:81060. [↑339](#)
- [168] V. V. Kisil. Möbius transformations and monogenic functional calculus. *Electron. Res. Announc. Amer. Math. Soc.*, **2** (1):26–33, 1996. [On-line](#). [↑15](#), [256](#), [302](#), [303](#), [371](#)
- [169] V. V. Kisil. Plain mechanics: Classical and quantum. *J. Natur. Geom.*, **9** (1):1–14, 1996. E-print: [arXiv:funct-an/9405002](#). [↑339](#), [371](#)
- [170] V. V. Kisil. Analysis in $\mathbf{R}^{1,1}$ or the principal function theory. *Complex Variables Theory Appl.*, **40** (2):93–118, 1999. E-print: [arXiv:funct-an/9712003](#). [↑15](#), [34](#), [105](#), [126](#), [224](#), [232](#), [234](#), [241](#), [249](#), [252](#), [265](#), [272](#), [273](#), [274](#), [364](#), [370](#), [372](#), [375](#)
- [171] V. V. Kisil. Relative convolutions. I. Properties and applications. *Adv. Math.*, **147** (1):35–73, 1999. E-print: [arXiv:funct-an/9410001](#), [On-line](#). Zbl933.43004. [↑287](#), [365](#)
- [172] V. V. Kisil. Two approaches to non-commutative geometry. *Complex methods for partial differential equations* (Ankara, 1998), pages 215–244, Kluwer Acad. Publ., Dordrecht, 1999. E-print: [arXiv:funct-an/9703001](#). [↑xiii](#), [232](#), [265](#)
- [173] V. V. Kisil. Wavelets in Banach spaces. *Acta Appl. Math.*, **59** (1):79–109, 1999. E-print: [arXiv:math/9807141](#), [On-line](#). [↑234](#), [249](#), [250](#), [253](#), [254](#), [255](#), [257](#), [273](#), [281](#), [287](#), [302](#), [303](#), [342](#), [364](#), [365](#)
- [174] V. V. Kisil. Umbral calculus and cancellative semigroup algebras. *Z. Anal. Anwendungen*, **19** (2):315–338, 2000. E-print: [arXiv:funct-an/9704001](#). Zbl0959.43004. [↑250](#)
- [175] V. V. Kisil. *Spaces of analytical functions and wavelets—Lecture notes*, 2000. 92 pp. E-print: [arXiv:math.CV/0204018](#). [↑265](#), [273](#), [274](#)
- [176] V. V. Kisil. Meeting Descartes and Klein somewhere in a noncommutative space. In A. Fokas, J. Halliwell, T. Kibble, and B. Zegarlinski (eds.) *Highlights of mathematical physics* (London, 2000), pages 165–189, Amer. Math. Soc., Providence, RI, 2002. E-print: [arXiv:math-ph/0112059](#). [↑xiii](#), [15](#), [265](#)
- [177] V. V. Kisil. Quantum and classical brackets. *Internat. J. Theoret. Phys.*, **41** (1):63–77, 2002. E-print: [arXiv:math-ph/0007030](#). [On-line](#). [↑337](#), [339](#)
- [178] V. V. Kisil. Tokens: an algebraic construction common in combinatorics, analysis, and physics. *Ukrainian mathematics congress—2001 (ukrainian)*, pages 146–155, Natsional. Akad. Nauk Ukraïni Ìnst. Mat., Kiev, 2002. E-print: [arXiv:math.FA/0201012](#). [↑250](#)
- [179] V. V. Kisil. Two slits interference is compatible with particles’ trajectories. In A. Khrennikov (ed.) *Quantum theory: Reconsideration of foundations*, pages 215–226, Växjö University Press, 2002. E-print: [arXiv:quant-ph/0111094](#). [↑341](#)
- [180] V. V. Kisil. Monogenic calculus as an intertwining operator. *Bull. Belg. Math. Soc. Simon Stevin*, **11** (5):739–757, 2004. E-print: [arXiv:math.FA/0311285](#), [On-line](#). [↑302](#), [303](#), [371](#)
- [181] V. V. Kisil. p-Mechanics as a physical theory: an introduction. *J. Phys. A: Math. Theor*, **37** (1):183–204, 2004. E-print: [arXiv:quant-ph/0212101](#), [On-line](#). Zbl1045.81032. [↑319](#), [333](#), [335](#), [337](#), [339](#), [340](#), [342](#), [343](#), [354](#), [359](#), [371](#)
- [182] V. V. Kisil. Spectrum as the support of functional calculus. *Functional analysis and its applications*, pages 133–141, Elsevier, Amsterdam, 2004. E-print: [arXiv:math.FA/0208249](#). [↑15](#), [256](#), [289](#), [302](#), [303](#), [372](#)
- [183] V. V. Kisil. p-mechanics and field theory. *Rep. Math. Phys.*, **56** (2):161–174, 2005. E-print: [arXiv:quant-ph/0402035](#), [On-line](#). Zbl1088.81067. [↑371](#)
- [184] V. V. Kisil. A quantum-classical bracket from p-mechanics. *Europhys. Lett.*, **72** (6):873–879, 2005. E-print: [arXiv:quant-ph/0506122](#), [On-line](#). [↑342](#), [371](#)
- [185] V. V. Kisil. Erlangen program at large–0: Starting with the group $SL_2(\mathbf{R})$. *Notices Amer. Math. Soc.*, **54** (11):1458–1465, 2007. E-print: [arXiv:math/0607387](#), [On-line](#). Zbl1137.22006. [↑19](#), [36](#), [149](#), [154](#), [157](#), [160](#), [162](#), [172](#), [183](#), [191](#), [197](#), [207](#), [210](#), [370](#), [371](#)
- [186] V. V. Kisil. Fillmore–Springer–Cnops construction implemented in GiNaC. *Adv. Appl. Clifford Algebr.*, **17** (1):59–70, 2007. [On-line](#). A more recent version: E-print: [arXiv:cs.MS/0512073](#). The latest documentation, source files, and live ISO image are at the project page: <http://moebinv.sourceforge.net/>. Zbl05134765. [↑50](#), [160](#), [161](#), [163](#), [178](#), [197](#), [211](#), [379](#), [383](#)
- [187] V. V. Kisil. Two-dimensional conformal models of space-time and their compactification. *J. Math. Phys.*, **48** (7):073506, 2007. E-print: [arXiv:math-ph/0611053](#). Zbl1144.81368. [↑162](#), [197](#)

- [188] V. V. Kisil. Comment on “Do we have a consistent non-adiabatic quantum-classical mechanics?” by Agostini F. et al. *Europhys. Lett. EPL*, **89**:50005, 2010. E-print: [arXiv:0907.0855](#). ↑[242](#), [342](#), [371](#)
- [189] V. V. Kisil. Computation and dynamics: Classical and quantum. *AIP Conference Proceedings*, **1232** (1):306–312, 2010. E-print: [arXiv:0909.1594](#). ↑[338](#)
- [190] V. V. Kisil. Erlangen program at large—2: Inventing a wheel. The parabolic one. *Zb. Pr. Inst. Mat. NAN Ukr. (Proc. Math. Inst. Ukr. Ac. Sci.)*, **7** (2):89–98, 2010. E-print: [arXiv:0707.4024](#). ↑[36](#), [119](#), [172](#), [173](#), [205](#), [354](#)
- [191] V. V. Kisil. Erlangen program at large—1: Geometry of invariants. *SIGMA*, **6** (076):45, 2010. E-print: [arXiv:math.CV/0512416](#). MR2011i:30044. Zbl1218.30136. ↑[14](#), [49](#), [50](#), [160](#), [161](#), [162](#), [172](#), [173](#), [197](#), [205](#), [272](#), [273](#), [276](#), [279](#), [283](#), [284](#), [348](#), [355](#), [370](#), [371](#), [372](#), [375](#), [376](#)
- [192] V. V. Kisil. Wavelets beyond admissibility. In M. Ruzhansky and J. Wirth (eds.) *Progress in analysis and its applications*, pages 219–225, World Sci. Publ., Hackensack, NJ, 2010. E-print: [arXiv:0911.4701](#). Zbl1269.30052. ↑[249](#), [280](#), [284](#), [287](#)
- [193] V. V. Kisil. Covariant transform. *Journal of Physics: Conference Series*, **284** (1):012038, 2011. E-print: [arXiv:1011.3947](#). ↑[15](#), [266](#), [287](#), [288](#), [302](#), [303](#)
- [194] V. V. Kisil. Erlangen program at large—2 1/2: Induced representations and hypercomplex numbers. *Известия Коми научного центра УрО РАН [Izvestiya Komi nauchnogo centra UrO RAN]*, **1** (5):4–10, 2011. E-print: [arXiv:0909.4464](#). ↑[15](#), [144](#), [241](#), [244](#), [245](#), [320](#), [321](#), [335](#), [347](#), [348](#), [369](#), [372](#)
- [195] V. V. Kisil. Erlangen Programme at Large 1.1: Integral transforms and differential operators. *in preparation*, 2011. ↑[269](#), [270](#), [272](#), [311](#)
- [196] V. V. Kisil. Erlangen Programme at Large 3.2: Ladder operators in hypercomplex mechanics. *Acta Polytechnica*, **51** (4):44–53, 2011. on-line. E-print: [arXiv:1103.1120](#). ↑[16](#), [109](#), [173](#), [205](#), [242](#), [339](#)
- [197] V. V. Kisil. Erlangen programme at large: An overview. In S. V. Rogosin and A. A. Koroleva (eds.) *Advances in applied analysis*, pages 1–94, Birkhäuser Verlag, Basel, 2012. E-print: [arXiv:1106.1686](#). ↑[xiii](#), [276](#), [279](#), [280](#), [283](#), [284](#), [287](#), [288](#), [289](#), [320](#), [359](#), [360](#), [361](#), [362](#), [364](#), [372](#)
- [198] V. V. Kisil. *Geometry of Möbius transformations: Elliptic, parabolic and hyperbolic actions of $SL_2(\mathbf{R})$* . Imperial College Press, London, 2012. Includes a live DVD. Zbl1254.30001. ↑[149](#), [150](#), [151](#), [153](#), [154](#), [156](#), [157](#), [159](#), [160](#), [161](#), [162](#), [163](#), [172](#), [173](#), [178](#), [182](#), [183](#), [187](#), [191](#), [196](#), [197](#), [205](#), [207](#), [210](#), [211](#), [276](#), [279](#), [283](#), [284](#), [321](#)
- [199] V. V. Kisil. Hypercomplex representations of the Heisenberg group and mechanics. *Internat. J. Theoret. Phys.*, **51** (3):964–984, 2012. E-print: [arXiv:1005.5057](#). Zbl1247.81232. ↑[16](#), [109](#), [242](#), [320](#), [321](#), [334](#), [351](#), [356](#), [360](#), [371](#), [372](#)
- [200] V. V. Kisil. Is commutativity of observables the main feature, which separate classical mechanics from quantum?. *Известия Коми научного центра УрО РАН [Izvestiya Komi nauchnogo centra UrO RAN]*, **3** (11):4–9, 2012. E-print: [arXiv:1204.1858](#). ↑[109](#), [162](#), [321](#)
- [201] V. V. Kisil. Operator covariant transform and local principle. *J. Phys. A: Math. Theor.*, **45**:244022, 2012. E-print: [arXiv:1201.1749](#). On-line. ↑[250](#), [276](#), [281](#), [359](#)
- [202] V. V. Kisil. Boundedness of relative convolutions on nilpotent Lie groups. *Zb. Pr. Inst. Mat. NAN Ukr. (Proc. Math. Inst. Ukr. Ac. Sci.)*, **10** (4–5):185–189, 2013. E-print: [arXiv:1307.3882](#). ↑[366](#)
- [203] V. V. Kisil. Induced representations and hypercomplex numbers. *Adv. Appl. Clifford Algebras*, **23** (2):417–440, 2013. E-print: [arXiv:0909.4464](#). Zbl1269.30052. ↑[162](#), [173](#), [205](#), [261](#), [278](#)
- [204] V. V. Kisil. Calculus of operators: Covariant transform and relative convolutions. *Banach J. Math. Anal.*, **8** (2):156–184, 2014. E-print: [arXiv:1304.2792](#), on-line. ↑[287](#), [359](#), [364](#), [365](#), [366](#)
- [205] V. V. Kisil. The real and complex techniques in harmonic analysis from the point of view of covariant transform. *Eurasian Math. J.*, **5**:95–121, 2014. E-print: [arXiv:1209.5072](#). On-line. ↑[359](#), [362](#)
- [206] V. V. Kisil. Uncertainty and analyticity. In V. V. Mityushev and M. V. Ruzhansky (eds.) *Current trends in analysis and its applications*, pages 583–590, Springer International Publishing, 2015. E-print: [arXiv:1312.4583](#). ↑[363](#)
- [207] V. V. Kisil. *MoebInv illustrations*, 2015. YouTube playlist: <https://goo.gl/Z9GULO>. ↑[172](#), [173](#), [203](#)
- [208] V. V. Kisil. Remark on continued fractions, Möbius transformations and cycles. *Известия Коми научного центра УрО РАН [Izvestiya Komi nauchnogo centra UrO RAN]*, **25** (1):11–17, 2016. E-print: [arXiv:1412.1457](#), on-line. ↑[160](#), [161](#), [162](#), [166](#), [191](#), [197](#), [205](#)
- [209] V. V. Kisil. Poincaré extension of Möbius transformations. *Complex Variables and Elliptic Equations*, **62** (9):1221–1236, 2017. E-print: [arXiv:1507.02257](#). ↑[157](#), [160](#), [161](#), [162](#), [168](#), [173](#), [194](#), [197](#), [205](#)

- [210] V. V. Kisil. Symmetry, geometry and quantization with hypercomplex numbers. In I. M. Mladenov, G. Meng, and A. Yoshioka (eds.) *Geometry, integrability and quantization XVIII*, pages 11–76, Bulgar. Acad. Sci., Sofia, 2017. E-print: [arXiv:1611.05650](https://arxiv.org/abs/1611.05650). ↑162
- [211] V. V. Kisil. An extension of Möbius–Lie geometry with conformal ensembles of cycles and its implementation in a GiNaC library. *Proc. Int. Geom. Cent.*, **11** (3):45–67, 2018. E-print: [arXiv:1512.02960](https://arxiv.org/abs/1512.02960). Project page: <http://moebinv.sourceforge.net/>. ↑67, 148, 150, 153, 178, 179, 194, 197, 205, 375, 379, 387
- [212] V. V. Kisil. Möbius–Lie geometry and its extension. In I. M. Mladenov, G. Meng, and A. Yoshioka (eds.) *Geometry, integrability and quantization XX*, pages 13–61, Bulgar. Acad. Sci., Sofia, 2019. E-print: [arXiv:1811.10499](https://arxiv.org/abs/1811.10499). ↑150, 153, 194, 205
- [213] V. V. Kisil. MoebInv library: Demo, v5, 2019. doi: [10.24433/CO.9934595.v5](https://doi.org/10.24433/CO.9934595.v5). ↑379
- [214] V. V. Kisil. MoebInv library: Jupyter notebooks, v0.3, 2019. <https://github.com/vvkisil/MoebInv-notebooks>. ↑379
- [215] V. V. Kisil. MoebInv: C++ libraries for manipulations in non-Euclidean geometry. *SoftwareX*, **11**:100385, 2020. doi: [10.1016/j.softx.2019.100385](https://doi.org/10.1016/j.softx.2019.100385). ↑147, 148, 153
- [216] V. V. Kisil. Cycles cross ratio: a Jupyter notebook. *GitHub*, 2021. <https://github.com/vvkisil/Cycles-cross-ratio-Invitation>. ↑147, 152, 153, 154, 155
- [217] V. V. Kisil. Cycles cross ratio: an invitation. *Elem. Math.*, **78** (2):49–71, 2023. E-print: [arXiv:2105.05634](https://arxiv.org/abs/2105.05634), doi: [10.4171/EM/471](https://doi.org/10.4171/EM/471). ↑147
- [218] V. V. Kisil and J. Reid. Conformal parametrisation of loxodromes by triples of circles. In S. Bernstein (ed.) *Topics in Clifford analysis: Special volume in honor of Wolfgang Sprößig*, pages 313–330, Birkhäuser, Cham, 2019. E-print: [arXiv:1802.01864](https://arxiv.org/abs/1802.01864). ↑160, 161, 162, 163, 166, 167, 173
- [219] J. R. Klauder. Coherent states for the hydrogen atom. *J. Phys. A*, **29** (12):L293–L298, 1996. ↑266
- [220] J. R. Klauder and B.-S. Skagerstam (eds.) *Coherent states: Applications in physics and mathematical physics*. World Scientific Publishing Co., Singapore, 1985. ↑249, 250, 280, 281
- [221] F. Klein. *Elementary mathematics from an advanced standpoint. Arithmetic, algebra, analysis*. Dover Publications Inc., Mineola, NY, 2004. Translated from the third German edition by E. R. Hedrick and C. A. Noble, Reprint of the 1932 translation. ↑xiii
- [222] F. Klein. *Elementary mathematics from an advanced standpoint. Geometry*. Dover Publications Inc., Mineola, NY, 2004. Translated from the third German edition and with a preface by E. R. Hendrik and C. A. Noble, Reprint of the 1949 translation. ↑xiii
- [223] A. W. Knap and N. R. Wallach. Szegő kernels associated with discrete series. *Invent. Math.*, **34** (3):163–200, 1976. ↑232
- [224] J. Kollár and S. Mori. *Birational geometry of algebraic varieties*. Cambridge Tracts in Mathematics, vol. 134. Cambridge University Press, Cambridge, 2008. With the collaboration of C. H. Clemens and A. Corti. Paperback reprint of the hardback edition 1998. Zbl1143.14014. ↑144
- [225] A. N. Kolmogorov. И. М. Яглом, “Принцип относительности Галилея и неевклидова геометрия” (рецензия) [I. M. Yaglom, “Galileo’s principle of relativity and noneuclidean geometry” (review)]. *Uspehi Mat. Nauk*, **26** (3(159)):247–249, 1971. Review of [339]. <http://mi.mathnet.ru/umn5223>. ↑xiv
- [226] B. G. Konopelchenko and W. K. Schief. Menelaus’ theorem, Clifford configurations and inversive geometry of the Schwarzian KP hierarchy. *J. Phys. A*, **35** (29):6125–6144, 2002. ↑166, 375
- [227] B. G. Konopelchenko and W. K. Schief. Reciprocal figures, graphical statics, and inversive geometry of the Schwarzian BKP hierarchy. *Stud. Appl. Math.*, **109** (2):89–124, 2002. ↑166, 375
- [228] B. G. Konopelchenko and W. K. Schief. Conformal geometry of the (discrete) Schwarzian Davey–Stewartson II hierarchy. *Glasg. Math. J.*, **47** (A):121–131, 2005. ↑166, 375
- [229] N. G. Kononenko. Algebras of Differential Invariants for Geometrical Quantities on Affine Line. *Visn., Ser. Fiz.-Mat. Nauky, Kyiv. Univ. Im. Tarasa Shevchenka*, **2008** (2):9–15, 2008. ↑375
- [230] N. G. Kononenko and V. V. Lychagin. Differential Invariants of Nonstandard Projective Structures. *Dopov. Nats. Akad. Nauk Ukr., Mat. Pryr. Tekh. Nauky*, **2008** (11):10–13, 2008. Zbl1164.53313. ↑375
- [231] P. Koosis. *Introduction to H_p spaces*. Cambridge Tracts in Mathematics, vol. 115. Cambridge University Press, Cambridge, Second, 1998. With two appendices by V. P. Havin [Viktor Petrovich Khavin]. ↑258, 260, 263, 275, 277, 282, 285, 290

- [232] Ö. Köse. Kinematic differential geometry of a rigid body in spatial motion using dual vector calculus: Part-I. *Applied Mathematics and Computation*, **183** (1):17–29, 2006. [↑265](#)
- [233] S. G. Krantz. *Explorations in harmonic analysis. With applications to complex function theory and the Heisenberg group*. Applied and Numerical Harmonic Analysis. Birkhäuser Boston Inc., Boston, MA, 2009. With the assistance of Lina Lee. [↑263](#), [275](#)
- [234] V. V. Kravchenko and S. M. Torba. Construction of Transmutation Operators and Hyperbolic Pseudoanalytic Functions. *ArXiv e-prints*, August 2012. [↑375](#)
- [235] V. V. Kravchenko. *Applied pseudoanalytic function theory*. Frontiers in Mathematics. Birkhäuser Verlag, Basel, 2009. With a foreword by Wolfgang Sproessig. [↑375](#)
- [236] M. G. Kreĭn. On Hermitian operators with directed functionals. *Akad. Nauk Ukrain. RSR. Zbirnik Prac' Inst. Mat.*, **1948** (10):83–106, 1948. [MR14:56c](#), reprinted in [\[237\]](#). [↑253](#)
- [237] M. G. Kreĭn. *Избранные Труды. II [Selected papers. II]*. Akad. Nauk Ukrainy Inst. Mat., Kiev, 1997. [MR96m:01030](#). [↑401](#)
- [238] J. P. S. Kung (ed.) *Gian-carlo rota on combinatorics: Introductory papers and commentaries*. Contemporary Mathematicians, vol. 1. Birkhäuser Verlag, Boston, 1995. [↑250](#)
- [239] S. Lang. *Algebra*. Addison-Wesley, New York, 1969. [↑20](#)
- [240] S. Lang. $SL_2(\mathbb{R})$. Graduate Texts in Mathematics, vol. 105. Springer-Verlag, New York, 1985. Reprint of the 1975 edition. [↑3](#), [4](#), [15](#), [19](#), [33](#), [125](#), [186](#), [243](#), [245](#), [246](#), [249](#), [252](#), [255](#), [258](#), [271](#), [338](#), [339](#), [346](#), [364](#), [370](#)
- [241] M. A. Lavrent'ev and B. V. Shabat. *Проблемы Гидродинамики и Их Математические Модели. [Problems of hydrodynamics and their mathematical models]*. Izdat. "Nauka", Moscow, Second, 1977. [↑37](#), [136](#), [144](#), [242](#), [373](#), [375](#)
- [242] J.-M. Lévy-Leblond. Une nouvelle limite non-relativiste du groupe de Poincaré. *Ann. Inst. H. Poincaré Sect. A (N.S.)*, **3**:1–12, 1965. [↑337](#)
- [243] M. Libine. Hyperbolic Cauchy integral formula for the split complex numbers. *ArXiv e-prints*, December 2007. [↑375](#)
- [244] V. B. Lidskiĭ. On the theory of perturbations of nonselfadjoint operators. *Ž. Vyčisl. Mat. i Mat. Fiz.*, **6** (1):52–60, 1966. [↑308](#)
- [245] E. Liflyand. Hausdorff operators on Hardy spaces. *Eurasian Math. J.*, **4** (4):101–141, 2013. [↑276](#)
- [246] G. L. Litvinov. The Maslov dequantization, and idempotent and tropical mathematics: a brief introduction. *Zap. Nauchn. Sem. S.-Peterburg. Otdel. Mat. Inst. Steklov. (POMI)*, **326** (Teor. Predst. Din. Sist. Komb. i Algoritm. Metody. 13):145–182, 282, 2005. E-print: [arXiv:math/0507014](#). [↑141](#)
- [247] S. G. Low. Noninertial Symmetry Group of Hamilton's Mechanics, March 2009. E-print: [arXiv:0903.4397](#). [↑355](#)
- [248] G. W. Mackey. *Mathematical foundations of quantum mechanics*. W. A. Benjamin, Inc., New York, Amsterdam, 1963. [↑316](#)
- [249] M. Magee, H. Oh, and D. Winter. Expanding maps and continued fractions, 2014. E-print: [arXiv:1412.4284](#). [↑207](#)
- [250] Y. I. Manin. *Mathematics as metaphor*. American Mathematical Society, Providence, RI, 2007. Selected essays of Yuri I. Manin, With a foreword by Freeman J. Dyson. [↑322](#)
- [251] V. Mazorchuk. *Lectures on $\mathfrak{sl}_2(\mathbb{C})$ -modules*. Imperial College Press, London, 2010. [↑246](#), [338](#), [350](#), [351](#)
- [252] A. McIntosh. Clifford algebras, Fourier theory, singular integral operators, and partial differential equations on Lipschitz domains. In J. Ryan (ed.) *Clifford algebras in analysis and related topics*, pages 33–88, CRC Press, Boca Raton, 1995. [↑263](#), [275](#)
- [253] I. P. Mel'nichenko and S. A. Plaksa. *Коммутативные алгебры и пространственные потенциалы* [Commutative algebras and spatial potential fields]. Inst. Math. NAS Ukraine, Kiev, 2008. [↑375](#)
- [254] W. Miller Jr. *Lie theory and special functions*. Mathematics in Science and Engineering, vol. 43. Academic Press, New York, 1968. [↑15](#), [17](#)
- [255] J. J. Milne. *An elementary treatise on cross-ratio geometry: with historical notes*. Cambridge: The University Press, 1911. <https://archive.org/details/elementarytreati00milnuoft/page/n5/mode/2up>. [↑147](#), [156](#)

- [256] R. Mirman. *Quantum field theory, conformal group theory, conformal field theory. Mathematical and conceptual foundations, physical and geometrical applications*. Nova Science Publishers Inc., Huntington, NY, 2001. ↑375
- [257] V. V. Mityushev and S. V. Rogosin. *Constructive methods for linear and nonlinear boundary value problems for analytic functions. Theory and applications*. Chapman & Hall/CRC Monographs and Surveys in Pure and Applied Mathematics, vol. 108. Chapman & Hall/CRC, Boca Raton, FL, 2000. ↑261, 274, 276, 291
- [258] J. P. Morais, S. Georgiev, and W. Sprößig. *Real quaternionic calculus handbook*. Birkhäuser/Springer, Basel, 2014. ↑205
- [259] J. Moro, J. V. Burke, and M. L. Overton. On the Lidskii-Vishik-Lyusternik perturbation theory for eigenvalues of matrices with arbitrary Jordan structure. *SIAM J. Matrix Anal. Appl.*, **18** (4):793–817, 1997. ↑308
- [260] A. E. Motter and M. A. F. Rosa. Hyperbolic calculus. *Adv. Appl. Clifford Algebras*, **8** (1):109–128, 1998. ↑375
- [261] K. A. Mustafa. The groups of two by two matrices in double and dual numbers, and associated Möbius transformations. *Adv. Appl. Clifford Algebr.*, **28** (5):Art. 92, 25, 2018. E-print: [arXiv:1707.01349](https://arxiv.org/abs/1707.01349). ↑156, 162, 172, 173, 205
- [262] T. Needham. *Visual complex analysis*. The Clarendon Press Oxford University Press, New York, 1997. ↑3
- [263] U. Niederer. Maximal kinematical invariance group of the harmonic oscillator. *Helv. Phys. Acta*, **46** (2):191–200, 1973. ↑327
- [264] N. K. Nikolski. *Operators, functions, and systems: an easy reading. Vol. 1: Hardy, Hankel, and Toeplitz*. Mathematical Surveys and Monographs, vol. 92. American Mathematical Society, Providence, RI, 2002. Translated from the French by Andreas Hartmann. ↑263, 275, 277, 280, 282, 294, 295
- [265] N. K. Nikolski. *Operators, functions, and systems: an easy reading. Vol. 2: Model operators and systems*. Mathematical Surveys and Monographs, vol. 93. American Mathematical Society, Providence, RI, 2002. Translated from the French by Andreas Hartmann and revised by the author. ↑263, 275
- [266] N. K. Nikol'skii. *Treatise on the shift operator. Spectral function theory*. Springer-Verlag, Berlin, 1986. With an appendix by S. V. Hruščev [S. V. Khrushchëv] and V. V. Peller, Translated from the Russian by Jaak Peetre. ↑256, 301
- [267] P. J. Olver. *Applications of Lie groups to differential equations*. Springer-Verlag, New York, Second, 1993. ↑304
- [268] P. J. Olver. *Equivalence, invariants, and symmetry*. Cambridge University Press, Cambridge, 1995. ↑304, 305
- [269] P. J. Olver. *Classical invariant theory*. London Mathematical Society Student Texts, vol. 44. Cambridge University Press, Cambridge, 1999. ↑51, 101
- [270] A. L. Onishchik and R. Sulanke. *Projective and Cayley-Klein geometries*. Springer Monographs in Mathematics. Springer-Verlag, Berlin, 2006. ↑194, 375
- [271] *VirtualBox—powerful x86 and AMD64/Intel64 virtualization product*. Oracle, 2011. URL: <http://www.virtualbox.org>. ↑381
- [272] *Open virtual machine—the open source implementation of VMware Tools*. OVMTP, 2011. URL: <http://open-vm-tools.sourceforge.net/>. ↑381
- [273] J. R. Parker. *Hyperbolic spaces*. University of Durham, 2007. URL: <http://maths.dur.ac.uk/~dma0jrp/img/HSjyvaskyla.pdf>. ↑14, 177
- [274] J. F. Paydon and H. S. Wall. The continued fraction as a sequence of linear transformations. *Duke Math. J.*, **9**:360–372, 1942. ↑207, 209
- [275] P. Pech. *Selected topics in geometry with classical vs. computer proving*. World Scientific Publishing Co. Pte. Ltd., Hackensack, NJ, 2007. ↑xiv, 172
- [276] D. Pedoe. *Circles: A mathematical view*. MAA Spectrum. Mathematical Association of America, Washington, DC, 1995. Revised reprint of the 1979 edition, With a biographical appendix on Karl Feuerbach by Laura Guggenbuhl. ↑45, 147, 151, 156, 160, 161, 172, 197
- [277] R. Penrose. The complex geometry of the natural world. In O. Lehto (ed.) *Proceedings of the International Congress of Mathematicians. Vol. 1*, 2, pages 189–194. Academia Scientiarum Fennica, Helsinki, 1980. Held in Helsinki, August 15–23, 1978. ↑322

- [278] I. Percival and D. Richards. *Introduction to Dynamics*. Cambridge etc.: Cambridge University Press. VIII, 228 p., 1982. ↑355
- [279] A. Perelomov. *Generalized coherent states and their applications*. Texts and Monographs in Physics. Springer-Verlag, Berlin, 1986. ↑249, 250, 251, 281
- [280] F. Pérez and B. E. Granger. IPython: a system for interactive scientific computing. *Computing in Science and Engineering*, 9 (3):21–29, May 2007. URL: <http://ipython.org>. ↑384
- [281] V. N. Pilipchuk. *Nonlinear Dynamics. Between Linear and Impact Limits*. Lecture Notes in Applied and Computational Mechanics, vol. 52. Springer, Berlin, 2010. ↑144, 321, 375
- [282] V. N. Pilipchuk. Non-smooth spatio-temporal coordinates in nonlinear dynamics, January 2011. E-print: [arXiv:1101.4597](https://arxiv.org/abs/1101.4597). ↑144, 375
- [283] V. N. Pilipchuk, I. V. Andrianov, and B. Markert. Analysis of micro-structural effects on phononic waves in layered elastic media with periodic nonsmooth coordinates. *Wave Motion*, 63:149–169, 2016. ↑375
- [284] R. I. Pimenov. Unified axiomatics of spaces with maximal movement group. *Litov. Mat. Sb.*, 5:457–486, 1965. Zbl0139.37806. ↑94, 157, 191, 338, 375
- [285] G. Piranian and W. J. Thron. Convergence properties of sequences of linear fractional transformations. *Michigan Math. J.*, 4:129–135, 1957. ↑207, 209
- [286] S. Plaksa. Commutative algebras of hypercomplex monogenic functions and solutions of elliptic type equations degenerating on an axis. In H. G. W. Begehr (ed.) *Further progress in analysis. Proceedings of the 6th international ISAAC congress, Catania, Italy, July 25–30, 2005*, pages 977–986, World Scientific, Hackensack, NJ, 2009. ↑375
- [287] G. Pólya and G. Szegő. *Problems and theorems in analysis. I Series, integral calculus, theory of functions*. Classics in Mathematics. Springer-Verlag, Berlin, 1998. Translated from the German by Dorothee Aeppli, Reprint of the 1978 English translation. ↑xiv
- [288] L. S. Pontryagin. *Обобщения чисел [Generalisations of numbers]*. Библиотечка “Квант” [Library “Kvant”], vol. 54. “Nauka”, Moscow, 1986. ↑36
- [289] I. R. Porteous. *Clifford algebras and the classical groups*. Cambridge Studies in Advanced Mathematics, vol. 50. Cambridge University Press, Cambridge, 1995. ↑51, 84, 161, 162, 339
- [290] R. M. Porter. Differential invariants in Möbius geometry. *J. Natur. Geom.*, 3 (2):97–123, 1993. ↑194, 205
- [291] R. M. Porter. Möbius invariant quaternion geometry. *Conform. Geom. Dyn.*, 2:89–106, 1998. ↑194, 205
- [292] R. M. Porter. Quaternionic Möbius transformations and loxodromes. *Complex Variables Theory Appl.*, 36 (3):285–300, 1998. ↑194, 205
- [293] R. M. Porter. Local geometry of circles and loxodromes. *J. Anal.*, 15:211–219, 2007. ↑194, 205
- [294] O. V. Prezhdo and V. V. Kisil. Mixing quantum and classical mechanics. *Phys. Rev. A* (3), 56 (1):162–175, 1997. E-print: [arXiv:quant-ph/9610016](https://arxiv.org/abs/quant-ph/9610016). ↑339
- [295] J. Ryan. Inner product algebras and the function theory of associated Dirac operators. *Miniconference on Operators in Analysis (Sydney, 1989)*, pages 213–226, Austral. Nat. Univ., Canberra, 1990. ↑191
- [296] W. W. Sawyer. *Prelude to mathematics*. Popular Science Series. Dover Publications, New York, 1982. ↑48, 101
- [297] W. K. Schief and B. G. Konopelchenko. A novel generalization of Clifford’s classical point-circle configuration. Geometric interpretation of the quaternionic discrete Schwarzian Kadomtsev-Petviashvili equation. *Proc. R. Soc. Lond. Ser. A Math. Phys. Eng. Sci.*, 465 (2104):1291–1308, 2009. ↑166, 375
- [298] M. Schottenloher. *A mathematical introduction to conformal field theory*. Lecture Notes in Physics, vol. 759. Springer-Verlag, Berlin, Second, 2008. ↑103, 104
- [299] H. Schwerdtfeger. Moebius transformations and continued fractions. *Bull. Amer. Math. Soc.*, 52:307–309, 1946. ↑207, 209
- [300] H. Schwerdtfeger. *Geometry of complex numbers: Circle geometry, Moebius transformation, non-Euclidean geometry*. Dover Books on Advanced Mathematics. Dover Publications Inc., New York, 1979. A corrected reprinting of the 1962 edition. ↑7, 45, 147, 148, 149, 151, 156, 160, 161, 191, 197, 207, 210
- [301] I. E. Segal. *Mathematical problems of relativistic physics*. Proceedings of the Summer Seminar (Boulder, Colorado, 1960), vol. II. American Mathematical Society, Providence, R.I., 1963. ↑235
- [302] I. E. Segal. *Mathematical cosmology and extragalactic astronomy*. Pure and Applied Mathematics, vol. 68. Academic Press [Harcourt Brace Jovanovich Publishers], New York, 1976. ↑105, 106, 111

- [303] I. R. Shafarevich and A. O. Remizov. *Linear algebra and geometry*. Springer, Heidelberg, 2013. Translated from the 2009 Russian original by David Kramer and Lena Nekludova. ↑147, 150, 156
- [304] R. W. Sharpe. *Differential geometry. Cartan's generalization of Klein's Erlangen program*. Graduate Texts in Mathematics, vol. 166. Springer-Verlag, New York, 1997. With a foreword by S. S. Chern. ↑375
- [305] M. A. Shubin. *Pseudodifferential operators and spectral theory*. Springer-Verlag, Berlin, Second, 2001. Translated from the 1978 Russian original by Stig I. Andersson. ↑24
- [306] B. Simon. *Szegő's theorem and its descendants. Spectral theory for L^2 perturbations of orthogonal polynomials*. M. B. Porter Lectures. Princeton University Press, Princeton, NJ, 2011. ↑45, 52, 148, 149, 154, 159, 162, 194, 197, 199, 205
- [307] O. Skavhaug and O. Certik. *swiGiNaC—a Python interface to GiNaC, built with SWIG*, 2010. URL: <http://swiginac.berlios.de/>. ↑383
- [308] G. Sobczyk. The hyperbolic number plane. *College Math Journal*, **26** (4):268–280, 1995. ↑375
- [309] *Debian—the universal operating system*. Software in the Public Interest, Inc., 1997. URL: <http://www.debian.org/>. ↑379
- [310] F. Sommen. Monogenic functions on surfaces. *J. Reine Angew. Math.*, **361**:145–161, 1985. ↑191
- [311] A. B. Sossinsky. *Geometries*. Student Mathematical Library, vol. 64. American Mathematical Society, Providence, RI, 2012. ↑48, 375
- [312] H. M. Srivastava, V. K. Tuan, and S. B. Yakubovich. The Cherry transform and its relationship with a singular Sturm-Liouville problem. *Q. J. Math.*, **51** (3):371–383, 2000. ↑350
- [313] E. M. Stein. *Singular integrals and differentiability properties of functions*. Princeton Mathematical Series, No. 30. Princeton University Press, Princeton, N.J., 1970. ↑291
- [314] E. M. Stein. *Harmonic analysis: Real-variable methods, orthogonality, and oscillatory integrals*. Princeton Mathematical Series, vol. 43. Princeton University Press, Princeton, NJ, 1993. With the assistance of Timothy S. Murphy, Monographs in Harmonic Analysis, III. ↑254, 259, 260, 261, 263, 275, 277, 278, 283, 284, 286, 287, 289, 291, 292, 293
- [315] G. F. Steinke. Topological circle geometries. *Handbook of incidence geometry*, pages 1325–1354, North-Holland, Amsterdam, 1995. ↑72, 375
- [316] I. Stewart and D. Tall. *Algebraic number theory and Fermat's last theorem*. A K Peters, Ltd., Natick, MA, Third, 2002. ↑170
- [317] R. Sulanke. Submanifolds of the Möbius space. II. Frenet formulas and curves of constant curvatures. *Math. Nachr.*, **100**:235–247, 1981. ↑194
- [318] B. Sz.-Nagy and C. Foias. *Harmonic analysis of operators on Hilbert space*. North-Holland Publishing Company, Amsterdam, 1970. ↑255
- [319] J. L. Taylor. A general framework for a multi-operator functional calculus. *Advances in Math.*, **9**:183–252, 1972. ↑371
- [320] M. E. Taylor. *Pseudodifferential operators*. Princeton Mathematical Series, vol. 34. Princeton University Press, Princeton, N.J., 1981. ↑365, 367
- [321] M. E. Taylor. *Noncommutative harmonic analysis*. Mathematical Surveys and Monographs, vol. 22. American Mathematical Society, Providence, RI, 1986. ↑17, 19, 25, 125, 224, 233, 245, 249, 271, 331, 339
- [322] A Torre. A note on the general solution of the paraxial wave equation: a Lie algebra view. *Journal of Optics A: Pure and Applied Optics*, **10** (5):055006 (14pp), 2008. ↑327, 334, 339, 350
- [323] A Torre. Linear and quadratic exponential modulation of the solutions of the paraxial wave equation. *Journal of Optics A: Pure and Applied Optics*, **12** (3):035701 (11pp), 2010. ↑327, 339
- [324] E. E. Tyrtshnikov. *A brief introduction to numerical analysis*. Birkhäuser Boston Inc., Boston, MA, 1997. ↑308
- [325] S. Ulrych. Relativistic quantum physics with hyperbolic numbers. *Phys. Lett. B*, **625** (3–4):313–323, 2005. ↑347, 348, 375
- [326] S. Ulrych. Representations of Clifford algebras with hyperbolic numbers. *Adv. Appl. Clifford Algebr.*, **18** (1):93–114, 2008. ↑348
- [327] S. Ulrych. Considerations on the hyperbolic complex Klein-Gordon equation. *J. Math. Phys.*, **51** (6):063510, 8, 2010. ↑321, 375
- [328] V. A. Uspenskiĭ. *Что такое нестандартный анализ? [What is non-standard analysis?]*. “Nauka”, Moscow, 1987. With an appendix by V. G. Kanovëi. ↑96

- [329] N. L. Vasilevski. On the structure of Bergman and poly-Bergman spaces. *Integral Equations Operator Theory*, **33** (4):471–488, 1999. ↑[364](#)
- [330] N. L. Vasilevski. *Commutative algebras of Toeplitz operators on the Bergman space*. Operator Theory: Advances and Applications, vol. 185. Birkhäuser Verlag, Basel, 2008. ↑[194](#), [196](#), [199](#), [205](#)
- [331] G. R. Veldkamp. On the use of dual numbers, vectors and matrices in instantaneous, spatial kinematics. *Mechanism and Machine Theory*, **11** (2):141–156, 1976. ↑[375](#)
- [332] J. C. Vignaux and A. Durañona y Vedia. Sobre la teoría de las funciones de una variable compleja hiperbólica [On the theory of functions of a complex hyperbolic variable]. *Univ. nac. La Plata. Publ. Fac. Ci. fis. mat.*, **104**:139–183, 1935. Zbl[62.1122.03](#). ↑[375](#)
- [333] N. Ja. Vilenkin. *Special functions and the theory of group representations*. Translations of Mathematical Monographs, vol. 22. American Mathematical Society, Providence, R. I., 1968. Translated from the Russian by V. N. Singh. ↑[15](#), [17](#), [220](#), [221](#), [223](#)
- [334] J. Vince. *Geometric algebra for computer graphics*. Springer-Verlag London, Ltd., London, 2008. ↑[160](#)
- [335] V. S. Vladimirov. *Equations of mathematical physics*. Marcel Dekker, New York, 1971. ↑[138](#)
- [336] A. Vourdas. Analytic representations in quantum mechanics. *J. Phys. A*, **39** (7):R65–R141, 2006. ↑[337](#)
- [337] P. M. H. Wilson. *Curved spaces. From classical geometries to elementary differential geometry*. Cambridge University Press, Cambridge, 2008. ↑[113](#), [115](#)
- [338] C. E. Wulfman. *Dynamical Symmetry*. World Scientific, 2010. ↑[335](#), [339](#), [350](#), [355](#)
- [339] I. M. Yaglom. *A simple non-Euclidean geometry and its physical basis*. Heidelberg Science Library. Springer-Verlag, New York, 1979. Translated from the Russian by Abe Shenitzer, with the editorial assistance of Basil Gordon. ↑[xiv](#), [3](#), [5](#), [13](#), [40](#), [45](#), [46](#), [75](#), [84](#), [90](#), [91](#), [94](#), [95](#), [96](#), [100](#), [102](#), [103](#), [109](#), [110](#), [111](#), [116](#), [117](#), [119](#), [131](#), [136](#), [137](#), [140](#), [147](#), [148](#), [156](#), [157](#), [162](#), [191](#), [210](#), [242](#), [320](#), [347](#), [353](#), [375](#), [400](#)
- [340] Da. Yang, Do. Yang, and X. Fu. The Hardy space H^1 on non-homogeneous spaces and its applications—a survey. *Eurasian Math. J.*, **4** (2):104–139, 2013. ↑[278](#)
- [341] C. Zachos. Deformation quantization: Quantum mechanics lives and works in phase-space. *Internat. J. Modern Phys. A*, **17** (3):297–316, 2002. E-print: [arXiv:hep-th/0110114](#). ↑[319](#), [343](#)
- [342] D. N. Zejlinger. *Комплексная Линейчатая Геометрия. Поверхности и Конгруенции. [Complex lined geometry. Surfaces and congruency]*. GTTI, Leningrad, 1934. ↑[320](#), [375](#)
- [343] G. Zöll. *Residuenkalkül in der Clifford–analysis und die Möbius transformationen in den Euklidischen räumen*. Ph.D. Thesis, 1987. ↑[191](#)
- [344] A. Zygmund. *Trigonometric series. Vol. I, II*. Cambridge Mathematical Library. Cambridge University Press, Cambridge, Third, 2002. With a foreword by Robert A. Fefferman. ↑[276](#)

Index

- \mathbb{A} (point space), 37
- A subgroup, 4, 32
- A -orbit, 4, 38, 132
- A' subgroup, 32, 41, 114, 127
- A'' subgroup, 43
- A' -orbit, 43
- \mathbb{C} (complex numbers), 37
- $\check{C}_{\check{\sigma}}$ (ghost cycle), 78
- \mathbb{D} (dual numbers), 37
- \mathbb{D}_{σ} (unit disk), 126
- F subgroup, 29
- F' subgroup, 29
- \bar{F} subgroup, 29
- $\mathcal{G}(\rho)$, 230
- \mathbb{H}^1 (Heisenberg group), 19
- K subgroup, 4, 15, 32, 114
- K -orbit, 4, 38, 38–40, 43, 57, 104, 106, 132
- M map, 48, 101
- N subgroup, 4, 32
- N -orbit, 4, 38, 132
- N' subgroup, 32, 41, 114
- N' -orbit, 43
- \mathbb{O} (double numbers), 37
- \mathbb{O} (two-fold cover of double numbers), 105
- \mathbb{O}^+ (hyperbolic upper half-plane), 105
- P (projection from the projective space), 123
- $\mathbb{P}^1(\mathbb{A})$ (projective space), 53
- \mathbb{P}^3 (projective space), 48
- Q map, 48, 72, 101
- $\mathbb{R}_{\check{\sigma}}^{\check{s}}$ (cycle representing the real line), 83
- \mathbb{R} (projective real line), 30
- \mathbb{R}^* (hyperreals), 100
- S (section to the projective space), 54
- $SL_2(\mathbb{R})$ group, 3, 19
- $SU(1, 1)$ group, 126
- T_{σ} (unit cycle), 126
- Z (the centre of the Heisenberg group), 324
- $Z_{\check{\sigma}}^{\check{s}}(y)$ ($\check{\sigma}$ -zero-radius cycle), 62
- Z_{∞} (zero-radius cycle at infinity), 101
- $[z_1, z_2, z_3, z_4]$ (cross ratio), 53
- $\Lambda(g)$, 223
- $SL_2(\mathbb{R})$, 276, 279, 283, 297
- $SL_2(\mathbb{R})$ group
 - Hardy representation, 220
 - representation, 243–244
 - in Banach space, 303
- $Sp(2)$, 324
- \mathbb{H}^n (Heisenberg group), 324
- \mathbb{J}^n (jet space), 305
- \cos_{σ} , 44
- δ_{jk} , 220
- ∞ (point at infinity), 102
- \perp (perpendicularity), 95
- \overrightarrow{AB} (directed interval), 92
- $\langle \cdot, \cdot \rangle$, 220
- σ -cosine, 44, 64, 91
- σ -sine, 44, 91
- σ -tangent, 43
- \sin_{σ} , 44
- \dashv (f-orthogonality), 85
- \tan_{σ} , 43
- tr , 221
- $a\alpha + b$ group, 3, 3, 19, 38, 253, 257, 258, 266–268, 278, 282, 285, 288
 - Haar measure, 26
 - invariant measure, 278
 - left regular representation, 278
 - representation, 219, 251
 - co-adjoint, 279
 - quasi-regular, 278
- ε (parabolic unit), 3
- ϵ (infinitesimal), 96
- \mathfrak{h}_1 (Lie algebra of the Heisenberg group), 325
- i (imaginary unit), 3
- ι (hypercomplex unit), 3, 36, 373
- \check{i} (hypercomplex unit in cycle space), 7, 48
- j (hyperbolic unit), 3
- k -normalised cycle, 13, 57, 63, 64, 89, 91, 103, 388

- $l_c(\overrightarrow{AB})$ (length from centre), 92
- $l_f(\overrightarrow{AB})$ (length from focus), 92
- ω (symplectic form), 324
- p map, 21, 108, 224
- r map, 21, 108, 224
- s map, 21, 108, 224
- σ ($\sigma := \iota^2$), 4, 37
- $\check{\sigma}$ ($\check{\sigma} := \check{\iota}^2$), 48
- $\check{\sigma}$ -focus, 56, 122
- \mathfrak{sl}_2 (Lie algebra), 25
- χ (Heaviside function), 78
- $\check{\square}$, *see* CAS exercise
- Abel summation, 276
- abelian group, *see* commutative group
- about hearing a drum's shape, 9
- absolute time, 110, 136, 378
- abstract group, 17, 20
- acceleration, 110
- action
 - derived, 5, 25, 30, 38
 - transitive, 3, 20, 22, 38
- adjoint representation, 53, 221
- admissible
 - mother wavelet, 294
- admissible vector, 230
- admissible wavelet, 249, 251, 257, 281, 284
- affine
 - group, *see* $ax + b$ group
- affine group, *see* $ax + b$ group
- algebra
 - associative, 373
 - Clifford, 14, 50, 51, 80, 253, 339, 369, 371, 375
 - cycle matrix, 376
 - Möbius map, 376
 - matrix similarity, 376
 - commutative, 373
 - homomorphism, 301
 - Lie, 22–25, 53
 - Weyl, 323, 325
- algebraically-closed, 373
- analysis
 - complex, 15
 - functional, 47
 - harmonic, 15
 - multiresolution, 253
 - non-Archimedean, *see* non-standard
 - non-standard, 96, 100
- analytic
 - contravariant calculus, 302
 - function on discrete sets, 370
- annihilation operator, *see* ladder operator
- annulus, 274
- Apollonian gasket, 48
- approximation
 - identity, of the, 278
- Archimedes, 96, 374
- arithmetic of infinity, 30
- arrow, time, of, 105, 111
- associative algebra, 373
- associativity, 17
- astronomy, extragalactic, 106, 111
- Asymptote, 379, 385
- asymptote, hyperbola, of, 39, 374
- Atiyah–Singer index theorem, 4
- atom, 259, 286
- atomic
 - decomposition, 260, 287
- automatic theorem proving, 387
- automorphism
 - group, of, 326
 - inner, 327
 - outer, 327
- Baker–Campbell–Hausdorff formula, 326
- Benz
 - parallelism, 72
- Bergman
 - integral, 15
 - space, 15, 249, 252, 274, 370
- birational geometry, 144
- Birkhoff orthogonality, *see* perpendicular
- Blaschke
 - product, 307
- boundary effect on the upper half-plane, 9, 56, 63, 71, 78, 85
- bracket
 - Moyal, 343, 344
 - hyperbolic, 337, 349
 - Poisson, 355
- calculus
 - contravariant, 256, 371
 - analytic, 302
 - covariant, 255, 307, 310, 311, 371
 - Berezin, 255
 - functional, 256, 301, 370, 371
 - covariant, 289
 - Riesz–Dunford, 256
 - support, *see* spectrum
 - symbolic, *see* covariant calculus
 - umbral, 250
- Calderón–Zygmund
 - decomposition, 293
- Campbell–Hausdorff formula, *see* Baker–Campbell–Hausdorff formula
- cancellation, formula for cross ratio, 54
- cancellation, formula for cross-ratios, 122

- cancellative semigroup, 250
- canonical transformation, 108
- Carleson
 - measure, 295
 - norm, 295
- Cartan
 - subalgebra, 246
- CAS, *xiv*, 49, 96, 375, 379–389
 - pyGiNaC, 383
 - swiGiNaC, 383
 - exercise, 34, 38, 39, 42, 44, 49, 50, 54, 58, 60, 63–67, 70, 71, 78–84, 86, 89–93, 95–99, 101, 115, 121, 130, 131, 144
- case
 - elliptic, 4, 37
 - hyperbolic, 4, 37
 - parabolic, 4, 37
- Casimir operator, 271
- categorical viewpoint, 10, 69
- category theory, 10
- Cauchy integral, 15, 251, 271–273, 276, 282, 297, 304, 370
- Cauchy integral formula, 228
- Cauchy–Riemann
 - operator, 15
- Cauchy–Riemann operator, 267, 288, 297
- Cauchy–Schwarz inequality, 65–67, 71
- Cauchy–Riemann operator, 270, 271, 347, 370
- causal, 341
- causal orientation, 105, 111
- Cayley transform, 125, 131, 272
 - cycle, of, 129
 - elliptic, 125
 - hyperbolic, 125
 - parabolic, 128
- centre
 - cycle, of, 8, 37, 46, 55, 57, 91, 122, 128, 374, 378
 - ellipse, of, 374
 - hyperbola, of, 374
 - length from, 14, 92, 92, 93, 126–128
- character, 331
 - group, of, 222
- character of a group, 222
- character of representation, 221
- characteristic
 - function, 255
- circle, 45, 374
 - imaginary, 46, 55, 58, 61
 - parabolic (Yaglom term), 75, 378
 - unit, *see* elliptic unit cycle
- classes of equivalent representations, 220
- classic
 - Fock–Segal–Bargmann representation, 353
 - probability, 355
- Schrödinger representation, 353
- classical mechanics, 108, 342
 - Hamiltonian, 323
- Clifford
 - algebra, 14, 50, 51, 80, 253, 339, 369, 371, 375
 - cycle matrix, 376
 - Möbius map, 376
 - matrix similarity, 376
- Clifford algebras, 14
- co-adjoint
 - representation, 333
 - orbit, 333
 - representation of $\alpha x + b$ group, 279
- coaxial cycles, 40, 58
- coefficients
 - matrix, 227
 - representational, 227
- coherent state, *see* wavelet
- coherent states, 227
- commutation
 - relation
 - Heisenberg, 323, 326
 - Weyl, 323
- commutation relation, Heisenberg, 25
- commutative
 - algebra, 373
 - group, 18
- commutator, 24, 337, 339
- commuting operator, 223
- compactification, 101
- complex
 - analysis, 15
 - numbers, 34, 373
- complex numbers, 283
- computer algebra system, *see* CAS
- concentric, 8, 46, 58, 97, 128
 - parabolas, 56, 129
- concurrent cycles, 74
- conyclic, 54
- condition, Vahlen, 80, 84
- cone, 5, 373
 - light, 41, 63, 72, 81, 98, 105, 110
 - infinity, at, 103, 105
- configuration
 - space, 342, 344, 349, 354, 356
- confocal, 97
 - parabolas, 129
- conformal
 - infinitesimally, 99
 - space-time, 104
- conformality, 14, 93
 - parabolic, 144
- congruence, matrix, of, 52
- conic section, 4, 5, 39, 373

- conjugated subgroups, 21
- conjugation, 20, 53
 - cycles, of, 12, 97
- constant curvature, 102
- constant Planck, 337, 354
- construction
 - Fillmore–Springer–Cnops, 7, 48, 128, 369
 - operator, 311
 - Gelfand–Naimark–Segal, 10, 60
- continuous
 - wavelet transform, 281
- continuous group, 18
- contour line, 38, 93, 95, 139
- contravariant
 - calculus, 256, 371
 - analytic, 302
 - spectrum, 302, 303, 305, 307
 - stability, 308
 - symbol, 255
 - transform, 284, 297
- contravariant transform, 256, 364
- convolution, 26, 339
 - relative, 287, 365
- convolution operator, 26
- correspondence
 - Kirillov, 52
- coset space, 21
- covariant
 - calculus, 255, 307, 310, 311, 371
 - Berezin, 255
 - functional calculus, 289
 - pencil, 310
 - spectral distance, 308
 - symbol, 254
 - symbolic calculus, 254
 - transform, 249, 280, 297
 - induced, 265
 - inverse, *see* contravariant transform
- cover, two-fold
 - hyperbolic plane, 105, 127
- creation operator, *see* ladder operator
- cross ratio, 53, 151
 - cancellation formula, 54
 - cycles, 85, 151, 189
 - projective, 54, 54
- cross-ratio, 122
 - cancellation formula, 122
 - projective, 123
- curvature, 38
 - constant, 102
- curve length, 114
- cycle, 5, 45, 47, 161, 312, 373
 - ö-product, 60, 69, 91
 - Cayley transform, 129
- centre, 8, 37, 46, 55, 57, 91, 122, 128, 374, 378
- concentric, 97
- confocal, 97
- conjugation, 12, 97
- cross ratio, 85, 151, 189
- diameter, 89, 378
- equation, 7, 45, 47
- f-ghost, 86
- flat, 46
- focal length, 56, 89
- focus, 8, 37, 56, 89, 122, 128, 374
- ghost, 78, 83
- infinitesimal radius, of, 96, 96–100, 131
- inversion, 82, 82–84, 86, 103
- isotropic, 11, 71
- matrix, 7, 48
 - Clifford algebra, 376
- normalised, 9, 57
 - det-, 57, 62, 64, 85, 89, 103, 388
 - k-, 13, 57, 63, 64, 89, 91, 103, 388
 - norm, 64
- orthogonality, 50, 98
- parabolic (Yaglom term), 378
- positive, 61, 115
- radius, 13, 58, 89, 388
 - infinitesimal, of, 96, 96–100
 - zero, 97
- reflection, 12, 82, 82–84, 130
- selfadjoint, 75, 85, 122, 378
- similarity, 79, 130, 388
 - Clifford algebra, 376
- space, 7, 48, 101, 161, 378
 - unit
 - elliptic, 126
 - hyperbolic, 127
 - parabolic, 128
 - zero-radius, 9, 11, 51, 61, 62–66, 71–73, 89, 97, 101, 103, 120, 378
 - elliptic, 63
 - hyperbolic, 63
 - infinity, at, 101
 - parabolic, 63
- cycles
 - coaxial, 40, 58
 - concurrent, 74
 - disjoint, 66, 71, 73
 - f-orthogonal, 12, 14, 85, 95, 131, 388
 - intersecting, 66, 71, 73
 - orthogonal, 7, 10, 46, 69, 69–79, 82–83, 115, 131, 388
 - pencil, xiv, 58, 64, 66–67, 72–74, 387
 - orthogonal, 73, 80, 84
 - radical axis, 40, 58
 - tangent, 58, 66, 73

- Descartes–Kirillov condition, 66
- cyclic vector, 222
- De Donder–Weyl formalism, 371
- decomposable
 - representation, 223
- decomposition atomic, 260, 287
- decomposition Calderón–Zygmund, 293
- decomposition Iwasawa, 4, 33, 37, 369
- defect operator, 255
- degeneracy parabolic, 78, 129
- dequantisation Maslov, 141
- derivation
 - inner, 337, 339
- derived action, 5, 25, 30, 38
- Descartes–Kirillov
 - condition for tangent circles, 66
- det-normalised cycle, 57, 62, 64, 85, 89, 103, 388
- determinant, 9
- diameter, cycle, of, 89, 378
- discrete series, 231
- directing functional, 253
- directrix, 8, 39
 - parabola, of, 56, 374
- discrete
 - analytic function, 370
 - geometry, 369
 - spectrum, 370
- discriminant, 61
- disjoint cycles, 66, 71, 73
- disk, unit, 125
 - elliptic, 126, 126
 - hyperbolic, 127
 - metric, 131, 135
 - parabolic, 128
- distance, 13, 90, 90, 93, 126, 127, 135
 - conformal, 93
 - covariant spectral, 308
 - inversive between cycles, 64
- distinct, essentially, 54, 123
- divisor, zero, 4, 35, 36, 41, 53, 102, 138, 352, 373
- domain
 - non-simply connected, 274
 - simply connected, 274
- double, 3
- double number, 337, 347, 352
- double numbers, 3, 36, 284, 373
- doubling condition, 278
- dual, 3
- dual number, 337, 353, 353–356
- dual numbers, 3, 35, 35, 373
- dual object, 223
- dual space, 223
- dyadic
 - squares, 277, 289, 297
- dynamics non-linear, 144, 375
- e-centre, 46
- e-focus, 56
- eigenvalue, 245, 246, 305, 307
 - generalised, 309
 - quadratic, 311
- element, ideal, 101
- ellipse, 374
 - centre, 374
 - focus, 374
- elliptic
 - case, 4, 37
 - Cayley transform, 125
 - rotation, 126
 - unit
 - cycle, 126
 - disk, 126, 126
 - upper half-plane, 34, 41
 - zero-radius cycle, 63
- EPAL, *see* Erlangen programme at large, 14
- EPH classification, 4, 37, 121
- equation
 - discrete
 - integrability of, 375
 - dynamics in p-mechanics, 339
 - Hamilton, 337, 354
 - heat, 138, 267
 - Heisenberg, 337, 343
 - quadratic, 373
 - Schrödinger, 327
- equivalent representations, 220
- Erlangen programme, ii, xiii, xiii, 3, 3
 - at large, xiii, 14
- essentially distinct, 54, 123
- Euclidean
 - geometry, xiii, 96
 - space, 94
- Euler
 - formula, 137, 377
 - operator, 38
- exact representation, 220
- exponential map, 23, 32
- extension
 - Poincaré, 177
 - Poincaré, 53
- extragalactic astronomy, 106, 111
- f-ghost cycle, 86
- f-orthogonality, 12, 14, 85, 95, 98, 120, 131, 388
- factorisation
 - Wiener–Hopf, 253
- faithful representation, 220

- fiducial operator, 249, 280
- fiducial vector, 227
- field
 - quantum, 371
- Fillmore–Springer–Cnops construction, 7, 48, 128, 369
 - operator, 311
- finite dimensional
 - representation, 220
- fixed point
 - Möbius map, of, 31, 33, 98, 126
- flat cycles, 46
- focal
 - length, 40, 89, 97, 110
 - cycle, of, 56
 - parabola, of, 56
 - orthogonality, *see* f-orthogonality
- Fock–Segal–Bargmann
 - representation, 333, 335, 356, 362
 - classic (parabolic), 353
 - hyperbolic, 348
 - representations, 341
 - space, 253, 335, 347, 357, 371
 - transform, 362
- focus, 61, 89
 - cycle, of, 8, 37, 56, 122, 128, 374
 - ellipse, of, 374
 - elliptic, 56
 - hyperbola, of, 39, 374
 - hyperbolic, 56
 - length from, 14, 92, 92, 93, 99, 128
 - p-conformality, 144
 - parabola, of, 8, 39, 56, 374
 - parabolic, 56
- form, symplectic, 53, 54, 108, 324, 326, 376
- formalism
 - paravector, 375
 - vector, 375
- formula
 - Baker–Campbell–Hausdorff, 326
 - Campbell–Hausdorff, *see* Baker–Campbell–Hausdorff formula
 - cancellation for cross ratio, 54
 - cancellation for cross-ratios, 122
 - Euler, 137, 377
 - reconstruction, 257, 284
 - Sokhotsky–Plemelj, 276
- FSB
 - representation, *see* Fock–Segal–Bargmann representation
 - space, *see* Fock–Segal–Bargmann space
- FSCc, *see* Fillmore–Springer–Cnops construction
- function
 - characteristic, 255
 - Gauss, *see* Gaussian, 234
 - Heaviside, 10, 30, 78
 - Hermite, *see* Hermite polynomial
 - norm of, 47
 - orthogonality of, 47
 - parabolic cylinder, *see* Weber–Hermite function
 - polyanalytic, 271
 - special, 15
 - Weber–Hermite, 350, 352
- functional analysis, 47
- functional calculus, 256, 301, 370, 371
 - covariant, 289
 - Riesz–Dunford, 256
 - support, *see* spectrum
- functional directing, 253
- functional invariant, 256, 284
- functional model, 255, 301, 308, 371
- functions
 - trigonometric
 - σ -, 43
 - parabolic, 136
- Galilean
 - orthogonality, 95
 - space-time, 110, 136
 - transformation, 110
- Gårding space, 230
- Gauss
 - function, *see* Gaussian
 - measure, 235
- Gaussian, 228, 234, 235, 252, 267, 282, 344, 348, 349, 361, 362
- Gelfand–Naimark–Segal construction, 10, 60, 60
- generalised
 - eigenvalue, 309
- generator
 - quadratic, 335
 - subgroup, of, 245
- geodesics, 118, 113–123, 131, 135, 145
- geometrical quantisation, 337
- geometry, 369
 - birational, 144
 - commutative, xiii
 - discrete, 369
 - Euclidean, xiii, 96
 - hyperbolic, 37
 - Lobachevsky, xiii, 37, 258, 270, 369
 - non-commutative, xiii, 15, 312
 - representational, 47
 - Riemann, 37, 113
- ghost cycle, 78, 83
- GiNaC, *see* CAS, 382

- GNS construction, *see* Gelfand–Naimark–Segal construction, 10
- GNU, 379
- General Public License (GPL), 379
 - Linux, 379
 - emulator, 380, 381
- GPL, *see* GNU General Public License
- grand maximal function, 254, 283
- ground state, 227
- group, 3, 17
- $SL_2(\mathbb{R})$, 3, 19, 20, 276, 279, 283, 297
 - Hardy representation, 220
 - Lie algebra, 25
 - one-dimensional subgroup, 22
- $Sp(2)$, *see also* $SL_2(\mathbb{R})$, 338
- $SU(1, 1)$, *see also* $SL_2(\mathbb{R})$, 255
- $\alpha x + b$, 3, 19, 29, 38, 253, 257, 258, 266–268, 278, 282, 285, 288
- Haar measure on, 26
 - invariant measure, 278
 - Lie algebra, 23–24
 - one-dimensional subgroup, 22
- abelian, *see* commutative group
- abstract, 17, 20
- affine, *see* $\alpha x + b$ group, *see* $\alpha x + b$ group automorphism of, 326
- inner, 327
 - outer, 327
- characters, of, 222
- commutative, 18
- continuous, 18
- Heisenberg, 3, 16, 19, 324, 323–329, 337, 339–357, 371
- centre, 324
 - Fock–Segal–Bargmann representation, 362
 - Fock–Segal–Bargmann representation, 333
 - Haar measure on, 26
 - induced representation, 331
 - invariant measure, 331
 - Lie algebra, 24, *see* Weyl algebra
 - one-dimensional subgroup, 22
 - polarised, 325
 - Schrödinger representation, 220
- Heisenberg–Weyl, *see* Heisenberg group, 323
- law, *see* group multiplication
- Lie, 19, 22
- nilpotent, 326
- locally compact, 18
- multiplication, 17
- non-commutative, 18
- representation, 219
- linear, 15
- Schrödinger, 327, 346
- symplectic, 324, 327, 334, 339, 346
- transformation, 17, 20
- unimodular, 331
- Weyl, *see* Heisenberg group, 323
- h-centre, 46
- h-focus, 56
- Haar measure, 25, *see* invariant measure, *see* invariant measure
- $\alpha x + b$ group, on, 26
 - Heisenberg group, on, 26
- half-plane, 310
- boundary effect, 9, 56, 63, 71, 78, 85
 - invariance, 34, 35, 104, 105
 - lower, 20, 40, 43
 - non-invariance, 35, 104, 105
 - upper, 20, 40, 43, 125, 364
 - elliptic, 34, 41
 - hyperbolic, 35, 105
 - parabolic, 35, 41
- Hamilton
- equation, 337, 354
- Hamiltonian, 108
- classical mechanics, 323
 - quadratic, 108
- Hardy pairing, 257, 258, 285
- Hardy space, 15, 249, 251, 261, 271, 273, 277, 279, 282, 291, 302, 308, 370
- generalised, 261
 - generalized, 278, 289, 292
- Hardy–Littlewood
- maximal functions, 253, 260, 277, 283, 290, 297
- harmonic
- analysis, 15
 - oscillator, 108, 327, 335, 339, 340, 343, 346, 349, 355
 - quantum, 109
 - repulsive (hyperbolic), 350
- heat
- equation, 138, 267
 - kernel, 138, 267
- Heaviside function, 10, 10, 30, 78, 78
- Heisenberg
- commutation relation, 25, 323, 326
 - equation, 337, 343
 - group, 3, 16, 19, 324, 323–329, 337, 339–357, 371
 - centre, 324
 - Fock–Segal–Bargmann representation, 333, 362
 - Haar measure, 26
 - induced representation, 331
 - invariant measure, 331
 - Lie algebra, 24
 - one-dimensional subgroup, 22

- polarised, 325
 - Schrödinger representation, 220
- Heisenberg group, 3
- Heisenberg–Weyl
 - group, *see* Heisenberg group, 323
- Hermite
 - polynomial, 346, 352
- Hilbert space, 47, 60
- Hilbert transform, 291
- homogeneous space, 20, 20–22
- homomorphism
 - algebraic, 301
- horizon, 121
- horocycle, 9, 63, 66
- Huygens principle, 113
- hyperbola, 46, 374
 - asymptote, 39, 374
 - centre, 374
 - focal length, 40, 110
 - focus, 39, 374
- hyperbolic
 - case, 4, 37
 - Cayley transform, 125
 - Fock–Segal–Bargmann representation, 348
 - geometry, 37
 - harmonic oscillator, 350
 - Moyal bracket, 337, 349
 - plane
 - two-fold cover, 105, 127
 - probability, 349
 - rotation, 127
 - Schrödinger representation, 349
 - unharmonic oscillator, 349
 - unit
 - cycle, 127
 - disk, 127
 - unit (j), 3
 - upper half-plane, 35, 105
 - zero-radius cycle, 63
- hyperboloid, 102
- hypercomplex number, 357
- hypercomplex numbers, 279
- hypercomplex unit (u), 3, 373
- hyperreal
 - number, 100
- ideal element, 101
- idempotent mathematics, 141
- identity, 18
 - approximation of the, 278
 - Jacobi, 24
 - Pythagoras’
 - parabolic, 137, 139
- imaginary
 - circle, 46, 55, 58, 61
 - unit (i), 3
- indefinite product, 60
- index refractive, 107
- induced covariant transform, 265
- induced representation, 53, 109, 144, 224, 234, 241, 304, 337
 - Heisenberg group, of, 331
 - induced wavelet transform, 234
- induction, 241
- inequality
 - Cauchy–Schwarz, 65–67, 71
 - triangle, 113, 119, 142
- infinite dimensional representation, 220
- infinitesimal
 - number, 96, 100
 - radius cycle, 96, 96–100, 131
- infinitesimally conformal, 99
- infinity
 - arithmetic, of, 30
- inner automorphism of group, 327
- inner derivation, 337, 339
- inner product, 47
 - Frobenius, 60
 - norm of vector, 89
- integrability of discrete equation, 375
- integral
 - Bergman, 15
 - Cauchy, 15, 251, 271–273, 276, 282, 297, 304, 370
 - Poisson, *see* Poisson kernel, *see* Poisson kernel
- interference, 341, 345, 355
- intersecting cycles, 66, 71, 73
- intertwining map, 49
- intertwining operator, 223, 250, 260, 265, 266, 287, 288, 290, 302, 309, 361
- interval
 - space-like, 110, 115
 - time-like, 110, 115
- invariant, 256, 284
 - functional, 256, 284
 - measure, 249, 251, 257, 278, 281, 284, 285
 - Heisenberg group, 331
 - metric, 113–123, 139
 - pairing, 256, 284
 - subset, 20
 - subspace, 289
 - vector fields, 23
- invariant measure, 25
- invariant subspace, 222
- inverse, 18
 - covariant transform, *see* contravariant transform
- inverse wavelet transform, 229

- inversion
 - circles, in (Yaglom term), 378
 - first kind, of the (Yaglom term), 84
 - in a cycle, 82, 82–84, 86, 101, 103
 - second kind, of the (Yaglom term), 84, 378
- inversive distance between cycles, 64
- IPython, 383
- irreducible
 - representation, 278, 289
- irreducible representation, 222
- isotropic cycles, 11, 71
- isotropy subgroup, 20, 40–44, 127, 129
 - orbit, 43, 65
- Iwasawa decomposition, 4, 33, 37, 369
- Jacobi identity, 24
- jet, 305, 306, 309, 337
 - bundle, 305
- joint
 - spectrum, 303
- Jordan
 - normal form, 306
- Jordan's normal form of a matrix, 222
- kernel heat, 138, 267
- kernel Poisson, 252, 271, 276, 282, 297
 - conjugated, 282, 291
- kernel reproducing, 232
- Kirillov
 - correspondence, 52
 - Descartes–Kirillov condition for tangent circles, 66
 - orbit method, 53
- Krein directing functional, 253
- Krein space, 60, 244, 337
- Kronecker delta, 220
- ladder operator, 245–248, 270, 272, 346–348, 350–353, 355–357
- Laplace operator, 15, 267, *see* Laplacian, 288
- Laplacian, 270, 271, 370
- Lebesgue measure, 25
- left regular representation, 223, 331
 - $\alpha x + b$ group, 278
- left shift, 18, 20, 21, 23
- lemma
 - Schur's, 224
- length, 14, 92
 - conformal, 93
 - curve, of, 114
 - focal, of a cycle, 56, 89
 - focal, of a hyperbola, 40, 110
 - focal, of a parabola, 56
 - from centre, 14, 92, 92, 93, 126–128
 - from focus, 14, 92, 92, 93, 97, 99, 128
 - p-conformality, 144
- Lidskii theorem, 308
- Lie
 - algebra, 22–25, 53
 - commutator, 24
 - Heisenberg group, *see* Weyl algebra
 - groups, 19, 22
- lifting, 332
- light
 - cone, 41, 63, 72, 81, 98, 104, 105, 110
 - infinity, at, 103–105
 - speed, of, 110
- limit
 - semiclassical, 337, 342
- line
 - contour, 38, 93, 95, 139
 - Menger, 118
 - parallel, 67
 - special (Yaglom term), 378
 - spectral, 109, 111
- linear space, 47
- linear-fractional transformations, *see* Möbius map
- linearization procedure, 219
- Littlewood–Paley operator, 253
- Littlewood–Paley theory, 277
- Lobachevsky
 - geometry, xiii, 37, 258, 270, 369
- locally compact group, 18
- loop, 22
- Lorentz–Poincaré transformation, 110
- lower half-plane, 20, 40, 43
- lowering operator, *see* ladder operator
- Möbius map, 3
 - fixed point, 31, 33, 98, 126
- main problem
 - of representation theory, 223
- map
 - M, 48, 101
 - Q, 48, 72, 101
 - p, 21, 108, 224
 - r, 108
 - s, 21, 108, 224
 - r, 21, 224
 - exponential, 23, 32
 - intertwining, 49
- Möbius, 3, 17, 20, 252, 255, 269, 274, 307, 310, 311
 - Clifford algebra, 376
 - on cycles, 7, 49

- on the real line, 30
 - preserving orthogonality, 72
- Maslov dequantisation, 141
- mathematics
 - idempotent, 141
 - tropical, 141
- matrix
 - congruence, 52
 - cycle, of, 7, 48
 - Clifford algebra, 376
 - Jordan normal form, 306
 - Jordan's normal form of, 222
 - similarity, 49, 388
 - Clifford algebra, 376
 - transfer, 107
- matrix coefficients, 227
- matrix elements, 220
- maximal function
 - grand, 254, 283
- maximal functions, 278
 - Hardy–Littlewood, 253, 260, 277, 283, 290, 297
 - non-tangential, 258, 285, 297
 - vertical, 258, 285, 297
- measure, 25
 - Carleson, 295
 - Gauss, 235
 - Haar, 25, *see* invariant measure, *see* invariant measure
 - invariant, 249, 251, 257, 278, 281, 284, 285
 - Heisenberg group, 331
 - Lebesgue, 25
 - left invariant, 25
- mechanics
 - classical, 108, 342
 - Hamiltonian, 323
 - quantum, 16, 103, 108
- Menger line, 118
- metaplectic representation, *see* oscillator representation
- method
 - orbit, 279
 - orbits, of, 337, 369
- metric, 113
 - invariant, 113–123, 139
 - monotonous, 117
 - unit disk, 131, 135
- Mexican hat
 - wavelet, 282
- minimal
 - polynomial, 307
- Minkowski space, 61
- Minkowski space-time, 52, 106, 110
- Möbius map, 3, 17, 20, 252, 255, 269, 274, 307, 310, 311
 - Clifford algebra, 376
 - on cycles, 7, 49
 - on the real line, 30
- model
 - functional, 255, 301, 308, 371
- modulus, parabolic, 139
- monad, 100
- monotonous metric, 117
- mother wavelet, 15, 227, 251, 281, 304
 - admissible, 294
- Moyal bracket, 343, 344
 - hyperbolic, 337, 349
- multiresolution analysis, 253
- netbook, 380
- nilpotent
 - Lie group, 326
- nilpotent unit, *see* parabolic unit
- non-Archimedean analysis, *see* non-standard analysis
- non-commutative
 - geometry, xiii, 15
 - group, 18
 - space, xiii
- non-commutative geometry, 312
- non-linear dynamics, 144, 375
- non-locality, 10, 12, 71, 76
- non-simply connected domain, 274
- non-standard
 - analysis, 96, 100
 - monad, 100
- non-tangential
 - maximal functions, 258, 285, 297
- non-trivial invariant subspaces, 222
- norm
 - Carleson, 295
 - function, of, 47
 - inner product, from, 89
 - parabolic, 139
- norm-normalised cycle, 64
- normal
 - subgroup, 21
- normalised cycle, 9, 57
 - det-, 57, 62, 64, 85, 89, 103, 388
 - k-, 13, 57, 63, 64, 89, 91, 103, 388
 - norm-, 64
- nucleus, 259, 286
- number
 - double, 337, 347, 352
 - dual, 337, 353, 353–356
 - hypercomplex, 357
 - infinitesimal, 96, 100
 - prime, 222
 - system, 36

- signature, 46
- numbers
 - complex, 34, 283, 373
 - double, 3, 36, 284, 373
 - dual, 3, 35, 373
 - hypercomplex, 279
 - split-complex, *see* double numbers
- numerical
 - range, 255
- observable, 339
- one-dimensional subgroup, 22
 - $\alpha x + b$ group, of, 22
 - group $SL_2(\mathbb{R})$, of, 22
 - Heisenberg group, of, 22
- open source, 379
- operator
 - annihilation, *see* ladder operator
 - Casimir, 271
 - Cauchy–Riemann, 15, 267, 288, 297
 - Cauchy-Riemann, 270, 271, 347, 370
 - commuting, 223
 - convolution, 26
 - creation, *see* ladder operator
 - defect, 255
 - Euler, 38
 - fiducial, 249, 280
 - Fillmore–Springer–Cnops construction, 311
 - integral
 - singular, 261, 277, 291, 297
 - intertwining, 223, 250, 260, 265, 266, 287, 288, 290, 302, 309, 361
 - ladder, 245–248, 270, 272, 346–348, 350–353, 355–357
 - Laplace, 15, 267, *see* Laplacian, 288
 - Littlewood–Paley, 253
 - lowering, *see* ladder operator
 - power bounded, 370
 - pseudo-differential, 24
 - pseudodifferential, 255
 - quasinilpotent, 370
 - raising, *see* ladder operator
 - Toeplitz, 370
 - unitary, 25, 221
- optics, 327
 - illusion, 81
 - paraxial, 107
- orbit, 20
 - co-adjoint representation, 333
 - isotropy subgroup, 43, 65
 - method, 279, 337, 369
 - method of Kirillov, 53
 - subgroup A' , of, 43
 - subgroup A , of, 4, 38, 132
 - subgroup K , of, 4, 38, 38–40, 43, 57, 104, 106, 132
 - subgroup N , of, 4, 38, 132
 - subgroup N' , of, 43
- orders
 - zero, of, 307
- orientation causal, 105, 111
- orthocenter, 74
- orthogonal cycles, *see* orthogonality of cycles
- orthogonal pencil of cycles, 73, 80, 84
- orthogonality
 - cycles, of, 7, 10, 46, 50, 69, 69–79, 82–83, 98, 115, 131, 388
 - focal, *see* f-orthogonality
 - function, of, 47
 - Galilean, 95
 - preserving map, 72
 - relation, 296
 - second kind, of the, *see* f-orthogonality
- orthonormal basis, 220
- oscillator
 - harmonic, 108, 327, 335, 339, 340, 343, 346, 349, 355
 - quantum, 109
 - repulsive (hyperbolic), 350
 - representation, 334
 - unharmonic, 340, 344, 355
 - hyperbolic, 349
- outer
 - automorphism of group, 327
- p-centre, 46
- p-focus, 56
- p-mechanics, 339
 - dynamic equation, 339
 - observable, 339
 - state, 341
- p-mechanisation, 340
- packet, wave, 109
- pairing
 - Hardy, 257, 258, 285
 - invariant, 256, 284
- parabola, 46, 374
 - directrix, 8, 39, 56, 374
 - focal length, 56
 - focus, 8, 39, 56, 374
 - vertex, 8, 56, 374
- parabolas
 - concentric, 129
 - confocal, 129
- parabolic
 - case, 4, 37
 - Cayley transform, 128
 - circle (Yaglom term), 75, 378

- cycle (Yaglom term), 378
- cylinder function, *see* Weber–Hermite function
- degeneracy, 78, 129
- Fock–Segal–Bargmann representation, 353
- modulus, 139
- norm, 139
- probability, *see* classic probability
- Pythagoras’ identity, 137, 139
- Schrödinger representation, 353
- trigonometric functions, 136
- unit
 - cycle, 128
 - disk, 128
- unit (ϵ), 3
- upper half-plane, 35, 41
- zero-radius cycle, 63
- parallel
 - line, 67
- parallelism, Benz, 72
- paravector formalism, 375
- paraxial optics, 107
- PDO, *see* pseudo-differential operator, 255
- pencil
 - covariant, 310
 - cycles, of, xiv, 58, 64, 66–67, 72–74, 387
 - orthogonal, 73, 80, 84
- periodic table, 36
 - chemical elements, of, xiii
- perpendicular, 14, 94
- phase space, 108, 335, 338, 342, 344, 346, 348
 - tangent space of, 108
- Planck
 - constant, 337, 354
- plane
 - hyperbolic
 - two-fold cover, 105, 127
- Plato’s cave, 7, 7, 55
- Poincaré extension, 53, 177
- point
 - cycle, of, 64, 91
 - infinity, at, 102
 - power, of, xiv, 40, 46, 64, 91, 388
 - space, 7, 48, 161, 378
- Poisson
 - bracket, 355
- Poisson kernel, 252, 271, 276, 282, 297
 - conjugated, 282, 291
- polar
 - projection, *see* stereographic projection
- polyanalytic function, 271
- polynomial
 - Hermite, 346, 352
 - minimal, 307
- Pontrjagin space, 60
- positive cycle, 61, 115
- power
 - cycle, of, 64, 91
 - point, of, xiv, 40, 46, 64, 91, 388
 - Steiner, *see* power of a point
- power bounded operator, 370
- primary
 - representation, 278, 303, 305, 311
- primary representation, 223
- prime number, 222
- principal
 - value, 261, 277, 291
- principle
 - Huygens, 113
 - similarity and correspondence, 352, 357
- probability
 - classic (parabolic), 355
 - hyperbolic, 349
 - quantum, 337, 341, 344
- product
 - Blaschke, 307
 - cycle, 60, 69, 91
 - indefinite, 60
 - inner, 47
 - Frobenius, 60
 - norm of vector, 89
- projection
 - polar, *see* stereographic
 - stereographic, 102
- projective
 - cross ratio, 54, 54
 - cross-ratio, 123
 - real line, 30
 - double cover, 31
- projective space, 7, 48, 51, 53, 142, 373
- prolongation, 304
- pseudo-differential operator, 24
- pseudodifferential operator, 255
- $\mathcal{P}\mathcal{T}$ -symmetry, 337
- pulling, 332
- pyGiNaC, 383
- Pythagoras’
 - identity
 - parabolic, 137, 139
- Python, 383, 384
- Pyzo, 383
- quadratic
 - eigenvalue, 311
 - equation, 373
 - discriminant, 61
 - generator, 335
 - Hamiltonian, 108
- quadric, 373

- quantisation
 - geometrical, 337
- quantum
 - field, 371
 - harmonic oscillator, 109
 - mechanics, 16, 103, 108
 - probability, 337, 341, 344
- quantum mechanics, 339
- quasi-regular
 - representation of $\alpha x + b$ group, 278
- quasinilpotent operator, 370
- Quaternions, 14
- quotient group, 21
- radical axis
 - cycles, of, 40, 58
- radius cycle, of, 13, 58, 89, 388
- Radon transform, 254
- raising operator, *see* ladder operator
- range
 - numerical, 255
- ray, 107, 113
 - reflection, 374
- real line, 3
 - $\alpha x + b$ map, 21, 25
 - Möbius map, 30
 - projective, 30
 - double cover, 31
- reconstruction formula, 257, 284
- red shift, 106, 111
- reduced wavelet transform, *see* induced wavelet transform, 265
- reducible representation, 222
- reference system, 109
- reflection
 - in a cycle, 12, 82, 82–84, 101, 130
 - ray, of, 374
- refractive index, 107
- regular representation, 223
- relation
 - orthogonality, 296
- relation of equivalence, 220
- relative
 - convolution, 287
- relative convolution, 365
- relativity, 109
- representation, 219
 - $SL_2(\mathbb{R})$ group, 243–244
 - in Banach space, 303
 - $\alpha x + b$ group, 251
 - co-adjoint, 279
 - quasi-regular, 278
 - adjoint, 53, 221
 - character of, 221
 - co-adjoint, 333
 - orbit, 333
 - coefficients, *see* wavelet transform, *see* wavelet transform
 - complementary series, 252, 370
 - continuous, 219
 - decomposable, 223
 - discrete series, 243, 249, 252, 370
 - exact, 220
 - faithful, 220
 - finite dimensional, 220
 - Fock–Segal–Bargmann, 333, 335, 356, 362
 - classic (parabolic), 353
 - hyperbolic, 348
 - FSB, *see* Fock–Segal–Bargmann representation group
 - linear, 15
 - Heisenberg group
 - classic (parabolic), 353
 - hyperbolic, 349
 - Schrödinger, 334
 - induced, 53, 109, 144, 224, 234, 241, 304, 337
 - Heisenberg group, of, 331
 - infinite dimensional, 220
 - irreducible, 222, 278, 289
 - left regular, 225, 331
 - $\alpha x + b$ group, 278
 - linear, 219
 - linearization, 219
 - metaplectic, *see* oscillator representation
 - oscillator, 334
 - primary, 223, 278, 303, 305, 311
 - principal series, 252, 370
 - reducible, 222
 - regular
 - left, 223
 - Schrödinger, 220, 334, 341, 342, 347, 351, 360
 - classic (parabolic), 353
 - hyperbolic, 349
 - series
 - discrete, 231
 - Shale–Weil, *see* oscillator representation
 - square integrable, 227, 230, 249, 251, 257, 265, 281, 284, 294
 - trivial, 220
 - unitary, 221
 - representation of a group, 219
 - representation space, 220
 - representation theory
 - main problem of, 223
 - representational coefficients, 227

- representational geometry, [47](#)
- representations, [219](#)
 - equivalent, [220](#)
 - unitary, [221](#)
 - Fock–Segal–Bargmann, [341](#)
 - linear, [241](#)
- reproducing kernel, [232](#)
- repulsive
 - harmonic oscillator, [350](#)
- resolvent, [256](#), [301](#), [303](#), [310](#)
- restriction of representation, [222](#)
- Riemann
 - geometry, [37](#), [113](#)
 - mapping theorem, [274](#)
 - sphere, [102](#)
- right shift, [18](#), [20](#), [23](#)
- rotation, [41](#), [114](#)
 - elliptic, [126](#)
 - hyperbolic, [127](#)
 - parabolic
 - tropical, [142](#)
- scalar product, [220](#)
- Schrödinger
 - equation, [327](#)
 - group, [327](#), [346](#)
 - representation, [334](#), [341](#), [342](#), [347](#), [351](#), [360](#)
 - classic (parabolic), [353](#)
 - hyperbolic, [349](#)
- Schrödinger representation, [220](#)
- Schur’s lemma, [224](#)
- section, [21](#)
- section conic, [4](#), [5](#), [39](#), [373](#)
- selfadjoint cycle, [75](#), [85](#), [122](#), [378](#)
- semiclassical
 - limit, [337](#), [342](#)
- semigroup
 - cancellative, [250](#)
- set
 - total, [227](#)
- Shale–Weil representation, *see* oscillator representation
- shift
 - left, [18](#), [20](#), [21](#), [23](#)
 - red (astronomy), [106](#), [111](#)
 - right, [18](#), [20](#), [23](#)
- signature, number systems, of, [46](#)
- similarity
 - cycles, of, [79](#), [130](#), [388](#)
 - Clifford algebra, [376](#)
 - matrix, of, [49](#), [388](#)
 - Clifford algebra, [376](#)
- simply connected domain, [274](#)
- singular
 - integral operator, [261](#), [277](#), [291](#), [297](#)
 - SIO, *see* singular integral operator
 - seesingular integral operator, [291](#)
 - Sokhotsky–Plemelj formula, [276](#)
 - source
 - open, [379](#)
 - space
 - Bergman, [15](#), [249](#), [252](#), [274](#), [370](#)
 - commutative, [xiii](#)
 - configuration, [342](#), [344](#), [349](#), [354](#), [356](#)
 - cycle, [161](#)
 - cycles, of, [7](#), [48](#), [101](#), [378](#)
 - Euclidean, [94](#)
 - Fock–Segal–Bargmann, [253](#), [335](#), [347](#), [357](#), [371](#)
 - FSB, *see* Fock–Segal–Bargmann space
 - Gårding , [230](#)
 - Hardy, [15](#), [249](#), [251](#), [261](#), [271](#), [273](#), [277](#), [279](#), [282](#), [291](#), [302](#), [308](#), [370](#)
 - generalised, [261](#)
 - generalized, [278](#), [289](#), [292](#)
 - Hilbert, [47](#), [60](#)
 - Krein, [60](#), [244](#), [337](#)
 - linear, [47](#)
 - Minkowski, [61](#)
 - non-commutative, [xiii](#)
 - phase, [108](#), [335](#), [338](#), [342](#), [344](#), [346](#), [348](#)
 - tangent space of, [108](#)
 - point, [7](#), [48](#), [161](#), [378](#)
 - Pontrjagin, [60](#)
 - projective, [7](#), [48](#), [51](#), [53](#), [142](#), [373](#)
 - tangent, [23](#), [53](#), [85](#), [113](#)
 - phase space, of, [108](#)
 - space-like interval, [110](#), [115](#)
 - space-time, [104](#), [109](#)
 - Galilean, [110](#), [136](#)
 - Minkowski, [52](#), [106](#), [110](#)
 - special
 - function, [15](#)
 - line (Yaglom term), [378](#)
 - spectral covariant distance, [308](#)
 - spectral line, [109](#), [111](#)
 - spectrum, [301](#), [304](#)
 - contravariant, [302](#), [303](#), [305](#), [307](#)
 - stability, [308](#)
 - discrete, [370](#)
 - joint, [303](#)
 - mapping, [301](#)
 - speed, light, of, [110](#)
 - sphere, Riemann, [102](#)
 - split-complex numbers, *see* double numbers
 - square integrable
 - representation, [249](#), [251](#), [257](#), [265](#), [281](#), [284](#), [294](#)
 - square integrable representation, [227](#), [230](#)
 - squares

- dyadic, 277, 289, 297
- stability
 - contravariant spectrum, 308
- state, 341
 - coherent, *see* wavelet
 - ground, 227
 - vacuum, *see* mother wavelet, *see* mother wavelet
- Steiner power, *see* power of a point
- stereographic projection, 102
- stopping time argument, 289, 297
- subalgebra
 - Cartan, 246
- subgroup, 19
 - A, 4, 32
 - orbit, 4, 38, 132
 - A', 32, 41, 110, 127, 137
 - A'', 43
 - F, 29
 - F', 29
 - F̄, 29
 - K, 4, 15, 32, 114, 137
 - orbit, 4, 38, 38–40, 43, 57, 104, 106, 132
 - N, 4, 32
 - orbit, 4, 38, 132
 - N', 32, 41, 110, 114, 137
 - orbit, 43
 - A', 114
 - orbit, 43
 - conjugated, 21
 - generator, 245
 - isotropy, 20, 40–44, 127, 129
 - orbit, 43, 65
 - normal, 21
 - one-dimensional, 22
- subrepresentation, 222
- subset, invariant, 20
- subspace
 - invariant, 222, 289
- summation
 - Abel, 276
- support
 - functional calculus, *see* spectrum
- swiGiNaC, 383
- symbol
 - contravariant, 255
 - covariant, 254
- symbolic calculus, *see* covariant calculus
 - covariant, 254
- symplectic form, 53, 54, 108, 324, 326, 376
- symplectic group, 324, 327, 334, 339, 346
- symplectic transformation, 241, 242, 338, 350
- system, reference, 109
- tangent, 10, 57, 70–71, 76, 78, 95, 121
 - cycles, 58, 66, 73
 - Descartes–Kirillov condition, 66
 - lines, 67
 - space, 23, 53, 85, 113
 - phase space, of, 108
- Taylor series, 15
- tent, 277, 284, 295
- theorem
 - automatic proving, 387
 - Lidskii, 308
 - main of arithmetic, 222
 - Riemann mapping, 274
 - spectral mapping, 301
- theory
 - Littlewood–Paley, 277
- time
 - absolute, 110, 136, 378
 - arrow, 105, 111
 - time-like interval, 110, 115
- Toeplitz
 - operator, 370
- token, 250
- total set, 227
- trace, 9, 221
- transfer matrix, 107
- transform
 - Cayley, 125, 131, 272
 - cycle, of, 129
 - elliptic, 125
 - hyperbolic, 125
 - parabolic, 128
 - contravariant, 256, 284, 297, 364
 - covariant, 249, 280, 297
 - induced, 265
 - inverse, *see* contravariant transform
 - Fock–Segal–Bargmann, 362
 - Hilbert, 291
 - Radon, 254
 - wavelet, 15, 227, *see* wavelet transform, 281, 297
 - continuous, 281
 - induced, 234
 - reduced, *see* induced wavelet transform
- transformation
 - canonical, 108
 - Galilean, 110
 - group, 17, 20
 - linear-fractional, *see* Möbius map
 - Lorentz–Poincaré, 110
 - Möbius, *see* Möbius map
 - symplectic, 241, 242, 338, 350
- transitive, 3, 20, 22, 38
- triangle inequality, 113, 119, 142

- trigonometric
 - functions
 - σ -, 43
 - parabolic, 136
- trivial representation, 220
- tropical
 - mathematics, 141
 - parabolic rotation, 142
- umbral calculus, 250
- unharmonic
 - oscillator, 340, 344, 355
 - hyperbolic, 349
- unimodular
 - group, 331
- unit
 - circle, *see* elliptic unit cycle, 273
 - cycle
 - elliptic, 126
 - hyperbolic, 127
 - parabolic, 128
 - disk, 125, 273
 - elliptic, 126, 126
 - hyperbolic, 127
 - metric, 131, 135
 - parabolic, 128
 - hyperbolic (j), 3
 - hypercomplex (t), 3, 373
 - imaginary (i), 3
 - nilpotent, *see* parabolic unit
 - parabolic (ϵ), 3
- unitary equivalent representations, 221
- unitary operator, 25, 221
- unitary representation, 221
- upper half-plane, 20, 40, 43, 125, 364
 - boundary effect, 9, 56, 63, 71, 78, 85
 - elliptic, 34, 41
 - hyperbolic, 35, 105
 - parabolic, 35, 41
- vacuum state, *see* mother wavelet, *see* mother wavelet
 - wavelet
- vacuum vector, 227
- vacuum vector of quantum mechanics, 234
- Vahlen condition, 80, 84
- value
 - principal, 261, 277, 291
- vector
 - admissible, 230
 - cyclic, 222
 - fiducial, 227
 - vacuum, 227
- vector fields, invariant, 23
- vector formalism, 375
- vertex, parabola, of, 8, 56, 374
- vertical
 - maximal functions, 258, 285, 297
- wave, 113
 - packet, 109
- wavelet, 3, 249, 251, 265, 269, 280, 281, 304
 - admissible, 249, 251, 257, 281, 284
 - Mexican hat, 282
 - mother, 15, 227, 251, 281, 304
 - admissible, 294
 - transform, 15, 251, 281, 297, 304, 347
 - continuous, 281
 - induced, *see* induced covariant transform
 - reduced, 265
- wavelet transform, 227
 - induced, 234
 - inverse, 229
 - reduced, *see* induced wavelet transform
- wavelets, 227
- Weber–Hermite function, 350, 352
- Weyl
 - algebra, 323, 325
 - commutation relation, 323
 - group, *see* Heisenberg group, 323
- Wiener–Hopf factorisation, 253
- Yaglom term
 - inversion
 - circles, in, 378
 - second kind, of, 378
 - parabolic
 - circle, 378
 - cycle, 378
 - special line, 378
- zero divisor, 4, 35, 36, 41, 53, 102, 138, 352, 373
- zero order, of, 307
- zero-radius cycle, 9, 11, 51, 61, 62–66, 71–73, 89, 97, 101, 103, 120, 378
- infinity, at, 101